

猪口孝一教授退職記念教室業績集

(2013～2021)

日本医科大学血液内科学教室

Chromatin Structure of the Human Dihydrofolate Reductase Gene Promoter

MULTIPLE PROTEIN-BINDING SITES*

(Received for publication, August 7, 1985)

Takashi Shimada, Koiti Inokuchi, and Arthur W. Nienhuis

From the Clinical Hematology Branch, National Heart, Lung, and Blood Institute, National Institutes of Health, Bethesda, Maryland 20205

The chromatin structure of the promoter region of the human dihydrofolate reductase gene was determined using a variety of nucleases including DNase I, micrococcal nuclease, several restriction endonucleases, exonuclease III, and *Bal31*. Two separate regions from -670 to -340 (the distal hypersensitive region) and from -170 to +150 (the proximal hypersensitive region) were shown to be essentially free of proteins as indicated by their accessibility to both endo- and exonucleases. Within the proximal hypersensitive region, one protein appears to be bound at the start site for transcription. A 170-base pair fragment between the two hypersensitive regions was highly resistant to all nucleases tested. Multiple barriers against exonuclease digestion and resistance to dissociation by high salt concentrations suggest that more than one protein is tightly bound to this region. The upstream sequence from -670 and the downstream sequence from +150 were shown to be packaged into nucleosomes. The selective accessibility of certain sites to micrococcal nuclease cutting indicates that the initial nucleosomes are phased upstream from the distal hypersensitive region. There appears to be a protein bound between the phased nucleosomes and the upstream boundary of the distal hypersensitive region. These results suggest that the normal nucleosome array is interrupted by about 900 base pairs of nucleosome-free DNA to which several nuclear proteins bind in a DNA sequence-specific manner.

Gene regulation is thought to be mediated by interaction of nuclear proteins with specific DNA sequences in control regions of genes. Such control regions included promoters and enhancers, often identified as nucleosome-free, DNase I-hypersensitive sites where protein binding may occur. Protein DNA sequence-specific interactions have been demonstrated at the promoter and/or enhancer for several specialized genes including globin (Emerson and Felsenfeld, 1984), immunoglobulin (Ephrussi *et al.*, 1985), myc (Siebenlist *et al.*, 1984), heat shock (Wu, 1984 a, 1984b; Parker and Topol, 1984), and the SV40 early region (Tjian, 1979; Dynan and Tjian, 1983; Gidoni *et al.*, 1984). A role for specific binding proteins in the regulation of constitutively expressed genes has not been defined.

We have cloned and molecular characterized one constitu-

tively expressed gene, that for dihydrofolate reductase (Chen *et al.*, 1984; Shimada and Nienhuis, 1985). The gene is DNase I-insensitive and fully methylated over its 30-kilobase coding region, but the promoter and immediate 5'-flanking sequences are undermethylated and DNase I-hypersensitive. Thus, transcriptional control is likely to be exerted at the promoter region. We have designed experiments to determine whether there are molecules that bind at specific sites in this region of the gene.

These studies were facilitated by use of cells resistant to methotrexate (MTX^r), an inhibitor of dihydrofolate reductase, in which there are many copies of the dihydrofolate reductase gene. Our previous studies had shown that all copies of the dihydrofolate reductase gene in such cells have the same methylation pattern and structure in chromatin (Shimada and Nienhuis, 1985). Recently, Wu (1984a) has developed an *in situ* exonuclease III protection technique that maps sequences within nuclease-hypersensitive regions in chromatin onto which regulatory proteins are bound. This method and related strategies designed to detect protection of specific sequences from nuclease digestion were used to map multiple binding sites within the dihydrofolate reductase promoter region.

MATERIALS AND METHODS

Reagents—Restriction enzymes were obtained from New England BioLabs, Bethesda Research Laboratories, or Worthington. Deoxyribonuclease I (DNase I) and micrococcal nuclease were obtained from Worthington, exonuclease III and *Bal31* from New England BioLabs, and *S₁* nuclease from P-L Biochemicals. Nylon membrane filters (GeneScreen Plus) were obtained from New England Nuclear.

Southern Blot Analysis—Standard agarose gels were used to resolve restricted DNA. Southern transfer to GeneScreen Plus, hybridization, filter washing, and rehybridization conditions were according to the protocol provided by New England Nuclear. The following molecular probes were used in various hybridization experiments: Ex probe that contains the human dihydrofolate reductase coding sequences for exons 2-6, F probe that contains the 5'-flanking region from the *EcoRI* site at -1252 to the *RsaI* site at -994, I probe that contains the intron I sequence from the *RsaI* site at +209 to the *EcoRI* site at +524, S probe that contains sequences between -565 and -115 (0.45-kilobase *ScaI-SstII* fragment), and the IX probe that contains sequences between +209 and +469 (0.26-kilobase *RsaI-XhoI* fragment). These probes were isolated by agarose gel electrophoresis and rendered radioactive by nick translation using standard methodology.

Cell Culture and Isolation of Nuclei—MTX-resistant (Yoder *et al.*, 1983) and sensitive HeLa cells were grown as previously described (Shimada and Nienhuis, 1985). Nuclei were isolated from these cells essentially according to published techniques except that 0.1 mM phenylmethylsulfonyl fluoride (PMSF) was added to all buffers used

* The costs of publication of this article were defrayed in part by the payment of page charges. This article must therefore be hereby marked "advertisement" in accordance with 18 U.S.C. Section 1734 solely to indicate this fact.

¹ The abbreviations use are: MTX, methotrexate; bp, base pairs; PMSF, phenylmethylsulfonyl fluoride; EGTA, ethylene glycol bis(β-aminoethyl ether)-N,N,N',N'-tetraacetic acid.

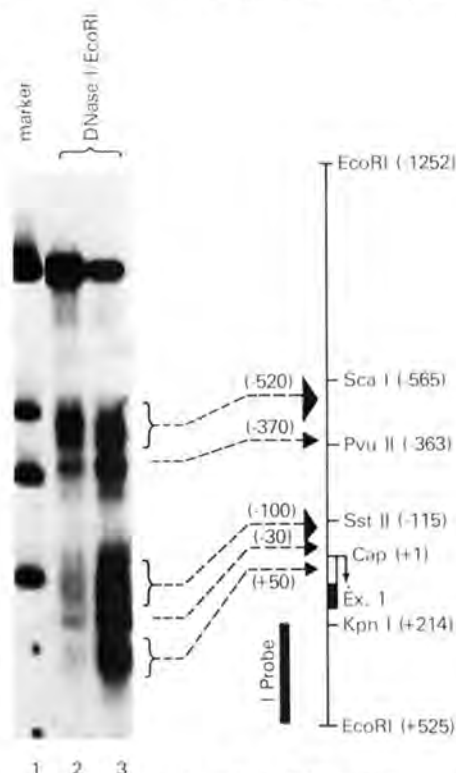


Fig. 1. Detailed mapping of the DNase I-hypersensitive sites in the 5' end region of the human dihydrofolate reductase genes. Nuclei were isolated from the MTX-resistant HeLa cells and digested with DNase I at 1.0 (lane 2) and 3.0 (lane 3) $\mu\text{g}/\text{ml}$ at 37 °C for 10 min. DNA was extracted, digested with *EcoRI*, and blot-hybridized with the I probe. Size markers of appropriate length were obtained as follows: aliquots of the 1.78-kilobase *EcoRI* fragment (–1252 to +525) were singly restricted with *ScaI*, *PvuII*, *SstII*, or *RsaI* and the digested samples were mixed (lane 1). The large arrowheads indicate the DNase I-hypersensitive sites or regions. Values are indicated in base pairs from the initiation site of transcription.

for extraction, and cells were lysed in a final concentration of 1.0% Nonidet P-40 in buffer R (10 mM Tris-HCl, pH 7.5, 10 mM NaCl, 3 mM MgCl_2 , 0.1 mM PMSF) containing 0.25 M sucrose.

Mapping of Endonuclease-sensitive Sites. Isolated nuclei and purified DNA from MTX-resistant HeLa cells were suspended in buffer R for DNase I digestion, in buffer M (50 mM Tris-HCl, pH 7.4, 60 mM KCl, 3 mM CaCl_2 , 0.34 M sucrose, and 0.1 mM PMSF) for micrococcal nuclease digestion, or in buffer E (50 mM Tris-HCl, pH 7.5, 50 mM NaCl, 5 mM MgCl_2 , 0.1 mM EGTA, 0.5 mM dithiothreitol, 0.3 M sucrose, and 0.1 mM PMSF) for restriction enzyme digestion. The nuclei were incubated with increasing amounts of endonucleases under conditions described under "Results." DNA was purified, restricted with enzymes as specified, and analyzed by Southern blot hybridization.

Exonuclease Protection Assay. The exonuclease III protection assay was performed essentially according to the methods defined by Wu (1984a). Nuclei were suspended in buffer E at a concentration equivalent to 0.25 mg of DNA/ml and incubated with 1,000 units/ml of the specified restriction enzyme and variable amounts of exonuclease III for 30 min at 37 °C. Digestion was terminated by addition of an equal volume of 2 \times lysis buffer (1% sodium dodecyl sulfate, 0.6 M NaCl, 20 mM EDTA, 20 mM Tris-HCl, pH 7.5), and DNA was prepared as described (Shimada and Nienhuis, 1985). The DNA was digested with *S₁* nuclease in 30 mM sodium acetate, pH 4.5, 50 mM NaCl, and 1 mM ZnCl_2 . The concentrations of DNA and *S₁* nuclease were 0.2 mg/ml and 30 units/ml, respectively. Southern blot analysis

was performed by standard methods. For the protection assay that utilized *Bal31*, the nuclei were first digested with a specified restriction enzyme alone in buffer E. After 30 min, the nuclei were recovered by centrifugation (1 min at $10,000 \times g$) and resuspended in buffer B (20 mM Tris-HCl, pH 8.0, 150 mM NaCl, 12 mM MgCl_2 , 12 mM CaCl_2 , 1 mM EDTA, 0.3 M sucrose, and 0.1 mM PMSF) at a concentration equivalent to 0.25 mg of DNA/ml and incubated with various amounts of *Bal31* for 30 min at 30 °C. The DNA was then purified by standard methods, exposed to *S₁* nuclease as described above, repurified, restricted with a specified enzyme, and analyzed by the Southern blotting method. To determine whether the molecules that block exonuclease III progression could be extracted with salt, isolated nuclei were incubated at a concentration equivalent to 70 μg of DNA/ml in buffer R containing 0–2 M NaCl for 30 min at 4 °C. The nuclei were recovered by centrifugation at $10,000 \times g$ for 1 min and then resuspended in buffer E and analyzed according to the standard method for defining exonuclease III protection sites.

RESULTS

Mapping of Endonuclease-hypersensitive Regions in the Dihydrofolate Reductase Gene Promoter. Recently, we found several DNase I cutting sites in the promoter region (Shimada and Nienhuis, 1985). These have now been mapped more precisely. DNA samples extracted from DNase I-treated nuclei were restricted with *EcoRI* and electrophoresed on a long 2% agarose gel with restriction endonuclease fragments derived from the cloned dihydrofolate reductase gene run on adjacent lanes as size markers (Fig. 1). Two separate regions from –600 to –350 (the distal hypersensitivity region) and from –150 to +100 (the proximal hypersensitivity region) were shown to be sensitive to DNase I. The 200 bp between the two hypersensitive regions were highly resistant. Five discrete DNase I cutting sites were mapped at –520, –370, –100, –30, and +50. Two small segments between –440 and –400 and between –10 and +20 seem to be relatively resistant to DNase I.

Data obtained on the exposure of isolated nuclei to various restriction endonucleases further defined the positions of the hypersensitive regions (Fig. 2). For example, exposure of isolated nuclei to *HaeIII* revealed preferential cutting at sites –400 and –110 bp upstream from the cap site with relative protection of two sites between the two hypersensitive regions and those downstream within the coding sequences (Fig. 2A). A site immediately in front of the cap site (–4) is nonetheless relatively resistant. Similarly, exposure of nuclei to *HhaI* resulted in detection of four sites that lie within the hypersensitive regions that exhibit preferential cutting compared to sites within coding sequences (Fig. 2B). The boundaries of the hypersensitive regions were further defined using *HinfI*, *RsaI*, *AluI*, and *DdeI* as shown in Fig. 2.

The Hypersensitive Regions Are Nucleosome-free and the Upstream Nucleosomes Are Phased on DNA. A typical nucleosome ladder was observed when DNA from micrococcal nuclease-digested nuclei were hybridized on Southern blots to a coding sequence probe (Ex), indicating that nucleosomes are distributed normally over the coding region (Fig. 3A). Analogous Southern blots were probed with the F probe derived from the 5'-flanking region and the I probe containing the first intron. A ladder pattern was observed indicating the presence of nucleosomes, although a smear rather than discrete bands appears in the region of the gel corresponding to higher multiples (Fig. 3, B and D). This occurs because the adjacent hypersensitive region lacks discrete internucleosome cutting sites. In contrast, the S probe (–565 to –115) that includes the nuclear DNase I cutting site did not detect a nucleosome ladder pattern, indicating that this region is nucleosome-free (Fig. 3C). With limit digestion, the S probe detected a 200-bp fragment that may correspond to the seg-

Chromatin Structure of the Dihydrofolate Reductase Gene Promoter

1447

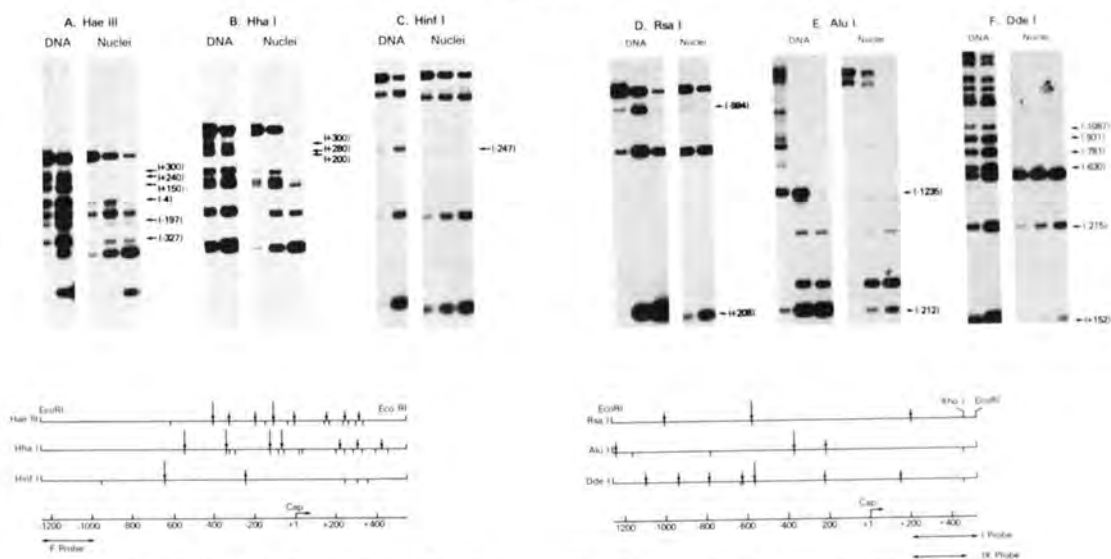


FIG. 2. Mapping of restriction endonuclease-sensitive sites. Isolated nuclei and purified DNA from MTX-resistant HeLa cells were partially digested with *Hae*III (A), *Hha*I (B), *Hinf*I (C), *Rsa*I (D), *Alu*I (E), or *Dde*I (F). DNA was purified and restricted with *Eco*RI (A-D) or *Xho*I (E and F) and blot-hybridized with the F probe (A-C), the I probe (D), or the IX probe (E). The fragments missing or of diminished intensity by protection of certain sites in nuclear chromatin are shown by arrows on the blots. The restriction maps are shown below. The long arrows indicate restriction endonuclease-sensitive sites. The short arrows indicate restriction endonuclease-resistant sites.

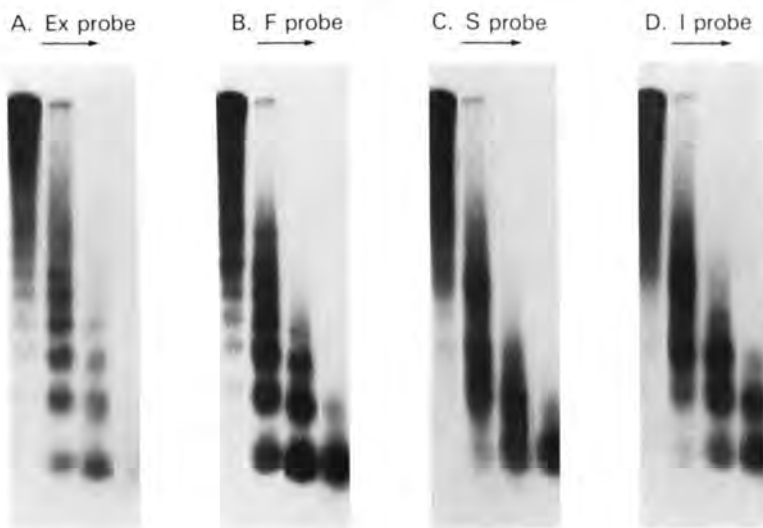
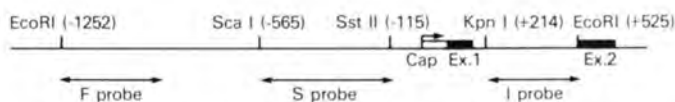


FIG. 3. Nucleosomal patterns produced by micrococcal nuclease. Isolated nuclei from MTX-resistant HeLa cells were digested with micrococcal nuclease in increasing concentration (0.2, 1.0, 5.0, and 20.0 units/ml, indicated by the direction of the arrow above each blot), at 37 °C for 5 min. DNA was extracted and blot-hybridized with the Ex probe (A), the F probe (B), the S probe (C), or the I probe (D).



ment between -350 and -150 that also fails to be cut by DNase I.

Evidence suggesting phasing of the upstream nucleosomes was obtained by the comparison of micrococcal nuclease diges-

tion of nuclear DNA and purified DNA. During the early stages of digestion, micrococcal nuclease exhibits preferential cutting at specific sites as shown by the analysis of purified DNA exposed to the enzyme (Fig. 4; Fittler and Zachau, 1979).

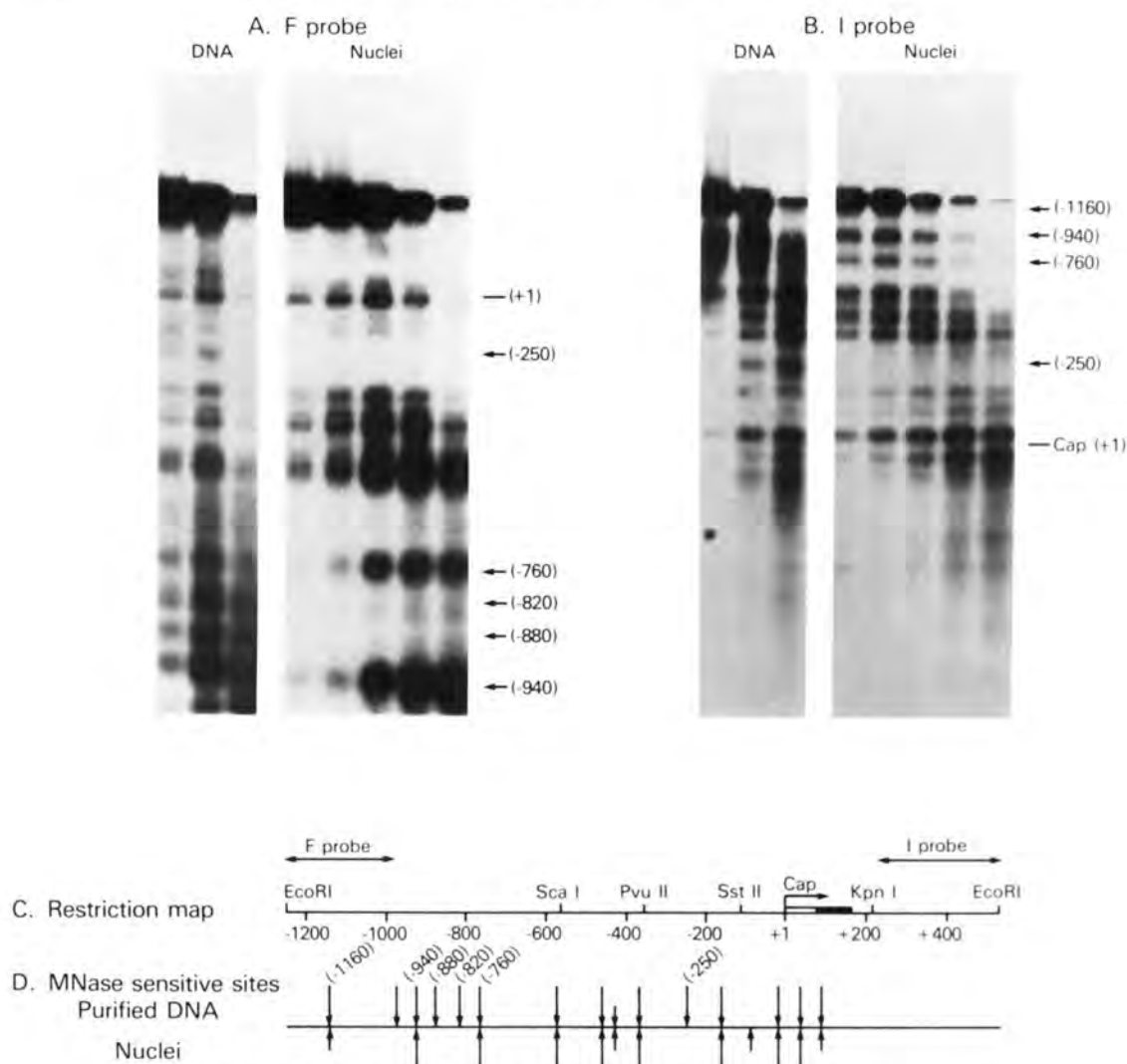


FIG. 4. Mapping of micrococcal nuclease-sensitive sites. Isolated nuclei and purified DNA from MTX-resistant HeLa cells were digested with micrococcal nuclease (*MNase*) in increasing concentration (0.05, 0.1, 0.2, 0.5, and 1.0 units/ml for nuclei digestion and 0.15, 0.5, and 1.5 units/ml for purified DNA digestion, from left to right) at 37 °C for 5 min. DNA was extracted, restricted with *EcoRI*, and blot-hybridized with the F probe (A) or the I probe (B). Panel D shows micrococcal nuclease-sensitive sites. The arrows above the line indicate micrococcal nuclease preferential cutting sites in purified DNA. The arrows below the line indicate micrococcal nuclease-sensitive sites in nuclear chromatin.

Several discrete cutting sites were observed when both nuclei and purified DNA from HeLa cells containing multiple copies of the dihydrofolate reductase genes were lightly digested with micrococcal nuclease, restricted completely with *EcoRI*, and analyzed on Southern blot by the indirect end-labeling method (Fig. 4). In nuclear digestions, the sites of initial cleavage are thought to lie in linker regions between nucleosomes. Cutting sites at -860 and -820, seen on digestion of purified DNA, were not cut on exposure of nuclei to micrococcal nuclease, suggesting that nucleosomes are protecting these sites. In contrast, the sites at -1160, -940, and -760 are cleaved equally in purified DNA and nuclei consistent

with the fact that these sites lie between nucleosomes. A nucleosome ladder is observed on analysis of Southern blots of nuclear DNA with the intron probe (I probe), indicating the presence of nucleosomes, but the lack of discrete micrococcal nuclease cutting sites in this region of purified DNA prevented determining whether these nucleosomes are also phased.

In the two DNase I-hypersensitive regions, many preferential micrococcal nuclease cutting sites were mapped, and these sites were all equally sensitive to micrococcal nuclease in isolated nuclei with the exception of the site at -250. This site was cut in purified DNA but protected in isolated nuclei;

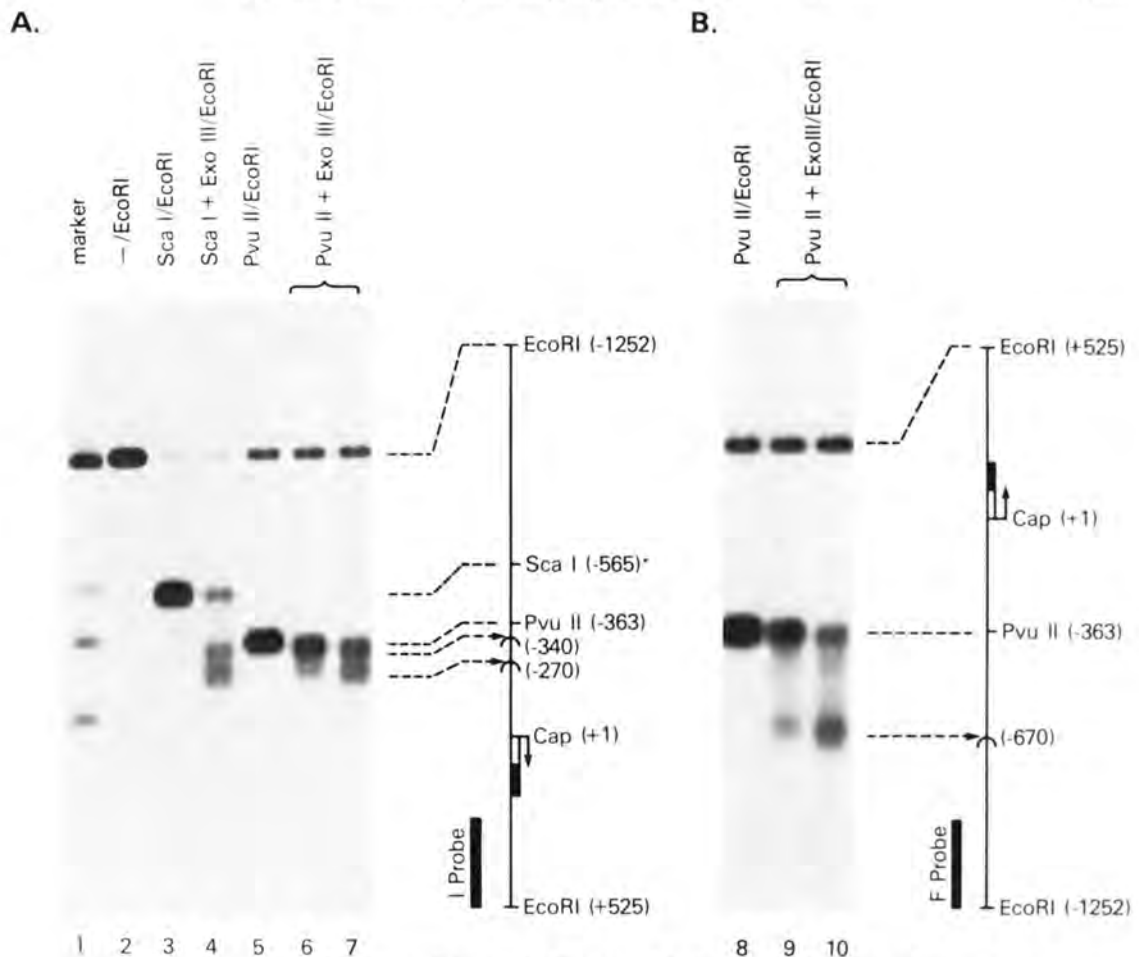


FIG. 5. Exonuclease III-protected sites in the 5' region of the human dihydrofolate reductase gene in MTX-resistant HeLa cells. Isolated nuclei were digested with *Sca*I (lanes 3 and 4) or *Pvu*II (lanes 5-10) and exonuclease III at 1600 units/ml (lanes 6 and 9) or 8000 units/ml (lanes 4, 7, and 10) at 37 °C for 30 min. DNA was purified, trimmed with *S*₁ nuclease, restricted with *Eco*RI, and blot-hybridized with the I probe (A) or the F probe (B). Exonuclease III stop positions are indicated by the arrows.

this site may lie in the protected segment that falls between the two DNase I-sensitive regions.

Mapping the Boundaries of the Hypersensitive Regions with Exonucleases: Detection of Multiple Protein-binding Sites—Nuclei were exposed to a restriction endonuclease with a cutting site within one of the hypersensitive regions and to an exonuclease that digested the DNA from this site until it encountered a specific block. After this digestion, DNA was purified, trimmed with *S*₁ nuclease, restricted with *Eco*RI, and analyzed by Southern blotting. The positions of blocks to further exonuclease digestion during the nuclear incubations were mapped on these Southern blots by the indirect end-labeling method (Fig. 5).

In the experiments exhibited in Fig. 5A, *Sca*I (-565) or *Pvu*II (-363) were used, and both enzymes cut within the distal hypersensitive region. The first block to downstream progression of exonuclease III occurred at -340 just inside the *Pvu*II site. This position corresponds to the 3' boundary

of the distal hypersensitive region as defined with various endonucleases (see above). Exonuclease III molecules that penetrated this block were blocked again at position -270. Exonuclease III molecules that started from the *Pvu*II site were also blocked at the same positions. The same filter was rehybridized to the F probe in an experiment designed to define the 5' boundary of the distal hypersensitive region (Fig. 5B). Exonuclease III molecules progressed upstream from the *Pvu*II site to -670. Thus, the segment of DNA between -670 and -340 is completely unprotected from exonuclease III digestion.

Previous data had shown that the two dihydrofolate reductase gene copies in MTX-sensitive cells and the multiple gene copies in resistant HeLa cells exhibited the same methylation pattern and DNase I hypersensitivity of the promoter region (Shimada and Nienhuis, 1985). The *Sca*I and *Pvu*II sites in nuclei from MTX-sensitive cells were accessible for digestion (Fig. 6), verifying the presence of the distal hypersensitive

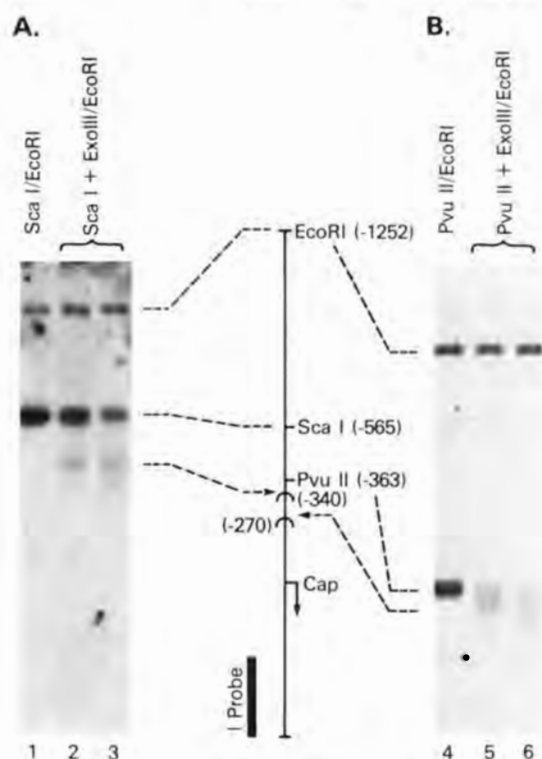


FIG. 6. Exonuclease III-protected sites in the 5' region of the human dihydrofolate reductase gene in MTX-sensitive HeLa cells. Isolated nuclei were digested with *ScaI* (A) or *PvuII* (B) and exonuclease III at 1600 units/ml (lanes 2 and 5) or 8000 units/ml (lanes 3 and 6) at 37°C for 30 min. The purified DNA was processed as described for Fig. 5 and blot-hybridized with the I probe.

region in these cells. The blocks to exonuclease III progression at -340 and -270 defined in nuclei of MTX-resistant cells were also observed on the analysis of DNA from MTX-sensitive cells, although the relevant bands were less discrete and well defined (Fig. 6).

Exonuclease III could not be used to map the boundaries of the proximal hypersensitive region as this enzyme only digests 3' to 5' if the 3' end is recessed or the end in blunt (Wu, 1984a). No appropriate restriction sites are present in the proximal hypersensitive region. Hence, we used another enzyme with exonuclease activity, *Bal31*. To verify that *Bal31* could be used in this fashion, nuclei digested with *ScaI* were treated with *Bal31* (Fig. 7A). The same blocks defined with exonuclease III at -340 and -270 were observed with *Bal31*. Some *Bal31* molecules penetrated the block at -270 but were stopped at -230 when low concentrations of the enzyme was used. At high concentrations, only the blocks at -340 and -230 were observed. The upstream boundary of the distal hypersensitive region at -670 was also detected with *Bal31* as shown by rehybridization of the same blot to an appropriate probe (Fig. 7D).

The boundaries of the proximal hypersensitive region were mapped with *Bal31* (Fig. 7, B and C). *SstII*, an enzyme that cuts within this region at -115, was used to make the initial cut. A block to upstream progression of *Bal31* was observed at -170 (Fig. 7C). A weak block to downstream progression

was observed at +1 with a strong block at +150 (Fig. 7B). Thus, this hypersensitive region extends from -170 to +150. Most of exon 1 is free of nucleosomes.

As a control, purified DNA restricted with *ScaI*, *PvuII*, or *SstII* was incompletely digested with either exonuclease III or *Bal31*. The DNA was then purified, digested with *EcoRI*, and analyzed by Southern blots. No apparent blocks to progression of these enzymes on naked DNA were observed (data not shown), consistent with the previous control experiments of Wu (1984a).

High Affinity Binding of Molecules to DNA between the Proximal and Distal Hypersensitive Regions—The sequences between -340 and -170 are protected from exonuclease and endonuclease digestion, presumably by virtue of sequence-specific binding of particular molecules. The resistance of these molecules to dissociation by salt was studied (Fig. 8). Aliquots of nuclei were first incubated with various concentrations of NaCl and, then after removal of the salt, were digested with *ScaI* in a large volume of buffer E (estimated ratio of nuclei and buffer = 1:100). The blocks to exonuclease III progression that defined the downstream boundary of the distal hypersensitive region were unaltered by prior incubation of nuclei in 0.5 M NaCl. With a 1 M NaCl wash, the blocks to exonuclease III progression were both moved upstream nearly 100 nucleotides, whereas a 2 M NaCl wash rendered the DNA completely susceptible to exonuclease III digestion.

DISCUSSION

The features of chromatin structure at the 5' end of the dihydrofolate reductase gene are summarized in Fig. 9. There are two regions of DNA that appear to be essentially free of proteins as indicated by their sensitivity to several endo- and exonucleases. Within the proximal of these segments, one protein appears to be bound at, or very close to, the start site for transcription. One or more molecules are tightly bound to the 170-bp segment of DNA between the hypersensitive regions; tight binding is suggested by resistance to disassociation by high salt concentrations. The nucleosomes upstream from the distal hypersensitive region are phased on DNA. The coding sequences of the gene are covered with nucleosomes beginning at approximately the boundary between exon 1 and intron 1. Several proteins must interact with specific DNA sequences to create and preserve these features of chromatin structure.

The proximal hypersensitive region is bounded upstream by the tightly binding molecules at position -170 and by nucleosomes beginning at +150. The corresponding nucleosomes on the mouse dihydrofolate reductase gene have been shown to contain ubiquitinated H2A histones perhaps facilitating nucleosome disassociation during transcription of the dihydrofolate reductase gene (Barsoum and Varshavsky, 1985). Presumably, sequence-specific interaction of a non-histone chromosomal protein is involved in establishing this boundary between nucleosome-free DNA in the hypersensitive region and the nucleosomes on the body of the gene.

The nature of the tight binding molecules between -170 and -340 is uncertain. Conceivably, a single nucleosome might occupy this position although the protected segment of DNA is longer than that usually associated with a single nucleosome. The exonuclease III block at -260 and the *Bal31* block at -230 would be difficult to explain based on known features of nucleosome structure. Perhaps the bound proteins are involved in gene regulation, or alternatively, this region of the DNA might interact with the nuclear matrix (Agutter and Richardson, 1980). Proteins that are part of the nuclear

Chromatin Structure of the Dihydrofolate Reductase Gene Promoter

1451

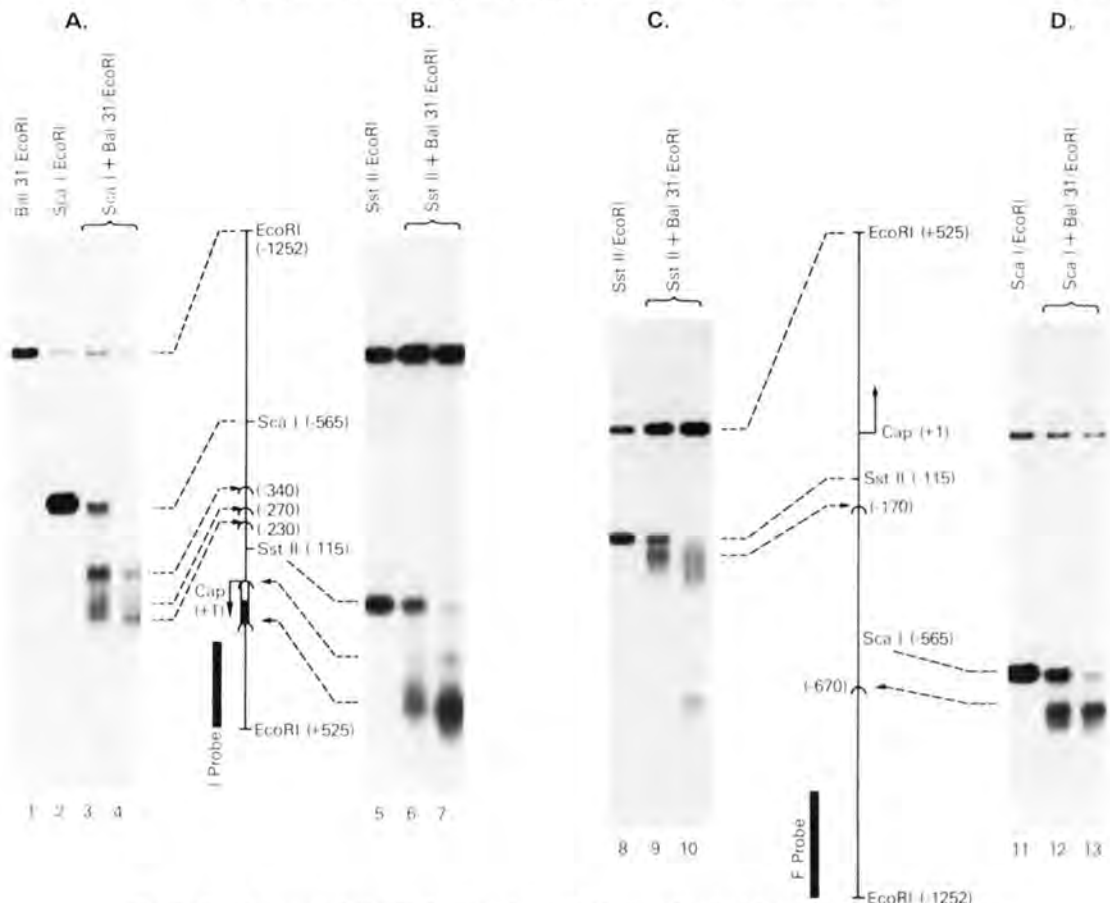


FIG. 7. *Bal31*-protected sites in the 5' region of the human dihydrofolate reductase gene in MTX-resistant HeLa cells. Isolated nuclei were digested with *ScaI* (A and D) or *SstII* (B and C) in buffer E at 37 °C for 30 min. The nuclei recovered by centrifugation were resuspended in buffer B and digested with *Bal31* at 3 units/ml (lanes 3, 6, 9, and 12) or 15 units/ml (lanes 4, 7, 10, and 13). The purified DNA was processed as described for Fig. 5 and blot-hybridized with the I probe (A and B) or the F probe (C and D). *Bal31* stop positions are indicated by the arrows.

matrix are known to be resistant to disassociation of DNA by high salt concentrations (Hentzen *et al.*, 1984). Only 140 nucleotides are free between the tight binding molecules at -170 and the TATA box. This is barely sufficient for entry of an RNA polymerase II molecule that has a molecular weight of more than 500,000 (Lewis and Burgess, 1982; Sentenac, 1985). Perhaps the molecules tightly bound between -170 and -340 slide on the DNA double helix to allow polymerase entry in a manner analogous to their apparent movement on exposure of isolated nuclei to 1.0 M NaCl (Fig. 8). Alternatively, the tightly bound molecules might facilitate polymerase binding at the TATA box specifically. Another formal possibility is that polymerase binding occurs in the distal hypersensitive region and that removal of the tightly bound molecules during DNA replication allows the polymerase access to the dihydrofolate reductase gene.

Several features of the distal hypersensitive region are of interest. Homology between the mouse and human genomes is found in this region (Chen *et al.*, 1984; McGrogan *et al.*, 1985). A RNA polymerase II initiation site has been identified

on the opposite strand to the human dihydrofolate reductase coding sequences at position -600 by *in vitro* transcription of DNA in nuclear extracts (Chen *et al.*, 1984). However, there is no homology between mouse and human DNA at this position. Relatively abundant very short RNA molecules are also transcribed *in vivo* from the opposite strand of the mouse genome but beginning 250-300 bp from the dihydrofolate reductase translational start site (Farnham *et al.*, 1985; Crouse *et al.*, 1985). The relevance of these observations to dihydrofolate reductase gene expression and the general function of this region of DNA remains unresolved.

The nucleosomes upstream from the distal hypersensitive region are phased on the DNA double helix. The selective accessibility of certain upstream sites to micrococcal nuclease cutting provides evidence for phasing. The sensitive sites are thought to lie within the internucleosome regions, whereas protected sites are thought to be present in nucleosome-associated DNA. There are 90 nucleotides between the exonuclease III and *Bal31* blocks at -670 and the position of the first nucleosome, as predicted by the micrococcal nuclease

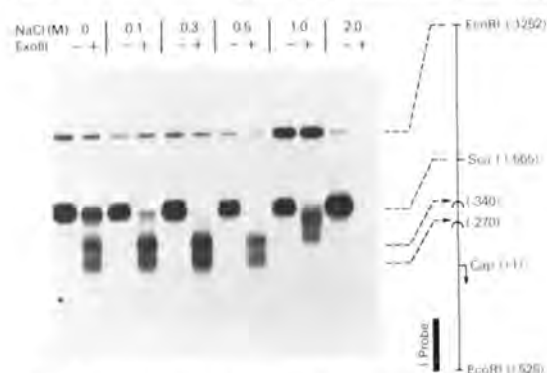


FIG. 8. Sensitivity of the exonuclease III-protected sites to salt extraction. Isolated nuclei from MTX-resistant HeLa cells were incubated in 0–2 M NaCl. The nuclei recovered by centrifugation were digested with *ScaI* and exonuclease III (*ExoIII*) at 1000 and 8000 units/ml, respectively. The purified DNA was processed as described for Fig. 5 and blot-hybridized with the I probe.

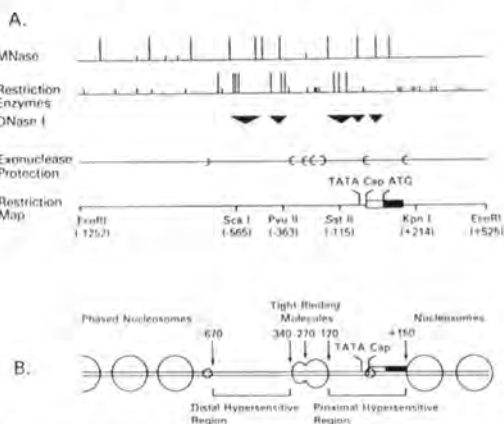


FIG. 9. A, summary of the map of endonuclease-sensitive sites and exonuclease stop sites in the promoter region of the dihydrofolate reductase gene. a, micrococcal nuclease (*MNase*) sensitive sites; b, restriction endonuclease-sensitive (the long bars indicate sensitive sites; the short bars indicate protected sites); c, *Dnase I*-hypersensitive sites; d, exonuclease protection sites; e, a restriction map. B, schematic representation of the features of chromatin structure at the 5' end of the dihydrofolate reductase gene.

data, beginning at –760. Presumably a protein is bound at this position. Phasing of nucleosomes at this boundary of the distal hypersensitive region is therefore most likely due to interaction of this non-histone chromosomal protein, both with specific DNA sequences and with some portion of the first nucleosome (Kornberg, 1981). An alternative mechanism namely DNA sequence-specific interaction with a portion of the nucleosome for which there is evidence in other systems (Thomas and Simpson, 1985), seems less likely.

The levels of dihydrofolate reductase mRNA are known to vary throughout the cell cycle with the highest levels present during DNA synthesis (Hendrickson *et al.*, 1980; Leys and Kellems, 1981). Several studies have suggested that modulation occurs by post-transcriptional mechanisms (Leys and

Kellems, 1981; Kaufman and Sharp, 1983; Leys *et al.*, 1984). However, a recent study using cells synchronized by physical methods indicates that the dihydrofolate reductase gene is transcribed mainly during the G₁-S transition of the cell cycle (Farnham and Schimke, 1985). Thus, there is a temporal link between DNA replication and dihydrofolate reductase gene transcription. Of interest is the resemblance between the structural features of the dihydrofolate reductase promoter region and the "gap" of the SV40 minichromosome (Saragosti *et al.*, 1982). In each there are two hypersensitive regions separated by tightly binding molecules. The SV40 gap contains sequences involved in DNA replication and SV40 gene transcription. The cells utilized in our studies were mainly confluent and quiescent so that the features of chromatin defined are most likely those of the nontranscribed and non-replicating dihydrofolate reductase gene. Studies that utilize synchronized cells may elucidate any potential relationship between replication, transcription, and chromatin structure of the dihydrofolate reductase gene.

Acknowledgement—We wish to thank Inogene Surrey for help in preparation of this manuscript.

REFERENCES

- Agutter, P. S., and Richardson, J. C. (1980) *J. Cell Sci.* **44**, 395–435.
 Barsoum, J., and Varshavsky, A. (1985) *J. Biol. Chem.* **260**, 7688–7697.
 Chen, M.-J., Shimada, T., Moulton, A. D., Cline, A., Humphries, R. K., Maizel, J., and Nienhuis, A. W. (1984) *J. Biol. Chem.* **259**, 3933–3943.
 Crouse, G. F., Leys, E. J., McEwan, R. N., Frayne, E. G., and Kellems, R. E. (1985) *Mol. Cell Biol.* **5**, 1847–1858.
 Dynan, W. S., and Tjian, R. (1983) *Cell* **35**, 79–87.
 Ephrussi, A., Church, G. M., Tonegawa, S., and Gilbert, W. (1985) *Science* **227**, 134–140.
 Emerson, B. M., and Felsenfeld, G. (1984) *Proc. Natl. Acad. Sci. U.S.A.* **81**, 95–99.
 Farnham, P. J., and Schimke, R. T. (1985) *J. Biol. Chem.* **260**, 7675–7680.
 Farnham, P. J., Abrams, J. M., and Schimke, R. T. (1985) *Proc. Natl. Acad. Sci. U.S.A.* **82**, 3978–3982.
 Fittler, F., and Zachau, H. G. (1979) *Nucleic Acids Res.* **7**, 1–13.
 Gidoni, D., Dynan, W. S., and Tjian, R. (1984) *Nature* **312**, 409–413.
 Hendrickson, S. L., Wu, J.-S. R., and Johnson, L. F. (1980) *Proc. Natl. Acad. Sci. U.S.A.* **77**, 5140–5144.
 Hentzen, P. C., Rho, J. H., and Bekhor, I. (1984) *Proc. Natl. Acad. Sci. U.S.A.* **81**, 304–307.
 Kaufman, R. J., and Sharp, P. A. (1983) *Mol. Cell Biol.* **3**, 1598–1608.
 Kornberg, R. (1981) *Nature* **292**, 579–580.
 Lewis, M. K., and Burgess, R. R. (1982) in *The Enzymes* (Boyer, P. D., ed) Vol. 15, pp. 109–153. Academic Press, New York.
 Leys, E. J., and Kellems, R. E. (1981) *Mol. Cell Biol.* **1**, 961–971.
 Leys, E. J., Crouse, G. F., and Kellems, R. E. (1984) *J. Cell Biol.* **98**, 180–187.
 McGrogan, M., Simonsen, C. C., Smouse, D. T., Farnham, P. J., and Schimke, R. T. (1985) *J. Biol. Chem.* **260**, 2307–2314.
 Parker, C. S., and Topol, J. (1984) *Cell* **37**, 273–283.
 Saragosti, S., Cereghini, S., and Yaniv, M. (1982) *J. Mol. Biol.* **160**, 133–146.
 Sentenac, A. (1985) *Crit. Rev. Biochem.* **18**, 31–90.
 Shimada, T., and Nienhuis, A. W. (1985) *J. Biol. Chem.* **260**, 2468–2474.
 Siebenlist, U., Hennighausen, L., Battey, J., and Leder, P. (1984) *Cell* **37**, 381–391.
 Thomas, F., and Simpson, R. T. (1985) *Nature* **315**, 250–252.
 Tjian, R. (1979) Cold Spring Harbor Symp. Quant. Biol. **43**, 655–662.
 Wu, C. (1984a) *Nature* **309**, 229–234.
 Wu, C. (1984b) *Nature* **311**, 81–84.
 Yoder, S. S., Roberson, B. L., Leys, E. J., Hook, A. G., Al-Ubaidi, M., Yeung, C.-Y., Kellems, R. E., and Berger, S. M. (1983) *Mol. Cell Biol.* **3**, 819–828.

*Original article***Transforming genes and chromosome aberrations in therapy-related leukemia and myelodysplastic syndrome*****K. Inokuchi¹, N. Amuro², M. Futaki¹, K. Dan¹, T. Shinohara³, S. Kuriya⁴, T. Okazaki², and T. Nomura¹**¹ The Third Department of Internal Medicine, Nippon Medical School, Tokyo, Japan² The Department of Biochemistry, Nippon Medical School, Tokyo, Japan³ The Department of Human Genetics, Japan Red Cross Medical Center, Tokyo, Japan⁴ The Third Department of Internal Medicine, Iwate Medical School, Morioka, Japan

Received October 8, 1990 / Accepted February 26, 1991

Summary. The presence of activated transforming genes was investigated in four patients with therapy-related leukemia and in three with therapy-related myelodysplastic syndrome. DNA of bone marrow cells from six of the patients exhibited transforming activity in the tumorigenicity assay. Five of the six patients who were positive in the tumorigenicity assay contained activated *N-ras* oncogenes, and three contained activated *K-ras* oncogenes. Thus, concurrent activation of *N-ras* and *K-ras* oncogenes was observed in two patients.

In vitro DNA amplification followed by oligonucleotide dot-blot analysis was used to investigate mutations in codons 12, 13, and 61 of the *N-ras* and *K-ras* oncogenes. Two patients exhibited an *N-ras* mutation, substituting aspartic acid (GAT) for glycine (GGT), and three patients exhibited an *N-ras* codon 13 mutation, substituting valine (GTT) for glycine. Two patients exhibited *K-ras* codon 12 mutations, substituting aspartic acid (GAT) or cysteine (TGT) for glycine (GGT), respectively, and one case exhibited a *K-ras* codon 61 mutation, substituting lysine (AAA) for glutamic acid (CAA). Cytogenetic analysis revealed that loss of chromosome 7 was frequent (four patients: 57%). Our data indicate that activation of *N-ras* and *K-ras* genes, as well as loss of heterozygosity for specific alleles on chromosome 7, plays a more important role in the leukemogenesis of both therapy-related leukemia and myelodysplastic syndrome.

Key words: *N-ras* oncogene – Therapy-related leukemia – Myelodysplastic syndrome – Chromosome

Introduction

Therapy-related leukemia represents a separate entity in the spectrum of acute myelogenous leukemia [7, 18, 19]. It has several characteristic clinical features including a preleukemic phase [1, 23, 27]. Therapy-related leukemia is resistant to chemotherapy and generally has an ominous prognosis. Cytogenetic studies have shown that therapy-related leukemia, including myelodysplastic syndrome, is characterized by nonrandom chromosomal abnormalities [18, 20]. Abnormalities of chromosomes 5 and 7 are frequently observed, but the genetic basis of therapy-related leukemogenesis remains unknown. Investigation of leukemias has been extended to the molecular level in recent years in order to elucidate the mechanisms involved in leukemogenesis [12, 13, 17]. Human leukemia cells have been found to contain activated transforming genes. The majority of these cases of activated oncogenes thus far reported have been identified as involving the *N-ras* oncogene, and the minority of them have been identified as *K-* and *H-ras* oncogenes by using NIH/3T3 assay [5, 12]. More recently, the polymerase chain reaction (PCR) method and the synthetic oligomer method have detected point mutations of *ras* oncogenes [9, 22]. The cases of mutated *ras* oncogene are also predominantly in the *N-ras* oncogene [9, 22]. These mutations, which are not present in normal cells, occur in codon 12, 13, or 61 of the *N-ras* oncogene. The studies were conducted on cases of de novo human leukemia and myelodysplastic syndrome. In the present study, we characterized the transforming gene and chromosomal aberrations of therapy-related leukemia and myelodysplastic syndrome.

Materials and methods*Patients*

Cells were prepared from the bone marrow of four patients with acute myeloblastic leukemia and three patients with myelodysplastic syndrome. All patients had undergone previous chemotherapy, and one patient had received radiation therapy for another malignancy.

* This work was supported in part a Grant-in-Aid for Scientific Research from the Ministry of Education, Science and Culture of Japan

Offprint requests to: K. Inokuchi, The Third Department of Internal Medicine, Nippon Medical School, Sendagi 1-1-5, Bunkyo-ku, Tokyo 113, Japan

nant disease. The clinical and cytogenetic results have been published previously for only two of these patients [14, 25]. A summary of the clinical and cytogenetic characteristics of the patients is shown in Table 1. The latent period from the start of previous chemotherapy to development of leukemia or myelodysplastic syndrome ranged from 36 to 133 months.

Cell culture and transfection

NIH/3T3 cells were kindly provided by S.A., Aaronson. The cells were maintained in Dulbecco's modified Eagle medium containing 10% calf serum and 50 µg/ml gentamicin. Genomic DNA was extracted by standard proteinase-K treatment and phenol-chloroform treatment of mononuclear cells of heparinized bone marrow aspirates from the patients and normal volunteers. The cells (2×10^5 cells per 60-mm culture dish) were transfected by the standard CaPO₄ precipitation method [11], as described elsewhere [29].

In vitro transfection assay

DNA was precipitated at a final concentration of 40 µg/ml. The recipient culture was inoculated with 0.5 ml of DNA precipitate without removing the culture medium and then incubated for 12 h at 37°C. The medium was changed at 2-day intervals, and the foci of transformed cells were counted 12–15 days after exposure to DNA. Each DNA (100 µg) sample was assayed using four or five recipient cultures in each experiment. SV40 (pMK16/SV40) was employed as a positive control.

Tumorigenicity assay

The method was a modification of that described by Fasano et al. [10]. Genomic DNA (60 µg) was mixed with 4 µg of plasmid pSV2neo and transfected by the standard CaPO₄ coprecipitation method [11]. The precipitate was incubated at 37°C for 12 h. Forty-eight hours later, the cells were trypsinized, replated, and subjected to selection with G418 at 400 µg/ml of medium. Fourteen to 21 days after transfection, cells were removed from the plates by trypsinization, giving > 500 colonies. Samples of 5×10^6 cells were resuspended in 0.5 ml of cold medium. This suspension was then injected subcutaneously into athymic nude mice, and the develop-

ment of tumors was scored. The observation period for tumor formation was limited to 80 days after injection.

Analysis of DNA from transformed cells

DNA prepared from representative clones was subjected to Southern blot analysis for detection of human repetitive sequences and human proto-oncogene sequences. High-molecular-weight DNA (20 µg) was digested with appropriate restriction endonucleases, electrophoresed through 0.8% agarose gels, and blotted onto nylon filters (Gene Screen Plus; New England Nuclear). The resulting blots were hybridized with a nick-translated ³²P-labeled DNA probe [15].

Synthetic oligonucleotide probes

The oligonucleotides (20-mers) were prepared by an asynchronous simultaneous synthesis strategy using the solid-phase phosphite triester method by an Applied Biosystems model A380 DNA synthesizer. The oligomers used for the analyses of *ras* gene mutations were the same as described by Vries et al. [30]. The oligomers were end-labeled using [γ -³²P]-ATP (New England Nuclear) and T₄-polynucleotide kinase. The kinase-treated probes were separated from the unincorporated ATP by chromatography on a Sephadex G50 column. The specific activities were more than 5×10^5 cpm/pmol.

Polymerase chain reaction

DNA amplification in vitro was performed as described by Saiki et al. [28]. Each DNA (500 ng) was mixed with 100 pmol of upstream (5'-) and downstream (3'-) primers complementary to the sequences surrounding the codon to be screened, in 100 µl of 50 mM Tris-HCl, pH 8.5, 15 mM (NH₄)₂SO₄, 10 mM MgCl₂, 10 mM β -mercaptoethanol, and 0.2 mg/ml of bovine serum albumin. After incubation at 95°C for 7 min, 2 U of Taq polymerase (Biotec International Ltd.) and the four deoxynucleotide triphosphates (to a final concentration of 1 mM each) were added to the mixture. PCR was started by incubation at 65°C for 1 min, followed by denaturation at 95°C for 30 s and then annealing at 50°C for 30 s. After 40 cycles of amplification, 1 U of Taq polymerase was added to the mixture, and another 20 cycles of amplification were carried out [22].

Table 1. Summary of clinical data and cytogenetic analysis

Patient no.	Primary disease	Age/sex	Therapy (total dose in mg)	Latent period (months)	Secondary disease (FAB type)	Survival (months)	Karyotype
1.	Multiple myeloma	63/F	Melphalan (2620) vincristine (108)	96	M6	18	47,XX,+8
2.	Gastric cancer	58/F	5-Fluorouracil	133	M4	10	46,XX,-8,3p-,+mar
3.	Polycythemia vera	59/M	Pipobroman (45 600) melphalan (2250)	131	M1	6	45,XY,-7,+der(1), t(1;7)(p11;p11)
4.	Prostatic cancer	76/M	5-Fluorouracil (31 500), MMC (126), Ctx (12 200)	60	M4	7	45,XX,-7
5.	Multiple myeloma	65/F	Melphalan (2040) vincristine (102)	54	RAEB-t	3	45,XX,-5,-7,-15, 17p+,+2mar
6.	Prostatic cancer	64/M	Estramustine (403,200), Adm (90), carboquone (9), radiation 60 Gy	36	CMMoL	24+	46,XY
7.	Uterine cancer	68/F	Melphalan (144) Ctx (1,200), 5-fluorouracil (3000), Adm (120) bleomycin (60)	54	RAEB	30	45,XX,-7

Abbreviations: FAB, French-American-British; MMC, mitomycin C; Ctx, cyclophosphamide; Adm, doxorubicin; +, still alive; RAEB, refractory anemia with excess of blasts; RAEB-t, RAEB in transformation; CMMoL, chronic myelomonocytic leukemia

Dot-blot hybridization

Dot-blot hybridization was performed as described by Vries et al. [30]. DNA (10 μ l) amplified in vitro was spotted onto nylon filters (Gene Screen Plus; New England Nuclear). The filters were pre-hybridized at 50°C for 2 h in 5 \times SSPE (10 mmol/l sodium phosphate, pH 7.0, 0.18 mol/l NaCl, and 1 mmol/l EDTA), 7% SDS, 100 μ g/ml sonicated and denatured salmon sperm DNA, and 5 \times Denhardt's solution and hybridized for 3 h at 50°C in the presence of 1 ng α^{32} P-labeled oligomer probe. Hybridization filters were washed twice in 2 \times SSPE, 0.1% SDS, for 5 min at room temperature and once in 5 \times SSPE, 0.1% SDS, for 30 min at 50°C. A final high-stringency wash was performed for 10 min at 59°C for N-*ras* 61 and K-*ras* 61 probes, at 63°C for N-*ras* 12/13 and K-*ras* 12/13 probes. The exposure to Kodak XAR films was performed for 4 h at -70°C with intensifying screens.

Chromosome analysis

Cytogenetic study was performed by the conventional trypsin-Giemsa banding technique. The bone marrow cells were processed by a direct method [15].

Results

In vitro focus-forming assay

A DNA sample exhibiting a transforming activity of > 0.01 foci per microgram of DNA in an assay was evaluated as "positive" [12]. High-molecular-weight DNA of bone marrow cells from one of four patients with therapy-related leukemia and from three patients with therapy-related myelodysplastic syndrome exhibited transforming activity in the in vitro focus-forming assay (Table 2). The DNA of marrow cells from normal subjects did not exhibit significant transforming activity (Table 2). All of the transformants of transfected NIH/3T3 cells were transplantable into nude mice.

Tumorigenicity assay

The DNA of bone marrow cells from three of the four patients with therapy-related leukemia and from all of the three patients with therapy-related myelodysplastic syndrome exhibited transforming activity in the tumorigenicity assay (Table 2). The tumors arising in nude mice became apparent between 12 and 60 days after injection of transfected cells.

Identification of the oncogenes

All the transformants detected in the tumorigenicity assay were analyzed by Southern blotting for the presence of human repetitive sequences using the probe Blur-8, representative of human Alu sequences (data not shown). The results indicated that all transformants carried human Alu sequences. In view of evidence relating the transforming genes of leukemia and myelodysplastic syndrome to the *ras* family of oncogenes, we analyzed the transformant DNA using the probes for the *ras* family. We found that *ras* genes were responsible for the activity

of all of the six DNA samples that were positive in the tumorigenicity assay (five N-*ras* and three K-*ras*) (Figs. 1 and 2). Two samples concurrently bore two kinds of transforming genes that were members of the *ras* family. H-*ras* probe detected no human-specific fragments (data not shown).

Mutations of *ras* genes

Activation of *ras* genes usually results from mutations within codons 12, 13, and 61 [5, 17]. We sought to deter-

Table 2. Transforming genes of therapy-related leukemia and MDS

Patient no. (FAB)	In vitro focus-forming assay (positive/total tested)	Tumorigenicity of transfected cells (positive/total tested)	Transforming gene
1 (M6)	0/4	4/4	N- <i>ras</i> , K- <i>ras</i>
2 (M4)	2/4	1/4	N- <i>ras</i>
3 (M1)	0/4	0/4	
4 (M4)	0/4	1/4	N- <i>ras</i>
5 (RAEB-t)	1/4	1/4	N- <i>ras</i>
6 (CMML)	2/4	2/4	N- <i>ras</i> , K- <i>ras</i>
7 (RAEB)	0/5	1/4	K- <i>ras</i>
8*	0/12	0/11	

* Normal subjects

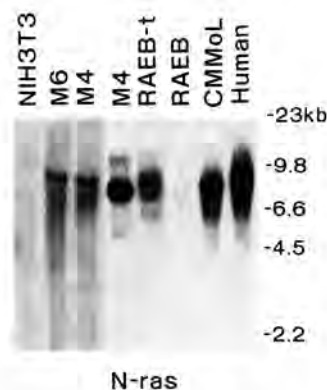


Fig. 1. Detection of human-specific N-*ras* band in NIH/3T3 transfectants derived from the patients. DNA (10 μ g/lane) was digested with *Eco*R I, subjected to electrophoresis in 0.8% agarose gels, and transferred to nylon membranes. The membrane was probed with the human N-*ras* exon probe that contained a portion of exon 1 (0.5-kb *Hind* III fragment). The positions of migration of the λ Hind III-digested DNA markers are indicated on the right. The position of human-specific N-*ras* band is 9.2 kb. Lanes: NIH/3T3, NIH/3T3 DNA; M6, patient-1 NIH/3T3 transformant DNA; M4 (left), patient-2 NIH/3T3 transformant DNA; M4 (right), patient-4 NIH/3T3 transformant DNA; RAEB-t, patient-5 NIH/3T3 transformant DNA; RAEB, patient-7 NIH/3T3 transformant DNA; CMML, patient-6 NIH/3T3 transformant DNA; Human, normal human cellular DNA

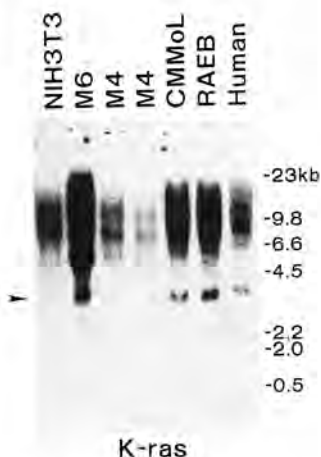


Fig. 2. Detection of human-specific *K-ras* band in NIH/3T3 transfectants. A Southern blot of *EcoR* I-digested DNAs (10 µg/lane) was probed using a v-*K-ras* (0.3-kb *Sst* II-*Xba* I fragment). Positions of migration and sizes of *Hind* III-digested λDNA and *Hae* III-digested ø×DNA markers are indicated. Arrowhead indicates the position of a 3.0-kb human-specific fragment hybridized with the probe. Patient-5 NIH/3T3 transformant DNA had no human-specific *K-ras* band, although the data are not shown here. Lanes: NIH/3T3, NIH/3T3 DNA; M6, patient-1 NIH/3T3 transformant DNA; M4, patient-2 NIH/3T3 transformant DNA; M4, patient-4 NIH/3T3 transformant DNA; CMMoL, patient-6 NIH/3T3 transformant DNA; RAEB, patient-7 NIH/3T3 transformant DNA; Human, normal human cellular DNA

mine the nature of the mutations in the active *ras* genes detected by transfection with DNA. As Fig. 3 shows, we could detect mutations when at least 1% of total cells carried mutational *N-ras* oncogene following the protocol described in *Methods*. To check whether the amplification by PCR was successful or not, we tested the hybridization signal with the corresponding wild-type probe. *N*- and *K-ras* point mutations within codons 12, 13, and 61 were investigated using hybridization of mutation-specific oligomers to in vitro-amplified DNA samples obtained from mononuclear cells from the bone marrow of the seven patients (Fig. 4). Mutations in *K*- and *N-ras* were detected by hybridization of mutation-specific oligomers to in vitro-amplified DNA samples in three of the four leukemia patients and in all of the three myelodysplastic patients (Fig. 4). The first case (patient 1) had a *K-ras* codon 12 mutation substituting aspartic acid (GAT) for glycine (GGT) (Fig. 4). The second case (patient 6) had a *K-ras* codon 12 mutation substituting cysteine (TGT) for glycine. The third case (patient 7) had a *K-ras* codon 61 mutation substituting lysine (AAA) for glutamic acid (CAA). Two patients (patients 1 and 2) exhibited an *N-ras* codon 12 mutation, substituting aspartic acid (GAT) for glycine (GGT), and three patients (patients 4, 5, and 6) exhibited an *N-ras* codon 13 mutation, substituting valine (GTT) for glycine (Fig. 4).

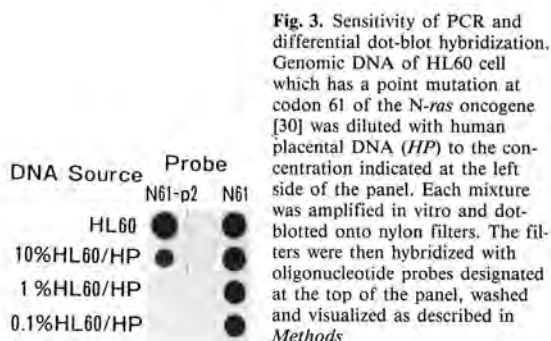


Fig. 3. Sensitivity of PCR and differential dot-blot hybridization. Genomic DNA of HL60 cell which has a point mutation at codon 61 of the *N-ras* oncogene [30] was diluted with human placental DNA (HP) to the concentration indicated at the left side of the panel. Each mixture was amplified in vitro and dot-blotted onto nylon filters. The filters were then hybridized with oligonucleotide probes designated at the top of the panel, washed and visualized as described in *Methods*

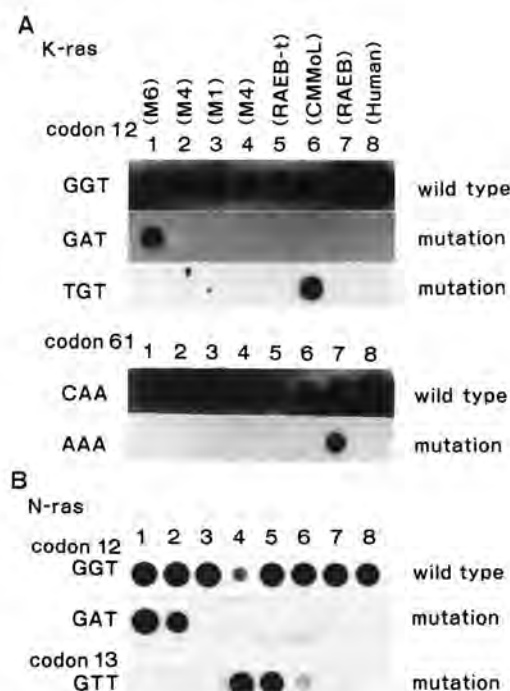


Fig. 4. Hybridization of mutation-specific oligomers to in vitro-amplified DNAs obtained from mononuclear cells of bone marrow from seven patients. DNA from mononuclear cells was amplified in vitro, dot-blotted, and hybridized with K12, K61, and N12 wild-type oligomers and with the appropriate mutant probes. Grid numbers and the corresponding amplified DNAs are as follows: 1, patient-1; 2, patient-2; 3, patient-3; 4, patient-4; 5, patient-5; 6, patient-6; 7, patient-7; 8, normal human cellular DNA. The first, fourth, and sixth rows demonstrate the presence of the *K-ras* codon 12 and 61 wild-type sequence and *N-ras* codon 12 wild-type sequence, respectively. Second row, presence of a point mutation containing aspartic acid (GAT) substituted for normal glycine (GGT); third row, presence of a point mutation containing cysteine (TGT) in place of normal glycine (GGT); fifth row, presence of a point mutation containing lysine (AAA) substituted for normal glutamic acid (CAA); seventh row, presence of a point mutation containing aspartic acid (GAT) substituted for normal glycine (GGT); eighth row, presence of a point mutation containing valine (GTT) substituted for normal glutamic acid (GGT)

Chromosome analysis

The results of karyotyping are shown in Table 1. Most (86%) of the patients had a chromosomal aberration. Five of the seven had hypodiploidy in their blast cells. Four of the seven had an aberration which was loss of all of chromosome 7. Loss of the short arm of chromosome 3 was seen in patient 2.

Discussion

The importance of the *ras* family of oncogenes in the process of leukemogenesis is indicated by the frequency of their activation in human de novo leukemia. Recent studies using a polymerase chain reaction and synthetic oligonucleotide probe for acute myeloid leukemia cases indicate that approximately 20%–40% have mutated *ras* genes [2, 22]. Moreover, the incidence of mutation of *ras* genes in chronic myelogenous leukemia and acute lymphoblastic leukemia is low [21, 24]. This mutation originally was detected by both an in vitro focus-forming assay and a tumorigenicity assay. The activation is nearly always attributable to point mutations, especially at codons 12, 13, or 61 of the *N-ras* oncogene [5, 9, 13], and sometimes of either the *K-ras* oncogene or the *H-ras* oncogene in human leukemia and myelodysplastic syndrome [6, 21]. However, little is known of the genetic events of therapy-related leukemia and myelodysplastic syndrome.

In the present study, we demonstrated that activation of *N-ras* oncogenes and/or activation of *K-ras* oncogenes may occur in acute myelogenous leukemia and myelodysplastic syndrome related to chemotherapy. In an animal experiment, murine lymphomas induced by intraperitoneal injection of the chemical carcinogen *n*-nitrosomethylurea had a higher frequency (51%) of *ras* oncogene activation [8]. Activated *K-ras* genes were predominant, and two examples had concurrent *K-* and *N-ras* gene point mutations in the same lymphoma. In fresh leukemia cells from an AML patient, concurrent activation of *K-ras* and *N-ras* due to point mutation was reported [16]. Recently, a laboratory reported studies on leukemia and myelodysplastic syndrome related to chemotherapy using rapid PCR dot-blot screening for point mutations within codons, 12, 13, and 61 in the *ras* gene family [3, 26]. The first report detected an *N-ras* point mutation at codon 13 in one of nine cases following intensive treatment with alkylating agents [26]. The second report detected *N-ras* point mutations in two cases following intensive chemotherapy. The rates of *N-ras* point mutations in these reports seem to be contradictory.

We detected both the activated *K-ras* and *N-ras* oncogene in leukemia cells by tumorigenicity assay and found both *K-ras* and *N-ras* mutations at codon 12, 13, and 61 in six of seven patients. In addition, no activation of the *H-ras* gene in tumor DNAs was detected, in agreement with the report of Diamond et al. [8]. Using the tumorigenicity assay, we detected concurrently activated *K-ras* and *N-ras* oncogenes in patients 1 and 6. However, we could not decide from our studies whether the cell sam-

ples investigated consist of two different cell types, one with an *N-ras* and another with a *K-ras* activation, or whether both activations involve the genome of the monoclonal cell population in patients 1 and 6. Moreover, even if the latter possibility is correct, it remains unknown whether the mutations of two *ras* genes in a patient sufficiently explain the development of leukemia. In addition, the efficacy of PCR on the wild-type allele of exon 1 of *N-ras* of cells from patient 4 (M4 AML) was low (Fig. 4B), suggesting loss of the wild-type allele in some leukemic cells.

We wonder whether genetic damage occurs at nonrandom sites on chromosomes during long-term chemotherapy. In addition to nonrandom chromosomal aberrations, activated *N-ras* or/and *K-ras* genes were observed in six of our seven patients. Although the number of patients is small, the rate is about 86%. Activated *N-ras* or/and *K-ras* genes should play more important roles in the leukemogenesis of therapy-related leukemia and MDS than in de novo leukemia and MDS. High rates of aberrations of chromosomes 5 and 7 are well known [20], and deletion 3p is sometimes seen in therapy-related leukemia [4]. Whether some of the growth factor genes or other oncogenes located in chromosomes 5 and 7 might play a pathogenetic role in therapy-related leukemia remains unclear and is a subject for study. The presence of both activated *ras* genes and nonrandom chromosome aberrations in the preleukemic phase, MDS, suggests that both events may be important early events in therapy-related leukemogenesis. We speculate that concurrent activation of *N-ras* or/and *K-ras* and aberration of chromosome 7 might be common in therapy-related leukemia and MDS.

Acknowledgements. We are grateful to P. L. Deininger for providing probe *Blur-8*, to R. W. Ellis for *v-K-ras*, K. Shimizu for *N-ras* probe, and S. A. Aaronson for NIH/3T3 cells. We also thank K. Ozawa and T. Shimada for helpful discussions, I. Komiya of Douai Memorial Hospital, who referred patient material and clinical specimens for this study, and S. Inokuchi for help with preparation of the manuscript.

References

1. Anderson RL, Bagby GC, Richert-Boe K, Magenis RE, Koler RD (1981) Therapy-related preleukemic syndrome. *Cancer* 47: 1867–1871
2. Bar-Eli M, Ahuja H, Gonzalez-Cadavid N, Foti A, Cline MJ (1989) Analysis of *N-ras* exon-1 mutations in myelodysplastic syndromes by polymerase chain reaction and direct sequencing. *Blood* 73: 281–283
3. Bartram CR, Ludwig W, Hiddemann W, Lyons J, Buschle M, Ritter J, Harbott J, Frohlich A, Janssen JW (1989) Acute myeloid leukemia: analysis of *ras* gene mutations and clonality defined by polymorphic X-linked loci. *Leukemia* 3: 247–256
4. Benitez J, Carbonell F, Ferro T, Prieto F, Fayos JS (1986) Cytogenetic studies in 18 patients with secondary blood disorders. *Cancer Genet Cytogenet* 22: 309–317
5. Bos JL, Toksoz D, Marshall CJ, Verlaan-de Vries M, Veeneman GH, Vander Eb AJ, Van Boom JH, Janssen JW, Steenvoorden ACM (1985) Amino acid substitutions at codon 13 of the *N-ras* oncogene in human acute myeloid leukemia. *Nature* 315: 726–730
6. Bos JL, Vries MV, van der Eb AJ, Janssen JW, Delwel R,

- Lowenberg B, Colly LP (1987) Mutations in *N-ras* predominate in acute myeloid leukemia. *Blood* 69: 1237-1241
7. Coltman C (1982) Treatment-related leukemia. In: Bloomfield CD (ed) *Acute leukemia*. Martinus Nijhoff, The Hague, p 61
 8. Diamond LE, Guerrero I, Pellicer A (1988) Concomitant K- and *N-ras* gene point mutations in clonal murine lymphoma. *Mol Cell Biol* 8: 2233-2236
 9. Farr CJ, Saiki RK, Erlich HA, McCormick F, Marshall CJ (1988) Analysis of RAS gene mutations in acute myeloid leukemia by polymerase chain reaction and oligonucleotide probes. *Proc Natl Acad Sci USA* 85: 1629-1633
 10. Fasano O, Birnbaum D, Edlund L, Fogh J, Wigler M (1984) New human transforming genes detected by a tumorigenicity assay. *Mol Cell Biol* 4: 1695-1705
 11. Graham JF, van der Eb AJ (1973) A new technique for the assay of infectivity of human adenovirus 5 DNA. *Virology* 52: 456-467
 12. Hirai H, Tanaka S, Azuma M, Anraku Y, Kobayashi Y, Fujisaria M, Okabe T, Urabe T, Takaku F (1985) Transforming genes in human leukemia cells. *Blood* 66: 1371-1378
 13. Hirai H, Kobayashi Y, Mano H, Hagiwara K, Maru Y, Omine M, Mizoguchi H, Nishizima J, Takaku F (1987) A point mutation at codon 13 of the *N-ras* oncogene in myelodysplastic syndrome. *Nature* 327: 430-432
 14. Inokuchi K, Tajika K, Ito T, Ogata K, Yamada T, Tanabe Y, Ohki I, Dan K, Kuriya S, Nomura T, Shinohara T (1988) Secondary myelodysplastic syndrome with monosomy 7. *Jpn J Clin Hematol* 29: 718-722
 15. Inokuchi K, Komiya I, Dan K, Kuriya S, Shinohara T, Nomura T (1990) TdT-positive, SmIg-negative B precursor cell leukemia with Burkitt morphology: a case report. *Leuk Lymph* 2: 251-255
 16. Janssen JWJ, Lyons J, Steenvoorden ACM, Seliger H, Bartram CR (1987) Concurrent mutations in two different *ras* genes in acute myelocytic leukemias. *Nucleic Acid Res* 15: 5669-5680
 17. Janssen JWJ, Steenvoorden ACM, Lyons J, Anger B, Bohlke JU, Bos JL, Seliger H, Bartram CR (1987) RAS gene mutations in acute and chronic myelocytic leukemias, chronic myeloproliferative disorders and myelodysplastic syndromes. *Proc Natl Acad Sci USA* 84: 9228-9232
 18. Kantarjian HM, Keating MJ, Walters RS, Smith TL, Cork A, McCredie K, Freirech EJ (1986) Therapy-related leukemia and myelodysplastic syndrome: clinical, cytogenetic, and prognostic features. *J Clin Oncol* 4: 1748-1757
 19. Koeffler P, Rowley J (1985) Therapy-related acute non-lymphocytic leukemia. In: Wiernik P, Canellos G, Kyle R et al. (eds) *Neoplastic Diseases of the blood*. Churchill Livingstone, New York, p 357
 20. LeBeau MM, Albain KS, Larson RA, Vardiman JW, Davis EM, Blough RR, Golomb HM, Rowley JD (1986) Clinical and cytogenetic correlations in 63 patients with therapy-related myelodysplastic syndromes and acute nonlymphocytic leukemia: further evidence for characteristic abnormalities of chromosomes no. 5 and 7. *J Clin Oncol* 4: 325-345
 21. Liu E, Hjelle B, Bishop M (1988) Transforming genes in chronic myelogenous leukemia. *Proc Natl Acad Sci USA* 85: 1952-1956
 22. Mano H, Ishikawa F, Hirai H, Takaku F (1989) Mutations of *N-ras* oncogene in myelodysplastic syndromes and leukemias detected by polymerase chain reaction. *Jpn J Cancer Res* 80: 102-106
 23. Michels SD, McKenna RW, Arthur DC, Brunning RD (1985) Therapy-related acute myeloid leukemia and myelodysplastic syndrome: a clinical and morphologic study of 65 cases. *Blood* 65: 1364-1372
 24. Neri A, Knowles DM, Greco A, McCormick F, Dalla-Favera R (1988) Analysis of RAS oncogene mutations in human lymphoid malignancies. *Proc Natl Acad Sci USA* 85: 9268-9272
 25. Ogata K, Futaki M, Inokuchi K, Gomi S, Ohki I, Kuwabara T, Dan K, Kuriya S, Nomura T, Shinohara T (1989) Successful treatment of secondary erythroleukemia with androgen. *Jpn J Clin Hematol* 30: 1079-1083
 26. Pedersen-Bjergaard J, Janssen WG, Lyons J, Philip P, Bartram CR (1988) Point mutation of the *ras* proto-oncogenes and chromosome aberrations in acute nonlymphocytic leukemia and preleukemia related to therapy with alkylating agents. *Cancer Res* 48: 1812-1817
 27. Pedersen-Bjergaard J, Larsen SO (1982) Incidence of acute nonlymphocytic leukemia, and acute myeloproliferative syndrome up to 10 years after treatment of Hodgkin's disease. *N Engl J Med* 307: 965-971
 28. Saiki RK, Gelfand DH, Stoffel S, Scharf SJ, Higuchi R, Horn GT, Mullis KB, Erlich HA (1988) Primer-directed enzymatic amplification of DNA with a thermostable DNA polymerase. *Science* 239: 487-491
 29. Shimada T, Inokuchi K, Nienhuis AW (1987) Site-specific demethylation and normal chromatin structure of the human dihydrofolate reductase gene promoter after transfection into CHO cells. *Mol Cell Biol* 7: 2830-2837
 30. Vries MV, Bogaard ME, van den Elst H, van Boom J, van der Eb AJ, Bos JL (1986) A dot-blot screening procedure for mutated *ras* oncogenes using synthetic oligo-deoxynucleotides. *Gene* 50: 313-320

THE RELATIONSHIP BETWEEN THE SITE OF BREAKPOINTS
WITHIN THE *bcr* GENE AND THROMBOPOIESIS OF
PHILADELPHIA-POSITIVE CHRONIC MYELOCYTIC LEUKEMIAKOITI INOKUCHI,* MAKOTO FUTAKI,* TAKASHI YAMADA,* YOSHIHIRO TANABE,*
KAZUO DAN,* TAMIKO SHINOHARA,† SHIN-ICHIRO KURIYA‡ and TAKEO NOMURA*

* The Third Department of Internal Medicine, Nippon Medical School, Tokyo, Japan; † The Department of Human Genetics, Japan Red Cross Medical Center, Hiroo, Tokyo, Japan and ‡ The Third Department of Internal Medicine, Iwate Medical School, Iwate, Japan

(Received 1 September 1990. Revision accepted 13 April 1991)

Abstract—We determined the position of the breakpoint within the *bcr* gene in 22 patients with Philadelphia-positive chronic myelocytic leukemia using conventional Southern-blots and analyzed its relationship to thrombopoiesis. After DNA digestion with restriction endonucleases (Hind III, Bam HI and Bgl II), we localized the breakpoint in *bcr* using two genomic probes. The location of the breakpoint within the *bcr* was assigned to one of five zones. Breakpoints in zones 1 and 2 were grouped as "5'", and those in zones 3, 4 and 5 as "3'". Thus we subdivided patients with *bcr* rearrangements into those with genomic breaks at either 5' or 3' of the Bam HI site, just upstream of exon 3. Nine patients had 5' breakpoints and 13 patients had 3' breakpoints. The platelet counts of 3' patients were significantly higher than those of 5' patients ($139.5 \text{ vs } 27.4 \times 10^9/\text{l}$; $p < 0.03$). The megakaryocyte counts from bone marrow histological sections in 3' patients ($n = 12$) and 5' patients ($n = 7$) were $63.4/\text{mm}^2$ and $19.5/\text{mm}^2$, respectively, with a significant difference of $p < 0.006$. The mean number of megakaryocyte progenitor cells assayed by *in vitro* cloning was $128.3/2 \times 10^5$ bone marrow cells for 3' patients ($n = 7$) compared with 46.3 for 5' patients ($n = 4$). These results suggest that Philadelphia-positive CML patients with 3' breakpoints have higher thrombopoietic activity than patients with 5' breakpoints.

Key words: CML, *bcr* gene, thrombopoiesis, breakpoint site, Philadelphia chromosome, platelet.

INTRODUCTION

A SHORTENED chromosome 22, designated as the Philadelphia (Ph1) chromosome, is observed in the leukemic cells of more than 90% of chronic myelocytic leukemia (CML) patients [1]. The Ph1 chromosome, which can be considered to be the first karyotypic marker consistently present in a human neoplasm, is the result of a reciprocal translocation between chromosomes 9 and 22, $t(9;22)(q34;q11)$ [2]. This translocation moves the *c-abl* proto-oncogene from chromosome 9 to chromosome 22 [3]. The breakpoint of chromosome 22 has been shown to be clustered within a limited region of about 5.8 kb, referred to as the breakpoint cluster region (*bcr*) [4, 5]. Almost all patients have genomic breakpoints between exons b2 and b3 or between exons b3 and b4 of *bcr* [6]. The two chimeric genes may be distinguished by Southern-blot analysis. The first indication that precise location of the breakpoint on

chromosome 22 might have some clinical significance came from a study by Schaefer-Rego *et al.* [7]. Next, a study by Eisenberg *et al.* [8] showed that the mean duration of the chronic phase for patients who had progressed to blast crisis was significantly shorter for patients with a 3'-breakpoint site, consisting of zones 4 and 5 (Fig. 1), than for those with a 5'-breakpoint site, consisting of zones 1, 2 and 3, within the *bcr*. Even a small difference in the location of the breakpoint within the *bcr* gene may cause a change in the amino acid sequence of the fused protein, which in turn may affect the clinical features of CML patients. We report here that CML patients with a 3' breakpoint (zones 3, 4 and 5) within the *bcr* gene have higher thrombopoietic activity than those with a 5' breakpoint (zones 1 and 2).

MATERIALS AND METHODS

Patients

The 22 patients included in this study were all diagnosed as having Ph1-positive CML in the chronic phase of the leukemia, and all were without evidence of acceleration.

Correspondence to: Dr Koiti Inokuchi, The Third Department of Internal Medicine, Nippon Medical School, 1-1-5 Sendagi, Bunkyo-ku, Tokyo 113, Japan.

Diagnosis was established by the standard clinical and hematological criteria [9, 10]. All patients were untreated until the time of the study. In all patients the following clinical and hematologic laboratory data at diagnosis were recorded. All samples of peripheral blood and bone marrow were obtained in the chronic phase at diagnosis after informed consent was obtained.

Many patients were treated with hydroxyurea from diagnosis until the appearance of blastic phase, and some were treated with busulfan.

Cell isolation

Isolation of mononuclear cells from heparinized blood or bone marrow aspirate was performed by Ficoll-Conray (Lymphoprep, Norway) density gradient centrifugation [11]. The interface cells were collected and washed three times with Iscove's modified Dulbecco's medium (IMDM, Gibco Laboratories, U.S.A.).

Extraction and restriction analysis of DNA

High molecular weight DNA was extracted from the mononuclear cells. After genomic DNA was digested with restriction endonucleases (Hind III, Bam HI and Bgl II), 20 µg of digested DNA was size-fractionated by 0.8% standard agarose gel electrophoresis and blotted onto nylon membrane filters (Gene Screen Plus, New England Nuclear, U.S.A.). Hybridization was done according to the protocol provided by New England Nuclear, as described previously [12, 13]. The filter-bound DNA fragments were hybridized to nick-translated [³²P]DNA probes at 63°C and visualized on autoradiograms.

DNA probes

The genomic probe of a 1.2 kb Hind III-Bgl II fragment (1.2HBg, Fig. 1) was obtained from Oncogene Science, Inc. (Mineola, U.S.A.). DNAs for which the breakpoint could not be determined with this probe were analyzed with a 0.6 HB probe [14]. (This probe was a gift from Dr S. Hirose, Tokyo Medical and Dental University, Japan.)

Analysis of the bone marrow megakaryocyte progenitors (CFU-Meg)

Mononuclear bone marrow cells were separated by centrifugation on a Ficoll-metrizoate gradient and washed three times. CFU-Meg was assayed in plasma clot according to Vainchenker *et al.* [15] in a modified form [16]. Briefly, 5×10^5 cells were cultured in 1 ml of IMDM containing 2×10^{15} M 2-mercaptoethanol, 10% deionized bovine serum albumin (Armour, U.S.A.), 10% phytohemagglutinin-stimulated leukocyte-conditioned medium, 10% human AB citrated plasma, 10% citrated calf plasma and 0.26 µg CaCl₂. Culture dishes were incubated at 37°C in a 100% humidified 5% CO₂ atmosphere for 12 days. The cultures were fixed in neutralized buffered formalin and washed with phosphate-buffered saline (PBS). The dishes were subsequently incubated at room temperature for 45 min with rabbit anti-human factor VIII-related antigen (Dakopatts, Denmark). After washing with PBS, the dishes were treated with biotin-labeled goat anti-rabbit IgG antibodies followed by avidin-biotin-peroxidase complex (Vector Lab., U.S.A.). Then the dishes were incubated in H₂O₂-diaminobenzidine solution. The peroxidase-positive, brown-colored colonies were enumerated *in situ* under a microscope at a magnification of 100×. A cluster of three

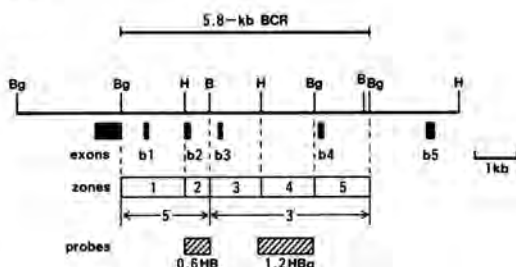


FIG. 1. Restriction map of the *bcr* locus. Exons (b1–b5) are indicated by vertical black boxes below the map. The two probes (0.6 HB and 1.2 HBg) used in this study are indicated by horizontal hatched boxes. Zone numbers are indicated in horizontal open boxes. The line above the map denotes the region designated as *bcr*; B, BamH I; Bg, Bgl II; H, Hind III. Demarcations of the zones are as defined by Mills *et al.* [17].

TABLE 1. DETERMINATION OF LOCATION OF BREAKPOINT USING 1.2 HBg PROBE

Breakpoint group	5'		3'	
Zone	1, 2	3	4	5
Hind III	G*	G	R†	R
BamH I	G	R	R	R
Bgl II	R	R	R	G

* Germline configuration.

† Rearranged band present.

or more brown-colored cells was counted as a megakaryocyte colony.

RESULTS

Analysis of the breakpoint site within the BCR

DNAs of 22 patients with CML were digested with restriction endonucleases Hind III, Bam HI and Bgl II. Using the 1.2 HBg and 0.6 HB probes, rearranged bands were detected in DNAs from all the patients. By digesting the DNA with three restriction enzymes separately, the location of the breakpoint within the *bcr* was assigned to one of five zones as described by Ken I. Mills (Fig. 1, Table 1) [17]. Breakpoints in zones 1 and 2 were grouped as 5', and those in zones 3, 4 and 5 as 3'. Figure 2 shows the Southern-blot results of four respective CML patients. According to this classification, 9 patients had 5' breakpoints and 13 patients had 3' breakpoints.

Clinical correlations

The data regarding the site of the *bcr* breakpoint and the patients' clinical and hematologic features are summarized in Table 2. To standardize our analysis, we compared only the laboratory and clinical

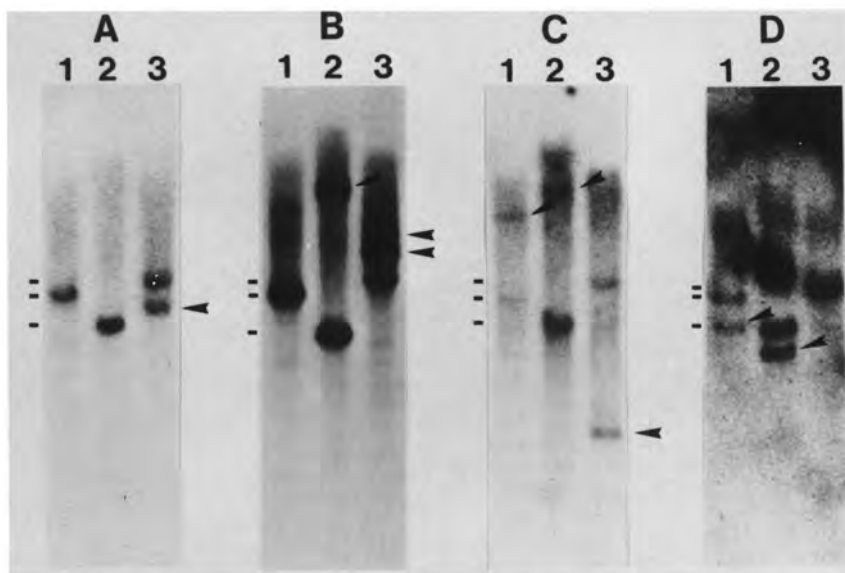


FIG. 2. Southern-blots of four CML patients in each zone with 1.2 HBg probe. DNAs were extracted from mononuclear cells of bone marrow aspirate. DNAs from these patients were digested with restriction endonucleases Hind III, BamH I and Bgl II, respectively. Patients examined: panel A, zone 1-2; B, zone 3; C, zone 4; D, zone 5. Lane 1, Hind III; lane 2, BamH I; lane 3, Bgl II. Horizontal bars show germline bands (5.0, 4.4 and 3.3 kb). The arrow heads indicate the rearranged bands.

TABLE 2. CLINICAL AND HEMATOLOGIC DATA OF 22 CML PATIENTS ACCORDING TO THE POSITION OF THE BREAKPOINT

Breakpoint group	No.	Age median (range, years)	Sex M/F	Spleen palpable	Hb (g/dl) (range)	WBC ($\times 10^9/l$) (range)	Basophils ($\times 10^9/l$) (range)	NAP score (range)
5'	9	47 (25-71)	2/7	7	11.6 (8.2-15.1)	113 (37-519)	7.5 (1.9-11.5)	39.9 (5-119)
3'	13	49 (32-86)	7/6	8	11.5 (7.0-15.4)	92 (13-422)	6.5 (0.4-22.5)	54.5 (5-145)

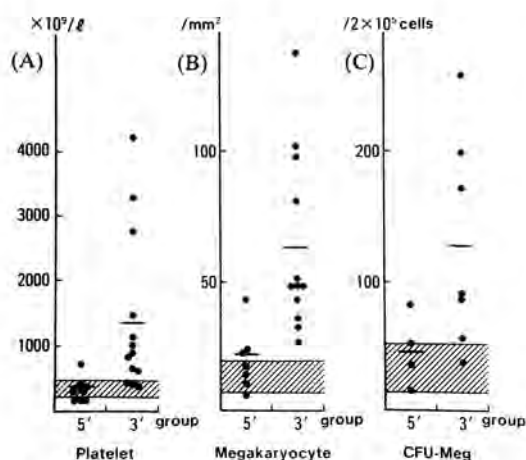


FIG. 3. The correlation of thrombopoiesis with the location of the breakpoint zone. A: correlation of platelet count with the location of the breakpoint group. Platelet count is that at diagnosis. The normal range is indicated by the hatched box. The bars indicate the mean values. B: correlation of megakaryocyte count with the location of the breakpoint group (5'; $n = 7$, 3'; $n = 12$). Megakaryocytes were counted under a light microscope on histological sections prepared from bone marrow aspirates collected at diagnosis. The normal range is indicated by the hatched box. Bars: mean values. C: correlation of colonies of CFU-Meg with the location of the breakpoint group (5'; $n = 4$, 3'; $n = 7$). The normal range of five hematologically normal subjects is indicated by the hatched box. Bars: mean values.

features obtained at the time of diagnosis. There were few differences in the initial laboratory values for hemoglobin, WBC count, NAP score or basophil count between the patients with breakpoints in groups 5' and 3' (p is not significant). The clinical features such as age, sex and size of the spleen were similar in both groups. We could not find any correlation between the location of the BCR breakpoint and the duration of survival.

Relation of breakpoint-site to thrombopoiesis

On the other hand, there was an increase in the platelet count in patients with breakpoints in group 3' compared with those in group 5' (1395 vs $274 \times 10^9/l$, $p < 0.03$) (Fig. 3A). There was also a significant

difference in the megakaryocyte count between the 12 patients with breakpoints in group 3' and 7 patients in group 5' (63.4 vs $19.5/mm^2$, $p < 0.006$) as shown in Fig. 3B. The count of CFU-Meg for each patient examined is shown in Fig. 3C. The average count of CFU-Meg for patients with 5' ($n = 4$) and 3' ($n = 7$) breakpoints was 46.3 and 128.3 per 2×10^5 mononuclear cells, respectively (p is not significant).

DISCUSSION

Ph1-positive CML is thought to be a clonal myeloproliferative disorder resulting from oncogenic transformation of a bone marrow stem cell. In the chronic phase, the disease phenotype is characterized by pronounced granulocytosis and thrombocytosis of the peripheral blood and increased myeloid and megakaryocyte compartments in the hypercellular bone marrow.

Recently, our understanding of the pathogenesis of CML has been greatly advanced due to molecular biology. Ph1-positive CML is characterized by the presence of a *bcr* rearrangement. Schaefer-Rego *et al.* [7] performed restriction mapping of breakpoints in 26 patients with Ph1-positive CML. They suggested that there might be a correlation between 3' breakpoints and blastic crisis. Eisenberg *et al.* [8] reported a significant excess of patients with 3' breakpoints already in transformation compared with patients still in the chronic phase among 71 patients with CML. Mills *et al.* [17] studied 22 patients with CML and found that the median duration of the chronic phase was about 4 times longer in the 5' group. Other studies have failed to confirm an association between the location of the breakpoint within the *bcr* and the progression of disease in CML. We again failed to detect any difference in the duration of survival between the 5' and 3' patient groups. Our findings do not, therefore, support the notion that the precise position of the breakpoint within the *bcr* influences the duration of the chronic phase. Although a number of attempts have been made in connecting the breakpoint-site and the duration of survival, studies correlating breakpoint-sites and the clinical features have been few. Shtalrid *et al.* [18],

Jaubert *et al.* [19] and Morris *et al.* [20] reported a correlation between the site of the *bcr* breakpoint and the patients' clinical and hematologic features. They found that there were no differences in the initial laboratory values (hemoglobin, WBC count and platelet count) or clinical features (age, sex and palpable spleen) between the 5' and 3' groups.

In the present study, we found a striking correlation between the site of the breakpoint and thrombopoiesis in 22 Ph1-positive CML cases. The conflicting findings among authors are very difficult to explain. The first possibility is that there were five patients in group 3', who had platelet counts in excess of $1000 \times 10^9/l$ in our analysis. The five with marked thrombocytosis (23%) of 22 patients is reasonable rate according to the report of Mason *et al.* [21]. They report that twenty-nine of the 71 patients have platelet counts in excess of $1000 \times 10^9/l$, with the highest count in the series at $7000 \times 10^9/l$ during their course. But we considered that it was possible that marked thrombopoiesis was associated with early appearance of blastic formation. The median duration of the chronic phase for the five patients was 40.8 months (range 20–89). There was no trend for shorter duration of the chronic phase in the five patients. In addition, there was no suggestion that these five patients had any clinical features distinct from other CML patients in the chronic phase except marked thrombocytosis during their course. The next possibility is that the definition of the breakpoint group within the *bcr* adopted by us is slightly different from that of others. We subdivided patients with *bcr* rearrangement into those with genomic breaks of either 5' or 3' of the Bam HI site, just upstream of exon 3. Jaubert *et al.* subdivide patients into those with genomic breaks of either 5' or 3' of the central Hind III site, just downstream of exon 3. When we subdivided patients into two groups using the central Hind III site according to Jaubert *et al.*, we could obtain no correlation between the site of the breakpoint and thrombopoiesis. Because of this, the sites of the breakpoint in two of the 5 patients who had platelet counts in excess of $1000 \times 10^9/l$ were in zone 3. Shtalrid *et al.* and Morris *et al.* subdivide patients into three or four groups that are the same as our zones. Although they reported no correlation between the breakpoint sites and platelet counts, we infer that the platelet counts among the 3 laboratories show a similar tendency to ours.

Both the megakaryocyte counts and the mean number of megakaryocyte progenitor cells, in addition to platelet counts, in patients with group 3' were increased compared with those with group 5' in our analysis. After giving careful consideration, we concluded that CML patients with 3' breakpoints

have higher thrombopoietic activity than patients with 5' breakpoints.

Acknowledgements—We would like to thank Dr S. Hiro-sawa for the 0.6 HB probe, the blood-research group of the Third Department of Internal Medicine for supplying blood samples and Dr S. Inokuchi for the excellent secretarial support.

REFERENCES

- Rowley J. D. (1973) A new consistent chromosomal abnormality in chronic myelogenous leukemia identified by quinacrine fluorescence and Giemsa staining. *Nature* **243**, 290.
- De Klein A., van Kessel A. G., Grosveld G., Bartram C. R., Hagemeijer A., Bootsma D., Spur N. K., Heisterkamp N., Groffen J. & Stephenson J. R. (1982) A cellular oncogene is translocated to the Philadelphia chromosome in chronic myelogenous leukemia. *Nature* **300**, 765.
- Heisterkamp N., Stephenson J. R., Groffen J., Hansen P. F., de Klein A., Bartram C. R. & Grosveld G. (1983) Localization of the *c-abl* oncogene adjacent to a translocation breakpoint in chronic myelocytic leukemia. *Nature* **306**, 239.
- Groffen J., Stephenson J. R., Heisterkamp N., de Klein A., Bartram C. R. & Grosveld G. (1984) Philadelphia chromosomal breakpoints are clustered within a limited region, *bcr*, on chromosome 22. *Cell* **36**, 93.
- Heisterkamp N., Stam K., Groffen J., de Klein A. & Grosveld G. (1985) Structural organization of the *bcr* gene and its role in the Ph' translocation. *Nature* **316**, 758.
- Shtivelman E., Lifshitz B., Gale R. P. & Canaani E. (1985) Fused transcripts of *abl* and *bcr* genes in chronic myelogenous leukemia. *Nature* **315**, 550.
- Schaefer-Rego K., Dudek H., Popenoe D., Arlin Z., Mears J. G., Bank A. & Leibowitz D. (1987) CML patients in blast crisis have breakpoints localized to a specific region of the *BCR*. *Blood* **70**, 448.
- Eisenberg A., Silver R., Soper L., Arlin Z., Coleman M., Bernhardt B. & Benn P. (1988) The location of breakpoints within the breakpoint cluster region (*bcr*) of chromosome 22 in chronic myeloid leukemia. *Leukemia* **2**, 642.
- Spier A. S. D., Bain B. J. & Turner J. E. (1977) The peripheral blood in chronic granulocytic leukemia: Study of 50 untreated Philadelphia-positive cases. *Scand. J. Haemat.* **18**, 25.
- Cervantes F. & Rozman C. (1982) A multivariate analysis of prognostic factors in chronic myeloid leukemia. *Blood* **60**, 1298.
- Hoffman R. & Yang H. H. (1985) Definition of the regulatory factors required for human megakaryocyte colony formation. *Clin. Res.* **30**, 546A.
- Shimada T., Inokuchi K. & Nienhuis A. W. (1986) Chromatin structure of the human dihydrofolate reductase gene promoter. Multiple protein-binding sites. *J. biol. Chem.* **261**, 1445.

13. Inokuchi K., Komiya I., Dan K., Kuriya S., Shinohara T. & Nomura T. (1990) TdT-positive, SmIg-negative B precursor cell leukemia with Burkitt Morphology: A case report. *Leukemia lymphoma* **2**, 251.
14. Hirosawa S., Aoki N., Matsushima H. & Shibuya M. (1988) Undetectable *bcr-abl* rearrangements in some CML patients are due to a deletion mutation in the *bcr* gene. *Am. J. Hemat.* **28**, 33.
15. Vainchenker W., Bouguet J., Guichard J. & Breton-Gorius J. (1979) Megakaryocyte colony formation from human bone marrow precursors. *Blood* **54**, 940.
16. Ogata K., Kuriya S., Dan K. & Nomura T. (1989) Partial purification of human urinary megakaryocyte colony-stimulating factor. *Expl Hemat.* **57**, 19.
17. Mills K. I., MacKenzie E. D. & Birnie G. D. (1988) The site of the breakpoint within the *bcr* is a prognostic factor in Philadelphia-positive CML patients. *Blood* **72**, 1237.
18. Shtalrid M., Talpaz M., Kurzrock R., Kantarjian H., Trujillo J., Gutterman J., Galina Y. & Mark B. (1988) Analysis of breakpoints within the *bcr* gene and their correlation with the clinical course of Philadelphia-positive chronic myelogenous leukemia. *Blood* **72**, 485.
19. Jaubert J., Martiat P., Dowding C., Ifrah N. & Goldman J. M. (1990) The position of the M-BCR breakpoint does not predict the duration of chronic phase or survival in chronic myeloid leukemia. *Br. J. Haemat.* **74**, 30.
20. Morris S. W., Daniel L., Ahmed C. M. I., Elias A. & Lebowitz P. (1990) Relationship of *bcr* breakpoint to chronic phase duration, survival, and blast crisis lineage in chronic myelogenous leukemia patients presenting in early chronic phase. *Blood* **75**, 2035.
21. Mason J. E., DeVita V. T. & Canellos G. P. (1974) Thrombocytosis in chronic granulocytic leukemia: Incidence and clinical significance. *Blood* **44**, 483.

RAPID COMMUNICATION

A Possible Correlation Between the Type of *bcr-abl* Hybrid Messenger RNA and Platelet Count in Philadelphia-Positive Chronic Myelogenous Leukemia

By Koiti Inokuchi, Tokiko Inoue, Arinobu Tojo, Makoto Futaki, Koichi Miyake, Takashi Yamada, Yoshihiro Tanabe, Ichiro Ohki, Kazuo Dan, Keiya Ozawa, Shigetaka Asano, and Takeo Nomura

The Philadelphia (Ph1) chromosome, in which the hybrid *bcr-abl* gene is formed, is thought to be the initial event in chronic myelogenous leukemia (CML). The position of the breakpoint within the breakpoint cluster region (*bcr*) on Ph1 chromosome and the splicing pattern determine the species of the fused *bcr-abl* messenger RNA (mRNA). We tried to detect the two types of fused mRNAs in 57 chronic-phase cases of Ph1-positive CML using the polymerase chain reaction procedure (RT-PCR). The *bcr* exon 2/*abl* exon 2 fused mRNA (b2-a2) was detected in 17 patients, the *bcr* exon

3/*abl* exon 2 fused mRNA (b3-a2) was detected in 34 patients, and both types of mRNA were detected in six patients. The platelet counts of patients who expressed b3-a2 mRNA or both types were significantly higher than those of patients who expressed only b2-a2 ($841.5 \pm 373.5 \times 10^3/L$; $P < .015$), although there was no significant difference in the white blood cell counts or hemoglobin. This finding suggests a possibility that the type of *bcr-abl* mRNA may affect the thrombopoietic activity in CML.

© 1991 by The American Society of Hematology.

A SHORTENED chromosome 22, designated as the Philadelphia (Ph1) chromosome, is observed in the leukemic cells of more than 90% of chronic myelogenous leukemia (CML) patients.¹ The Ph1 chromosome, which can be considered to be the first karyotypic marker consistently present in a human neoplasm, is the result of a reciprocal translocation between chromosomes 9 and 22, t(9;22)(q34;q11).² This translocation moves the *c-abl* proto-oncogene from chromosome 9 to chromosome 22.³ The breakpoint of chromosome 22 has been shown to be clustered within a limited region of about 5.8 kb, referred to as the breakpoint cluster region (*bcr*).^{4,5} Almost all of the patients have genomic breakpoints between exons b2 and b3 or between exons b3 and b4 within *bcr*.⁶ The two chimeric genes may be distinguished by Southern blot analysis. The first indication that the precise location of the breakpoint on chromosome 22 might have some clinical significance came from a study by Schaefer-Rego et al.⁷ Next, a study by Eisenberg et al.⁸ showed that the mean duration of the chronic phase for patients who had progressed to blast crisis was significantly shorter for patients with a 3'-breakpoint site than for those with a 5'-breakpoint site within the *bcr*. Many studies have reported on this controversial point.⁹⁻¹¹ Even a small difference in the location of the breakpoint within the *bcr* gene may cause a change in the amino acid sequence of the fused protein, which in turn may affect the clinical features of CML patients. Recently, we reported that CML patients with a 3' breakpoint within the *bcr* gene have higher thrombopoietic activity than those with a 5' breakpoint.¹²

Here, we tried to ascertain the relationship between thrombopoiesis and the two potential types of fused *bcr-abl* messenger RNAs (mRNAs) using the polymerase chain reaction (RT-PCR) in 57 CML patients. As expected, we found that patients with fused b3-a2 mRNA had higher platelet counts than those with fused b2-a2 mRNA.

MATERIALS AND METHODS

Patient population. Blood and bone marrow samples were obtained from 57 Ph1-positive CML patients in the chronic phase of the disease. Most of the patients had not received therapy before RNA analysis. The clinical data of each patient are that at diagnosis.

RT-PCR for detection of *bcr-abl* fusion mRNA. The total RNA of mononuclear cells was extracted by the CsCl method.¹³ RT-PCR was performed using the methods described by Roth et al.¹⁴ and by Kawasaki et al.¹⁵ with a slight modification.¹⁶ Approximately 2 µg of total RNA was used as the template with 10 U of avian myeloblastosis virus reverse-transcriptase (Boehringer-Mannheim, Indianapolis, IN) for 1 hour at 37°C in 50 mmol/L Tris-HCl, pH 8.3, 50 mmol/L KCl, 8 mmol/L MgCl₂, 10 mmol/L dithiothreitol, dNTPs at 500 µmol/L each in a total volume of 50 µL with 0.05 OD₂₆₀ units of oligo-primer (*abl*-RT: 5'-AACGAAAAGGTTGGGGTC-3', antisense strand). Ten microliters of the reverse transcriptase reaction mixture was adjusted to PCR conditions (10 mmol/L Tris-HCl pH 8.3, 50 mmol/L KCl, 15 mmol/L MgCl₂, 2 mmol/L dithiothreitol, 200 µmol/L dNTPs) with 0.0125 OD₂₆₀ units of one of two sets of primers (the first set, A: 5'-AGCATGGCCTTCAGGGTGCA-CAGCCGCAACGGCAA-3', coding strand, and B: 5'-TCAC-TGGGTCCAGCGAGAAGGTTTTCCTTGGAGTT-3', antisense strand; the second set, C: 5'-GGAGCTGCAGATGCTGACCAAC-3', coding strand and D: 5'-TCAGACCTGAGGCTCAAAGTC-3', antisense strand) and 2 U of Taq polymerase (Thermus aquaticus DNA polymerase; Perkin Elmer Cetus, Norwalk, CT) in a 50 µL reaction volume (Fig 1). PCR of 40 cycles was performed, consisting of 30 seconds at 94°C (denaturation), 30 seconds at 55°C (annealing), and 1 minute at 75°C (extension). Finally, the PCR products (20 µL) were phenol-extracted, ethanol-precipitated, and electrophoresed through a 2% agarose gel. The PCR products were visualized directly in ethidium bromide-stained gels, photographed, and transferred onto Gene Screen Plus membranes (New England Nuclear, Boston, MA). Southern hybridization was performed using a 0.6HB probe corresponding to the *bcr* exon 2 (provided by Dr S. Hirose, Tokyo Medical and Dental University), or two kinds of oligonucleotides (E: 5'-GCTGAAGGGCTTT-

From the Third Department of Internal Medicine, Nippon Medical School; and the Department of Hematology-Oncology, the Institute of Medical Science, the University of Tokyo, Tokyo, Japan.

Submitted August 26, 1991; accepted September 17, 1991.

Address reprint requests to Koiti Inokuchi, MD, PhD, The Third Department of Internal Medicine, Nippon Medical School, Sendagi 1-1-5, Bunkyo-ku, Tokyo 113, Japan.

The publication costs of this article were defrayed in part by page charge payment. This article must therefore be hereby marked "advertisement" in accordance with 18 U.S.C. section 1734 solely to indicate this fact.

© 1991 by The American Society of Hematology.

0006-4971/91/7812-0029\$3.00/0

bcr-abl mRNA (8.5kb)

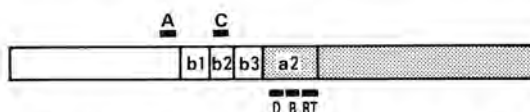


Fig 1. Schematic representation of the *bcr-abl* mRNA with position of oligomers numbered A, B, C, and D used in the PCR reaction, and *abl*-RT oligomer for making cDNA synthesis as described.^{14,15} (□) *bcr*-specific sequences; (■) *abl*-specific sequences.

TGAAGCTCT3', specific for *bcr* exon3/*abl* exon 2; and F: 5'-GCTGAAGGGCTTCTCTTATTGATG-3', specific for *bcr* exon2/*abl* exon 2).¹⁵

RESULTS

RNA samples from 57 CML patients were analyzed for specific *bcr-abl* mRNA. The *bcr-abl* mRNA junctions were amplified by the RT-PCR method using two pairs of primers. The two junctions, *bcr2-abl2* and *bcr3-abl2*, were identified by their electrophoretic mobility and hybridization to *bcr* exon2 (0.6HB) probe or junction-specific oligoprobes. An example of the RT-PCR analysis in which a pair of primers (primers A and B) was used is shown in Fig 2. The RT-PCR products of RNA samples from K562 cells and five CML patients were electrophoresed and subsequently visualized by ethidium bromide staining and hybridization to the 0.6HB probe. The 319-bp RT-PCR product is the band specific for *b3-a2* mRNA, while the 244-bp RT-PCR product is specific for *b2-a2* mRNA. The RT-PCR

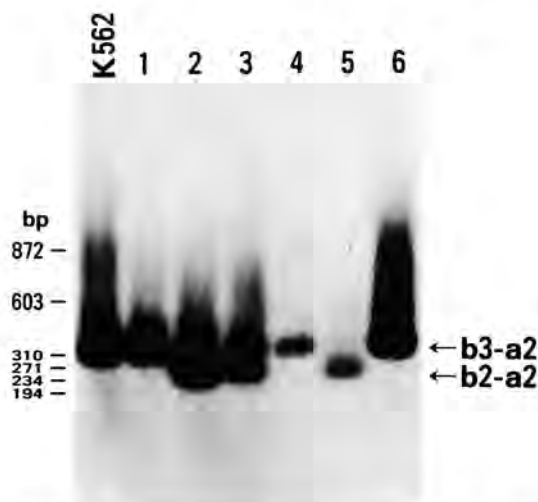


Fig 2. Examples of Southern blot hybridization of RT-PCR products of the *bcr-abl* mRNA in Ph1-positive patients. Products from RT-PCR analyses were size-fractionated by 2.0% agarose gel electrophoresis, transferred to a nylon membrane, and hybridized to a 0.6HB probe. K562 cells and patients 1, 4, and 6 have the *b3a2* junction. Patients 2 and 5 have the *b2a2* junction only. Patient 3 produces both junctional products.

analysis of 57 patients showed the presence of *b3-a2* mRNA in 34 cases and *b2-a2* mRNA in 17 cases, and coexpression of both junctions in six cases. The relationship between the type of *bcr-abl* mRNA and platelet count is shown in Fig 3. The platelet counts of patients expressing *b3-a2* mRNA were significantly higher than those of patients expressing only *b2-a2* mRNA ($841.5 \text{ v } 373.5 \times 10^9/\text{L}$; $P < .015$). We also examined the relationship with the white blood cell count and hemoglobin, but no significant correlations were found.

DISCUSSION

Ph1-positive CML is thought to be a clonal myeloproliferative disorder resulting from oncogenic transformation of a bone marrow stem cell. In the chronic phase, the disease phenotype is characterized by pronounced granulocytosis and thrombocytosis in peripheral blood and increased myeloid and megakaryocyte compartments in the hypercellular bone marrow.

Recently, our understanding of the pathogenesis of CML has been greatly advanced by the molecular studies. Ph1-positive CML is characterized by the presence of a *bcr* rearrangement. Attempts have been made to elucidate the relationship between the breakpoint site and the duration of survival or the other clinical features by Southern analysis at the DNA level. Shtalrid et al,⁹ Jaubert et al,¹⁰ and Morris et al¹¹ reported that there was a significant correla-

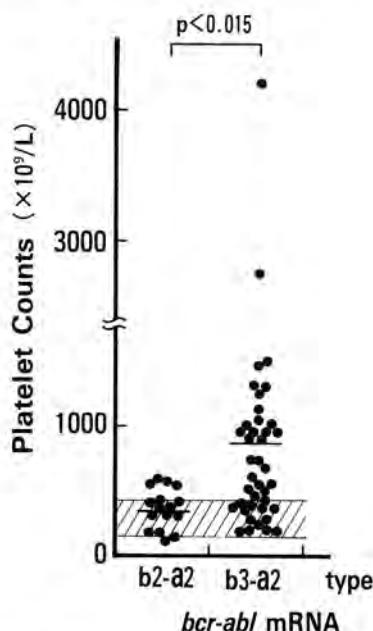


Fig 3. Correlation of platelet count with the type of *bcr-abl* mRNA. The platelet counts were obtained at diagnosis before the therapy. The normal range is indicated by the hatched box. The bars indicate the mean values. The significance of platelet counts in both types was tested with the Wilcoxon-2 sample test.

tion between the site of the *bcr* breakpoint and the duration of survival. CML patients have one of two *bcr-abl* mRNA types or both.^{14,17} Application of the RT-PCR method to determine the type of *bcr-abl* mRNA in CML patients has made it easier to identify the site of the *bcr* rearrangement. The studies using the RT-PCR method are now prevailing in this research area.^{17,18} Recently, we found that CML patients with a 3' breakpoint site within the *bcr* gene have a tendency to have higher thrombopoietic activity than those with a 5' breakpoint.¹² Therefore, to confirm this preliminary observation, we extensively studied the relationship between the type of *bcr-abl* mRNA and the patient's platelet count in 57 Ph1-positive CML cases using the PCR method. As expected, the platelet counts were higher in the patients expressing b3-a2 mRNA.

A recent study reported similar finding in Ph1-positive essential thrombocythemia.¹⁹ The b3-a2 type mRNA was observed in five patients and the b2-a2 type mRNA was

observed in only one patient. In our present study, 16 patients who had platelet counts of more than $900 \times 10^9/L$ expressed only b3-a2 type mRNA, and almost all of the patients with b2-a2 type mRNA had a platelet count of less than $600 \times 10^9/L$. There were no apparent differences in hematologic findings between the patients with b3-a2 type mRNA and the CML patients with b2-a2 type mRNA, except for the platelet count. Thus, we speculate that the type of *bcr-abl* mRNA may affect the thrombopoietic activity in CML, although we are currently unable to explain why the platelet count correlates with the type of *bcr-abl* mRNA.

ACKNOWLEDGMENT

We thank Dr S. Hirokawa for the 0.6HB probe, the blood-research group of the Third Department of Internal Medicine of the Nippon Medical School for supplying blood samples, and Dr S. Inokuchi for help with the preparation of the manuscript.

REFERENCES

- Rowley JD: A new consistent chromosomal abnormality in chronic myelogenous leukemia identified by quinacrine fluorescence and giemsa staining. *Nature* 243:290, 1973
- De Klein A, van Kessel AG, Grosveld G, Bartram CR, Hagemeijer A, Bootsma D, Spur NK, Neisterkamp N, Groffen J, Stephenson JR: A cellular oncogene is translocated to the Philadelphia chromosome in chronic myelogenous leukemia. *Nature* 300:765, 1982
- Heisterkamp N, Stephenson JR, Groffen J, Hansen PF, de Klein A, Bartram CR, Grosveld G: Localization of the *c-abl* oncogene adjacent to a translocation breakpoint in chronic myelocytic leukemia. *Nature* 306:239, 1983
- Groffen J, Stephenson JR, Heisterkamp N, de Klein A, Bartram CR, Grosveld G: Philadelphia chromosomal breakpoints are clustered within a limited region, *bcr*, on chromosome 22. *Cell* 36:93, 1984
- Heisterkamp N, Stam K, Groffen J, de Klein A, Grosveld G: Structural organization of the *bcr* gene and its role in the Ph' translocation. *Nature* 316:758, 1985
- Shtivelman E, Lifshitz B, Gale RP, Canaani E: Fused transcripts of *abl* and *bcr* genes in chronic myelogenous leukemia. *Nature* 315:550, 1985
- Schaefer-Rego K, Dudek H, Popenoe D, Arlin Z, Mears JG, Bank A, Lebowitz D: CML patients in blast crisis have breakpoints localized to a specific region of the BCR. *Blood* 70:448, 1987
- Eisenberg A, Silver R, Soper L, Arlin Z, Coleman M, Bernhardt B, Bann P: The location of breakpoints within the breakpoint cluster region (*bcr*) of chromosome 22 in chronic myeloid leukemia. *Leukemia* 2:642, 1988
- Shtalrid M, Talpaz M, Kurzrock R, Kantarjian H, Trujillo J, Gutterman J, Galina Y, Mark B: Analysis of breakpoints within the *bcr* gene and their correlation with clinical course of Philadelphia-positive chronic myelogenous leukemia. *Blood* 72:485, 1988
- Jaubert J, Martiat P, Dowding C, Ifrah N, Goldman JM: The position on the M-BCR breakpoint does not predict the duration of chronic phase or survival in chronic myeloid leukemia. *Br J Haematol* 74:30, 1990
- Morris SW, Daniel L, Ahmed CMI, Elias A, Lebowitz P: Relationship of *bcr* breakpoint to chronic phase duration, survival, and blast crisis lineage in chronic myelogenous leukemia patients presenting in early chronic phase. *Blood* 75:2035, 1990
- Inokuchi K, Futaki M, Yamada T, Tanabe Y, Dan K, Shinohara T, Kuriya S, Nomura T: The relationship between the site of breakpoints within the *bcr* gene and thrombopoiesis of Philadelphia-positive chronic myelocytic leukemia. *Leuk Res* (in press)
- Chirgwin JM, Przybyla AE, MacDonald RJ, Rutter WJ: Isolation of biologically active ribonucleic acid from sources enriched in ribonuclease. *Biochemistry* 18:5294, 1979
- Roth MS, Antin JH, Bingham EL, Ginsburg D: Detection of Philadelphia chromosome-positive cells by the polymerase chain reaction following bone marrow transplant for chronic myelogenous leukemia. *Blood* 74:882, 1989
- Kawasaki ES, Clark SS, Coyne MY, Smith SD, Champlin R, Witte ON, McCormick FP: Diagnosis of chronic myeloid and acute lymphocytic leukemias by detection of leukemia-specific mRNA sequences amplified in vitro. *Proc Natl Acad Sci USA* 85:5698, 1988
- Futaki M, Inokuchi K, Dan K, Nomura T: Activation of *bcr-abl* fusion gene and *ras* oncogenes in chronic myelogenous leukemia. *Leuk Lymphoma* (in press)
- Morgan GJ, Hernandez A, Chan LC, Hughes T, Martiat P, Wiedemann LM: The role of alternative splicing patterns of BCR/ABL transcripts in the generation of the blast crisis of chronic myeloid leukemia. *Br J Haematol* 76:33, 1990
- Marcelle C, Gale RP, Prokocimer M, Berrebi A, Merle-Beral H, Canaani E: Analysis of BCR-ABL mRNA in chronic myelogenous leukemia patients and identification of a new BCR-related sequence in human DNA. *Gene Chromosomes Cancer* 1:172, 1989
- Martiat P, Ifrah N, Rassool F, Morgan G, Giles F, Gow J, Goldman JM: Molecular analysis of Philadelphia positive essential thrombocythemia. *Leukemia* 3:563, 1989

INTHEM 00115

N-*RAS* activation in the terminal stage of undifferentiated chronic myeloproliferative disease

Koiti Inokuchi^a, Makoto Futaki^a, Koichi Miyake^a, Tetsuo Kuwabara^a, Tamiko Shinohara^b, Kazuo Dan^a and Takeo Nomura^a

^aThird Department of Internal Medicine, Nippon Medical School, Tokyo, Japan and ^bDepartment of Human Genetics, Japan Red Cross Medical Center, Tokyo, Japan

(Received 16 May 1991, accepted 27 November 1991)

The relationship between activation of the N-*RAS* gene and the leukemic progression of undifferentiated chronic myeloproliferative disease (UCMPD) was investigated in a 71-year-old male. Hematologically, it was difficult to differentiate the UCMPD from chronic myelogenous leukemia. Chromosomal analysis revealed no Philadelphia chromosome (Ph¹), and DNA analysis revealed no *BCR* rearrangement (*BCR*[−]) either at the beginning or in the terminal stages of the disease. We performed a tumorigenicity assay, using NIH3T3 cells, and molecular analysis, using the polymerase chain reaction (PCR) and direct sequencing. The DNA of leukemic cells at the beginning of the leukemic progression did not show any abnormalities, but at the terminal stage of the disease the DNA showed a point mutation in codon 12 (GGT→GCT) of the N-*RAS* gene. Interestingly, a codon 13 mutation (GGT→GTT) was also detected by tumorigenicity assay. These observations suggest that the activated N-*RAS* gene contributes to the hematologic progression of UCMPD.

Key words: N-*RAS* oncogene; Philadelphia chromosome; *BCR* rearrangement; Undifferentiated chronic myeloproliferative disease; Chronic myelogenous leukemia

Introduction

Chronic myelogenous leukemia (CML) is characterized by the presence of the Philadelphia chromosome (Ph¹) or by the *BCR* gene rearrangement [1]. Recent clinical, hematologic, and cytogenetic evidence suggests that Ph¹-negative/*BCR*-negative CML (Ph¹[−]/*BCR*[−] CML) is a heterogeneous mixture of disorders rather than typical

CML [2–5]. With the recent proposal of criteria for the classification of myelodysplastic syndromes (MDS) by the French–American–British (FAB) group, it has become apparent that many cases of Ph¹[−]/*BCR*[−] CML are examples of MDS [2,3]; some of these are undifferentiated chronic myeloproliferative disease (UCMPD), the pathogenesis of which is still unclear. We encountered a patient with UCMPD and a history of pancytopenia; this state preceding a CML-like leukemoid reaction is extremely unusual. We performed cytogenetic and molecular studies at different stages of the leukemic progression in this patient, and in this paper we discuss the relationship between N-*RAS* activation

Correspondence: Koiti Inokuchi, M.D., The Third Department of Internal Medicine, Nippon Medical School, 1-1-5 Sendagi, Bunkyo-ku, Tokyo 113, Japan.

and the leukemic progression of UCMPD from the pancytopenic state in the patient.

Materials and Methods

Case history

A 71-year-old male was found to have a hemoglobin level of 9.9 g/dl and a hematocrit value of 32.4% in October 1988. His white blood cell (WBC) count was $2.3 \times 10^9/l$ (5% bands, 21% segmented neutrophils, 71% lymphocytes, 1% eosinophils and 2% monocytes), and the platelet count was $105 \times 10^9/l$. For about 12 months, his pancytopenic state showed little change (Fig. 1).

In December 1989, he was referred to our hospital because of an abrupt increase in the leukocyte count. Physical examination revealed splenomegaly with a spleen tip palpable 2 cm below the left costal margin, and an enlarged liver palpable 2 cm below the right costal margin, but no lymphadenopathy. On admission, the peripheral blood study revealed a hemoglobin level of 9.4 g/dl, red blood cell count of $3.1 \times 10^{12}/l$ (reticulocytes: 10%), platelet count of $110 \times 10^9/l$, and WBC of $23.0 \times 10^9/l$, with a differential of 2% blasts, 1% promyelocytes, 28% myelocytes, 5% metamyelocytes, 20% bands, 32% segmented neutrophils, 12% lymphocytes, and 3/200 erythro-

blasts. Bone marrow aspiration revealed a hypercellular marrow with a myeloid/erythroid ratio of 10.0. Megakaryocytes were increased in number but normal in morphology. The serum vitamin B₁₂ level was more than 1600 µg/ml (normal: 210–945 µg/ml, and the leukocyte alkaline phosphates score was 9 (normal: 170–285). A diagnosis of CML in the chronic phase was made. Despite these hematologic findings, examination of the bone marrow and peripheral blood failed to reveal the Philadelphia chromosome.

Because of the remarkable leukocytosis, antileukemic therapy with hydroxyurea, 1.5 g daily, was commenced in April 1990. At that time, the hematological data were: WBC $247.8 \times 10^9/l$, hemoglobin 6.4 g/dl, and platelet count $53.0 \times 10^9/l$. Despite the administration of 1.5 g of hydroxyurea daily, the remarkable leukocytosis did not cease, so higher doses, up to 3.0 g, were administered subsequently. However, the WBC count did not change in response to these escalating doses. Progressive leukocytosis terminated in a pulmonary hemorrhage, and the patient died in May 1990. Autopsy revealed severe hemorrhage in both lungs.

Southern blot analysis

High-molecular-weight DNA was extracted from mononuclear cells obtained from bone mar-

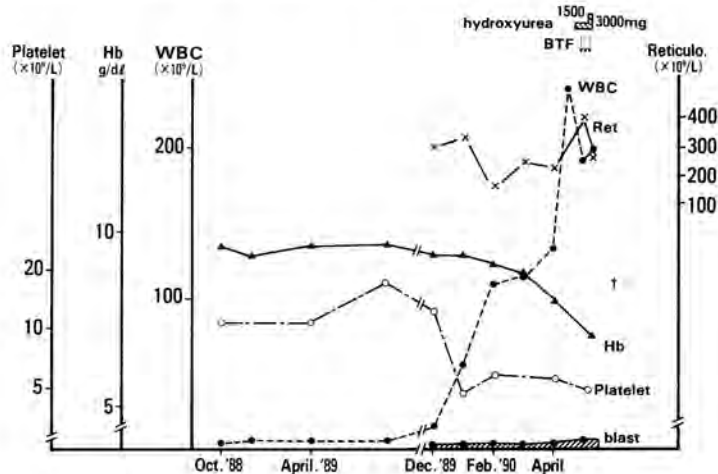


Fig. 1. Patient's clinical course. BTF, blood transfusion.

row aspirates by Ficoll-Hypaque gradient centrifugation. After genomic DNA was digested with restriction endonucleases, the digested DNA was size-fractionated by 0.8% agarose gel electrophoresis and transferred to a nylon membrane filter as described previously [6].

Tumorigenicity assay

The tumorigenicity assay was performed by the CaPO₄ method, with slight modification, described previously [7,8]. In brief, genomic DNA (60 µg) was mixed with 4 µg of plasmid pSV2neo and transfected into NIH3T3 cells by the standard CaPO₄ coprecipitation method [9]. The precipitate was incubated at 37°C for 12 h. Forty-eight hours later, the cells were trypsinized, replated, and subjected to selection with G418 at 400 µg per ml of medium. Fourteen to 21 days after transfection, cells producing > 500 colonies were removed from the plates by trypsinization. Samples, 5 × 10⁶ cells, were resuspended in 0.5 ml of cold medium. This suspension was then injected subcutaneously into athymic nude mice, and the emergence of tumors was scored. The observation period for tumor formation was limited to 80 days after injection. DNA prepared from representative tumors was subjected to Southern blot analysis for the detection of human repetitive and oncogene sequences.

PCR and direct sequencing

The PCR reaction was performed in a DNA Thermal Cycler (Perkin-Elmer/Cetus Corp. UK) with slight modification of the original PCR procedure of Saiki et al. [10]. Two hundred ng of DNA from either mononuclear cells or NIH3T3 transformant cells was incubated with 0.5 U of Taq DNA polymerase (Perkin-Elmer/Cetus Corp. UK) and with 200 ng of each of two synthetic 20-mer oligonucleotides spanning the 5' and 3' ends of the target sequence (5':5'-ATGACTGAGTACAACTGGT-3', coding strand; 3':5'-CTATGGTGGGATCATATTCA-3', antisense strand). A 109-bp amplified fragment was electrophoresed on 2.0% agarose, sliced from the gel, electroeluted, purified with phenol and ethanol-precipitated.

Direct nucleotide sequencing was performed using a modification of the method of Radich et al. [11]. Six µl of total annealing mixture containing

approximately 20–60 ng of PCR DNA product, 20 pmol of oligonucleotide primer, 1 µl of 5 × Sequenase buffer, and 10% dimethyl sulfoxide (DMSO) was boiled for 2 min, snap-cooled on dry ice, and then placed on wet ice. Four microliters of labelling mixture, consisting of 1 µl of 0.1 mol/l DTT, 1 µl of ³⁵S-dATP, and 2 µl of 1:8 diluted Sequenase enzyme was then added. This mixture was then divided equally and placed in four tubes, which contained respectively, 2 µl of a deoxy/dideoxy nucleotide "chase" mixture (80 µM dGTP, dATP, dCTP, dTTP, 50 mmol/l NaCl, and 8 µM ddGTP [tube G], 8 µM ddATP [tube A], 8 µM ddTTP [tube T], and 8 µM ddCTP [tube C]). These tubes were incubated at 41°C for 2 min, followed by the addition of 4 µl of formamide stop mixture. After being boiled for 2 min, 6 µl aliquots were loaded and electrophoresed on an 8% polyacrylamide/7 M urea gel.

Results

DNA obtained from the patient's bone marrow mononuclear cells was analyzed by Southern hybridization to a breakpoint cluster region probe (Fig. 2). The DNA was digested with three restriction endonucleases, i.e., *Hind*III, *Bam*HI, and *Bg*II. No *BCR* rearrangement band was seen. Northern hybridization was also performed on mRNA derived from the patient's bone marrow mononuclear cells. No 8.5-kb aberrant transcript was seen when the filters were probed with the *c-ABL* universal probe (data not shown). The clinical characteristics at the time of the sampling of bone marrow cells are shown in Table 1. The results of tumorigenicity assays are shown in Table 2 and Fig. 3. At the time of admission (the beginning of the leukocytosis), the patient's DNA did not have the capacity to transform NIH3T3 cells. However, in the terminal stage of the disease, his DNA did have this capacity, and an activated *N-RAS* gene was detected (Fig. 3).

Figure 4 depicts the antisense of *N-RAS* exon-1 segments from DNA of different stages, and the DNA of NIH3T3 transformant cells. DNA at the terminal stage revealed a mutation in codon 12 (GGT→GCT), whereas DNA obtained on admission had not shown any mutation. Another point

TABLE 1

Clinical characteristics at the time of sampling of bone marrow cells

	Peripheral blood				Bone marrow		
	Hb (g/dl)	WBC ($\times 10^9/l$)	Blast (%)	Platelet ($\times 10^9/l$)	Cellularity	Blast (%)	Cytogenetics
December 1989	9.4	29.5	4.0	110	Hypercellular	2.4	46,XY
April 1990	6.4	247.8	2.0	53	Hypercellular	2.6	46,XY

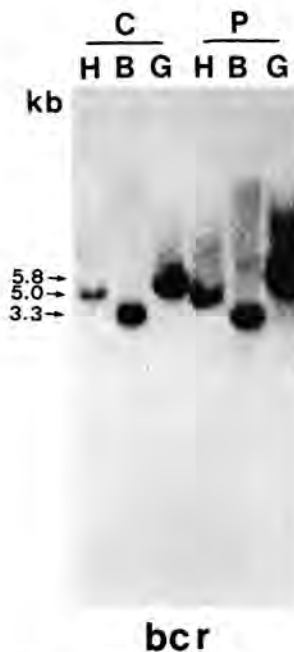


Fig. 2. Southern blot analysis of *bcr* gene rearrangements in the present patient. The restriction enzymes were *Hind*III (H), *Bam*HI (B), and *bg*/II (G). Blotting membranes were hybridized to a *bcr* universal probe (Oncogene Sciences, Mineola, NY). Lane C: DNA from a hematologically normal subject. Lane P: DNA from the patient. Bands corresponding to germline fragments are indicated by arrows. Sizes (kb) are indicated on the left.

mutation was detected in codon 13 (GGT→GTT) of the *N-RAS* gene of NIH3T3 transformant cells.

Discussion

The Philadelphia chromosome is observed in 90% of CML patients. It has been reported that

TABLE 2

Transforming gene at the time of bone marrow cell sampling

	Transforming activity ^a (positive/total tested)	Transforming gene
December 1989	0/4	—
April 1990	2/4	<i>N-RAS</i> gene ^b
Normal subjects	0/11	—

^aTransfected NIH3T3 cells were injected subcutaneously into athymic nude mice. After 80 days, the number of tumors formed was scored.

^bTransformant DNA was subjected to Southern blot analysis using the human *N-RAS* 1st exon (*Hind*III-*Hind*III) probe. The human *N-RAS* gene was detected in the transformant DNA.

5% of CML cases were *Ph*¹-/*BCR*⁻ [12] and Wiedemann et al. have suggested that these *Ph*¹-/*BCR*⁻ CML cases should be reclassified as atypical CML or chronic myelomonocytic leukemia (CMML) [12]. These investigators stated that the main hematologic features that distinguish atypical CML from typical CML are that in the former (a) some myelocytes, metamyelocytes, and neutrophils have morphological abnormalities such as hypogranularity and irregular multisegmentation; (b) basophils are either absent, or present in small percentages; (c) the percentage of monocytes is increased; and (d) the platelet count is often $< 150 \times 10^9/l$. Our present patient had mild thrombocytopenia and no basophilia, but there were no morphological abnormalities in the three cell types and no monocytosis. The present case satisfied all the above criteria for typical CML except for (d). Other criteria for *Ph*¹-/*BCR*⁻ CML, as described by Kantarjian et al. are: (a) a hypercellular marrow with granulocytic hyperplasia; (b) peripheral leukocytosis ($> 20 \times 10^9/l$) with a left maturation shift in granulocytic elements;

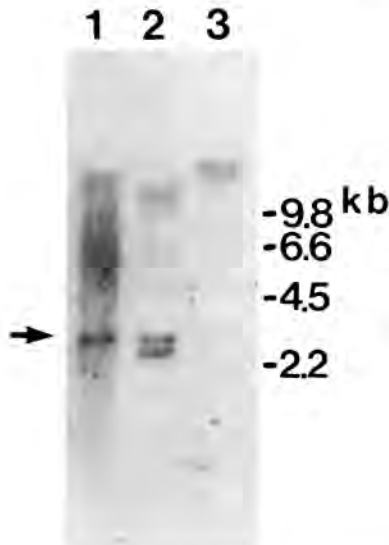


Fig. 3. Presence of the human *N-RAS* gene in DNA of nude mouse tumor. The restriction enzyme was *Pst*I. Blotting membranes were hybridized to *N-RAS* exon 1 (*Hind*III-*Hind*III fragment). Lane 1: human control. Lane 2: DNA from nude mouse tumor. Lane 3: NIH3T3 cell. Human-specific bands are indicated by an arrow. Sizes (kb) are indicated on the right.

(c) absence of the Ph^1 chromosome in cytogenetic studies; and (d) absence of *BCR* rearrangement [13]. The present case satisfied all these criteria for Ph^1 -/*BCR*⁻ CML. Interestingly, the state of pancytopenia had continued for at least one year before the leukocytosis developed. In addition, the

patient had remarkable reticulocytosis ($200\text{--}400 \times 10^9/\text{l}$) in the state of leukocytosis. These two characteristics are extremely rare events in Ph^1 -/*BCR*⁻ CML.

Taking into account the reports of Travis et al. [2] and Pugh et al. [3], the present disease might be diagnosed as UDCMPD. The criteria for a diagnosis of UDCMPD include (a) splenomegaly; (b) a leukoerythroblastic picture; (c) absence of the Ph^1 chromosome; and (d) absence of significant bone marrow fibrosis. The present case satisfied all these criteria. We diagnosed the present case as UDCMPD after taking into account the absence of morphological abnormality, although there is still the possibility that this disease was unclassifiable myelodysplastic syndrome, the criteria for which are still obscure.

Two groups of investigators have studied *RAS* gene mutations in Ph^1 -/*BCR*⁻ CML patients, using PCR, oligonucleotide hybridization, and direct sequencing [14,15]. Hirsch-Ginsberg et al. studied six patients with Ph^1 -/*BCR*⁻ CML and 30 patients with CMML for the presence of *RAS* oncogene point mutations [14]. None of the six Ph^1 -/*BCR*⁻ CML patients had mutations in the *RAS* oncogenes, while 17 (57%) of the 30 CMML patients did. These investigators suggested that *RAS* mutations appeared to be associated with CMML, but not with Ph^1 -/*BCR*⁻ chronic phase CML. Cogswell et al. found *N-RAS* point mutations in three of seven Ph^1 -/*BCR*⁻ CML cases and in both of two cases of unclassifiable myelo-

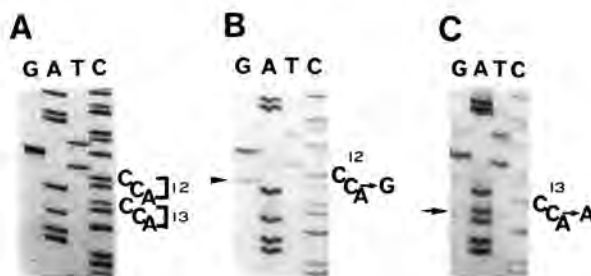


Fig. 4. Mutation analyses of codons 12 and 13 of the *N-RAS* gene at diagnosis (A), in the terminal stage (B), and in NIH3T3 transformant cells (C). The 3' and 5' primers were used for in vitro amplification, and the 3' primer was also used as the sequencing primer. (A) Direct sequence of an amplified fragment of the antisense strand at diagnosis. (B) Direct sequence of an amplified fragment of the antisense strand at the terminal stage. Lanes, from left to right, are: G, A, T and C. The mutant "G" nucleotide, indicated by an arrowhead, is present in the second nucleotide of *N-RAS* codon 12. The mutant "A" nucleotide, indicated by an arrow, is present in the second nucleotide of *N-RAS* codon 13.

proliferative syndrome (MPS) [15]. The fundamental difference between the findings of these two studies may lie in the criteria used to differentiate CMML and MPS from $\text{Ph}^1^-/\text{BCR}^-$ CML. The mutation involved in the *N-RAS* genes of each of the two MPS cases in the Cogswell et al. study was in the 12th codons; a polar amino acid (glycine) was replaced by a basic amino acid (arginine) or a polar amino acid (serine) [15]. The *N-RAS* mutation detected in our present case is a new mutation in the 12th codon: glycine was replaced by alanine, a nonpolar amino acid. In leukemia, a Gly-to-Asp substitution is the most common mutation of the *N-RAS* gene (60–80%) [16,17]. The substitution of an amino acid other than aspartic acid for glycine seems to be a minor mutation in leukemia, but a major mutation in UCMPD or MPS. The allele containing Gly-to-Ala in the present case was biologically less active than the allele containing Gly-to-Ser or Gly-to-Asp, using the in vitro NIH3T3 transformation assay [17]. Differences in amino acid substitution in the *N-RAS* gene may affect not only the capacity to transform NIH3T3 cells but also the course of leukemia progression. The present GGT→GCT mutation in codon 12 of the *N-RAS* gene may be one of the triggers which induce the clonal expansion of leukemic cells, although this mutation of the patient's DNA could not be detected at the time of admission by the PCR-direct sequencing technique [18]. The present UCMPD case also showed evidence that the normal differentiation capacity of hematopoietic cells was undisturbed by the mutated *RAS* gene. Unfortunately, we were unable to perform cytogenetic or molecular studies during the preceding pancytopenic stage in this patient. At the beginning of the leukocytosis, we were unable to find any *N-RAS* mutation or tumor formation by tumorigenicity assay, whereas we were able to detect the *N-RAS* point mutation when the disease was in the terminal stage. These time-course observations indicate that a minor *N-RAS*-activated clone grew to become a dominant clone during the process of the leukemic progression of UCMPD.

Interestingly, a codon 13 mutation substituting valine (GTT) for glycine (GGT) was detected in NIH3T3 transformant cells by the tumorigenicity

assay. Why did the tumorigenicity assay detect a mutation in codon 13 (GTT) instead of in codon 12 (GCT)? Although we are currently unable to explain why the tumorigenicity assay detected the mutation in codon 13 (GTT), one possibility is that this assay itself might lead to artifactual mutations during transfection and selection. A second possibility is that a new leukemic clone with a mutation in codon 13 had just appeared and existed as a quite minor clone in the terminal stage, and that this new leukemic clone had the capacity to transform NIH3T3 cells. Since the sensitivity of the tumorigenicity assay may be higher than that of the PCR-direct sequencing technique, the tumorigenicity assay was able to detect a mutation in codon 13 of the *N-RAS* gene [11,19]. The PCR-direct sequencing technique is capable of detecting an *N-RAS* point mutation only if this mutation is present in 10% of the cell samples [11].

The results of these molecular studies on the present UCMPD case provide a chance to elucidate the role of aberrant *N-RAS* genes in leukemogenesis. Although the frequency of *RAS* activation in $\text{Ph}^1^-/\text{BCR}^-$ CML does not seem to be high, further analysis of *RAS* activation in these cases, including UCMPD, will certainly help us to understand the role of *RAS* genes in leukemogenesis. Moreover, we speculate that such molecular markers will prove useful for a better classification of $\text{Ph}^1^-/\text{BCR}^-$ CML than can be achieved on the basis of morphology alone.

References

- 1 Groffen J, Stephenson JR, Heisterkamp N, de Klein A, Bartram CR, Grosveld G. Philadelphia chromosomal breakpoints are clustered within a limited region, bcr, on chromosome 22. *Cell* 1989;36:93–96.
- 2 Travis LB, Pierre RV, DeWald GW. Ph^1 -negative chronic granulocytic leukemia: A nonentity. *Am J Clin Pathol* 1986;85:186–193.
- 3 Pugh WC, Pearson M, Vardiman JW, Rowley JD. Philadelphia chromosome-negative chronic myelogenous leukemia: a morphological reassessment. *Br J Haematol* 1985;60:457–467.
- 4 Groupe Francais de Cytogenetique Hematologique. Cytogenetics of acutely transformed chronic myeloproliferative syndromes without a Philadelphia chromosome. *A*

- multicenter study of 55 patients. *Cancer Genet Cytogenet* 1988;32:157-168.
- 5 Groupe Francais de Cytogenetique Hematologique. Cytogenetics might elucidate the etiology of acute transformation of chronic myeloproliferative syndromes without a Philadelphia chromosome. *Eur J Haematol* 1989;43:86-87.
 - 6 Inokuchi K, Komiya I, Dan K, Kuriya S, Shinohara T, Nomura T. TdT-positive, SmIg-negative B precursor cell leukemia with Burkitt morphology: A case report. *Leukem Lymphom* 1990;2:251-255.
 - 7 Shimada T, Inokuchi K, Nienhuis AW. Site-specific demethylation and normal chromatin structure of the human dihydroforate reductase gene promoter after transfection into CHO cells. *Mol Cell Biol* 1987;7:2830-2837.
 - 8 Inokuchi K, Amuro N, Futaki M, et al. Transforming genes and chromosome aberrations in therapy-related leukemia and myelodysplastic syndrome. *Ann Hematol* 1991;62:211-216.
 - 9 Graham JF, Van der Eb AJ. A new technique for the assay of infectivity of human adenovirus 5 DNA. *Virology* 1973;52:456-467.
 - 10 Saiki RK, Gelfand DH, Stoffel S, et al. Primer-directed enzymatic amplification of DNA with a thermostable DNA polymerase. *Science* 1988;239:487-491.
 - 11 Radich JP, Kopecky KJ, Willman CL, et al. N-ras mutations in adult de novo acute myelogenous leukemia: Prevalence and clinical significance. *Blood* 1990;76:801-807.
 - 12 Wiedemann LM, Karhi KK, Shivji MKK, et al. The correlation of breakpoint cluster region rearrangement and p210 phl/abl expression with morphological analysis of Ph-negative chronic myeloid leukemia and other myeloproliferative diseases. *Blood* 1988;71:349-355.
 - 13 Kantarjian HM, Shtalrid M, Kurzrock R, et al. Significance and correlations of molecular analysis results in patients with Philadelphia chromosome-negative chronic myelogenous leukemia and chronic myelomonocytic leukemia. *Am J Med* 1988;85:639-644.
 - 14 Hirsch-Ginsberg C, LeMaistre AC, Kantarjian H, et al. Ras mutations are rare events in Philadelphia chromosome-negative/bcr gene rearrangement-negative chronic myelogenous leukemia, but are prevalent in chronic myelomonocytic leukemia. *Blood* 1990;76:1214-1219.
 - 15 Cogswell PC, Morgan R, Dunn M, et al. Mutations of the ras protooncogenes in chronic myelogenous leukemia: A high frequency of ras mutations in bcr/abl rearrangement-negative chronic myelogenous leukemia. *Blood* 1989;74:2629-2633.
 - 16 Farr CJ, Saiki RK, Erlich HA, et al. Analysis of ras gene mutations in acute myeloid leukemia by polymerase chain reaction and oligonucleotide probes. *Proc Natl Acad Sci USA* 1988;85:1629-1633.
 - 17 Neri A, Knowles DM, Greco A, et al. Analysis of ras oncogene mutations in human lymphoid malignancies. *Proc Natl Acad Sci USA* 1988;85:9268-9292.
 - 18 Hirai H, Okada M, Mizoguchi H, et al. Relationship between an activated N-ras oncogene and chromosomal abnormality during leukemic progression from myelodysplastic syndrome. *Blood* 1988;71:256-258.

RELATIONSHIP OF THE TYPE OF *BCR-ABL* HYBRID mRNA TO CLINICAL COURSE AND TRANSFORMING ACTIVITY IN PHILADELPHIA-POSITIVE CHRONIC MYELOGENOUS LEUKEMIA

MAKOTO FUTAKI, KOITI INOKUCHI, HIROKI MATSUOKA, KOICHI MIYAKE, KAZUO DAN and TAKEO NOMURA

The Third Department of Internal Medicine, Nippon Medical School, Tokyo, Japan

(Received 13 February 1992. Revision accepted 4 July 1992)

Abstract—We studied the type of *bcr-abl* mRNA for 34 patients with chronic myelogenous leukemia and analyzed for correlations among the mRNA type, the clinical outcome and the transforming activity using the tumorigenicity assay. There was no difference in the distribution of the mRNA-types (b2-a2 and b3-a2) between clinical phases. We found no correlation between the two types of *bcr-abl* mRNA and the chronic phase duration or survival. The DNA from 12 of 20 chronic phase patients and all five blastic phase patients showed transforming activity. Although there was no difference in the positive rate of transforming activity among the two mRNA-type groups, the blastic phase patients showed a tendency to have higher transforming activity.

Key words: CML, Philadelphia chromosome, *bcr-abl* mRNA, transforming activity, prognosis.

INTRODUCTION

THE Philadelphia chromosome (Ph¹), a derivative of chromosome 22 due to a t(9;22) translocation, is present in more than 90% of the patients of chronic myelogenous leukemia (CML) [1]. Ph¹ is associated with a rearrangement of the *c-abl* proto-oncogene on chromosome 9 [1–3]. The breakpoint on chromosome 22 is located within a limited region of about 5.8 kb, referred to as the breakpoint cluster region (*bcr*), comprising four small exons [4, 5]. Almost all patients have genomic breakpoints between exons b2 and b3 or between exons b3 and b4 within the *bcr* [6]. A small difference in the location of the breakpoint within the *bcr* may cause a change in the amino acid sequences of the fused protein, which in turn may affect the clinical course of CML patients.

Many authors have reported on whether the clinical course of CML patients was dependent on the location of the *bcr*-breakpoint [7–13]. Previously, we reported that the tumorigenicity assay using NIH3T3 cells was more useful than the *in vitro* transforming assay for determining the transforming activity in CML patients [14]. Thus, to obtain further information on the biological role of the *bcr-abl* fusion gene in CML, we examined the expression-type of

the *bcr-abl* chimeric mRNA in 34 CML patients and analyzed for correlations between the mRNA type, the clinical course and the transforming activity using the tumorigenicity assay.

MATERIALS AND METHODS

Patients

Thirty-four patients with Ph¹-positive CML, 29 in the chronic phase and five in the blastic phase, were studied for analysis of *bcr-abl* mRNA. Among them, 20 chronic phase patients and the five blastic phase patients were also studied for transforming activity using the tumorigenicity assay.

Cell preparation and extraction of DNA and RNA

Mononuclear cells were obtained by Ficoll-Hypaque centrifugation (Lymphoprep, Neegard, Norway) of the bone marrow of the patients and 11 normal volunteers after receiving informed consent. High molecular-weight DNA was extracted from the mononuclear cells by digesting the nuclei with proteinase K followed by phenol/chloroform extraction and ethanol precipitation [15]. The total RNA was isolated using isothiocyanate and super-centrifugation with CsCl [16].

Analysis of bcr-abl fusion mRNA by polymerase chain reaction (PCR)

The total RNA, extracted by the CsCl method, was subjected to reverse transcription and the polymerase chain reaction (RT/PCR). RT/PCR was performed using the methods described by Roth *et al.* [17], with slight modification [18]. cDNA synthesized by the reverse tran-

Correspondence to: Makoto Futaki, The Third Department of Internal Medicine, Nippon Medical School, 1-1-5, Sendagi, Bunkyo-ku, Tokyo 113, Japan.

TABLE 1. SUMMARY OF CLINICAL AND MOLECULAR CHARACTERIZATIONS AND TRANSFORMING ASSAY IN 34 CML PATIENTS

Patient No.	Age/sex	Clinical stage	Type of <i>bcr-abl</i> mRNA	Tumorigenicity assay	Detected transforming <i>ras</i> gene
1	47/F	CP	b2a2	—	—
3	65/M	CP	b2a2	+	
4	36/M	CP	b2a2	—	
7	72/M	CP	b2a2	—	
8	27/M	CP	b2a2	—	
14	32/M	CP	b2a2	+	
21	33/M	CP	b2a2	+	
26	47/F	CP	b2a2	+	
27	33/F	CP	b2a2	ND	
28	50/F	CP	b2a2	ND	
2	39/F	CP	b3a2	+	K- <i>ras</i>
11	59/M	CP	b3a2	+	
12	36/F	CP	b3a2	+	
18	58/M	CP	b3a2	—	
19	53/M	CP	b3a2	+	
22	49/F	CP	b3a2	+	
24	48/F	CP	b3a2	—	
30	34/M	CP	b3a2	ND	
32	71/M	CP	b3a2	ND	
33	41/F	CP	b3a2	ND	
34	46/M	CP	b3a2	ND	N- <i>ras</i>
6	36/M	CP	b2a2, b3a2	+	
9	41/F	CP	b2a2, b3a2	—	
15	39/F	CP	b2a2, b3a2	+	
23	53/M	CP	b2a2, b3a2	+	
29	25/F	CP	b2a2, b3a2	ND	
31	86/F	CP	b3a2, b2a2	ND	
35	64/F	CP	b2a2, b3a2	ND	
10	54/F	CP	—	—	
13	47/F	BP	b2a2	+	
16	39/F	BP	b2a2	+	—
17	46/M	BP	b3a2	+	—
20	53/M	BP	b3a2	+	—
25	64/F	BP	b2a2, b3a2	+	—

ND, not done; CP, chronic phase; BP, blastic phase; +, positive; —, negative.

scriptase was used for the PCR analysis. PCR of 40 cycles was performed, consisting of 30 s at 94°C (denaturation), 30 s at 55°C (annealing), and 1 min at 72°C (extension). The PCR products were phenol-extracted, ethanol-precipitated and electrophoresed through a 2% agarose gel. The gels were photographed, and the amplified DNA was transferred on to a nylon filter and hybridized to ³²P-labeled oligomers corresponding to a part of the *bcr* exon 2. The amplimers and oligonucleotide probes used for this study were synthesized with an Applied Biosystems DNA synthesizer. The sequences of the oligomers are:

abl-RT (antisense strand):

5'-AACGAAAAGGTTGGGGTC-3'

bcr-1 (coding strand):

5'-AGCATGGCCTTCAGGGTGACAGCCGCAACGGCAA-3'

abl-1 (antisense strand):

5'-TCACTGGGTCCAGCGAGAAGGTTTTCCTTGAGATT-3'

Two fragments are originated by the use of these amplimers. The fragment of 392 bp shows a junction between *bcr* exon 3 and *abl* exon II (b3-a2 type of *bcr-abl* mRNA),

while the fragment of 317 bp indicates a junction between *bcr* exon 2 and *abl* exon II (b2-a2 type of *bcr-abl* mRNA).

Tumorigenicity assay using nude mice

The tumorigenicity assay was performed by a modification of the technique of Fasano *et al.* [14, 19, 20]. In brief, co-transfection of NIH3T3 cells with genomic DNA (60 µg) and the plasmid pSV2Neo (4 µg), which contains a dominant neomycin resistance-selectable marker, was performed by the standard CaPO₄ coprecipitation method. After G418 selection for 14–21 days, G418-resistant colonies were harvested and removed from the plates by trypsinization. Five million cells were resuspended in 0.5 ml of cold medium. This suspension was then injected into subcutaneous sites of athymic nude mice. Tumors which arose 20 ~ 30 days after the inoculation of the NIH3T3 cells transfected with DNA were analyzed. Tumors detected in the tumorigenicity assay were subjected to Southern-blotting for the presence of human repetitive sequences using the probe Blur-8, representative of human *Alu*

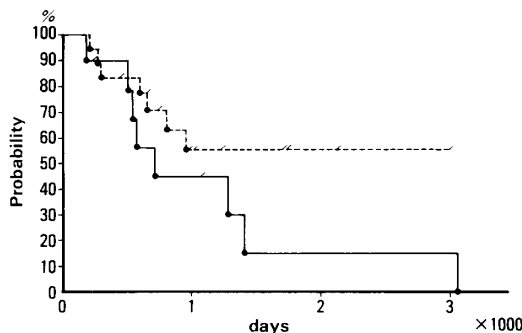


FIG. 1. Kaplan-Meier curves for chronic phase duration in CML patients expressing only b2-a2 type mRNA (—) and b3-a2 type mRNA (·····).

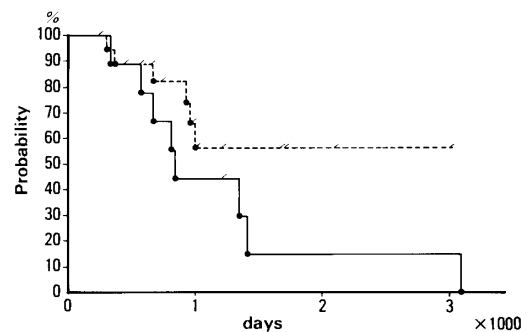


FIG. 2. Kaplan-Meier curves for survival in CML patients expressing only b2-a2 type mRNA (—) and b3-a2 type mRNA (·····).

sequences. The result carrying human *Alu* sequences indicates positive transforming activity. We also analyzed the transformant DNA using the probes for the *ras* family [14].

Statistical analysis

The chronic phase duration and the survival time of the patients with the two types of *bcr-abl* mRNA were compared by computerized Kaplan-Meier life-table analysis, followed by Mantel-Cox analysis to test for significance. The significance of differences in the distribution of the clinical phase and the positivity of the transforming activity between two mRNA types was assessed by the chi-square test. The probability of a significant difference in the transforming activity between two clinical phase groups was determined by the same test.

RESULTS

Expression type of *bcr-abl* chimeric mRNA

The expression type of *bcr-abl* mRNA was analyzed by the RT/PCR method in 29 chronic phase patients and the five blastic phase patients. The *bcr-abl* mRNAs were detected in 33 patients (Table 1). In one patient (No. 10), no message was found. The RT/PCR analysis revealed the presence of b2-a2 mRNA (*bcr* exon 2 and *abl* exon II junction) in 12 cases, and b3-a2 mRNA (*bcr* exon 3-*abl* II junction) in 13 cases, and co-expression of both types of mRNA in eight cases. There was no difference in the distribution of the three types of mRNA expression between the chronic phase and blastic phase patients.

Relationship between the type of *bcr-abl* mRNA and clinical course

The median duration of the chronic phase and the survival time were calculated to be 32.9 months and 34.9 months, respectively. The relationships between the type of *bcr-abl* mRNA and the clinical course in 28 chronic phase patients are shown in Figs 1 and 2. The mean duration of the chronic phase and the

survival time showed no significant differences between the patients expressing only b2-a2 type mRNA and the patients expressing b3-a2 type mRNA.

Correlation between the type of *bcr-abl* mRNA and transforming activity

The results of the tumorigenicity assay are shown in Table 1. Eleven normal human cellular DNAs did not form tumors. The DNA from bone marrow cells from the patients showed positive transforming activity in 12 of 20 cases of CML in the chronic phase, and in all five blastic phase cases. The transformed NIH3T3 cells detected in the tumorigenicity assay were analyzed by Southern-blotting for the presence of human repetitive sequences using the probe Blur-8, representative of human *Alu* sequences. All of them carried human *Alu* sequences (data not shown). Six of 10 patients expressing b2-a2 mRNA were positive for transforming activity, while 11 of 14 patients expressing b3-a2 mRNA were positive. No significant correlation was detected between the transforming activity and the type of *bcr-abl* mRNA. On the other hand, the blastic phase patients showed a high incidence of transforming activity (100%) compared with the chronic phase patients (60%), although the difference was not statistically significant. *N-ras* activation was found in one chronic phase sample and *K-ras* activation in another chronic phase sample among the 17 transformants.

DISCUSSION

Previous studies indicated that the *bcr-abl* fusion gene gives rise to a chimeric tyrosine protein kinase with transforming potential [21-24]. Since the contribution of *bcr* exon 3 to the chimeric protein is variable, the question has arisen as to whether the

existence of exon b3 of *bcr* in *bcr-abl* mRNA might influence the clinical course of CML. In previous studies, conflicting results regarding this point have been reported at the DNA level [7–13]. Schaefer-Rego *et al.* [7] suggested that there might be a correlation between the 3' breakpoint and blastic crisis. Eisenberg *et al.* [8] reported a significant excess of patients with a 3' breakpoint already in transformation compared with patients still in the chronic phase. Mills *et al.* [9] suggested a correlation between the site of the breakpoint and the length of the chronic phase. They showed that patients with a 5' breakpoint had a longer chronic phase. On the other hand, some authors reported no significant differences in the chronic phase duration or survival time among patients with the breakpoint site within the *bcr* gene [10–13]. RNA analysis using a PCR-based technique has been developed. Two distinct types of mRNA (b2–a2 and b3–a2) encoded in the *bcr-abl* fusion gene can now be detected by the technique. Few reports have discussed a correlation between the type of mRNA and the disease phase or the duration of chronic phase with conflicting results [25–27]. This relationship thus remains controversial and unclear. Our present study using the RT/PCR method failed to demonstrate a correlation between the type of transcripts and the duration of the chronic phase or survival.

One or both of two types of *bcr-abl* mRNA, one with *bcr* exon 3 sequences and the other without, exist in the cells of CML patients [17, 25–27]. These two mRNAs encode proteins differing by 25 amino acids encoded in exon 3 [6]. The small difference in the fused proteins may directly or indirectly affect the transforming activity. We studied the transforming activity using the tumorigenicity assay and analyzed its relationship with the two types of *bcr-abl* mRNA. In the present study, although, transforming activity was detected in 17 of 25 cases, it did not correlate with the subtype of *bcr-abl* mRNA. Thus, our transformation results may be irrelevant to the splicing type.

In previous studies using the NIH3T3 transfection assay, human cellular transforming genes were detected in tumors by their ability to induce the transformation of NIH3T3 cells [28]. The tumorigenicity assay using NIH3T3 cells based on gene transfer and tumorigenesis was sensitive for detecting activated transforming genes [20]. Most detected transforming genes in human hematopoietic malignancies are related to the *ras* family [29]. Although recent studies using the polymerase chain reaction and synthetic oligonucleotide probes for acute myeloid leukemia and myelodysplastic syndrome patients indicate that approximately 20–40% have

mutated *ras* genes [30–32], their incidence in chronic myelogenous leukemia has ranged widely in a variety of patients studied, with most of the mutations found in blastic phase [33–35]. In our earlier study using the tumorigenicity assay, N-*ras* and K-*ras* oncogene activations were detected in two of 14 chronic phase patients of chronic myelogenous leukemia, but no *ras* activation could be detected in either of two blastic phase patients [14]. Although activation of the *ras* gene family was detected in the present study in only two of 17 cases as shown in Table 1, a higher incidence of transforming activity was found in the DNA of the blastic phase patients than the chronic phase patients. There might be a possibility that activation of an additional unknown oncogene cooperates with the *bcr-abl* gene in the more aggressive stage. Liu *et al.* reported that an unidentified transforming gene is detected in a CML case using the same assay system as ours [33]. Little is known about CML evolution from a chronic to a more advanced stage at the molecular level. More detailed information on the chimeric *bcr-abl* mRNA and the determination of the oncogenic activities of the proteins they encode are necessary to elucidate the pathogenesis of CML.

REFERENCES

1. Rowley J. D. (1973) A new consistent abnormality in chronic myelogenous leukaemia identified by quinacrine fluorescence and giemsa staining. *Nature* **243**, 290.
2. De Klein A., van Kessel A. G., Grosveld G., Bartram C. R., Hagemeijer A., Bootsma D., Spur N. K., Heisterkamp N., Groffen J. & Stephenson J. R. (1982) A cellular oncogene is translocated to the Philadelphia chromosome in chronic myelogenous leukaemia. *Nature* **300**, 765.
3. Heisterkamp N., Stephenson J. R., Groffen J., Hansen P. F., de Klein A., van Kessel A. G., Bartram C. R. & Grosveld G. (1983) Localization of the *c-abl* oncogene adjacent to a translocation breakpoint in chronic myelocytic leukaemia. *Nature* **306**, 239.
4. Groffen J., Stephenson J. R., Heisterkamp N., de Klein A., Bartram C. R. & Grosveld G. (1984) Philadelphia chromosomal breakpoints are clustered within a limited region, *bcr*, on chromosome 22. *Cell* **36**, 93.
5. Heisterkamp N., Stam K., Groffen J., de Klein A. & Grosveld G. (1985) Structural organization of the *bcr* gene and its role in the Ph¹ translocation. *Nature* **316**, 758.
6. Shtivelman E., Lifshitz B., Gale R. P. & Canaani E. (1985) Fused transcripts of *abl* and *bcr* genes in chronic myelogenous leukemia. *Nature* **315**, 550.
7. Schaefer-Rego K., Dudek H., Popenoe D., Arlin Z., Mears J. G., Bank A. & Leibowitz D. (1987) CML patients in blastic crisis have breakpoints localized to a specific region of the *BCR*. *Blood* **70**, 448.
8. Eisenberg A., Silver R., Soper L., Arlin Z., Coleman M., Bernhardt B. & Bann P. (1988) The location of

- breakpoints within the breakpoint cluster region (*bcr*) of chromosome 22 in chronic myeloid leukemia. *Leukemia* **2**, 642.
9. Mills K. I., Mackenzie E. D. & Birnie G. D. (1988) The site of the breakpoint within the *bcr* is a prognostic factor in Philadelphia-positive CML patients. *Blood* **72**, 1237.
 10. Shtalrid M., Talpaz M., Kurzrock R., Kantarjian H., Trujillo J., Gutterman J., Yoffe G. & Blick M. (1988) Analysis of breakpoints within the *bcr* gene and their correlation with the clinical course of Philadelphia-positive chronic myelogenous leukemia. *Blood* **72**, 485.
 11. Jaubert J., Martiat P., Dowding C., Ifrah N. & Goldman J. M. (1990) The position on the M-BCR breakpoint does not predict the duration of chronic phase or survival in chronic myeloid leukaemia. *Br. J. Haemat.* **74**, 30.
 12. Morris S. W., Daniel L., Ahmed C. M. I., Elias A. & Lebowitz P. (1990) Relationship of *bcr* breakpoint to chronic phase duration, survival, and blastic crisis lineage in chronic myelogenous leukemia patients presenting in early chronic phase. *Blood* **75**, 2035.
 13. Inokuchi K., Futaki M., Yamada T., Tanabe Y., Dan K., Shinohara T., Kuriya S. & Nomura T. (1991) The relationship between the site of breakpoints within the *bcr* gene and thrombopoiesis of Philadelphia-positive chronic myelocytic leukemia. *Leukemia Res.* **15**, 1067.
 14. Futaki M., Inokuchi K., Dan K. & Nomura T. (1991) Activation of *bcr-abl* fusion gene and *ras* oncogenes in chronic myelogenous leukemia. *Leukemia and Lymphoma* **5**, 163.
 15. Inokuchi K., Komiya I., Dan K., Kuriya S., Shinohara T. & Nomura T. (1990) TdT-positive, SmIg-negative B precursor cell leukemia with Burkitt morphology: a case report. *Leukemia and Lymphoma* **2**, 251.
 16. Chirgwin J. M., Przybyla A. E., MacDonald R. J. & Rutter W. J. (1979) Isolation of biologically active ribonucleic acid from sources enriched in ribonuclease. *Biochemistry* **18**, 5294.
 17. Roth M. S., Antin J. H., Bingham E. L. & Ginsburg D. (1989) Detection of Philadelphia chromosome-positive cells by polymerase chain reaction following bone marrow transplant for chronic myelogenous leukemia. *Blood* **74**, 882.
 18. Inokuchi K., Inoue T., Tojo A., Futaki M., Miyake K., Yamada T., Tanabe Y., Ohki I., Dan K., Ozawa K., Asano S. & Nomura T. (1991) A possible correlation between the type of *bcr-abl* hybrid messenger RNA and platelet count in Philadelphia-positive chronic myelogenous leukemia. *Blood* **78**, 3125.
 19. Inokuchi K., Amuro N., Futaki M., Dan K., Shinohara T., Kuriya S., Okazaki T. & Nomura T. (1991) Transforming genes and chromosome aberrations in therapy-related leukemia and myelodysplastic syndrome. *Ann. Hemat.* **62**, 211.
 20. Fasano O., Birnbaum D., Edlund L., Fogh J. & Wigler M. (1984) New human transforming genes detected by a tumorigenicity assay. *Mol. Cell. Biol.* **4**, 1695.
 21. MacLaughlin J., Chianese E. & Witte O. N. (1987) *In vitro* transformation of immature hematopoietic cells by the P210 BCR-ABL oncogene product of the Philadelphia chromosome. *Proc. natn. Acad. Sci. U.S.A.* **84**, 6558.
 22. Daley G. Q. & Baltimore D. (1988) Transformation of an interleukin 3-dependent hematopoietic cell line by the chronic myelogenous leukemia-specific P210^{bcr/abl} protein. *Proc. natn. Acad. Sci. U.S.A.* **85**, 9312.
 23. Lugo T. G. & Witte O. N. (1989) The BCR-ABL oncogene transforms Rat-1 cells and cooperates with v-myc. *Mol. Cell. Biol.* **9**, 1263.
 24. Daley G. Q., van Etten R. A. & Baltimore D. (1990) Induction of chronic myelogenous leukemia in mice by the P210^{bcr/abl} gene of the Philadelphia chromosome. *Science* **247**, 824.
 25. Morgan G. J., Hernandez A., Chan L. C., Hughes T., Martiat P. & Wiedemann L. M. (1990) The role of alternative splicing patterns of BCR/ABL transcripts in the generation of the blast crisis of chronic myeloid leukaemia. *Br. J. Haemat.* **76**, 33.
 26. Marcelle C., Gale R. P., Prokocimer M., Berrebi A., Merle-Beral H. & Canaani E. (1989) Analysis of BCR-ABL mRNA in chronic myelogenous leukemia patients and identification of a new BCR-related sequence in human DNA. *Gene Chrom. Cancer* **1**, 172.
 27. Mills K. I., Sproul A. M., Leibowitz D. & Burnett A. K. (1991) Mapping of breakpoints, and relationship to BCR-ABL RNA expression, in Philadelphia-chromosome-positive chronic myeloid leukaemia patients with a breakpoint around Exon 14 (b3) of the BCR gene. *Leukemia* **5**, 937.
 28. Krontiris T. G. & Cooper G. M. (1981) Transforming activity of human tumor DNAs. *Proc. natn. Acad. Sci. U.S.A.* **78**, 1181.
 29. Hirai H., Tanaka S., Azuma M., Anraku Y., Kobayashi Y., Fujisawa M., Okabe T., Urabe A. & Takaku F. (1985) Transforming genes in human leukemia cells. *Blood* **66**, 1371.
 30. Bos J. L., Vries M. V., van der Eb A. J., Janssen J. W. G., Delwel R., Lowenberg B. & Colly L. P. (1987) Mutation in N-ras predominate in acute myeloid leukemia. *Blood* **69**, 1237.
 31. Farr C. J., Saiki R. K., Erlich H. A., McCormick F. & Marshall C. J. (1988) Analysis of *ras* gene mutations in acute myeloid leukemia by polymerase chain reaction and oligonucleotide probes. *Proc. natn. Acad. Sci. U.S.A.* **85**, 1629.
 32. Hirai H., Kobayashi Y., Mano H., Hagiwara K., Maru W., Omine M., Mizoguchi H., Mishizima J. & Takaku F. (1987) A point mutation at codon 13 of the N-ras oncogene in myelodysplastic syndrome. *Nature* **327**, 430.
 33. Liu E., Hjelle B. & Bishop J. M. (1988) Transforming genes in chronic myelogenous leukemia. *Proc. natn. Acad. Sci. U.S.A.* **85**, 1952.
 34. Janssen J. W. G., Steenvorden A. C. M., Lyons J., Anger B., Bohlke J. U., Bos J. L., Seliger H. & Bartram C. R. (1987) *Ras* gene mutations in acute and chronic myelocytic leukemias, chronic myeloproliferative disorders and myelodysplastic syndromes. *Proc. natn. Acad. Sci. U.S.A.* **84**, 9228.
 35. Collins S. J., Howard M., Andrews D. F., Agura E. & Radich J. (1989) Rare occurrence of N-ras point mutations in Philadelphia chromosome positive chronic myeloid leukemia. *Blood* **73**, 1028.

EXPRESSION OF THE DCC GENE IN MYELODYSPLASTIC SYNDROMES AND OVERT LEUKEMIA

KOICHI MIYAKE, KOITI INOKUCHI, KAZUO DAN and TAKEO NOMURA

Third Department of Internal Medicine, Nippon Medical School, Tokyo, Japan

(Received 26 February 1993. Revision accepted 4 May 1993)

Abstract—To evaluate the molecular events in the genome that are associated with myelodysplastic syndromes (MDS) and the development of leukemia, we investigated the expression of the deleted in colorectal carcinoma (DCC) gene by the reverse transcriptase-polymerase chain reaction (RT-PCR) method in 24 MDS cases and in 7 overt leukemia cases that progressed from MDS. Expression of the DCC gene was absent or extremely reduced in 2 of the 24 MDS cases, and those 2 cases developed overt leukemia within 6 months. Moreover, in 5 of the 7 cases of overt leukemia that developed from MDS, expression of the DCC gene was absent or extremely reduced. These findings suggest that inactivation of the DCC gene may be the late event that triggers the progression of MDS to leukemia.

Key words: DCC gene, tumor suppressor gene, myelodysplastic syndromes, overt leukemia, leukemogenesis.

INTRODUCTION

THE MYELODYSPLASTIC syndromes (MDS) represent a preleukemic condition and comprise a group of acquired clonal disorders of hematopoietic stem cells. About 30% of MDS cases develop acute myelogenous leukemia (AML) [1]. These distinctive preleukemic and leukemic stages are an important model for analyzing the molecular mechanism of leukemogenesis. Mutations of *ras* family genes [2-7], *c-fms* gene [8, 9] and *p53* gene [10] have been detected in some MDS cases, and these genetic alterations are thought to contribute to the development or progression of MDS. However, the molecular mechanisms of the development and progression of MDS remain largely unclear.

The deleted in colorectal carcinoma (DCC) gene, located in the chromosome 18q21.3 region, was identified as a candidate tumor suppressor gene in

colorectal carcinoma [11]. While the DCC gene was expressed in almost all normal tissues, its expression was greatly reduced or absent in 88% (15 of 17) of colorectal carcinoma cell lines [11], 81% (13 of 16) of invasive colorectal carcinomas [12], 73% (8 of 11) of pancreatic carcinoma cell lines and 50% (4 of 8) of ductal pancreatic adenocarcinomas [13]. These findings suggest that inactivation of the DCC gene is involved not only in colorectal carcinoma but also in pancreatic carcinoma. There is also a possibility that inactivation of the DCC gene is involved in other human malignancies, including MDS and leukemia. To evaluate the role of the DCC gene in leukemogenesis, we analyzed expression of the DCC gene in 24 MDS cases and seven cases of overt leukemia progressed from MDS.

MATERIALS AND METHODS

Patients

Twenty-four MDS cases, including 7 with refractory anemia (RA), 2 with RA with ring sideroblasts (RARS), 6 with RA with excess of blasts (RAEB), 7 with RAEB in transformation (RAEB-t) and two with chronic myelomonocytic leukemia (CMML), as well as 7 cases with overt leukemia progressed from MDS were investigated. Diagnosis was made according to the French-American-British (FAB) classification [14]. Twenty-two healthy volunteers were also investigated after obtaining informed consent.

Cell preparation and extraction of RNA

Mononuclear cells were obtained by Ficoll-Hypaque centrifugation (Lymphoprep, Norgard, Norway) of the bone

Abbreviations: DCC, deleted in colorectal carcinoma; AML, acute myelogenous leukemia; MDS, myelodysplastic syndromes; RA, refractory anemia; RARS, refractory anemia with ring sideroblasts; RAEB, refractory anemia with excess of blasts; RAEB-t, refractory anemia with excess of blasts in transformation; CMML, chronic myelomonocytic leukemia; FAB, French-American-British; RT-PCR, reverse transcriptase-polymerase chain reaction; cDNA, complementary DNA.

Correspondence to: Koichi Miyake, M.D., The Third Department of Internal Medicine, Nippon Medical School, 1-1-5 Sendagi, Bunkyo-ku, Tokyo 113, Japan (Tel: (03) 3822-2131; Fax: (03) 5685-1793).

TABLE 1. EXPRESSION OF THE DCC GENE IN MDS AND OVERT LEUKEMIA PROGRESSED FROM MDS

Diagnosis	No. of cases examined	No. of cases with reduced or absent expression
MDS	24	2
RA	7	0
RARS	2	0
RAEB*	6	1
RAEB-t*	7	1
CMML	2	0
Overt leukemia*	7	5
Normal control†	22	0

* 2 of the 6 RAEB cases, 2 of the 7 RAEB-t cases and 4 of the 6 overt leukemia cases are shown in Table 2.

† Bone marrow samples of normal healthy volunteers were examined.

marrow of the patients and 22 normal volunteers. The total RNA was extracted by the CsCl method [15]. The integrity of the RNA samples was determined by formaldehyde-agarose gel electrophoresis, and degraded RNA samples were rejected.

Analysis of DCC expression by reverse transcriptase-polymerase chain reaction (RT-PCR)

RT-PCR was performed using a Gene Amp RNA PCR kit (Perkin-Elmer Cetus, Norwalk, CT) according to the instructions of the manufacturer. cDNA was synthesized with 1 µg of total RNA using a 3'-primer, DCC 2. PCR was performed with 20 µl of cDNA reaction mixture by using each oligonucleotide primer (DCC 1 and DCC 2). Amplifications were performed in an automated thermocycler for 35 cycles consisting of 1 min at 95°C

(denaturation), 1 min at 60°C (annealing), and a final elongation at 60°C for 7 min. After amplification, 10 µl of the PCR products were electrophoresed through a 4% NuSieve 3:1 (FMC Corp., Rockland, ME) agarose gel. The PCR products were visualized directly in ethidium bromide-stained gels, photographed and transferred onto Gene Screen Plus membranes (New England Nuclear, Boston, MA). Hybridization was performed according to the protocol provided by New England Nuclear, as described previously [16]. The filters were hybridized with ³²P-labeled DCC cDNA probe (pDCC1.65) [11], which consisted of nucleotides 591–2250 of the cDNA (provided by Dr B. Vogelstein, John Hopkins Oncology Center), and then visualized on autoradiograms. To demonstrate the intactness of the RNA, we examined the expression of β-actin mRNA [17] as a control using oligonucleotide primers (actin 1 and actin 2) by the same RT-PCR method, except that 20 cycles were run. The sequences of the oligomers were as follows:

DCC 1: 5'-TTCCGCCATGGTTTTTAAATCA-3' (sense strand)

DCC 2: 5'-AGCCTCATTTTCAGCCACACA-3' (antisense strand) [11]

actin 1: 5'-AACGGCTCCGGCATGTGCAA-3' (sense strand)

actin 2: 5'-CTTCTGACCCATGCCACCA-3' (antisense strand) [17].

RESULTS

We examined the expression of the DCC gene in the 24 MDS cases and the 7 overt leukemia cases progressed from MDS. While we found normal expression of the DCC gene in all of the normal control samples, expression of the DCC gene was



FIG. 1. RT-PCR analysis of DCC expression in 4 patients at the time of MDS and after progression to overt leukemia. The case numbers of the samples are the same as those in Table 2. Bone marrow samples from healthy volunteers were examined as the normal controls. To demonstrate the intactness of the RNA, expression of the β-actin gene was also examined.

TABLE 2. CHARACTERISTICS OF 4 PATIENTS AT THE TIME OF MDS AND AFTER PROGRESSION TO OVERT LEUKEMIA

Case no.	Age/sex	Diagnosis	Disease duration (mo)	Peripheral blood				BM blast (%)	Karyotype	Expression of DCC gene
				WBC (/ μ l)	Hb (g/dl)	Platelet ($\times 10^4$ / μ l)	blast (%)			
1	59/F	RAEB-t AML	2	2100	11.0	10.2	6	21.0	46, XX	Normal
			8	1800	6.9	0.5	33	79.6	46, XX, 10q-, 10q+, 11q-, +mar	Absent
2	66/F	RAEB-t AML	3	6200	8.1	7.7	2	22.4	46, XX	Normal
			34	137,000	5.3	3.0	79	77.4	46, XX, inv(9p+q-)	Reduced
3	42/M	RAEB AML	1	13,100	8.2	3.7	2	11.6	46, XY, t(6p-;9q+)	Absent
			3	8500	7.5	1.5	1	42.6	46, XY, t(6p-;9q+)	Absent
4	59/M	RAEB AML	2	6300	8.4	15.4	1	18.4	Not done	Normal
			5	5700	7.1	2.8	5	34.0	45, XY, 5q-, 7q-, 11q+, 12P-, -21, -22, +mar	Absent

absent or extremely reduced in 2 of the 24 MDS cases, and those two cases developed overt leukemia within 6 months. Moreover, in 5 of the 7 cases of overt leukemia which had progressed from MDS, expression of the DCC gene was absent or extremely reduced. These results are compiled in Table 1.

In this study, 4 patients were able to be examined in both the MDS stage and the overt leukemia stage. The first case was a 59-year-old woman with 21% blasts in the bone marrow and normal expression of the DCC gene at diagnosis. Six months later, when she developed overt leukemia, expression of the DCC gene had vanished (Fig. 1, Case 1). The second case was a 66-year-old woman with 22.4% blasts in the bone marrow with normal DCC expression at diagnosis. When she developed overt leukemia from RAEB-t 31 months later, expression of the DCC gene was found to be extremely reduced (Fig. 1, Case 2). The third case was a 42-year-old man with 11.6% blasts in the bone marrow at diagnosis, and expression of the DCC gene was almost all absent since the time of the RAEB stage (Fig. 1, Case 3). The fourth case was a 59-year-old man with 18.4% blasts in the bone marrow and normal DCC expression. Only 3 months later, when his disease progressed to overt leukemia, expression of the DCC gene had vanished (Fig. 1, Case 4). The characteristics of these 4 patients are presented in Table 2.

DISCUSSION

The molecular mechanism of leukemogenesis has been thought to be based on a multiple-step process [18], such as activation of oncogenes and inactivation of tumor suppressor genes. It has been reported that activation of the *N-ras*, *K-ras* and *H-ras* genes plays a role in the pathogenesis of some cases of MDS [2-7]. Recently, mutation of the *c-fms* gene in codon

301 or 969 was reported in 9 of 67 MDS cases [8] and in 6 of 33 MDS cases [9], and a mutated *p53* gene was also reported in 5 of 151 cases of MDS [10]. However, the molecular mechanisms of the development and progression of MDS remain unclear. We examined the expression of the DCC gene in 24 MDS cases and 7 cases of overt leukemia progressed from MDS. Expression of the DCC gene was extremely reduced or absent in 2 of the 24 MDS cases. One patient was in the RAEB stage, and the other case was in the RAEB-t stage. Moreover those two patients progressed to overt leukemia within 6 months. In overt leukemia, expression of the DCC gene was extremely reduced or absent in 5 of the 7 cases. These findings suggest that inactivation of the DCC gene is a late event in the progression to overt leukemia and contributes to leukemogenesis in some MDS cases.

A part of the DCC gene sequence was identified by Fearon *et al.* in 1990 [11]. However, even now, full-length cDNA is unknown. The predicted amino acid sequence of DCC shows homology with neural cell adhesion molecules and other related cell surface glycoproteins [11], but the detailed function of the DCC protein is also unclear. Recently, Tanaka *et al.* reported that introduction of chromosome 18 into a human colorectal cell line, COK Fu, suppressed its tumorigenicity [19], and Narayanan *et al.* demonstrated the first direct biological evidence of a possible role of DCC protein by the antisense RNA method [20]. These reports suggest that the DCC gene plays a role as a tumor suppressor gene in tumorigenesis.

The mechanisms of absent or reduced DCC expression are unclear. In colorectal carcinoma, allelic deletions were detected in 71% and somatic mutations in 13% of colorectal carcinoma specimens analyzed [11]. In order to examine the structural

abnormalities in the DCC gene, we performed Southern blot analysis using a pDCC1.65 cDNA probe in 24 MDS cases and in 7 overt leukemia cases that progressed from MDS. However, no definitive rearrangements or deletions were observed (data not shown). Thus, it is necessary to conduct a detailed study such as of point mutations in the DCC gene.

To conclude, our findings of absent or reduced DCC expression in 2 of 24 MDS cases and 5 of the 7 overt leukemia cases suggested that the DCC gene plays an important role in the leukemogenesis of MDS as a tumor suppressor gene. It will be necessary to study a large number of cases and the details of the mechanism of inactivation of the DCC gene in order to elucidate the molecular mechanisms of the leukemogenesis of MDS.

Acknowledgements—We thank Dr Bert Vogelstein for kindly providing the pDCC1.65 probe and Dr Tamiko Shinohara for performing the chromosome analyses.

REFERENCES

- Koeffler H. P. (1986) Myelodysplastic syndromes (pre-leukemia). *Semin. Hemat.* **23**, 284.
- Hirai H., Kobayashi Y., Mano H., Hagiwara K., Maru Y., Omine M., Mizoguchi H., Nishida J. & Takaku F. (1987) A point mutation at codon 13 of the *N-ras* oncogene in myelodysplastic syndrome. *Nature* **327**, 430.
- Liu E., Hjelle B., Morgan R., Hecht F. & Bishop J. M. (1987) Mutations of *Kirsten-ras* proto-oncogene in human preleukemia. *Nature* **300**, 186.
- Janssen J. W. G., Steenvoorden A. C. M., Lyons J., Anger B., Bohlke J. U., Bos J. L., Seliger H. & Bartram C. R. (1987) *Ras* gene mutation in acute and chronic myelocytic leukemias, chronic myeloproliferative disorders, and myelodysplastic syndromes. *Proc. natn. Acad. Sci. U.S.A.* **84**, 9228.
- Lyons J., Janssen J. W. G., Bartram C., Layton M. & Mufti G. J. (1988) Mutation of *Ki-ras* and *N-ras* oncogene in myelodysplastic syndromes. *Blood* **71**, 1707.
- Padua R. A., Carter G., Hughes D., Gow J., Farr C., Oscier D., McCormick F. & Jacobs A. (1988) *Ras* mutations in myelodysplasia detected by amplification, oligonucleotide hybridization, and transformation. *Leukemia* **2**, 503.
- Yunis J. J., Boot A. J. M., Mayer M. G. & Bos J. L. (1989) Mechanisms of *ras* mutation in myelodysplastic syndrome. *Oncogene* **4**, 609.
- Ridge S. A., Worwood M., Oscier D., Jacobs A. & Padua R. A. (1990) FMS mutations in myelodysplastic, leukemic, and normal subjects. *Proc. natn. Acad. Sci. U.S.A.* **87**, 1377.
- Tobal K., Pagliuca A., Bhatt B., Bailey N., Layton D. M. & Mufti G. J. (1990) Mutation of the FMS gene (M-CSF receptor) in myelodysplastic syndromes and acute myeloid leukemia. *Leukemia* **4**, 486.
- Jonveaux Ph., Fenaux P., Quiquandon I., Pignon J. M., Lai J. L., Loucheux-Lefebvre M. H., Goossens M., Bauters F. & Berger R. (1991) Mutations in the *p53* gene in myelodysplastic syndromes. *Oncogene* **6**, 2243.
- Fearon E. R., Cho K. R., Nigro J. M., Kern S. E., Simons J. W., Ruppert J. M., Hamilton S. R., Preisinger A. C., Thomas G., Kinzler K. W. & Vogelstein B. (1990) Identification of chromosome 18q gene that is altered in colorectal cancers. *Science* **247**, 49.
- Kikuchi-Yanoshita R., Konishi M., Fukunari H., Tanaka K. & Miyaki M. (1992) Loss of expression of the DCC gene during progression of colorectal carcinomas in familial adenomatous polyposis and non-familial adenomatous polyposis patients. *Cancer Res.* **52**, 3801.
- Hohne M. W., Halatsh M-E., Kahl G. F. & Weinert R. J. (1992) Frequent loss of expression of the potential tumor suppressor gene DCC in ductal pancreatic adenocarcinoma. *Cancer Res.* **52**, 2616.
- Bennet J. M., Catovsky D., Daniel M. T., Flandrin G., Galton D. A. G., Gralnick H. R. & Sultan C. (1982) The French-American-British (FAB) cooperative group. Proposal for the classification of the myelodysplastic syndromes. *Br. J. Haemat.* **51**, 189.
- Chirgwin J. M., Przybyla A. E., MacDonald R. J. & Rutter W. J. (1979) Isolation of biologically active ribonucleic acid from sources enriched in ribonuclease. *Biochemistry* **18**, 5294.
- Inokuchi K., Futaki M., Yamada T., Tanabe Y., Dan K. & Nomura T. (1991) The relationship between the site of breakpoints within the BCR gene and thrombopoiesis of Philadelphia-positive chronic myelocytic leukemia. *Leukemia Res.* **15**, 1067.
- Nakajima-Iijima S., Hamada H., Reddy P. & Kaku-naga T. (1985) Molecular structure of the human cytoplasmic β -actin gene: interspecies homology of sequences in the introns. *Proc. natn. Acad. Sci. U.S.A.* **82**, 6133.
- Weinberg R. A. (1989) Oncogene, antioncogene, and molecular bases of multistep carcinogenesis. *Cancer Res.* **49**, 3713.
- Tanaka K., Oshimura M., Kikuchi R., Seki M., Hayashi T. & Miyaki M. (1991) Suppression of tumorigenicity in human colon carcinoma cells by introduction of normal chromosome 5 or 18. *Nature* **349**, 340.
- Narayanan R., Lawlor K. G., Schaapveld R. O. J., Cho K. R., Vogelstein B., Tran P. B. V., Osborne M. P. & Telang N. T. (1992) Antisense RNA to the putative tumor-suppressor gene DCC transforms Rat-1 fibroblasts. *Oncogene* **7**, 553.

p53 and N-ras Mutations in Two New Leukemia Cell Lines Established From a Patient With Multilineage CD7-Positive Acute Leukemia

By Junko Abo, Koiti Inokuchi, Kazuo Dan, and Takeo Nomura

Two new myeloid cell lines (K051 and K052) were established from a patient with multilineage CD7-positive acute leukemia. The K051 and K052 were established from the patient's bone marrow cells at diagnosis and at relapse, respectively. The K051 cell expressed myeloid-associated antigens (CD13 and CD33), a platelet-associated antigen (CD41), and an erythroid antigen (glycophorin A). The K052 cell expressed myeloid-associated antigens (CD13, CD14, and CD33), lymphoid markers (CD2, CD5, and CD7), and HLA-DR. Chromosome analysis of both cell lines showed a 17p- chromosome. Both cell lines were investigated for aberrations of the p53 gene and the N-ras gene. A p53 mutation detected in both cell lines consisted of a C → T substitution in codon 248. An N-ras mutation detected only in the K052 cell consisted of a G → C substitution in codon 13. Expression of the multidrug resistance

gene (MDR1) was also investigated by the semiquantitative reverse transcriptase-polymerase chain reaction (RT-PCR). MDR1-mRNA was more highly expressed by the K052 cell than the K051 cell, being equivalent to that in HEL cells. The functional MDR1-protein against vincristine was also observed, and its function was inhibited by verapamil and Cyclosporin A. The K052 cells were capable of phenotypic or morphologic differentiation after being incubated with granulocyte colony-stimulating factor, interleukin-2, phorbol 12-myristate 13-acetate, or 1,25-dihydroxyvitamin D₃. In contrast, the K051 cells responded phenotypically to retinoic acid. Thus, the K051 and K052 cell lines will be useful for investigating the cellular and molecular events in leukemogenesis and differentiation, and the mechanism of expression of the MDR1 gene.

© 1993 by The American Society of Hematology.

SEVERAL INVESTIGATORS have shown that alteration of the p53 gene may be involved in the progression of chronic myeloid leukemia (CML) from the chronic phase to blast crisis.¹⁻³ It has also been shown that the development of leukemia in some patients with myelodysplastic syndrome (MDS) may be related to chromosomal abnormalities or *ras* oncogene activation.^{4,5} Many studies have also reported evidence of *ras* activation and p53 gene mutations in a significant percentage of acute myelogenous leukemia (AML) cases.⁶⁻⁸ Here, two unique cell lines with p53 and N-ras mutations were established from a patient suffering from the CD7-positive acute myeloid leukemia (CD7 + AML) at different stages.

The CD7 + AML are considered to be of an early hematopoietic cell origin, capable of multilineage differentiation.⁹⁻¹¹ Accordingly, to confirm the multilineage characteristics of the established cell lines, we attempted to induce expression of differentiation with various inducers.¹¹⁻¹⁴

Because original blasts were refractory to therapy, both cell lines were also investigated for expression of the multidrug resistance (MDR1) gene¹⁵ and functional resistance to vincristine (VCR).¹⁶

The present report describes the establishment and characterization of two new CD7+ cell lines with p53 gene and N-ras gene mutations, established from the same patient at different stages. Additional consideration of the clonal evolution of the present case of CD7 + AML is performed through molecular study of both cell lines.

MATERIALS AND METHODS

Case history. A 46-year-old man was admitted to the hospital of Nippon Medical School because of malaise and a high fever on March 22, 1991. Hematologic examinations showed a hemoglobin level of 5.0 g/dL and a hematocrit value of 17.5%. His white blood cell count was $5.0 \times 10^9/L$ (78% blasts, 1% promyelocytes, 1% metamyelocytes, 3% segmented neutrophils, and 17% lymphocytes), and the platelet count was $5 \times 10^9/L$. Bone marrow examination showed a hypercellular marrow containing 58% myeloblasts. He was diagnosed as having acute myeloblastic leukemia (M2) in accordance with the French-American-British (FAB) criteria.¹⁷ How-

ever, immunophenotypically blasts had characteristics of CD7 + AML. The induction therapy was started on March 25th.¹⁸ The marrow was in a state of remission on May 9, 1991. After two cycles of consolidation therapy were administered, his bone marrow relapsed into recurrent disease (35% myeloblasts and 5% promyelocytes). His leukemic cells were refractory to many other chemotherapy regimens.^{19,21} He died on December 6, 1991 of irreversible septic shock.

Establishment of cell lines. Bone marrow mononuclear cells (MNC) were separated by density gradient centrifugation using Ficoll-Hypaque (specific gravity 1.077; Lymphoprep; Nyegaard, Oslo, Norway) at both diagnosis and relapse of the AML. The MNC were washed three times with Alpha medium (GIBCO, Grand Island, NY) supplemented with 10% fetal calf serum (FCS), 2×10^{-3} mol/L glutamine, and 100 µg/mL gentamicin (Schering Pharmaceutical Corp, Kenilworth, NJ). The cells were cultured in the supplemented Alpha medium with 10% FCS in culture flasks at 37°C in a humidified atmosphere containing 5% CO₂. After 2 weeks, the culture medium was replaced with fresh medium. After initial growth was noted, the cells were propagated in vitro with replacement of the medium containing 10% FCS without addition of growth factors twice weekly.

Immunologic marker studies. The surface markers of leukemic blasts and the cell lines were determined by direct immunofluorescence using flow cytometry on a FACS II (Becton-Dickinson; Sunnyvale, CA) flow cytometer, as previously described.²² The cells were incubated with appropriately diluted fluorescein isothiocyanate (FITC)-conjugated MoAb for 30 minutes at 4°C. The cells were then washed twice, and the percentages of positive cells deter-

From the Hematological Division of the Third Department of Internal Medicine, Nippon Medical School, Tokyo, Japan.

Submitted January 4, 1993; accepted July 2, 1993.

Address reprint requests to Koiti Inokuchi, MD, PhD, The Third Department of Internal Medicine, Nippon Medical School, 1-1-5 Sendagi, Bunkyo-ku, Tokyo 113, Japan.

The publication costs of this article were defrayed in part by page charge payment. This article must therefore be hereby marked "advertisement" in accordance with 18 U.S.C. section 1734 solely to indicate this fact.

© 1993 by The American Society of Hematology.

0006-4971/93/8209-0008\$3.00/0

mined by flow cytometry. To determine the background fluorescence, control cells were stained with FITC-conjugated normal mouse immunoglobulin. Epstein-Barr virus nuclear antigen (EBNA) was assayed by anticomplement immunofluorescence.²³

Cytogenetic studies. Cytogenetic studies were performed by the conventional trypsin-Giemsa banding technique.²⁴ The cells were processed by a direct method. The karyotype was determined by both direct microscopic analysis and photography.

Polymerase chain reaction (PCR) and direct sequencing of the *N-ras* gene. The PCR reaction and direct sequencing were performed according to our original protocol.²⁵ The PCR reaction was performed in a DNA Thermal Cycler (Perkin-Elmer/Cetus Corp, Norwalk, CT). Two hundred nanograms of DNA from cells was incubated with 0.5 U of Taq DNA polymerase (Perkin-Elmer/Cetus Corp) and with 200 ng of each of two synthetic 20-mer oligonucleotides spanning the 5' and 3' ends of the target sequence (5'-5'-ATGACTGAGTACAACTGGT-3', coding strand; 3'-5'-CT-ATGGTGGGATCATATTCA-3', antisense strand). A 109-bp amplified fragment was electrophoresed on 2.0% agarose, sliced from the gel, electroeluted, purified with phenol and ethanol precipitated. The fragments were subjected to direct sequencing as described below.

Reverse transcriptase (RT)-PCR and direct sequencing of the *p53* gene. The RT-PCR reaction was performed with a slight modifica-

Table 1. Immunophenotypes of K051 and K052 Cell Lines and Original Bone Marrow Cells at Different Stages

CD	Bone Marrow Cells		Cell Lines	
	Diagnosis	Relapse	K051	K052
CD2 (Leu 5)	14.1	3.2	1.1	39.2
CD3 (Leu 4)	8.8	1.0	3.5	0.4
CD5 (Leu 1)	9.1	7.3	0.3	36.1
CD7 (Leu 9)	50.1	53.1	8.7	99.6
CD10 (CALLA)	0.3	0.1	0.4	3.0
CD13 (MY 7)	70.1	99.7	98.2	100.0
CD14 (MY 4)	6.6	0.4	2.4	28.9
CD19 (Leu 12)	1.0	0.2	0.4	1.0
CD20 (Leu 16)	3.4	0.2	3.6	1.6
CD33 (MY 9)	16.6	63.6	46.1	99.6
CD34 (HPCA-2)	ND	ND	1.8	31.4
CD41 (GP IIb/IIIa)	0.7	5.5	42.2	25.8
Glycophorin A	16.0	1.1	71.2	23.8
HLA-DR	65.0	98.3	1.3	99.2

The immunophenotypes of the blood MNC from bone marrow cells and cell lines K051 and K052 were assayed by direct immunofluorescence assay. The denoted percentage of cell lines is mean number of that of positive cells of three experiments.

Abbreviation: ND, not done.

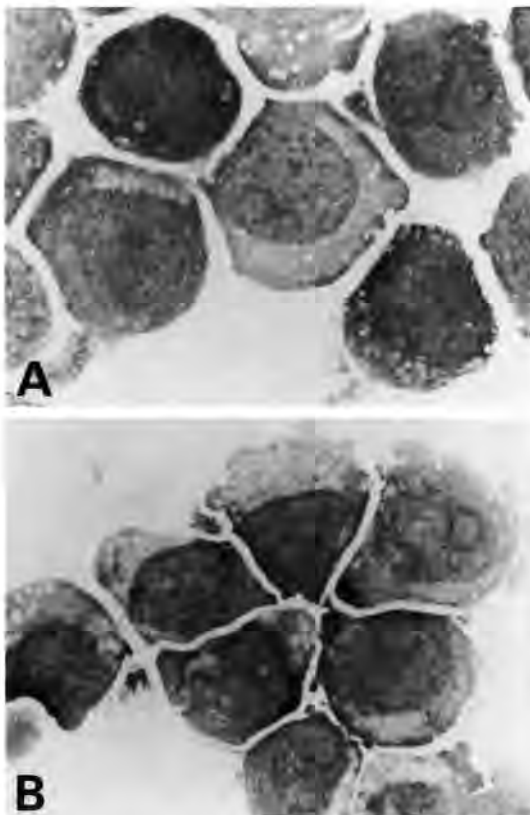


Fig 1. Cytocentrifuge preparations of K051 cells (A) and K052 cells (B) (Wright-Giemsa stain; original magnification $\times 1,000$).

tion of the original PCR procedure of Sugimoto et al.²⁶ All primers used were the same as those of Sugimoto et al. Using the nucleotide numbers of the sequence published by Zakut-Houri et al.,²⁷ the sense primers were: ST1, TCTGTGACTGCACGTACTC (residues 361-380); SN2, ACGTACTCCCTGCCCTCAA (residues 373-392); and SC3, GCGTGTGGAGTATTTGGATG (residues 603-622). The antisense primers were: AST1, CACGGATCTGAA-GGGTGAAA (residues 1000-981); ASN2, GTCTTCCAGTGT-GATGATCC (residues 777-758); and ASC3, TATTCTCCATCC-AGTGGTTT (residues 980-961). Complementary DNA was synthesized from 1 μ g of total cellular RNA from bone marrow MNC using 100 ng of 3'-primer AST1 and 200 U of Moloney murine leukemia virus (M-MLV) RT (Bethesda Research Laboratories, Gaithersburg, MD) in 25 μ L of solution containing 200 μ mol/L each of all four dNTPs, 80 U of RNase inhibitor, 50 mmol/L Tris-HCl (pH 8.3), 75 mmol/L KCl, 10 mmol/L dithiothreitol, and 3 mmol/L MgCl₂. The reaction was allowed to proceed for 60 minutes at 37°C, and the reaction solution was used as the substrate for the PCR. The PCR reaction was performed in a DNA Thermal Cycler (Perkin-Elmer/Cetus Corp) with slight modification of our original protocol.²⁸ To the RT reaction solution, 25 μ L of a solution containing 250 μ mol/L each of all four dNTPs, 100 ng of 5'-primer ST1, 10 mmol/L Tris-HCl (pH 8.3), 50 mmol/L KCl, and 3 U of Taq DNA polymerase (Perkin-Elmer/Cetus Corp) was added. The reaction conditions and cycle number were as previously described. A second PCR was performed for direct sequencing. Primers SN2 and ASN2 were used to amplify the 5'-side fragment, whereas primers SC3 and ASC3 were used for the 3'-side fragment. One microliter of RT-PCR reaction solution was used in a 50-cycle second PCR with a 10-fold reduction of one of the primers. The resulting single-stranded DNA was purified and sequenced by the dideoxy chain termination method. The sequencing primers were the reduced primers of the second PCR.

Direct nucleotide sequencing was performed using a modification of the method of Radich et al.²⁹ Six microliters of the total annealing mixture containing approximately 20 to 60 ng of PCR DNA product, 20 pmol of oligonucleotide primer, 1 μ L of 5 \times Se-

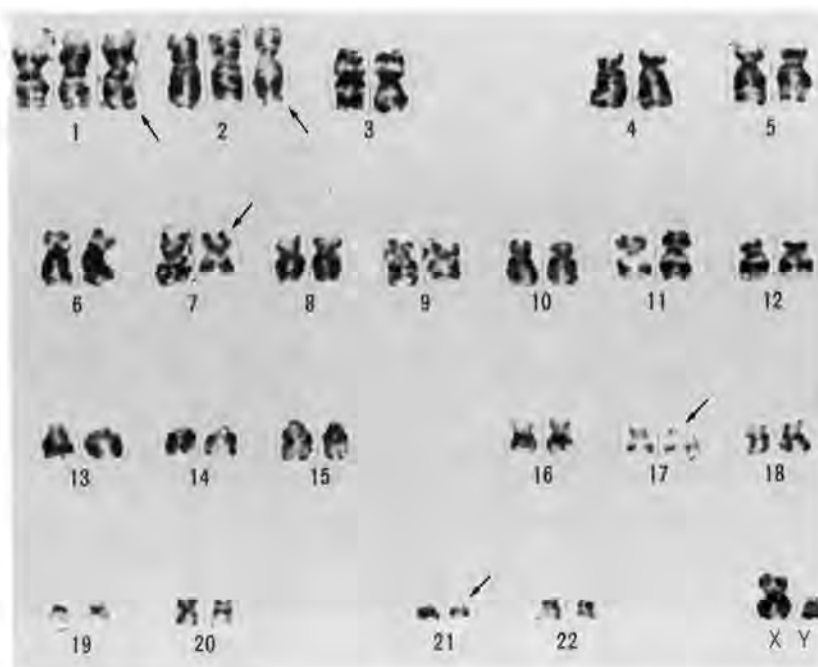


Fig 2. Karyotype of K051 cells by G-banding shows 48, XY, +1, +2, 7q-, 17p-, 21q-.

quenase buffer (United States Biochemical Co, Cleveland, OH) and 10% dimethyl sulfoxide was boiled for 2 minutes, snap-cooled on dry ice, and then placed on wet ice. Four microliters of labeling mixture, consisting of 1 μ L of 0.1 mol/L DTT, 1 μ L of 35 S-dATP, and 2 μ L of 1:8 diluted Sequenase enzyme was then added. This mixture was then divided equally and placed in four tubes that contained, respectively, 2 μ L of a deoxy/dideoxy nucleotide "chase" mixture (80 μ mol/L dGTP, dATP, dCTP, dTTP, 50 mmol/L NaCl) and 8 μ mol/L ddGTP [tube G], 8 μ mol/L ddATP [tube A], 8 μ mol/L ddTTP [tube T], and 8 μ mol/L ddCTP [tube C]. These tubes were incubated at 41°C for 2 minutes, followed by addition of 4 μ L of a formamide stop mixture. After boiling for 2 minutes, 6 μ L aliquots were loaded and electrophoresed on an 8% polyacrylamide/7 mol/L urea gel.

Semiquantitative RT-PCR analysis of MDR1 gene expression. The semiquantitative RT-PCR analysis of MDR1 gene expression was performed according to the protocol of Noonan et al with slight modification.³⁰ Complementary DNA was synthesized from 100 ng of total cellular RNA from each cell line using 100 ng of MDR-2, GGCTAGAAACAA-ATAGTGAAAACAA (an antisense primer; residues 2283-2260), or 100 ng of β_2 -microglobulin (β_2 m)-2 GTGTGAACCATGTGACTTTGTAC (an antisense primer; residues 1598-1574), and 200 U of M-MLV RT in 25 μ L of solution as described above.³¹ After RT reaction, the RT reaction solution was supplemented with 24 μ L of a solution containing 250 μ mol/L each of all four dNTPs, 100 ng of MDR-1, AAGCTTAGT-ACCAAAGAGGCTCTG (a sense primer; residues 2041-2064), or β_2 m-1, ACCCCCACTGAAAAAGATGA (a sense primer; residues 1543-1562), 10 mmol/L Tris-HCl (pH 8.3), 50 nmol/L KCl, 3 U of Taq DNA polymerase, and 1 μ L of [α - 32 P]dCTP. The reactions were performed for 25 cycles to obtain linearity in the PCR product. After the PCR reaction, each 10- μ L sample was resolved on a 3.0% agarose gel in Tris-acetate buffer and stained with ethidium bromide. The products were transferred to nylon filters (Gene

Screen Plus; New England Nuclear, Boston, MA). The resulting blots were exposed to Kodak XAR films (Eastman Kodak, Rochester, NY). A P-gp-overexpressing cell line, HEL, was used as a positive control, and K562 cells were used as a negative control.³²

Assays of VCR-resistance and of reversal of resistance by verapamil (VER) and cyclosporin A (CSA). The cells were suspended in fresh medium in 24-well dishes (Costar, Cambridge, MA) at 2.0×10^5 /mL. The cells were cultured in the presence of graded concentrations of VCR (Shionogi, Osaka, Japan) for 72 hours and counted with a Coulter Counter (Multisizer; Coulter Electronics Ltd, Luton, England). Drug sensitivity was expressed in terms of the concentration of VCR required for 50% inhibition of cell growth (IC_{50}).^{32,33} To observe the degree of reversal of VCR-resistance, each cell line was treated with graded concentrations of VCR in the presence of a given concentrations of VER (Eizai, Tokyo, Japan) or CSA (Sandoz, Tokyo, Japan). Each drug was dissolved in physiologic saline and diluted in Alpha growth medium to an appropriate concentration immediately before each experiment. The degree of reversal of resistance by VER or CSA was expressed as an α -fold decrease by dividing the IC_{50} value in the absence of VER or CSA by that in the presence of VER or CSA. The cells treated with VER or CSA alone served as one control to determine if VER or CSA alone had a growth-inhibitory effect on the cultured cells.

Attempt at cell differentiation by various inducers. The cells were suspended in Alpha medium containing 10% FCS without growth factors. The cells were plated at a concentration of 5×10^6 cells/mL in a 24-well tissue culture plate in a total volume of 2 mL of Alpha medium supplemented with either: (1) 500 ng/mL of granulocyte colony-stimulating factor (G-CSF; Sankyo, Tokyo, Japan); (2) 80 U/mL of interleukin-2 (IL-2; Genzyme, Boston, MA) + 5% phytohemagglutinin; (3) 200 ng/mL of phorbol 12-myristate 13-acetate (PMA; Wako Chemical, Tokyo, Japan); (4) 1 μ mol/L of 1,25-dihydroxyvitamin D3 (1,25(OH) $_2$ D $_3$; Sigma, St Louis, MO) or (5) 5 μ mol/L of retinoic acid (RA; Sigma). On day 7, the immuno-

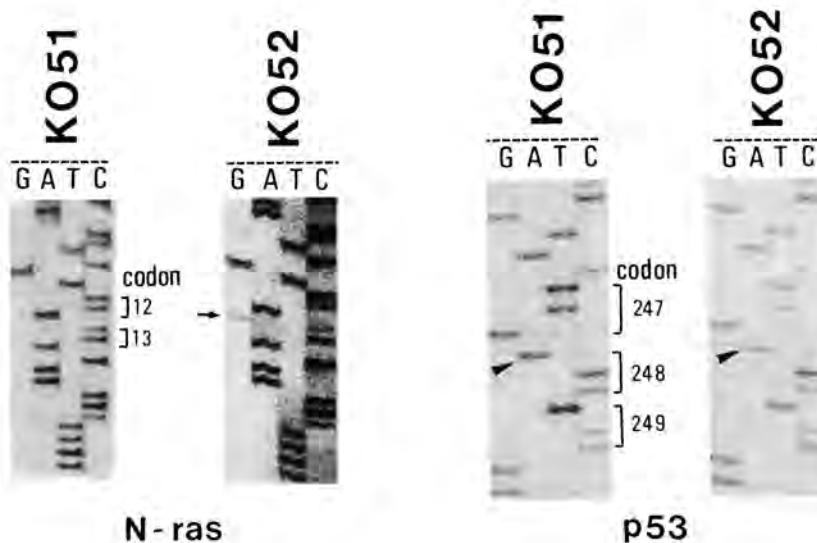


Fig 3. Mutation analyses of N-ras gene and p53 gene in both cell lines. Autoradiographs show direct sequences of an amplified fragment of the antisense strand. Lanes, from left to right, are: G, A, T, and C. The mutant nucleotides are indicated by arrowheads and an arrow.

phenotype of cells in each medium was examined as described above, and the morphology of the cells was determined from Wright-Giemsa-stained cytospin slide preparations.

RESULTS

Establishment of cell lines. The cultured cells began to proliferate 2 weeks after the start of the culture. After subcloning by the limiting dilution technique, the subcloned cells grew well in suspension, and the cell lines were subsequently established. The cells established from bone marrow obtained at diagnosis and at relapse were named K051 cells and K052 cells, respectively. The cells have now been maintained in continuous culture for 1.5 years. The doubling time was 48 hours for both cell lines.

Morphology and cytochemistry. The K051 cells had a folded nucleus with several nucleoli and vacuoles in basophilic cytoplasm (Fig 1A). The K052 cells had a round nucleus with several nucleoli and occasional azurophilic granules in basophilic cytoplasm (Fig 1B). Both cell lines were positive for peroxidase stain and Sudan black B stain, but negative for nonspecific esterase stain and periodic acid-Schiff stain. Electron microscopic analysis showed that

most of the K051 and the K052 cells measured 15 to 20 μm and 12 to 18 μm , respectively, in diameter, and that perinuclear cytoplasmic fibrils were seen in many K051 cells.

Immunophenotype. Some differences between K051 and K052 were detected in their surface phenotypes (Table 1). Phenotypically, both cell lines were positive for CD13 and CD33. K051 cells were positive for the megakaryocyte-associated antigen (CD41) and the erythroid-associated antigen (glycophorin A). K052 cells were positive for lymphoid-associated antigens (CD2, CD5, and CD7), monocyte-associated antigens (CD14) and HLA-DR. Both cell lines were negative for EBNA.

Cytogenetics. The patient's blast cells at diagnosis showed normal chromosomes. On the other hand, the patient's blasts at relapse and the two cell lines showed a 17p-chromosome aberration, as shown in Fig 2 and Table 2.

Detection of N-ras and p53 genes mutations. Figure 3 depicts the antisense of N-ras exon 1 segments from the DNA and the antisense of p53-cDNA of both the K051 and K052 cell lines. We observed neither involvement of codon 12 or 13 of the N-ras gene nor a point mutation of the p53 gene in the leukemic cells at diagnosis. However, the K051

Table 2. Summary of Cytogenetic and Molecular Analyses of K051 and K052 Cell Lines and Patient's Original Blasts at Different Clinical Stages

	Original Blasts		Cell Lines	
	Diagnosis	Relapse	K051	K052
Karyotype	46,XY (40/40)*	46,XY,17p- (40/40)	48,XY,+1,+2,7q-,17p-,21q- (39/40)	49,XY,1p-,1q-,+1,+8,9q-,10q+,+13,+13,-15,17p- (28/40) 50,XY,+3,7q+,+8,10q+,+13,17p- (7/40)
N-ras gene	Normal	GGT \rightarrow CGT at codon 13	Normal	GGT \rightarrow CGT at codon 13
p53 gene	Normal	CGG \rightarrow TGG at codon 248	CGG \rightarrow TGG at codon 248	CGG \rightarrow TGG at codon 248

* The number of karyotypes shown/the number of metaphases examined. All of the karyotypes of both cell lines had a 17p- abnormality.

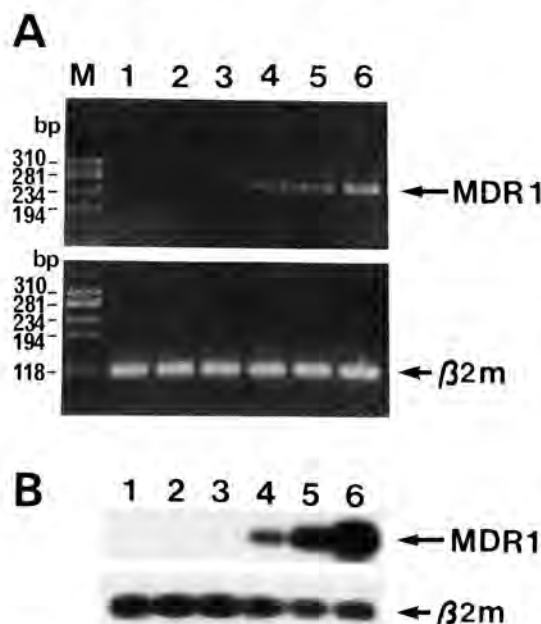


Fig 4. Quantitation of MDR1 mRNA by the RT-PCR assay. The total RNA of HEL cell, which shows high expression of MDR1 gene, was diluted with K562 RNA to the concentrations indicated below. (A) The ethidium-bromide-stained gel. The upper panel shows the RT-PCR products of MDR1-mRNA. The lower panel shows that of the β_2m . One hundred nanograms of total RNA was analyzed. The number of PCR cycles was 25. After RT-PCR with ^{32}P -dCTP, the products were electrophoresed on 3% agarose gel. The lanes represent K562 in HEL at dilutions of (1) K562 alone, (2) 1,000:1, (3) 500:1, (4) 100:1, (5) 20:1, and (6) HEL alone. Lane M: marker ϕ X 174, digested with *Hae* III. Arrows indicated MDR1-product (243 bp) and β_2m -product (115 bp). (B) Autoradiogram of the same gel. After staining with ethidium bromide, the gel was blotted onto a nylon membrane filter and the products were visualized on autoradiograms. The thin MDR1 band in lane 3 was visible on autoradiograms.

cells, which were established from leukemic cells obtained at diagnosis, showed a p53 mutation at codon 248 (C \rightarrow T) (Table 2). On the other hand, both the leukemic cells at relapse and the K052 cells showed the same mutation (C \rightarrow T) at codon 248 of the p53 gene and a G \rightarrow C substitution in codon 13 of the N-ras gene.

Semiquantitative analysis of MDR1 gene expression. As Figure 4 shows, we were able to detect MDR1-mRNA when at least 0.2% of the total cells expressed the MDR1 gene. Only a 243-bp product spanning exons 16-18 was seen in photographs of both ethidium-bromide staining and autoradiography (Figs 4 and 5). β_2m was chosen as an internal control for the MDR1 gene expression. Using this assay, the level of MDR1-mRNA in the K052 cell was at least as high as that in the HEL cell (Fig 5). MDR1-mRNA was expressed in the K051 cell, but the level was relatively low compared with that in the K052 cell (Fig 5).

VCR resistance and reversal of resistance by VER or

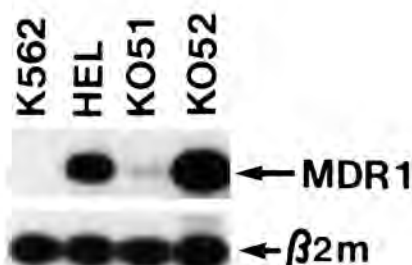


Fig 5. RT-PCR for detection of MDR1-mRNA in the K051 and the K052 cells. The upper panel shows the RT-PCR product of MDR1-mRNA in each cell line. The lower panel shows that of β_2m . The name of the individual cell line is indicated in the picture. One hundred nanograms of total RNA was analyzed for 25 PCR cycles.

CSA. Table 3 shows the IC_{50} values of VCR in the four cell lines in the presence or absence of 5.0 μ g/mL of VER or CSA. The IC_{50} values of VCR in the K051, K052, and HEL cells but not the K562 cell were decreased dramatically in the presence of 5 μ g/mL of VER or CSA. On the other hand, no significant potentiation of the growth-inhibitory activity of VCR by VER or CSA was observed in the K562 cell. Reversal of VCR resistance by VER or CSA at 0.5 μ g/mL in K052 was also observed and greater than that in K051 (data not shown).

Phenotypic and morphologic changes in the K051 and K052 cells induced by various inducers. RA induced phenotype of the K051 cell to erythroid-predominant antigen (Table 4). The K052 cells were capable of phenotypically or morphologically differentiating in the medium containing various inducers. In the absence of any inducer, the K052 cells have predominantly a myeloblastic morphology, and show high levels of expression of T-cell and myeloid-associated antigens. As shown in Table 4, IL-2 induced striking changes in the phenotype of the K052 cell characteristic of lympho-monocytic differentiation. PMA induced the phe-

Table 3. VCR Resistance and Effect of CSA and VER on the Growth-Inhibitory Activity of VCR

Cell Line	IC_{50} * (nmol/L) of VCR (x-fold decrease)†		
	None	VER (5.0 μ g/mL)	CSA (5.0 μ g/mL)
K562	1.0	0.8 (1.3)	1.0 (1.0)
HEL	43.2	8.0 (5.4)	10.0 (4.3)
K051	6.4	1.0 (6.4)	1.9 (3.4)
K052	47.5	1.4 (33.9)	2.2 (21.6)

* The cells (2.0×10^5 /mL) were cultured in the presence of graded concentrations of drug for 72 hours and counted with a Coulter Counter. Drug sensitivity was expressed in terms of the concentration of drug required for 50% inhibition of cell growth (IC_{50}). Each number is the mean of triplicate experiments.

† x-Fold decrease was obtained by dividing the IC_{50} value in the absence of VER or CSA by that in the presence of VER or CSA. Significant potentiation ($P < .01$) of drug sensitivity to VCR by both modifiers was observed in three MDR-positive cell lines in comparison with those in the control MDR-negative K562 cell line.

Table 4. Comparative Study of Cell Surface Markers of K051 and K052 Cells After Incubation With Different Inducers

CD	K051		K052				
	None	RA	None	G-CSF	IL-2	PMA	D3
CD2 (Leu 5)	1.1	0.8	39.2	14.0	29.5	3.4	5.8
CD3 (Leu 4)	3.5	0.8	0.4	1.0	10.8	9.2	0.7
CD5 (Leu 1)	0.3	0.4	36.1	6.7	19.0	2.4	1.3
CD7 (Leu 9)	8.7	3.7	99.6	91.1	95.0	7.4	98.5
CD10 (CALLA)	0.4	0.1	3.0	1.9	8.8	1.5	0.2
CD13 (MY 7)	98.2	82.0	100.0	99.8	99.0	98.9	99.6
CD14 (MY 4)	2.4	0.5	28.9	32.3	56.2	2.5	31.3
CD19 (Leu 12)	0.4	0.2	1.0	0.2	10.0	1.6	0.3
CD20 (Leu 16)	3.6	0.5	1.6	1.5	12.5	1.5	0.5
CD33 (MY 9)	46.1	5.2	99.6	97.5	95.6	13.4	97.4
CD34 (HPCA-2)	1.8	0.8	31.4	8.6	30.2	12.1	26.3
CD41 (IIb/IIIa)	42.2	2.0	25.8	12.3	12.7	6.0	1.8
Glycophorin A	71.2	96.4	23.8	12.3	10.6	9.1	1.1
HLA-DR	1.3	1.7	99.2	93.7	95.4	23.0	87.8

K051 or K052 cells were cultured in the presence of one inducer for 7 days. Cell differentiation and immunophenotypic analysis were performed as described in Materials and Methods. The results are expressed as the percentage of positive cells in three experiments.

notype of the K052 cell to become predominantly a myeloid-associated phenotype. Although G-CSF and $1,25(\text{OH})_2\text{D}_3$ did not induce any phenotypic changes in the K052 cell, they were able to induce morphologic changes, as shown in Fig 6.

DISCUSSION

The K051 cell line was established from leukemic cells at diagnosis. The K051 cell had a p53 mutation, although the leukemic cells at diagnosis had no mutations of either the *N-ras*, p53 gene, or deletion of 17p. The PCR-direct sequencing technique is capable of detecting an *N-ras* point mutation only if this mutation is present in 10% of the cell samples.³⁴ Taking the cytogenetic and RT-PCR data into consideration, we speculate that a new leukemic clone carrying both the p53 mutation and 17p-deletion represented a minor clone of less than 1% to 10% in the presentation sample. This quite minor clone was established as the K051 cell line. As the disease progressed, this minor clone expanded possibly because of acquisition of the *N-ras* mutation. This clone with two mutations acquired strong drug-resistance and the capacity for leukemic progression. The new, progressed clone was established as the K052 cell line.

The presence of the same p53 and *N-ras* mutations in the relapse sample and the K052 cell line indicates that these changes arose in the patient and were not an artifact of culture.

Coordinated loss of one copy of the p53 gene and mutation of the remaining copy have been reported in many human malignancies.^{35,36} Both mutations and allelic loss generally occur near the time of transition from a benign to malignant state in colorectal tumorigenesis,³⁷ and from the chronic phase to the acute phase in CML.¹⁻³ In the present case, leukemic cells with both mutations and allelic loss already existed at the time of presentation.

One of the mechanisms of drug-resistance in cancer is said to be associated with high expression of the P-glycoprotein encoded by the *MDR1* gene normally found at substantial levels in many organs.^{38,39} Expression of the *MDR1* gene in cancers is increased following relapse after chemotherapy, suggesting that *MDR1* expression might be selected in tumor populations exposed to chemotherapy.⁴⁰ As shown in Fig 5, the K051 (having p53 mutation) and K052 (having p53 and *N-ras* mutations) cells expressed a small and large amount of mRNA of the *MDR1* gene, respectively. Expression of a functionally active *MDR1* protein by

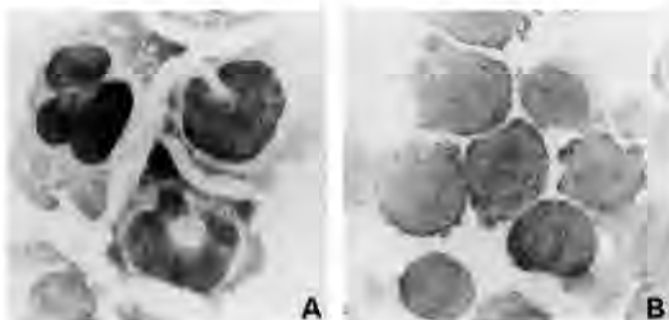


Fig 6. Morphology of G-CSF- or $1,25(\text{OH})_2\text{D}_3$ -induced K052 cells. K052 cells were incubated with G-CSF (500 ng/mL) or $1,25(\text{OH})_2\text{D}_3$ ($1 \mu\text{mol/L}$) for 7 days. Following the incubation, the cytospin preparations of cells were stained with Wright-Giemsa stain and examined by light microscopy (Wright-Giemsa stain; original magnification $\times 1,000$). (A) Cells induced by G-CSF have kidney-shaped or segmented nuclei. (B) Cells induced by $1,25(\text{OH})_2\text{D}_3$ contain many basophilic granules.

the K051 and K052 cells was demonstrated using assay of VCR-resistance reversal by VER or CSA. The MDR1 gene might be regulated positively as a result of activation of *ras* and inactivation of the p53 tumor suppressor gene.⁴¹ Thus, we speculated that the emergence of multidrug resistance might be closely associated with p53 and N-ras mutations.

The original blasts of the FAB-M2 patient had characteristics of multilineage CD7 + AML phenotypically. A high level of CD7 expression, concurrent CD2 expression in the original blasts, and high levels of expression of T-cell, platelet, and erythroid antigens on both cell lines are evidence of the multilineage nature of the cell of origin. The unusual multiple antigen phenotype of the K052 cell supports the concept that these cells originated from multilineage cells. As shown in Table 1, the immunophenotypes of the K051 and the K052 cells are quite different. There are also marked differences between the phenotypes of the cell lines and the respective samples from which they were obtained. Although we are currently unable to explain these marked differences among the cell lines and the original samples, one possibility is that CD7 + AML may have multilineage characteristics and change phenotype easily.

The K051 and K052 cells may be useful for investigating the cellular and molecular events in leukemogenesis and drug resistance. Moreover, these cell lines may be productive models for investigating the process of differentiation.

ACKNOWLEDGMENT

We thank Dr Hisamaru Hirai and Dr Koichi Sugimoto for kindly providing the primers of RT-PCR analysis, Dr Tamiko Shinohara for performing the chromosome analysis, Dr Sachiko Inokuchi for performing the ultrastructural study, Dr Koichi Miyake for helpful discussions, and the Japanese Cancer Research Resources Bank for providing cell lines.

REFERENCES

- Ahujia H, Bar-Eli M, Advani SH, Benchimol S, Cline MJ: Alterations in the p53 gene and the clonal evolution of the blast crisis of chronic myelocytic leukemia. *Proc Natl Acad Sci USA* 86:6783, 1989
- Kelman Z, Prokocimer M, Peller S, Kahn Y, Rechavi G, Manor Y, Cohen A, Rotter V: Rearrangements in the p53 gene in Philadelphia chromosome positive chronic myelogenous leukemia. *Blood* 74:2318, 1989
- Mashal R, Shtalrid M, Talpaz M, Kantarjian H, Smith L, Beran M, Cork A, Trujillo J, Gutterman J, Deisseroth A: Rearrangement and expression of p53 in the chronic phase and blast crisis of chronic myelogenous leukemia. *Blood* 75:180, 1990
- Hirai H, Okada M, Mizoguchi H, Mano H, Kobayashi Y, Nishida J, Takaku F: Relationship between an activated N-ras oncogene and chromosomal abnormality during leukemic progression from myelodysplastic syndrome. *Blood* 71:256, 1991
- Melaní C, Haliassos A, Chomel JC, Miglino M, Ferraris AM, Gaetani GF, Kaplan JC, Kitzis A: Ras activation in myelodysplastic syndromes: Clinical and molecular study of the chronic phase of the disease. *Br J Haematol* 74:408, 1990
- Needleman SW, Krans MH, Srivastava SK, Levine PH, Aaronson SA: High frequency of N-ras activation in acute myelogenous leukemia. *Blood* 67:753, 1986
- Bos JL, Verlaan-de Vries M, van der Eb AJ, Janssen JW, Delwel R, Lowenberg B, Colly LP: Mutations in N-ras predominate in acute myeloid leukemia. *Blood* 69:1237, 1986
- Janssen JW, Steenvoorden ACM, Lyons J, Anger B, Bohlke JU, Bos JL, Seliger H, Bartram CR: *Ras* gene mutations in acute and chronic myelocytic leukemias, chronic myeloproliferative disorders, and myelodysplastic syndromes. *Proc Natl Acad Sci USA* 84:9228, 1987
- Coco FL, Rossi GD, Pasqualetti D, Lopez M, Diverio D, Tagliata R, Fenu S, Mandelli F: CD7 positive acute myeloid leukemia: A subtype associated with cell immaturity. *Br J Haematol* 73:480, 1989
- Zutter MM, Martin PJ, Hanke D, Kidd PG: CD7⁺ acute non-lymphocytic leukemia: Evidence for an early multipotential progenitor. *Leuk Res* 14:23, 1990
- Kurtzberg J, Waldmann TA, Davey MP, Bigner SH, Moore JO, Herschfield MS, Haynes BF: CD7⁺, CD4⁺, CD8⁺ acute leukemia: A syndrome of malignant pluripotent lymphohematopoietic cells. *Blood* 73:381, 1989
- Roverd G, Santoli D, Damsky C: Human promyelocytic leukemia cells in culture differentiate into macrophage-like cells when treated with a phorbol diester. *Proc Natl Acad Sci USA* 76:2779, 1979
- Mangelsdorf DJ, Koeffler HP, Donaldson CA, Pike JW, Haussler MR: 1,25-dihydroxyvitamin D₃-induced differentiation in a human promyelocytic leukemia cell line (HL-60): Receptor-mediated maturation to macrophage-like cells. *J Cell Biol* 98:391, 1984
- Breitman TR, Selonick SE, Collins SJ: Induction of differentiation of the human promyelocytic leukemia cell line (HL-60) by retinoic acid. *Proc Natl Acad Sci USA* 77:2936, 1980
- Chen CJ, Chin JE, Ueda K, Clark DP, Pastan I, Gottesman MM, Roninson IB: Internal duplication and homology with bacterial transport proteins in the *mdr1* (p-glycoprotein) gene from multidrug-resistant human cells. *Cell* 47:381, 1986
- Tsuruo T, Iida H, Tsukagoshi S, Sakurai Y: Overcoming of vincristine resistance in P388 leukemia in vivo and in vitro through enhanced cytotoxicity of vincristine and vinblastine by verapamil. *Cancer Res* 41:1967, 1981
- Bennett JM, Catovsky D, Daniel M-T, Flandrin G, Galton DAG, Gralnick HR, Sultan C: Proposals for the classification of the acute leukemias. *Br J Haematol* 33:451, 1976
- Nagura E, Yamada K: A controlled randomized clinical trial of adult acute leukemia. *Jpn J Clin Hematol* 26:821, 1985
- Sauter C, Fehr J, Frick P, Gmuer J, Honnegger H, Martz G: Acute myelogenous leukemia: Successful treatment of relapse with cytosine arabinoside, VP 16-213, vincristine and vinblastine (A-Triple-V). *Eur J Clin Oncol* 18:733, 1982
- Kantarjian HM, Estey EH, Plunkett W, Keating MJ, Walters RS, Jacoboni S, McCredie KB, Freireich EJ: Phase I-II clinical and pharmacologic studies of high-dose cytosine arabinoside in refractory leukemia. *Am J Med* 81:387, 1986
- Ho AH, Lipp T, Ehninger G, Illiger H, Meyer P, Freund M, Hunstein W: Combination of mitoxantrone and etoposide in refractory acute myelogenous leukemia—An active and well-tolerated regimen. *J Clin Oncol* 6:213, 1988
- Inokuchi K, Komiya I, Dan K, Kuriya S, Shinohara T, Nomura T: TdT-positive, Smlg-negative B precursor cell leukemia with Burkitt morphology: A case report. *Leuk Lymphom* 2:251, 1990
- Reedman BM, Klein G: Cellular localization of an Epstein-Barr virus (EBV)-associated complement-fixing antigen in producer and non-producer lymphoblastoid cell lines. *Int J Cancer* 11:499, 1973
- Inokuchi K, Amuro N, Futaki M, Dan K, Shinohara T, Kuriya S, Okazaki T, Nomura T: Transforming genes and chromosome aberrations in therapy-related leukemia and myelodysplastic syndrome. *Ann Hematol* 62:211, 1991

25. Inokuchi K, Futaki M, Miyake K, Kuwabara T, Shinohara T, Dan K, Nomura T: *N-ras* activation in the terminal stage of undifferentiated chronic myeloproliferative disease. *Int J Hematol* 56:9, 1992
26. Sugimoto K, Toyoshima H, Sakai R, Miyagawa K, Hagiwara K, Hirai H, Ishikawa F, Takaku F: Mutations of the p53 gene in lymphoid leukemia. *Blood* 77:1153, 1991
27. Zakut-Houri R, Bientz-Tadmor B, Givol D, Oren M: Human p53 cellular tumor antigen: cDNA sequence and expression in COS cells. *EMBO J* 4:1251, 1985
28. Inokuchi K, Inoue T, Tojo A, Futaki M, Miyake K, Yamada T, Tanabe Y, Ohki I, Dan K, Ozawa K, Asano S, Nomura T: A possible correlation between the type of bcr-abl hybrid messenger RNA and platelet count in Philadelphia-positive chronic myelogenous leukemia. *Blood* 78:3125, 1991
29. Radich JP, Kopecky KJ, Willman CL, Weick J, Head D, Appelbaum F, Collins SJ: *N-ras* mutations in adult de novo acute myelogenous leukemia: Prevalence and clinical significance. *Blood* 76:801, 1990
30. Noonan KE, Beck C, Holzmayer TA, Chin JE, Wunder JS, Andrulis IL, Gazdar AF, Willman CL, Griffith B, Von Hoff DD, Roninson IB: Quantitative analysis of MDR1 (multidrug resistance) gene expression in human tumors by polymerase chain reaction. *Proc Natl Acad Sci USA* 87:7160, 1990
31. Miyachi H, Takemura Y, Yonekura S, Komatsuda M, Nagao T, Arimori S, Ando Y: MDR1 (multidrug resistance) gene expression in adult acute leukemia: correlations with blast phenotype. *Int J Hematol* 57:31, 1993
32. Ishida Y, Ohtsu T, Hamada H, Sugimoto Y, Tobinai K, Minato K, Tsuruo T, Shimoyama M: Multidrug resistance in cultured human leukemia and lymphoma cell lines detected by a monoclonal antibody, MRK16. *Jpn J Cancer Res* 80:1006, 1989
33. Ishida Y, Shimada Y, Shimoyama M: Synergistic effect of cyclosporin A and verapamil in overcoming vincristine resistance of multidrug-resistant cultured human leukemia cells. *Jpn J Cancer Res* 81:834, 1990
34. Radich JP, Kopecky KJ, Willman CL, Weick J, Head D, Appelbaum F, Collins SJ: *N-ras* mutations in adult de novo acute myelogenous leukemia: Prevalence and clinical significance. *Blood* 76:801, 1990
35. Isobe M, Emanuel BS, Givol D, Oren M, Croce CM: Localization of gene for human p53 tumor antigen to band 17p13. *Nature* 320:84, 1986
36. Hansen MF, Cavenee WK: Genetics of cancer predisposition. *Cancer Res* 47:5518, 1987
37. Baker SJ, Preisinger AC, Jessup JM, Paraskera C, Markowitz S, Willson JKV, Hamilton S, Vogelstein B: p53 mutations occur in combination with 17p allelic deletions as late events in colorectal tumorigenesis. *Cancer Res* 50:7717, 1990
38. Fojo AT, Ueda K, Slamon DJ, Poplack DG, Gottesman MM (1987) Expression of a multidrug-resistance gene in human tumors and tissues. *Proc Natl Sci USA* 84:265, 1987
39. Thiebaut F, Tsuruo T, Hamada H, Gottesman MM, Pastan I, Willingham MC: Cellular localization of the multidrug-resistance gene product P-glycoprotein in normal human tissues. *Proc Natl Sci USA* 84:7735, 1987
40. Goldstein LJ, Galski H, Fojo A, Willingham M, Lai S-L, Gazdar A, Pirker R, Green A, Crist W, Brodeur GM, Lieber M, Cossman J, Gottesman MM, Pastan I: Expression of a multidrug resistance gene in human cancers. *J Natl Cancer Inst* 81:116, 1989
41. Chin K-V, Ueda K, Pastan I, Gottesman MM: Modulation of activity of the promoter of the human MDR1 gene by ras and p53. *Science* 255:459, 1992



0145-2126(95)00059-3

ESTABLISHMENT AND CHARACTERIZATION OF A VILLOUS LYMPHOMA CELL LINE FROM SPLENIC B-CELL LYMPHOMA

Koiti Inokuchi,* Junko Abo,* Hidemi Takahashi,† Koichi Miyake,* Sachiko Inokuchi,‡
Kazuo Dan* and Takeo Nomura*

*Third Department of Internal Medicine, Nippon Medical School, Tokyo, Japan; †Department of Microbiology and Immunology, Nippon Medical School, Tokyo, Japan; and ‡Division of Nephrology, Department of Medicine, Juntendo University School of Medicine, Tokyo 113, Japan

(Received 23 September 1994. Accepted 21 April 1995)

Abstract—A new B-cell line (VL51) with cytoplasmic villi was established from a female patient with splenic lymphoma with circulating villous lymphocytes (SLVL). The patient exhibited a clinical picture characteristic of SLVL, including massive enlargement of the spleen. Tartrate-resistant acid phosphatase (TRAP)-negative villous lymphocytes were seen in the peripheral blood, bone marrow (BM) and both red and white pulps of the spleen. Monoclonality of the VL51 cell line was confirmed by clonal genotype abnormalities in the immunoglobulin heavy chain (IgH) gene and the T-cell receptor β (TCR β) gene. Evidence for commitment of phenotype of the VL51 cell line to the B lineage was also shown by the immunophenotype, including expression of CD10, CD19, CD20 and surface immunoglobulins. The VL51 cells were positive for Epstein-Barr virus nuclear antigen (EBNA). The VL51 cell line is the first SLVL cell line to be established, and it is expected to be useful in clarifying the leukemogenesis of SLVL.

Key words: Splenic lymphoma with villous lymphocytes, hairy cell leukemia, cell line, IgH, TCR β , rearrangement.

Introduction

Hairy-cell leukemia (HCL) is a well-defined clinico-pathological entity with several highly distinctive features [1, 2]. Variant forms of HCL (vHCL) with intermediate features between HCL and B-cell lymphoma have been reported [3–5]. A characteristic type of diffuse lymphoma with circulating lymphocytes which resemble hairy cells deserves special attention for its differential diagnosis from HCL. This was recently reported by Melo *et al.*, who termed it “splenic lymphoma with circulating villous lymphocytes (SLVL)”, which is a rare splenomegalic non-Hodgkin’s lymphoma variant [6–8].

In this paper, we report a newly established B-cell line derived from a patient with SLVL. We elucidated the characteristics of this cell line in terms of its cytochemistry, immunophenotype, cytogenetics and genotype. Dual characteristic rearrangements of the immunoglobulin heavy chain (IgH) and T-cell receptor β (TCR β) genes were found.

Materials and Methods

Case report

A 70-year-old female was admitted to our hospital on 19 February 1988 because of malaise. Physical examination revealed remarkable splenomegaly with the spleen tip palpable 20 cm below the left costal margin, and lymphadenopathy. Her hemoglobin level was 8.2 g/dl, the platelet count was 111,000/ μ l, and the white blood cell (WBC) count was 1,800/ μ l with 62% atypical lymphocytes. The atypical lymphocytes had cytoplasmic villi which were visible with an optical microscope and an electron microscope (Fig. 1). A bone marrow aspirate (Fig. 2) revealed nodular type infiltration by hairy cell-like lymphocytes (11%), which were negative for acid phosphatase staining. A mild M band composed of IgG was found. Enlarged para-aortic lymph nodes were detected by a computed tomography examination. Splenectomy was performed on 8 April 1988. Histological examination of the spleen showed diffuse lymphoma cell infiltration into both the white and red pulps, with a diagnosis of SLVL (Fig. 3). After splenectomy, the patient’s WBC count increased to 13,000/ μ l (villous lymphocytes: 42.5%). In June 1988, chemotherapy with five courses of CHOP therapy [9] was started, and this resulted in a good response. The patient’s disease is clinically stable and in remission at present.

Establishment of cell lines

Splenic mononuclear cells (MNC) were separated by density gradient centrifugation using Ficoll-Hypaque (specific

Correspondence to: K. Inokuchi, Division of Hematology, The Third Department of Internal Medicine, Nippon Medical School, 1-1-5 Sendagi, Bunkyo-ku, Tokyo 113, Japan.

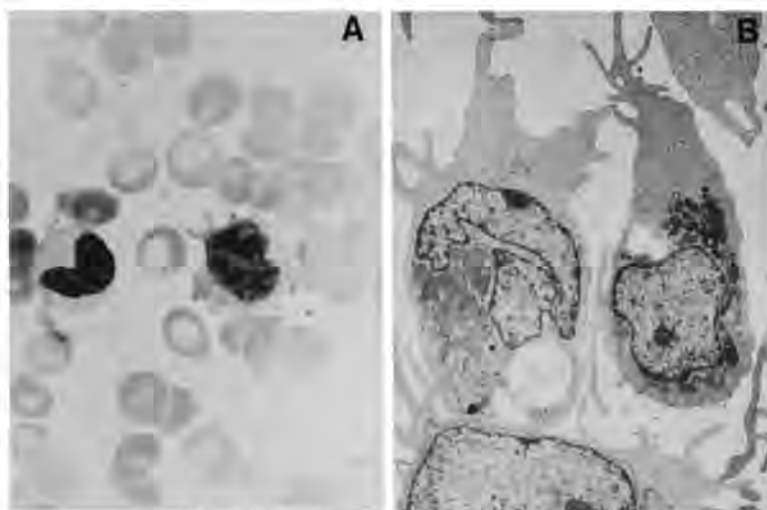


Fig. 1. Morphological examination of peripheral blood. Light microscopy (H and E stain, $\times 1000$) (A) and electron microscopy (TEM $\times 2500$) (B) of peripheral villous lymphocyte. A mature neutrophil and a villous lymphocyte are shown in (A). Villous lymphocytes have scant cytoplasm with irregular long projections and partially localized villi. The irregular projections show an uneven distribution all around the membrane. There are many mitochondria and some vesicles.

gravity 1.077; Lymphoprep, Nyegaard, Oslo, Norway). The cells were then washed three times with alpha medium (Flow Laboratories, Inglewood, CA, U.S.A.) supplemented with 20% fetal calf serum (FCS), 2×10^{-3} mol/l glutamine, and 100 μ g/ml gentamicin (Schering Corp., Kenilworth, NJ, U.S.A.). The cells were cultured in the supplemented alpha medium (Gibco, Grand Island, NY, U.S.A.) in culture flasks (Falcon #3013, Becton-Dickinson, Cockville, MD, U.S.A.) at 37°C in a humidified atmosphere containing 5% CO_2 . After 2 weeks, the culture medium was replaced with fresh medium. After initial growth was noted, cells were propagated *in vitro* with medium replacement twice weekly.

Transmission electron microscopy

Cell pellets were fixed in 2% phosphate-buffered glutaraldehyde for 2 h, followed by post-fixation with 1% phosphate-buffered osmium tetroxide for 1 h. Specimens were dehydrated in graded ethanols, dealcoholized with propylene oxide, and embedded in EPON812. Ultrathin sections were prepared, followed by double-staining with uranyl acetate and lead citrate. They were observed with a Hitachi S-800 electron microscope (Hitachi Ltd., Tokyo, Japan) [10].

Scanning electron microscopy

The MNC of peripheral blood and the established cells were centrifuged at 3000 rpm for 5 min in a Hitachi 05PR-22 refrigerated centrifuge at 4°C . The sediments were placed on poly-L-lysine-coated round and thin glasses, 1.5 cm in diameter, for 10 min. The specimens were then fixed with

2% EM grade glutaraldehyde–0.1 M phosphate buffer and dehydrated in a graded series (50, 70, 90, 95 and 100%) of ethyl alcohol. The specimens were then dried with carbon dioxide by the critical-point method. After drying, the specimens were coated with an alloy of 60% gold–40% palladium in an Eiko engineering sputter coater IB type 5 and observed with a Hitachi S-800 scanning electron microscope, operating at 10 kV acceleration [11].

Immunological marker studies

Cells were immunophenotyped by flow cytometry on a FACS II (Becton-Dickinson, Sunnyvale, CA, U.S.A.) flow cytometer, as described previously [12, 13]. Mouse monoclonal antibodies against CD2 (T11), CD5 (T1), CD25 (IL2R), CD20 (B1), CD10 (CALLA), CD19 (B4), CD13 (My 7) and CD33 (My 9) were obtained from Coulter Clone (Hialeah, FL, U.S.A.) and I2 (HLA-DR), CD34 (HPCA-1) from Becton-Dickinson (Mountain View, CA, U.S.A.). The mouse IgG1 (Coulter Clone) was used as a control. The cells were incubated for 30 min at 4°C with an appropriate dilution of each monoclonal antibody. The labeled cells were washed three times in cold phosphate-buffered saline (PBS) and stained with fluorescein-conjugated goat antimouse IgG (Tago, Burlingame, CA, U.S.A.). The cells were then washed, fixed and analyzed by flow cytometry (indirect immunofluorescence). Tests for surface immunoglobulin utilized FITC-conjugated goat anti-human IgG, IgA, IgM, κ and λ by direct immunofluorescence. To test for EB virus infection, the cells were tested for the presence of EB virus nuclear antigen using the method of Reedman and Klein. [14].

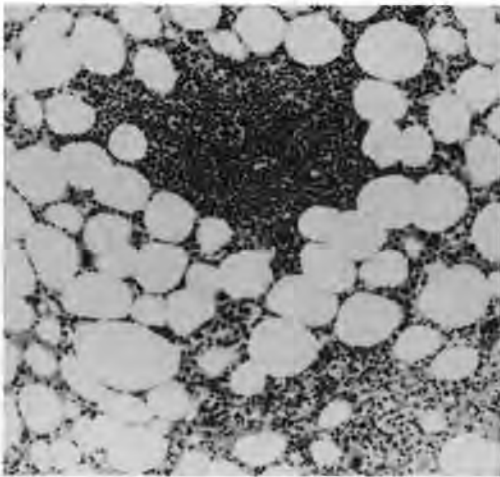


Fig. 2. Bone marrow morphology (Trepphine) shows a nodular, lymphocytic pattern of involvement (H and E: $\times 200$).

Cytogenetic studies

Cytogenetic studies were performed by the conventional trypsin-Giemsa banding technique [15]. The cells were processed by a direct method. Metaphase cells of peripheral blood were also examined from both short-term unstimulated cultures and cultures stimulated with a B-cell specific mitogen, concanavalin A (Con-A). The karyotype was determined by both direct microscopic analysis and photography [16].

DNA isolation and gene analysis

DNA was extracted as described previously. Briefly, the cells were incubated at 37°C overnight in 10 mmol/l Tris-HCl, pH 8.0, 100 mmol/l NaCl, and 1 mmol/l EDTA containing 1% (wt/vol) sodium dodecylsulphate (SDS) and 100 μ g proteinase K/ml buffer. High-molecular-weight DNA was obtained after extraction with phenol, incubation with DNase-free RNase A, further extraction with phenol/chloroform (1:1, vol/vol), and precipitation at -20°C with 2 volumes of ethanol and 1/10 volume of a 3 mol/l sodium acetate solution. Digestion was carried out with *EcoR* I or *Hind* III in the buffer recommended by the supplier at 37°C for 6 h by using 3.0 U of enzyme/ μ g of DNA. The digestion products were separated by size on 0.8% agarose gels and transferred to nylon filters (Gene Screen Plus). The human immunoglobulin gene probe used was the joining region (JH) of the μ -Ig gene [17]. The JH probe was kindly provided by Dr T. Honjo through the Japanese Cancer Research Resources Bank (JCRB). A T-cell β -receptor gene probe (TC β 1) was obtained from Oncor (Gaithersburg, MD, U.S.A.).

Results

Establishment of cell lines

Proliferation of the cultured cells was noted 5 weeks from the start of the culture. At that stage, subcloning was performed by the limiting-dilution technique.

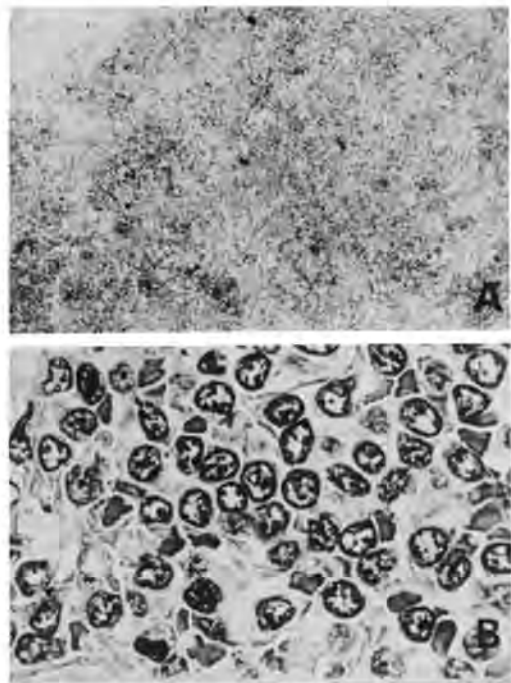


Fig. 3. Histological examination of splenic tissue. Numerous immature lymphocytes are infiltrating both the red and white pulps. The normal structure of the spleen is almost destroyed by the infiltrating immature lymphocytes. (H and E: (A) $\times 40$, (B) $\times 400$).

Thereafter, subcloned cells grew well in suspension. The established cell line, designated VL51, has now been maintained continuously for over 5 years in liquid suspension. We have already confirmed that this cell line can be frozen in a viable form without consequent alteration of its functional characteristics after thawing. The VL51 cells have a doubling time of approximately 70–80 h.

Morphology, cytochemistry and electron microscopy

The VL51 cell line showed cytoplasmic projections when observed by light microscopy (Fig. 4A). Both peripheral blood mononuclear cells (MNC) and the VL51 cells were positive for α -naphthyl butylate esterase staining, but negative for acid phosphatase, Sudan Black B and PAS staining. In the ultrastructural examinations, prominent cytoplasmic projections were observed (Fig. 4B,C).

Immunological marker analysis

The phenotypes of both MNCs and VL51 are shown in Table 1. Both MNCs and VL51 were positive for

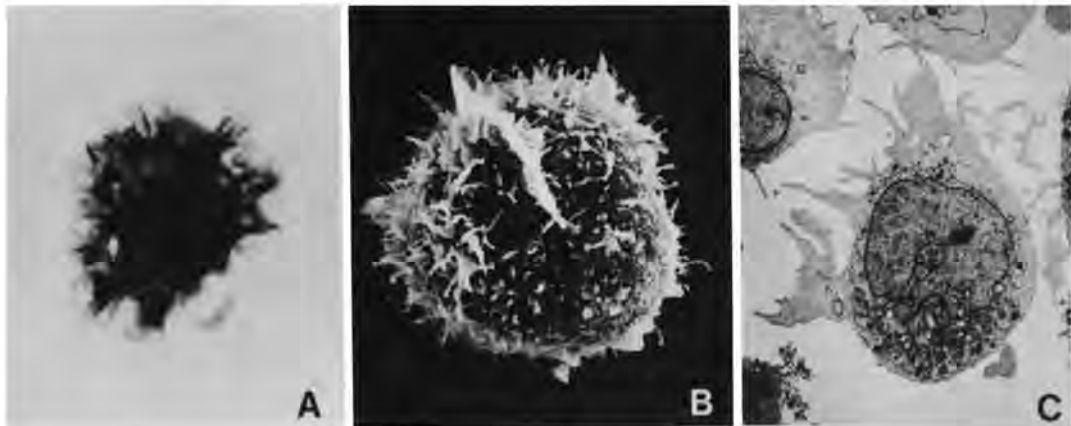


Fig. 4. Morphology of VL51 cells. Light microscopy shows numerous cytoplasmic villi and projections. These villi and long projections are irregular and unevenly distributed on many VL51 cells (A). VL51 cells are characterized by long projections and numerous villi, usually unevenly distributed ((B) SEM $\times 3500$, (C) TEM $\times 5000$). The many broad-based projections of VL51 cells tend to have a polar distribution. TEM shows that the VL51 cells possess an eccentric nucleus, many cytoplasmic mitochondria and several vesicles.

CD10, CD19, CD20, HLA-DR and λ . VL51 was positive for CD25, which is expressed by activated B-cells. These results are consistent with a B-cell lymphoproliferative disorder. However, the VL51 cells are not typical hairy cells because they did not exhibit CD11c, which is usually seen on typical hairy cells [7]. Unexpectedly, VL51 cells were positive for CD34. During establishment of the cell line, CD34 may have been activated. The VL51 cells were positive for EBNA.

Cytogenetic studies

Chromosomal analyses of both MNCs and the VL51 cell line showed a normal karyotype of 46,XX.

IgH and TCR β gene configurations of MNCs and VL51 cell line

To confirm the clonality and lineage of the VL51 cell line, DNA was isolated from MNCs and the VL51 cell line, and the configurations of IgH and TCR β genes were determined. The results of IgH gene and TCR β gene analyses indicated the same clonal rearrangements in both MNCs and the VL51 cell line, as shown in Fig. 5. IgH analysis after *Hind* III digestion detected the presence of rearranged bands in both alleles, and no germline band in VL51 cells (Fig. 5A; Lane 3 of *Hind* III digestion). The TCR β probe detected rearrangement of one allele of the TCR β gene when the genomic DNA was digested with *Hind* III and *Eco*R I (Fig. 5B).

Discussion

HCL is easily diagnosed from peripheral blood smears and BM biopsy specimens, and demonstration of TRAP activity of the leukemic cells is further substantiation of the diagnosis. However, there are

Table 1. Immunological marker profile of peripheral blood and VL51 cell line

Marker	Positive cells (%)	
	Peripheral blood	VL51 cell
CD2 (T11)	25.3	0.4
CD5 (T1)	92.5	0.2
CD10 (CALLA)	68.7	63.0
CD11c (LeuM5)	N.D.	0.1
CD13 (My7)	N.D.	1.7
CD19 (B4)	75.2	72.2
CD20 (B1)	62.1	92.2
CD25 (IL-2R)	1.1	35.7
CD33 (My9)	N.D.	8.0
CD34 (HPCA-1)	N.D.	55.6
HLA-DR	77.8	91.4
SIgG	N.D.	41.6
SIgM	N.D.	2.8
SIgA	N.D.	1.9
SIgD	N.D.	3.1
κ	5.2	1.5
λ	61.3	90.1

N.D., not done.

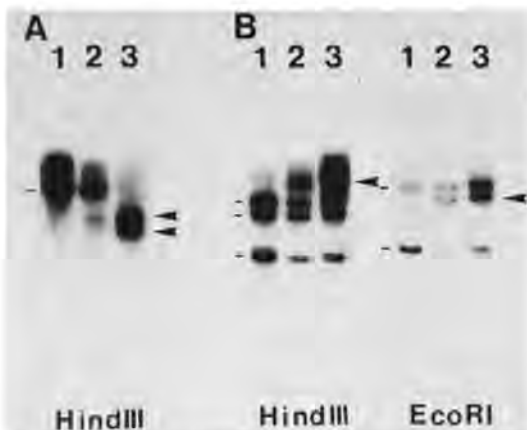


Fig. 5. Southern blot analyses of the IgH gene (A) and TCR β gene (B). Genomic DNA from normal human MNC, peripheral blood MNC and VL51 cells was hybridized with the JH probe or TC β 1 probe after *Hind* III or *Eco*RI restriction enzyme digestion. Germ-line bands are indicated by small vertical bars. The length of the JH-containing germ-line is 20.0 kb, and that of the TCR β gene is 10, 8 and 3.8, and 12 and 4.2 kb, respectively. The rearranged bands are indicated by arrowheads. Lane 1: DNA from normal human MNC as control; Lane 2: DNA from peripheral blood MNC; Lane 3: DNA from VL51 cells.

circumstances in which diagnosis of HCL may be difficult. Recently, Melo *et al.* described SLVL, which shares many clinical findings with HCL [6]. SLVL patients show splenomegaly with lymphadenopathy. The leukemic cells in the PB are often confused with the cells of HCL in that they have many cytoplasmic projections [6, 7]. However, these projections are distributed unevenly on the cell surface. The present case had many of the clinical findings of SLVL as described by Melo *et al.*, rather than those of HCL. The atypical lymphocytes of the present case had cytoplasmic projections and villi, which were distributed unevenly in the peripheral blood. Also, the massively enlarged spleen showed infiltration of atypical lymphocytes in both the red and white pulps and disruption of the normal spleen structure due to the infiltration, in contrast to the diffuse red pulp infiltration that is characteristic of HCL [6].

Phenotypically, SLVL cells are usually TRAP $^-$, CD10 $^+$, CD11c $^+$ and CD25 $^-$ [6]. Cytochemical and surface marker analyses revealed that the atypical lymphocytes of the present case were negative in the TRAP stain and did not exhibit CD11c, which is seen in many typical HCL cases. CD11c $^-$ is occasionally seen in some SLVL cases [18]. In addition, the atypical lymphocytes were characterized as clonal B-cells by virtue of their expression of surface Ig of a single light

chain isotype and B-cell associated markers, CD19 and CD20. In addition to the pattern of splenic involvement and phenotypical markers of villous lymphocytes, other SLVL-related clinical markers such as anemia, thrombocytopenia, monoclonal gammopathy of IgG were also present in this patient [6–8].

The latest classification of lymphoid neoplasms was proposed by the International Lymphoma Study Group (ILSG) [19]. SLVL is in the entity of "splenic marginal zone lymphoma with or without villous lymphocytes (SMZL)" in peripheral B-cell neoplasms and identical to HCL. The pattern of involvement of the spleen is in both the red and white pulps, with a mantle and/or marginal zone pattern in the white pulp. There was almost total destruction of the patient's splenic tissue due to preferential infiltration into both pulps. The spleen of the patient showed massive enlargement, extending 20 cm below the costal margin. Thus, after careful consideration, the final diagnosis was SLVL which is called SMZL by the ILSG.

The established VL51 cells have prominent cytoplasmic villi and also showed a B-cell lineage in the immunological marker analyses. The cell line's monoclonality was confirmed by analysis of the IgH and TCR genes. Both alleles of the IgH gene were rearranged, and no germline was detected. Analysis of the TCR gene revealed the presence of a rearrangement of one allele. Cleary *et al.* reported that splenic hairy cells of 11 untreated HCL patients revealed rearrangement of the IgH gene, but the configuration of the TCR β gene remains unclear [20]. Recently, a variant HCL case [21] and a T-cell HCL case [22], both of which had IgH and TCR rearrangements, were reported. We recently reported a SLVL case which had dual rearrangements of the IgH and TCR genes [23]. The present case was also an SLVL case having dual rearrangements of the IgH and TCR genes. Although rearrangement of TCR may be present in about 10% of B-cell malignancies, we speculate that there is a possibility that SLVL sometimes has a genotypically aberrant configuration.

Establishment of many hairy cell lines has been reported to date [24, 25]. However, SLVL has never previously been cloned. The VL51 cell line is expected to be useful for analysis of the pathogenesis of SLVL and B-cell malignancies.

References

1. Paguet G. B., Satya-Prakash K. L. & Agee J. F. (1988) Cytochemical, cytogenetic, immunophenotypic and tumorigenic characterization of two hairy cell lines. *Blood* 71, 422.
2. Korsmeyer S. J., Greene W. C., Cossman J., Hsu S., Jensen J. P., Neckers L. M., Marshall S. L., Bakhshi A., Depper J. M., Leonard W. J., Jaffe E. S. & Waldmann T. A. (1983) Rearrangement and expression of immunoglobulin genes

- and expression of Tac antigen in hairy cell leukemia. *Proc. natn. Acad. Sci. USA* **80**, 4522.
3. Palutke M., Tabaczka P., Mirchandani I. & Goldfarb, S. (1981) Lymphocytic lymphoma simulating hairy cell leukemia: a consideration of reliable and unreliable diagnostic features. *Cancer* **48**, 2047.
 4. Cawley J. C., Burns G. F. & Hayhoe F. G. A. (1980) Chronic lymphoproliferative disorder with distinctive features: a distinct variant of hairy-cell leukemia. *Leukemia Res.* **4**, 547.
 5. Catovsky D., O'Brien M., Melo J. V., Wardle J. & Brozovic M. (1984) Hairy cell leukemia (HCL) variant: an intermediate disease between HCL and B prolymphocytic leukemia. *Semin. Oncol.* **11**, 362.
 6. Melo J. V., Hegde U., Parreira A., Thompson L., Lampert I. A. & Catovsky D. (1987) Splenic B cell lymphoma with circulating villous lymphocytes: differential diagnosis of B cell leukaemias with large spleens. *J. clin. Pathol.* **40**, 642.
 7. Mulligan S. & Catovsky D. (1992) Splenic lymphoma with villous lymphocytes. *Leukemia Lymphoma* **6**, 97.
 8. Rousselet M. C., Gardembas-Pain M., Renier G., Chevallier A. & Ifran N. (1992) Splenic lymphoma with circulating villous lymphocytes; report of a case with immunologic and ultrastructural studies. *Am. J. Clin. Pathol.* **97**, 147.
 9. McKelvey E. M., Gottlieb J. A., Wilson H. E., Haut A., Talley R. W., Stephens R., Lane M., Gamble J. F., Jones S. E., Grozea P. N., Gutterman J., Coltman Jr. C. & Moon T. E. (1976) Hydroxyl daunomycin (adriamycin) combination chemotherapy in malignant lymphoma. *Cancer* **38**, 1484.
 10. Inokuchi S., Sakai T., Shirato I., Tomino Y. & Koide H. (1993) Ultrastructural changes in glomerular epithelial cells in acute puromycin aminonucleoside nephrosis: a study by high-resolution scanning electron microscopy. *Virchows Archiv A Pathol. Anat.* **423**, 111.
 11. Shirato I., Tomino Y. & Koide H. (1990) Detection of "activated platelets" in the urinary sediments using a scanning electron microscope in patients with IgA nephropathy. *Am. J. Nephrol.* **10**, 186.
 12. Abo J., Inokuchi K., Dan K. & Nomura T. (1993) p53 and N-ras mutations in two new leukemia cell lines established from a patient with multilineage CD7-positive acute leukemia. *Blood* **82**, 2829.
 13. Inokuchi K., Komiya I., Dan K., Kuriya S., Shinohara T. & Nomura T. (1990) TdT-positive, SmIg-negative B precursor cell leukemia with Burkitt morphology: a case report. *Leukemia Lymphoma* **2**, 251.
 14. Reedman B. M. & Klein G. (1973) Cellular localization of an Epstein-Barr virus (EBV)-associated complement-fixing antigen in producer and non-producer lymphoblastoid cell lines. *Int. J. Cancer* **11**, 499.
 15. Shinohara T., Takuwa N., Morishita K., Leki R., Yokota J., Nakayama E., Asano S. & Miwa S. (1983) Chronic myelomonocytic leukemia with a chromosome abnormality (46,XY,20q-) in all dividing myeloid cells: evidence for clonal origin in a multipotent stem cell common to granulocyte, monocyte, erythrocyte and thrombocyte. *Am. J. Hematol.* **15**, 289.
 16. ICNS (1985) *An International System for Human Cytogenetic Nomenclature* (Harnden D. G., Path F. R. C. & Klinger H. P., Eds). Karger Medical and Scientific, Basel.
 17. Takahashi N., Nakai S. & Honjo T. (1980) Cloning of human immunoglobulin S gene and comparison with mouse μ gene. *Nucleic Acids Res.* **8**, 5983.
 18. Bassan R., Neonato M. G., Abbate M., Motta T., Barbui T. & Rambaldi A. (1991) Monoclonal lymphocytosis with villous lymphocytes: a chronic lymphoproliferative disease of CD11c+ B-cells. *Leukemia* **5**, 799.
 19. Harris N. L., Jaffe E. S., Stein H., Banks P. M., Chan J. K. C., Cleary M. L., Delsol G., De Wolf-Peters C., Falini B., Gatter K. C., Grogan T. M., Isaacson P. G., Knowles D. M., Mason D. Y., Muller-Hermelink H., Pileri S. A., Piris M. A., Ralfkiaer E. & Warnke R. A. (1994) A revised European-American classification of lymphoid neoplasms; a proposal from the International Lymphoma Study Group. *Blood* **84**, 1361.
 20. Cleary M. L., Wood G. S., Warnke R., Chao J. & Sklar J. (1984) Immunoglobulin gene rearrangements in hairy cell leukemia. *Blood* **64**, 99.
 21. Giardina S. L., Young H. A., Faltynek C. R., Jaffe E. S., Clark J. W., Steis R. G., Urba W. J., Mathieson B. J., Gralnick H., Lawrence J., Overton W. R. & Longo D. L. (1988) Rearrangement of both immunoglobulin and T-cell receptor genes in a prolymphocytic variant of hairy cell leukemia patient resistant to interferon-alpha. *Blood* **72**, 1708.
 22. Palumbo A. P., Corradini P., Battaglio S., Omede P., Coda R., Boccadoro M. & Pileri A. (1991) Dual rearrangement of immunoglobulin and T-cell receptor genes in a case of T-cell hairy-cell leukemia. *Eur. J. Haematol.* **46**, 71.
 23. Hanawa H., Abo J., Inokuchi K., Tanosaki S., Matsuoka H., Miyake K., Futaki M., Dan K. & Nomura T. (1995) Dual rearrangement of immunoglobulin and T-cell receptor genes in a case of splenic lymphoma with villous lymphocytes. *Leukemia Lymphoma* **18**, 357.
 24. Sairenji T., Spiro R. C., Reisert P. S., Paquin L., Sakamoto K., Shibuya A., Sullivan J. L., Katayama I. & Humphreys R. E. (1983) Analysis of transformation with Epstein-Barr virus and phenotypic characteristics of lymphoblastoid cell lines established from patients with hairy cell leukemia. *Am. J. Hematol.* **15**, 361.
 25. Miyoshi I., Hiraki S., Tsubota T., Hujita T., Masuji H., Nishi Y. & Ikuro K. (1981) Hairy cell leukemia: establishment of a cell line and its characteristics. *Cancer* **47**, 60.

DCC Protein Expression in Hematopoietic Cell Populations and Its Relation to Leukemogenesis

Koiti Inokuchi, Koichi Miyake, Hidemi Takahashi,* Kazuo Dan, and Takeo Nomura

Division of Hematology, Department of Internal Medicine, Nippon Medical School, Tokyo 113, Japan; and *Department of Immunology, Nippon Medical School, Tokyo 113, Japan

Abstract

Using flow cytometry and immunoprecipitation (IP), we have investigated the deleted in colon cancer (DCC) protein expression on the bone marrow (BM) and peripheral blood (PB) cells of 16 normal subjects, 17 myelodysplastic syndrome (MDS) patients, and 10 acute myelogenous leukemia (AML) patients.

With regard to the BM mononuclear cells (BM-MNCs) of normal subjects, the DCC protein expression ranged from 6.6 to 57.0%. Two-color flow cytometry revealed that among the BM-MNCs the DCC protein was clearly expressed on the CD14+, CD13+, and factor 8+ cells, whereas it was low on the CD19+ and CD7+ cells and did not express on the CD34+, CD8+, and the glycophorin A+ cells. Further, the DCC protein expression was not seen on the PB CD11b+ and CD13+ cells. The IP results revealed that the 180-kD DCC protein was detected on the MNCs of both the BM and PB cells by the antibodies AF5, specific for the DCC extracellular domain, and G97-449, specific for the cytoplasmic domain.

In contrast, flow cytometry did not detect the DCC protein on any BM-MNC MDS lineages (0.1–1.5%) or on AML leukemic cells (0.1–0.9%). The IP results indicated that the AF5 antibody did not detect the DCC protein on BM-MNCs of three of five MDS patients and four of five AML patients; however, the G97-449 antibody detected the 180-kD DCC protein in two MDS patients in whom AF5 had detected greatly reduced DCC band.

These findings suggest that the DCC protein presence appears to be associated with normal hematopoiesis, and that its absence on the surfaces of the BM-MNCs and AML cells may contribute to the MDS and AML pathogenesis. (*J. Clin. Invest.* 1996. 97:852–857.) Key words: myelodysplastic syndromes • acute myelogenous leukemia • hematopoiesis

Introduction

The deleted in colorectal carcinoma (DCC)¹ gene has been identified as a possible tumor-suppressor gene (1). Consistent with its possible function as a tumor-suppressor gene, DCC gene expression has been shown to be markedly decreased or absent in many cancers (2), including leukemia (3, 4) and myelodysplastic syndromes (MDS) (5, 6). The predicted nucleic acid sequence of human DCC cDNA from fetal brain tissue indicates that the DCC gene encodes a 1,447-amino acid transmembrane protein having extensive similarity to neural cell adhesion molecules and other cell-surface glycoproteins (7, 8). The DCC protein is composed of four immunoglobulin-like and six fibronectin type III-like extracellular domains, and a cytoplasmic domain (1).

So far, DCC expression studies have focused on DCC gene expression. Expression studies of the DCC protein have been limited for colon and neural tissues particularly at the cellular level (8, 9). Although important roles of the DCC protein in control of growth of the normal intestine and colon carcinoma have been emphasized, little is known about the DCC protein's function and antioncogenicity. Thus, we investigated DCC protein expression of mononuclear cells (MNCs) in normal subjects and patients with MDS and acute myelogenous leukemia (AML).

Methods

Patients for DCC protein expression. 10 untreated AML patients and 17 untreated MDS patients, consisting of 6 with refractory anemia (RA), 2 with RA with ringed sideroblasts, 5 with RA with an excess of blasts (RAEB), and 4 with RAEB in transformation, were investigated after obtaining informed consent. Diagnosis was made according to the French-American-British classification (10). 16 healthy volunteers were also investigated for DCC protein expression.

Reverse transcriptase (RT)-PCR for detection of DCC mRNA. 48 patients with MDS and 53 with AML were examined by RT-PCR. The total RNA of bone marrow (BM) MNCs was extracted by the CsCl method (11). RT-PCR was performed as described previously (3). Briefly, cDNA synthesis was performed first using an oligonucleotide primer (DCC2: 5'-AGCCTCATTTTCAGCCACACA-3', antisense strand). PCR was performed with 10 µl of cDNA reaction mixture by using 0.0125 OD₂₆₀ (optical density) units of each oligo-

Address correspondence to Koiti Inokuchi, MD, Division of Hematology, Department of Internal Medicine, Nippon Medical School, 1-1-5 Sendagi, Bunkyo-ku, Tokyo 113, Japan. Phone: 3-3822-2131x775; FAX: 3-5685-1793.

Received for publication 6 July 1995 and accepted in revised form 13 November 1995.

J. Clin. Invest.

© The American Society for Clinical Investigation, Inc.
0021-9738/96/02/0852/06 \$2.00

Volume 97, Number 3, February 1996, 852–857

1. **Abbreviations used in this paper:** AML, acute myelogenous leukemia; BM, bone marrow; DCC, deleted in colorectal carcinoma; IP, immunoprecipitation; MDS, myelodysplastic syndromes; MNC, mononuclear cell; PB, peripheral blood; PE, phycoerythrin; RA, refractory anemia; RAEB, RA with an excess of blasts; RT, reverse transcriptase; SBA, soybean agglutinin.

nucleotide primer (DCC1: 5'-TTCGCCCATGGTTTAAATCA-3', coding strand; and DCC2: antisense strand). These oligonucleotide primers are the same ones used by Fearon et al. (1). PCR of 35 cycles was performed, consisting of 30 s at 94°C, 30 s at 55°C, and 1 min at 75°C (12). 20 µl of the PCR products was phenol-extracted, ethanol-precipitated, and electrophoresed through a 3.5% agarose gel (NuScience 3:1 agarose; FMC Corp. BioProducts, Rockland, ME). The PCR products were visualized directly in ethidium bromide-stained gels and photographed.

Separation of CD13+, CD14+, and CD34+ for RT-PCR analysis. For RT-PCR analysis of DCC gene expression in the CD13+ and CD14+ populations, these populations were sorted with a FACStar Plus® (Becton Dickinson, San Jose, CA) using FITC-conjugated MY4 (CD14) or MY7 (CD13) (Becton Dickinson) from BM-MNCs. The purity of these cells obtained by sorting was 97 and 96%, respectively.

For CD34+ isolation, CD34+ cells were first enriched from MNCs using an anti-CD34 antibody-coated MicroCELLector flask (Applied Immune Sciences, Inc., Santa Clara, CA) and then sorted using FITC-conjugated HPCA1 (CD13; Becton Dickinson) (13, 14).

BM-MNCs were suspended in Dulbecco's phosphate-buffered Ca/Mg-free saline containing 1 mmol/liter EDTA (DPBSE) at a concentration of 5×10^6 cells/ml. The cells were loaded into AIS MicroCELLector SBA (Applied Immune Sciences, Inc.) containing covalently immobilized soybean agglutinin (SBA) and incubated for 45 min at room temperature. The nonadherent (SBA-) cells were removed, and 2×10^7 cells were subsequently loaded into AIS MicroCELLector CD34- flasks, which contained a covalently immobilized anti-CD34 monoclonal antibody, ICH3. After incubation for 1 h at room temperature, the nonadherent cells (CD34-) were removed, and the adherent cells (CD34+) were collected after physical agitation in DPBSE containing 10% FBS. The enriched cells (45% positivity for CD34) were collected and washed with Dulbecco's PBS containing 0.1% sodium azide. FITC-conjugated HPCA1 antibody was added to the cells, followed by incubation for 30 min at 4°C. The cells were washed twice with DPBS-azide and sorted with a FACStar Plus®. The purity of the obtained CD34+ was 97%. Total RNA extraction from each population was performed with RNeasy™ solvent (Qiagen/Biotecx Laboratories, Houston, TX).

Flow cytometric analysis. MNCs were obtained by Ficoll-Hypaque centrifugation (Lymphoprep, Neegard, Norway) of BM cells or peripheral blood (PB) collected from the patients and normal volunteers. The DCC protein expression was examined by an indirect immunofluorescence technique. Briefly MNCs were dispensed at 2×10^5 cells/tube and incubated with 100 µl of PBS containing 100 nM of an anti-DCC mAb, AF5 (Oncogene Science, Inc., Manhasset, NY) specific for the extracellular domain, and 0.1% azide for 60 min on ice. After washing with PBS, the cells were incubated with 50 µl of phycoerythrin (PE)- or FITC-conjugated goat anti-mouse IgG1 antibody at 4°C for 30 min. The samples were then washed, fixed, and analyzed with a FACScan® (Becton Dickinson). FITC- or PE-conjugated MY4, MY7, HPCA1, Leu9 (CD7), Leu12 (CD19), Leu2a (CD8), Leu 15 (CD11b), anti-factor 8, and anti-glycophorin A were used for staining surface membrane antigens, as described elsewhere (15). CD34-rich cells (mean: 40.8%, $n = 4$) prepared with an anti-CD34 antibody-coated CELLector flask (Applied Immune Sciences, Inc.) (13) were subjected to two-color FACS® analysis of CD34 and AF5. Each two-color analysis experiment was performed at least four times. When two-color FACS® analysis of Leu 15 and AF5 was performed, cells in the granulocyte gate of PB were the test materials.

Immunoprecipitation (IP) analysis. 2×10^7 MNC were metabolically labeled with 10 µCi/ml of [³⁵S]methionine and [³⁵S]cysteine for 3.5 h in methionine- and cysteine-free RPMI 1640 medium containing 10% dialyzed FBS. After labeling, the cells were washed with PBS and lysed in 500 µl of RIPA buffer (50 mM Tris-HCl, pH 7.5, 150 mM NaCl, 5 mM EDTA, 1% NP-40, 0.5% deoxycholate, and 0.1% SDS with protease inhibitors (1 mM PMSF, 50 µg/ml aprotinin, 5 µg/ml leupeptin)). Cell debris was removed by cen-

trifugation. The supernatant was precleared by incubation with rabbit serum and protein A-Sepharose on ice for 30 min. The precleared lysates were assayed for incorporation, and $1-3 \times 10^7$ cpm was used for each IP. The supernatant was then incubated with an mAb, AF5 (20 µg/ml) or G97-449 (specific for the cytoplasmic domain, 20 mg/ml; Pharmingen, San Diego, CA) for 1 h on ice. DCC-specific immunoprecipitates were recovered with 30 µl of a 50% suspension of protein A-Sepharose and washed two times with NP-40 buffer (50 mM Tris, pH 8.0, 1.0% NP-40, 50 mM NaCl) and once with 10 mM Tris (pH 8.0). The proteins released from the immunoprecipitates by Laemmli's sample buffer were subsequently analyzed by electrophoresis on 5-25% SDS-PAGE (16). After drying, the gels were exposed to films. The protein concentration was determined by Bio-Rad protein assay (Bio Rad Laboratories, Hercules, CA).

Results

DCC protein is expressed on cell surface of specific lineages of normal BM and PB cells. Fig. 1 B and Table I show the results of a normal volunteer by single-color flow cytometric analysis. The DCC protein was detected at rates of 6.6-57.0% ($n = 16$; mean: 31.4%). To clarify which cell lineages of MNCs express the DCC protein, two-color flow cytometric analysis was performed. Fig. 2 shows a typical example of a normal individual, and Table II summarizes the data. The DCC protein was expressed in high positivity on CD14+, CD13+, and factor 8+ cells among BM-MNCs. CD19+ and CD7+ cells were also positive, whereas CD34+ and glycophorin A+ cells were negative for the DCC protein. CD11b+, CD13+, and CD8+ cells

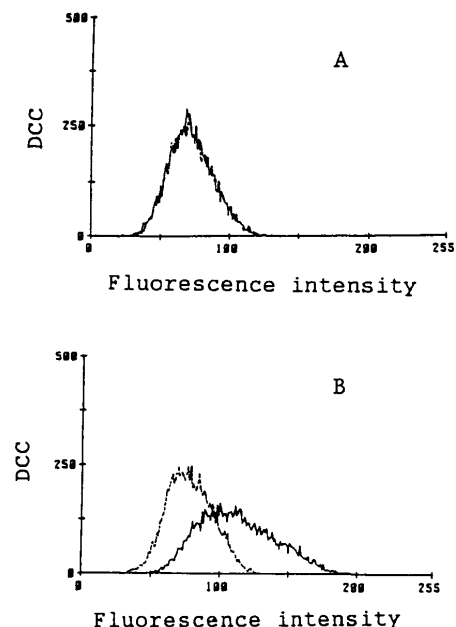


Figure 1. Single-color flow cytometric analysis of DCC expression on MNCs from an MDS case (A) and a normal volunteer (B). Cells were incubated with AF5 mAb, followed by FITC-labeled goat anti-mouse IgG. Cells were analyzed by single-color fluorescence using a FACScan® flow cytometer. The percentage of positive cells was 0.2 and 55.4%, respectively. Solid lines, AF5; dashed lines, control mouse IgG.

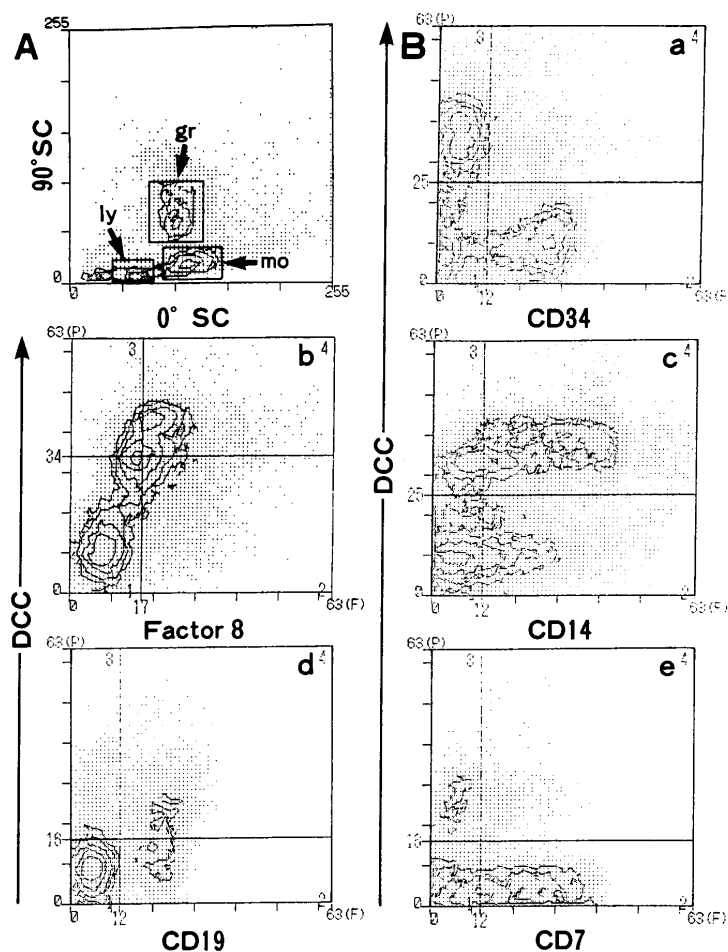


Figure 2. Example of analysis of DCC protein expression on surface MNCs from normal BM and PB. **A** depicts the light scattering of BM-MNCs. Viable MNCs were gated with forward scatter (x-axis) against side-ward scatter (y-axis). Lymphocyte (*ly*), monocyte (*mo*), and granulocyte (*gr*) gates were created. (**B**) x-axis: **a**, CD34-FITC intensity in all gates; **b**, factor 8-FITC intensity in *ly* gate; **c**, CD14-FITC intensity in *mo* gate; **d**, CD19-FITC intensity in *ly* gate; **e**, CD7-FITC intensity in *ly* gate. y-axis: **a–e**, PE-labeled DCC intensity.

of PB were also negative. Thus, two-color flow cytometric analysis revealed that the monocyte lineage was consistently DCC positive and that the granulocyte lineage was transiently DCC positive in the immature stage. B cell lineages were weakly positive, although T cell lineages were low positive or negative for DCC. After fractionating BM-MNC of normal volunteers, expression of the DCC gene in the CD13+, CD14+, and CD34+ populations was investigated by RT-PCR analysis (Fig. 3). The RT-PCR data paralleled the abundance of the immunoreactive DCC protein on BM-MNC. No PCR product of the DCC transcript, or the DCC protein, could be detected from CD34+ cells.

DCC protein is absent from cell surface of BM-MNCs of MDS/AML patients. Although the DCC protein was expressed on MNCs from normal volunteers, it was not detected (0.1–1.5%) in any of the 17 MDS or 10 AML patients, as shown in Fig. 1 *A* and Table I. Two-color flow cytometric analysis also showed that the DCC protein was not expressed in the MDS patients. BM-MNCs of the MDS contain the same populations as that of normal subjects. Thus, in the MDS pa-

tients, the CD14+, CD13+, and factor 8+ populations of BM-MNCs were all negative for the DCC protein (data not shown), whereas these cell lineages from normal volunteers were positive.

Loss of antigenicity of the DCC protein on cell surface of BM-MNC from MDS/AML patients. Because the DCC transcript was detected by RT-PCR analysis in 80 of 101 MDS/AML patients, as shown in Fig. 4 and summarized in Table III, we speculated that the antigenicity of the DCC protein must have been reduced or lost even in cases having a DCC-specific RT-PCR product. To confirm this speculation, IP analysis was performed of BM-MNC from normal volunteers and MDS/AML patients. As shown in Fig. 5, *A* and *B*, the DCC protein from normal MNCs migrated at the region of a molecular mass of ~180 kD. On the other hand, the DCC band corresponding to 180 kD could not be detected in an AML (M0) patient (lane 5) or an MDS (RAEB) patient (lane 7) (Fig. 5 *B*). A reduced amount of DCC protein was detected in an RA patient (Fig. 5 *B*, lane 6). These three AML/MDS patients have a DCC-specific RT-PCR product. Two antibodies specific for either the

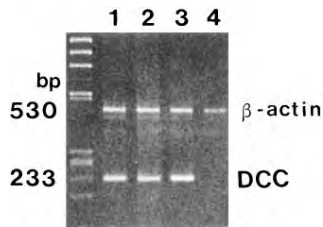


Figure 3. RT-PCR analysis of expression of the DCC of purified CD34+, CD14+, and CD13+ cells from normal BM-MNCs. Isolated CD34+ cells were prepared in an anti-CD34 antibody-coated CELLector flask followed by cell sorting as

described in Methods. CD14+ and CD13+ cells were prepared by cell sorting. cDNA was synthesized from 0.0125 OD₂₆₀ units of total RNA. After cDNA was synthesized using a DCC2 primer, PCR was performed using DCC1 and DCC2 primers. The PCR products (233 bp) were size fractionated by 3% agarose gel electrophoresis. Expression of the β-actin gene is shown at 530 bp as an internal control. Lane 1 shows BM-MNCs from healthy volunteers; lane 2, CD13+ cells; lane 3, CD14+ cells; lane 4, CD34+ cells. The left lane shows markers of λ DNA fragments digested by HindIII and φx 174 DNA fragments digested by HaeIII.

extracellular or cytoplasmic domain were used to examine for the DCC protein by IP analysis in another MDS patient having a DCC-specific RT-PCR product. An ~180-kD DCC protein was obviously detected by the G97-449 antibody (specific for the cytoplasmic domain of the DCC protein), whereas a band with greatly reduced intensity and the same mobility, as shown in lane 2 of Fig. 5 C, was detected by the AF5 antibody (specific for the extracellular domain). Table IV compiles the qualitative levels of DCC expression by various assays in selected MDS/AML patients. DCC-RNA was detectable by the more sensitive RT-PCR assay in many patients. The normal-sized DCC protein was detected by G97-449 and/or AF5 antibody in some RT-PCR-positive patients (MDS-1, -2, AML-1, and -2 in Table IV).

Discussion

The DCC gene, which has been postulated to be a tumor-suppressor gene, was first identified in a colon cancer study by Fearon et al., in which they found that the tissue of 71% of their colon cancer patients showed an allelic DCC deletion and that 88% of these patients showed a reduced DCC expression, in contrast to the DCC expression seen in most normal tissues (1). Further, the DCC expression has been found to be low or lost in patients with pancreatic (17), esophageal (18), prostatic (19), and other carcinomas (2, 20). Also, in leukemia

Table I. Positivity for the DCC Protein

Sources of BM-MNC		DCC positivity (%)
Normal	(n = 16)	6.6–57.0 (mean: 31.4)
MDS	(n = 17)	0.1–1.5 (mean: 0.9)
AML	(n = 10)	0.1–0.9 (mean: 0.5)

Single-color flow cytometry analysis of BM-MNC was performed by indirect immunofluorescence assay. An anti-DCC mAb, AF5, specific for the extracellular domain of DCC, was used. The detailed patients with MDS or AML are presented in Methods.

cases, we and other investigators have found that DCC gene inactivation in some instances appears to contribute to leukemogenesis (3–6). However, while these findings suggest that a loss in the DCC expression is critical to cancer development, little is known about DCC mechanisms that may mediate tumoral suppression.

Similarly, the role that the DCC protein plays in cellular development and differentiation also remains unclear. It has been reported that the DCC protein was found in the axons of the central and peripheral nervous system and in differentiated cell types of the intestine (9). Further, a recent study suggests that the DCC protein may stimulate the PC12 neuritic outgrowth in a manner similar to neural cell adhesion molecules and N-cadherin (7). Cell-cell interaction through the DCC protein was required to stimulate PC12 to differentiate morphologically. Given these considerations, we thus have speculated that the participation of the DCC protein in both cellular development and differentiation occurs in a hematopoietic manner.

This study found that the DCC protein expression in CD34+ cells is very low, whereas in mature cells, i.e., the CD14+, CD13+, CD19+, and the factor 8+ cells, the DCC protein expression is high. These findings are consistent with a previous study in which the DCC protein was found in differentiated cell types of the normal intestine (9); of great interest is that the DCC protein content was very low in the CD8+ (T cells and NK cells) subsets, the erythrocyte lineage, and the CD11b subset of the mature granulocyte lineage. An uneven DCC protein distribution in normal hematopoiesis strongly supports the hypothesis that the DCC protein may act on differentiation pathways and that a cell's fate is determined by the cell-to-cell interaction (7).

With regard to oncogenesis, the first direct evidence that the DCC gene is functionally a tumor suppressor was obtained from an experimental animal study (21), wherein it was found

Table II. DCC Protein Positivity by Two-Color Flow Cytometric Analysis of Normal BM- and PB-MNC

CD+ cells	CD34	CD14	CD13	CD11b	Fact.8	Gly.A	CD19	CD7	CD8
BM	+/- (4)	++ (11)	++/+ (12)		++/+ (6)	- (10)	+ (5)	+/- (5)	
PB		++/+ (6)	- (8)	- (4)			+/- (6)	+/- (7)	- (5)

++, > 50%; +, 20–50%; +/-, 5–10%; -, 0–5%. Fact.8, Factor 8; Gly.A, glycophorin A. Numbers in parentheses represent numbers of study, respectively.

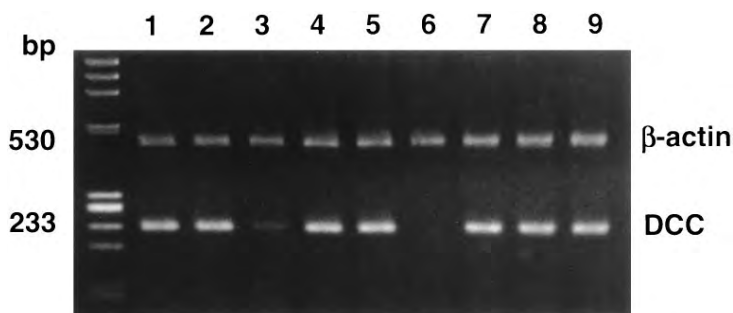


Figure 4. RT-PCR analysis of expression of the DCC gene in MDS/AML patients. After cDNA was produced using a DCC2 primer, PCR was performed using DCC1 and DCC2 primers. The PCR products (233 bp) were size fractionated by 3% agarose gel electrophoresis. Expression of the β -actin gene is shown at 530 bp as an internal control. Lanes 1 and 2 are control samples from BM-MNCs from healthy volunteers. Lanes 3–5 are BM-MNCs from MDS patients. Lanes 6–9 are BM-MNCs from AML patients. Expression of the DCC gene was reduced in lane 3 and absent in lane 6. The left lane shows marker of λ DNA/HindIII fragments and ϕ x 174 DNA/HaeIII fragments.

that the wild-type, full-length DCC gene expression inhibited tumor growth in human epithelial cells (1811-NMU-T1) in subcutaneous tissue of nude, athymic mice. In contrast, a truncated DCC gene is unable to suppress tumorigenesis, since it lacks the major portion of the cytoplasmic carboxy domain of the DCC protein.

Our previous observation that there is very low expression or absent expression of DCC on MNC from AML and MDS

patients supports previous DCC gene expression studies. Thus, it may be that some BM-MNCs of MDS or leukemic cells that show an apparent RNA expression of the DCC gene are expressing an aberrant protein after a reduction in their antigenicity.

Although the results shown in Fig. 5 C appear to suggest that the AF5 antibody may be less efficient at immunoprecipitating DCC than the G97-449 antibody, based on the summary provided in Table IV, two other possibilities that may account for poor IP may be a loss in the specific antigenicity of the extracellular (or cytoplasmic) domain or a disturbance in the DCC protein transport to the cell surface due to an unknown disorder. In this regard, since the AF5 antibody was suffi-

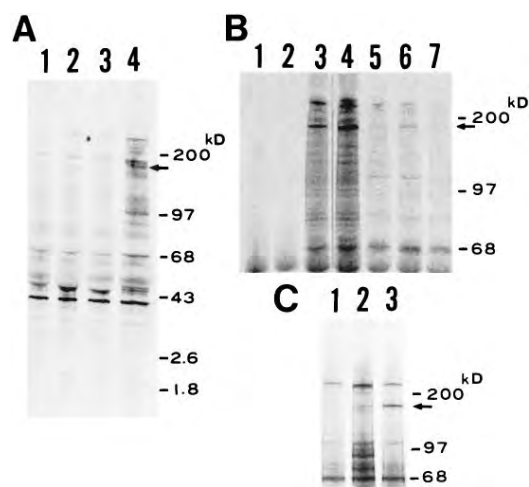


Figure 5. Characterization of DCC molecule identified by anti-DCC mAbs. IP analysis of normal PB (A). Lanes 1–3 show bands immunoprecipitated by three types of control mouse IgG1, IgG1, and IgG2a, (Becton Dickinson and DAKO, Copenhagen, Denmark). Lane 4 shows a DCC-specific 180-kD band identified by AF5 mAb. IP analysis of BM-MNCs from a normal volunteer and from two MDS patients and one AML patient using AF5 and G97-449 mAbs (B). Lanes 1 and 2 show two types of IgG1 (Becton Dickinson and DAKO) immunoprecipitates of normal BM-MNCs, and lanes 3 and 4 show G97-449 and AF5 immunoprecipitates of the same normal BM. Lane 5 shows an AF5 immunoprecipitate of an AML (M0) patient. Lanes 6 and 7 show AF5 immunoprecipitates of two MDS (RA and RAEB) patients. IP analysis of BM-MNCs of an MDS (RA) patient using AF5 and G97-449 mAbs (C). Lane 1 is control IgG1 immunoprecipitate; lane 2, AF5 immunoprecipitate; lane 3, G97-449 immunoprecipitate. Arrows indicate DCC-specific bands. The relative mobilities of molecular mass markers are indicated at the right side of each figure.

Table III. Expression of the DCC Gene in MDS/AML Patients

Disease	No. of patients examined	No. of patients with reduced DCC expression	No. of patients with absent DCC expression
MDS			
RA	16	1	0
RARS	3	0	0
RAEB	14	2	1
RAEB-t	15	2	1
Total	48	5	2
AML			
M0	3	1	1
M1	12	1	3
M2	16	3	2
M3	7	0	1
M4	10	1	0
M5	2	0	0
M6	3	0	1
Total	53	6	8
Normal sample	24	0	0

Expression of the DCC gene was analyzed by RT-PCR as described in Methods and reference 3. 48 untreated MDS patients and 53 AML patients were analyzed by RT-PCR assay. 24 healthy volunteers were also investigated. AML and MDS were diagnosed according to the French-American-British criteria (10). Compared with the density of the DCC product of the normal sample, no band for the product was surmised to represent absent DCC expression, whereas reduced density was interpreted as reduced DCC expression. RARS, RA with ringed sideroblasts; RAEB-t, RAEB in transformation.

Table IV. DCC mRNA and Protein Expression in Selected MDS/AML Patients

Patients	RT-PCR	FACS®	IP	
			AF5	G97-449
Normal	+	+	+	+
MDS				
MDS-1	+	—	+-	+
MDS-2	+	—	+-	+
MDS-3	+	—	—	ND
MDS-4	+-	—	—	—
MDS-5	—	—	—	—
AML				
AML-1	+	—	—	+-
AML-2	+	—	+	—
AML-3	+-	—	—	ND
AML-4	—	—	—	—
AML-5	—	—	—	ND

The qualitative levels of DCC expression were determined by various assays in normal subjects and MDS/AML patients. The assays for DCC protein include FACSscan® flow cytometric analysis and IP using AF5 or G97-449 mAbs. mRNA was assayed by RT-PCR. Three normal samples were investigated. ND, assay not done for the individual patient. +, results of DCC assay were positive; +-, result of DCC assay was reduced; —, result of DCC assay was negative.

ciently efficient at immunoprecipitating the DCC of normal BM-MNCs (Table IV and Fig. 5 B) and, unlike the G97-449 antibody, it detected a sufficient intensity in the DCC band of an AML patient (AML-2; Table IV), it may be that either or both of these two possibilities may be the reason(s).

The DCC role in normal hematopoiesis and leukemogenesis is certain to be better understood once its ligand and effector molecules are more clearly characterized.

Acknowledgments

We thank the many physicians who referred their patients for study. We thank Drs. K.R. Cho, L. Hedrick, and B. Vogelstein for providing DCC plasmids. We also thank S. Inokuchi and H. Hanawa for preparing the manuscript.

This study was supported in part by a Grand-in-Aid for Scientific Research on Priority Areas (No. 06671116) from the Ministry of Education, Science and Culture of Japan.

References

1. Fearon, E.R., K.R. Cho, J. M. Nigro, S.E. Kern, J.W. Simons, J.M. Rupert, S.R. Hamilton, A.C. Preisinger, G. Thomas, K.W. Kinzler, and B. Vogel-

stein. 1990. Identification of a chromosome 18q gene that is altered in colorectal cancers. *Science (Wash. DC)*. 247:49–56.

2. Scheek, A.C., and S.W. Coons. 1993. Expression of the tumor suppressor gene DCC in human gliomas. *Cancer Res.* 53:5605–5609.

3. Miyake, K., K. Inokuchi, K. Dan, and T. Nomura. 1993. Alterations in the deleted in colorectal carcinoma gene in human primary leukemia. *Blood*. 82:927–930.

4. Porfiri, E., L.M. Secker-Walker, A.V. Hoffbrand, and J.F. Hancock. 1993. DCC tumor suppressor gene is inactivated in hematologic malignancies showing monosomy 18. *Blood*. 81:2696–2701.

5. Miyake, K., K. Inokuchi, K. Dan, and T. Nomura. 1993. Expression of the DCC gene in myelodysplastic syndromes and overt leukemia. *Leuk. Res.* 17: 785–788.

6. Miyake, K., K. Inokuchi, and T. Nomura. 1994. Expression of the DCC gene in human hematological malignancies. *Leuk. & Lymphoma*. 16:13–18.

7. Pierceall, W.E., K.R. Cho, R.H. Getzenberg, M.A. Reale, L. Hedrick, B. Vogelstein, and E.R. Fearon. 1994. NIH3T3 cells expressing the deleted in colorectal cancer tumor suppressor gene product stimulate neurite outgrowth in rat PC12 pheochromocytoma cells. *J. Cell Biol.* 124:1017–1027.

8. Reale, M.A., G. Hu, A.J. Zafar, R.H. Getzenberg, S.M. Levine, and E.R. Fearon. 1994. Expression and alternative splicing of the deleted in colorectal cancer (DCC) gene in normal and malignant tissues. *Cancer Res.* 54:4493–4501.

9. Hedrick, L., K.R. Cho, E.R. Fearon, T.-C. Wu, K. W. Kinzler, and B. Vogelstein. 1994. The DCC gene product in cellular differentiation and colorectal tumorigenesis. *Genes & Dev.* 8:1174–1183.

10. Bennett, J.M., D. Catovsky, M.T. Daniel, G. Flandrin, D.A.G. Galton, H.R. Gralnick, C. Sultan, The French-American-British (FAB) Co-operative Group. 1982. Proposals for the classification of the myelodysplastic syndromes. *Br. J. Haematol.* 51:303–306.

11. Chirgwin, J.M., A.E. Przybyla, R.J. MacDonald, and W.J. Rutter. 1979. Isolation of biologically active ribonucleic acid from sources enriched in ribonuclease. *Biochemistry*. 18:5294–5299.

12. Inokuchi, K., T. Inoue, A. Tojo, M. Futaki, K. Miyake, T. Yamada, Y. Tanabe, I. Ohki, K. Dan, K. Ozawa, et al. 1991. A possible correlation between the type of bcr-abl hybrid messenger RNA and platelet count in Philadelphia-positive chronic myelogenous leukemia. *Blood*. 78:3125–3127.

13. Lebkowski, J.S., L.R. Schain, D. Okrongly, R. Levinsky, M.J. Harvey, and T.B. Okarma. 1992. Rapid isolation of human CD34 hematopoietic stem cells. Purging of human tumor cells. *Transplantation (Baltimore)*. 53:1011–1019.

14. Hatzfeld, J., M.-L. Li, E.L. Brown, H. Sookdeo, J.-P. Levesque, T. O'Toole, C. Gurney, S.C. Clark, and A. Hatzfeld. 1991. Release of early human hematopoietic progenitors from quiescence by antisense transforming growth factor B1 or Rb oligonucleotides. *J. Exp. Med.* 174:925–929.

15. Abo, J., K. Inokuchi, K. Dan, and T. Nomura. 1993. p53 and N-ras mutations in two new leukemia cell lines established from a patient with multilineage CD7-positive acute leukemia. *Blood*. 82:2829–2836.

16. Inokuchi, K., Y. Goto, Y. Terashi, N. Amuro, and R. Shukuya. 1984. Changes in the activity of submitochondrial protein synthesis in the liver of bullfrog tadpole, *Rana catesbeiana*, during metamorphosis. *Comp. Biochem. Physiol.* 77B:733–735.

17. Hohne, M.W., M.-E. Halatsch, G.F. Kahl, and R.J. Weinle. 1992. Frequent loss of expression of the potential tumor suppressor gene DCC in ductal pancreatic adenocarcinoma. *Cancer Res.* 52:2616–2619.

18. Miyake, S., K. Nagai, K. Yoshino, M. Oto, M. Endo, and Y. Yuasa. 1994. Point mutations and allelic deletion of tumor suppressor gene DCC in human esophageal squamous cell carcinomas and their relation to metastasis. *Cancer Res.* 54:3007–3010.

19. Gao, X., K.V. Honn, D. Grignon, W. Sakr, and Y.Q. Chen. 1993. Frequent loss of expression and loss of heterozygosity of the putative tumor suppressor gene DCC in prostatic carcinomas. *Cancer Res.* 53:2723–2727.

20. Chenevix-Trench, G., J. Leary, J. Kerr, J. Michel, R. Kefford, T. Hurst, P.G. Parsons, M. Friedlander, and S.K. Khoo. 1992. Frequent loss of heterozygosity on chromosome 18 in ovarian adenocarcinoma which does not always include the DCC locus. *Oncogene*. 7:1059–1065.

21. Klingelhutz, A.J., L. Hedrick, K.R. Cho, and J.K. McDougall. 1995. The DCC gene suppresses the malignant phenotype of transformed human epithelial cells. *Oncogene*. 10:1581–1586.

Establishment of a Cell Line With Variant *BCR/ABL* Breakpoint Expressing P180BCR/ABL From Late-Appearing Philadelphia-Positive Acute Biphenotypic Leukemia

Koiti Inokuchi,^{1*} Tamiko Shinohara,² Makoto Futaki,¹ Hideki Hanawa,¹ Sakae Tanosaki,¹ Hiroki Yamaguchi,¹ Takeo Nomura,³ and Kazuo Dan¹

¹Division of Hematology, Department of Internal Medicine, Nippon Medical School, Tokyo, Japan

²The Okinaka Memorial Institute for Medical Research, Tokyo, Japan

³Nippon Medical School, Tokyo, Japan

In acute leukemia (AL) with a late-appearing Philadelphia (la-Ph) translocation, it is unclear whether these translocations arise from the same molecular event as classical Ph translocations. In order to elucidate the molecular events of la-Ph and subsequent translocations of la-Ph leukemia, we performed molecular analysis on the complex rearrangements, in a cell line, MY, which was established from bone marrow mononuclear cells of a patient with a la-Ph acute biphenotypic leukemia. This la-Ph, expressing an acute lymphoblastic leukemia (ALL)-type *BCR/ABL* transcript, produces a novel P180BCR/ABL fusion protein reflecting deletion of 174 bases (58 amino acids) encoded by the $\alpha 2$ exon of the *ABL* gene. An immune complex kinase assay showed that this protein had autophosphorylation activity. Fluorescence in situ hybridization (FISH) in conjunction with G-banding analysis revealed that the initial der(9)t(9;22)(q34;q11) progressed to a der(9)(9pter→9q34::22q11→22q13::5q11.2→5q15::10q23→10qter) by, first, a three-way translocation among the der(9)t(9;22)(q34;q11), chromosome 5, and the normal chromosome 22, and then a subsequent translocation with chromosome 10. Moreover, both the end-stage leukemic cells of the patient and the MY cell line had another translocation, t(X;12)(p11.2;p13). The 12p breakpoint was located near the *ETV6* gene by analysis of pulsed-field gel electrophoresis, but transcription of *ETV6* was unaffected. Tumorigenicity analysis indicated that an additional translocation, t(2;3)(p16;q29), may have caused a more malignant clone, because only MY cells with the t(2;3)(p16;q29) were capable of growing subcutaneously in nude mice within 40 days. The molecular events of leukemogenesis and leukemic progression in the present la-Ph AL occurred by accumulation of unique translocations. This cell line, MY, expressing a novel variant P180BCR/ABL protein with a deletion of the $\alpha 2$ exon of the *ABL* gene, may be useful for elucidating the pathophysiology of this fusion protein and for studying *ETV6*-related leukemogenesis and t(2;3), as well as the molecular mechanisms of the complex translocations. *Genes Chromosomes Cancer* 23:227–238, 1998. © 1998 Wiley-Liss, Inc.

INTRODUCTION

The Philadelphia (Ph) translocation, t(9;22)(q34;q11.2), is found in most patients with chronic myelogenous leukemia (CML) and in subsets of patients with acute lymphoblastic leukemia (ALL) and acute myelogenous leukemia (AML). The *ABL* gene on chromosome 9 is usually translocated to the 8.5 kb major breakpoint cluster region (M-bcr) in the *BCR* gene on chromosome 22 (De Klein et al., 1982). This chimeric *BCR/ABL* gene expresses a chimeric 8.5 kb *BCR/ABL* transcript that encodes a p210 tyrosine kinase (P210BCR/ABL). In most patients with Ph-positive ALL, the *ABL* gene is translocated to a more 5' minor breakpoint region (m-bcr) in the first intron of the *BCR* gene. As a result, the e1-a2 mRNA (a 7.0 kb *BCR/ABL* transcript) is translated into a P185BCR/ABL tyrosine kinase (Chan et al., 1987). These translocations are critical for leukemogenesis because transgenic mice bearing the P185BCR/ABL or P210BCR/ABL fusion

gene develop hematologic features similar to those of human acute leukemias or CML (Daley et al., 1990; Voncken et al., 1992).

The late appearance of the Ph chromosome, which is of interest in leukemogenesis and leukemic progression, has been documented in some leukemias (Najfeld et al., 1989; Katsuno et al., 1994). However, little has been done to investigate the molecular events in la-Ph patients. Late-appearing Ph is frequently associated with additional chromosomal abnormalities. The present leukemia and leukemic cell line also had additional translocations of 12p13, in which the *ETV6* gene is located, and a t(2;3)(p16;q29).

In order to elucidate the molecular events of leukemogenesis and leukemic progression of la-Ph

*Correspondence to: Koiti Inokuchi, M.D., Ph.D., Division of Hematology, Department of Internal Medicine, Nippon Medical School, 1-1-5 Sendagi, Bunkyo-ku, Tokyo 113, Japan.

Received 16 September 1997; Accepted 14 April 1998

TABLE 1. Surface Marker Analysis of Original Leukemic Cells and MY Cells

CD	Positive cells (%)		
	Onset	Second relapse	MY cells
CD2	15.8	40.4	0.9
CD3	16.0	32.6	0.8
CD5	25.6	30.2	1.5
CD7	16.8	35.5	0.8
CD10	94.6	55.9	98.1
CD13	98.9	29.7	99.1
CD14	15.5	4.9	0.7
CD19	99.5	52.3	98.4
CD20	99.3	40.9	3.9
CD33	99.0	4.6	2.5
CD34	62.5	68.4	70.5
CD41	0.9	8.3	0.4
Glycophorin A	4.5	3.3	0.8
HLA-DR	97.4	82.5	100.0

leukemia, we performed a molecular analysis on this rearrangement. We found expression of a variant P185BCR/ABL tyrosine kinase, and we determined the breakpoint near the *ETV6* gene and investigated the tumorigenic capacity of the novel translocation t(2;3).

MATERIALS AND METHODS

Case Report

A 52-year-old woman was diagnosed as having acute biphenotypic leukemia. The peripheral leukocyte count at diagnosis was $188 \times 10^9/L$ with 92% lymphoblasts. Hemoglobin was 10 g/dL, and the platelet count was $52 \times 10^9/L$. The bone marrow (BM) aspirate showed hypercellular BM containing 92% lymphoblasts. The spleen was moderately enlarged, but there was no hepatomegaly, mediastinal mass, or central nervous system (CNS) involvement at diagnosis. The immunophenotype of the leukemic cells is summarized in Table 1. Leukemic cells expressed B-lymphoid markers (CD10, 19, and 20), myeloid markers (CD13, 33, and 34), and HLA-DR. The leukemic cells were positive for periodic acid-Schiff (PAS) but negative for peroxidase, chloroacetate esterase, and α -naphthyl butyrate esterase. Cytogenetic analysis of BM mononuclear cells (MNCs) at diagnosis revealed a normal karyotype. Induction chemotherapy was begun immediately, but remission was not obtained, and a Ph clone emerged. After further induction chemotherapy, a remission was obtained, but the patient soon relapsed. Cytogenetic analysis now revealed a complex Ph with additional chromosomal abnormalities (Table 2). After that, the leuke-

mia became refractory to chemotherapy regimens. At 9 months after diagnosis, the leukemic cells acquired a more complex rearrangement and a t(X;12) (Table 2). The patient died 10 months after diagnosis.

Establishment of a Cell Line

BM-MNCs were harvested 9 months after diagnosis and were separated by density gradient centrifugation using Ficoll-Hypaque. The cells were washed three times with IMDM 1640 medium (GIBCO, Grand Island, NY) supplemented with 10% fetal calf serum (FCS), 2×10^{-3} mol/L glutamine, and 100 μ g/mL gentamicin (Schering Pharmaceutical, Kenilworth, NJ). The cells were cultured in Alpha medium supplemented with 10% FCS at 37°C in a humidified atmosphere containing 5% CO₂. After 1 week, the culture medium was replaced with fresh medium. After initial growth was noted, the cells were propagated in vitro twice weekly by replacement of medium containing 10% FCS without addition of growth factors.

Immunologic Marker Studies

Surface markers of the leukemic blasts and of the cell lines were determined by direct immunofluorescence using flow cytometry on a FACS II (Becton-Dickinson, Sunnyvale, CA) flow cytometer, as previously described (Abo et al., 1993). Cells were incubated with appropriately diluted fluorescein isothiocyanate (FITC)-conjugated MoAb for 30 min at 4°C. Cells were washed twice, and the percentage of positive cells was determined. To determine background fluorescence, we stained control cells with FITC-conjugated normal mouse immunoglobulin.

Cytogenetic Studies

Cytogenetic studies were performed by the conventional trypsin-Giemsa banding technique (Abo et al., 1993). The bone marrow cells at diagnosis and relapse stages as well as established cell line cultures were processed by a direct method. The karyotype was determined by both direct microscopic analysis and photography.

Reverse Transcriptase-Polymerase Chain Reaction and Sequencing of the BCR/ABL mRNA

Total RNA of cells was extracted by RNeasy. Reverse transcriptase-polymerase chain reaction (RT-PCR) was carried out with minor modifications of the original method (Inokuchi et al., 1997a). Complementary DNA was prepared from 200 ng of total RNA using random 9-mers and reverse trans-

TABLE 2. Summary of Sequential Cytogenetic Analyses of Leukemic Cells from the Patient

Disease state and time (time after diagnosis)	Karyotype	Number of metaphases
Onset	46,XX	20/20 cells
Induction failure (2 months)	46,XX,t(9;22)(q34;q11) other karyotype ^a with 46,XX,t(9;22)(q34;q11)	6/20 cells
First relapse (6 months)	46,XX,t(9;22)(q34;q11),-20,add(21)(q22) 46,X,t(X;12)(p11.2;p13),der(5)(5pter→5q11.2::22q11→22qter), der(9)(9pter→9q34::5q11.2→5qter),del(10)(q11.2),+14,-17,+19, der(22)(22pter→22q11::9q34→9qter),del(22)(q11) 46,X,t(X;12)(p11.2;p13), der(5)(5pter→5q11.2::22q11→22qter), der(9)(9pter→9q34::5q11.2→5qter), del(10)(q11.2), -13,+19,-20,der(22)(22pter→22q11::9q34→9qter), del(22)(q11)	14/20 cells 18/20 cells 1/20 cells 1/20 cells
Second relapse (9 months)	46,XX,der(5)(5pter→5q11.2::22q11→22qter), der(9)(9pter→9q34::5q11.2→5qter),del(10)(q11.2),inv(12)(p13q13), der(22)(22pter→22q11::9q34→9qter),del(22)(q11) 46,X,t(X;12)(p11.2;p13),der(5)(5pter→5q11.2::22q11→22qter), der(9)(9pter→9q34::5q11.2→5qter), der(10)(10pter→10q23::5q15→5qter), der(22)(22pter→22q11::9q34→9qter), del(22)(q11) 47,XX,der(5)(5pter→5q11.2::22q11→22qter), der(9)(9pter→9q34::5q11.2→5qter),inv(12)(p13q13), der(22)(22pter→22q11::9q34→9qter),del(22)(q11),+mar 44,X,t(X;12)(p11.2;p13),-2,der(5)(5pter→5q11.2::22q11→22qter), der(9)(9pter→9q34::5q11.2→5q15::10q23→10qter), der(10)(10pter→10q23::5q15→5qter),-18, der(22)(22pter→22q11::9q34→9qter),del(22)(q11) 46,XX	11/20 cells 5/20 cells 2/20 cells 1/20 cells 1/20 cells

^aNonspecific aberration.

criptase. The cDNA was amplified by e-1 (5'-CCGAGGCCACCATCGTTGGGCGTCC-3') and abl-2 (5'-GTTTCTCCACACTGTTGACTG-3'). The PCR products were electrophoresed on a 2% agarose gel, stained with ethidium bromide, Southern-transferred, and hybridized to a 5' end-labeled *ABL*-exon oligonucleotide probe (5'-GTAGCATC-TGAGTTTGAGCCTGAG-3').

After RT-PCR, products were electrophoresed on a 2% agarose gel and stained with ethidium bromide; the 201 bp fragment was sliced from the gel, electroeluted, purified with phenol, and ethanol-precipitated. The fragments were subcloned into the *EcoRV* site of a pGEM-5Zf (+/-) cloning vector. Transfected cells were plated onto Luria-Beriani (LB)-ampicillin agar plates containing 5-bromo-4-chloro-3-indolyl- β -D-galactoside (X-Gal) and isopropylthio- β -D-galactoside (IPTG). White colonies were transferred to a fresh LB-ampicillin agar plate containing X-Gal and IPTG and cultured overnight for secondary selection. Confirmed white colonies were then transferred into 150 ml of LB medium containing 50 mg/mL ampicillin and cultured at 37°C for 4 hr. The cultures were centrifuged, resuspended in 20 mL of water, and heated at 98°C for 10 min. After centrifugation, the resulting supernatants were used for PCR with T7 or SP6 primers. The PCR products were sequenced by using an ABI sequencer with dye terminators (Perkin Elmer, Warrington, U.K.). All sequences were confirmed by sequencing in both orientations.

Kinase Assay for BCR/ABL Protein

An immune complex kinase assay for BCR/ABL protein was performed (Wada et al., 1995). Cells were solubilized at 1×10^7 cells/ml in lysis buffer [0.15 M NaCl, 50 mM Tris-HCl (pH 7.4), 1% Triton X-100, 1% sodium deoxycholate, 0.1% SDS, 5 mM EDTA, 2 mM phenylmethylsulfonyl fluoride, 500 units/mL aprotinin, 0.1 mM ZnCl₂, and 0.1 mM Na₃SO₄] at 4°C for 20 min. The lysates were clarified by centrifugation at $10,000 \times g$ for 10 min and pretreated with rabbit sera for 15 min, and then with protein A-Sepharose (Pharmacia, Tokyo, Japan) for 45 min at 4°C. Immunoprecipitation was performed by the addition of 3 μ l of anti-ABL antibody (8E9; Pharmingen, San Diego, CA) at 4°C for 2 hr. Immune complexes were collected in protein A-Sepharose and washed extensively with 50 mM Tris-HCl buffer (pH 7.4). The in vitro immune complex kinase assay was performed in the presence of 10 μ Ci [γ -³²P]ATP (>3000 Ci/mmol; Amersham International, Amersham, UK) with 20

mM MnCl₂ and 20 mM HEPES buffer (pH 7.0) at 4°C for 30 min. The samples were analyzed by 5–15% gradient SDS-PAGE (Inokuchi et al., 1997b).

Pulsed-Field Gel Electrophoresis (PFGE) and Synthesis of *ETV6* cDNA Probe

Cells were embedded in 0.75% low-melting-temperature agarose at a concentration of 2×10^7 cells per mL. Cells were treated with 1 mg of proteinase K per mL overnight at 50°C, then inactivated with phenylmethylsulfonyl fluoride. Restriction endonuclease digestion of 2×10^6 cells was accomplished with 200 units of enzyme in 0.3 mL of restriction buffer at 37°C overnight. Digested DNA was electrophoresed on a CHEF-DR II apparatus (Amersham) and incubated with *ETV6* cDNA probe containing nucleotides (nt) 10–149 using a standard technique.

The *ETV6* probe was made using an RT-PCR method (Inokuchi et al., 1997a). Total RNA from normal bone marrow cells was prepared and complementary DNAs (cDNAs) were prepared with the *ETV*-a1 primer (5'-ATGGTTCTGATGCAGTATGACCTC-3'; 458–482). The cDNA was amplified by nested PCR using the first primer set *ETV*-s1 (5'-TCGCTGTGAGACATGTCTGAGACT-3'; 13–36) and *ETV*-a2 (5'-GTGTATAGAGTTTC-CAGGGTGGAA-3'; 425–449), and the second primer set, *ETV*-s2 (5'-GCTCAGTGTGACATTAAGCAGGAA-3'; 40–64). The RT-PCR products of *ETV6* cDNA were subcloned into the *EcoRV* site of the pGEM-5Zf (+/-) cloning vector, and transfected cells were plated onto Luria-Beriani (LB)-ampicillin agar plates exactly as above. Positive cells were selected, and supernatants were used for PCR as above. The PCR products were sequenced in both orientations.

Fluorescence In Situ Hybridization Analysis

The Vysis LSI *BCR-ABL* translocation probe (Vysis, Downers Grove, IL) detects *BCR/ABL* gene fusions in metaphase cells (Yamaguchi et al., 1998) and can be used for identifying either of the two breakpoint regions, major or minor, on chromosome 22. This probe is a mixture of a *BCR* probe labeled directly with Spectrum Green and an *ABL* probe labeled directly with Spectrum Orange. The *ABL* probe begins between exons 4 and 5 and continues for about 200 kb toward the telomere of chromosome 9. The *BCR* probe begins between *BCR* exons 13 and 14 (*M-bcr* exons 2 and 3) and extends to the centromeric region on chromosome 22 for

approximately 300 kb, crossing well beyond the m-bcr region.

The probes specific to chromosome 5, 22, or 9 used for chromosome painting were purchased from Vysis and labeled by standard nick translation using biotin-11-dUTP (Sigma, St. Louis, MO) or digoxigenin-11-dUTP (Boehringer Mannheim, Germany). Two-color fluorescence in situ hybridization (FISH) with various probe combinations was carried out. One hundred to 150 ng of the probe was denatured, allowed to preanneal with unlabeled human Cot-1 DNA (10 to 15 μ g) at 37°C for 20 min, and then hybridized overnight. Biotinylation was detected with avidin-fluorescein isothiocyanate (Vector Laboratories, Burlingame, CA), biotinylated goat antiavidin (Vector Laboratories), and a second layer of avidin-FITC. Digoxigenin-labeled probes were detected with mouse antidigoxigenin (TRITC) (Boehringer) and goat antirabbit IgG-TRITC (Boehringer). Chromosomes were counterstained with 1 mg/mL of 4,6-diaminido-2-phenylindole dihydrochloride (DAPI) and mounted in antifade solution. Results were analyzed on a conventional fluorescence microscope, Olympus BH2-RFC (Olympus, Tokyo, Japan), and photographed on Fuji D1600 film (Fuji Film, Tokyo, Japan).

Tumorigenicity Assay

This assay was a modification of the original technique (Inokuchi et al., 1991). Five $\times 10^6$ cells were resuspended in 0.5 mL of cold medium. Cells were then injected into subcutaneous sites of athymic nude mice. Tumors that arose within 40 days after inoculation indicated a positive tumorigenicity assay.

RESULTS

Establishment of the Cell Line MY and Its Chromosomal Evolution

BM-MNCs were cultured, and proliferation was noted 3 weeks after the start of culture. The established cell line, designated MY (Fig. 1), has now been maintained continuously for more than 2 years in a suspension culture. We have confirmed that this cell line can be frozen without subsequent alteration of its functional characteristics after thawing. MY cells have a doubling time of approximately 48 hr.

At establishment of the cell line, MY cells had two of the four karyotypes demonstrated at second relapse, as shown in Tables 2 and 3. When MY cells were cultured for 1 year, their karyotype evolved

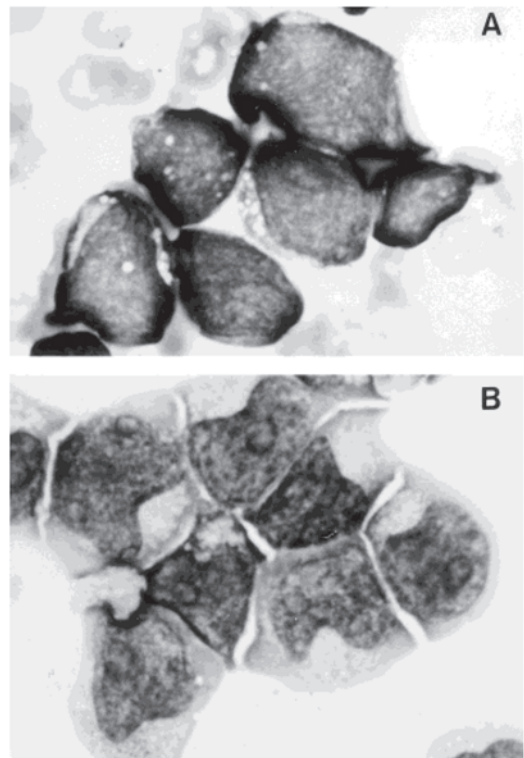


Figure 1. Morphology of the original leukemic cells from bone marrow at second relapse (A) and of MY cells at establishment (B). Wright-Giemsa staining. Magnification 1,000 \times .

(Table 3 and Fig. 2). The clone characterized by a complex rearrangement involving the der(9)t(9;22) became the major clone. Also, a t(2;3)(p16;q29) was subsequently found, and MY cells with the t(2;3) were noted in the major clone. With limiting dilution methods we successfully isolated the subclones M12 and M13, which differed only by M12 having the t(2;3)(p16;q29).

Cell Surface Marker Analysis

The summary of cell surface markers of the original leukemic cells at onset and relapse and MY cells is shown in Table 2. MY cells were positive for CD10, CD19, CD13, CD34, and HLA-DR, but negative for CD33.

Molecular Analysis of BCR/ABL mRNA

The smaller chimeric BCR/ABL product was detected by the ABL-exon oligonucleotide probe (Fig. 3A), but was not detected by the junction oligonucleotide probe (data not shown). To clarify whether the PCR product was an atypical BCR/ABL mRNA, the RT-PCR product was sliced, subcloned

TABLE 3. Sequential Cytogenetic Analyses of MY Cells and Subclones

Cell line	Karyotype	Number of metaphases per 20 cells
Cell line at establishment	46,XX,der(5)(pter→5q11.2::22q11→22qter),der(9)(pter→9q34::5q11.2→5qter),inv(12)(p13q13),der(22)(22pter→22q11::9q34→9qter),del(22)(q11)	14
1 year after establishment	46,X,t(X;12)(p11.2;p13),der(5)(pter→5q11.2::22q11→22qter),der(9)(pter→9q34::5q11.2→5q15::10q23→10qter),der(10)(10pter→10q23::5q15→5qter),der(22)(22pter→22q11::9q34→9qter),del(22)(q11)	6
	46,XX,der(5)(pter→5q11.2::22q11→22qter),der(9)(pter→9q34::5q11.2→5qter),del(10)(q23),inv(12)(p13q13),der(22)(22pter→22q11::9q34→9qter),del(22)(q11)	3
	46,X,t(X;12)(p11.2;p13),der(5)(pter→5q11.2::22q11→22qter),der(9)(pter→9q34::5q11.2→5q15::10q23→10qter),der(10)(10pter→10q23::5q15→5qter),der(22)(22pter→22q11::9q34→9qter),del(22)(q11)	8
	46,X,t(X;12)(p11.2;p13),t(2;3)(p16;q29),der(5)(pter→5q11.2::22q11→22qter),der(9)(pter→9q34::5q11.2→5q15::10q23→10qter),der(10)(10pter→10q23::5q15→5qter),der(22)(22pter→22q11::9q34→9qter),del(22)(q11)	9
	46,X,t(X;12)(p11.2;p13),t(2;3)(p16;q29),der(5)(pter→5q11.2::22q11→22qter),der(9)(pter→9q34::5q11.2→5q15::10q23→10qter),der(10)(10pter→10q23::5q15→5qter),der(22)(22pter→22q11::9q34→9qter),del(22)(q11)	20
M12 clone	46,X,(X;12)(p11.2;p13),der(5)(pter→5q11.2::22q11→22qter),der(9)(pter→9q34::5q11.2→5q15::10q23→10qter),der(10)(10pter→10q23::5q15→5qter),der(22)(22pter→22q11::9q34→9qter),del(22)(q11)	20



Figure 2. Karyotype of MY cells by Giemsa banding technique: 46,X,t(X;12)(p11.2;p13),t(2;3)(p16;q29),der(5)(5pter→5q11.2::22q11→22qter),der(9)(9pter→9q34::5q11.2→5q15::10q23→10qter),der(10)(10pter→10q23::5q15→5qter),der(22)(22pter→22q11::9q34→9qter),del(22)(q11). Abnormal chromosomes are indicated by arrows.

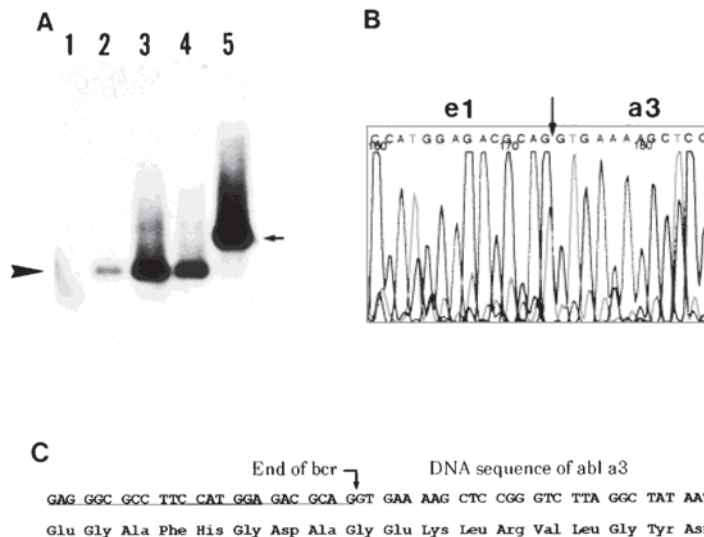


Figure 3. A new *BCR/ABL* mRNA. **A**: RT-PCR analysis of m-BCR type *BCR/ABL* mRNA. Lane 1: RT-PCR product of total RNA from leukemic cells at diagnosis. Lane 2: From leukemic cells after two induction courses. Lane 3: From established MY cells. Lane 4: From clone M12. Lane 5: From OM9;22 cells with m-*BCR* (Ohyashiki et al., 1993). **B**: Sequence analysis of the cloned PCR product of e1-a3 mRNA.

The chromatograms show part of the 5'–3' sequence upstream of the *BCR/ABL* junction. A vertical arrow indicates the position of the junction. **C**: Nucleotide sequences and amino acid residues of the junction region of the *BCR/ABL* mRNA expressed in MY cells. The new fragment was 174 bases shorter than the original e1-a2 and had in-frame junction between *BCR* exon e1 and *ABL* exon a3.

into cloning vector, and sequenced. Sequencing revealed a new minor *BCR/ABL* that was 174 bases shorter than the standard minor *BCR/ABL*. These 174 bases corresponded with the a2 exon of the

ABL gene (Fig. 3B). The new junction between *BCR* exon e1 and *ABL* exon a3 resulted in a 58-amino-acid deletion from the protein associated with an intact a2 exon (Fig. 3C).

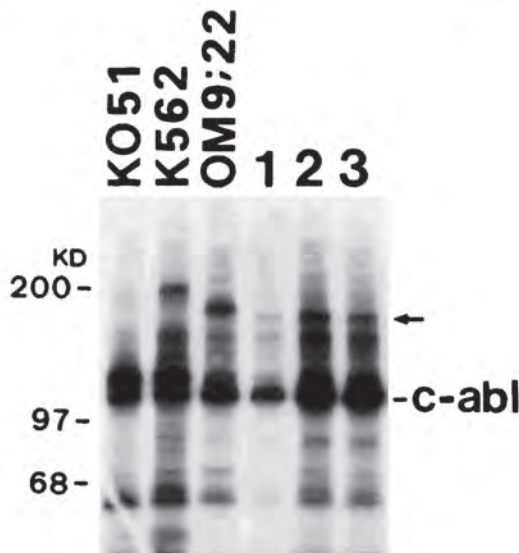


Figure 4. Kinase assay for BCR/ABL protein. An immune complex kinase assay was performed on the anti-ABL antibody immunoprecipitates. Arrow indicates the new P180BCR/ABL. Lane KO51: KO51 cell without Ph translocation. Lane K562: K562 cell with M-BCR. Lane OM9;22: OM9;22 cell with m-bcr. Lane 1: MY cell. Lane 2: Clone M12. Lane 3: Clone M13.

Kinase Assay for BCR-ABL Protein

Cell lines K562 and OM9;22 were used as positive controls for p210 and p190 BCR-ABL proteins, respectively. MY cells and clones M12 and M13 had a 180 kDa BCR-ABL protein with kinase activity (Fig. 4). This is consistent with the nucleotide sequence determination, suggesting a shorter protein.

FISH Analysis of BCR and ABL genes

In order to clarify the precise chromosomal location of the *BCR* and *ABL* genes, we performed two-color FISH with *BCR* and *ABL* YACs on MY cells. FISH showed red signals of the *ABL* gene bound to chromosomes 9 and the Ph, der(22)t(9;22), as shown in Figure 5A. Faint red signals are also present at the center region of the long arm of der(9). Green signals of the *BCR* gene were bound to chromosomes der(5)t(5;22) and the Ph. Yellow signals showed formation of a chimeric *BCR/ABL* on the Ph. There were no *BCR* gene signals on the der(22)t(22;22).

FISH Analysis of der(9)

To examine the mechanism of formation of the complex der(9), we performed two-color FISH with chromosome-specific library DNAs for chromo-

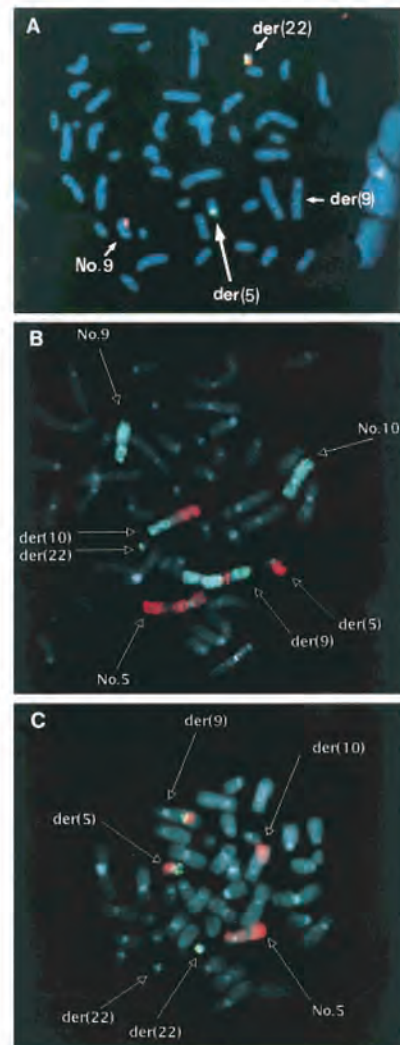


Figure 5. FISH analysis of MY cells. **A:** Metaphase with a two-color hybridization. The *BCR* probe was labeled with Spectrum Green (green). The *ABL* probe was labeled with Spectrum Orange (red). Metaphase cells were counterstained with DAPI. The *BCR/ABL* fusion gene was detected as yellow. Two green hybridization signals of the *BCR* gene were detected on chromosomes der(5) and der(9). The yellow signals of the *BCR/ABL* fusion gene were detected on der(22)t(9;22). **B:** Metaphase cells after two-color FISH with chromosome 9-specific (green), chromosome 10-specific (green), and chromosome 5-specific (red) library DNAs. Der(10) and der(9) were painted green and red. **C:** Metaphase cells after two-color FISH with chromosome 5-specific (red) and chromosome 22-specific (green) DNAs. Center part of the der(9) long arm was painted red and green.

somes 5, 9, 10, and 22 on the metaphase cells. The chromosome 10-specific library DNA (green) painted the distal part of the long arm of der(9), and the proximal part was painted by chromosome 5-specific library DNA (red), which adjoins the chromosome 10-specific part (Fig. 5B). The area

between the chromosome 9-specific and the chromosome 5-specific parts was not painted; this was the area in which chromosome 22 containing the *BCR* gene was originally translocated (Fig. 5C). The chromosome 22-specific library was confirmed between chromosomes 5-specific and chromosome 9-specific libraries of the long arm of the der(9) (Fig. 5C). Thus, FISH analysis demonstrated a complex translocation involving chromosomes 5, 9, 10, and 22. In conjunction with G-banded analysis, the der(9) was interpreted as der(9)(9pter→9q34::22q11.2→22q13::5q11.2→5q15::10q23→10qter).

FISH Analysis of Chromosomes der(5), der(10), and der(22)

The chromosome 22-specific library also painted the distal part of the long arm of der(5). In addition, the chromosome 5-specific library painted the distal part of the long arm of der(10) (Fig. 5B). The der(22) was painted only by the chromosome 22-specific library (Fig. 5C). Thus, FISH analysis in conjunction with G-banding analysis demonstrated that the der(5) was a der(5)(5pter→5q11.2::22q11→22qter), the der(22)(q11) was a der(22)t(22;22), or in long form, der(22)(22pter→22q11::22q13→22qter), and the der(10) was a der(10)(10pter→10q23::5q11.2→5qter), as shown in Figure 6.

Identification of the Breakpoint of t(X;12)(p11.2;p13) by PFGE

To determine whether the *ETV6* (*TEL*) gene is located near the breakpoint in 12p13 rearrangements, we performed PFGE analysis. High-molecular-weight DNA was digested with three different rare cutting enzymes (*Mlu*I, *Not*I, and *Sac*II), separated by PFGE, and hybridized with the 5' part of the *ETV6* cDNA probe. DNA fragments cut by *Mlu*I or *Sac*II revealed normal hybridization patterns with fragments similar to those of cells without an abnormal chromosome 12. DNA digested with *Not*I revealed an abnormal 750 kb band, as shown in Figure 7. However, Northern blot analysis did not reveal an abnormally sized *ETV6* transcript (data not shown).

Tumorigenicity in the Nude Mouse and t(2;3)(p16;q29)

The ability of MY cells to grow in the nude mouse was tested by injection of cells. MY cells and the M12 clone exhibiting the t(2;3)(p16;q29) had the ability to grow as subcutaneous nodules within 40 days. In contrast, the M13 clone exhibiting no t(2;3)(p16;q29) abnormality did not grow as quickly,

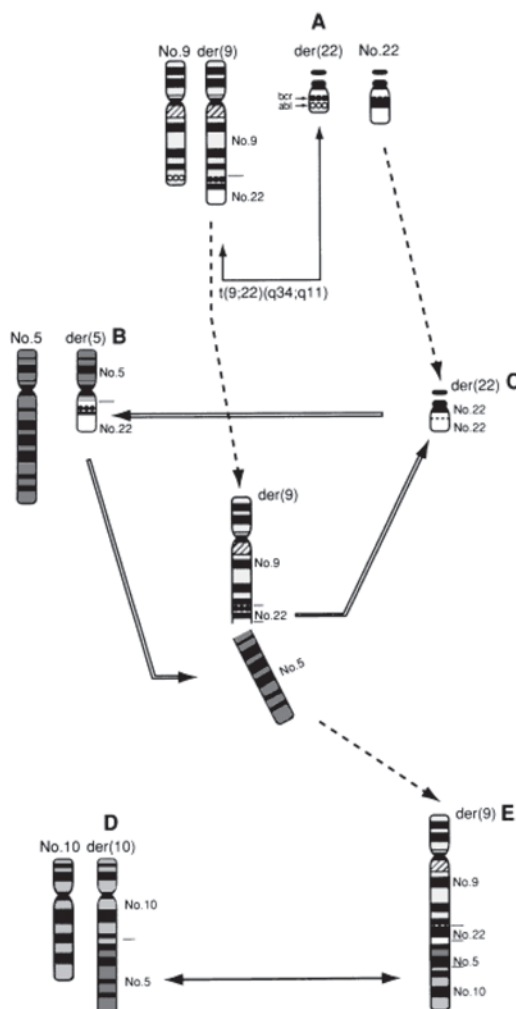


Figure 6. Model of the mechanism of complex rearrangement. The first translocation is t(9;22)(q34;q11); the secondary is a three-way translocation among der(9)t(9;22)(q34;q11), chromosome 5, and the normal chromosome 22. The third translocation occurs between the der(9)t(9;22) with chromosome 5 material and chromosome 10. The final der(9) can be written in long format as follows: der(9)(9pter→9q34::22q11.2→22q13::5q11.2→5q15::10q23→10qter) and as der(22)(22pter→22q11::22q13→22qter). The final abnormal complex translocations are indicated as A to E. A: der(22)(22pter→22q11.2::9q34→9qter); B: der(5)(5pter→5q11.2::22q11→22qter); C: der(22)(22pter→22q11::22q13→22qter); D: der(10)(10pter→10q23::5q11.2→5qter); and E: der(9)(9pter→9q34::22q11→22q13::5q11.2→5q15::10q23→10qter).

forming subcutaneous nodules in 3 months. Tumor cells derived from growth of MY cells had only one karyotype, which was the same as that of the M12 clone, containing the t(2;3)(p16;q29).

DISCUSSION

The Ph chromosome is commonly associated with CML and occasionally with ALL as an early

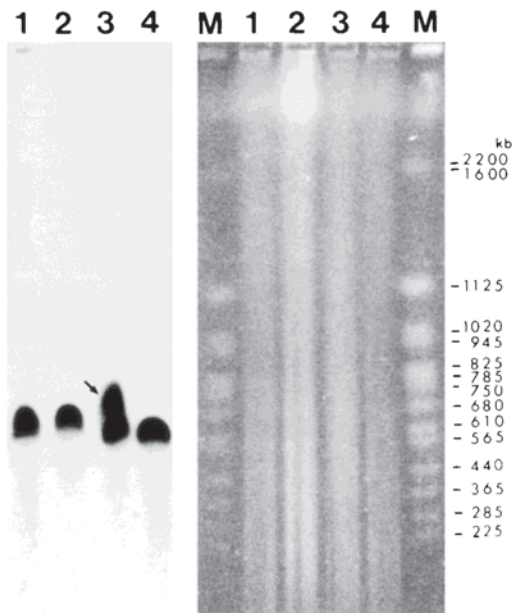


Figure 7. *ETV6* gene by PFGE. MY cells were digested with *NotI*, separated by PFGE, and probed with the 5' *ETV6* cDNA probe. The wild-type 610 kb band is seen in normal samples and MY cells. One new band (750 kb) is seen in MY cells. Lanes M in ethidium bromide staining photo indicate molecular markers. An arrow indicates aberrant band. Lane 1: K562; lane 2: HL60; lane 3: MY; lane 4: original leukemic cells at diagnosis.

event of the leukemogenesis. Recently, the late appearance of the Ph in the course of leukemias has been reported (Najfeld et al., 1989; Katsuno et al., 1994). Thus, the Ph translocation suggests that the *BCR/ABL* fusion product may be important not only in leukemogenesis, but also in leukemic progression. However, the molecular implications of a la-Ph are not well understood. Many cases with la-Ph have been documented as having other karyotype abnormalities, such as translocation and deletion of other chromosomes (Najfeld et al., 1989; Katsuno et al., 1994). In the la-Ph case presented here, leukemic cells developed a complex rearrangement involving chromosomes 5, 9, 10, and the normal 22. Sequential G-banding and FISH revealed the precise construction of this variant complex translocation, namely, $\text{der}(9)(9\text{pter} \rightarrow 9\text{q}34::22\text{q}11.2 \rightarrow 22\text{q}13::5\text{q}11.2 \rightarrow 5\text{q}15::10\text{q}23 \rightarrow 10\text{qter})$, $\text{der}(22)(22\text{pter} \rightarrow 22\text{q}11.2::9\text{q}34 \rightarrow 9\text{qter})$, $\text{der}(22)(22\text{pter} \rightarrow 22\text{q}11.2::22\text{q}13 \rightarrow 22\text{qter})$, etc., as illustrated in Figure 6.

Although a one-step mechanism of three-way or four-way translocation in a complex Ph has been reported (McKeithan et al., 1992; Koduru et al.,

1993), the present complicated rearrangement has not been reported previously.

One of the interesting molecular events in this case was la-Ph producing a variant *BCR/ABL* transcript with a deleted exon 2 of the *ABL* gene. The breakpoint of the *ABL* gene is probably located in intron 2, because the *ABL* cDNA probe did not detect a rearrangement of the *ABL* gene, when the genomic DNA was digested with *HindIII*, *BamHI*, or *BglII* (data not shown). This variant ALL-type *BCR/ABL* transcript encoded a functional P180BCR/ABL protein with tyrosine kinase activity. In this tyrosine kinase assay, the signals on the autoradiogram suggested that the activity of the variant P180BCR/ABL is similar to standard P185BCR/ABL and P210BCR/ABL containing the $\alpha 2$ sequence. The deleted 58 amino acids are therefore unlikely to influence the phosphorylation activity of the variant P180BCR/ABL. The kinase domain of the *ABL* gene shows strong homology with the kinase domain of the *SRC* oncogene and is called the src-homology 1 region (SH1) (Pawson, 1988). Two additional homology regions have been described in the *ABL* gene, the SH2 and SH3 regions (Pawson, 1988; Stahl et al., 1988). The SH3 region is proposed to have a negative regulatory function on the kinase domain (SH1) of the *ABL* gene. Because of the deletion of the $\alpha 2$ sequence, which encodes 17 N-terminal amino acids in a stretch of 50 amino acids of the SH3 region, this *BCR/ABL* product may therefore have enhanced tyrosine kinase activity.

Using the present tumorigenicity assay with a latent period of 3 months, OM9;22 cells, which contain the P185BCR/ABL, 1p- and 3q- abnormalities (Ohayashiki et al., 1993), and the M13 clone formed subcutaneous nodules. However, OM9;22 and the M13 clone formed no tumors with a latent period of 40 days. Thus, the M13 clone expressing P180BCR/ABL and OM9;22 expressing P185BCR/ABL both seem to have the capacity to grow subcutaneously in nude mice. Both BCR/ABL proteins have similar activity to form tumors. However, both may be weaker than the M12 clone. As described above, there is evidence that only the M12 clone exhibiting the $t(2;3)(p16;q29)$ in many MY cell clones was able to form a subcutaneous tumor in only 40 days. This indicates that, first, P180BCR/ABL has a similar capacity to P185BCR/ABL to make cells grow subcutaneously in nude mice and, second, $t(2;3)(p16;q29)$ may confer a greater capacity for tumorigenicity in cooperation with P180BCR/ABL. Further characterization of the biological effect of P180BCR/ABL is a future project.

The present tumorigenicity analysis revealed that the MY cells with the t(2;3)(p16;q29) were more aggressive. Although the t(2;3)(p16;q29) has not been described previously in the literature, it is possible that t(2;3)(p16;q29) is related to more malignant progression in this case. This translocation may have been acquired during in vitro culture. Further characterization of the biological effect of t(2;3)(p16;q29) is another future project.

The Ph translocation producing P180BCR/ABL is very rare. To our knowledge, only one case with this variant P180BCR/ABL has been reported (Soekarman et al., 1990). This case was also la-Ph. Thus, we speculate that la-Ph may sometimes possess the variant P180BCR/ABL protein without codons from exon a2. One ALL and one CML case with variant P210BCR/ABL proteins lacking ABL exon a2 were also reported (Soekarman et al., 1990; van der Plas et al., 1991).

The three-way translocation involving the der(9)t(9;22)(q34;q11), chromosome 5, and the normal chromosome 22 was the second molecular event. Subsequent translocations, t(X;12)(p11.2;p13), and between chromosome 10 and the der(9) (9pter→9q34::22q11.2→22q13::5q11.2→5qter), must have occurred in a later step, as suggested by sequential cytogenetic analysis. With regard to the translocation t(X;12)(p11.2;p13), a putative transcription factor belonging to the ETS family of DNA-binding proteins, the *ETV6* gene, is located at 12p13 (Golub et al., 1994; Baens et al., 1996). To determine whether the translocation breakpoint occurred around the *ETV6* gene, we performed PFGE analysis. PFGE demonstrated a new 750 kb band after digestion with *NotI*. However, the more frequent cutters, *MluI* and *SacII*, revealed normal hybridization patterns; furthermore, Northern blotting revealed no abnormal transcript of the *ETV6* gene in MY cells (data not shown). Thus, the translocation breakpoint was close to the *ETV6* gene, but the *ETV6* gene is unlikely to be affected. The *CDKN1B* gene or D12S178 loci may be aberrant in this translocation, because these are neighboring genes rearranged in hematologic malignancies (Kim et al., 1996; Wlodarska et al., 1996).

In conclusion, MY cells have several translocations in addition to the t(9;22), all of which are unique aberrations (Mitelman and Heim, 1988; Heim and Mitelman, 1992). In leukemias with la-Ph, these complex translocations may sometimes occur and accumulate. We have elucidated several steps in the rearrangement in this case. To our knowledge, leukemia cell lines with an e1-a3 translocation have never been reported. MY cells may be

a useful tool for cloning unknown genes involved in the development of leukemia. This cell line is also a useful model for multistep leukemogenesis.

ACKNOWLEDGMENTS

We thank Drs. K. Ohyashiki and JH. Ohyashiki for providing OM9;22 cells. We also thank Dr. S. Inokuchi for preparing the manuscript.

REFERENCES

- Abo J, Inokuchi K, Dan K, Nomura T (1993) p53 and N-ras mutations in two new leukemia cell lines established from a patient with multilineage CD7-positive acute leukemia. *Blood* 82:2829–2836.
- Baens M, Peeters P, Guo C, Aerssens J, Marynen P (1996) Genomic organization of TEL: The human ETS-variant gene 6. *Genome Res* 6:404–413.
- Chan LC, Karhi KK, Rayter SI, Heisterkamp N, Eridani S, Powles R, Lawler SD, Groffen J, Foulkes JG, Greaves MF, Wiedemann LMA (1987) Novel abl protein expressed in Philadelphia chromosome-positive acute lymphoblastic leukemia. *Nature* 325:635–637.
- Daley GQ, Van Etten RA, Baltimore D (1990) Induction of chronic myelogenous leukemia in mice by the p210^{bcral} gene of the Philadelphia chromosome. *Science* 247:824–830.
- De Klein A, van Kessel AG, Grosveld G, Bartram CR, Hagemeijer A, Bootsma D, Spur NK, Heisterkamp N, Groffen J, Stephenson JR (1982) A cellular oncogene is translocated to the Philadelphia chromosome in chronic myelogenous leukemia. *Nature* 300:765–767.
- Golub TR, Barker GF, Lovett M, Gilliland DG (1994) Fusion of PDGF receptor to a novel ets-like gene, tel, in chronic myelomonocytic leukemia with t(5;12) chromosomal translocation. *Cell* 77:307–316.
- Heim S, Mitelman F (1992) Cytogenetic analysis in the diagnosis of acute leukemia. *Cancer* 70:1701–1709.
- Inokuchi K, Amuro N, Futaki M, Dan K, Shinohara T, Kuriya S, Okazaki T, Nomura T (1991) Transforming genes and chromosome aberrations in therapy-related leukemia and myelodysplastic syndrome. *Ann Hematol* 62:211–216.
- Inokuchi K, Futaki M, Hanawa H, Tanosaki S, Yamaguchi H, Iwakiri R, Nomura T, Dan K (1997a) Heterogeneous expression of bcr-abl fusion mRNA in a patient with Philadelphia-chromosome-positive acute lymphoblastic leukemia. *Br J Haematol* 97:837–840.
- Inokuchi K, Miyake K, Takahashi H, Dan K, Nomura T (1997b) DCC protein expression in hematopoietic cell populations and its relation to leukemogenesis. *J Clin Invest* 97:852–857.
- Katsuno M, Yamashita S, Sadamura S, Umemura T, Hirata J, Nishimura J, Nawata H (1994) Late-appearing Philadelphia chromosome in a patient with acute nonlymphocytic leukemia derived from myelodysplastic syndrome: detection of P210- and P190-type bcr/abl fusion gene transcripts at the leukemic stage. *Br J Haematol* 87:51–56.
- Kim DH, Moldwin RL, Vignon C, Bohlander SK, Suto Y, Giordano L, Gupta R, Fears S, Nucifora G, Rowley JD, Smith SD (1996) TEL-AML1 translocations with TEL and CDKN2 inactivation in acute lymphoblastic leukemia cell lines. *Blood* 88:785–794.
- Koduru PRK, Goh JC, Pergolizzi RG, Lichtman SM, Broome JD (1993) Molecular characterization of a variant Ph1 translocation t(9;22;11)(q34;q11;q13) in chronic myelogenous leukemia (CML) reveals the translocation of the 3'-part of BCR gene to the chromosome band 11q13. *Oncogene* 8:3239–3247.
- McKeithan TW, Warshawsky L, Espinosa R III, Le Beau MM (1992) Molecular cloning of the breakpoints of a complex Philadelphia chromosome translocation: Identification of a repeated region on chromosome 17. *Proc Natl Acad Sci USA* 89:4923–4927.
- Mitelman F, Heim S (1988) Consistent involvement of only 71 of the chromosomal bands of the human genome in primary neoplasia-associated rearrangements. *Cancer Res* 48:7115–7119.
- Najfeld V, Cuttner J, Figur A, Kawasaki ES, Witte ON, Clark SS (1989) P185^{BCR-ABL} in two patients with late-appearing Philadelphia chromosome-positive acute nonlymphocytic leukemia. *Leukemia* 3:841–846.
- Ohyashiki K, Miyauchi J, Ohyashiki JH, Saito M, Yaguchi M, Inatomi Y, Nakazawa S, Wada H, Mizutani S, Matsuo Y, Minowada J, Toyama K (1993) Interleukin-7 enhances colony growth and

- induces CD20 antigen of a Ph+ acute lymphoblastic leukemia cell line, OM9;22. *Leukemia* 7:1034–1040.
- Pawson T (1988) Noncatalytic domains of cytoplasmic protein-tyrosine kinases: Regulatory elements in signal transduction. *Oncogene* 3:491–495.
- Soekarman D, Van Denderen J, Moret M, Meeuwssen T, Van Baal J, Hagemeijer A, Grosveld G (1990) A novel variant of the bcr–abl fusion product in Philadelphia chromosome-positive acute lymphoblastic leukemia. *Leukemia* 4:397–403.
- Stahl ML, Ferenz CR, Kelleher KL, Kriz RW, Knopf JL (1988) Sequence similarity of phospholipase C with the noncatalytic region of src. *Nature* 332:269–272.
- Van der Plas DC, Soekarman D, van Gent AM, Grosveld G, Hagemeijer A (1991) bcr–abl mRNA lacking abl exon a2 detected by polymerase chain reaction in a chronic myelogenous leukemia patient. *Leukemia* 5:457–461.
- Voncken JW, Griffiths S, Greeves MF, Pattengale PK, Heisterkamp N, Groffen J (1992) Restricted oncogenicity of BCR/ABL p190 in transgenic mice. *Cancer Res* 52:4534–4539.
- Wada H, Mizutani S, Nishimura J, Usuki Y, Kohsaki M, Komai M, Kaneko H, Sakamoto S, Delia D, Kanamaru A, Kakishita E (1995) Establishment and molecular characterization of a novel leukemic cell line with Philadelphia chromosome expressing p230 BCR/ABL fusion protein. *Cancer Res* 55:3192–3196.
- Wlodarska I, Marynen P, La Starza R, Mecucci C, Van den Berghe (1996) The ETV6, CDKN1B and D12S178 loci are involved in a segment commonly deleted in various 12p aberrations in different hematological malignancies. *Cytogenet Cell Genet* 72:229–235.
- Yamaguchi H, Inokuchi K, Shinohara T, Dan K (1998) Extramedullary presentation of chronic myelogenous leukemia with P190 BCR/ABL transcripts. *Cancer Genet Cytogenet* 102:74–77.

BRIEF COMMUNICATION

Establishment of a Cell Line With *AML1-MTG8*, *TP53*, and *TP73* Abnormalities From Acute Myelogenous Leukemia

Koiti Inokuchi,^{1,*} Hiroyuki Hamaguchi,² Masafumi Taniwaki,³ Hiroki Yamaguchi,¹ Sakae Tanosaki,¹ and Kazuo Dan¹

¹Division of Hematology, Department of Internal Medicine, Nippon Medical School, Tokyo

²Department of Hematology, Musashino Red Cross Hospital, Tokyo

³Third Department of Internal Medicine, Kyoto Prefectural University of Medicine, Kyoto, Japan

Gene alterations accumulate during the progression of acute myelogenous leukemia (AML) to a malignant clone. Here, a new myeloid cell line, designated YSK-21, with the balanced t(8;21)(q22;q22) and the unbalanced der(1)t(1;17)(p36;q21), was established. YSK-21 grows well in a medium containing recombinant human granulocyte colony-stimulating factor (rhG-CSF), granulocyte-macrophage colony-stimulating factor (rhGM-CSF), or interleukin-3 (rhIL-3). Molecular analysis using the reverse transcriptase-polymerase chain reaction (RT-PCR) and fluorescence in situ hybridization (FISH) revealed that t(8;21)(q22;q22) resulted in an *AML1-MTG8* fusion transcript. FISH and spectral karyotyping (SKY) in conjunction with G-banding analysis revealed a der(1)t(1;17)(p36;q21) chromosomal translocation, which appeared in the clone developed from the original leukemic cells. Molecular analysis of the *TP73* gene on 1p36 and the *TP53* gene revealed a deletion of one-allele in *TP73* with partial demethylation of another allele in the initial clone of YSK, and a point mutation consisting of an A→T substitution in codon 288 of the *TP53* gene in the developed clone of YSK-21. YSK-21 cells, expressing aberrant *AML1-MTG8*, *TP53*, and *TP73* protein molecules, may be useful for elucidating the pathophysiology of these aberrant proteins and for studying the der(1)t(1;17)(p36;q21) chromosomal translocation. © 2001 Wiley-Liss, Inc.

The t(8;21)(q22;q22) translocation is found in many patients with acute myelogenous leukemia (AML-M2) (Trujillo et al., 1979). This translocation synthesizes an *AML1-MTG8* fusion transcript which contributes to leukemogenesis (Miyoshi et al., 1993).

Recently, the *TP73* gene, showing significant homology to *TP53*, as well as functional similarity, was discovered on the short arm (p36) of chromosome 1 (Kaghad et al., 1997). The p73 protein inhibits cell growth and can induce apoptosis (Jost et al., 1994). Monoallelic expression of p73 may have particular significance for tumors which display 1p36 loss of heterozygosity (LOH) as a tumor-suppressor gene. However, it remains unclear whether the *TP73* gene plays a role in tumorigenesis. Evidence of monoallelic expression of p73 in normal peripheral blood cells has been reported, but p73 participation in leukemogenesis remains uncertain (Jost et al., 1994).

The present report describes the establishment of a novel cell line, YSK-21, having an *AML1-MTG8* fusion transcript, aberrant *TP73* in an unbalanced translocation of der(1), and a *TP53* gene mutation.

A 45-year-old man had pyrexia and purpura in May 1992. The white blood cell count was $6.2 \times 10^9/L$ with 68% myeloblasts. The bone marrow

(BM) was hypercellular with 74.2% myeloblasts. Cytogenetic analysis of BM cells showed 45,X,-Y,t(8;21)(q22;q22). The leukemic cells expressed CD13 (88.6%) and CD33 (48.5%). The cells were positive for myeloperoxidase (MPO) and chloroacetate esterase (CAE). A diagnosis of AML (M2) was made. Induction chemotherapy was started immediately, and complete remission (CR) was obtained. He relapsed in March 1994. Cytogenetic analysis showed the same abnormal karyotype as that at onset. A second CR was obtained in April 1994. However, the patient relapsed again in March 1995. After further induction chemotherapy, a third remission was obtained. In September, 1995, he received a bone marrow transplant from a sibling and achieved a fourth CR. In January, 1996, he relapsed again, with karyotype evolution to 45,X,-Y,der(1)t(1;17)(p36;q21),t(8;21)(q22;q22). His leukemic cells were refractory, and he died in May 1996.

*Correspondence to: Koiti Inokuchi, M.D., Ph.D., Division of Hematology, Department of Internal Medicine, Nippon Medical School, 1-1-5 Sendagi, Bunkyo-ku, Tokyo 113, Japan.
E-mail: inokuchi@nms.ac.jp

Received 4 December 2000; Accepted 16 April 2001

Peripheral blood mononucleated cells (PB-MNCs) obtained at the third relapse were separated using Ficoll-Hypaque. The cells were cultured in RPMI 1640 medium (Gibco, Grand Island, NY) supplemented with 10% FCS and 10 ng/ml of GM-CSF (Yamamoto et al., 1997; Inokuchi et al., 1998). After initial growth was noted, the cells were propagated in vitro twice weekly by replacement of the medium containing 10% FCS and 10 ng/ml of GM-CSF.

Cytogenetic studies were performed by the conventional trypsin-Giemsa banding technique (Abo et al., 1993). The bone marrow cells at diagnosis and relapse and the cells of the established cell line, YSK-21, were processed by a direct method.

Complementary DNA (cDNA) was prepared from 200 ng of total RNA using R3 (5'-ATT-GCTGAAGCCATTGGGTG-3'; residues 2300-2319) and reverse transcriptase (Miyoshi et al., 1993). The cDNA was amplified with S1 (5'-CTTCACTCTGACCATCACTG-3'; residues 2013-2032) and R3 (5'-GTGCTTCTCAGTACGATTTC-3'; residues 2108-2127) (Miyoshi et al., 1993). MTG8 cDNA as an internal control was amplified with C1 (5'-GACTCACCTGTGGATGTGAA-3'; residues 2040-2160) and A1 (5'-TCAAGGCTGTAGGAGAATGG-3'; residues 2265-2184). PCR was performed using a slight modification of our original protocol. After the RT-PCR products (145 bp) were electrophoresed on a 2% agarose gel, they were stained with ethidium bromide.

The probes used in this assay were bacteriophage DNA libraries from sorted human chromosome 1 (WCP1), purchased from Vysis (Downers Grove, IL). The probes were labeled by standard nick-translation using biotin-11-dUTP (Sigma, St. Louis, MO). The biotin-labeled probes were detected with fluorescein isothiocyanate (FITC) (Vector Laboratories, Burlingame, CA). Chromosomes were counterstained with 1 µg/mL of 4,6-diaminido-2-phenylindole dihydrochloride (DAPI) and mounted in antifade solution. The results were analyzed using a conventional fluorescence microscope, Olympus BH2-RFC (Olympus, Tokyo, Japan).

For a spectral karyotyping (SKY) study, slides were freshly prepared from chromosome suspensions that had been stored in methanol/acetic acid at -20°C. SKY was performed without prior knowledge of the chromosomal aberrations identified by G-banding. Eight metaphase cells were analyzed by SKY. A SKY™ kit containing chromosome painting probes was purchased from Applied

Spectral Imaging (ASI, Israel). SKY analysis was performed according to the ASI protocol (Veldman et al., 1997). Chromosome hybridization was performed directly using the SKY™ hybridization mix, in which probe DNA was labeled with rhodamine, Texas-Red, Cy5, FITC, and Cy5.5, according to the SCI protocol. Chromosomes were counterstained with DAPI and covered with paraparaphenylene-diamine. Image acquisition was performed using an SD200 Spectral Bio-imaging System (ASI, Israel). The spectral information was displayed and analyzed using software provided by ASI.

RT-PCR for detecting the *TP73* mRNA was performed with a minor modification of the original procedure (Inokuchi et al., 1997). Using the nucleotide numbers corresponding to human *TP73* cDNA deposited in the EMBL database under accession number Y11416 EMBL, the following primers were created. The sense primer was p73-5', CAGCAGTC-CAGCACGGCCAA (residues 504-523), while the antisense primer was p73-3', TTCTTGCGGAG-CTCTCGTT (residues 1056-1075). A cDNA was synthesized from 250 ng of total cellular RNA using primer random 9-mer and 200 U of Moloney murine leukemia virus. RT-PCR products were electrophoresed on 2% agarose gel and stained with ethidium bromide.

The 572-bp PCR fragment was sliced from the gel, electroeluted, purified with phenol, and precipitated with ethanol. The fragments were subcloned into the *EcoRV* site of a pGEM-5Zf (+/-) cloning vector (Inokuchi et al., 1997). The PCR products were sequenced using an ABI sequencer with dye terminators (Perkin Elmer, Warrington, UK). All sequences were confirmed by sequencing in both orientations. The 572-bp cDNA fragment was used for Southern analysis.

For the *TP73* gene analysis, DNA extractions were performed as described previously (Miyake et al., 1993). The blotting filters for Southern blotting were hybridized with a ³²P-labeled 572-bp cDNA probe.

To identify LOH of the *TP73* gene, the *SlyI* polymorphic site in exon 2 was selected (Mai et al., 1998). Genomic PCR was performed using primers located in introns 1 and 2, followed by *SlyI* digestion. Primers P1 and P2 (5'-CAGGAGGACAGAG-CACGAG-3' and 5'-CGAAGGTGGCTGAGGC-TAG-3') were used to perform PCR. Ten µl of the PCR product (229 bp) was then digested overnight with *SlyI*. The PCR products with the A/T polymorphic allele were digested into 157-bp and 72-bp bands. PCR products were electrophoresed on 2% agarose gel and stained with ethidium bromide.

TABLE 1. Surface Marker Analysis of Original Leukemic Cells and YSK-21 Cells

CD	Positive cells (%)	
	Third relapse	YSK-21 cells
CD1	0.2	1.2
CD2	1.6	3.3
CD3	2.0	1.9
CD5	1.7	0.7
CD7	1.7	20.1
CD10	0.6	1.4
CD13	43.4	79.8
CD14	0.2	2.4
CD19	1.7	2.3
CD20	1.0	3.5
CD33	22.2	48.5
CD34	81.3	59.3
CD41	ND	2.6
Glycophorin A	ND	1.2
HLA-DR	88.6	99.8

Surface markers of the leukemic blasts and the cell line were determined by direct immunofluorescence using a FACS II (Becton-Dickinson, Sunnyvale, CA) flow cytometer (Abo et al., 1993). ND: not done.

Methylation-specific PCR (MSP) analysis of the methylation patterns within the CpG island of the *TP73* gene in exon 1 (sequence -110-bp to -42-bp relative to the translocation starting point, GenBank accession number Y11416) was performed as described elsewhere (Corn et al., 1999). The primer sequences of *TP73* for the methylated reaction were 5'-GGACGTAGC-GAAATCGGGGTTC-3' (sense) and 5'-ACCC-CGAACATCGACGTCCG-3' (antisense), and for the unmethylated reaction they were 5'-AGG-GGATGTAGTGAAATTGGGGTTT-3' and 5'-ATCACAACCCCAACATCAACATCCA-3' (antisense). PCR products were loaded directly onto nondenaturing 2.5–15% polyacrylamide gels and stained with ethidium bromide.

Mutations of the *TP53* genes were detected by our standard protocol (Abo et al., 1993).

PB-MNCs obtained after the third relapse were cultured, and proliferation was noted 3 weeks after the start of culture. The established cell line, designated YSK-21 (Fig. 2A), has now been maintained continuously for more than 3 years. Table 1 summarizes the cell surface markers of the original leukemic cells at the third relapse and YSK-21 cells. YSK-21 cells are positive for CD7, CD13, CD33, CD34, and HLA-DR. YSK-21 cells have a doubling time of approximately 48 hr. Addition of rhG-CSF, rhGM-CSF, or rhIL-3 at a concentration of 10 ng/ml stimulated the growth of YSK-21 cells approximately threefold after 8 days of culture,

although they did not proliferate well with rhIL6 or rhTPO (data not shown). The cytokine dependency of YSK-21 cells has not changed from the time of establishment.

At establishment of the cell line, YSK-21 cells had two karyotypes, i.e., 45,X,-Y,der(1)t(1;17)(p36;q21),t(8;21)(q22;q22) in 16 cells and 45,idem,der(21)t(1;21)(q31;p11) in four cells (Table 2). After YSK-21 cells were cultured for 1 year, the major clone had the der(21)t(1;21)(q31;p11) (Fig. 1A).

The original leukemic cells and YSK-21 had the specific 145-bp PCR product of chimeric *AML1/MTG8* mRNA of t(8;21)(q22;q22) (Fig. 1B).

We also subjected the metaphase cells to whole chromosome 1 painting and SKY. The chromosome 1-specific DNA painted the distal part of the short arm of der(21), while the distal part of the short arm of der(1) was not painted (Fig. 2B). SKY revealed that the distal part of the short arm of chromosome 17 was translocated to the distal part of the short arm of der(1) (Fig. 2C). SKY and chromosome 1 painting also revealed formation of the complex der(21). Thus, FISH and SKY analysis in conjunction with G-banding analysis revealed that the final karyotype of YSK-21 was 45,X,-Y,der(1)t(1;17)(p36;q21), t(8;21)(q22;q22), der(21)t(1;21)(q31;p11).

For molecular characterization of the der(1) abnormality, the *TP73* gene was analyzed to elucidate its status in YSK-21 cells.

High-molecular-weight DNA was analyzed. DNA fragments cut with *Hind* III revealed normal hybridization patterns with one-half or less density, as shown in Figure 3A. Using the C/T polymorphism of exon 2 for allele-specific analysis, the original leukemic cells at onset had both alleles with two types of *Sst*I polymorphic site, while loss of the A/T allele was shown in the YSK-21 clone having the der(1) (Fig. 3B). A methylation study of the *TP73* 5'CpG island by MSP showed that one C/G allele was partially methylated and demethylated (Fig. 3C). All these molecular data revealed that one *TP73* allele was lost and another allele was partially demethylated in the YSK-21 clone having the der(1) chromosome. RT-PCR analysis detected the *TP73* transcripts (Fig. 3D). No mutation was detected in the DNA-binding domain of the *TP73* transcript (data not shown). Figure 3E illustrates a *TP53* mutation in codon 288 (A→T) of the final clone of YSK-21 cells. No point mutations were detected in codons 12, 13, and 61 of the *RAS*N gene (data not shown).

Balanced translocations of chromosomes are common mechanisms of leukemogenesis (Mitel-

CELL LINE WITH ABERRANT TP53, TP73, AND AML1-MTG8

185

TABLE 2. Summary of Sequential Cytogenetic Analysis and TP73 and TP53 Mutations of Leukemic Cells From the Patient

Disease state	Karyotype	Number of metaphase cells	One-allele deletion and mutation of the other TP53 gene	One-allele deletion of the TP73 gene
Onset	45,X,-Y,t(8;21)(q22;q22)	20/20 cells	Normal	Normal
First relapse	45,X,-Y,t(8;21)(q22;q22)	20/20 cells	ND	ND
Second relapse	45,X,-Y,t(8;21)(q22;q22)	20/20 cells	ND	ND
Third relapse	45,X,-Y,der(1)(p36;q21), t(8;21)(q22;q22)	20/20 cells	Normal	One-allele deletion
Cell line at establishment	45,X,-Y,der(1)(p36;q21), t(8;21)(q22;q22)	16/20 cells	ND	ND
	45,X,-Y,der(1)(p36;q21), t(8;21)(q22;q22),der(21)t(1;21)(q31;p11)	4/20 cells		
1 year after establishment	45,X,-Y,der(1)(p36;q21), t(8;21)(q22;q22),der(21)t(1;21)(q31;p11)	20/20 cells	Point mutation at codon 288	One-allele deletion

ND; not done.

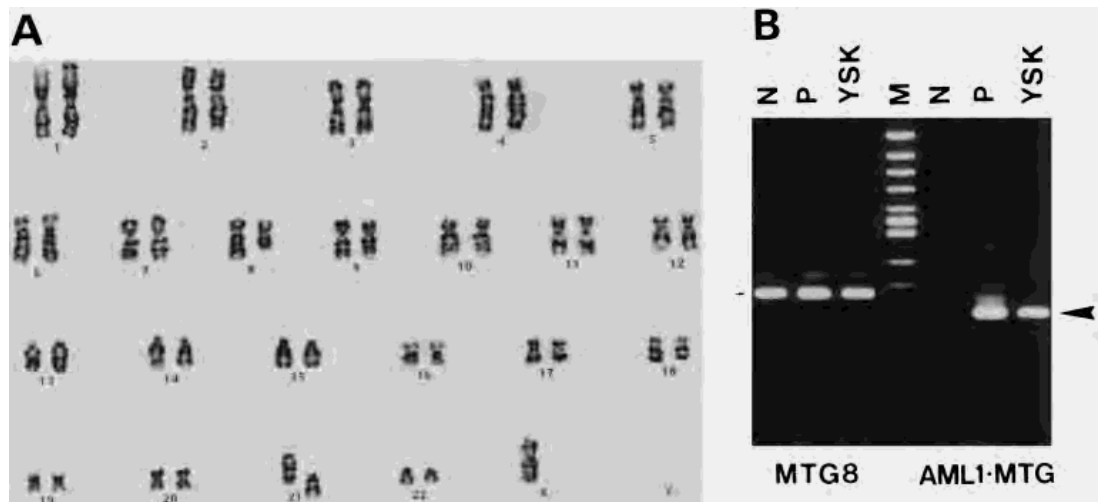


Figure 1. Karyotype of YSK-21 cells and RT-PCR product of AML1/MTG8. **A:** 45,X,-Y,der(1)(p36;q21),t(8;21)(q22;q22),der(21)t(1;21)(q31;p11). **B:** RT-PCR product of total RNA from YSK-21 cells. Lanes N; from normal lymphocytes. Lanes P; from original leukemic cells. Lanes YSK; from YSK-21 cells. Lane M; molecular marker of *HincII*-digested ϕ x DNA. The horizontal bar on the left indicates the RT-PCR product of the MTG8 transcript as an internal control. The arrowhead on the right indicates AML1/MTG8.

man et al., 1997). The t(8;21)(q22;q22) is one of the most common AML chromosomal aberrations with a single structural abnormality. Clinically, patients with AML having t(8;21) are known to show a good response to combined chemotherapy (Trujillo et al., 1979). The present case responded well to the first induction chemotherapy. There was no cytogenetic evolution or mutation of the *RAS* and *TP53* genes at the first and second relapses. However, cytogenetic evolution of der(1) chromosome occurred at the third relapse. After acquisition of

der(1) at the third relapse, the leukemic cells became more refractory to chemotherapy. A balanced t(1;17) (p36;q21) is a structural abnormality sometimes seen in AML and malignant lymphoma (Mitelman et al., 1997). However, the der(1) chromosome in the present case is a unique unbalanced translocation between chromosomes 1 and 17. This unbalanced translocation caused a deletion of one allele in the *TP73* gene of the recurrent leukemic cells. The other allele of the *TP73* gene was partially demethylated, and a small amount of *TP73*

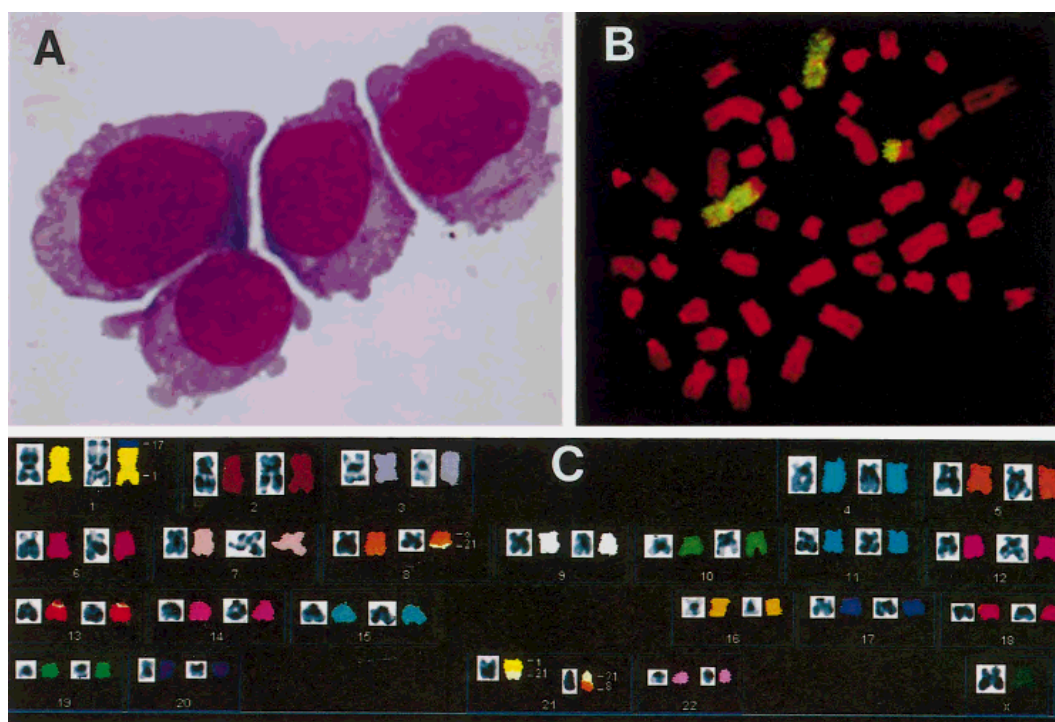


Figure 2. Morphology (A), FISH (B), and SKY (C) analyses of YSK-21 cells. **A:** YSK-21 cells at establishment. Wright-Giemsa staining. Magnification $\times 1,000$. **B:** Metaphase cells after FISH with chromosome 1-specific (green) library DNAs. The short arm of der(21), der(1), and normal chromosome 1 were painted green. The short arm of der(1)

was not stained. **C:** SKY of YSK-21 metaphase cells. Translocations of chromosome 17 material to the short arm of chromosome 1 and the long arm of chromosome 1 to the short arm of chromosome 21, which were not detectable by G-banding analysis, t(8;21) were detected.

transcript was detected by RT-PCR (Fig. 3D). Partial methylation of one allele of the *TP73* gene is an abnormal methylation status in normal blood cells (Jost et al., 1997). HL60 cells and U937 cells were reported to be predominantly methylated and fully methylated, respectively (Corn et al., 1999). Lower expression from one allele, which was partially methylated, may be one cause of the higher viability of YSK-21 cells.

TP73 protein has structural and functional similarity to TP53, including the ability to promote apoptosis when overexpressed in vitro and to up-regulate *TP53*-responsive genes involved in cell-cycle control, such as *CDKN1A* (Jost et al., 1997). Thus, a one-allele deletion in the *TP73* gene may influence the cell viability, as it does in *TP53*.

Both *TP53* and *TP73* are induced by cisplatin (Gong et al., 1999). Because TP53 and TP73 are regulated by parallel pathways that are independently regulated (Levero et al., 1999), the final clone of YSK-21 with both aberrant TP53 and TP73 might acquire a greater growth advantage by

blocking these parallel pathways of tumor suppression and apoptosis.

The clone characterized by a complex rearrangement involving the der(21) chromosome became the final major clone. This translocation was an unbalanced translocation like the der(1), which may endow YSK-21 cells with a growth advantage. The surface of established YSK-21 cells became positive for CD7, although the original leukemic cells at third relapse were negative for CD7 (Table 1). We cannot explain why cells became positive for CD7.

To our knowledge, this is the first report of a leukemia cell line with *AML1/MTG8*, aberrant TP53, and aberrant TP73. The YSK-21 cells may be a useful tool for studying the pathophysiological mechanisms of apoptosis through the TP53 and TP73 signal pathways.

ACKNOWLEDGMENT

We thank Dr. S. Inokuchi for preparing the manuscript.

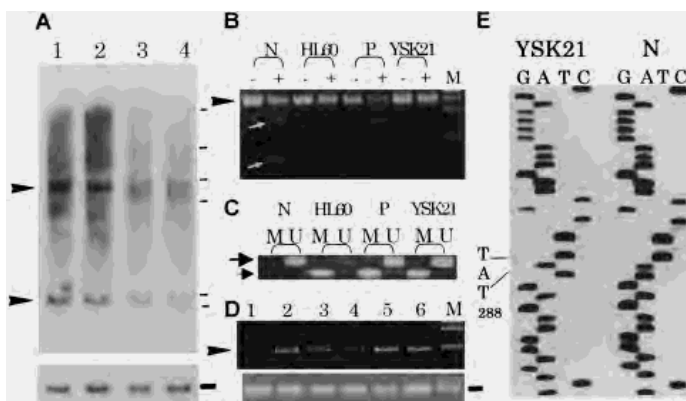


Figure 3. Characterization of the *TP73* gene and mutation of the *TP53* gene. **A:** Southern analysis using a *TP73* cDNA probe. Genomic DNA was digested with *Hind*III and separated on 1.2% agarose gel. After blotting, the membrane was probed with a *TP73* cDNA probe. Lane 1: normal MNC-BM; Lane 2: original leukemic cells at onset; Lane 3: original leukemic cells at third relapse; Lane 4: YSK-21 cells. Arrowheads indicate the genomic *TP73* bands (2.1 and 5.0 kb, respectively). The horizontal bar in the lower panel shows 1.7-kb *Hind*III-digested bcr bands of the bcr gene as an internal control (Inokuchi et al., 1991). The horizontal bars in the upper panel indicate DNA weight markers of λ DNA digested with *Hind*III (23.1, 9.4, 6.6, 2.3, and 2.0 kb, respectively). **B:** One-allele deletion in *TP73* gene of YSK-21 cells. PCR was performed for 35 cycles, consisting of 20 seconds at 95°C (denaturation), 15 seconds at 60°C (annealing), and 30 seconds at 72°C (extension). Sty I polymorphism, detected by agarose gel electrophoresis of Sty I-digested genomic PCR products, was lost in the YSK-21 cells. Lanes N: DNA from normal healthy BM cells; Lanes HL60: DNA from HL60 cells; Lanes P: DNA from original cells at onset; Lanes YSK21: DNA from YSK-21 cells; Lane M: marker of *Hae* III-digested ϕ x DNA (271, 234, 194 and 118 bp, respectively). + lanes indicate the presence of StyI-digested genomic PCR products (157 and 72 bp indicated by white arrows). – lanes indicate nondigested lanes (229 bp; arrow head),

respectively. **C:** Methylation of the *TP73* promoter region CpG island. PCR was performed for 35 cycles, consisting of 30 sec at 95°C (denaturation), 30 sec at 61°C for the methylation reaction and 58°C for the demethylation reaction (annealing), and 30 sec at 72°C (extension). Visible PCR product in the lanes marked M indicates the presence of methylated *TP73* gene (small arrow), while the product in the U lanes indicates the presence of demethylated *TP73* gene (large arrow). Lanes N: DNA from normal healthy BM cells; Lanes HL60: DNA from HL60 cells; Lanes P: DNA from original cells at onset; Lanes YSK21: DNA from YSK-21 cells. **D:** RT-PCR analysis of *TP73* mRNA. Arrowhead indicates the amplified PCR product of *TP73* cDNA (672 bp). Lane 1: RNA from BALL-1 cells, in which the *TP73* gene is not expressed; Lane 2: RNA from normal BM cells; Lane 3: RNA from HL60 cells, in which expression of the *TP73* gene is decreased; Lane 4: RNA from YSK-21 cells at 1 year after establishment; Lane 5: RNA from original leukemic cells; Lane 6: RNA from K562 cells; Lane M: markers consisting of λ DNA digested with *Hind*III and *Hae* III-digested ϕ x DNA. The lower panel shows the RT-PCR (115 bp) product of the β_2 -microglobulin transcript as an internal control. **E:** Nucleotide sequence of the *TP53* gene of YSK-21 cells. YSK; YSK-21 cells at 1 year after establishment; N: normal control.

REFERENCES

- Abo J, Inokuchi K, Dan K, Nomura T. 1993. p53 and N-ras mutations in two new leukemia cell lines established from a patient with multilineage CD7-positive acute leukemia. *Blood* 82:2829–2836.
- Corn PG, Kuerbitz SJ, Van Noesl MM, Esteller M, Compitello N, Baylin SB, Herman JG. 1999. Transcriptional silencing of the p73 gene in acute lymphoblastic leukemia and Burkitt's lymphoma is associated with 5' CpG island methylation. *Cancer Res* 59:3352–3356.
- Gong JG, Costanzo A, Tamg HQ, Melino G, Kaelin WG, Levrero M, Wang JYJ. 1999. The tyrosine kinase c-Abl regulates p73 in apoptotic response to cisplatin-induced DNA damage. *Nature* 399:806–809.
- Inokuchi K, Futaki M, Yamada T, Yanabe Y, Dan K, Shinohara T, Kuriya S, Nomura T. 1991. The relationship between the site of breakpoints within the bcr gene and thrombopoiesis of Philadelphia-positive chronic myelocytic leukemia. *Leuk Res* 15:1067–1073.
- Inokuchi K, Futaki M, Hanawa H, Tanosaki S, Yamaguchi H, Iwakiri R, Nomura T, Dan K. 1997. Heterogeneous expression of bcr-abl fusion mRNA in a patient with Philadelphia-chromosome-positive acute lymphoblastic leukemia. *Br J Haematol* 97:837–840.
- Inokuchi K, Shinohara T, Futaki M, Hanawa H, Tanosaki S, Tamaguchi H, Nomura T, Dan K. 1997. Establishment of a cell line with variant BCR/ABL breakpoint expressing P180BCR/ABL from late-appearing Philadelphia-positive acute biphenotypic leukemia. *Genes Chromosomes Cancer* 23:227–238.
- Jost CA, Marin MC, Kaelin WG Jr. 1997. p73 is a human p53-related protein that can induce apoptosis. *Nature* 389:191–194.
- Kaghad M, Bonnet H, Yang A, Creancier L, Biscan JC, Valent A, Minty A, Chalou P, Lelias JM, Dumont X, Ferrara P, McKeon F, Caput D. 1997. Monoallelically expressed gene related to p53 at 1p36, a region frequently deleted in neuroblastoma and other human cancers. *Cell* 90:809–819.
- Levrero M, De Laurenzi V, Costanzo A, Gong J, Melino G, Wang JYJ. 1999. Structure, function and regulation of p63 and p73. *Cell Death Differ* 6:1146–1153.
- Mai M, Yokomizo A, Qian C, Yang P, Tindall DJ, Smith DI, Liu W. 1998. Activation of p73 silent allele in lung cancer. *Cancer Res* 58:2347–2349.
- Mitelman F, Mertens F, Johansson B. 1997. A breakpoint map of recurrent chromosomal rearrangements in human neoplasia. *Nat Genet* 15:417–474.
- Miyake K, Inokuchi K, Dan K, Nomura T. 1993. Alterations in the deleted in colorectal carcinoma gene in human primary leukemia. *Blood* 82:927–930.
- Miyoshi H, Kozu T, Shimizu K, Enomoto K, Maseki N, Kaneko Y, Kamada N, Ohki M. 1993. The t(8;21) translocation in acute myeloid leukemia results in production of an AML1-MTG8 fusion transcript. *EMBO J* 12:2715–2721.
- Trujillo JM, Cork A, Ahearn MJ, Youness EL, McCredie KB. 1979. Hematologic and cytologic characterization of 8/21 translocation acute granulocytic leukemia. *Blood* 53:695–706.
- Veldman T, Vignon C, Schrock E, Rowley JD, Ried T. 1997. Hidden chromosome abnormalities in hematological malignancies detected by multicolour spectral karyotyping. *Nat Genet* 15:406–410.
- Yamamoto K, Hamaguchi H, Nagata K, Kobayashi M, Tanimoto F, Taniwaki M. 1997. Establishment of a novel human acute myeloblastic leukemia cell line (YNH-1) with t(16;21), t(1;16) and 12q13 translocations. *Leukemia* 11:599–608.

Abnormality of c-kit oncoprotein in certain patients with chronic myelogenous leukemia – potential clinical significance

K Inokuchi, H Yamaguchi, M Tarusawa, M Futaki, H Hanawa, S Tanosaki and K Dan

Division of Hematology, Department of Internal Medicine, Nippon Medical School, Tokyo, Japan

Chronic myelogenous leukemia (CML) is characterized by the Philadelphia (Ph) chromosome and *bcr/abl* gene rearrangement which occurs in pluripotent hematopoietic progenitor cells expressing the c-kit receptor tyrosine kinase (KIT). To elucidate the biological properties of KIT in CML leukemogenesis, we performed analysis of alterations of the c-kit gene and functional analysis of altered KIT proteins. Gene alterations in the c-kit juxtamembrane domain of 80 CML cases were analyzed by reverse transcriptase and polymerase chain reaction-single strand conformation polymorphism (RT-PCR-SSCP). One case had an abnormality at codon 564 (AAT→AAG, Asn→Lys), and six cases had the same base abnormality at codon 541 (ATG→CTG, Met→Leu) in the juxtamembrane domain. Because the change from Met to Leu at codon 541 was a conservative one which was also observed in the normal population and normal tissues of CML patients, it probably represents a polymorphic variation. Although samples of hair roots and leukemic cells from the chronic phase of one CML patient showed no abnormality, an abnormality at codon 541 (ATG→CTG, Met→Leu) was found only at blastic crisis (BC) of this case. In the case with the abnormality at codon 564, the mutation was detected only in a sample of leukemic cells collected at BC. To examine the biological consequence and biological significance of these abnormalities, murine KIT^{L540} and KIT^{K563} expression vectors were introduced into interleukin-3 (IL-3)-dependent murine Ba/F3 cells to study their state of tyrosine phosphorylation and their growth rate. Ba/F3 cells expressing KIT^{WT}, KIT^{L540} and KIT^{K563} showed dose-dependent tyrosine phosphorylation after treatment with increasing concentrations of recombinant mouse stem cell factor (rmSCF). The cells expressing KIT^{L540} and KIT^{K563} were found to have greater tyrosine phosphorylation than cells expressing KIT^{WT} at 0.1 and 1.0 ng/ml of rmSCF. The Ba/F3 cells expressing KIT^{K563} proliferated in response to 0.1 and 1.0 ng/ml of rmSCF as well as IL-3. The Ba/F3 cells expressing KIT^{L540} showed a relatively higher proliferative response to 0.1 ng/ml of rmSCF than the response of cells expressing KIT^{WT}. These mutations and *in vitro* functional analyses raise the possibility that the KIT abnormalities influence the white blood cell counts ($P < 0.05$) and survival ($P < 0.04$) of CML patients.

Leukemia (2002) 16, 170–177. DOI: 10.1038/sj/leu/2402341

Keywords: c-kit; CML; Ba/F3; WBC

Introduction

Philadelphia (Ph) chromosome is the cytogenetic hallmark of chronic myelogenous leukemia (CML) and is found in up to 95% of CML patients.¹ The demonstration of *bcr/abl* mRNA is accepted as a reliable diagnostic marker for CML, and in some cases this evidence is more reliable than the Ph chromosome.² The clinical signs and hematological findings probably depend partly on the presence of P210^{BCR/ABL}, which plays a central role in the pathogenesis of the chronic phase of CML.³ According to the breakpoint site of the *bcr* gene in most CML

patients, there are two *bcr/abl* mRNAs for P210^{BCR/ABL}, one with and one without exon b3 (b3-a2 type and b2-a2 type).⁴ In a smaller number of CML patients, there are two other types of *bcr/abl* mRNAs based on the breakpoint positions of the *bcr* gene, ie m-*bcr* and μ -*bcr* for P190^{BCR/ABL} and P230^{BCR/ABL}, respectively.^{5,6} Extensive studies have been performed on the subtypes of the *bcr/abl* gene and their relation to the prognosis and clinical features.^{7,8} The established findings regarding the influence of the subtype of the *bcr/abl* gene (b3-a2 or b2-a2) on the clinical characteristics have been similar for each subtype, except for a higher platelet count in patients with the b3-a2 type.^{4,9} P190^{BCR/ABL} in CML may be associated with monocytosis, and P230^{BCR/ABL} may be associated with the chronic neutrophilic leukemia variant and marked thrombocytosis.^{6,10} Other molecular factors which might control the clinical features and hematological characteristics remain unclear.

Recently, the stem cell factor (SCF) c-kit signal system (KIT/SCF) has been shown to play a crucial role in hematopoiesis.¹¹ The c-kit receptor tyrosine kinase (KIT) is expressed on progenitor stem cells as well as mast cells. SCF synergizes *in vitro* with other cytokines to increase the number and size of colonies of hematopoietic progenitors.¹² Thus, we speculated that the KIT/SCF system possibly controls the hematological characteristics of CML.

The present study was designed to investigate the mutations of the c-kit gene and the relationship between the *in vitro* function of mutant c-kit and the biological features of CML patients.

Materials and methods

Patients

We studied 116 bone marrow (BM) or peripheral blood (PB) samples obtained from 80 patients with CML in various clinical phases: 65 in chronic phase (CP), seven in accelerated phase (AP), and 44 in blastic crisis (BC). The diagnosis of CML was made on the basis of clinical features, hematological data and Ph chromosome. In 34 patients, both cytogenetic and molecular analyses were performed in more than two phases, ie CP and BC (30 patients), CP and AP (two patients), and CP, AP and BC (two patients). Sixty-eight normal BM or PB samples were obtained to study mutation and polymorphism of the c-kit gene. These samples were obtained with the patients' and normal volunteers' informed consent.

Cells

Ba/F3,¹³ a murine IL-3-dependent pro-B lymphoid cell line, was cultured in RPMI 1640 medium supplemented with 10% fetal calf serum (FCS) and 10% WEHI-3 cell conditioned medium.

Correspondence: K Inokuchi, Division of Hematology, Department of Internal Medicine, Nippon Medical School, 1-1-5 Sendagi, Bunkyo-ku, Tokyo 113, Japan; Fax: 81-3-5814-6934.
 Received 19 December 2000; accepted 3 October 2001

Extraction of RNA and DNA

The total RNA of BM or PB leukocytes was extracted with an RNazol kit (Biotex Laboratories, Houston, TX, USA), which was based on a technique described previously.¹⁴ The total cellular DNA was extracted from BM and PB cells by protease K digestion, phenol-chloroform extraction and ethanol precipitation.

RT-PCR of *c-kit* mRNA

RT-PCR was performed as described elsewhere.¹⁵ The sense primers were: kit560-1, 5'-CTGTTCACTCCTTGCTGAT-3' (residues 1582-1601); kit560-2, 5'-TTCGTAATCGTACCTGGCAT-3' (residues 1605-1624); kit816-1, 5'-ATCATGGAGGATGACGAGTTG-3' (residues 2287-2306); and kit816-2, 5'-CTAGACTTAGAAGACTTGCT-3' (residues 2310-2329). The antisense primers were: kit560-3, 5'-CATGTGATTACCAAGGTAA-3' (residues 1955-1974); kit560-4, 5'-GCTCCAAGTAGATTACAAT-3' (residues 1978-1997); kit816-3, 5'-ATTTCCAGCAGGTGCGTGTC-3' (residues 2698-2717); and kit816-4, 5'-TTTTTGGGGATCTGCATCC-3' (residues 2742-2761). Complementary DNA was synthesized from 500 ng of total cellular RNA extracted from cells using 100 ng of primer kit560-4 for analysis of the sequence in the juxtamembrane domain or kit816-4 for analysis of the phosphotransferase domain. Briefly, RT reaction mixture contained 32 U of avian myeloblastosis virus (AMV) RT (Takara Biochemicals, Shiga, Japan) in 25 μ l of a solution containing 200 μ mol/l each of all four dNTPs, 80 U of RNase inhibitor, 50 mmol/l Tris-HCl (pH 8.3), 75 mmol/l KCl, 10 mmol/l dithiothreitol and 3 mmol/l MgCl₂. The reaction was allowed to proceed for 60 min at 37°C, and the reaction mixture was used as the PCR substrate. A 35-cycle PCR reaction was performed in a DNA Thermal Cycler with slight modification of our original protocol.⁴ Briefly, 25 μ l of the RT reaction solution was mixed with a mixture containing 250 μ mol/l of each of all four dNTPs, 100 ng of 5'-primer ST1, 10 mmol/l Tris-HCl (pH 8.3), 50 mmol/l KCl, 3 U of Taq DNA polymerase (Takara Biochemicals) and 100 ng of primers kit560-1 and kit560-4 or primers kit816-1 and kit816-4. The reaction conditions and cycle number were the same as those described above. A second PCR was performed for direct sequencing. Primers kit560-2 and kit560-3 or primers kit816-2 and kit816-3 were used to amplify the first PCR products, whereas primers SC3 and ASC3 were used for the 3'-fragment.

Single-stranded conformation polymorphism (SSCP) gel analysis

Detection of *c-kit* mutations was performed by SSCP gel analysis. The 5'-ends of primers (100 pmol) were labeled with γ -³²P-ATP (3000 Ci/mmol) and polynucleotide (5 U, Boehringer-Mannheim; Mannheim, Germany) in 10 μ l of 50 mM Tris-HCl, pH 8.3, 10 mM MgCl₂ and 5 mM DTT at 37°C for 30 min. The PCR mixture contained 10 pmol of each of the labeled primers, 2 nmol each of the four deoxynucleotides, 0.1 μ g of sample cDNA or DNA, and 0.25 U of Taq polymerase in 10 μ l of the buffer provided in the GeneAmp kit. The PCR products were mixed with 10 volumes of a loading buffer containing 95% formamide, 20 mM EDTA, 0.05% bromophenol blue and 0.05% xylene cyanol, denatured at 94°C for 5 min, quenched on ice and applied (1 μ l/lane) to

a 10% polyacrylamide gel containing 90 mM Tris-borate, pH 8.3, 4 mM EDTA, and 10% glycerol. Electrophoresis was performed at 40 W for 3 h at 18° with cooling using a water jacket. The gel was dried on a filter paper and exposed to X-ray film at -80° for 1-24 h with an intensifying screen.

Sequence analysis of the *c-kit* gene

After the RT-PCR products were separated on 2% agarose gels and stained with ethidium bromide, the amplified fragment was excised from the gel, electroeluted, purified with phenol and precipitated with ethanol. The fragments were subcloned into the *EcoRV* site of the pGEM-5Zf(+/-) cloning vector.¹⁶ The transfected cells were plated on to Luria-Berani (LB)-ampicillin agar plates containing 5-bromo-4-chloro-3-indolyl- β -D-galactoside (X-Gal), isotransferred to fresh LB-ampicillin agar plates containing X-Gal and isopropylthio- β -D-galactoside, and cultured overnight for secondary selection. White colonies were transferred into 150 ml of LB medium containing 50 mg/ml ampicillin and cultured at 37°C for 4 h. The cultures were sedimented by centrifugation, resuspended in 20 ml of water and heated at 98°C for 10 min. After centrifugation, the supernatants were amplified by PCR using the T7 or SP6 primer. Three to five clones of the three independent PCR products were sequenced using a Model 377 ABI sequencer with dye terminators (Perkin Elmer, Warrington, UK). All sequences were confirmed in both orientations. A mutation was defined as when three or more clones showed the same abnormality of the base sequence.

Site-directed mutagenesis and transfection

To examine for functional abnormality of *c-kit* mutations in activation of *c-kit* tyrosine kinase activity, site-directed mutagenesis was performed using murine *c-kit* cDNA as described by Furitsu et al.¹⁷ The genes encoding murine wild-type *c-kit* and *c-kit* c-DNA with a mutation at codon 814 (GAC→GTC) in the *XbaI* site of the expression vector, pEF-BOS, were used as wild and mutant controls.¹⁸ These two *c-kit* expression vectors were kindly provided by Prof Y Kanakura (Osaka University, Osaka, Japan). To generate genes containing L-540, two oligonucleotide sets of 5'-GCAT-TATTGTGCTGATTCTGACCTACAAAT-3' and 3'-CAGAA TCAGCACAATAATGCATCATGCCC-5' were synthesized, annealed to the template and extended. To generate genes containing K-563, two oligonucleotide sets of 5'-GAGGAGA TAAGTGGAAACAATTATGTTTAC-3' and 3'-ATTGTTTCC ACTTATCTCCTCAACAACCTTCC A-5' were synthesized, annealed to the template and extended, according to the instructions accompanying the ExSite PCR-Based Site-Directed Mutagenesis kit (Stratagene, La Jolla, CA, USA). Fifteen temperature-cycles of PCR were performed to extend and incorporate mutation primers by Pfu Turbo DNA polymerase, resulting in formation of mutated circular strands. Methylated parental DNA template was digested with 10 U of Dpl. The mutated double-stranded plasmid was transformed into XL1-Blue *E. coli* cells to expand the plasmid after repairing the nicks with T4 DNA ligase. The *c-kit* cDNA and expression vectors were sequenced to confirm the mutations and absence of artifact abnormalities.

The expression vectors containing wild-type and mutated *c-kit* cDNA (10 μ g) were transfected by electroporation into 5 \times 10⁷ Ba/F3 cells with pSV2Neo (0.2 μ g), which encodes and

expresses the neomycin-resistant protein. The Ba/F3 cells were cultured in RPMI 1640 containing 10% FCS 600 $\mu\text{g}/\text{ml}$ G418 (Calbiochem-Novabiochem, San Diego, CA, USA) and 10% WEHI-3 cell-conditioned medium. After selection with G418 and limiting dilution of the cells, expression of KIT was confirmed by flow cytometry.

Flow cytometry

To detect cell surface expression of KIT, cells were incubated with fluorescein isothiocyanate (FITC)-conjugated anti-KIT (2B8 clone; PharMingen, San Diego, CA, USA) MoAb at 4°C for 30 min and analyzed on a FACScan (Becton Dickinson, Los Angeles, CA, USA).¹⁵

Immune complex kinase assay

The procedures of immunoprecipitation, gel electrophoresis and immunoblotting were performed according to the methods described previously.¹⁹ The cells were washed with PBS and lysed in 500 μl of RIPA buffer (50 mM Tris-HCl, pH 7.5, 150 mM NaCl, 5 mM EDTA, 1% NP-40, 0.5% deoxycholate, and 0.1% SDS with protease inhibitors (1 mM PMSF, 50 $\mu\text{g}/\text{ml}$ of antipain, 5 $\mu\text{g}/\text{ml}$ of aprotinin, and 2 $\mu\text{g}/\text{ml}$ of leupeptin)). Cell debris was removed by centrifugation. The supernatant was precleared by incubation with protein-G Sepharose (Pharmacia, Uppsala, Sweden) on ice for 30 min. The precleared lysates were incubated with anti-mouse c-kit MoAb, 2B8 (PharMingen) for 1 h on ice and with Protein-G Sepharose for 30 min on ice to collect antigen-antibody complexes. The immunoprecipitates were washed three times with NP-40 buffer (50 mM Tris, pH 8.0, 1.0% NP-40, 50 mM NaCl) containing protease inhibitors. The proteins released from the immunoprecipitates by Laemli's sample buffer were subsequently analyzed by electrophoresis on 5–25% SDS-PAGE. The proteins were electrophoretically transferred from the gel on to a nitrocellulose membrane. After the transfer, the filter was blocked by incubation in 1% BSA/Tween-PBS (1.37 M NaCl, 27 mM KCl, 81 mM Na_2HPO_4 , 15 mM KH_2PO_4 , 1% Tween-20, 1% BSA). Immunoblotting was performed with an antiphosphotyrosine MoAb (Py20; PharMingen) or anti-c-kit antibody, and detected with HRP-conjugated goat anti-mouse IgG (Santa Cruz Biotechnology, Santa Cruz, CA, USA). All immunoprecipitates were detected with HRP-conjugated goat anti-mouse IgG and visualized by autoradiography.

Semiquantification of the photographic signals was performed using an MCID image analysis system (Imaging Research, St Catharines, Ontario, Canada). The entire width of the lane was analyzed with appropriate background subtraction. All bands in one photograph were analyzed together. The relative intensity was defined as the ratio of the KIT phosphorylation signals to KIT^{V814} signals at 15 min incubation.

Cell proliferation assay

Proliferation of cells was quantified by ³H-thymidine incorporation. Briefly, the cells were washed twice with IMDM medium, and triplicate aliquots of cells (5×10^4) suspended in 200 μl of Cosmedium-001 (Cosmo Bio Co., Tokyo, Japan) were cultured in 96-well microtiter plates for 72 h at 37°C in the presence of various concentrations of rmIL-3 or rmSCF, provided by Kirin Brewery Company, Ltd. At 72 h after

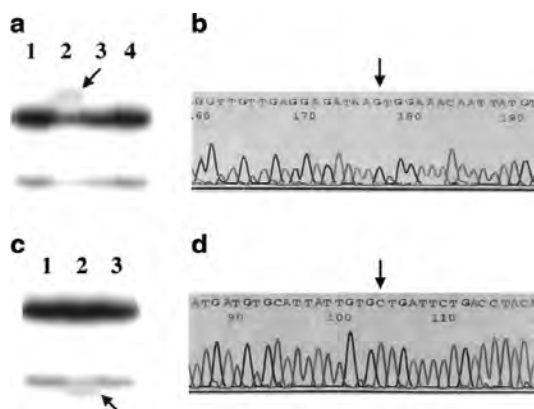


Figure 1 RT-PCR-SSCP analysis and sequencing of the cloned RT-PCR products of the c-kit gene of the CML cases detected abnormalities. (a) and (b) show the RT-PCR-SSCP and sequence of the RT-PCR products of case 1. (c) and (d) show the RT-PCR-SSCP and sequence of the RT-PCR products of case 2. (a) Lane 1: RT-PCR product of RNA sample from chronic phase; lane 2: RT-PCR product of blastic crisis; lane 3: RT-PCR product of hair root; lane 4: RT-PCR product of skin. The arrow indicates an abnormal band. (b) Sequence of the cloned RT-PCR product of blastic crisis sample. The arrow indicates a one-base change (codon 564, AAT→AAG). (c) Lane 1: RT-PCR product of RNA sample from chronic phase; lane 2: RT-PCR product of blastic crisis; lane 3: RT-PCR product of hair root. The arrow indicates an abnormal band. (d) Sequence of the cloned RT-PCR product of blastic crisis sample. The arrow indicates a one-base change (codon 541, ATG→CTG).

initiation of the culture, 0.5 μCi ³H-thymidine (specific activity, 5 Ci/mmol; Amersham, Arlington Heights, IL, USA) was added to each well. Five hours later, the cells were harvested with a semi-automatic cell harvester (Pharmacia), and the incorporation of ³H-thymidine was measured with a liquid scintillation counter.

Determination of the type of bcr/abl mRNA

Reverse transcriptase-polymerase chain reaction analysis (RT-PCR) for determination of the type of bcr/abl mRNA was carried out as described previously.^{4,16} Briefly, complementary DNA (cDNA) was prepared from 250 ng of total RNA using an antisense ABL cDNA primer. Primers bcr-1 and abl-1 were used for PCR for p210 mRNA, whereas primers e-1 and abl-1 were used for p190 mRNA. The PCR products were electrophoresed through a 2.5% agarose gel, stained with ethidium bromide, Southern-transferred and hybridized.

Table 1 Frequency of c-kit abnormality in CML patients and hematologically healthy volunteers

Abnormality	CML patients with abnormality/total CML patients (positive rate)	Healthy volunteers with abnormality/Total hematologically healthy volunteers (positive rate)
Mutation at codon 564	1/80 (1.3%)	0/68 (0%)
Mutation at codon 541	6/80 (7.5%)	1/68 (1.5%) ^a

^a*P* < 0.05 compared with 80-patient CML group.

Table 2 Summary of CML patients with a c-kit abnormality

Case No.	Sex/Age (yr)	Abnormality of c-kit			WBC ^b (μl)	Plt ^c (×10 ³ /μl)	Hb ^d (g/dl)	Bcr/abl type	Additional chromosomal abnormality in BC	Survival duration (months)	Giant splenomegaly	Treatment
		Codon	Nucleotide/ Amino acid	Sample for detection								
1	M/52	564	AAT→AAG Asn→Lys	BC	100600	2.60	13.0	B2a2	del(3)(q21q23)	41	Yes	IFN+HU→VP
2	M/57	541	ATG→CTG Met→Leu	BC	11200	35.8	13.7	B3a2	+X	61	No	IFN→VP
3	M/23	541	ATG→CTG Met→Leu	CP, BC, skin, HR	276800	32.8	10.2	B3a2	15q-, 17q+	94	Yes	IFN+HU→VP
4	F/36	541	ATG→CTG Met→Leu	CP, BC, skin, HR	67000	37.0	13.1	B3a2	ND	32	No	IFN+HU→VP
5	F/45	541	ATG→CTG Met→Leu	CP, BC, skin, HR	178000	30.4	12.0	B3a2	None	75+	Yes	IFN+HU
6	F/44	541	ATG→CTG Met→Leu	CP, BC, skin, HR	52000	34.0	9.0	Minor	None	11	Yes	HU→VP
7	M/64	541	ATG→CTG Met→Leu	BC, skin ^a	75700	7.5	8.9	Minor	t(9;14)(q34;q32)	7	No	VP

Normal range of neutrophil alkaline phosphatase (NAP): 150–350.

^aRNA samples of BC and skin were able to be analyzed.

^bNumbers were those at diagnosis of CP.

CP, chronic phase; BC, blastic crisis; HR, hair root; ND, not done; IFN, interferon-α; HU, hydroxyurea; VP, combined therapy with vincristine and prednisolone.

Statistical analysis

Statistical analysis was performed using the Statview (Brain Power, Calabashes, CA, USA) software package for the Macintosh personal computer. Comparisons of groups were analyzed using Fisher's exact test for 2×2 tables. Values of $P < 0.05$ were considered significant.

Results

c-kit mutations in CML patients

Eighty CML cases were screened for mutations in the coding region of the c-kit gene by RT-PCR-SSCP. Expression of the c-kit gene was detected in all 80 CML patients by RT-PCR. Seven cases showed aberrant bands on RT-PCR-SSCP gels. Sequencing of the RT-PCR fragments which showed aberrant bands on the RT-PCR-SSCP gels revealed one of the seven cases had an abnormality at codon 564 (AAT→AAG, Asn→Lys) in the juxtamembrane domain, while six cases had an abnormality at codon 541 (ATG→CTG, Met→Leu) (Figure 1). These two base abnormalities were observed in cDNA clones generated from three independent PCR products. Sixty-eight normal BM aspirate samples were obtained from hematologically healthy volunteers after obtaining informed consent and used as normal controls. One of the 68 healthy normal BM samples had the same migration pattern by SSCP and the same alteration as that of our CML patients at codon 541 in which ATG was changed to CTG, resulting in a change in the encoded amino acid from Met to Leu (Table 1). The same codon 541 abnormality was detected in RNA samples from skin and hair roots of cases 3, 4, 5 and 6 (Table 2). Because the amino acid substitution was a conservative one which was also observed in the normal population and normal tissues of the CML patients, it probably represents a polymorphic variation. Intriguingly, however, RNA samples from the hair roots and leukemic cells at CP of case 2 were demonstrated to have no abnormality, whereas this case showed the same abnormality at codon 541 (ATG→CTG, Met→Leu) in the leukemic cells at BC. Thus, we think the alteration of codon 541, in which ATG was changed to CTG, occurred

during leukemic progression of case 2. In case 1, the abnormality at codon 564 was detected only in an RNA sample from leukemic cells at BC (Figure 1).

c-kit receptor tyrosine kinase

In order to determine the functional role of c-kit abnormalities in ligand-independent activation of c-kit products, expression vectors containing normal or mutated murine c-kit genes were transfected into a murine IL-3-dependent cell line, Ba/F3 cells.

We used site-directed mutagenesis to construct two mutant murine c-kitR expression vectors: c-kit^{K563} coding for substitution of Lys for Asn at codon 563, and c-kit^{L540} coding for substitution of Leu for Met at codon 540, which correspond to Lys-564 and Leu-541 of abnormal human c-kitR, respectively. These murine c-kit-expression vectors were co-transfected into the Ba/F3 murine IL-3-dependent cell line with pSV2Neo, which contains the *neomycin* resistance gene, by electroporation. As a negative control, the pEF-BOS vector, without the c-kit gene, was transfected into Ba/F3 cells. After selection in a G418-containing medium for 2 weeks, surface expression of KIT on the transfected cells was examined with DX2, an anti-mouse c-kit MoAb. Flow cytometric analysis showed that, although transfection of Ba/F3 cells with the pEF-BOS vector alone resulted in no expression of KIT, Ba/F3 cells transfected with pEF-BOS-KIT^{WT}, pEF-BOS-KIT^{V814}, pEF-BOS-KIT^{K563} or pEF-BOS-KIT^{L540} showed abundant surface expression of KIT^{WT}, KIT^{V814}, KIT^{K563} or KIT^{L540} on their surface, respectively (Figure 2a).

State of tyrosine phosphorylation of KIT^{K563} or KIT^{L540}

To examine the state of KIT-tyrosyl phosphorylation in the transfected Ba/F3 cells, the cells were deprived of serum and growth factors for 12 h and then stimulated with 0.1, 1 or 100 ng/ml of rmSCF for 15 min. KIT was then immunoprecipitated and assayed by immunoblotting with either antiphosphotyrosine MoAb or anti-c-kit MoAb. As shown in Figure 2b, when wild-type or mutated c-kit genes were transfected into Ba/F3, the c-kit gene products were synthesized in the cells as 145-

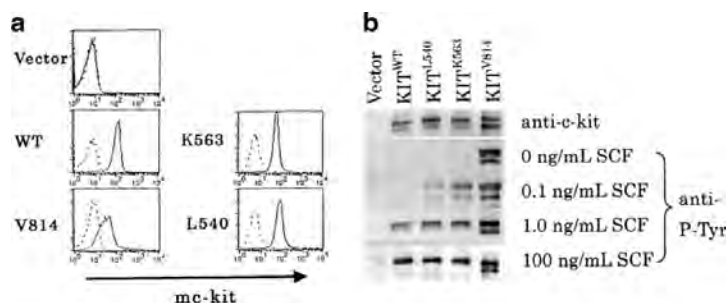


Figure 2 Flow cytometric analysis and tyrosine phosphorylation of Ba/F3^{Vector}, Ba/F3- KIT^{WT}, Ba/F3- KIT^{V814}, Ba/F3- KIT^{K563} and Ba/F3- KIT^{L540}. (a) Flow cytometric analysis of the surface binding of a monoclonal anti-c-kit antibody to Ba/F3 cells transfected with pEF-BOS vector alone (Vector), pEF-BOS-KIT^{WT}, pEF-BOS-KIT^{V814}, pEF-BOS-KIT^{K563} or pEF-BOS-KIT^{L540}. Cells were incubated with either FITC-conjugated negative-control antibody (—) or 2B8 (—), washed and analyzed on a FACScan. (b) Tyrosine phosphorylation of KIT in Ba/F3 cells expressing KIT^{WT}, KIT^{V814}, KIT^{K563} and KIT^{L540}. KIT was immunoprecipitated with an anti-c-kit MoAb (2B3) from lysates of the indicated cells before and after stimulation with rmSCF (0, 0.1, 1.0 or 100 ng/ml). The immunoprecipitates were separated by SDS-PAGE and then immunoblotted with antiphosphotyrosine (anti-P-Tyr) MoAb (second to fifth rows). The immunoprecipitates of Ba/F3 cells were cultured with 0 ng/ml of SCF, divided into two aliquots, separated by SDS-PAGE, and then immunoblotted with anti-c-kit (2B3) (first row). All immunoprecipitates were detected with HPR-conjugated goat anti-mouse IgG and visualized by autoradiography.

and 125-kDa proteins, respectively. Immunoblotting with an antiphosphotyrosine MoAb showed that increased phosphotyrosine was observed in KIT^{V814} regardless of rmSCF stimulation. In contrast, KIT^{WT}, KIT^{L540} and KIT^{K563} were dose-dependently phosphorylated on tyrosine after treatment with increasing concentrations of rmSCF. KIT^{L540} and KIT^{K563} were found to be more phosphorylated on tyrosine than KIT^{WT} at 0.1 and 1.0 ng/ml of rmSCF (Figure 2).

Repeated semi-quantification of immunoblots (Figure 3a) and the time course for the induction using a narrower range of concentrations between 0 and 1.0 ng/ml of rmSCF (Figure 3b) successfully showed dose-dependent activation of KIT^{L540} and KIT^{K563} as well as KIT^{WT}, although KIT^{V814} and KIT^{K563} showed relatively higher efficiency than KIT^{WT} between 0.1 and 1.0 ng/ml of rmSCF (Figure 3).

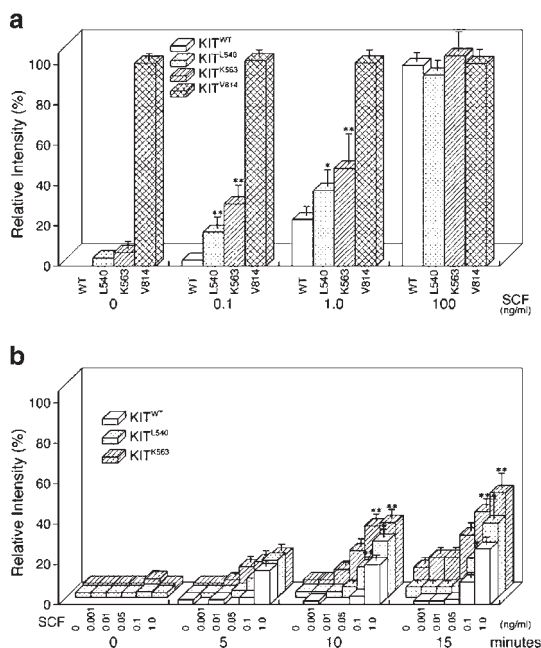


Figure 3 Semiquantification of tyrosine-phosphorylation signals of KIT in Ba/F3 cells expressing KIT^{WT}, KIT^{V814}, KIT^{K563} and KIT^{L540}. (a) Semiquantification of tyrosine-phosphorylation signals of KIT in Ba/F3 cells expressing KIT^{WT}, KIT^{V814}, KIT^{K563} and KIT^{L540} in Figure 2b. The representative data from three independent experiments are shown with error bars. The relative intensities of tyrosine-phosphorylation signals of KIT in Ba/F3 cells expressing KIT^{WT}, KIT^{K563} and KIT^{L540} compared with those of KIT^{V814} are given as the mean \pm s.d. for three independent experiments. (b) Time course of tyrosine-phosphorylation signals of KIT in Ba/F3 cells expressing KIT^{WT}, KIT^{V814}, KIT^{K563} and KIT^{L540}. Incubation times were 0, 5, 10 and 15 min. SCF concentrations were six points between 0 and 1.0 ng/ml. Relative intensities of tyrosine-phosphorylation signals of KIT in Ba/F3 cells expressing KIT^{WT}, KIT^{K563} and KIT^{L540} compared with those of KIT^{V814} are given as the mean \pm s.d. for three independent experiments. Significantly higher values were obtained for Ba/F3 cells expressing KIT^{K563} or KIT^{L540} compared with those expressing KIT^{WT}. * $P < 0.05$; ** $P < 0.01$.

KIT^{L540} and KIT^{K563} modulation in IL-3-dependent Ba/F3 growth

To determine if KIT^{L540} and KIT^{K563} could modulate IL-3- or SCF-dependent growth, Ba/F3 cells expressing KIT^{WT}, KIT^{V814}, KIT^{L540} or KIT^{K563} were cultured in the presence of 0 to 100 ng/ml of rmlL-3 or 0 to 1000 ng/ml of rmSCF for 72 h, followed by measurement of cell proliferation using ³H-thymidine uptake assay (Figure 4). It was demonstrated that rmlL-3 induced dose-dependent proliferation whereas rmSCF induced no proliferation in the parental Ba/F3 or pEF-BOS-transfected Ba/F3 cells. In addition to the proliferative response to rmlL-3, Ba/F3 cells expressing KIT^{WT}, KIT^{K563} and KIT^{L540} induced dose-dependent proliferation in response to rmSCF over the range of 0.1 to 1000 ng/ml, indicating functional expression of KIT^{WT}, KIT^{K563} and KIT^{L540}. KIT^{K563} induced a higher proliferative response to 0, 0.1 and 1 ng/ml of rmSCF than KIT^{WT}. The proliferative response to 0.1 ng/ml of rmSCF by Ba/F3 cells expressing KIT^{L540} was relatively higher than the response by cells expressing KIT^{WT}. In contrast, Ba/F3 cells expressing KIT^{V814} proliferated even in the absence of both rmlL-3 and rmSCF.

Clinical features of CML patients with c-kit abnormality

Table 2 shows the relationships between the clinical data and the molecular characteristics of the seven CML cases with a c-kit abnormality. Three kinds of bcr/abl junctions, ie the b2-a2 and b3-a2 types of major bcr breakpoint, and the minor bcr/abl type of minor bcr breakpoint, are shown in Table 2. One of the seven CML cases with c-kit gene alterations had the b2-a2 type, while four had the b3-a2 type. Intriguingly, two CML patients with a c-kit abnormality had the rare, minor bcr/abl type. Case 6 had extramedullary onset, and case 7 had received 5-FU medication for several years for esophageal cancer. As shown in Table 2, the platelet counts of all seven cases at diagnosis of CP were within or below the normal range, regardless of the type of bcr/abl junction. The platelet counts of CML with 564^{Lys}-541^{Leu}-KIT were marginally lower ($P < 0.07$, Table 3) than the counts of CML with wild-type KIT (WT-KIT). The WBC count at diagnosis of six mutated cases was markedly higher than the other 73 cases of CML with KIT^{WT} ($P < 0.05$, Table 3). The WBC count was relatively low in case 2 with a normal c-kit gene in CP. The mean survival duration of the seven CML patients with 564^{Lys}-541^{Leu}-KIT was 45.9 months, while that of the CML patients without any KIT abnormality was 69.6 months (Table 3). 564^{Lys}-KIT and 541^{Leu}-KIT may be prognostic factors ($P < 0.04$), as shown in Table 3.

Discussion

The interstitial cells of Cajal (ICCs) and hematopoietic stem cells express both KIT and CD34. Gastrointestinal stromal tumors (GISTs) may originate from the ICCs.²⁰ CML may originate from hematopoietic stem cells that are double-positive for KIT and CD34. High expression of c-kit has been demonstrated on CD34⁺ cells from chronic-phase CML patients.²⁰ Here, we successfully demonstrated that the juxtamembrane domain mutant occurs in some CML cells which are double-positive for KIT and CD34 as well as in ICCs. The juxtamembrane domain mutant is found in GISTs.²¹ The juxtamembrane

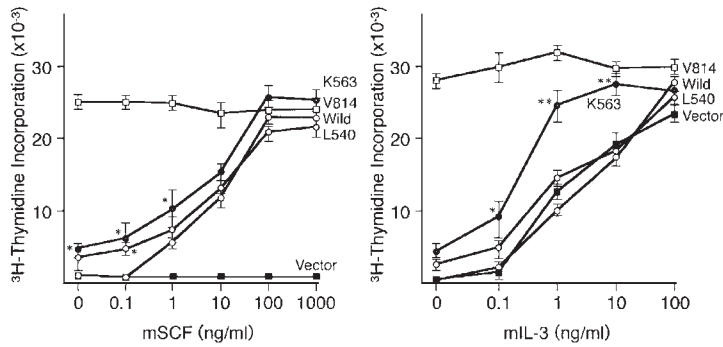


Figure 4 Proliferation of Ba/F3 cells in response to various concentrations of rmSCF (left panel) and rmlL3 (right panel). Quadruplicate aliquots of cells expressing KIT^{WT}, KIT^{V814}, KIT^{K563} or KIT^{L540} were cultured with each factor, and cell proliferation was measured by ³H-thymidine incorporation assay. The results are shown as the mean \pm s.d. for three separate experiments. Wild, V814, K563 and L540 mean Ba/F3 cells expressing KIT^{WT}, KIT^{V814}, KIT^{K563} and KIT^{L540}, respectively. Vector means Ba/F3 cells transfected with the pEF-BOS vector. Significantly higher values were obtained for Ba/F3 cells expressing KIT^{K563} or KIT^{L540} compared with those expressing KIT^{WT}. * $P < 0.05$; ** $P < 0.01$.

Table 3 Summary of total CML patients of the two groups

	CML with c-kit mutation (n = 7)	CML with WT c-kit (n = 73)
Mean age \pm s.d. (yr)	45.9 \pm 13.6	44.6 \pm 16.5
Male	4	40
Female	3	33
WBC ($\times 10^4/\mu$ l)	12.5 \pm 8.7 (n = 6) ^c	7.0 \pm 5.8 ($P < 0.05$) ^b
Platelet ($\times 10^4/\mu$ l)	29.07 \pm 10.1	69.8 \pm 64.4 ($P < 0.07$) ^b
Overall survival (months)	45.9 \pm 32.5	69.6 \pm 22.4 ($P < 0.04$) ^a

^aLog rank P value.

^bStudent's t -test.

^cCase 2 having WT-KIT in CP was omitted.

domain mutant is also found in mast cell leukemia.²² The tyrosine kinase domain mutant occurs only in human and murine mast cell leukemia, but the mechanism of tumorigenesis differs between the juxtamembrane domain mutant and the tyrosine kinase domain mutant. The former, the juxtamembrane domain mutant, is constitutively dimerized and activated without binding SCF, whereas the latter, the tyrosine kinase domain mutant, is constitutively activated without forming dimers.²³ In GISTs, mutations are located within an 11-amino acid stretch (Lys-550 to Val-560).²¹ The tyrosine kinase and proliferation of Ba/F3 cells expressing these mutated KIT proteins were constitutively activated without SCF.²¹ Another report shows two major types of deletion mutations involving codons 550–565 and codons 566–580, stretches which were especially common in GISTs.²² In murine mastocytoma cells, the mutation is deletion of a 7-amino acid stretch (Thr-573 to His-579).²⁴ Point mutations/polymorphism at codon 564 or 541 is within or near these stretches involved in GIST mutations and deletion mutations of murine mastocytoma, although these mutations resulted in these mutant KITs not being constitutively activated. These *in vitro* biological differences may be partly due to differences in the mutation type, such as deletions of many nucleotides or one nucleotide mutation.

The 541^{Leu}-KIT mutation may be one of polymorphism, since it is found even in normal healthy people. In our CML patients, however, the frequency of the 541^{Leu}-KIT polymorphism was relatively more common compared with in normal individuals (Table 1). This higher frequency in CML was partly due to a newly occurring mutation at BC, such as in case 2.

The Ba/F3-cell proliferation-inducing activity of KIT^{L540} was the same as that of KIT^{WT}. Tyrosine kinase activation of KIT^{L540} was slightly higher than that of KIT^{WT} in medium containing 0.1 ng/ml of SCF. The tyrosine kinase activation and Ba/F3-cell proliferation activities of KIT^{K563} were relatively higher than those of wild-type KIT in medium containing between 0.1 and 1.0 ng/ml of SCF. Based on these *in vitro* data on tyrosine kinase activation and proliferation activities, KIT^{L540} and KIT^{K563} do not have exactly the same function as KIT^{WT}. Unlike KIT^{WT}, KIT^{L540} and KIT^{K563} may cause very low levels of spontaneous tyrosine kinase activation and cell proliferation even without SCF, as shown in Figures 3 and 4. These findings may indicate that 541^{Leu}-KIT does not fall within the category of polymorphism. This is because the KIT abnormality of these cases was more common (8.8%) than in the normal healthy cases (1.5%; $P < 0.05$).

We speculate that these tiny differences in *in vitro* function may influence the clinical phenotype of CML. Recently, an internal tandem duplication (ITD) of the juxtamembrane (JM) domain-coding sequence of the FLT3 gene in acute myeloid leukemia patients was found to lead to leukocytosis and shorter survival.²⁵ The KIT and FLT3 proteins are members of the class III receptor tyrosine kinase family.²⁶ The ITD mutant of FLT3 is constitutively dimerized and autophosphorylated on tyrosine residues.²⁷ The KIT^{L540} and KIT^{K563} abnormalities of JM may be more easily dimerized and autophosphorylated than KIT^{WT} between 0 and 1.0 ng/ml SCF. This phenomenon may result in a tiny change in the structure of the KIT molecule which causes CML cells to undergo greater proliferation and culminates in shorter survival of CML patients.

Overall, the present analysis found that these c-kit mutations do not greatly affect the pathogenesis of CML, although the presence of these mutations resulted in clinical heterogeneity of the blood and a poorer prognosis for CML patients bearing a mutation vs CML patients with normal c-kit. The poor prognosis is probably due to the higher proliferation-inducing activities of 564^{Lys}-, 541^{Leu}-KIT than WT-KIT between

0 and 1.0 ng/ml SCF. The serum SCF concentration in our CML patients was between 0.5 and 1.5 ng/ml (preliminary data). Thus, CML blasts exposed to SCF concentrations between 0.5 and 1.5 ng/ml possibly undergo greater phosphorylation and proliferation.

Although our findings do not fully explain the mechanisms by which 564^{Lys}-, 541^{Leu}-KIT lead to clinical heterogeneity of CML, a small functional difference from KIT^{WT} is thought to be one cause of differences in the prognosis and the phenotype of leukocytosis in CML.

Acknowledgements

We thank Dr Y Kanakura for providing full-length murine c-kit expression vectors and Kirin Brewery Company, Ltd for providing rmlL-3 and rmSCF. This work was supported by Grants-in-Aid from the Ministry of Education, Science and Culture of Japan and the Takahashi Foundation.

References

- Groffen J, Stephenson JR, Heisterkamp N, de Klein A, Bartram CR, Grosveld G. Philadelphia chromosomal breakpoints are clustered within a limited region, bcr, on chromosome 22. *Cell* 1984; **36**: 93–99.
- Kantarjian HM, Smith TL, McCredie KB, Keating MJ, Walters RS, Talpaz M, Hester JP, Bligham G, Gehan E, Freireich EJ. Chronic myelogenous leukemia: a multivariate analysis of the associations of patient characteristics and therapy with survival. *Blood* 1985; **66**: 1326–1335.
- Shtivelman E, Lifshitz B, Gale RP, Canaani E. Fused transcripts of abl and bcr genes in chronic myelogenous leukemia. *Nature* 1985; **315**: 550–554.
- Inokuchi K, Inoue T, Tojo A, Futaki M, Miyake K, Yamada T, Tanabe Y, Ohki I, Dan K, Ozawa K, Asano S, Nomura T. A possible correlation between the type of bcr-abl hybrid messenger RNA and platelet count in Philadelphia-positive chronic myelogenous leukemia. *Blood* 1991; **78**: 3125–3127.
- Yamaguchi H, Inokuchi K, Shinohara T, Dan K. Extramedullary presentation of chronic myelogenous leukemia with p190 BCR/ABL transcripts. *Cancer Genet Cytogenet* 1998; **102**: 74–77.
- Yamagata T, Mitani K, Kanda Y, Yazaki Y, Hirai H. Elevated platelet count features the variant type of BCR/ABL junction in chronic myelogenous leukemia. *Br J Haematol* 1996; **94**: 370–372.
- Mills KI, Birnie GD. Does the breakpoint within the major breakpoint cluster region (M-bcr) influence the duration of the chronic phase in chronic myeloid leukemia? An analytical comparison of current literature. *Blood* 1991; **78**: 1155–1161.
- Shtalrid M, Talpaz M, Kurzrock R, Kantarjian H, Trujillo J, Guterman J, Galina Y, Mark B. Analysis of breakpoints within the bcr gene and their correlation with clinical course of Philadelphia-positive chronic myelogenous leukemia. *Blood* 1988; **72**: 485–490.
- Faderl S, Talpaz M, Estrov Z, O'Brien S, Kurzrock R, Kantarjian HM. The biology of chronic myeloid leukemia. *N Engl J Med* 1999; **341**: 164–172.
- Melo JV, Myint H, Galton DAG, Goldman JM. P190 BCR-ABL chronic myeloid leukemia: the missing link with chronic myelomonocytic leukemia? *Leukemia* 1994; **8**: 208–211.
- Ogawa M, Matsuzaki Y, Nishikawa S, Hayashi S-I, Kunisada T, Sudo T, Kina H, Nakauchi H, Nishikawa S-I. Expression and function of c-kit in hematopoietic progenitor cells. *J Exp Med* 1991; **174**: 63–71.
- Bernstein ID, Andrew RG, Zsebo KM. Recombinant human stem cell factor enhances formation of colonies by CD34⁺ and CD34⁺lin[−] cells, and the generation of colony-forming cell progeny from CD34⁺lin[−] cells cultured with interleukin-3, granulocyte colony-stimulating factor, or granulocyte-macrophage colony-stimulating factor. *Blood* 1991; **77**: 2316–2321.
- Palacios R, Steinmetz M. IL3-dependent mouse clone that express B-220 surface antigen, contain Ig genes in germ-line configuration, and generate B lymphocytes *in vivo*. *Cell* 1985; **41**: 727–734.
- Tanosaki S, Inokuchi K, Shimada T, Dan K. Relation between microsatellite instability and N-ras mutation and duration of disease free survival in patients with acute leukemia. *Cancer* 1998; **83**: 475–481.
- Abo J, Inokuchi K, Dan K, Nomura T. p53 and N-ras mutations in two new leukemia cell lines established from a patient with multilineage CD7-positive acute leukemia. *Blood* 1993; **82**: 2829–2836.
- Inokuchi K, Fukaki M, Hanawa H, Tanosaki S, Yamaguchi H, Iwakiri R, Nomura T, Dan K. Heterogenous expression of bcr-abl fusion mRNA in a patient with Philadelphia-chromosome-positive acute lymphoblastic leukemia. *Br J Haematol* 1997; **97**: 837–840.
- Furitsu T, Tsujimura T, Yono T, Ikeda H, Kitayama H, Koshimizu U, Sugahara H, Butterfield JH, Ashman LK, Kanayama Y, Matsuzawa Y, Kitamura Y, Kanakura Y. Identification of mutations in the coding sequence of the proto-oncogene c-kit in a human mast cell leukemia cell line causing ligand-dependent activation of c-kit. *J Clin Invest* 1993; **92**: 1736–1744.
- Mizushima S, Nagata S. pEF-BOS, a powerful mammalian expression vector. *Nucleic Acids Res* 1990; **18**: 5322.
- Inokuchi K, Miyake K, Takahashi H, Dan K, Nomura T. DCC protein expression in hematopoietic cell populations and its relation to leukemogenesis. *J Clin Invest* 1996; **97**: 852–857.
- Martin-Henao GA, Quiroga R, Sureda A, Garcia S. CD7 expression on CD34⁺ cells from chronic myeloid leukemia in chronic phase. *Am J Hematol* 1999; **61**: 178–186.
- Hirota S, Isozaki K, Moriyama Y, Hashimoto K, Nishida T, Ishiguro S, Kawano K, Hanada M, Kurata A, Takeda M, Tunio GM, Matsuzawa Y, Kanakura Y, Shinomura Y, Kitamura Y. Gain-of-function mutations of c-kit in human gastrointestinal stromal tumors. *Science* 1998; **279**: 577–580.
- Tsujimura T, Furitsu T, Morimoto M, Isozaki K, Nomura S, Matsuzawa Y, Kitamura Y, Kanakura Y. Ligand-independent activation of c-kit receptor tyrosine kinase in a murine mastocytoma cell line P-815 generated by a point mutation. *Blood* 1994; **83**: 2619–2626.
- Sakurai S, Fukasawa T, Chong JM, Tanaka A, Fukayama M. C-kit gene abnormalities in gastrointestinal stromal tumors (tumors of interstitial cells of Cajal). *Jpn J Cancer Res* 1999; **90**: 1321–1328.
- Tsujimura T, Morimoto M, Hashimoto K, Moriyama Y, Kitayama H, Matsuzawa Y, Kitamura Y, Kanakura Y. Constitutive activation of c-kit in FMA3 murine mastocytoma cells caused by deletion of seven amino acids at the juxtamembrane domain. *Blood* 1996; **87**: 273–283.
- Kiyoi H, Naoe T, Nakano Y, Yokota S, Minami S, Miyawaki S, Asou N, Kuriyama K, Jinnai I, Shimazaki C, Akiyama H, Saito K, Oh H, Moyoji T, Omoto E, Saito H, Ohno R, Ueda R. Prognostic implication of FLT3 and N-RAS gene mutations in acute myeloid leukemia. *Blood* 1999; **93**: 3074–3080.
- Matthews W, Jordan CT, Wiegand GW, Pardoll D, Lemischka IR. A receptor tyrosine kinase specific to hematopoietic stem and progenitor cell-enriched populations. *Cell* 1991; **65**: 1143–1152.
- Hayakawa F, Towatari M, Kiyoi H, Tanimoto M, Kitamura T, Saito H, Naoe T. Tandem-duplicated Flt3 constitutively activates STAT5 and MAP kinase and introduces autonomous cell growth in IL-3-dependent cell lines. *Oncogene* 2000; **19**: 624–631.

Loss of *DCC* Gene Expression Is of Prognostic Importance in Acute Myelogenous Leukemia

Koiti Inokuchi,¹ Hiroki Yamaguchi,
Hideki Hanawa, Sakae Tanosaki,
Kayo Nakamura, Miki Tarusawa, Koichi Miyake,
Takashi Shimada, and Kazuo Dan

Division of Hematology, Department of Internal Medicine and
Department of Biochemistry and Molecular Biology, Nippon Medical
School, Tokyo 113-8603, Japan

ABSTRACT

Purpose: Expression of the deleted in colorectal carcinoma (*DCC*) gene has been found to be lost in some patients with acute myelogenous leukemia (AML). Although this finding is critical to leukemogenesis, its prognostic significance remains uncertain. To evaluate this, loss of *DCC* gene expression in AML patients and their prognostic significance were investigated.

Experimental Design: A group of 170 patients with AML was analyzed. *DCC* gene expression in AML cells was determined by a semiquantitative reverse transcriptase-PCR. Simultaneous mutation analyses of the *p53*, *N-ras*, and *FLT3* genes were performed in all of the AML cells by single-strand conformation polymorphism and sequencing subsequent to PCR. The importance of loss of *DCC* expression was evaluated by Cox proportional analysis and the Kaplan-Meier method.

Results: Loss of *DCC* expression was detected in 47 patients (27.6%). The *p53*, *N-ras*, and *FLT3* mutations were detected in 20 (11.7%), 42 (24.7%), and 26 (15.2%) patients, respectively. The durations of overall survival (OS) and complete remission (CR) of the 47 *DCC*-negative AML patients were significantly shorter than that of the 123 *DCC*-positive patients ($P < 0.0045$ and <0.0060 , respectively). Univariate and multivariate analyses showed that loss of *DCC* expression was an unfavorable prognostic factor for both OS ($P < 0.0053$ and <0.0084 , respectively) and CR duration ($P < 0.0146$ and <0.0371 , respectively). The 64 *DCC*-positive patients with wild *p53*, *N-ras*, and *FLT3* had statistically better CR attainment compared with the other 106 patients ($P < 0.0001$).

Conclusions: Loss of *DCC* gene expression was shown to be an independent prognostic factor in AML patients. Thus,

loss of *DCC* gene expression might serve as an important molecular marker for predicting the CR duration and OS of patients with AML.

INTRODUCTION

Carcinogenesis is a multistep process in which accumulation of additional genomic alterations drives tumor progression (1, 2). Nonrandom chromosomal loss or deletion suggests that antioncogenes are also involved in AML² (3, 4). Mutations of the *p53* gene have been observed in AML, although the incidence of these events is lower than in solid tumors (5). Mutations of the *N-ras* gene are also associated with the pathogenesis of AML. *N-ras* gene mutations are found in 20–30% of AML patients (6, 7). An internal TD of exons 11 and 12 and mutation of aspartic acid at codon 835 (Asp835) in the *FLT3* gene are sometimes involved (in ~20% of AML patients; Ref. 8). The mutant *N-ras* and *FLT3* are ligand independently phosphorylated and play an important role in the proliferation of leukemia cells (9).

The *DCC* gene, which is deleted in colorectal cancer, has been identified as a possible tumor suppressor gene (10). *DCC* gene expression has been found to be lost in some patients with acute leukemias or myelodysplastic syndromes (11, 12). Although these findings suggest that a loss of *DCC* expression is critical to leukemogenesis, the *DCC* function that may mediate tumor suppression remains unclear (13). Recently, the *DCC* protein was found to transduce signals, resulting in activation of caspases (14) and inhibition of *cdk1* (15). These observations suggest that *DCC* protein product may suppress carcinogenesis.

To evaluate the role of the *DCC* gene in leukemias, we studied the expression of the *DCC* gene in AML using the RT-PCR and investigated its PS in relation to the duration of CR or the survival time. Because *p53* mutations, as well as *N-ras* and *FLT3* activation, have been detected in many AML patients and may influence the CR duration and survival time (9, 16, 17), simultaneous mutation analyses of the *p53*, *N-ras*, and *FLT3* genes, as well as cytogenetic analysis, were performed for all of the AML patients. The present study is the first report about simultaneous analyses of these genes.

PATIENTS AND METHODS

Patients. After obtaining informed consent, 170 patients with AML, who were classified by the FAB criteria into types M0–M7 (M0: $n = 15$; M1: $n = 39$; M2: $n = 58$; M3: $n = 18$; M4: $n = 23$; M5: $n = 12$; M6: $n = 3$; M7: $n = 2$), were

Received 12/5/01; revised 2/25/02; accepted 2/28/02.

The costs of publication of this article were defrayed in part by the payment of page charges. This article must therefore be hereby marked advertisement in accordance with 18 U.S.C. Section 1734 solely to indicate this fact.

¹ To whom requests for reprints should be addressed, at Division of Hematology, Department of Internal Medicine, Nippon Medical School, 1-1-5 Sendagi, Bunkyo-ku, Tokyo 113-8603, Japan. Phone: 81-3-3822-2131; Fax: 81-3-5814-6934; E-mail: inokuchi@nms.ac.jp.

² The abbreviations used are: AML, acute myelogenous leukemia; TD, tandem duplication; *DCC*, deleted in colorectal carcinoma; RT-PCR, reverse transcriptase-PCR; PS, prognostic significance; FAB, French-American-British; CR, complete remission; OS, overall survival; BMT, bone marrow transplantation.

evaluated. All these patients were untreated previously. None of them had secondary AML for another neoplasm. The 170 patients comprised 112 men and 58 women. The median age was 57 years (range, 15–79). The patients were treated at the Hospital of Nippon Medical School from 1986 through 2000. The induction regimens for AML patients comprised the same conventional chemotherapy (BHAC-DMP regimen), consisting of 170 mg/m² behenoyl cytarabine, 70 mg/m² 6-mercaptopurine, and 20 mg/m² prednisolone daily for 15 days and 25 mg/m² daunorubicin on days 1, 2, 5, 6, and 9. Fifteen cases of M0 AML were treated with the same BHAC-DMP regimen with 1.4 mg/m² vincristine on days 1 and 8 of the therapy (18). Cases aged ≥ 70 years were given a 70% dose of the same chemotherapy regimen. Eighteen M3 patients were treated with 45 mg/m² all-*trans* retinoic acid (19). After achieving CR, two courses of consolidation chemotherapy and six courses of intensification chemotherapy were administered. The duration of follow-up was 0.1–118 months (mean 20.6 months).

CR was defined as $<5\%$ blasts in normo-cellular bone marrow with normal levels of peripheral neutrophil and platelet counts. OS was calculated from the 1st day of therapy to death. CR duration for patients who achieved CR was measured from the date of CR to relapse or death. Nine patients who underwent BMT were censored at the date of BMT.

Analysis of *DCC* Expression by Semiquantitative RT-PCR. After obtaining informed consent, we prepared total RNA from the mononuclear cells of the bone marrow according to our standard protocols (11). *DCC* expression was analyzed by our standard RT-PCR protocol (11) and a semiquantitative RT-PCR protocol, as described previously (20).

Briefly, mononuclear cells of the bone marrow, which contains $\geq 90\%$ leukemic cells, were obtained by Ficol-Hypaque centrifugation (Lymphoprep, Neegard, Norway). The total RNA of mononuclear cells was extracted with an RNazol kit (Biotex Laboratories, Inc., Houston, TX) or by the CsCl method. The concentration of the RNA was determined by spectrophotometry, and semiquantitative RT-PCR was performed with slight modification. RNA (500 ng) was reverse transcribed using random 9-mer primer. Then the synthesized cDNA was subjected to PCR analysis. PCR was performed with 10 μ l of cDNA reaction mixture by using 0.0125 A_{260 nm} units of each oligonucleotide primer DCC1 and DCC2. These oligonucleotide primers are the same ones used by Fearon *et al.* (11). PCRs of 35 cycles for *DCC* and 25 cycles for β -actin were performed, consisting of 30 s at 94°C, 30 s at 55°C, and 1 min at 75°C. The RT-PCR reactions for *DCC* and β -actin were done in a multiplex fashion. The PCR products (10 μ l) were extracted with phenol, precipitated with ethanol, and electrophoresed. The PCR products were visualized directly in ethidium bromide-stained gels and photographed (Fig. 1). The quality of the RNA and the validity of the PCR amplifications were determined by RT-PCR of β -actin. Semiquantification of the photographic signals was performed using an MCID image analysis system (Imaging Research, Inc., St. Catharines, Ontario, Canada; Ref. 20). The entire width of the lane was analyzed with appropriate background subtraction. All bands in one photograph were analyzed together. The relative intensity was defined as the ratio of the *DCC* signal (233 bp) to that of β -actin (530 bp). As Fig. 1 shows, OIH-1 cells, (21) which show normal expression of the

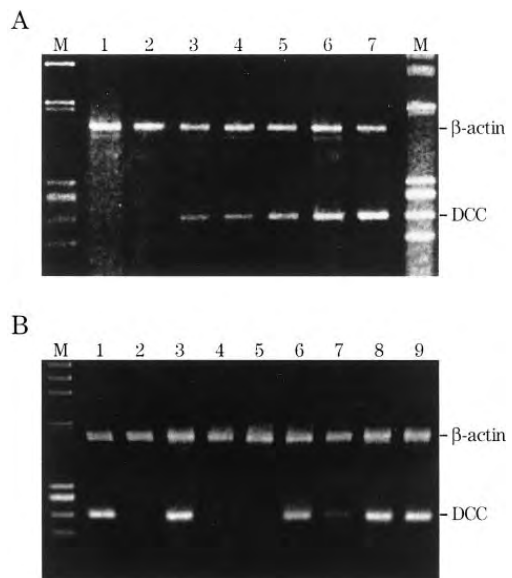


Fig. 1 A, quantitation of *DCC* mRNA by RT-PCR assay. The total RNA of OIH-1 cells was diluted with KML-1 RNA to the concentrations indicated. The lanes represent KML-1 in OIH-1 at dilutions of KML-1 alone (1), 50:1 (2), 20:1 (3), 10:1 (4), 5:1 (5), 2:1 (6), and OIH-1 alone (7). Lane M, molecular markers. B, RT-PCR assay of AML samples. Lane 1, OIH-1 cells; Lane 2, KML-1 cells; Lanes 3, 6, 8, and 9, *DCC*-positive samples; Lanes 4, 5, and 7, *DCC*-negative samples.

DCC gene, and KML-1 cells, (22) in which *DCC* expression is lost, were used to semiquantify the *DCC* mRNA.

A relative intensity of $\leq 10\%$ for the *DCC* products compared with that of β -actin was defined as negative *DCC* (*i.e.*, loss of *DCC* expression). A relative intensity of $\geq 11\%$ for the *DCC* products compared with that of β -actin was defined as positive *DCC* (*i.e.*, normal *DCC* expression). The semiquantitative RT-PCR was performed twice or three times for each patients.

Analysis of *N-ras* Gene Mutations. DNA from mononuclear cells of the bone marrow was prepared according to our standard protocols (23). Mutations of the *N-ras* gene were detected by our standard protocol as described previously (23, 24).

Analysis of *p53* Gene Mutations. Mutations of the *p53* genes were detected by our standard protocol as described previously (23).

Analysis of *FLT3* Gene Mutations. The PCR reaction was performed according to the procedure of Kiyoi *et al.* (25) Genomic PCR for TD mutation was performed using the primers 11F (5'-GCAATTTAGGTATGAAAGCCAGC-3') and 12R (5'-CTTTCAGCATTTTGACGGCAACC-3'). Genomic PCR for Asp835 mutation was performed using the primers 17F (5'-CCGCCAGGAACGTGCTTG-3') and 17R (5'-GCAGCCTCACATTGCCCC-3'; Ref. 26). The PCR mixture containing 500 ng of genomic DNA was incubated with 0.5 unit of Takara

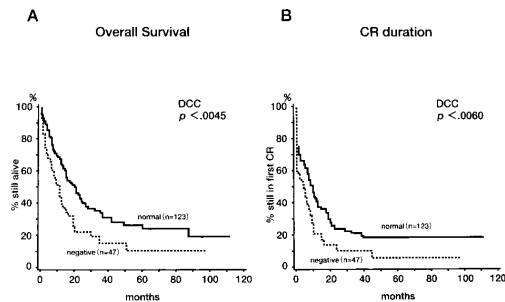


Fig. 2 Kaplan-Meier analysis of OS (A) and CR duration (B) of the 170 patients according to DCC expression. CR duration and OS of AML patients, classified as DCC negative and DCC positive.

Taq DNA polymerase (Takara, Shiga, Japan). Denaturing, annealing, and extension steps were performed at 94°C for 30 s, 56°C for 1 min (for TD), or 59°C for 1 min (for Asp835) and 72°C for 2 min, respectively, for 35 cycles, including an initial 3-min denaturation step at 94°C and a final extension step at 72°C for 10 min. The PCR products were visualized directly in ethidium bromide-stained agarose gels and photographed.

The sequences of abnormal-sized *FLT3*-TD products were determined according to our original protocols (27). The PCR products of abnormal size were cut out from an agarose gel and purified. The fragments were subcloned into the *Eco* RV site of pGEM-5Zf(+/−) cloning vector. The PCR products were sequenced using an ABI sequencer with dye terminators (Perkin-Elmer, Warrington, United Kingdom). All sequences were confirmed by sequencing in both orientations.

The PCR products of *FLT3*-Asp835 were digested with *Eco* RV and subjected to electrophoresis on an agarose gel. If the PCR products showed undigested band, the PCR products directly sequenced on a DNA sequencer (310; Applied Biosystems, Foster City, CA) using a BigDye terminator cycle sequencing kit (Applied Biosystems).

Statistical Methods. OS was calculated from the 1st day of therapy until death. Patients who underwent BMT were excluded from the study on the date of the transplant.

The following patient characteristics before treatment were analyzed: age, sex, FAB classification, peripheral WBC count, cytogenetic findings, *N-ras* mutation, *p53* mutation, *FLT3* mutations, and DCC expression. Analysis of frequencies was performed using Fisher's exact test for 2 × 2 tables or Pearson's χ^2 test for larger tables. Survival probabilities were estimated by the Kaplan-Meier method, and differences in the survival distributions between the DCC-positive and DCC-negative groups were tested with the Log-rank statistic (28). The PS of the study variables was assessed using the Cox proportional hazards model. These statistic analyses were performed with SAS ver6.12 software (SAS Institute, Inc., Cary, NC). For all analyses, the *P*s were two tailed, and a *P* < 0.05 was considered statistically significant.

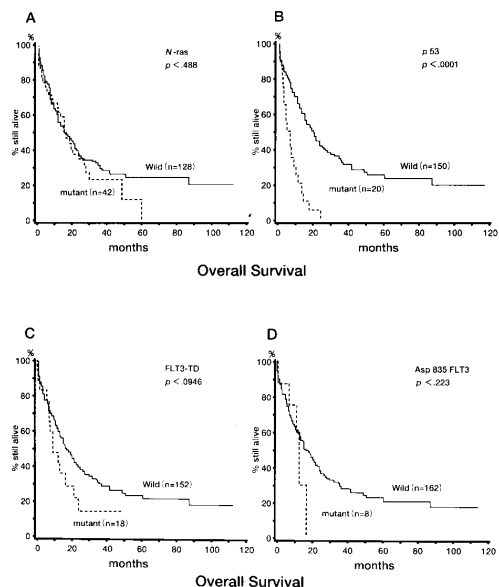


Fig. 3 Kaplan-Meier analysis of OS of the 170 patients according to mutations of *N-ras* (A), *p53* (B), *FLT3*-TD (C), and Asp835*FLT3* (D), respectively. OS of patients, classified as mutant and wild-type *N-ras*, *p53*, *FLT3*-TD, and Asp835*FLT3*, respectively.

RESULTS

Loss of DCC Expression. We identified normal DCC expression (DCC positive) in 123 patients (M0: *n* = 10; M1: *n* = 27; M2: *n* = 41; M3: *n* = 13; M4: *n* = 20; M5: *n* = 8; M6: *n* = 2; M7: *n* = 2) and loss of DCC expression (DCC negative) in 47 patients (M0: *n* = 5; M1: *n* = 13; M2: *n* = 17; M3: *n* = 5; M4: *n* = 3; M5: *n* = 4; M6: *n* = 1; M7: *n* = 0). The DCC-negative group comprised 16 women and 31 men. The survival time and CR duration of the DCC-negative AML patients were shorter than those of the DCC-positive patients, and these differences were significant (*P* < 0.0045 and < 0.0060, respectively; Log-rank test), as shown in Fig. 2, A and B.

Analysis of *N-ras*, *p53*, and *FLT3* Mutations. *N-ras* gene mutation was detected in 42 (M0: *n* = 1; M1: *n* = 12; M2: *n* = 10; M3: *n* = 2; M4: *n* = 9; M5: *n* = 5; M6: *n* = 1; M7: *n* = 1) of the 170 patients (24.7%). Mutations at codons 12, 13, and 61 were observed in 28, 13, and 5 patients, respectively. Nine of the 42 patients had multiple mutations at codon 12, and 1 had a multiple mutation at codon 13. Of the total *N-ras* gene point mutations found in the 42 patients, a G to A transition was the most frequent (32 of 51). A G to T transition was found less often (8 of 39). We could not discriminate, here, whether one leukemia sample contained multiple subclones of cells, each with a different *N-ras* mutation, or whether >1 bp in the codon was mutated in every cell of the malignant clone. No correlation was found between *N-ras* mutation and the survival time (*P* < 0.488; Fig. 3A) or between *N-ras* mutation and the CR duration (*P* < 0.314; Fig. 4A).

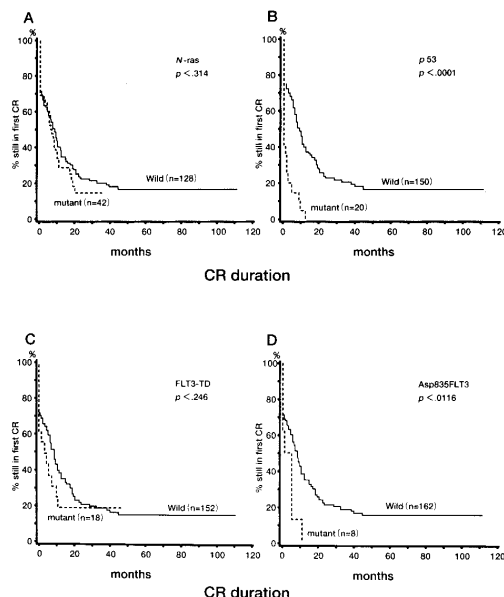


Fig. 4 Kaplan-Meier analysis of CR duration of the 170 patients according to mutations of *N-ras* (A and B), *p53* (C and D), and *FLT3* (E and F), respectively. CR duration of patients, classified as mutant and wild-type *N-ras*, *p53* and *FLT3*-TD, and Asp835*FLT3*, respectively.

p53 gene mutations were detected in 20 (M0: $n = 4$; M1: $n = 5$; M2: $n = 7$; M3: $n = 0$; M4: $n = 3$; M5: $n = 1$; M6: $n = 0$; M7: $n = 0$) of the 170 patients (11.7%). Mutations at codons 248 and 278 were observed in each of 2 patients. Although the mutant *N-ras* group did not show a significantly shorter survival than the wild-type *N-ras* group, the mutant *p53* group had a significantly shorter survival time ($P < 0.0001$; Fig. 3B) and a significantly shorter CR duration than the wild *p53* group ($P < 0.0001$; Fig. 4B).

A genomic fragment corresponding to exon 11 to exon 12 of the *FLT3* gene was amplified by PCR. Mutation of *FLT3*-TD was detected in 18 (M0: $n = 1$; M1: $n = 5$; M2: $n = 2$; M3: $n = 3$; M4: $n = 5$; M5: $n = 2$; M6: $n = 0$; M7: $n = 0$) of the 170 patients (10.4%). In 5 of these 18 patients, amplified germ-line bands were more weakly observed than each abnormal band, suggesting a loss of the normal allele. Sequence analysis confirmed that the size of the TD fragment was from 18 to 105 bp coded in frame transcripts. A part of exon 11 was duplicated. No correlation was found between *FLT3*-TD mutation and the survival time ($P < 0.0946$; Fig. 3C) or between *FLT3*-TD mutation and CR duration ($P < 0.246$; Fig. 4C).

Asp835 Mutation of *FLT3* (*FLT3*-Asp835) was detected in 8 (M0: $n = 0$; M1: $n = 2$; M2: $n = 2$; M3: $n = 0$; M4: $n = 1$; M5: $n = 1$; M6: $n = 0$; M7: $n = 0$) of the 170 patients (4.7%). In 5 of these 8 patients, *EcoRV*-cutted germ-line bands were more weakly observed than each abnormal band, suggesting a loss of the normal allele. The first nucleotide G of Asp835 was most frequently substituted with T (six of eight mutations). No

correlation was found between *FLT3* mutation and the survival time ($P < 0.223$; Fig. 3D). However, the correlation was found between *FLT3* mutation and the CR duration ($P < 0.0116$; Fig. 4D).

The AML Subgroup with no Mutations Correlated More Closely with CR Duration and OS. In the total of 170 patients, 28 patients had loss of *DCC* expression with wild-type *N-ras*, *p53*, and *FLT3* genes (negative *DCC*/wild *N-ras*, *p53*, and *FLT3*), 64 patients had normal *DCC* expression with wild-type *N-ras*, *p53*, and *FLT3* genes (positive *DCC*/wild *N-ras*, *p53*, and *FLT3*), 59 patients had normal *DCC* expression with one or more of mutant-type *N-ras*, *p53*, and *FLT3* genes (positive *DCC*/mutant *N-ras*, *p53*, *FLT3*), and 19 patients had loss of *DCC* expression with one or more of mutant-type *N-ras*, *p53*, and *FLT3* genes (negative *DCC*/mutant *N-ras*, *p53*, and *FLT3*). The clinical characteristics of these four groups were compared (Table 1). The 64 positive *DCC*/wild *N-ras*, *p53*, and *FLT3* group had statistically better CR attainment compared with the other 106 patients ($P < 0.0001$). Especially, the positive *DCC*/wild *N-ras*, *p53*, and *FLT3* group had statistically better CR attainment compared with the negative *DCC*/wild *N-ras*, *p53*, and *FLT3* and the positive *DCC*/mutant *N-ras*, *p53*, and *FLT3* groups ($P < 0.0005$ and < 0.0001 , respectively). The OS and CR duration were further analyzed for these four groups.

The OS of the positive *DCC*/wild *N-ras*, *p53*, and *FLT3* group was significantly different from the other groups ($P < 0.0006$, < 0.0001 , and < 0.0004 , respectively; Fig. 5A). The CR duration of the positive *DCC*/wild *N-ras*, *p53*, and *FLT3* group was significantly different from the other groups ($P < 0.0008$, < 0.0001 , and < 0.0003 , respectively; Fig. 5B).

Unfavorable Prognostic Factors for OS or CR Duration. The prognosis of AML patients depends on factors such as the age, initial WBC counts, FAB type classification, karyotype, and immune phenotype (Tables 2 and 3). Among these factors, cytogenetic data are thought to be the most important prognostic factor. On the basis of cytogenetic findings, the 170 patients were segregated into three groups: a good risk group ($n = 33$) was defined by a karyotype of t(8;21), t(15;17), or inv(16); a poor risk group ($n = 26$) by t(9;22), 11q23 alterations, del(5), or del(7); and a standard risk group ($n = 111$) by normal or other altered karyotypes. Univariate and multivariate analyses for the OS or CR duration were performed (Tables 2 and 3).

Univariate analysis showed that unfavorable prognostic factors for the OS included the following: male gender ($P < 0.0163$), FAB type other than M2 and M3 ($P < 0.0089$), age of ≥ 60 years ($P < 0.0033$), poor risk karyotype compared with good risk karyotype ($P < 0.0001$), and mutant *p53* ($P < 0.0001$), loss of *DCC* expression ($P < 0.0053$), and *FLT3*-Asp835 ($P < 0.0232$; Table 1). Multivariate analysis for OS showed that the poor risk karyotype compared with the good risk karyotype was the strongest unfavorable factor (relative risk, 0.149; $P < 0.0001$), followed by mutant *p53* ($P < 0.0002$), mutant *FLT3*-TD ($P < 0.0072$), and loss of *DCC* expression ($P < 0.0084$). Leukocytosis, FAB type, mutant *N-ras*, mutant *FLT3*-Asp835, and male gender were less important.

Univariate analysis showed that unfavorable prognostic factors for the CR duration were the following: male gender ($P < 0.0162$), FAB type classification other than M2 and M3 ($P < 0.0041$), age of ≥ 60 years ($P < 0.0167$), poor risk

Table 1 Clinical characteristics of 170 patients with AML^a

	Total (n = 170)	Positive DCC/wild N-ras, p53, and FLT3 (n = 64)	Negative DCC/wild N-ras, p53, and FLT3 (n = 28)	Positive DCC/mutant N-ras, p53, and FLT3 (n = 59)	Negative DCC/mutant N-ras, p53, and FLT3 (n = 19)
Men/women	112/58	39/25	15/13	45/14	16/3
Age	55.4 (15–79)	56.2 (15–79)	57.9 (15–76)	55.5 (17–78)	49.1 (23–74)
WBC (10 ⁹ /liter)	26.2 (0.6–483)	26.4 (0.7–124)	15.9 (0.7–121)	51.0 ^b (0.6–333)	69.9 ^b (4.7–483)
FAB					
M0	15	4	3	6	2
M1	39	10	8	17	4
M2	58	27	10	14	7
M3	18	9	4	4	1
M4	23	9	0	11	3
M5	12	3	2	5	2
M6	3	1	1	1	0
M7	2	1	0	1	0
Cytogenetics					
Poor risk	26	8	6	9	3
Standard risk	111	45	10	41	15
Good risk	33	11	12	9	1
Outcome					
CR	121	57	16 (<i>P</i> < 0.0005) ^c	33 (<i>P</i> < 0.0001) ^c	15
Failure	49	7	12	26	4

^a Mean (range) values are indicated for age and WBCs. The numbers of cases are shown for FAB type, cytogenetics, and outcome.

^b *P* < 0.0375 and 0.029 compared with the negative DCC/wild N-ras, p53, and FLT3 group by Mann-Whitney's *U* test, respectively.

^c Compared with the positive DCC/wild N-ras, p53, and FLT3 group, respectively.

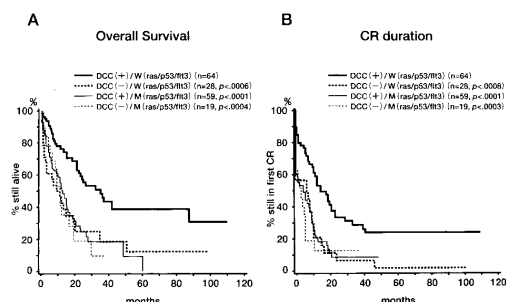


Fig. 5 Kaplan-Meier analysis of OS (A) and CR duration (B) of the four types of AML patient groups with wild- or mutant-type N-ras, p53, and FLT3 according to DCC expression (Table 1). DCC+, DCC positive; DCC-, DCC negative; W, wild; M, mutant. The FLT3 implies TD and Asp835 mutations of the FLT3 gene.

karyotype compared with good risk karyotype (*P* < 0.0001), loss of *DCC* expression (*P* < 0.0146), mutant *p53* (*P* < 0.0001) and mutant *FLT3*-Asp835 (*P* < 0.0268), as shown in Table 3. Multivariate analysis for CR duration showed that poor risk karyotype was the strongest unfavorable factor (*P* < 0.0001; relative risk, 0.189), followed by mutant *p53* (*P* < 0.0003), mutant *FLT3*-TD (*P* < 0.0235), loss of *DCC* expression (*P* < 0.0371), and age of ≥ 60 years (*P* < 0.0392), and. Mutant *FLT3*-Asp835 was only a marginal prognostic factor (*P* < 0.0616). Leukocytosis, mutant N-ras, and male gender were less important.

DISCUSSION

In the present study, we showed that loss of *DCC* expression is significantly associated with CR duration and OS. In our

Table 2 Unfavorable prognostic factors for OS in 170 patients^a

Prognostic factors	Univariate	Multivariate
	<i>P</i>	<i>P</i> Relative risk (95% confidence limits)
Sex	0.0163	0.3504
Age	0.0033	0.0204
FAB types other than M2 and M3	0.0089	0.6631
WBC count	0.0111	0.6376
Cytogenetics ^b	0.0001	0.0001
Loss of <i>DCC</i> expression	0.0053	0.0084
Mutant <i>p53</i>	0.0001	0.0002
Mutant N-ras	0.4918	0.2473
Mutant <i>FLT3</i> -TD	0.1000	0.0072
Mutant <i>FLT3</i> -Asp835	0.0232	0.4800

^a Karyotypes were segregated into three groups.

^b Comparison between the good risk and poor risk karyotype groups.

previous analysis of acute leukemia, expression of the *DCC* gene was absent in 20–30% of AML patients, in some of whom allelic loss in the *DCC* gene was observed (11, 12). In the 37 DCC-negative patients, allelic loss in the *DCC* gene was observed in only 2 AML patients with loss of *DCC* expression (data not shown; Ref. 11). Another 35 AML patients had no abnormality at the Southern level. Cytogenetic analysis also revealed 3 patients had monosomy 18 abnormality, and 2 AML patients had 18q21 abnormality. Thus, no abnormality of chromosome 18 was observed by G banding in 32 AML patients with loss of *DCC*. In colorectal tumorigenesis, loss of *DCC* expression was present exclusively in colorectal tumors harboring intragenic loss of heterozygosity in the *DCC* gene (29). The excellent correlation between loss of *DCC* and intragenic *DCC* loss of heterozygosity suggests that this may be an important

Table 3 Unfavorable prognostic factors for CR duration in 170 patients^a

Prognostic factors	Univariate	Multivariate	
	P	P	Relative risk (95% confidence limit)
Sex	0.0162	0.3598	
Age	0.0167	0.0392	1.20 (0.81–1.76)
FAB types other than M2 and M3	0.0041	0.4861	
WBC count	0.1038	0.7637	
Cytogenetics ^b	0.0001	0.0001	0.189 (0.092–0.39)
Loss of <i>DCC</i> expression	0.0146	0.0371	0.659 (0.44–0.97)
Mutant <i>p53</i>	0.0001	0.0003	0.367 (0.21–0.63)
Mutant <i>N-ras</i>	0.3485	0.3067	
Mutant <i>FLT3</i> -TD	0.2849	0.0235	0.505 (0.28–0.91)
Mutant <i>FLT3</i> -Asp835	0.0268	0.0616	0.485 (0.22–1.03)

^a Karyotypes were segregated into three groups.^b Comparison between the good risk and poor risk karyotype groups.

mechanism of *DCC* inactivation and supports the role of *DCC* in human colorectal tumorigenesis (29). Recently, we found hypermethylation of the GC-rich region of the *DCC* gene in many leukemic cell lines.³ Hypermethylation of the *DCC* gene may be one of the cause of loss of *DCC* gene expression. In leukemia, loss of *DCC* expression more likely is an epigenetic phenomenon that is associated with an unfavorable prognosis, but it is likely to be partly independent of intragenic loss of heterozygosity.

A recent report demonstrated that *DCC* regulates the activation of caspase-3 (14) and induces the following apoptosis or G₂-M cell cycle arrest, in which cdk1 activity is inhibited (15). This evidence has important implications regulating the suppression of leukemogenesis and also suggests that loss of *DCC* expression may be a prognostic factor. Interestingly, forced *DCC* expression induces apoptosis or cell cycle arrest of tumor cells regardless of their *p53* and retinoblastoma status, *i.e.*, whether they are wild type or mutant (15). Like the *p53* mutation, the present study shows that loss of *DCC* expression may be a prognostic marker in AML patients. One report has shown that forced *DCC* expression in transformed keratinocytes resulted in the suppression of tumorigenicity in nude mice (30). Another report has shown that forced *DCC* expression also affects the growth and tumorigenic properties of colonic cancer cells and is associated with elevated rates of cell shedding and apoptosis (31).

It is particularly interesting to investigate the multiplicity of gene alterations associated with AML. Multiplicity of the mutations of *N-ras*, *p53*, and *FLT3* in elderly patients with AML was reported recently. In elderly AML, *FLT3* and *ras* mutations were not associated with a poor clinical outcome, but mutation of the *p53* gene was associated with a worse OS. Our present results are consistent with these reports (32). Our results by Fisher's exact test suggest that the mutations of *N-ras*, *p53*, *FLT3*, and loss of *DCC* expression occurred independently,

although we could not entirely rule out the possibility that a weak adverse interaction exists between mutant *N-ras*, *p53*, *FLT3*, and loss of *DCC* expression. Because gene alterations are associated with aberrant signal transduction, these mutations may be additively or synergistically associated with leukemia progression. Intriguingly, the groups with one or more mutations had significantly less CR attainment and a poorer prognosis than the normal *DCC*/wild *N-ras*, *p53*, and *FLT3* group. These observations suggest that the *DCC* gene may functionally act as a tumor suppressor gene in leukemogenesis. However, the PS of the *p53* mutation is the most important factor in AML leukemogenesis, along with the poor risk karyotype. The present data, as well as those in previous reports (32), may indicate that the *p53* plays a more important role in leukemogenesis than the other genes.

Earlier reports indicate that *FLT3*-TD mutation is associated with OS. In the present study, unfortunately, *FLT3*-TD mutation did not show a correlation with a worse OS or short CR duration by Kaplan-Meier curves and the Log-rank test. However, *FLT3*-TD mutation was associated with the OS and the CR duration by multivariate analysis. The reasons for the discrepancy in these statistical analyses may be the sample size. *FLT3* mutation may be meaningful as a PS factor. The predictive value of *N-ras* mutations is still controversial from the present data and from other recent reports (8). The present study failed to find any correlation between *N-ras* mutation and CR duration or survival time, although mutations of *N-ras* may well be involved in the pathogenesis of AML.

As for the *DCC* gene, there is no report as to its PS in leukemias. Our present study revealed that loss of *DCC* expression is a useful and potent prognostic marker in AML patients. One recent study in patients with colorectal cancer dealt with the PS of the *DCC* protein in neoplasms (33). Although the function of the *DCC* gene as a tumor suppressor gene remains obscure, the present findings are of particular interest and are added to the current understanding of its role in cell differentiation and leukemogenesis (12).

REFERENCES

- Weinberg, R. A. Oncogenes, antioncogenes, and the molecular bases of multistep carcinogenesis. *Cancer Res.*, 49: 3713–3721, 1989.
- Fearon, E. R., and Vogelstein, B. A genetic model for colorectal tumorigenesis. *Cell*, 61: 759–767, 1990.
- Mrozek, K., Heinonen, K., de la Chapelle, A., and Bloomfield, C. D. Clinical significance of cytogenetics in acute myeloid leukemia. *Semin. Oncol.*, 24: 17–31, 1997.
- Caligiuri, M. A., Strout, M. P., and Gilliland, D. G. Molecular biology of acute myeloid leukemia. *Semin. Oncol.*, 24: 32–44, 1997.
- Wattel, E., Preudhomme, C., Hecquet, B., Vanrumbeke, M., Quesnel, B., Dervite, I., Morel, P., and Fenaux P. *p53* mutations are associated with resistance to chemotherapy and short survival in hematologic malignancies. *Blood*, 84: 3148–3157, 1994.
- De Melo, M. B., Lorand-Metze, I., Lima, C. S., Saad, S. T., and Costa, F. F. *N-ras* gene point mutations in Brazilian acute myelogenous leukemia patients correlated with a poor prognosis. *Leuk. Lymphoma*, 24: 309–317, 1997.
- Lee, Y. Y., Kim, W. S., Bang, Y. J., Jung, C. W., Park, S., Yoon, W. J., Cho, K. S., Jung T. J., and Choi, I. Y. Analysis of mutations of neurofibromatosis type 1 gene and *N-ras* gene in acute myelogenous leukemia. *Stem Cells*, 13: 556–563, 1995.

³ K. Nakayama and K. Inokuchi, *et al.*, unpublished data.

8. Kiyoi, H., Naoe, T., Nakano, Y., Yokota, S., Minami, S., Miyawaki, S., Asou, N., Kuriyama, K., Jinnai, I., Shimazaki, C., Akiyama, H., Saito, K., Oh, H., Motoji, T., Omoto, E., Saito, H., Ohno, R., and Ueda, R. Prognostic implication of FLT3 and N-ras gene mutations in acute myeloid leukemia. *Blood*, 93: 3074–3080, 1999.
9. Kiyoi, H., Towatari, M., Yokota, S., Hamaguchi, M., Ohno, R., Saito, H., and Naoe, T. Internal tandem duplication of the *FLT3* gene is a novel modality of elongation mutation which causes constitutive activation of the product. *Leukemia* (Baltimore), 12: 1333–1337, 1998.
10. Fearon, E. R., Cho, K. R., Nigro, J. M., Kern, S. E., Simons, J. W., Ruppert, J. M., Hamilton, S. R., Preisinger, A. C., Thomas, G., and Kinzler, K. W. Identification of a chromosome 18q gene that is altered in colorectal cancers. *Science* (Wash. DC), 247: 49–56, 1990.
11. Miyake, K., Inokuchi, K., Dan, K., and Nomura, T. Alteration in the deleted in colorectal carcinoma gene in human primary leukemia. *Blood*, 82: 927–930, 1993.
12. Inokuchi, K., Miyake, K., Takahashi, H., Dan, K., and Nomura, T. DCC protein expression in hematopoietic cell populations and its relation to leukemogenesis. *J. Clin. Invest.*, 97: 852–857, 1996.
13. Fazeli, A., Dickinson, S. L., Hermiston, M. L., Tighe R. V., Steen, R. G., Small, C. G., Stoeckli, E. T., Keino-Masu, K., Masu, M., Rayburn, H., Simons, J., Bronson, R. T., Gordon, J. L., Tessier-Lavigne, M., and Weinber, R. A. Phenotype of mice lacking functional Deleted in colorectal cancer (*Dcc*) gene. *Nature* (Lond.), 386: 796–804, 1997.
14. Mehlen, P., Rabizadeh, S., Snipas, S. J., Assa-Munt, N., Salvesen, G. S., and Breiden, D. E. The DCC gene product induces apoptosis by a mechanism requiring receptor proteolysis. *Nature* (Lond.), 395: 801–804, 1998.
15. Chen, Y. Q., Hsieh, J. T., Yao, F., Fang, B., Pong, R., Cipriano, S. C., and Krepulat, F. Induction of apoptosis and G2/M cell cycle arrest by DCC. *Oncogene*, 18: 2747–2754, 1998.
16. Neubauer, A., Dodge, R. K., George, S. L., Davey, F. R., Silver, R. T., Schiffer, C. A., Mayer, R. J., Ball, E. D., Wurster-Hill, D., and Bloomfield, C. D. Prognostic importance of mutations in the ras proto-oncogenes in *de novo* acute myeloid leukemia. *Blood*, 83: 1603–1611, 1994.
17. Singerland, J. M., Minden, M. D., and Benchimol, S. Mutation of the *p53* gene in human acute myelogenous leukemia. *Blood*, 77: 1500–1507, 1991.
18. Yokose, N., Ogata, K., Ito, T., Miyake, K., An, E., Inokuchi, K., Yamada, T., Gomi, S., Tanabe, Y., Ohki, I., Kuwabara, T., Hasegawa, S., Shinohara, T., Dan, K., and Nomura, T. Chemotherapy for minimally differentiated acute myeloid leukemia (AML-M0). *Ann. Hematol.*, 66: 57–70, 1993.
19. Iwakiri, R., Inokuchi, K., Dan, K., and Nomura, T. Marked basophilia in acute promyelocytic leukemia treated with all-*trans* retinoic acid: molecular analysis of the cell origin of the basophils. *Br. J. Haematol.*, 86: 870–872, 1994.
20. Inokuchi, K., Futaki, M., Dan, K., and Nomura, T. Possible correlation of b3-a2-type ber-abl messenger RNA defined by semiquantitative RT-PCR to platelet and megakaryocyte counts in Philadelphia-positive chronic myelogenous leukemia. *Intern. Med.*, 33: 189–192, 1994.
21. Hamaguchi, H., Inokuchi, K., Nara, N., Nagata, K., Yamamoto, K., Yagasaki, F., and Dan, K. Alterations in the colorectal carcinoma gene and protein in a novel human myeloid leukemia cell line with trisomy 18 established from overt leukemia after myelodysplastic syndrome. *Int. J. Hematol.*, 67: 153–164, 1998.
22. Ikezoe, T., Miyagi, T., Kubota, T., Taguchi, T., Ohtsuki, Y., Miyake, K., Inokuchi, K., Nomura, T., Koeffler, H. P., and Miyoshi, I. Inactivation of the DCC tumor suppressor gene in a B-cell lymphoma cell line with the alteration of chromosome 18. *Am. J. Hematol.*, 50: 124–132, 1995.
23. Abo, J., Inokuchi, K., Dan, K., and Nomura, T. p53 and N-ras mutations in two new leukemia cell lines established from a patient with multilineage CD7-positive acute leukemia. *Blood*, 82: 2829–2836, 1993.
24. Inokuchi, K., Amuro, N., Futaki, M., Dan, K., Kuriya, S., Shinohara, T., and Nomura, T. Transforming genes and chromosome aberrations in therapy-related leukemia and myelodysplastic syndrome. *Ann. Hematol.*, 62: 211–216, 1991.
25. Kiyoi, H., Naoe, T., Yokota, S., Nakao, M., Minami, S., Kuriyama, K., Takeshita, A., Saito, K., Hasegawa, S., Shimodaira, S., Tamura, J., Shimazaki, C., Matsue, K., Kobayashi, H., Arima, N., Suzuki, R., Morishita, H., Saito, H., Ueda, R., and Ohno, R. Internal tandem duplication of FLT3 associated with leukocytosis in acute promyelocytic leukemia. *Leukemia* (Baltimore), 11: 1447–1452, 1997.
26. Yamamoto, Y., Kiyoi, H., Nakano, Y., Suzuki, R., Kadera, Y., Miyawaki, S., Asou, N., Kuriyama, K., Yagasaki, F., Shimazaki, C., Akiyama, H., Saito, K., Nishimura, M., Motoji, T., Shinagawa, K., Takeshita, A., Saito, H., Ueda, R., Ohno, R., and Naoe, T. Activating mutation of D835 within the activation loop of FLT3 in human hematologic malignancies. *Blood*, 97: 2434–2439, 2001.
27. Inokuchi, K., Futaki, M., Hanawa, H., Tanosaki, S., Iwakiri, R., Nomura, T., and Nomura, T. Heterogenous expression of ber-abl fusion mRNA in a patient with Philadelphia-chromosome-positive acute lymphoblastic leukemia. *Br. J. Haematol.*, 97: 837–840, 1997.
28. Tanosaki, S., Inokuchi, K., Shimada, T., and Dan, K. Relation between microsatellite instability and N-ras mutation and duration of disease free survival in patients with acute leukemia. *Cancer* (Phila.), 83: 475–481, 1998.
29. Tarafa, G., Villanueva, A., Farre, L., Rodriguez, J., Reyes, G., Seminago, R., Olmedo, E., Paules, A. B., Peinado, M. A., Bachs, O., and Capella, G. DCC and SMAD4 alterations in human colorectal and pancreatic tumor dissemination. *Oncogene*, 19: 546–555, 2000.
30. Kleingelutz, A. J., Hedrick, L., Cho, K. R., and McDougal, J. K. The DCC gene suppresses the malignant phenotype of transformed human epithelial cells. *Oncogene*, 10: 1581–1586, 1995.
31. Velcich, A., Corner, G., Palumbo, L., and Augenlicht, L. Altered phenotype of HT29 colonic adenocarcinoma cells following expression of the DCC gene. *Oncogene*, 18: 2599–2606, 1999.
32. Stirewalt, D. L., Kopecky, K. J., Meshinchi, S., Appelbaum, F. R., Slovak, M. L., Willman, C. L., and Radich, J. P. FLT3, Ras, and TP53 mutations in elderly patients with acute myeloid leukemia. *Blood*, 97: 3589–3595, 2001.
33. Shibata, D., Reale, A., Lavin, P., Silverman, M., Fearon, E. R., Steele, G., Jessup, J. M., Loda, M., and Summerhayes, I. C. The DCC protein and prognosis in colorectal cancer. *N. Engl. J. Med.*, 335: 1727–1732, 1996.

Brief report

Myeloproliferative disease in transgenic mice expressing P230 Bcr/Abl: longer disease latency, thrombocytosis, and mild leukocytosis

Koiti Inokuchi, Kazuo Dan, Miyuki Takatori, Hidemasa Takahuji, Naoya Uchida, Mitsuharu Inami, Koichi Miyake, Hiroaki Honda, Hisamaru Hirai, and Takashi Shimada

P230 Bcr/Abl has been associated with indolent myeloproliferative disease (MPD). We generated transgenic mice expressing P230Bcr/Abl driven by the promoter of the long terminal repeat of the murine stem cell virus of the MSCV neo P230 BCR/ABL vector. Two founder mice exhibited mild granulocytosis and marked thrombocytosis and developed MPD. The disease of one founder

mouse, no. 13, progressed to extramedullary myeloblastic crisis in the liver at 12 months old. The other founder mouse, no. 22, was found to have chronic-phase MPD with large populations of megakaryocytes and granulocytes in an enlarged spleen. The transgenic progeny of no. 22 clearly exhibited MPD at 15 months old. These results showed that P230Bcr/Abl had leukemo-

genic properties and induced MPD. The phenotype of the MPD caused by P230Bcr/Abl was characterized by mild granulocytosis, a high platelet count, infiltration of megakaryocytes in some organs, and a longer disease latency compared with the MPD caused by P210Bcr/Abl. (Blood. 2003;102:320-323)

© 2003 by The American Society of Hematology

Introduction

The Bcr/Abl oncogene is formed by reciprocal translocation between chromosomes 9 and 22 and is associated with diverse human leukemias.¹ Three different forms of Bcr/Abl are associated with distinct forms of leukemia.^{2,3} Recently, a subset of patients was described who had Ph-positive myeloproliferative diseases (MPDs) resembling chronic myeloid leukemia (CML) but with very mild clinical symptoms, including a lower peripheral white blood cell (WBC) count consisting principally of neutrophilia, more severe thrombocytosis, less severe anemia, and delayed or absent transformation to blast crisis.⁴ These patients have a unique chimeric Bcr/Abl protein, P230 Bcr/Abl, that is formed with a breakpoint (μ breakpoint) located 3' to the common breakpoints.⁵ It was proposed that patients with P230 Bcr/Abl comprise a distinct clinical entity having a much more benign clinical course than that associated with the traditional P210 Bcr/Abl protein.⁶ P230Bcr/Abl protein contains additional Bcr coding sequences that are not found in P210 Bcr/Abl protein. These observations raise the question of whether different forms of the Bcr/Abl protein have intrinsically different leukemogenic activities in hematopoietic cells. Recently, there were 2 reports of mouse models created using in vitro retroviral-mediated gene transfer into hematopoietic cell lines and a primary bone marrow transplantation system.^{7,8}

To gain more insight into the molecular pathological function of P230 Bcr/Abl and its in vivo leukemogenic activity, we generated transgenic mice expressing P230 Bcr/Abl and investigated its leukemogenic activity and the disease phenotype.

Study design

Construction of the transgene and generation of MSCVneoP230 BCR/ABL transgenic mice

The MSCVneoP230 BCR/ABL vector, which was kindly provided by Dr R. Van Etten, Harvard Medical School, was cut at the *PvuII* and *SspI* sites (Figure 1A).^{7,9} The DNA fragment containing the long terminal repeats (LTRs) of murine stem cell virus (MSCV) (denoted as PCMV) and P230 BCR/ABL was microinjected into the pronuclei of eggs from C57BL/6N Crlj mice. The methods of microinjection and embryonal transfer were essentially described earlier.¹⁰ Transgenic mice were identified by polymerase chain reaction (PCR). Genomic DNA from tail-cut biopsy was subjected to PCR reaction. A 1020-base PCR product was identified as positive. Transgenic mice were also identified by Southern blotting of the DNA from tail-cut or spleen biopsy.¹¹

Flow cytometric analysis

The method of fluorescence-activated cell sorter (FACS) analysis was as described earlier.¹² Mononuclear blastic cells that had infiltrated in the liver of no. 13 were obtained by twice Ficoll-Hypaque centrifugation (Lymphoprep, Neebard, Norway) and incubated with a phycoerythrin (PE)- or fluorescein isothiocyanate (FITC)-conjugated monoclonal antibody (MoAb) and analyzed with a FACScan (Becton Dickinson, San Jose, CA). FITC- or PE-conjugated antibodies specific for CD45R/B220, Ly-6G (Gr-1), CD11b (Mac-1), CD34, CD3-e, CD61, and TER119 (BD Pharmingen, San Diego, CA) were used.

Southern and Northern blot analyses

The methods of Southern and Northern blot analyses were as described previously.^{11,13} The full Neo cDNA and 3' site of the *HindIII*-cut and *EcoRI*-cut fragment of BCR/ABL cDNA (Figure 1A) were used as probes.

From the Division of Hematology, Department of Internal Medicine, Department of Biochemistry and Molecular Biology, and Research Center for Life Science, Nippon Medical School, Tokyo, Japan; Department of Developmental Biology, Division of Radiation Biology and Medicine, Hiroshima University, Japan; and Department of Hematology/Oncology, Graduate School of Medicine, University of Tokyo, Japan.

Submitted October 22, 2002; accepted February 21, 2003. Prepublished online as *Blood* First Edition Paper, March 6, 2003; DOI 10.1182/blood-2002-10-3182.

Supported by a Grant-in-Aid from the Japanese Ministry of Health and Welfare.

Reprints: Koiti Inokuchi, Division of Hematology, Department of Internal Medicine, Nippon Medical School, 1-1-5 Sendagi, Bunkyo-ku, Tokyo 113-8603, Japan; e-mail: inokuchi@nms.ac.jp.

The publication costs of this article were defrayed in part by page charge payment. Therefore, and solely to indicate this fact, this article is hereby marked "advertisement" in accordance with 18 U.S.C. section 1734.

© 2003 by The American Society of Hematology

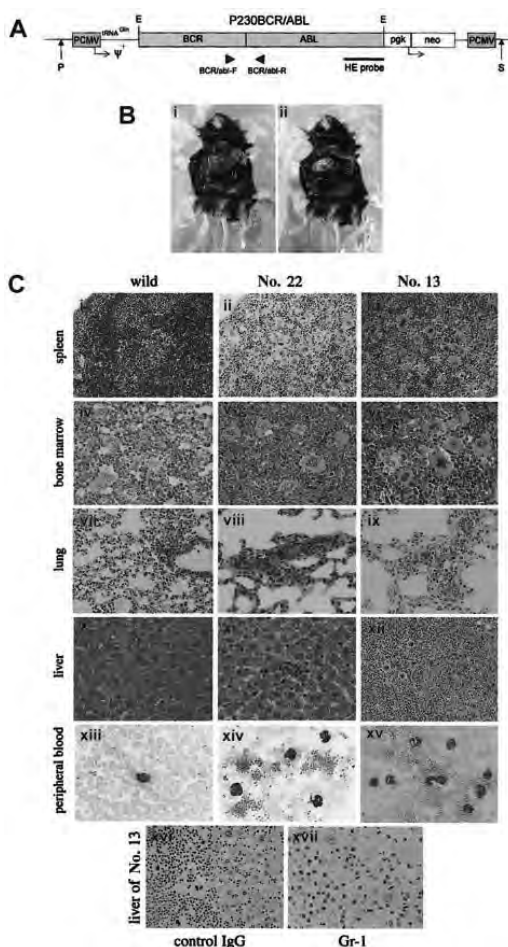


Figure 1. Schematic representation of the MSCVneo P230 BCR/ABL vector and macroscopic and histopathologic findings of founder mice no. 13 and no. 22. (A) The injection fragment for generating transgenic mice was made by cutting at *PvuI* and *SspI* sites of the bacterial plasmid, pUC19. Two vertical arrows indicate the cutting sites. P indicates *PvuI*; S, *SspI*. The nucleotide sequences of the primers for PCR were as follows: BCR/abl-F: 5'-TGACCAACTCGTGTGAACTCCAG-3'; and BCR/abl-R: 5'-CAGCAGATAC TCAGCGCATTTG-3'. (B) Macroscopic appearance of founder mouse no. 13 in the extramedullary blastic phase of MPD. (i) A markedly enlarged liver and a large volume of hemorrhage in the peritoneal cavity are seen. (ii) After removal of the liver, the enlarged spleen is visible. (C) Histopathologic findings of founder mice no. 13 and no. 22. Photomicrographs of hematoxylin and eosin-stained spleen (i-iii), bone marrow (iv-vi), lung (vii-ix), and liver (x-xii); Wright-Giemsa-stained peripheral blood (xiii-xv); from no. 22 (ii,v,viii,xi,xiv), no. 13 (iii,vi,ix,xii,xv-xvii), and a nontransgenic littermate mouse killed at 12 months of age (i,iv,vii,x,xiii). Panels xvi and xvii show the immunohistochemical findings of the liver stained with Gr-1 (xvii) and control IgG (xvi). Blasts were positive for Gr-1 (xvii) and control IgG (xvi). Original magnifications: $\times 200$ (i-iii); $\times 1000$ (panels xiii-xv); $\times 400$ (iv-xii, xvi); and $\times 800$ (xvii).

Western blotting and in vitro kinase assays

The methods were as described previously.¹⁴ Briefly, tissues were homogenized in RIPA lysis buffer with 1 mM phenylmethylsulfonyl fluoride (PMSF), 50 μ g/mL aprotinin, 5 μ g/mL aprotinin, and 2 μ g/mL leupeptin.¹² For detecting the p230bcr/abl transgene product, proteins were separated by sodium dodecyl sulfate–polyacrylamide gel electrophoresis (SDS-PAGE), transferred to nitrocellulose membranes, and probed with an anti-c-Abl MoAb, AB3 (Oncogene Science, Manhasset, NY). For in vitro kinase assay, 1 mg aliquots of total proteins were incubated with 1:200-diluted AB3 and

antimouse rat immunoglobulin G (IgG) (Sigma, St Louis, MO) coupled with protein A (Sigma). The immunoprecipitated proteins were washed and then incubated with 10 μ Ci (0.37 MBq) γ -³²P-adenosine triphosphate (γ -³²P-ATP) (Amersham, Arlington Heights, IL). The phosphorylated proteins were separated by SDS-PAGE, dried, and autoradiographed.

Results and discussion

Two founder mice developed MPD

We generated 2 founder mice, no. 13 and no. 22, that developed MPD. The WBC, platelet (Plt), and hemoglobin (Hb) were within their normal ranges until 7 months after birth. However, thereafter the Plt counts gradually increased. At 11 months after birth, WBC, Hb, and Plts of no. 13 were $6.5 \times 10^9/L$ ($65 \times 10^2/\mu L$), 99 g/L (9.9 g/dL), and $1867 \times 10^9/L$ ($186.7 \times 10^4/\mu L$), and at 12 months those of no. 22 were $9.1 \times 10^9/L$ ($91 \times 10^2/\mu L$), 92 g/L (9.2 g/dL), and $2437 \times 10^9/L$ ($243.7 \times 10^4/\mu L$), respectively. At 12 months after birth, no. 13 suddenly became moribund and subsequently died, and no. 22 was killed. At autopsy, no. 13 showed marked hepatomegaly with liver bleeding, splenomegaly, and ascites (Figure 1B). No. 22 was found to have marked splenomegaly and an enlarged liver.

Pathological examination revealed extramedullary expansion of the blastic cells in the liver of no. 13 (Figure 1Cxi). Many immature and mature granulocytes and many megakaryocytes were detected in the bone marrow, spleen, liver, and lung of both mice (Figure 1C). Blast cells were separated from the enlarged liver of no. 13, stained with MoAbs, and analyzed by the FACScan and immunohistopathological methods. The blasts were positive for CD34, Gr-1, and CD61 and partially positive for CD11b and CD45R (Figures 1Cxvii and 2A).

The clinical course and the results of these analyses showed that the disease of no. 13 had the characteristics of MPD with extramedullary blastic proliferation in the liver and that no. 22 mimicked the cardinal features of the chronic phase of human CML.

The transgenic progeny of no. 22 were maintained under continual observation. The WBC counts mildly increased after 11 months (Figure 2B). As for the differential count of the WBC, a steadily increased percent of granulocytes became apparent after 9 months of age (Figure 2B). The mean Plt counts for the transgenic progeny ($n = 20$) gradually increased after 9 months of age and reached $200 \times 10^4/\mu L$ (Figure 2B).

Expression of the p230Bcr/Abl transgene in transgenic mice

Southern blot analysis confirmed that no. 13 and no. 22 carry 10 and 5 copies of the p230Bcr/Abl transgene, respectively (data not shown). To confirm expression of the p230Bcr/Abl transgene, Northern blotting, Western blotting, and kinase assay were carried out using mRNAs or proteins extracted from the spleen, bone marrow, and liver cells. The p230Bcr/Abl mRNA and tyrosine-phosphorylated P230Bcr/Abl protein were detected in both mRNAs and proteins from no. 13 and the progeny of no. 22 (Figure 2C-E).

Many animal models of CML have proven to be invaluable for improving our understanding of the molecular pathophysiology of P210 Bcr/Abl.¹⁵ In transgenic mice, the p210 Bcr/Abl transgenic mouse using the mouse *tec* promoter system reproducibly developed CML-like disease.¹⁴

The present P230 Bcr/Abl transgenic mouse line using the MSCV promoter was characterized by modestly increased peripheral WBC counts (6×10^9 to $9.5 \times 10^9/L$ [6×10^3 to $9.5 \times 10^3/\mu L$]) composed predominantly of mature neutrophils, marked thrombocytosis (Plts 1300×10^9 to $3000 \times 10^9/L$ [130×10^4 to $300 \times 10^4/\mu L$]), and

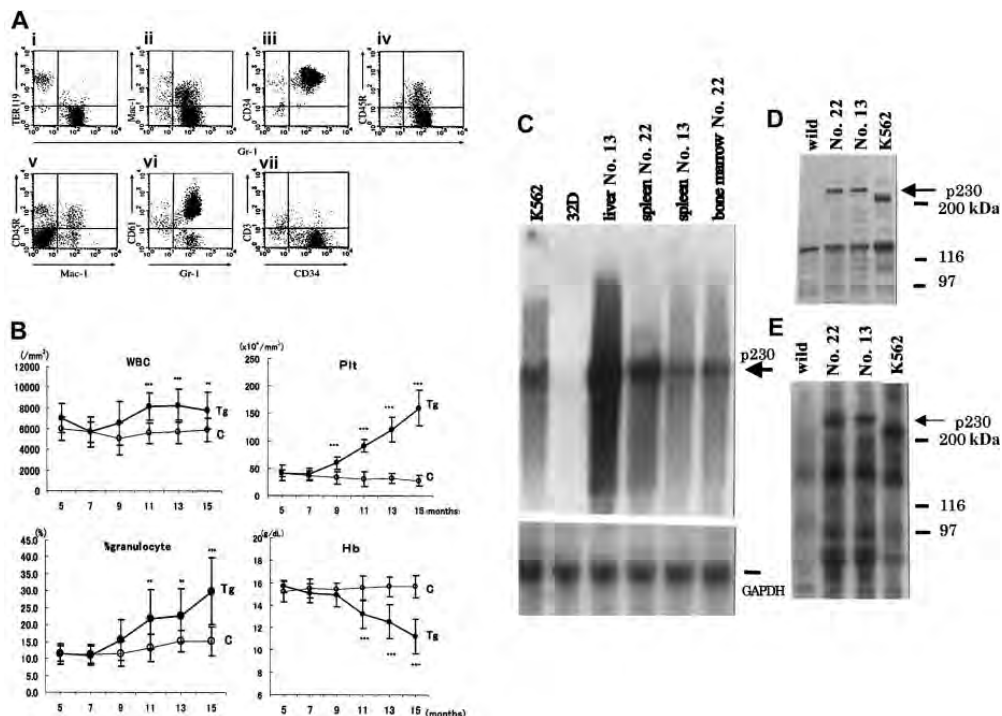


Figure 2. FACS analysis of leukemic mononuclear cells infiltrating the liver of founder mouse no. 13, comparison of hematologic parameters of transgenic progeny of no. 22, and molecular certification of p230 Bcr/Abl expression. (A) Surface marker analysis of leukemic cells infiltrating the liver of founder no. 13. (B) Comparison of hematologic parameters in the transgenic mice (n = 20; Tg, ●) and nontransgenic controls (n = 10; C, ○) from 5 months to 15 months. The data are shown as the mean values and standard deviations for each group. Time course of WBC count, platelet (Plt) count, the percentage (%) of granulocytes, and hemoglobin (Hb) are shown. ** $P < .01$; *** $P < .001$. (C) Northern blot analysis of p230 Bcr/Abl mRNA in tissues from no. 13 and no. 22 offspring. Lane K562: K562 cells as positive control; lane 32D: mouse 32D cells as negative control; lane liver no. 13; lane spleen no. 22; spleen cells of no. 22; lane spleen no. 13; spleen cells of no. 13; lane bone marrow no. 22: bone marrow cells of no. 22. The bottom bar shows the bands of glyceraldehyde-3-phosphate dehydrogenase (GAPDH) mRNA as an internal control. (D) P230 Bcr/Abl transgene product and (E) kinase activity of the p230 Bcr/Abl transgene product of the splenic cells. The expressed and phosphorylated P230 Bcr/Abl transgene products are indicated by arrows, and the positions of protein markers are shown on the right. The splenic cells of a 3-month-old F1 transgenic mouse were subjected to Western blot and immunoprecipitation analyses.

mild anemia (Hb97-127 g/L [9.7-12.7 g/dL]). All the transgenic offspring of no. 22 had an obvious phenotype of CML-like disease by around 15 months of age and showed massive infiltration of megakaryocytes and granulocytes mainly in the spleen and also in the liver and lung. The filial 3 (F3) Tg mice were confirmed to inherit a disease of MPD/CML phenotype. One of the disease phenotypic differences between the P210 and P230 Bcr/Abl transgenic mouse systems was the latency period.¹⁴ Latency until manifestation of disease in our transgenic mice was 7 months longer than that in the *tec* P210 Bcr/Abl system (8 months).¹⁴ Another difference was granulocytosis. Granulocytosis was milder than in the P210 Bcr/Abl transgenic mice.^{14,16} Peripheral thrombocytosis developed in both the P210 Bcr/Abl and the P230 Bcr/Abl transgenic mice, but infiltration of megakaryocytes in the spleen, liver, and lung was a unique characteristic of the P230 Bcr/Abl transgenic mice.^{14,16}

These disease findings of our transgenic mice might be due to the MSCV promoter function or the structure of the p230Bcr/Abl cDNA as well as b3a2-type p210Bcr/Abl cDNA.¹⁷ Previous reports suggested a positive correlation between thrombocytosis and the b3a2 type and p230Bcr/Abl type of Bcr/Abl transcripts in human CML.¹⁷⁻¹⁹ With its longer disease latency, our transgenic mice develop an MPD disease type with thrombocytosis. In this respect our transgenic mice may more accurately reflect the thrombopoietic characteristics of P230 Bcr/Abl in vivo. Human neutrophilic chronic myelogenous leukemia (CML-N) is known as a CML variant with a more benign clinical course than

CML.^{6,20} Such patients show the disease phenotype of Ph-positive essential thrombocythemia (ET)^{18,21} or CML with thrombocytosis.²²

Another leukemic model using the identical transgene has been reported using in vitro retroviral-mediated gene transfer/transplantation (T/T) system.⁷ Because the gene constructs used in that study are essentially the same as ours, it is unclear why the mice in these 2 studies showed different disease latency and disease phenotype. One possibility is that, unlike our transgenic mice, the recipient mice in the T/T study were exposed to various cytokines during in vitro culture and also in vivo engraftment, which might accelerate disease onset and affect disease phenotype.

In summary, we present a novel transgenic mouse line created using the P230 Bcr/Abl transgene to develop MPD mimicking CML-N or CML with thrombocytosis. This model will be valuable not only for investigating the biologic properties of P230 Bcr/Abl in vivo but also for analyzing the mechanism involved in the progression from chronic phase to blastic crisis.

Acknowledgments

We thank Dr R. Van Etten, Harvard Medical School, for providing the MSCVneoP230 BCR/ABL vector. We thank M. Kitoh, H. Yamaguchi, S. Inokuchi, and H. Matsuoka for their expert technical assistance.

References

- Shtivelman E, Lifshitz B, Gale RP, Canaani E. Fused transcript of *abl* and *bcr* genes in chronic myelogenous leukemia. *Nature*. 1985;315:550-554.
- Melo JV. The diversity of BCR-ABL fusion proteins and their relationship to leukemia type. *Blood*. 1996;88:2375-2384.
- Emilia G, Luppi M, Marasca R, Torelli G. Relationship between BCR/ABL fusion proteins and leukemia phenotype [letter]. *Blood*. 1997;89:3889.
- Pane F, Frigeri F, Sindona M, et al. Neutrophilic-chronic myeloid leukemia: distinct disease with a specific molecular marker (Bcr/Abl with C3/A2 junction). *Blood*. 1996;88:2410-2414.
- Briz M, Vilches C, Cabrera R, Fores R, Fernandez MN. Typical chronic myelogenous leukemia with e19a2 junction BCR/ABL transcript [letter]. *Blood*. 1997;90:5024.
- Verstovsek S, Lin H, Kantarjian H, et al. Neutrophilic-chronic myeloid leukemia: low levels of p230 BCR/ABL mRNA and undetectable p230 BCR/ABL protein may predict an indolent course. *Cancer*. 2002;94:2416-2425.
- Li S, Ilaria RL Jr, Million RP, et al. The P190, P210, and P230 forms of the BCR/ABL oncogene induce a similar chronic myeloid leukemia-like syndrome in mice but have different lymphoid leukemogenic activity. *J Exp Med*. 1999;189:1399-1412.
- Quackenbush RC, Reuther GW, Miller JP, et al. Analysis of the biologic properties of p230 Bcr-Abl reveals unique and overlapping properties with the oncogenic p185 and p210 Bcr-Abl tyrosine kinases. *Blood*. 2000;95:2913-2921.
- Hawley RG, Fong AZC, Burns BF, Hawley TS. Transplantable myeloproliferative disease induced in mice by an interleukin 6 retrovirus. *J Exp Med*. 1992;176:1149-1163.
- Hogan B, Constantini F, Lacy E. *Manipulating the Mouse Embryo*. Cold Spring Harbor, NY: Cold Spring Harbor Laboratory; 1986.
- Futaki M, Inokuchi K, Hanawa H, et al. Possible transforming activity of interferon regulatory factor 2 in tumorigenicity assay of NIH3T3 cells transfected with DNA from chronic myelogenous leukemia patients. *Leuk Res*. 1996;20:601-605.
- Inokuchi K, Miyake K, Takahashi H, et al. DCC protein expression in hematopoietic cell populations and its relation to leukemogenesis. *J Clin Invest*. 1996;97:852-857.
- Shinozawa I, Inokuchi K, Wakabayashi I, et al. Disturbed expression of the anti-apoptosis gene, *survivin*, and *EPR-1* in hematological malignancies. *Leuk Res*. 2000;24:965-970.
- Honda H, Oda H, Suzuki T, et al. Development of acute lymphoblastic leukemia and myeloproliferative disorder in transgenic mice expressing p210bcr/abl: a novel transgenic model for human Ph1-positive leukemias. *Blood*. 1998;91:2067-2075.
- Van Etten RA. Models of chronic myeloid leukemia. *Curr Oncol Rep*. 2001;3:228-237.
- Honda H, Hirai H. Model mice for BCR/ABL-positive leukemias. *Blood Cells Mol Dis*. 2001;27:265-278.
- Perego RA, Costantini M, Cornacchini G, et al. The possible influences of B2A2 and B3A2 BCR/ABL protein structure on thrombopoiesis in chronic myeloid leukaemia. *Eur J Cancer*. 2000;36:1395-1401.
- Yamagata T, Mitani K, Kanda Y, et al. Elevated platelet count features the variant type of BCR/ABL junction in chronic myelogenous leukaemia. *Br J Haematol*. 1996;94:370-372.
- Inokuchi K, Inoue T, Tojo A, et al. A possible correlation between the type of bcr/abl hybrid messenger RNA and platelet count in Philadelphia-positive chronic myelogenous leukemia. *Blood*. 1991;78:3125-3127.
- Pane F, Frigeri F, Sindona M, et al. Neutrophilic-chronic myeloid leukemia: a distinct disease with a specific molecular marker (BCR/ABL with C3/A2 junction). *Blood*. 1996;88:2410-2414.
- Wada H, Mizutani S, Nishimura J, et al. Establishment and molecular characterization of a novel leukemic cell line with Philadelphia chromosome expressing p230BCR/ABL fusion protein. *Cancer Res*. 1995;55:3192-3196.
- Saglio G, Guerrasio A, Rosso C, et al. New type of Bcr/Abl junction in Philadelphia chromosome-positive chronic myelogenous leukemia. *Blood*. 1990;76:1819-1824.

BRIEF COMMUNICATION

Antiangiogenic gene therapy of myeloproliferative disease developed in transgenic mice expressing P230 bcr/abl

K Miyake^{1,2,4}, K Inokuchi^{2,3,4}, N Miyake^{1,2}, K Dan³ and T Shimada^{1,2}

¹Department of Biochemistry and Molecular Biology, Nippon Medical School, Tokyo, Japan; ²Division of Gene Therapy Research, Center for Advanced Medical Technology, Nippon Medical School, Tokyo, Japan; and ³Department of Internal Medicine, Division of Hematology/Oncology, Nippon Medical School, Tokyo, Japan

Antiangiogenic gene therapy offers an attractive approach to the treatment of a variety of malignancies, including those of the hematological system. However, evaluation of this approach has been hampered by the lack of appropriate animal models. We have recently produced transgenic mice expressing P230 bcr/abl that develop myeloproliferative disease (MPD) closely resembling human chronic myelogenous leukemia. Using this MPD murine model, we examined the feasibility of systemic antiangiogenic gene therapy for hematological malignancy. An adenoviral vector containing the secreted endostatin gene was injected into the right quadriceps muscle of the MPD mice. The increased

endostatin level was detected for at least 6 months. Hematological parameters including platelet counts, granulocyte counts, and the hemoglobin concentration were improved by this gene therapy. Infiltration of megakaryocytes was also significantly inhibited in treated MPD mice. Reduction of the microvessel density was confirmed by histological examination. These results demonstrated, for the first time, that antiangiogenic gene therapy is effective to inhibit leukemogenesis caused by expression of the chimeric bcr/abl gene.

Gene Therapy (2005) 12, 541–545. doi:10.1038/sj.gt.3302427
 Published online 23 December 2004

Keywords: endostatin; bcr/abl; myeloproliferative disease; antiangiogenic gene therapy

A number of strategies for cancer gene therapy have been developed, but no definitive clinical efficacy has yet been demonstrated.¹ Targeted gene therapy of cancer cells using the suppressor oncogenes or the suicide genes has been hampered by the insufficient efficiency of current gene transfer technologies.^{2,3} Since angiogenesis is essential for both tumor growth and metastasis, antiangiogenic therapy may be an attractive new approach.^{4–6} Both local and systemic expression of antiangiogenic proteins such as angiostatin^{7,8} and endostatin^{9,10} have been attempted to treat various solid tumors to induce tumor dormancy.

Recent studies have suggested that the progression of hematological malignancies also relies on angiogenesis.¹¹ An increase in microvessel density in bone marrow (BM) specimens has been reported in leukemia patients.¹² Elevated levels of angiogenic factors such as basic fibroblast growth factor and vascular endothelial growth factor (VEGF) have been identified and are thought to be correlated with survival.^{13,14} Therefore, systemic antiangiogenic therapy is likely a promising therapy for hematological malignancies. However, the results of mouse

experiments are controversial. Scappaticci *et al*¹⁵ demonstrated synergistic antitumor activity and enhanced survival of mice bearing L1210 leukemic cells transduced with retroviral vectors expressing angiostatin and endostatin. In contrast, Eisterer *et al*¹⁶ reported that high levels of serum endostatin secreted from retrovirus transduced BM cells did not alter the growth of transplanted human leukemic cells. The reasons for this discrepancy are not known. One potential problem in these studies is the use of mice transplanted with leukemic cells. Since the development of leukemia from transplanted cells is different from the natural course of leukemogenesis, it should be important to establish a transgenic (tg) animal model in which leukemia develops from endogenous cells under the normal immunological surveillance.

We have recently succeeded in the generation of tg mice expressing P230 bcr/abl, which had leukemogenic properties and induced myeloproliferative disease (MPD).¹⁷ The progression of the disease in this murine model is similar to that of human neutrophilic myelogenous leukemia or chronic myelogenous leukemia with thrombocytosis. Reports have shown that BM microvessel density and serum VEGF are important for the development and prognosis of MPD.¹⁸ P230 bcr-abl has been associated with an indolent MPD as a distinct clinical entity.¹⁹ Thus, angiogenesis may be a critical step in MPD in tg mice expressing P230 bcr-abl. In the present study, we examined the feasibility of antiangiogenic gene therapy for hematological malignancies using this MPD

Correspondence: Professor T Shimada, Department of Biochemistry and Molecular Biology, Nippon Medical School, 1-1-5 Sendagi, Bunkyo-ku, Tokyo 113-8602, Japan

⁴These authors contributed equally to this work

Received 26 May 2004; accepted 27 October 2004; published online 23 December 2004

murine model. Since it is difficult to transduce all cancer cells, especially in hematological malignancies, systemic gene therapy appears to be preferable for the inhibition of tumor growth and metastases. Therefore, to obtain systemic expression of antiangiogenic protein, the recombinant adenovirus (Ad) vectors containing the secreted mouse endostatin driven by the CMV promoter (Ad-E; Invivo Gen, San Diego, CA, USA) were injected into the left quadriceps muscle of the 13- to 15-month-old MPD mice.

First, to analyze the duration of sustained expression of endostatin in Ad-E-injected MPD mice, the Ad-E (5×10^8 PFU) was injected into the right quadriceps muscle of the 13- to 15-month-old MPD mice and the concentration of serum endostatin was measured for 2–24 weeks using an enzyme-linked immunosorbent assay (ELISA) kit (ACCUCYTE murine endostatin; CytImmune Sciences, College Park, MD, USA). The background level of serum endostatin in control Ad vector expressing GFP (Ad-G)-injected mice was 56.0 ± 6.0 ng/ml, while injection of Ad-E increased the serum endostatin for at least 6 months (Figure 1). The concentration of serum endostatin peaked in the 4th week after injection (320 ± 20.5 ng/ml). At 6 months after the injection, serum endostatin was still significantly higher than the control value (86.2 ± 10.1 versus 51.8 ± 2.6 ng/ml, $P < 0.05$).

Since the MPD phenotype developed between 13 and 15 months after birth and the disease progress slowly, we analyzed the effect of systemic expression of endostatin 6 months after Ad-E injection. The results of peripheral blood (PB) examination at 6 months after Ad vector injection are presented in Table 1. MPD mice were characterized by a decreased concentration of hemoglobin and increased numbers of platelets and granulocytes. Compared to the control, MPD mice injected with Ad-G, injection of Ad-E showed significantly improved hemoglobin concentration (14.0 ± 0.84 versus 12.6 ± 0.85 ng/ml, $P < 0.01$), platelet count (98 ± 36 versus 144 ± 38 , $P < 0.05$), and granulocyte count (1021 ± 645 versus 3632 ± 473 , $P < 0.05$). Since huge splenomegaly was detected in MPD mice, we also analyzed the effect of endostatin on splenomegaly (Figure 2a and b). The longitudinal section area of the spleen was significantly reduced in Ad-E-injected MPD mice compared to Ad-G-injected mice (38.5 ± 13.4 versus 86.0 ± 24.5 mm², $P < 0.05$, $n = 9$). Histological examination showed that infiltration of mega-

karyocytes in the spleen and the BM was significantly inhibited in mice injected with Ad-E (Figure 2c and d and Table 1).

To confirm the mechanism of antiangiogenic gene therapy, we attempted to measure the microvessel density in the BM. Immunological staining with Factor VIII or CD31 did not give clear results because of the strong red color of the BM. However, the microvessels composed of one layer of endothelial cells were morphologically distinguishable from other cells in hematoxylin and eosin (H&E)-stained sections (Figure 3a–d). Compared with the age-matched wild-type mice, the number of microvessels in MPD mice transduced with a control vector (Ad-G) was increased (26.1 ± 2.6 versus 21.8 ± 8.2 /mm², $P < 0.05$). However, the area of microvessels was reduced (63.4 ± 26.8 versus 138.9 ± 58.2 μm²/mm², $P < 0.05$, $n = 9$), suggesting that massive infiltration of leukemic cells into the BM may decrease the area of vessels in the MPD BM. On the other hand, both the number (15.8 ± 4.5 versus 26.1 ± 2.6 /mm²,

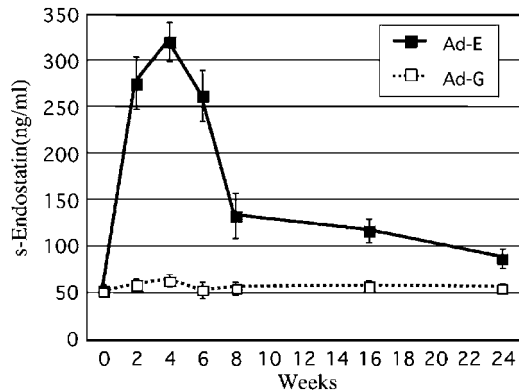


Figure 1 ELISA analysis for serum endostatin in Ad-E-injected mice. The Ad-E or Ad-G (5×10^8 PFU in 50 μl) were injected into the left quadriceps muscle of the 13 to 15-month-old MPD mice ($n = 3$) and the concentration of serum endostatin was measured for 2–24 weeks using a murine endostatin ELISA kit (ACCUCYTE murine endostatin; CytImmune Sciences, College Park, MD, USA) according to the manufacturer's instructions. Each result represents the mean value and standard deviation of three mice.

Table 1 Improvement of hematological parameters of MPD mice treated with Ad-E vector

Injected Ad vector (n)	Platelets ($\times 10^9$ /l) (82 ± 41) ^a	Granulocytes (μl) (174 ± 54.0)	Hemoglobin (g/dl) (15.2 ± 0.94)	Megakaryocytes	
				Spleen (longitudinal section) (10.3 ± 4.0)	Bone marrow (/mm ²) (12.3 ± 4.0)
Ad-G (9)	144 ± 38	3632 ± 473	12.6 ± 0.85	84.0 ± 40	13.6 ± 2.9
Ad-E (9)	$98 \pm 36^*$	$1021 \pm 645^*$	$14.0 \pm 0.84^{**}$	$43.0 \pm 12^{**}$	$7.6 \pm 3.3^*$

At 6 months after Ad injection, mice were killed and analyzed. PB was stained with Wright–Giemsa for differential analysis. Platelet counts, WBC counts and hemoglobin were determined with a blood cell counter for mouse PB (MICROS abc LC-152, Horiba, Tokyo, Japan). Tissue samples of the spleen and bone marrow were stained with H&E. Megakaryocytes were counted under a light microscope. Each result represents the mean value and standard deviation of nine mice. The statistical analysis was performed by the Student's *t*-test ($^*P < 0.05$, $^{**}P < 0.01$, compared to Ad-G).

^aThe normal values in nontransgenic age-matched mice of the same strain ($n = 20$).

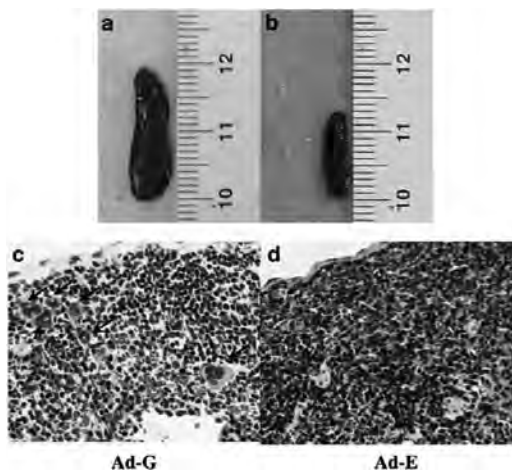


Figure 2 Macroscopic and microscopic examination of the spleen from mice injected with Ad-G or Ad-E. Tissue samples of the spleen of a mouse injected with Ad-G (a and c) and the spleen of a mouse injected with Ad-E (b and d). For pathological examination, they were fixed in 10% buffered formalin and embedded in paraffin. Sections were fixed on slides and stained with H&E by conventional techniques. The sections were viewed using a light microscope (Olympus, Tokyo, Japan). Arrows indicate megakaryocytes.

$P < 0.05$) (Figure 3e) and area (26.4 ± 15.7 versus $63.4 \pm 26.8 \mu\text{m}^2/\text{mm}^2$, $P < 0.05$) (Figure 3f) of microvessels in the femoral BM of Ad-E-injected mice were significantly reduced compared to control Ad-G-injected mice.

Here, we report for the first time that endostatin suppressed proliferative thrombopoiesis and granulopoiesis in MPD in tg mice expressing P230 bcr-abl. The most important point of this work is that we used a tg animal model for analyzing the effect of antiangiogenic gene therapy. Clinical trials of cancer gene therapy have so far been unsuccessful,^{2,3} although preclinical animal experiments are highly promising. One reason of the discrepancy between animal models and human patients may be that most of the animal models were generated by inoculation of established cancer cell lines into animals. The mechanisms of development of tumors from transplanted cells are different from the natural course of tumorigenesis. We demonstrated that antiangiogenic gene therapy is effective in treating the tg MPD model, in which leukemia was developed through the common leukemogenic pathway with the bcr/abl mutation. This murine model should prove valuable for the evaluation of other antileukemic therapies as well.

To analyze the effect of endostatin on BM cells obtained from MPD mice *in vitro*, we examined the proliferation capacity by 3-(4,5-dimethylthiazol-2-yl)-2,5-diphenyltetrazolium bromide (MTT) assay using a Cell Titer 96 aqueous nonradioactive cell proliferation assay kit (Promega, Madison, WI, USA), colony-forming units (CFUs) by methylcellulose assay of Ad-E- or Ad-G-transduced BM cells. However, we did not obtain any differences between Ad-E- and Ad-G-transduced BM cells in either proliferation capacity or the numbers of CFUs (data not shown). To analyze whether the presence

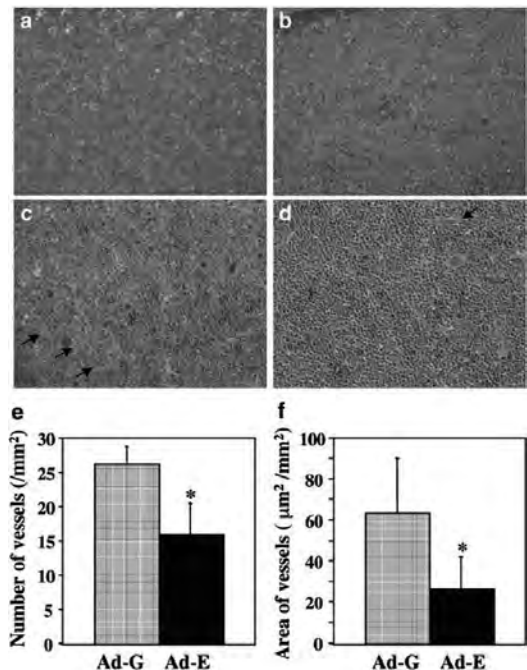


Figure 3 Microvessels in the center of the femoral BM. At 6 months after Ad vectors injection, tissue samples of BM sections ($6 \mu\text{m}$) from Ad-G-treated (a ($\times 100$) and c ($\times 400$)) or Ad-E-treated (b ($\times 100$) and d ($\times 400$)) mice were stained with H&E. Arrows indicate microvessels. The number of microvessels in the femoral BM of MPD mice (e) and the area of microvessel in the femoral BM of MPD mice (f) were quantified using an angiogenesis image analyzer (Kurabo, Okayama, Japan). Randomly selected four sections/animal from nine mice were examined. Arrows indicate megakaryocytes. The statistical analysis was performed by the Student's t-test using Statview (Brain Power, Calabasas, CA, USA) software package. Each result represents the mean value and standard deviation of nine mice (* $P < 0.05$).

of endostatin in Ad-E mice affects primarily the leukemic progenitor cells, we also analyzed expression of bcr-abl gene of CFUs using BM cells obtained from Ad-E- or Ad-G-injected mice by RT-PCR with bcr-abl-specific primer. Expression of bcr-abl gene was detected in all CFUs ($n = 20$) obtained from both Ad-E- and Ad-G-injected mice (data not shown). These results indicate that endostatin does not influence leukemic cell itself of MPD mice.

In this study, we analyzed the effect of systemic expression of endostatin administered by single injection of Ad vectors into the muscle. Recently, it was demonstrated that the serum level of endostatin was lower in chronic lymphocytic leukemia patients in advanced stage than in patients in early stage.²⁰ Therefore, the level of endostatin may have an important role on the progression of hematological malignancies. We think that it is logical to use endostatin for hematological malignancies. Skeletal muscle is an attractive target for gene therapy approaches for the treatment of myopathies and diseases requiring the secretion of proteins through the circulatory system because of its large size, good

capacity for protein synthesis, easy acquisition of sustained expression, and easy accessibility for intramuscular injection. Systemic administration of Ad vectors by intravenous was widely used for many types of gene therapy strategy.^{21–23} However, the toxicity to liver is a big problem of this method.^{24,25} When we checked transaminase (AST, ALT) in our Ad-injected mice, we did not detect the elevation of transaminase in any Ad-injected mice ($n=9$). However, using muscle-specific promoters or improving vector tropism for skeletal muscle may be useful to obtain safer and more efficient therapy after intramuscular administration of Ad vectors.

To study the utility of antiangiogenic gene therapy, we used Ad vectors, which are useful for transient expression of soluble proteins in muscle. On the other hand, adeno-associated virus (AAV) vectors have produced long-term expression of a therapeutic gene that is either integrated or an episomal vector genome.²⁶ Moreover, it was reported that AAV-1, AAV-5, and AAV-7 could transduce murine skeletal muscle more efficiently than the more widely used serotype AAV-2.^{27,28} Therefore, these AAV vectors may be more suitable for clinical trials of systemic antiangiogenic therapy targeting skeletal muscle.

An alternative approach for antiangiogenic gene therapy of hematological malignancy is the use of hematopoietic stem cells (HSCs) transduced with integrating vectors such as oncoretroviral or lentiviral vectors.²⁹ Long-term reconstitution with retroviral HSCs have been attained even in human clinical trials. As transplanted HSCs invade within the extravascular BM space, a high concentration of endostatin could be achieved at the site of malignant cell growth. We are currently attempting to evaluate this approach for long-term therapy of MPD model mice.

We demonstrated that an antiangiogenic strategy is effective to treat MPD of tg model mice. Although a first remission could be often achieved by rigorous chemotherapy programs, reappearance of the malignant cells is still a major concern in the treatment of leukemia. Antiangiogenic gene therapy may offer an important option for the establishment of the long-term anticancer state after remission induction of various hematological malignancies.

Acknowledgements

We thank Dr Izumu Saito for generous provision of plasmids and Ad vector, Dr Tsutomu Igarashi for expert technical assistance and helpful discussion. This work was supported in part by grants from the Ministry of Health and Welfare of Japan and the Ministry of Education, Science, and Culture of Japan.

References

- McCormick F. Cancer gene therapy: fringe or cutting edge? *Nat Rev Cancer* 2001; **1**: 130–141.
- Rainov NG, Ren H. Clinical trials with retrovirus mediated gene therapy – what have we learned? *J Neurooncol* 2003; **65**: 227–236.
- Zeimet AG, Marth C. Why did p53 gene therapy fail in ovarian cancer? *Lancet Oncol* 2003; **4**: 415–422.
- Weidner N, Semple JP, Welch WR, Folkman J. Tumor angiogenesis and metastasis – correlation in invasive breast carcinoma. *N Engl J Med* 1991; **324**: 1–8.
- O'Reilly MS et al. Angiostatin: a novel angiogenesis inhibitor that mediates the suppression of metastases by a Lewis lung carcinoma. *Cell* 1994; **79**: 315–328.
- O'Reilly MS et al. Endostatin: an endogenous inhibitor of angiogenesis and tumor growth. *Cell* 1997; **88**: 277–285.
- Tanaka T, Cao Y, Folkman J, Fine HA. Viral vector-targeted antiangiogenic gene therapy utilizing an angiostatin complementary DNA. *Cancer Res* 1998; **58**: 3362–3369.
- Ma HI et al. Intratumoral gene therapy of malignant brain tumor in a rat model with angiostatin delivered by adeno-associated viral (AAV) vector. *Gene Therapy* 2002; **9**: 2–11.
- Blezinger P et al. Systemic inhibition of tumor growth and tumor metastases by intramuscular administration of the endostatin gene. *Nat Biotechnol* 1999; **17**: 343–348.
- Sauter BV et al. Adenovirus-mediated gene transfer of endostatin *in vivo* results in high level of transgene expression and inhibition of tumor growth and metastases. *Proc Natl Acad Sci USA* 2000; **97**: 4802–4807.
- Moehler TM, Ho AD, Goldschmidt H, Barlogie B. Angiogenesis in hematologic malignancies. *Crit Rev Oncol Hematol* 2003; **45**: 227–244.
- Padro T et al. Increased angiogenesis in the bone marrow of patients with acute myeloid leukemia. *Blood* 2000; **95**: 2637–2644.
- Brunner B et al. Blood levels of angiogenin and vascular endothelial growth factor are elevated in myelodysplastic syndromes and in acute myeloid leukemia. *J Hematother Stem Cell Res* 2002; **11**: 119–125.
- Yetgin S, Yenicesu I, Cetin M, Tuncer M. Clinical importance of serum vascular endothelial and basic fibroblast growth factors in children with acute lymphoblastic leukemia. *Leukemia Lymphoma* 2001; **42**: 83–88.
- Scappaticci FA et al. Combination angiostatin and endostatin gene transfer induces synergistic antiangiogenic activity *in vitro* and antitumor efficacy in leukemia and solid tumors in mice. *Mol Ther* 2001; **3**: 186–196.
- Eisterer W et al. Unfulfilled promise of endostatin in a gene therapy – xenotransplant model of human acute lymphocytic leukemia. *Mol Ther* 2002; **5**: 352–359.
- Inokuchi K et al. Myeloproliferative disease in transgenic mice expressing P230 Bcr/Abl: longer disease latency, thrombocytosis, and mild leukocytosis. *Blood* 2003; **102**: 320–323.
- Verstovsek S et al. Prognostic significance of cellular vascular endothelial growth factor expression in chronic phase chronic myeloid leukemia. *Blood* 2002; **99**: 2265–2267.
- Verstovsek S et al. Neutrophilic-chronic myeloid leukemia: low levels of p230 BCR/ABL mRNA and undetectable BCR/ABL protein may predict an indolent course. *Cancer* 2002; **94**: 2416–2425.
- Gora-Tybor J, Blonski JZ, Robak T. Circulating proangiogenic cytokines and angiogenesis inhibitor endostatin in untreated patients with chronic lymphocytic leukemia. *Mediators Inflamm* 2003; **12**: 167–171.
- Green NK, Seymour LW. Adenoviral vectors: systemic delivery and tumor targeting. *Cancer Gene Ther* 2002; **9**: 1036–1042.
- Jiang Z, Feingold E, Kochanek S, Clemens PR. Systemic delivery of a high-capacity adenoviral vector expressing mouse CTLA4lg improves skeletal muscle gene therapy. *Mol Ther* 2002; **6**: 369–376.
- Ben-Gary H et al. Systemic interleukin-6 responses following administration of adenovirus gene transfer vectors to humans by different routes. *Mol Ther* 2002; **6**: 287–297.
- Brunetti-Pierri N et al. Acute toxicity after high-dose systemic injection of helper-dependent adenoviral vectors into nonhuman primates. *Hum Gene Ther* 2004; **15**: 35–46.

- 25 St George JA. Gene therapy progress and prospects: adenoviral vectors. *Gene Therapy* 2003; **10**: 1135–1141.
- 26 Buning H *et al*. AAV-based gene transfer. *Curr Opin Mol Ther* 2003; **5**: 367–375.
- 27 Chao H *et al*. Several log increase in therapeutic transgene delivery by distinct adeno-associated viral serotype vectors. *Mol Ther* 2000; **2**: 619–623.
- 28 Gao GP *et al*. Novel adeno-associated viruses from rhesus monkeys as vectors for human gene therapy. *Proc Natl Acad Sci USA* 2002; **99**: 11854–11859.
- 29 De Palma M, Venneri MA, Roca C, Naldini L. Targeting exogenous genes to tumor angiogenesis by transplantation of genetically modified hematopoietic stem cells. *Nat Med* 2003; **9**: 789–795.

Oral Administration of Imatinib to P230 BCR/ABL-Expressing Transgenic Mice Changes Clones with High *BCR/ABL* Complementary DNA Expression into Those with Low Expression

Mitsuharu Inami, Koiti Inokuchi, Hiroki Yamaguchi, Kazutaka Nakayama, Ayako Watanabe, Naoya Uchida, Sakae Tanosaki, Kazuo Dan

Division of Hematology, Department of Third Internal Medicine, Nippon Medical School, Tokyo, Japan

Received December 12, 2005; received in revised form June 16, 2006; accepted July 14, 2006

Abstract

The effect of imatinib on myeloproliferative disease in transgenic (Tg) mice expressing the P230 BCR/ABL transcript is unknown. To investigate this issue, we administered imatinib (30 mg/kg per day) orally to P230 BCR/ABL-expressing Tg mice for 30 days. Following imatinib administration, the enlarged spleen was significantly reduced to within the normal size range. Infiltrating megakaryocytes in the long-axis section of the spleen were also significantly reduced. However, the cellularity of the bone marrow was not affected. Fluorescence-activated cell-sorting analysis revealed that infiltrating mature granulocytes in the spleen were reduced in number. The numbers of infiltrating CD34, CD117, CD61, and CD11b populations were also reduced in immature populations of the spleen. Real-time quantitative polymerase chain reaction analysis of messenger RNA revealed a dramatic reduction in the *p230 BCR/ABL* transcript for CD34, CD117, CD61, and CD11b populations in both bone marrow cells and spleen cells. Western blotting and immunoprecipitation analysis also revealed a marked reduction in P230 BCR/ABL protein expression in both bone marrow cells and spleen cells. Thus, imatinib administration had the intriguing effect of replacing clones with high expression of *p230 BCR/ABL* complementary DNA with clones with very low expression. These data show that imatinib may still be capable of eliminating and eradicating clones with high *p230 BCR/ABL* expression and healing the disease phenotype in Tg mice. Pluripotent clones with very low *p230 BCR/ABL* expression still survive as immature CD34, CD117, CD61, and CD11b populations.

Int J Hematol. 2006;84:346-353. doi: 10.1532/IJH97.05186

© 2006 The Japanese Society of Hematology

Key words: P230 BCR/ABL; Transgenic mouse; Imatinib; Megakaryocyte; Myeloproliferative disease

1. Introduction

Chronic myeloid leukemia (CML) features a characteristic chromosome, the Philadelphia (Ph) chromosome. The Ph chromosome carries the *BCR/ABL* oncogene, which is formed by the reciprocal translocation of chromosomes 9 and 22 [1].

Imatinib mesylate (formerly STI571 or CGP57148B, hereafter imatinib) is a potent and relatively selective tyrosine kinase inhibitor of the BCR/ABL protein. Imatinib has

significant activity against P210 and P190 BCR/ABL in CML and acute lymphocytic leukemia [2-4]. However, there is no evidence that imatinib is also effective against P230 BCR/ABL, which is clinically characterized as chronic neutrophilic leukemia. Thus, we investigated whether imatinib has a selective inhibitory activity against the BCR/ABL tyrosine kinase of P230 BCR/ABL.

We generated transgenic (Tg) mice expressing P230 BCR/ABL driven by the MSCV neo P230 BCR/ABL vector [5]. Tg mice expressing P230 BCR/ABL complementary DNA (cDNA) were used in an in vivo model to confirm that imatinib is a potential drug for myeloproliferative disease (MPD) expressing P230 BCR/ABL.

The present report shows that imatinib eliminates the disease phenotype by removing hematologic cells expressing *p230 BCR/ABL* cDNA and allowing the proliferation of cells expressing low levels of *p230 BCR/ABL* cDNA.

Correspondence and reprint requests: Koiti Inokuchi, MD, PhD, Division of Hematology, Department of Internal Medicine, Nippon Medical School, 1-1-5 Sendagi, Bunkyo-ku, Tokyo 113-8603, Japan; 81-3-3822-2131; fax: 81-3-5814-6934 (e-mail: inokuchi@nms.ac.jp).

2. Methods

2.1. Imatinib Mesylate

Imatinib mesylate (STI571, CGP57148B) was donated by Witte-Maria Weber (Novartis Pharmaceuticals, Basel, Switzerland). Stock solutions of this compound were prepared to 5 mg/mL with distilled water, filtered, and stored at -20°C . Preparations used for animal experiments were made at the concentrations indicated below and kept at 4°C for a maximum of 4 days. Stock solutions of 5 mg/mL were administered to mice by gavage once a day. For the control Tg mice, distilled water was administered. The imatinib dose was chosen in accordance with the doses administered in previous published studies that have investigated the molecular mechanisms of imatinib resistance in a murine retroviral CML transduction and transplantation model. At first, we administered 50 mg/kg imatinib per day. However, all of the Tg mice had severe bone marrow suppression by day 7 (median white blood cell [WBC] count, $1.4 \times 10^9/\text{L}$; median hemoglobin concentration, 8.2 g/dL; median platelet count, $91 \times 10^9/\text{L}$); thus, we reduced the dosage to 30 mg/kg per day for this investigation. Administering imatinib at 30 mg/kg per day caused mild bone marrow suppression on day 20 (median WBC count, $5.5 \times 10^9/\text{L}$; median platelet count, $999.5 \times 10^9/\text{L}$), but it recovered by day 30. Administering imatinib at 3 mg/kg or 10 mg/kg per day caused neither bone marrow suppression nor a pharmacologic reaction in the spleen.

2.2. Tg Mice

We generated Tg mice that expressed P230 BCR/ABL driven by the promoter of the long terminal repeat of the murine stem cell virus of the MSCV neo P230 BCR/ABL vector [5].

2.3. Histologic Analysis of the Spleens of Tg Mice

Nine- to 13-month-old Tg mice with P230 BCR/ABL cDNA ($n = 24$) and wild-type mice of the same age were enrolled in this study. Imatinib was orally given at 30 mg/kg per day to 12 mice for 30 days. Because the imatinib-administered mice showed lowered activity levels and weight loss (median initial weight, 32 g; weight on day 30, 28 g), these Tg mice were sacrificed on the 30th day of oral administration. After the mice were sacrificed, the femur bone marrow and spleen tissue were obtained, fixed in neutrally buffered 10% formalin at room temperature for 24 hours, embedded in paraffin, and sectioned. All spleen sections were stained with hematoxylin and eosin for light microscopy. Immunostaining for megakaryocytes after formalin fixation was performed with purified rat antihuman CD62P (P-selectin) monoclonal antibody (BD Pharmingen, San Jose, CA, USA) and polyclonal rabbit antihuman von Willebrand factor conjugated with horseradish peroxidase (HRP) (Dako, Glostrup, Denmark) [5].

The megakaryocytes in the longitudinal section of the spleen were counted, and the long axis of the section was measured with Luna Vision, version 1.1 (Mitani, Fukui, Japan).

2.4. Flow Cytometric Analysis and Cell Purification

Mononuclear cells in the bone marrow and spleen from 4 Tg mice that had been treated with imatinib at 30 mg/kg for 30 days, 2 untreated control Tg mice with MPD, and 4 wild-type mice were evaluated by single-color flow cytometric analysis with a FACScan flow cytometer (BD Biosciences, San Jose, CA, USA) and fluorescein isothiocyanate (FITC)-conjugated monoclonal antibodies to CD117, TER-119, CD11b (Mac-1), and CD61, and phycoerythrin-conjugated monoclonal antibodies to CD34. All antibodies were purchased from BD Pharmingen (Franklin Lakes, NJ, USA). A minimum of 5000 events were acquired, and the data were analyzed with CellQuest software (BD Biosciences).

Mononuclear leukocytes (1×10^6) from wild-type mice, control Tg mice, and imatinib-administered Tg mice were separated from the bone marrow and spleen and were sorted by standard protocols with a MACS Mouse Cell Isolation kit (Miltenyi Biotec, Bergisch Gladbach, Germany), which is specific for CD34, CD117, CD11b, or FITC (indirect MicroBeads used for CD61 [Miltenyi Biotec]). Each sample was incubated with a specific monoclonal antibody (BD Biosciences) after incubation with MACS beads. The samples were added to an LS column (Miltenyi Biotec) in a magnetic field, and negative cell fractions were depleted. Fluorescence-activated cell-sorting (FACS) analysis established that all of the cells purified with a MACS Mouse Cell Isolation kit in the present study sorted cells with greater than 90% specificity (data not shown). After checking the purification results with the FACScan instrument, total RNA was extracted from the purified cells.

2.5. Real-Time Quantitative Polymerase Chain Reaction Analysis

Relative quantification of *BCR/ABL* gene expression in bone marrow cells and spleen cells (CD117⁺ cells, CD11b⁺ cells, CD34⁺ cells, and CD61⁺ cells) were measured by real-time quantitative polymerase chain reaction (RQ-PCR) analysis using the Gene Amp 5700 Sequence Detection System (Applied Biosystems, Foster City, CA, USA). Total RNA was extracted with the RNA STAT-60 reagent (Tel-Test, Friendswood, TX, USA) from each purified cell. One microgram of total RNA was used to construct cDNA by reverse transcription with an RNA PCR Kit (AMV), version 2.1 (TaKaRa Bio, Shiga, Japan) according to standard protocols. To quantify gene expression, we used the *glyceraldehyde-3-phosphate dehydrogenase (GAPDH)* gene as an endogenous control. Dilutions of a cDNA sample prepared from the total RNA of murine 32D cells transfected with *p230 BCR/ABL* cDNA were used to construct standard curves for the *BCR/ABL* and *GAPDH* amplifications. The specific probes and primers used in the RQ-PCR for the *BCR/ABL* gene segment coding for the adenosine triphosphate-binding site were TaqMan probe 5'-TCA TCC ACA GAG ATC TTG CTG CCC G-3' forward primer 5'-CCG TGG TGC TGC TGT ACA TG-3', and reverse primer 5'-GTT CTC CCCTAC CAG GCA GTT-3'. The primers and probes used for *GAPDH* were TaqMan Rodent GAPDH Control Reagents (Applied Biosystems). All samples were run twice.

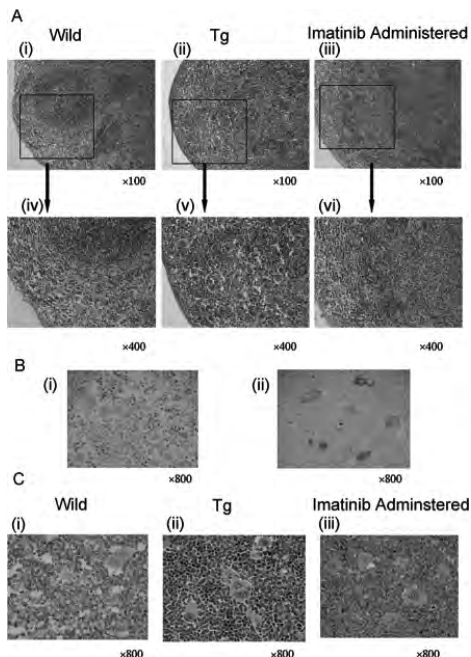


Figure 1. Histologic analysis of the spleen and bone marrow. The cryosection of the spleen was stained with hematoxylin and eosin (HE) for counting megakaryocytes with light microscopy, and the long axis of the section was measured. A, HE-stained sections of spleens from a wild-type mouse (i, iv), a control transgenic (Tg) mouse (ii, v), and an imatinib-administered mouse (iii, vi). B, Results of immunostaining of spleen cells with anti-CD62P (P-selectin) antibody (i) and with anti-von Willebrand factor/horseradish peroxidase antibody (ii). C, HE-stained bone marrow of wild-type mice (i), control Tg mice (ii), and imatinib-administered Tg mice (iii). Original magnifications are indicated beneath each panel.

2.6. Western Blotting and Immunoprecipitation

Purified spleen or bone marrow cells were suspended in RIPA lysis buffer (50 mM Tris-HCl [pH 7.4], 150 mM NaCl, 1 mM EDTA [pH 8.0], 1% Triton X-100, 0.1% sodium dodecyl sulfate [SDS], and 1% sodium deoxycholate) containing Complete, Mini, EDTA-Free Protease Inhibitor Cocktail Tablets (Roche Diagnostics, Mannheim, Germany) extraction solution and were lysed according to standard protocols. Cell lysates containing 30 μ g of protein were boiled with SDS sample buffer (20 mM sodium phosphate, 2% SDS, 0.001% bromophenol blue, 0.2 M dithiothreitol, and 2% glycerol) prior to SDS-polyacrylamide gel electrophoresis. The samples were electrophoresed with molecular weight markers (Biotinylated Protein Ladder Detection Pack; Cell Signaling Technology, Beverly, MA, USA), protein lysates of murine 32D cells transfected with *p230 BCR/ABL* cDNA as the positive control, and protein lysates of cells of the MV(4;11) cell line as the

negative control. After proteins were transferred to a polyvinylidene fluoride (PVDF) membrane from a 5%-to-25% gradient polyacrylamide gel, mouse antihuman Abl protein monoclonal antibody (BD Pharmingen) was incubated with 5% dry milk containing phosphate-buffered saline with polysorbate (Tween). PVDF membranes were incubated with HRP-linked antimouse antibody (BD Pharmingen) and HRP-linked antibiotin antibody (BD Pharmingen). Western blotting was performed with the ECL Plus Western Blotting Detection System (GE Healthcare, Piscataway, NJ, USA). Another membrane with the same amount of the same protein lysate was incubated with anti- β -actin antibody (BD Pharmingen) for normalization.

2.7. Statistical Analysis

Statistical analyses were performed with StatView software (SAS Institute, Cary, NC, USA). Data are expressed as the mean \pm SD unless otherwise indicated and have been compared by means of the unpaired Student *t* test. A *P* value of $<.05$ was considered statistically significant.

3. Results

3.1. Histologic Analyses of the Spleen and Bone Marrow Revealed That Imatinib Administration to Tg Mice Influenced the Length of the Long Axis of the Spleen and the Megakaryocyte Counts in the Spleen but Had No Influence on the Bone Marrow

The Tg mice were sacrificed on the 30th day of imatinib administration in order to analyze both bone marrow and spleen. Hematoxylin and eosin staining, anti-CD62 immunostaining (Figure 1B, i), and anti-von Willebrand factor immunostaining (Figure 1B, ii) of the spleen revealed that imatinib administration reduced the numbers of infiltrating large megakaryocytes (Figure 1A). However, there were no significant changes in bone marrow cellularity between the Tg control mice and the imatinib-administered Tg mice (Figure 1C).

The length of the long axis of the spleen was also significantly reduced to 10.7 ± 1.1 mm in the imatinib-administration group ($n = 7$), compared with 13.8 ± 5.3 mm in the control group ($n = 8$) ($P = .0065$; Figure 2A). The numbers of large megakaryocytes were also significantly reduced in the area of the long-axis section of spleens from the imatinib-administered group (132.6 ± 52.5 /section; $n = 7$) compared with the numbers in the control Tg group (321.8 ± 151.4 /section; $n = 8$) ($P = .008$; Figure 2B).

3.2. Imatinib Administration Markedly Reduced Mature Neutrophils in the Spleen but Had No Influence on the Bone Marrow

To evaluate the effect of imatinib on the phenotypic populations of infiltrated cells before and after imatinib administration, we performed a FACS analysis. The number of spleen cells of control Tg mice in area R1, which is strongly positive and weakly positive for CD11b and CD117

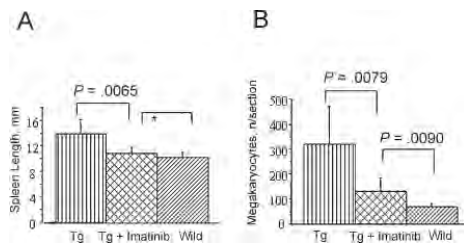


Figure 2. Histologic analysis of the spleen by counting megakaryocytes in the area and measuring the long axis of the spleen. Imatinib-administered transgenic (Tg) mice had a significantly decreased megakaryocyte count in the spleen section and a shorter long axis of the spleen. A, Length of the spleen long axis. B, The number of megakaryocytes per area of spleen section. Large mature megakaryocytes were counted in spleen sections stained with hematoxylin and eosin. Wild indicates wild-type mice; Tg, control Tg mice; Tg + imatinib, imatinib-administered Tg mice. * $P > .05$.

populations, respectively (Figure 3A, i), suggests that phenotypically mature granulocytes had increased. On the other hand, the numbers of cells in area R1 were markedly reduced in the imatinib-administered Tg mice (Figure 3B). The reduction in the number of cells noted in area R1 in the spleen was also detected in the bone marrow of imatinib-administered Tg mice (Figure 4). However, the frequencies of all 4 positive populations (CD117⁺, CD34⁺, CD61⁺, TER-119⁺) were maintained in area R2 spleen cells of Tg mice despite 30 days of imatinib administration (Figure 3A, iii). Area R2 consists of low-positive CD11b and high-positive CD117 populations, suggesting immature granulocytes. Thus, the FACS analysis revealed that the number of mature granulocytes (R1 area) was reduced in the spleens of imatinib-administered Tg mice. However, 30 days of imatinib administration had hardly any influence on the frequencies of CD117, CD34, CD61, and TER-119 cell populations in the immature population (R2 area) of the spleen. Figure 3C shows a cytospin cytocentrifuge analysis of sorted spleen cells. An examination of the sorted Mac-1⁺ (CD11b⁺) cells from area R1 showed mature granulocytes.

However, FACS analysis showed no significant changes in the cell populations of the bone marrow between imatinib-administered Tg mice and control Tg mice (Figure 4). A FACS analysis revealed that the cell populations of bone marrow were very different from those of the spleen. An R3 area, which is occupied by high-positive CD11b and low-positive CD117 cell populations, was not detected in spleen cells. The populations in area R1 were reduced. However, the populations in area R3 were increased in number (Figure 4).

3.3. High *BCR/ABL* Messenger RNA Expression among the Populations of Spleen Cells Was Markedly Reduced with Imatinib Administration

To evaluate the expression status of the *BCR/ABL* gene in each population, we tried to quantify *BCR/ABL* messenger RNA (mRNA) with the RQ-PCR method.

RQ-PCR analysis revealed that the infiltrated spleen cells had markedly higher *BCR/ABL* mRNA expression than bone marrow cells. In the control Tg mice, the CD117⁺, CD11b⁺, and CD61⁺ populations of the spleen showed higher expression than those of the bone marrow (Figure 5).

Following imatinib administration to Tg mice, RQ-PCR analysis revealed a significant 310-fold reduction in relative *p230 BCR/ABL* mRNA expression (0.1436 ± 0.0852 versus 44.445 ± 0.107) in the infiltrated spleen cells and a 9-fold reduction (0.4293 ± 0.078 versus 3.928 ± 0.1351) in the bone marrow cells of the imatinib-administered group, compared with the control group (Figure 5).

All populations of bone marrow cells and spleen cells of Tg mice ($n = 5$) showed reduced *BCR/ABL* mRNA levels after 30 days of imatinib administration compared with the levels of the control Tg mice ($n = 3$). *BCR/ABL* mRNA expression was also decreased in the purified cell populations of all CD34⁺, CD61⁺, CD117⁺, and CD11b⁺ bone marrow cells. Thus, the RQ-PCR analysis revealed that this mRNA was significantly reduced following imatinib administration to Tg mice (Figure 5).

3.4. Suppression of the P230 *BCR/ABL* Oncoprotein in Spleen Cells of Tg Mice Administered Imatinib

The influence of imatinib on the *BCR/ABL* oncoprotein was examined by Western blotting (Figure 6). Western blotting revealed that the *BCR/ABL* oncoprotein was significantly reduced after imatinib administration compared with control Tg mice. This result shows a good correlation between mRNA expression and protein expression.

4. Discussion

We generated Tg mice expressing *p230 BCR/ABL* cDNA by using the pMSCV P230 *BCR/ABL* cDNA vector [5]. P230 *BCR/ABL* Tg mice have a longer disease latency than P210 *BCR/ABL* Tg mice [6], which show mild granulocytosis, marked thrombocytosis, and the development of MPD with splenomegaly, as is seen in human chronic neutrophilic leukemia and CML with thrombocytosis.

In this study, we showed that infiltrating megakaryocytes expressing the CD61 antigen have higher *BCR/ABL* expression than progenitor cells such as c-kit⁺ (CD117⁺) cells, CD34⁺ cells, and mature myeloid cells such as CD11b⁺ cells. This phenomenon of *BCR/ABL* positivity may contribute to the phenotype of human MPD with marked thrombocytosis.

The oral administration of imatinib at a dosage of 30 mg/kg per day for 30 days to Tg mice significantly reduced the size of the enlarged spleen by removing infiltrated megakaryocytes and mature granulocytes (Figure 2). These cells in the megakaryocytic and myeloid lineages with high *p230 BCR/ABL* expression were eradicated. As is shown in the FACS analysis, the mature cell populations in area R1 (a mature granulocyte morphology) were reduced more significantly than the immature cell population (R2). In area R2, immature populations with 4 phenotypes (CD34, CD117, CD11b, and CD61 expression) were consistently present (Figure 3). However, these 4 populations were clearly reduced in number because imatinib administration reduced

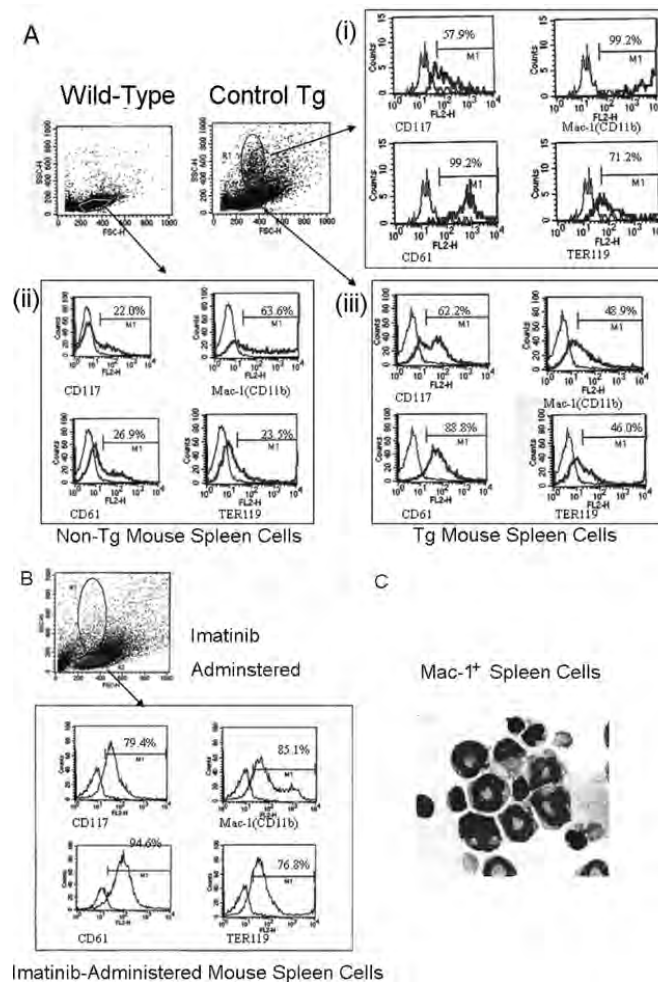


Figure 3. Fluorescence-activated cell-sorting (FACS) analysis of spleen cells from transgenic (Tg) mice after 30 days of imatinib administration. A, FACS analysis of spleen cells in 13-month-old wild-type and control Tg mice. B, FACS analysis of spleen cells in Tg mice administered imatinib for 30 days. The panels show flow cytometric side-scatter (SSC) and forward-scatter (FSC) properties. High SSC means high granularity, and high FSC means a large cell. The R1 (A, i) and R2 (A, ii and iii) regions indicate granular and mononuclear regions, respectively. C, Wright-Giemsa-stained sorted cells of area R1 spleen cells. CD34 indicates immature progenitor cells; CD61, megakaryocytes; CD11b, monocytes and neutrophils; CD117, immature progenitor cells.

the spleen size (volume) significantly. The higher frequencies of these 4 populations in area R2 may be due to clonal change. Clones in area R2 may have hardly any capacity for differentiation with imatinib administration. In other words, cells with high BCR/ABL expression were eliminated, and pluripotent cells with very low BCR/ABL expression consequently were selected and accumulated in area R2. Thus, imatinib had a sufficient capacity to inhibit the tyrosine kinase activity of P230 BCR/ABL and to eliminate high

BCR/ABL-expressing cells with a high capacity for proliferation and differentiation.

Despite the effect on the spleen, from the viewpoint of pathology, there were no effects on bone marrow cellularity in the imatinib-administered Tg mice. With respect to the FACS analysis of the bone marrow, we identified R3 populations that were not detected in the spleen. These mature cells may contribute to maintaining peripheral blood counts.

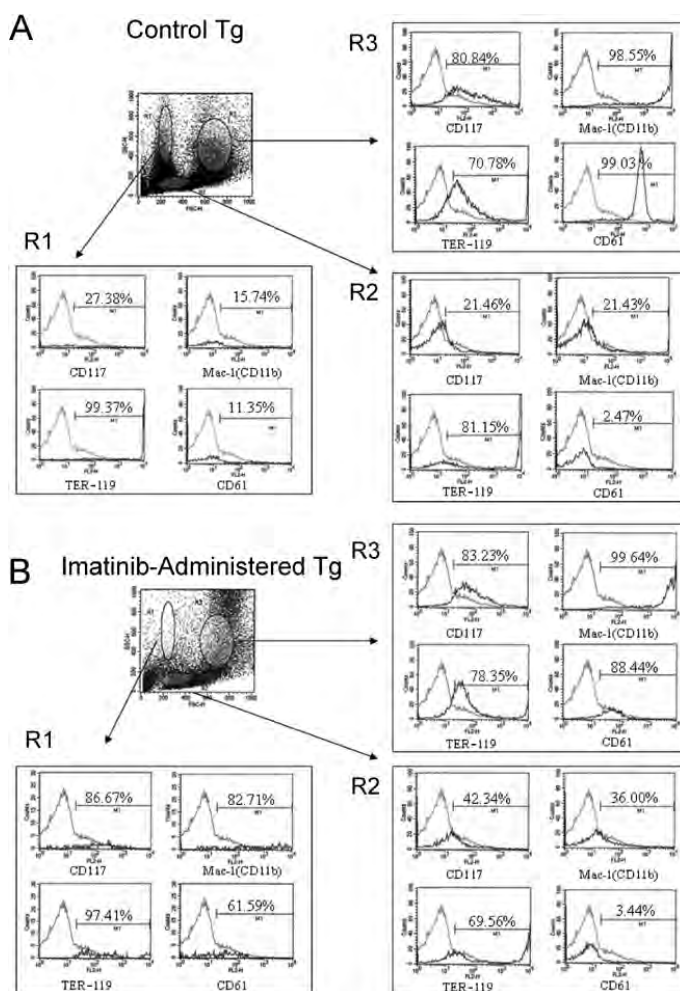


Figure 4. Fluorescence-activated cell-sorting (FACS) analysis of bone marrow cells from transgenic (Tg) mice after 30 days of imatinib administration. A, FACS analysis of control Tg mice (A) and Tg mice administered imatinib for 30 days (B).

There remains the question of why there was a difference in response between the bone marrow and the spleen of imatinib-administered Tg mice. The explanation is that spleen cells that expressed high *BCR/ABL* mRNA levels clearly were removed. On the other hand, mature cells in the bone marrow in area R3 were not affected. This difference may have been due to variations in the expression of *BCR/ABL* mRNA between the spleen and the bone marrow. Imatinib removed only cells with high *BCR/ABL* expression.

Because imatinib is an intrinsic tyrosine kinase inhibitor of the *BCR/ABL* protein, there could be no effect on mRNA transcription activity. However, a significant reduction in

BCR/ABL mRNA expression by imatinib was observed in the granulocytic and megakaryocytic cell population of the treated mice. Additionally, Western blotting revealed that administering imatinib also inhibited the expression of the P230 *BCR/ABL* oncoprotein. These data may indicate that cells with high *BCR/ABL* mRNA expression in the bone marrow are markedly reduced in exchange for cells with low *BCR/ABL* mRNA expression and consequently indicate the maintenance of residual infiltrated immature cells in the spleen.

However, it is difficult to normalize the elevated peripheral blood counts of Tg mice by administering 30 mg/kg per

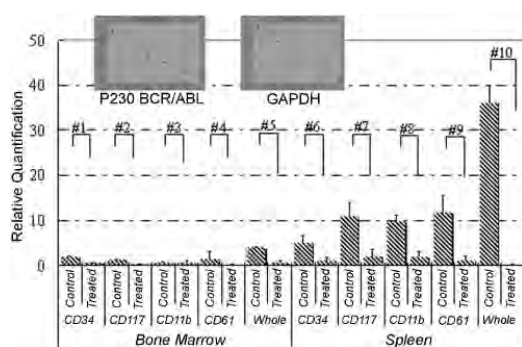


Figure 5. Relative quantification of BCR/ABL messenger RNA (mRNA) of cell populations in the spleen and bone marrow. Bars represent relative quantification of BCR/ABL mRNA of purified bone marrow and spleen cell populations of control transgenic (Tg) mice and Tg mice after 30 days of imatinib administration. For each experimental sample, the amounts of BCR/ABL mRNA and glyceraldehyde-3-phosphate dehydrogenase (GAPDH) mRNA were determined by real-time quantitative polymerase chain reaction analysis and comparison with the appropriate standard curve (insets). The BCR/ABL mRNA amount was divided by the GAPDH mRNA amount to obtain a normalized BCR/ABL mRNA value. All samples were analyzed in duplicate. All cell preparations purified with the MACS purification kit (Miltenyi Biotec) showed greater than 90% purity.

day of imatinib for 30 days, despite bone marrow suppression on day 20. However, there was a tendency toward decreased WBC counts on the 30th day in the Tg mice administered 30 mg/kg imatinib per day compared with the control Tg mice ($8.38 \pm 0.86 \times 10^9/L$ versus $7.92 \pm 0.22 \times 10^9/L$; $P = .5798$). In addition, hemoglobin concentrations were 12.43 ± 1.02 g/dL and 13.26 ± 0.95 g/dL ($P = .1388$) for the control and imatinib-administered groups, respectively, on the 30th day of administration, and the corresponding platelet counts were $1210 \pm 140 \times 10^9/L$ and $1100 \pm 540 \times 10^9/L$ ($P = .1226$). We speculated that the differences in the peripheral blood counts could not be the result of residual hematopoietic cells in the spleen and bone marrow expressing low levels of BCR/ABL and thereby partly contributing to maintaining the high platelet and leukocyte counts. Another speculation is that mature hematopoietic cells in area R3 of the bone marrow that are not affected by imatinib maintained the peripheral blood counts.

Low levels of BCR/ABL expression are sufficient to support growth factor independence [7]. Therefore, imatinib administration for 30 days was not able to affect the normalization of the peripheral blood count sufficiently. Normalization of the peripheral blood count could be achieved with a longer duration of imatinib administration in Tg mice, because all cells of Tg mice have the p230 BCR/ABL transgene and express the p230 BCR/ABL protein.

It is interesting that the RQ-PCR analysis revealed that 4 CD-positive populations of infiltrating cells in the spleen of control Tg mice had markedly higher BCR/ABL mRNA expression levels than the identical populations among

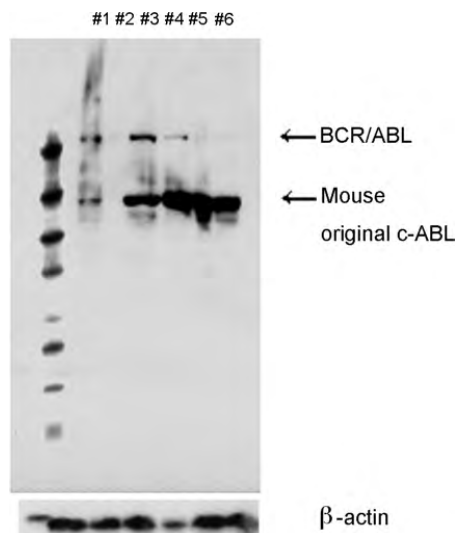


Figure 6. Western blotting of P230 BCR/ABL oncoproteins of bone marrow cells and spleen cells. The level of P230 BCR/ABL protein was normalized to that of β -actin, the product of a housekeeping gene. The left lane shows molecular weight markers. Lane 1, positive control (32D cells expressing p230 BCR/ABL cDNA); lane 2, negative control (MV[4;11] cell line expressing the MLL/AF4 fusion protein); lane 3, spleen of a control transgenic (Tg) mouse; lane 4, bone marrow of a control Tg mouse; lane 5, spleen of an imatinib-administered Tg mouse; lane 6, bone marrow of an imatinib-administered Tg mouse.

bone marrow cells. The reason for this difference could be that infiltrating cells in the spleen are more malignant clones that have lost the cell-cell interactions in the microenvironment of the bone marrow and that these cells are capable of deviation [8-10].

In human beings, normal hematopoiesis from Ph chromosome-negative hematopoietic cells recovered quickly in the bone marrow following imatinib-mediated eradication of Ph chromosome-positive leukemic cells. The time to the onset of a major cytogenetic response ranged from 2.4 to 19 months with once-daily imatinib administration. The median time to a complete hematologic response was 0.7 months [11]. On the other hand, previous reports of experiments with a murine bone marrow transduction and transplantation (BTT) model of CML indicated that imatinib induced hematologic responses and prolonged the lives of mice that received BCR/ABL-transfected bone marrow [12-14]. However, approximately 20% to 25% of the mice did not respond adequately to imatinib, and none of the imatinib-treated mice were cured of the CML-like MPD [12]. Because the human and murine models of CML have a heterogeneous phenotypic pattern, a longer period of administration may be needed for mice in the BTT model to confirm the efficacy on the peripheral blood of mice that showed no response. This is because some BTT models of CML that have responded to imatinib required 8 to 10 weeks to reach a maximal response.

Imatinib administered orally to Tg mice led to decreased levels of infiltrating cells with high BCR/ABL expression in the enlarged spleen. In particular, megakaryocytosis and granulocytosis in the spleen were clearly improved. Imatinib administration also changed the clone from cells with high BCR/ABL expression to cells with low BCR/ABL expression. This report is the first to show the effectiveness of imatinib on the P230 BCR/ABL oncoprotein and on Tg mice expressing P230 BCR/ABL cDNA.

References

1. Quackenbush RC, Reuther GW, Miller JP, Courtney KD, Pear WS, Pendergast AM. Analysis of the biologic properties of p230 Bcr-Abl reveals unique and overlapping properties with the oncogenic p185 and p210 Bcr-Abl tyrosine kinases. *Blood*. 2000;95:2913-2921.
2. Druker BJ, Tamura S, Buchdunger E, et al. Effects of a selective inhibitor of the Abl tyrosine kinase on the growth of Bcr-Abl positive cells. *Nat Med*. 1996;2:561-566.
3. le Coutre P, Mologni L, Cleris L, et al. In vivo eradication of human BCR/ABL-positive leukemia cells with an ABL kinase inhibitor. *J Natl Cancer Inst*. 1999;91:163-168.
4. Druker BJ, Talpaz M, Resta DJ, et al. Efficacy and safety of a specific inhibitor of the BCR-ABL tyrosine kinase in chronic myeloid leukemia. *N Engl J Med*. 2001;344:1031-1037.
5. Inokuchi K, Dan K, Takatori M, et al. Myeloproliferative disease in transgenic mice expressing P230 Bcr/Abl: longer disease latency, thrombocytosis, and mild leukocytosis. *Blood*. 2003;102:320-323.
6. Li S, Ilaria RL Jr, Million RP, Daley GQ, Van Etten RA. The P190, P210, and P230 forms of the BCR/ABL oncogene induce a similar chronic myeloid leukemia-like syndrome in mice but have different lymphoid leukemogenic activity. *J Exp Med*. 1999;189:1399-1412.
7. Cambier N, Chopra R, Strasser A, Metcalf D, Elefanti AG. BCR-ABL activates pathways mediating cytokine independence and protection against apoptosis in murine hematopoietic cells in a dose-dependent manner. *Oncogene*. 1998;16:335-348.
8. Calvi LM, Adams GB, Weibrecht KW, et al. Osteoblastic cells regulate the haematopoietic stem cell niche. *Nature*. 2003;425:841-846.
9. Zhang J, Niu C, Ye L, et al. Identification of the haematopoietic stem cell niche and control of the niche size. *Nature*. 2003;425:836-841.
10. Taichman RS. Blood and bone: two tissues whose fates are intertwined to create the hematopoietic stem-cell niche. *Blood*. 2005;105:2631-2639.
11. Kantarjian H, Sawyers C, Hochhaus A, et al. Hematologic and cytogenetic responses to imatinib mesylate in chronic myelogenous leukemia. *N Engl J Med*. 2002;346:645-652.
12. Wolff NC, Ilaria RL Jr. Establishment of a murine model for therapy-treated chronic myelogenous leukemia using the tyrosine kinase inhibitor STI571. *Blood*. 2001;98:2808-2816.
13. Ren R. The molecular mechanism of chronic myelogenous leukemia and its therapeutic implications: studies in a murine model. *Oncogene*. 2002;21:8629-8642.
14. Ilaria RL Jr. Animal models of chronic myelogenous leukemia. *Hematol Oncol Clin North Am*. 2004;18:525-543, vii.

ORIGINAL ARTICLE

Importance of *c-kit* mutation detection method sensitivity in prognostic analyses of t(8;21)(q22;q22) acute myeloid leukemia

S Wakita^{1,3}, H Yamaguchi^{1,3}, K Miyake², Y Mitamura¹, F Kosaka¹, K Dan¹ and K Inokuchi¹

¹Division of Hematology, Department of Internal Medicine, Nippon Medical School, Tokyo, Japan and ²Division of Gene Therapy Research Center for Advanced Medical Technology, Department of Biochemistry and Molecular Biology, Nippon Medical School, Tokyo, Japan

Recently, *c-kit* mutations have been reported as a novel adverse prognostic factor of acute myeloid leukemia with t(8;21)(q22;q22) translocation (t(8;21) AML). However, much remains unclear about its clinical significance. In this study, we developed a highly sensitive mutation detection method known as mutation-biased PCR (MB-PCR) and investigated the relationship between *c-kit* mutations and prognosis. When *c-kit* mutations were analyzed for 26 cases of t(8;21) AML using the direct sequence (DS) and MB-PCR, the latter had a much higher detection rate of *c-kit* mutations at initial presentation (DS 5/26(19.2%) vs MB-PCR 12/26(46.2%)). Interestingly for the three cases, in which *c-kit* mutations were observed only at relapse with the DS, *c-kit* mutations were detected at initial presentation using the MB-PCR. This result suggests that a minor leukemia clone with *c-kit* mutations have resistance to treatment and are involved in relapse. In univariate analyses, the presence of a *c-kit* mutation using DS was not an adverse prognostic factor ($P=0.355$), but was a factor when using MB-PCR ($P=0.014$). The presence of *c-kit* mutations with MB-PCR was also an independent adverse prognostic factor by multivariate analyses ($P=0.006$). We conclude that sensitivity of *c-kit* mutation detection method is important to predict prognosis for t(8;21) AML.

Leukemia (2011) 25, 1423–1432; doi:10.1038/leu.2011.104; published online 24 May 2011

Keywords: t(8;21) AML; *c-kit*; mutation; *FLT3ITD*; prognosis; sensitivity

Introduction

Acute myeloid leukemia (AML) has the highest incidence among adult leukemia and includes a variety of subtypes with varying pathology, responsiveness to treatment and prognoses.^{1,2} AML with the t(8;21)(q22;q22) translocation (t(8;21) AML), constitutes about 10% of all AMLs and has been considered an AML group with favorable prognosis based on its positive responsiveness to chemotherapy and high rate of complete remission.^{3–5} Many studies have reported that when high-dose Ara-C is used as post-remission therapy for t(8;21) AML, prognosis is good with overall disease-free survival rates of 50–70%.^{6–11}

However, although t(8;21) AML has good prognosis overall, about 40% of cases relapse, of which half become treatment resistant. In fact, reports suggest that the prognosis of t(8;21) AML following first relapse is just as poor as other relapsed

AMLs even when stem cell transplantation (SCT) is performed.^{12–15} Stratifying prognoses for t(8;21) AML become critical when determining, for example, SCT indications during the initial remission period. The white blood cell (WBC) count at initial examination,¹² WBC index,^{16,17} additional chromosomal aberrations such as del(9)¹⁸ and loss of sex chromosomes and CD56 positivity¹⁹ have been reported as adverse prognostic factors of t(8;21) AML. In recent years, *c-kit* mutations have also been proposed as a novel marker.^{20,21}

The *c-kit* gene is located on chromosome 4q11–12 and encodes a 145 kD type III receptor tyrosine kinase. It has five extracellular immunoglobulin-like domains, a juxtamembrane domain and an intracellular kinase domain. *c-kit* mutations have been found in gastrointestinal stromal tumors (70% or more), mastocytosis (90% or more) and germ cell tumors (about 10%).^{22,23} In addition, they have been reported in ~12–25% of cases of core-binding factor (CBF)–AMLs such as inv(16)(p13q22) and t(8;21) AML.²⁴ Normal *c-kit* sends proliferative cues into cells following stimulation by its ligand, stem cell factor and has an important role in early hematopoiesis.²⁵ On the other hand, mutant *c-kit* send proliferative signals into cells in a ligand-independent manner, and are considered class I aberrations, which have a role in leukemic cell proliferation.²⁶ In recent years, it has been reported that CBF–AML cases with *c-kit* mutations show a high rate of relapse and poor prognosis.^{20,21,27–29} Reflecting these reports, the National Comprehensive Cancer Network's (NCCN) 2009 guidelines considered t(8;21) AML with *c-kit* mutations to be an intermediate prognosis group. However, at present, much remains unclear about the significance of *c-kit* mutations as a prognostic factor for CBF–AML. For example, in inv(16)(p13q22) AML, prognosis of patients with or without mutation in *c-kit* exon 8 is not significantly different.²¹ Recently it is also reported that prognosis of pediatric CBF–AML patients with or without *c-kit* mutations is not significantly different.³⁰

The sensitivity of the detection method may be one reason why *c-kit* mutations remain an unclear prognostic factor for t(8;21) AML. A large majority of t(8;21) AML cases is classified as M2 by the French–American–British (FAB) Classification. Depending on the case, the proportion of leukemic cells may be less than 50%. In addition, nearly all *c-kit* mutations are heterozygous. It is possible that leukemic cells with *c-kit* mutations are quantitatively small populations at initial presentation and hence, not detectable with the direct sequence (DS) method. If the minor leukemic cells with *c-kit* mutations at initial presentation become treatment resistant and are involved in relapse, then a highly sensitive method to detect *c-kit* mutations is necessary in order to clarify the significance of *c-kit* mutations as a prognostic factor. Therefore, we used a highly sensitive mutation detection method known as mutation-biased

Correspondence: Dr H Yamaguchi, Division of Hematology, Department of Internal Medicine, Nippon Medical School, 1-1-5 Sendagi, Bunkyo-Ku, Tokyo 113-8603, Japan.

E-mail: y-hiroki@fd6.so-net.ne.jp

³These authors contributed equally to this work.

Received 6 August 2010; revised 28 February 2011; accepted 18 March 2011; published online 24 May 2011

PCR (MB-PCR) to detect *c-kit* mutations and investigated their significance as a prognostic factor for t(8;21) AML.

Patients and methods

Patient samples

We retrospectively analyzed 26 cases of t(8;21) AML treated at the Nippon Medical School and its affiliated facilities between January 1991 and January 2009. A search for *c-kit* mutations and *Fms-like tyrosine kinase 3 internal tandem duplications* (*Flt3 ITD*) was carried out on 26 initial diagnosis and 15 relapse cases where bone marrow or peripheral blood samples, in which 30% or more of the blast cells were available for use. Informed consents were obtained from the patients for genetic testing. This protocol was approved by our institutional review board.

Mutation analysis for *c-kit* and *Flt3 ITD*

Mononuclear cells from bone marrow or peripheral blood were isolated by density gradient centrifugation using lymphocyte separation medium (Organon, Durham, NC, USA). Genomic DNA of mononuclear cells was extracted with the QIAamp DNA Mini Kit (Qiagen, Hilden, Germany). PCR amplification of *c-kit* and *Flt3 ITD* was performed as previously described.^{31,32} Mutational analysis of the extracellular domain (exons 8 and 9), transmembrane domain (exon 10), juxtamembrane domain (exon 11) and the second intracellular kinase (TK) 2 domain (exons 17 and 18) of the *c-kit* gene was carried out with PCR followed by direct sequencing. Specific sequences of primers used for PCR and sequencing are available on request. To validate sequencing results, PCR products were inserted into the pCR2.1-TOPO vector using a TOPO TA cloning kit (Invitrogen, Carlsbad, CA, USA). Recombinant plasmids isolated from 8 to 12 white colonies were sequenced.

MB-PCR for *c-kit* mutations using QProbe

Quenching probe (QProbe) is a fluorescent probe in that a fluorescent substance is bound to cytosine on the terminal portion of the probe, which becomes quenched on hybridization with a complementary strand. With increasing temperature, the duplex unravels at a temperature (T_m) related to the strength of the bond between the QProbe and the complementary chain, at which point the fluorescence intensity recovers. T_m analysis is a technique to determine the degree of complementation between the QProbe and target nucleic acid by measuring the change in fluorescence intensity with increasing temperature.^{33,34} Here, we detected *c-kit* mutations using the QProbe method and a prototype of i-densy, a fully automated single nucleotide polymorphism genotyping systems.³⁴ Amplification was performed with MB-PCR for high-sensitivity detection of mutations using probes that perfectly matched the mutated form. In MB-PCR, the 3' terminal region of the primer is established as the mutation site, and allele-specific primers for wild-type and mutant primers are used for amplification. By adjusting the length of the primer, we devised a means by which the mutant form could be amplified more than the wild-type form. Furthermore, given the correlation between the proportion of the mutant form and the value of the fluorescence intensity detected by QProbe, it is possible to semiquantify the amount of mutations.

For sensitivity analysis, normal cells and clinical samples with heterozygous mutations were mixed and detection sensitivity was assessed. The ratio of each mutation was controlled by

adjusting the ratio of blast cells from the clinical samples. Detection sensitivity was also assessed using a mixture of DNA from a normal subject and *c-kit* mutations containing fragment generated by PCR and TA cloning from clinical samples.

Statistical analysis

Patient characteristics were compared using Chi-square, Fisher and *t* tests. In addition, we analyzed the cumulative incidence of relapse (CIR) using the Kaplan–Meier log-rank test. Prognostic factors for t(8;21) AML were analyzed with multivariate analyses using Cox proportional hazards. In order to extract independent events, those events with a *P*-value of 0.20 or less were analyzed using the backward stepwise model selection procedure. Statistical analyses were carried out using SPSS software (version 12.1.4; SPSS Inc., Chicago, IL, USA).

Results

Clinical characteristics of patients with t(8;21) AML

The clinical characteristics of patients are shown in Table 1. The median age was 50.3 years (range, 31–72 years) with 69.2% being males. Patients were followed-up for 3–112 months after initial presentation, with a median of 34.5 months. Of the 26 total t(8;21) AML cases, 15 (57.7%) relapsed.

Behenoyl cytosine arabinoside (BHAC)-DM-based, DNR/Ara-C and IDA/Ara-C regimens were used as induction therapies for 16, 7 and 3 cases, respectively. BHAC-DM-based regimen was a response-oriented individualized chemotherapy regimen using BHAC, dounorbicin (DNR) and 6-mercaptopurine (6-MP).^{35–38} All patients obtained complete remission by induction therapies. For post-remission consolidation, BHAC-based and HDAC-based regimens were administered in 14 and 12 cases, respectively. As t(8;21) AML was considered to have favorable prognosis, SCT was not given in any of the cases during the first remission period.

Evaluation of post-remission course revealed a range of 1–64 months until first relapse (median 16 months) and CIR of 45.2% at 1 year and 58.6% at 6 years. We further analyzed the impact of post-remission therapy, WBC counts at initial examination, WBC index and CD56 expression on relapse. However, post-remission therapies, initial WBC counts, WBC index and CD56 expression were not significantly associated with relapse, and therefore, remain of unclear prognostic significance. Specifically, BHAC-based regimen had CIR of 31.9% at 1 year and 48.9% at 6 years, whereas HDAC-based regimen resulted in CIR of 58.3% at 1 year and 66.7% at 6 years ($P=0.384$). When initial WBC counts were equal to or greater than 20 000/ μ l, CIR was 60.0% at 1 year and 80.0% at 6 years. When initial WBC counts were less than 20 000/ μ l, CIR was 36.2% at 1 year and 48.4% at 6 years ($P=0.4343$). WBC index were equal to or greater than 20, CIR was 43.2% at 1 year and 54.1% at 6 years. When WBC index were less than 20, CIR was 33.3% at 1 year and 66.7% at 6 years ($P=0.7569$). CD56 expression less than 10% was associated with CIR of 25.0% at 1 year and 52.4% at 6 years, whereas CD56 expression greater or equal to 10% resulted in CIR of 57.7% at 1 years and 66.2% at 6 years ($P=0.083$).

Comparison of chromosome analysis at initial presentation and at relapse

There were 14/26 cases (53.8%), in which a chromosomal aberration other than t(8;21)(q22;q22) was observed at initial presentation (Table 2). Among these, the most frequent was the

Table 1 Clinical and molecular characteristics of t(8;21)AML patients

Characteristics	Total		MB-PCR method	
	t(8;21)AML n = 26	Wild type n = 14	c-kit mutation(+) n = 12	P
			(D816V: 4, N822K: 8)	
Male/female	18/8	10/4	8/4	0.673
Age (years)				
Median (range)	50.3 (31–72)	50.2 (31–72)	50.4 (33–67)	1.000
<60	22	12	10	
≥60	4	2	2	
PS ≥2	1	1	0	
WBC (/μl)				
Median (range)	12858 (1400–42800)	12962 (1400–42800)	12745 (3900–29900)	0.928
<20 000	21	11	10	
≥20 000	5	3	2	
Hemoglobin (g/dl)				
Median (range)	7.48 (3.2–12.5)	6.73 (3.2–10.1)	8.36 (4.2–12.5)	0.148
≥10	21	13	8	
<10	5	1	4	
Platelet ($\times 10^4/\mu\text{l}$)				
Median (range)	2.26 (0.7–8.5)	2.43 (0.7–8.5)	2.08 (0.4–5.8)	0.654
% PB blast	49.8 (10.0–93.5)	58.7 (15.5–92.0)	48.2 (10.0–93.5)	0.770
Median (range)				
% BM blast	64.5 (30.4–95.0)	65.3 (37.6–95.0)	63.5 (30.4–90.0)	0.832
Median (range)				
WBC index				
Median (range)	70.6 (9.8–296.2)	67.4 (9.8–296.2)	74.8 (19.1–163.8)	0.792
<20	3	2	1	
≥20	23	12	11	
Extramedullary involvement	—	—	—	
CD56+				
<10%	13	9	4	0.238
≥10%	13	5	8	
Flt3 ITD				
Negative	24	13	11	
Positive	2	1	1	
Relapse rate (%)	57.7%	35.7%	83.3%	0.021
CIR				
Median	18 months	Not reached	11 months	0.014
% CIR at 1 year	45.2%	22.1%	72.5%	
% CIR at 6 years	58.6%	34.4%	81.7%	

Abbreviations: AML, acute myeloid leukemia; CIR, cumulative incidence of relapse; WBC, white blood cell.

loss of a sex chromosome, which was observed in 12 cases (46.2%) (–Y: 11 cases, –X: 1 case) (Table 2).

Of 15 relapsed cases, three were unacceptable for chromosomal analyses. Additional chromosomal aberrations were observed at relapse in 10/12 cases (83.3%), which was higher relative to the rate at initial presentation. New chromosomal aberrations were observed in 9/12 cases (75%). Furthermore, most of these cases were observed with two or more chromosomal aberrations in addition to t(8;21)(q22;q22). This suggests greater chromosomal instability at relapse compared with initial presentation. However, prognostic analyses did not show a significantly higher relapse rate (RR) for cases with additional chromosomal aberrations at initial examination

($P=0.400$). Specifically, cases with additional chromosomal aberrations at initial examination had CIR of 30.4% at 1 year and 53.6% at 6 years, whereas those without additional chromosomal aberrations at initial examination had CIR of 63.3% at 1 year and 6 years.

c-kit mutations detected by direct sequence analysis

We screened for *c-kit* mutations using DS on 26 initial presentation cases and 13 relapsed cases with t(8;21) AML, other two relapsed cases were not available for analysis. In initial presentation subject samples, mutations were observed in 5/26 cases (19.2%; three cases of D816V and two cases of

Table 2 Chromosomal aberrations, direct sequence and MB-PCR analysis of *c-kit* gene at initial presentation and relapse

	%Blast	Chromosome analysis	Direct sequence	MB-PCR
<i>At initial presentation</i>				
1	67.4%	46,XY,t(8;21)(q22;q22)	D816V	D816V
2	57.8%	45,X-Y,t(8;21)(q22;q22)	D816V	D816V
3	66.8%	46,XX,t(8;21)(q22;q22)	D816V	D816V
4	46.5%	46,XY,t(8;21)(q22;q22)	Wild	D816V
5	55.0%	46,XY,t(8;21)(q22;q22)	Wild	N822K
6	67.6%	45,X-Y,t(8;21)(q22;q22)	N822K	N822K
7	48.8%	45,X-Y,t(8;21)(q22;q22)	N822K	N822K
8	48.4%	46,XX,t(8;21)(q22;q22)	Wild	N822K
9	30.4%	46,XY,t(8;21)(q22;q22)	M541 L	N822K
10	80.0%	46,XX,t(1;13;21;8)(q21;q14;q22;q22)	Wild	N822K
11	90.0%	46,XX,t(8;21)(q22;q22)	M541 L, K546 K, L862 L	N822K
12	32.4%	45,X-Y,t(8;21)(q22;q22)	Wild	No signal
13	69.2%	45,X-Y,t(8;21)(q22;q22)	Wild	No signal
14	49.6%	45,X-Y,t(8;21)(q22;q22)	Wild	No signal
15	37.6%	45,X-Y,t(8;21)(q22;q22)	Wild	No signal
16	63.2%	46,XY,t(8;21)(q22;q22)	M541 L	No signal
17	90.0%	46,XY,t(8;21)(q22;q22)	Wild	N822K
18	62.8%	45,X-Y,t(8;21)(q22;q22)	Wild	No signal
19	54.8%	45,X-Y,t(8;21)(q22;q22)	Wild	No signal
20	95.0%	45,X-Y,t(8;21)(q22;q22)	Wild	No signal
21	44.2%	45,X-Y,t(8;21)(q22;q22)	Wild	No signal
22	70.0%	46,XX,t(8;21)(q22;q22)	Wild	No signal
23	95.0%	46,XX,t(8;21)(q22;q22)	Wild	No signal
24	79.8%	46,XY,t(8;21)(q22;q22)	Wild	No signal
25	62.6%	46,XX,t(8;13;21)(q22;q14;q22)	Wild	No signal
26	55.1%	45,X-Y,t(8;21)(q22;q22)	Wild	No signal
<i>At relapse</i>				
1	75.4%	46,XY,t(8;21)(q22;q22),t(1;2)(q42;q21)	D816V	D816V
2	82.4%	45,X-Y,t(8;21)(q22;q22),t(1;13)(p36;q14),del(11)(q23) 45,X-Y,t(8;21)(q22;q22),add(7)(q22)	D816V	D816V
3	42.0%	not acceptable	D816V	D816V
4	91.5%	45,X-Y,t(8;21)(q22;q22),t(1;22)(q21;q13) 45,X-Y,t(8;21)(q22;q22),add(2)(q33)	D816V	D816V
5	91.8%	45,X-Y,der(2)del(2)(p21)del(2)(q33),der(8)t(8;21)(q22;q22)t(8;14)(q22;q13),add(9)(p22),add(10)(q22),add(11)(q23),der(14)t(8;21)t(8;14),add(15)(q11),add(20)(q13),der(21)t(8;21)	D816V	D816V
6		Continuous first remission		
7	55.6%	45,X-Y,t(8;21)(q22;q22),add(2)(q21)	N822K	N822K
8	87.5%	46,XX,t(8;21)(q22;q22)	N822K	N822K
9	74.7%	46,XY,6q-,7q+, -11,t(8;21)(q22;q22),+mar	M541 L	No signal
10	42.2%	46,XX,t(1;13;21;8)(q21;q14;q22;q22)	Wild	No signal
11	55.0%	46,XX,t(8;21)(q22;q22)	M541 L, K546 K, L862 L	No signal
12	30.2%	Not acceptable	Wild	No signal
13	70.2%	45,X-Y,t(8;21)(q22;q22),12q-	Not acceptable	Not acceptable
14	30.0%	45,X-X,t(6;10)(q15;p13),t(8;21)(q22;q22) 45,X-X,t(8;21)(q22;q22),add(16)(q24)	Wild	No signal
15	8.0%	Not acceptable	Not acceptable	Not acceptable
16	35.2%	45,X-Y,t(8;21)(q22;q22),t(11;12)(p13;q24.3) 45,X-Y,t(8;21)(q22;q22),t(9;12)(q22;q13),t(11;12)(p13;q24.3)	M541 L	No signal
17		Drop out		
18		Continuous first remission		
19		Continuous first remission		
20		Continuous first remission		
21		Continuous first remission		
22		Continuous first remission		
23		Continuous first remission		
24		Continuous first remission		
25		Continuous first remission		
26		Continuous first remission		

N822K). In relapsed subject samples, mutations were observed in 7/15 cases (46.7%; five cases of D816V and two cases of N822K, two cases were not acceptable). All *c-kit* mutations localized to the A-loop of exon 17. Intriguingly, of the relapsed cases with *c-kit* mutations, three cases (two cases of D816V and one case of N822K) were not detected *c-kit* mutation at initial

presentation. Sequences of the detected *c-kit* mutations were D816V (GAT→GTC) and N822K (AAT→AAG). In addition to the above-mentioned mutations, we observed three cases of M541L (ATG→CTG; 11.5%), one case of K546K (AAA→AAG; 3.8%), and one case of L862L (CTG→CTC; 3.8%) as genetic polymorphisms (Table 2).

Establishment of a highly sensitive *c-kit* mutation detection method with MB-PCR

There were three cases, in which *c-kit* mutations were observed only at relapse using DS. For this reason, we surmised that minor

clone of leukemic cells with *c-kit* mutations at initial presentation had resistance to treatment and became involved in relapse. To prove this hypothesis, we established a highly sensitive method for detecting these *c-kit* mutations called MB-PCR. The

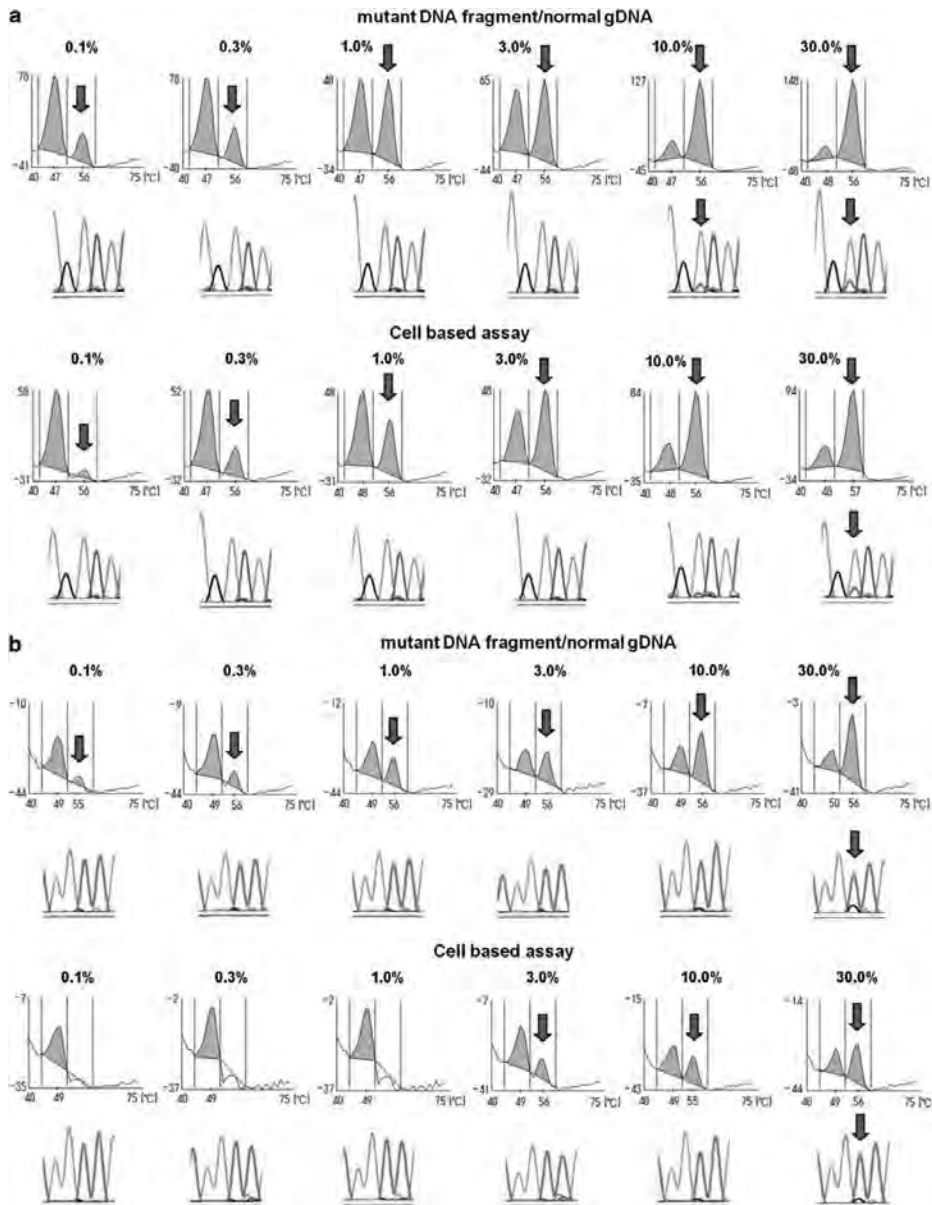


Figure 1 Comparison of detection sensitivities for *c-kit* exon 17 mutations. (a) Detection sensitivity for the D816V mutation. (b) Detection sensitivity for the N822K mutation. In (a) and (b), the upper panel shows the sensitivity analysis using a mixture of a mutated fragment and DNA from a normal subject. The lower panel shows sensitivity analysis using a mixed sample containing cells harboring mutations and normal cells. Sensitivity analysis was conducted using samples corresponding to 0.1, 0.3, 1, 3, 10 and 30% dilutions. The upper row in each panel shows results from MB-PCR. In contrast to wild-type *c-kit*, for which the complementary strand and QProbe separate at T_m values of 42–52 °C (D816V region) and 44–52 °C (N822K region), separation is observed at T_m values of 52–60 °C and 52–61 °C, respectively, for D816V and N822K mutations. The lower row of each panel shows results from the DS method. Arrows indicate waves of mutations.

sensitivity of detecting mutations using this method was tested by mixing cells containing D816V or N822K mutations with normal cells, which showed detection sensitivities of around 0.1% for D816V and 3.0% for N822K. Sensitivity analysis with a D816V- and N822K-containing fragment mixed with DNA from normal subjects produced a detection sensitivity of around 0.1% for both D816V and N822K. In contrast, the same sample subjected to the DS method resulted in a detection sensitivity of 10–30% for D816V and 30% for N822K. These results suggest that compared with the DS method, MB-PCR can detect mutations with much higher sensitivity (Figure 1).

Screening for c-kit mutations using highly sensitive mutation detection methods

When *c-kit* mutations of D816V and N822K were screened using MB-PCR, 12/26 of initial presentation samples were positive (46.2%; 4 cases of D816V and 8 cases of N822K). In 15 of relapse samples, two of them were not available for analyses, and seven of them were detected *c-kit* mutations (46.7%; five cases of D816V and two cases of N822K). In other words, MB-PCR offered a higher detection rate for *c-kit* mutations at initial presentation samples compared with DS.

MB-PCR was able to detect *c-kit* mutations at initial presentation or early stage for the three cases, in which *c-kit* mutations were observed only at relapse using DS. MB-PCR could detect *c-kit* mutations at initial presentation of case number 4 and 8, as well as at the first relapse of case number 5, for which *c-kit* mutations could not be detected using DS (Figure 2).

Although less prevalent than the D816V and N822K mutations, there has been reports of small deletion-type mutation in the T417–D419 region of exon 8 in *c-kit* (i.e., del419, del418–419 and Thr417Ile/del418–419). In order to analyze this exon 8 mutation, we generated a QProbe (QProbe^{T417–D419}) directed at the wild-type sequence. However, the T417–D419 deletion could not be detected in first presentation and relapsed t(8;21) AML samples.

Clinical significance of c-kit D816V and N822K mutations

The clinical progression of the 11 cases with detected *c-kit* mutations are shown in Figure 3 (one case was not included due to a short observation period). Five cases with the D816V observed at initial presentation using the MB-PCR method all eventually relapsed, and at relapse D816V remained positive in

all cases (Figure 3). For cases number 4 and 5 in particular, a low number of leukemic cells had D816V at initial presentation, which apparently became treatment resistant and amplified in subsequent relapse. Of the seven cases with N822K at initial presentation, six cases (86%) relapsed. Among these, however, N822K was observed in only two cases (33.3%) at relapse (Figure 3).

Significance of c-kit mutation as a prognostic factor in t(8;21) AML

Using DS and MB-PCR, we examined whether initial possession of a *c-kit* mutation has prognostic significance given the above MB-PCR results. No significant differences were found in clinical characteristics of case samples analyzed by both methods between those with or without *c-kit* mutations (Table 1 and Supplementary Table 1). By DS, there was a tendency for high RRs in the *c-kit* mutation (+) group, but this was not statistically significant (Figure 4a). Specifically, the *c-kit* mutation (+) group had a RR of 80.0% and CIR of 60.0% at 1 year and 80.0% at 6 years, while the *c-kit* mutation (–) group had a RR of 52.4% and CIR of 35.7% at 1 year and 52.8% at 6 years ($P=0.355$). However, with MB-PCR, the *c-kit* mutation (+) group had a statistically significant higher RR (Figure 4b). Specifically, the *c-kit* mutation (+) group had a RR of 83.3% and CIR of 72.5% at 1 year and 81.7% at 6 years, whereas the *c-kit* mutation (–) group had a RR of 35.7% and CIR of 22.1% at 1 year and 34.4% at 6 years ($P=0.014$).

Significance of c-kit mutation and Flt3ITD as a prognostic factor in t(8;21) AML

Flt3 ITD is observed in about 25% of all AMLs and is one of the gene mutations considered to be an adverse prognostic factor. However, among the 26 cases of t(8;21) AML examined, *Flt3* ITD was observed in only 2/26 (7.7%) cases at initial presentation, which is a lower incidence relative to *c-kit* mutations. In one case, *Flt3* ITD and *c-kit* mutations were observed simultaneously. All patients with *Flt3* ITD demonstrated relapse after short remission period. Considering the *Flt3* ITD (+) cases and/or MB-PCR *c-kit* mutation (+) cases together as the mutation (+) group, its relapse rate was shown to be significantly higher compared with those lacking both mutations (mutation (–) group: RR 30.8%, 1 year CIR 15.4%, 6 year CIR 34.2% versus mutation (+) group: RR 84.6%, 1 year CIR 74.8%, 6 year CIR 83.2%, $P=0.005$) (Figure 4c).

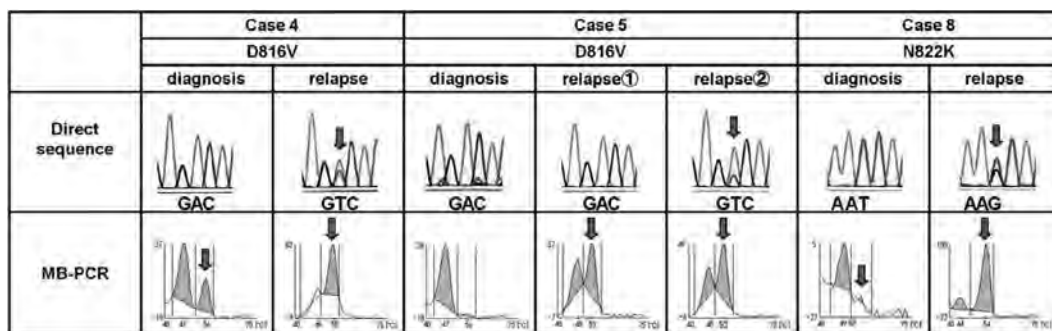


Figure 2 Detection of *c-kit* mutations with MB-PCR but not DS. The top and bottom panels, respectively, show results of the DS method and MB-PCR. For cases 4 and 8 at diagnosis and case 5 at first relapse, *c-kit* mutations were detected with MB-PCR but not with DS. Arrows indicate waves of mutations.

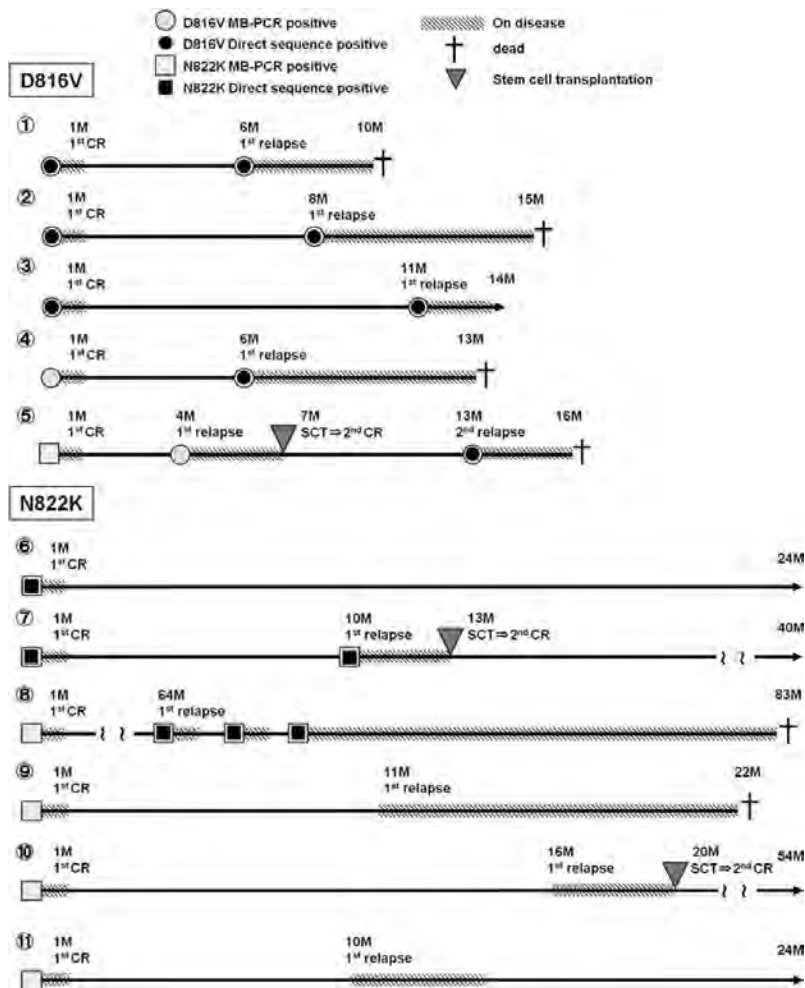


Figure 3 Clinical courses of patients with *c-kit* mutations D816V and N822K. The top panel shows five cases, in which the D816V mutation was observed; the bottom panel shows six cases, in which the N822K mutation was observed. For cases 4 and 5 of D816V and case 8 of N822K, mutations were detected with MB-PCR at an earlier time point than with the DS method. All five cases with detected D816V relapsed, at which time the mutation could be detected even with the DS method. In contrast, among the six cases for which N822K was detected, long-term remission was obtained in one case with chemotherapy alone (number 6). For three cases (number 9, 10 and 11), the N822K mutation was detected at initial presentation but not at relapse. CR, complete remission; M, month; SCT, stem cell transplantation.

Multivariate analyses

We carried out multivariate analyses with the backward stepwise model selection procedure on age (≥ 60 or < 60 years old), gender (male or female), additional chromosomal aberrations (yes or no), WBC count at initial examination ($\geq 20,000/\mu\text{l}$ or $< 20,000/\mu\text{l}$), hemoglobin ($\geq 10.0\text{g/dl}$ or $< 10.0\text{g/dl}$), and post-remission therapy (BHAC-based or HDAC-based) in order to establish the significance of *c-kit* mutations as prognostic factors for relapse of t(8;21)AML.

As a result, *c-kit* mutations and hemoglobin level at initial presentation were extracted as independent events by the backward stepwise model selection. Multivariate analyses with Cox proportional hazards revealed that MB-PCR detection of *c-kit* mutations (hazard ratio 5.074, $P=0.006$, 95%CI:

1.609–16.003) and *c-kit* mutation and/or *Flt3* ITD (hazard ratio 6.650, $P=0.003$, 95%CI: 1.948–22.695) were independent adverse prognostic factors. On the other hand, multivariate analyses revealed that hemoglobin level at initial presentation were not independent adverse prognostic factors ($P=0.11$).

Discussion

We present MB-PCR as a highly sensitive method for detecting gene mutations and showed that cases for which *c-kit* mutations were observed only at relapse using DS actually already harbored those mutations at initial presentation at a low level undetectable by DS. In this investigation, although we did not

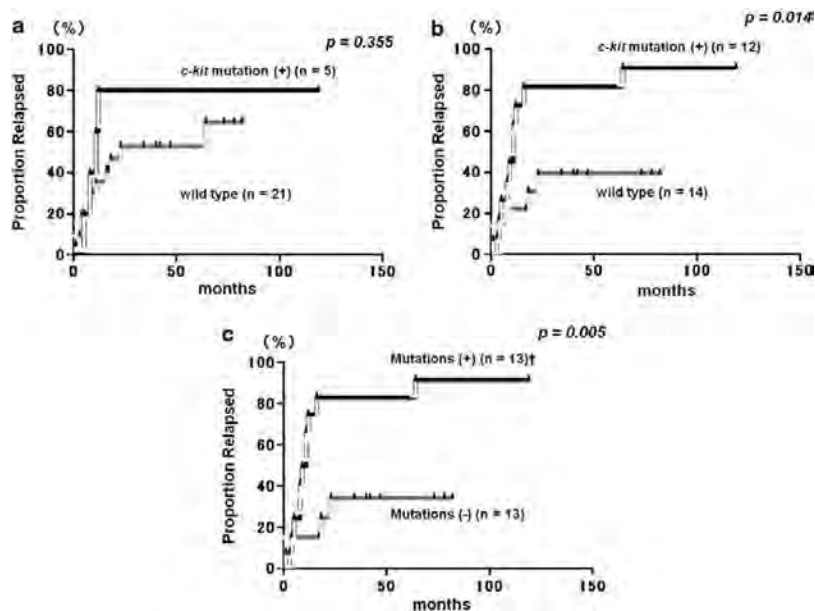


Figure 4 Relationship between presence of *c-kit* mutations and relapse. (a) Relationship between the presence of *c-kit* mutations and relapse with the DS method; (b) Relationship between the presence of *c-kit* mutations and relapse with the MB-PCR method; (c) Relationship between the presence of *c-kit* mutations with the MB-PCR method and *FLT3* ITD, and relapse. †: *c-kit* mutation (n = 11), *FLT3* ITD (n = 1), double positive (n = 1).

observe significant differences in relapse rates between cases with and without *c-kit* mutations using the DS method, we did observe a significant difference between cases with and without *c-kit* mutations using MB-PCR (Figures 4a and b). From the above, we conclude that high sensitive method of detecting *c-kit* mutation, such as MB-PCR method, is important to predict prognosis for t(8;21) AML.

These results suggest that a minor leukemia clone with *c-kit* mutation at initial presentation has resistance to treatment and becomes involved in relapse. There have been several recent reports of the role of leukemic stem cells in relapse of leukemia.^{39–44} The rare *c-kit* mutation-harboring leukemic cells at initial presentation thought to be involved in relapse may represent leukemic stem cells with *c-kit* mutations. In the future, we plan to analyze *c-kit* mutations in leukemic stem cell fractions using MB-PCR.

Aberrant *c-kit* in t(8;21) AML has been reported in the extracellular domain of exon 8, the juxtamembrane domain of exons 10 and 11, and the A-loop domain with tyrosine kinase activity of exon 17. Some previous *in vitro* studies report that the D816V mutation confers higher tumor growth and antiapoptotic potential compared with mutations in the extracellular domain of exon 8 or in the juxtamembrane domains of exons 10 and 11.^{45,46} Similar observations have been reported for *FLT3* mutations, which are class I mutations as found in *c-kit*. Specifically, mutations in the *FLT3* tyrosine kinase domain (TKD) confer lower tumor growth and antiapoptotic potential compared with *FLT3* ITD.^{47,48} These findings suggest that biological functions of *c-kit* mutations differ depending on the mutation site, which may affect responsiveness to treatments. In our study, we did not observe any mutations apart from D816V and N822K in the exon 17 A-loop. However, all cases with D816V at initial presentation eventually relapsed while preserving the D816V

mutation. In contrast, only one of three cases with N822K at initial presentation were detected N822K at relapse. This result suggests that D816V and N822K may differ functionally, even if this mutation is also in the same A-loop. Thus, we believe that functional analysis of both mutations will be necessary.

Although rare, mutations other than D816V, N822K, and the small T417-D419 deletion have been reported for t(8;21) AML. However, we detected no mutations other than D816V and N822K by screening exons 8–11, 17 and 18 using the both MB-PCR and DS method in relapse samples. On the basis of this, we conclude that at least for the cases examined in our study, *c-kit* mutations other than D816V and N822K were not major for relapse. In the future, we hope to investigate more cases and determine the clinical significance of rare *c-kit* mutations.^{20,27,49}

This investigation showed that aberrant *c-kit* at initial presentation in t(8;21)AML is associated with a significantly higher rate of relapse and shorter period of first remission. However, aberrations of unknown gene are involved in t(8;21) AML based on the following observations: a class I aberration must additionally occur in chimeric protein AML1-ETO for t(8;21)AML mouse model onset,^{50,51} *c-kit* mutations and *FLT3* ITD are not observed in about 50% of t(8;21) AML, and there are cases in which the N822K mutation disappeared at relapse. In addition, given report of positive responsiveness to high-dose Ara-C therapy and favorable prognosis of t(8;21) AML with *N-Ras* mutations, which is also a class I mutation,⁵² other class I mutations should also be examined.

Our results do not directly suggest that allogeneic SCT is indicated during the initial remission period for t(8;21) AML with *c-kit* mutations, as is the case with AML groups with poor prognosis. Recent reports have been inconclusive as to whether prognosis of t(8;21) AML after the first relapse is poor, like other relapsed AMLs,¹⁵ or still favorable.⁵³ However, as these results

were not stratified according to *c-kit* mutations, it remains unclear whether allogeneic SCT is indicated during the first remission period for t(8;21) AML with *c-kit* mutations. In addition, we have previously shown the utility of SCT using autologous disease-free peripheral blood stem cells in the first remission period of t(8;21) AML, including cases of *c-kit* mutations at initial presentation.³¹ This result is intriguing because it suggests that autologous peripheral blood stem cells without residual disease are useful against t(8;21) AML with *c-kit* mutations. Taking the above into consideration, future studies should investigate stratification of SCT indications during the first remission period according to genetic mutations such as *c-kit* mutations and *FLT3* ITD for t(8;21) AML, similar to current investigations for normal karyotype AML.

Finally, this is a retrospective study, and the number of patients examined was insufficient to carry out prognostic analysis. A large-scale prospective study is needed to clarify the utility of high-sensitivity analysis of *c-kit* mutations for t(8;21) AML in the clinical setting.

Conflict of interest

The authors declare no conflict of interest.

Acknowledgements

We thank Mitsuharu Hirai, Mariko Komori and ARKRAY, Inc. (Kyoto, Japan) for technical contribution to this work and providing QProbe and prototype of i-densy. SW and HY were the principal investigator and takes primary responsibility for the paper. SW, HY, KD and KI recruited the patients. SW, HY, YM and FK performed the laboratory work for this study. SW, HY, KD, KM and KI analyzed the data and wrote the paper. SW and HY contributed equally this work.

References

- Cheson BD, Cassileth PA, Head DR, Schiffer CA, Bennett JM, Bloomfield CD *et al.* Report of the National Cancer Institute-sponsored workshop on definitions of diagnosis and response in acute myeloid leukemia. *J Clin Oncol* 1990; **8**: 813–819.
- Byrd JC, Mrózek K, Dodge RK, Carroll AJ, Edwards CG, Arthur DC *et al.* Pretreatment cytogenetic abnormalities are predictive of induction success, cumulative incidence of relapse, and overall survival in adult patients with *de novo* acute myeloid leukemia: results from Cancer and Leukemia Group B (CALGB 8461). *Blood* 2002; **100**: 4325–4336.
- Ferrant A, Labopin M, Frasson F, Prentice HG, Cahn JY, Blaise D *et al.* Karyotype in acute myeloblastic leukemia: prognostic significance for bone marrow transplantation in first remission: a European Group for Blood and Marrow Transplantation study. Acute Leukemia Working Party of the European Group for Blood and Marrow Transplantation (EBMT). *Blood* 1997; **90**: 2931–2938.
- Grimwade D, Walker H, Oliver F, Wheatley K, Harrison C, Harrison G *et al.* The importance of diagnostic cytogenetics on outcome in AML: analysis of 1,612 patients entered into the MRC AML 10 trial. The Medical Research Council Adult and Children's Leukaemia Working Parties. *Blood* 1998; **92**: 2322–2333.
- Slovak ML, Kopecky KJ, Cassileth PA, Harrington DH, Theil KS, Mohamed A *et al.* Karyotypic analysis predicts outcome of preremission and postremission therapy in adult acute myeloid leukemia: a Southwest Oncology Group/Eastern Cooperative Oncology Group Study. *Blood* 2000; **96**: 4075–4083.
- Wolff SN, Herzog RH, Fay JW, Phillips GL, Lazarus HM, Flexner JM *et al.* High-dose cytarabine and daunorubicin as consolidation therapy for acute myeloid leukemia in first remission: long-term follow-up and results. *J Clin Oncol* 1989; **7**: 1260–1267.
- Weick JK, Kopecky KJ, Appelbaum FR, Head DR, Kingsbury LL, Balcerzak SP *et al.* A randomized investigation of high-dose versus standard-dose cytosine arabinoside with daunorubicin in patients with previously untreated acute myeloid leukemia: a Southwest Oncology Group study. *Blood* 1996; **88**: 2841–2851.
- Bloomfield CD, Lawrence D, Byrd JC, Carroll A, Pettenati MJ, Tantravahi R *et al.* Frequency of prolonged remission duration after high-dose cytarabine intensification in acute myeloid leukemia varies by cytogenetic subtype. *Cancer Res* 1998; **58**: 4173–4179.
- Schellong G, Pötter R, Brämswig J, Wagner W, Prott FJ, Dörffel W *et al.* High cure rates and reduced long-term toxicity in pediatric Hodgkin's disease: the German-Austrian multicenter trial DAL-HD-90. The German-Austrian Pediatric Hodgkin's Disease Study Group. *J Clin Oncol* 1999; **17**: 3736–3744.
- Brunet S, Esteve J, Berlanga J, Ribera JM, Bueno J, Martí JM *et al.* Treatment of primary acute myeloid leukemia: results of a prospective multicenter trial including high-dose cytarabine or stem cell transplantation as post-remission strategy. *Haematologica* 2004; **89**: 940–949.
- Gorin NC, Labopin M, Frasson F, Milpied N, Attal M, Blaise D *et al.* Identical outcome after autologous or allogeneic genodentical hematopoietic stem-cell transplantation in first remission of acute myelocytic leukemia carrying inversion 16 or t(8;21): a retrospective study from the European Cooperative Group for Blood and Marrow Transplantation. *J Clin Oncol* 2008; **26**: 3183–3188.
- Schlenk RF, Benner A, Krauter J, Büchner T, Sauerland C, Ehninger G *et al.* Individual patient data-based meta-analysis of patients aged 16 to 60 years with core binding factor acute myeloid leukemia: a survey of the German Acute Myeloid Leukemia Intergroup. *J Clin Oncol* 2004; **22**: 3741–3750.
- Marcucci G, Mrózek K, Ruppert AS, Maharry K, Kolitz JE, Moore JO *et al.* Prognostic factors and outcome of core binding factor acute myeloid leukemia patients with t(8;21) differ from those of patients with inv(16): a Cancer and Leukemia Group B study. *J Clin Oncol* 2005; **23**: 5705–5717.
- de Labarthe A, Pautas C, Thomas X, de Botton S, Bordessoule D, Tilly H *et al.* Allogeneic stem cell transplantation in second rather than first complete remission in selected patients with good-risk acute myeloid leukemia. *Bone Marrow Transplant* 2005; **35**: 767–773.
- Appelbaum FR, Kopecky KJ, Tallman MS, Slovak ML, Gundacker HM, Kim HT *et al.* The clinical spectrum of adult acute myeloid leukaemia associated with core binding factor translocations. *Br J Haematol* 2006; **135**: 165–173.
- Cairolì R, Grillo G, Beghini A, Tedeschi A, Ripamonti CB, Larizza L *et al.* C-Kit point mutations in core binding factor leukemias: correlation with white blood cell count and the white blood cell index. *Leukemia* 2003; **17**: 471–472.
- Nguyen S, Leblanc T, Fenaux P, Witz F, Blaise D, Pigneux A *et al.* A white blood cell index as the main prognostic factor in t(8;21) acute myeloid leukemia (AML): a survey of 161 cases from the French AML Intergroup. *Blood* 2002; **99**: 3517–3523.
- Schoch C, Haase D, Haeflrich T, Gudat H, Büchner T, Freund M *et al.* Fifty-one patients with acute myeloid leukemia and translocation t(8;21)(q22;q22): an additional deletion in 9q is an adverse prognostic factor. *Leukemia* 1996; **10**: 1288–1295.
- Baer MR, Stewart CC, Lawrence D, Arthur DC, Byrd JC, Davey FR *et al.* Expression of the neural cell adhesion molecule CD56 is associated with short remission duration and survival in acute myeloid leukemia with t(8;21)(q22;q22). *Blood* 1997; **90**: 1643–1648.
- Cairolì R, Beghini A, Grillo G, Nadali G, Elice F, Ripamonti CB *et al.* Prognostic impact of c-KIT mutations in core binding factor leukemias: an Italian retrospective study. *Blood* 2006; **107**: 3463–3468.
- Paschka P, Marcucci G, Ruppert AS, Mrózek K, Chen H, Kittles RA *et al.* Adverse prognostic significance of KIT mutations in adult acute myeloid leukemia with inv(16) and t(8;21): a Cancer and Leukemia Group B Study. *J Clin Oncol* 2006; **24**: 3904–3911.
- Heinrich MC, Blanke CD, Druker BJ, Corless CL. Inhibition of KIT tyrosine kinase activity: a novel molecular approach to the treatment of KIT-positive malignancies. *J Clin Oncol* 2002; **20**: 1692–1703.
- Roskoski Jr R. Structure and regulation of Kit protein-tyrosine kinase—the stem cell factor receptor. *Biochem Biophys Res Commun* 2005; **338**: 1307–1315.

- 24 Mrozek K, Bloomfield CD. Chromosome aberrations, gene mutations and expression changes, and prognosis in adult acute myeloid leukemia. *American Society of Hematology educational book* 2006; **2006**: 169–177.
- 25 Rönnstrand L. Signal transduction via the stem cell factor receptor/c-Kit. *Cell Mol Life Sci* 2004; **61**: 2535–2548.
- 26 Kuchenbauer F, Feuring-Buske M, Buske C. AML1-ETO needs a partner: new insights into the pathogenesis of t(8;21) leukemia. *Cell Cycle* 2005; **4**: 1716–1718.
- 27 Nanri T, Matsuno N, Kawakita T, Suzushima H, Kawano F, Mitsuya H et al. Mutations in the receptor tyrosine kinase pathway are associated with clinical outcome in patients with acute myeloblastic leukemia harboring t(8;21)(q22;q22). *Leukemia* 2005; **19**: 1361–1366.
- 28 Schnittger S, Kohl TM, Haeflrich T, Kern W, Hiddemann W, Spiekermann K et al. KIT-D816 mutations in AML1-ETO-positive AML are associated with impaired event-free and overall survival. *Blood* 2006; **107**: 1791–1799.
- 29 Boissel N, Leroy H, Brethon B, Philippe N, de Botton S, Auvrignon A et al. Acute Leukemia French Association (ALFA); Leucémies Aiguës Myéloblastiques de l'Enfant (LAME) Cooperative Groups. Incidence and prognostic impact of c-Kit, FLT3, and Ras gene mutations in core binding factor acute myeloid leukemia (CBF-AML). *Leukemia* 2006; **20**: 965–970.
- 30 Pollard JA, Alonzo TA, Gerbing RB, Ho PA, Zeng R, Ravindranath J et al. Prevalence and prognostic significance of KIT mutations in pediatric patients with core binding factor AML enrolled on serial pediatric cooperative trials for *de novo* AML. *Blood* 2010; **115**: 2372–2379.
- 31 Nakasone H, Izutsu K, Wakita S, Yamaguchi H, Muramatsu-Kida M, Usuki K. Autologous stem cell transplantation with PCR-negative graft would be associated with a favorable outcome in core-binding factor acute myeloid leukemia. *Biol Blood Marrow Transplant* 2008; **14**: 1262–1269.
- 32 Yamaguchi H, Hanawa H, Uchida N, Inamai M, Sawaguchi K, Mitamura Y et al. Multistep pathogenesis of leukemia via the MLL-AF4 chimeric gene/FLT3 gene tyrosine kinase domain (TKD) mutation-related enhancement of S100A6 expression. *Exp Hematol* 2009; **37**: 701–714.
- 33 Kurata S, Kanagawa T, Yamada K, Torimura M, Yokomaku T, Kamagata Y et al. Fluorescent quenching-based quantitative detection of specific DNA/RNA using a BODIPY((R)) FL-labeled probe or primer. *Nucleic Acids Res* 2001; **29**: E34.
- 34 Tanaka R, Kuroda J, Stevenson W, Ashihara E, Ishikawa T, Taki T et al. Fully automated and super-rapid system for the detection of JAK2V617F mutation. *Leuk Res* 2008; **32**: 1462–1467.
- 35 Ohno R, Kato Y, Nagura E, Murase T, Okumura M, Yamada H et al. Behenoyl cytosine arabinoside, daunorubicin, 6-mercaptopurine, and prednisolone combination therapy for acute myelogenous leukemia in adults and prognostic factors related to remission duration and survival length. *J Clin Oncol* 1986; **4**: 1740–1747.
- 36 Ohno R, Kobayashi T, Tanimoto M, Hiraoka A, Imai K, Asou N et al. Randomized study of individualized induction therapy with or without vincristine, and of maintenance-intensification therapy between 4 or 12 courses in adult acute myeloid leukemia. AML-87 Study of the Japan Adult Leukemia Study Group. *Cancer* 1993; **71**: 3888–3895.
- 37 Kobayashi T, Miyawaki S, Tanimoto M, Kuriyama K, Murakami H, Yoshida M et al. Randomized trials between behenoyl cytarabine and cytarabine in combination induction and consolidation therapy, and with or without ubenimex after maintenance/intensification therapy in adult acute myeloid leukemia. The Japan Leukemia Study Group. *J Clin Oncol* 1996; **14**: 204–213.
- 38 Miyawaki S, Kobayashi T, Tanimoto M, Kuriyama K, Murakami H, Yoshida M et al. Comparison of leukopenia between cytarabine and behenoyl cytarabine in JALSG AML-89 consolidation therapy. The Japan Adult Leukemia Study Group. *Int J Hematol* 1999; **70**: 56–57.
- 39 Bonnet D, Dick JE. Human acute myeloid leukemia is organized as a hierarchy that originates from a primitive hematopoietic cell. *Nat Med* 1997; **3**: 730–737.
- 40 Hope KJ, Jin L, Dick JE. Acute myeloid leukemia originates from a hierarchy of leukemic stem cell classes that differ in self-renewal capacity. *Nat Immunol* 2004; **5**: 738–743.
- 41 Gal H, Amariglio N, Trakhtenbrot L, Jacob-Hirsh J, Margalit O, Avigdor A et al. Gene expression profiles of AML derived stem cells; similarity to hematopoietic stem cells. *Leukemia* 2006; **20**: 2147–2154.
- 42 Dick JE. Stem cell concepts renew cancer research. *Blood* 2008; **112**: 4793–4807.
- 43 Misaghian N, Ligresti G, Steelman LS, Bertrand FE, Bäsecke J, Libra M et al. Targeting the leukemic stem cell: the Holy Grail of leukemia therapy. *Leukemia* 2009; **23**: 25–42.
- 44 Saito Y, Kitamura H, Hijikata A, Tomizawa-Murasawa M, Tanaka S, Takagi S et al. Identification of therapeutic targets for quiescent, chemotherapy-resistant human leukemia stem cells. *Sci Transl Med* 2010; **2**: 17a9.
- 45 Kohl TM, Schnittger S, Ellwart JW, Hiddemann W, Spiekermann K. KIT exon 8 mutations associated with core-binding factor (CBF)-acute myeloid leukemia (AML) cause hyperactivation of the receptor in response to stem cell factor. *Blood* 2005; **105**: 3319–3321.
- 46 Frost MJ, Ferrao PT, Hughes SP, Ashman LK. Juxtamembrane mutant V560GKit is more sensitive to Imatinib (STI571) compared with wild-type c-kit whereas the kinase domain mutant D816VKit is resistant. *Mol Cancer Ther* 2002; **1**: 1115–1124.
- 47 Choudhary C, Schwable J, Brandts C, Tickenbrock L, Sargin B, Kindler T et al. AML-associated FLT3 kinase domain mutations show signal transduction differences compared with FLT3 ITD mutations. *Blood* 2005; **106**: 265–273.
- 48 Mead AJ, Linch DC, Hills RK, Wheatley K, Burnett AK, Gale RE. FLT3 tyrosine kinase domain mutations are biologically distinct from and have a significantly more favorable prognosis than FLT3 internal tandem duplications in patients with acute myeloid leukemia. *Blood* 2007; **110**: 1262–1270.
- 49 Lasa A, Carricondo MT, Carnicer MJ, Perea G, Aventín A, Nomdedeu JF. A new D816 c-KIT gene mutation in refractory AML1-ETO leukemia. *Haematologica* 2006; **91**: 1283–1284.
- 50 Higuchi M, O'Brien D, Kumaravelu P, Lenny N, Yeoh EJ, Downing JR. Expression of a conditional AML1-ETO oncogene bypasses embryonic lethality and establishes a murine model of human t(8;21) acute myeloid leukemia. *Cancer Cell* 2002; **1**: 63–74.
- 51 Schessl C, Rawat VP, Cusan M, Deshpande A, Kohl TM, Rosten PM et al. The AML1-ETO fusion gene and the FLT3 length mutation collaborate in inducing acute leukemia in mice. *J Clin Invest* 2005; **115**: 2159–2168.
- 52 Neubauer A, Maharry K, Mrózek K, Thiede C, Marcucci G, Paschka P et al. Patients with acute myeloid leukemia and RAS mutations benefit most from postremission high-dose cytarabine: a Cancer and Leukemia Group B study. *J Clin Oncol* 2008; **26**: 4603–4609.
- 53 Kuwatsuka Y, Miyamura K, Suzuki R, Kasai M, Maruta A, Ogawa H et al. Hematopoietic stem cell transplantation for core binding factor acute myeloid leukemia: t(8;21) and inv(16) represent different clinical outcomes. *Blood* 2009; **113**: 2096–2103.

Supplementary Information accompanies the paper on the Leukemia website (<http://www.nature.com/leu>)

RCSD1-ABL1-positive B lymphoblastic leukemia is sensitive to dexamethasone and tyrosine kinase inhibitors and rapidly evolves clonally by chromosomal translocations

Koiti Inokuchi · Satoshi Wakita · Tsuneaki Hirakawa · Hayato Tamai · Norio Yokose · Hiroki Yamaguchi · Kazuo Dan

Received: 20 May 2011 / Revised: 29 July 2011 / Accepted: 29 July 2011 / Published online: 24 August 2011
© The Japanese Society of Hematology 2011

Abstract Recently, RCSD1 was identified as a novel gene fusion partner of the ABL1 gene. The RCSD1 gene, located at 1q23, is involved in t(1;9)(q23;q34) translocation in acute B lymphoblastic leukemia. Here we describe RCSD1-ABL1-positive B-cell acute lymphoblastic leukemia (ALL) followed by rapid clonal evolution exhibiting three rare reciprocal translocations. We performed breakpoint analysis of the transcript expressed by the RCSD1-ABL1 fusion gene. RT-PCR and sequence analyses detected transcription of a single RCSD1-ABL1 fusion gene variant, which had breakpoints in exon 3 of RCSD1 and exon 4 of ABL1. The RCSD1 portion of the RCSD1-ABL1 fusion transcript consists of exons 1, 2, and 3. Tyrosine kinase inhibitors, imatinib and dasatinib, coadministered with dexamethasone achieved transient clinical effects in the present RCSD1-ABL1-positive ALL. However, leukemic cells rapidly became refractory to this treatment following the subsequent development of three additional reciprocal chromosomal translocations, t(5;16)(q33;q24), dic(18;20)(p11.2;q11.2) and t(10;19)(q24;p13.3). The present RCSD1-ABL1-positive ALL may represent a state of high chromosomal instability.

Keywords RCSD1-ABL1 fusion gene · B lymphoblastic leukemia · Dexamethasone · TKI

1 Introduction

Chromosomal translocations are considered as the primary cause for leukemia, which ultimately determine the cell-lineage and regulate the etiology of the disease.

ABL1 is a gene located at 9q34 that codes for a protein with tyrosine kinase (TK) activity. The major fusion partner of ABL1 is BCR, which is involved in the t(9;22)(q34;q11.2) translocation, also known as a Philadelphia (Ph) chromosome. A BCR-ABL1 fusion gene in t(9;22)(q34;q11.2) is present in more than 90% of patients with chronic myelogenous leukemia (CML) and in 20% of B-cell acute lymphoblastic leukemia (B-ALL) patients [1, 2]. The BCR-ABL1 gene results in the formation of a chimeric BCR-ABL1 fusion transcript, which encodes a constitutively active ABL1 tyrosine kinase.

Several partner genes of ABL1 have also been reported. For example, ETV6, which is rearranged in t(9;12)(q34;p13) of acute leukemia and myeloproliferative neoplasms (MPN) [3, 4]. NUP214 and EML1 have been found to be rearranged with ABL1 in T-cell ALL [5, 6]. Recently, the identification of a novel ABL1 fusion partner, RCSD1, involved in a t(1;9)(q24;q34) translocation has been reported [7]. Only one case of ALL has been confirmed as RCSD1-ABL1-positive in the literature. Here we report a case of RCSD1-ABL1-positive ALL with rapid clonal evolution by three rare reciprocal chromosomal translocations.

2 Materials and methods

2.1 Patient profile

A 31-year-old man was admitted in February 2010 because of persistent fever and diffuse thoracic pain. Physical

K. Inokuchi (✉) · S. Wakita · T. Hirakawa · H. Tamai · N. Yokose · H. Yamaguchi · K. Dan
Division of Hematology, Department of Internal Medicine,
Nippon Medical School, 1-1-5 Sendagi, Bunkyo-ku,
Tokyo 113-8603, Japan
e-mail: inokuchi@nms.ac.jp

examination revealed no hepatomegaly. The spleen and nodular lymph nodes in both axillae were moderately enlarged. Computed tomography revealed no mediastinal enlargement or lymphadenopathy in the retroperitoneal region.

Peripheral blood cell counts were as follows: hemoglobin 11.2 g/dL, white blood cells 146,000/ μ L (neutrophils 9%, lymphocytes 1%, monocytes 0%, basophils 0%, blast cells 90%), and platelets 161,000/ μ L. The lactate dehydrogenase level was 865 U/L (normal <250 U/L). Bone marrow aspirate and biopsy were consistent with acute leukemia (AL). The medium- to large-sized blasts had a moderate amount of basophilic cytoplasm. Nuclei were round or oval and had finely stippled chromatin. The blast cells were positive for periodic acid-Schiff (PAS) but negative for peroxidase, chloroacetate esterase, and α -naphthyl butyrate esterase. The blast cell immunophenotypes were as follows: CD2 (–), CD3 (–), CD4 (–), CD5 (–), CD7 (–), CD8 (–), CD10 (+), CD19 (+), CD20 (–), CD22 (+), CD16 (–), CD56 (–), CD64 (–), CD11c (–), CD13 (+), CD14 (–), CD33 (+), CD36 (–), CD79a (+), CD117 (–), HLA-DR (+). As a result of these observations, a diagnosis of B-ALL was made. Cytogenetics revealed the karyotype of 46,XY,t(1;9)(q23;q34), inv(2)(p21q33) in 20/20 cells (Table 1, Fig. 2a).

The patient was treated with hyper-CVAD combination chemotherapy comprising cyclophosphamide, vincristine, doxorubicin, and dexamethasone [8, 9]. However, the disease did not achieve complete remission (CR), as shown in Fig. 1. Abscesses in the deep skin and deep vein thrombosis occurred in the left femoral vein of the central venous drip line. Therefore, the patient was treated with

combination chemotherapy comprising 800 mg of imatinib for 7 days and 40 mg of dexamethasone for 4 days followed by 140 mg of dasatinib daily. Because, there is evidence that dasatinib was effective to RCSD1-ABL1-positive ALL, as described by Mustjoki et al. [7], the patient was treated with imatinib followed by dasatinib. On day 74, lymphoblasts disappeared from the peripheral blood, but 15% remained in the bone marrow. A second course of hyper-CVAD with 140 mg of dasatinib daily was administered. Twenty days after therapy using 1.5 g of methotrexate and cytarabine (total dose; 18 g), lymphoblasts suddenly increased by 82% in a population of 42,000 leukocytes. Administration of 40 mg of dexamethasone for 4 days was highly effective in reducing lymphoblast count. Administration of triplicated dexamethasone and dasatinib achieved stable disease with partial remission in the bone marrow. However, during the seventh administration of dexamethasone, the disease recurred and there was no further response to treatment. The cytogenetic clonal evolution across the clinical course is shown in Table 1.

2.2 Fluorescence in situ hybridization (FISH) and spectral karyotyping (SKY) in conjunction with G-banding karyotype analysis

Karyotypic analyses were performed on unstimulated bone marrow cells after short-term culture. Chromosomes were G-banded and evaluated according to the International System for Human Cytogenetic Nomenclature (ISCN2005) [10, 11].

The Vysis LSI BCR, ABL dual color, dual fusion translocation probe (Abbott Laboratories, Abbott Park, IL)

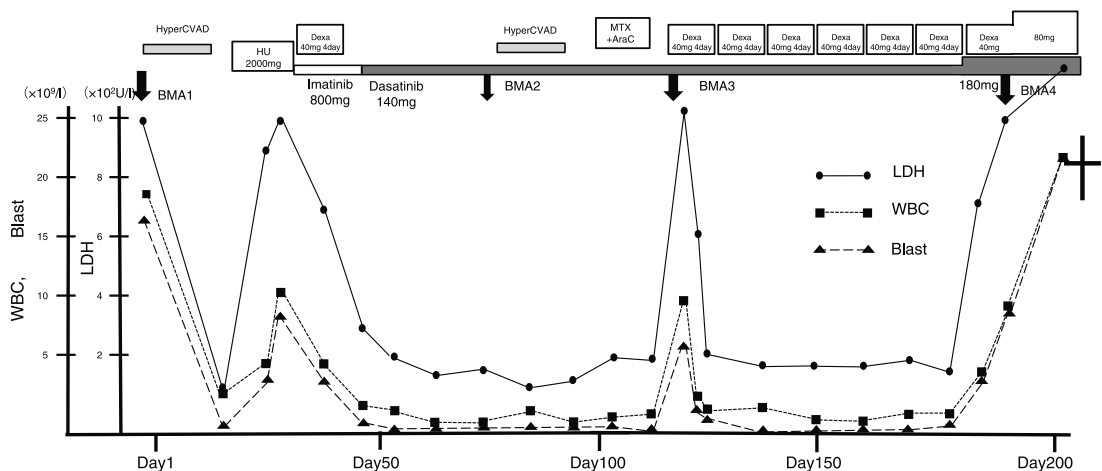


Fig. 1 Clinical course of the present patient. Ara-C cytarabine, BMA bone marrow aspiration, Dexamethasone, HU hydroxyurea, LDH lactate dehydrogenase, MTX methotrexate, WBC white blood cell count

Table 1 The cytogenetic clonal evolution during the clinical course

Date of bone marrow aspiration	Karyotype
Day 0 at diagnosis (BMA 1)	46,XY,t(1;9)(q23;q34),inv(2)(p21q33)[20]
Day 74 at the primary resistance stage (BMA 2)	45,XY,t(1;9)(q23;q34),inv(2)(q21q33), t(5;16)(q33;q24),dic(18;20)(p11.2;q11.2)[2]/ 46,XY[18]
Day 115 at the second clonal expansion (BMA 3)	45,XY,t(1;9)(q23;q34),inv(2)(q21q33), t(5;16)(q33;q24),dic(18;20)(p11.2;q11.2)[16]/ 46,XY,t(1;9)(q23;q34),inv(2)(q21q33), t(5;16)(q33;q24),der(19)t(17;19)(q21;p13.3), dic(18;20)(p11.2;q11.2),+21[4]
Day 180 of the final stage (BMA 4)	46,XY,t(1;9)(q23;q34),inv(2)(q21q33), t(5;16)(q33;q24),der(19)t(17;19)(q21;p13.3), dic(18;20)(p11.2;q11.2),+21[20]

BMA 1–4: BMA 1–4 in Fig. 1

was used to detect ABL1 and BCR genes in metaphase cells, as described previously [12]. SKY-FISH analysis was performed as described previously [13].

2.3 Cell preparation and extraction of RNA

After obtaining informed consent, clinical samples of bone marrow (BM) cells were obtained from the patient at diagnosis prior to treatment. Mononuclear cells (MNCs) were separated from the BM cells by Ficoll Hypaque centrifugation (Lymphoprep, Neegard, Norway). The blast cells represented more than 96% of the total cell population. The total RNA of BM MNCs at diagnosis was extracted with an RNazol kit (Biotex Laboratories, Inc., Houston, TX), which is based on a technique described previously [14].

2.4 Detection of the RCSD1-ABL1 fusion gene by reverse-transcription polymerase chain reaction (RT-PCR)

Complementary DNA (cDNA) was prepared from 0.5 µg of total RNA using a random hexamer primer. Amplification of the cDNA of the breakpoint site in the RCSD1-ABL1 fusion gene was performed for 30 cycles (denaturing at 98°C for 10 s, annealing at 60°C for 30 s, and extension at 72°C for 90 s) in a DNA thermal cycler. The sequences of the primers were SYN3044 F1 (5'-GGGACAGCGGGG ATCGTGAG-3') and SYN3044 R1 (5'-AGGAGCTGCAC CAGGTTAGG-3'). These two primers identify the fused site of both the RCSD1 and ABL1 transcripts. The PCR products were electrophoresed through a 1% agarose gel and then stained with ethidium bromide. The RCSD1-ABL1 amplified product was 626 nucleotides long. DNA sequences of the RCSD1-ABL1 amplified product were validated using the method described below.

2.5 Sequence analysis of the breakpoint site of the RCSD1-ABL1 fusion cDNA

The breakpoint site of the RCSD1-ABL1 fusion gene was amplified by PCR using SYN3044 F1 and SYN3044 R1 primers, as described above. Purified amplification products were sequenced with the Applied Biosystems 3130 Genetic Analyzer (Applied Biosystems, Foster City, CA, USA) in both directions using the BigDye Terminator v3.1 Cycle Sequencing Kit, as described previously [15].

3 Results

3.1 Cytogenetics

Cytogenetics revealed the karyotype of 46,XY,t(1;9)(q23;q34), inv(2)(p21q33) at diagnosis (Table 1; Fig. 1).

To clarify the precise chromosomal location of the BCR and ABL genes, we performed two-color FISH with BCR and ABL probes on blasts. FISH showed red signals of the ABL gene bound to chromosome 9, and showed faint signals of the ABL bound to der(1) t(1;9) and der(9) t(1;9), as shown in Fig. 2b. Therefore, part of the ABL gene was translocated to der(1) t(1;9). Green signals of the BCR gene were present on the long arms of both copies of chromosome 22. On day 74, following a partial response to treatment (15% of blasts remained in the bone marrow), of the 20 metaphase cells analyzed from an unstimulated 24-h culture, two showed the karyotype 46,XY,t(1;9)(q23;q34), inv(2)(q21q33), t(5;16)(q33;q24), dic(18;20) (p11.2;q11.2) and 18 showed normal karyotype (Table 2). During the clinical course, we also subjected the metaphase cells to G-banding cytogenetics and SKY-FISH. Subsequent clonal evolution was revealed cytogenetically. In the subsequent

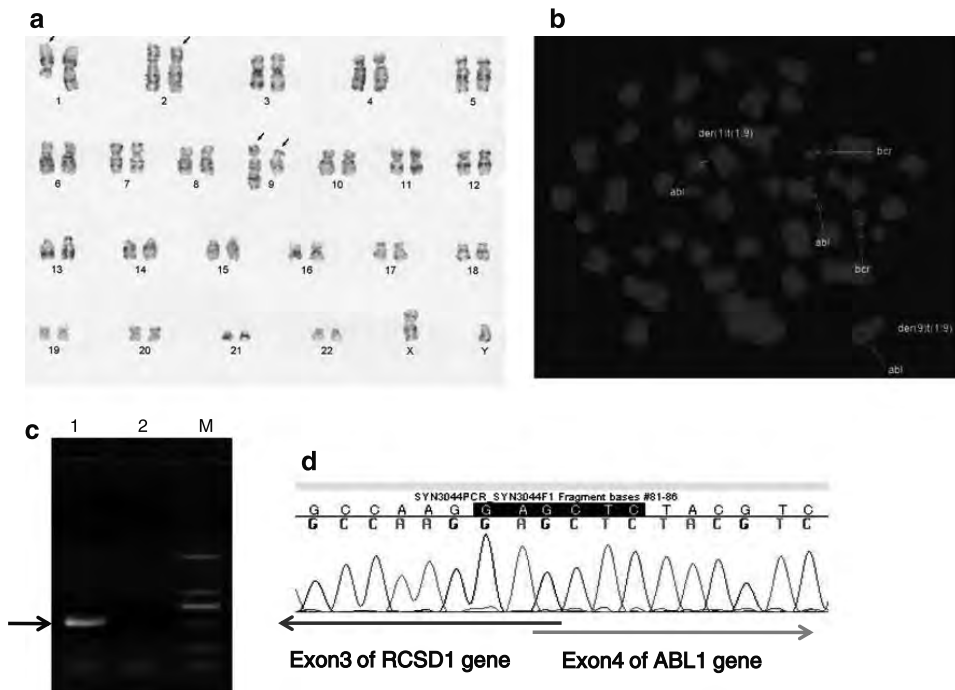


Fig. 2 Cytogenetic and molecular characterization of the t(1;9)(q24;q34) translocation. **a** G-banded karyotype showing the 46,XY,t(1;9)(q23;q34),inv(2)(p21q33). **b** FISH at metaphase revealed the divided existence of the *abl1* probe on der(1) and der(9). **c** Agarose gel of RT-PCR products. An arrow shows the amplified RCSD1-ABL1 products. The RCSD1-ABL1 amplified product was

626 nucleotides long. Lane M markers of 2,000, 1,000, 750, 500, 250 and 100 bp, respectively. Lane 1 RCSD1-ABL1 PCR (RT+). Lane 2 RCSD1-ABL1 PCR (RT-). **d** Sequence analysis of the RT-PCR product of the RCSD1-ABL1 cDNA. The chromatograms show part of the 5'-3' sequence upstream of the RCSD1-ABL1 junction

primary refractory phase on day 115, trisomy 21 and der(19)t(17;19)(q21;p13.3) was detected (Table 2). The karyotype 46,XY,t(1;9)(q23;q34), inv(2)(q21q33), t(5;16)(q33;q24), der(19)t(17;19)(q21;p13.3), dic(18;20)(p11.2;q11.2),+21 was the major clone in the final stage (Fig. 3).

3.2 Molecular analysis

RT-PCR analysis using both RCSD1 and ABL1 oligomers allowed us to amplify a 626-bp RCSD1-ABL1 fusion transcript (Fig. 2c). Sequencing revealed that the PCR product consisted of the first three exons of RCSD1 fused to the ABL1 gene starting from exon 4 extending to the kinase domain coding region (Fig. 2d). RT-PCR analysis did not detect the shorter PCR product consisting of the first two exons of RCSD1 fused to exon 4 of ABL1, as shown in Fig. 2c.

4 Discussion

Here, we report the identification of a new putative ABL1 fusion partner, RCSD1, involved in a t(1;9)(q24;q34)

translocation. Four ALL patients with t(1;9)(q24;q34) were reported (Table 2) [7, 16, 17]. All four patients were young males and each was diagnosed with B-cell or biphenotypic ALL. The three previous cases went into remission. After remission, allogeneic hematopoietic stem cell transplantation (HSCT) was performed in two of the three cases. However, all three cases experienced relapse of the disease. The present case did not achieve remission. Tyrosine kinase inhibitor (TKI), including imatinib and dasatinib, was effective in the treatment of the refractory phase of the third case and the present case [7].

Mustjoki et al. [7] reported two fusion transcripts consisting of the first three exons of RCSD1 fused to exon 4 of the ABL1 gene and the first two exons of RCSD1 fused to exon 4 of the ABL1 gene. The transcript expressed by the RCSD1-ABL1 fusion gene of the present case was exclusively of the type involving the fusion of the first three exons of RCSD1 with exon 4 of ABL1. Therefore, this type of RCSD1-ABL1 fusion appears to have greater leukemogenic activity than those involving the fusion of the first two exons of RCSD1 to exon 4 of ABL1.

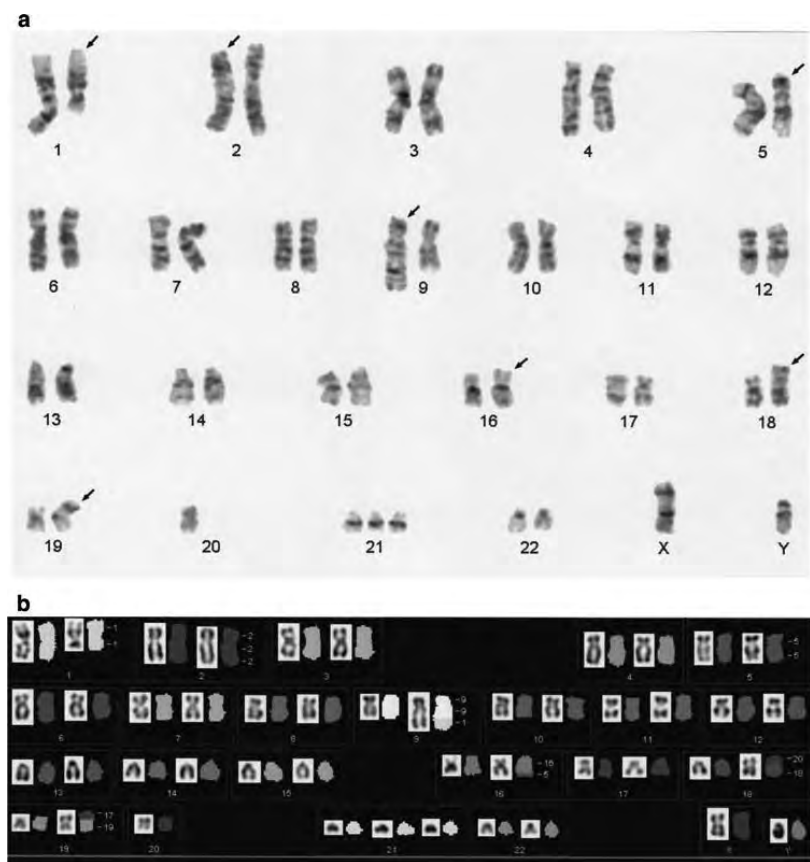


Fig. 3 Cytogenetic characterization of the karyotype at the Day 180. **a** G-banded karyotype showing the 46,XY,t(1;9)(q23;q34),inv(2)(q21q33),t(5;16)(q33;q24), der(19)t(17;19)(q21;p13.3),dic(18;20)(p11.2;q11.2),+21. **b** SKY-FISH revealed four types of translocations

Table 2 Literature reports of ALL with t(1;9)(q23–q24;q34)

Authors	Patient	Type of leukemia	Phenotype positive	Karyotype at diagnosis	Gene detected
Garcia et al. [16]	15-year-old boy	Biphenotypic leukemia	CD22, CD33, CD57	46,XY,t(1;9)(q23.3–q25;q34)[27]	ABL1
Braekeleer et al. [17]	11-year-old boy	B-cell acute leukemia	CD10, CD22, CD19, CD24, CD79a	46,Y,add(X)(p22),t(1;9)(q24;q34)[18] (karyotype at the time of relapse)	ABL1
Mustjoki et al. [7]	40-year-old male	Pre-B acute leukemia	CD10, CD19, CD22, nTdT, CD34, CD38, CD79a, HLA-DR	46,XY,t(1;9)(q24;q34)[5]	RCSD1-ABL1
Present case	31-year-old male	B-cell acute leukemia	CD10, CD13, CD19, CD22, CD33,CD34, CD79a, HLA-DR	46,XY,t(1;9)(q23;q34),inv(2)(p21q33)[20]	RCSD1-ABL1

The present case was ultimately resistant to Hyper-CVAD therapy, and TKIs and high-dose dexamethasone. We speculate that the resistance to combined chemotherapy and TKIs may be due to the activation of the additional

oncogenes by the three types of cytogenetic translocations that occurred subsequent to treatment.

The cytogenetic analysis in the ALL cases with t(1;9)(q23;q34) at the refractory phase has not yet been

reported in the previous three cases (Table 2). Although the ALL patients with t(1;9)(q23;q34) readily achieved remission and received a stem cell transplantation, these patients nevertheless experienced relapses shortly after treatment. Thus, ALL with t(1;9)(q23;q34) is a distinct category with a poor prognosis. The additional subsequent cytogenetic translocations may be one of the reasons for the poor prognosis. Dasatinib with dexamethasone therapy was transiently effective in the clonally evolved ALL with t(1;9)(q23;q34). The association of disease progression with cytogenetic clonal evolution of the present ALL case with t(1;9)(q22;q34) may provide important information on ALL that is refractory to treatment.

Here, we experienced a very rare RCSD1-ABL1-positive B-cell ALL followed by rapid clonal evolution exhibiting three rare additional translocations. The disease was primarily refractory to the standard chemotherapy, Hyper-CVAD, and methotrexate and cytarabine treatment. Combination chemotherapy comprising of TKIs, imatinib followed by dasatinib, and dexamethasone were transiently effective. Over the course of the disease, there is a possibility that cytogenetically cumulative evolution resulted in lymphoblasts that were resistant to hyper-CVAD and high-dose dexamethasone with high-dose dasatinib. The present RCSD1-ABL1-positive ALL may be in a state of high chromosomal instability manifesting as balanced and unbalanced reciprocal translocations.

References

1. De Klein A, Geurts van Kessel A, Gorsveld G, et al. A cellular oncogene is translocated to Philadelphia chromosome in chronic myelocytic leukemia. *Nature*. 1982;300:765–7.
2. De Klein A, Hagemeijer A, Bartram CR, Houwen R, et al. bcr rearrangement and translocation of the c-abl oncogene to Philadelphia positive acute lymphoblastic leukemia. *Blood*. 1986;68:1369–75.
3. Van Limbergen H, Beverloo HB, van Drunen E, Janssens A, et al. Molecular cytogenetic and clinical findings in ETV6/ABL1-positive leukemia. *Gene Chromosome Cancer*. 2001;30:274–82.
4. Meyer-Monard S, Muhlematter D, Streit A, Chase AJ, et al. Broad molecular screening of an unclassifiable myeloproliferative disorder reveals an unexpected ETV6/ABL1 fusion transcript. *Leukemia*. 2005;19:1096–9.
5. Graux C, Cools J, Melotte C, Quentmeier H, et al. Fusion of NUP214 to ABL1 on amplified episomes in T-cell acute lymphoblastic leukemia. *Nat Genet*. 2004;36:1084–9.
6. De Keersmaecker K, Graux C, Odero MD, Mentens N, et al. Fusion of EML1 to ABL1 in T-cell acute lymphoblastic leukemia with cryptic t(9;14)(q34;q32). *Blood*. 2005;105:4849–52.
7. Mustjoki S, Hernesniemi S, Rauhala A, Kahkonen M, et al. A novel dasatinib-sensitive RCSD1-ABL1 fusion transcript in chemotherapy-refractory adult pre-B lymphoblastic leukemia with t(1;9)(q24;q34). *Haematologica*. 2009;94:1469–71.
8. Thomas DA, Faderi S, Cortes J, O'Brien S, et al. Treatment of Philadelphia chromosome-positive acute lymphocytic leukemia with hyper-CVAD and imatinib mesylate. *Blood*. 2004;103:4396–407.
9. Ravandi F, O'Brien S, Thomas D, Faderi S, et al. First report of phase 2 study of dasatinib with hyper-CVAD for the frontline treatment of patients with Philadelphia chromosome-positive (Ph+) acute lymphoblastic leukemia. *Blood*. 2010;116:2070–7.
10. ISCN 2005. An international system for human cytogenetic nomenclature (2005). In: Shaffer LG, Tommerup N, editors. Basel: Karger publishers; 2005.
11. Abo J, Inokuchi K, Dan K, Nomura T. p53 and N-ras mutations in two new leukemia cell lines established from a patient with multilineage CD-7positive acute leukemia. *Blood*. 1993;82:2829–36.
12. Inokuchi K, Shinohara T, Futaki M, Hanawa H, et al. Establishment of a cell line with variant BCR/ABL breakpoint expression P180 BCR/ABL from late-appearing Philadelphia-positive acute biphenotypic leukemia. *Gene Chromosome Cancer*. 1998;23:227–38.
13. Inokuchi K, Hamaguchi H, Taniwaki M, Yamaguchi H, Tanosaki S. Establishment of cell line with AML1-MTG8, TP53, and TP73 abnormalities form acute myelogenous leukemia. *Gene Chromosome Cancer*. 2001;32:182–7.
14. Suessmuth Y, Elliott J, Percy MJ, Inami M, et al. A new polycythemia vera-associated SOCS3 SH2 mutant (SOCS3F136L) cannot regulate erythropoietin responses. *Br J Haematol*. 2009;147:450–8.
15. Inami M, Inokuchi K, Nakayama K, Tamura H, et al. Simultaneous novel BCR-ABL gene mutation and increased expression of BCR-ABL mRNA caused clinical resistance to STI571 in double-Ph-positive acute biphenotypic leukemia. *Int J Hematol*. 2003;78:173–5.
16. Garcia JRG, Bohlander SK, Angulo MG, Flores MAE, et al. A t(1;9)(q23.3 q25;q34) affecting the ABL1 gene in a biphenotypic leukemia. *Cancer Genet Cytogenet*. 2004;152:81–3.
17. Braekeller EDE, Douet-Guilbert N, Le Bris MJ, Berthou C, et al. A new partner gene fused to ABL1 in a t(1;9)(q24;q34)-associated B-cell acute lymphoblastic leukemia. *Leukemia*. 2007;21:2220–1.

ORIGINAL ARTICLE

Inhibition of S100A6 induces GVL effects in MLL/AF4-positive ALL in human PBMC-SCID mice

H Tamai¹, K Miyake^{2,3}, H Yamaguchi^{1,3}, T Shimada², K Dan¹ and K Inokuchi¹

Mixed-lineage leukemia (MLL)/AF4-positive ALL is associated with a poor prognosis even after allogeneic hematopoietic SCT (allo-HSCT). We reported previously that MLL/AF4-positive ALL shows resistance to TNF- α , which is the main factor in the GVL effect, by upregulation of S100A6 expression followed by interference with the p53–caspase 8–caspase 3 pathway *in vitro*. We examined whether inhibition of S100A6 can induce an effective GVL effect on MLL/AF4-positive ALL in a mouse model. MLL/AF4-positive ALL cell lines (SEM) transduced with lentiviral vectors expressing both S100A6 siRNA and luciferase (SEM-Luc-S100A6 siRNA) were produced. SEM-Luc-S100A6 siRNA cells and SEM-Luc-control siRNA cells were injected into groups of five SCID mice (1×10^7 /body). After confirmation of engraftment of SEM cells by *in vivo* imaging, the mice in each group were injected with 4.8×10^7 human PBMCs. SEM-Luc-S100A6 siRNA-injected mice showed significantly longer survival periods than SEM-Luc-control siRNA-injected mice ($P=0.002$). SEM-Luc-S100A6 siRNA-injected mice showed significantly slower tumor growth than those injected with SEM-Luc-control siRNA ($P<0.0001$). These results suggested that inhibition of S100A6 may be a promising therapeutic target for MLL/AF4-positive ALL in combination with allo-HSCT.

Bone Marrow Transplantation (2014) 49, 699–703; doi:10.1038/bmt.2014.18; published online 3 March 2014

Keywords: MLL; mixed lineage leukemia; MLL/AF4; S100A6; GVL

INTRODUCTION

Rearrangements of the mixed-lineage leukemia (MLL) gene located at 11q23 are common chromosomal abnormalities associated with acute leukemia, especially infant leukemia and secondary leukemia following treatment with DNA topoisomerase II inhibitors. In addition, 11q23/MLL abnormalities are now widely recognized as important prognostic factors in acute leukemia. Over 70 chromosomal partners of 11q23 have been identified to date, at least 50 of which have been cloned and characterized at the molecular level.¹ The prognosis of leukemia patients with MLL rearrangement varies widely depending on the partner gene, leukemia cell lineage, age of the patient, and treatment administered.¹ The most prevalent MLL rearrangement in ALL generates the MLL/AF4 fusion gene due to a t(4;11)(q21;q23) chromosomal translocation. Despite recent improvements in the overall treatment outcome for ALL patients, including allogeneic hematopoietic SCT (allo-HSCT), MLL/AF4-positive ALL is still associated with a poor prognosis.² One reason why MLL/AF4-positive ALL is resistant to allo-HSCT is that MLL/AF4-positive ALL escapes from TNF- α -mediated apoptosis, which is the main GVL effect, by upregulating the expression of S100A6.^{3,4}

S100A6 is a 10.5-kDa Ca^{2+} -binding protein belonging to the S100 protein family, which has been reported to interact with and alter the conformation of p53.^{5–8} Upregulation of S100A6 expression in MLL/AF4-positive ALL inhibits p53 acetylation followed by inhibition of upregulation of the caspase 8–caspase 3 apoptotic pathway in the presence of TNF- α .⁴ The present study was performed to examine whether inhibition of S100A6 induces GVL effects in an MLL/AF4-positive ALL *in vivo* model.

MATERIALS AND METHODS

Cell culture

The MLL/AF4-positive ALL cell line SEM was purchased from the American Type Culture Collection (ATCC; Manassas, VA, USA). The SEM cells were maintained in DMEM-high glucose (Sigma, St Louis, MO, USA) supplemented with 10% fetal bovine serum (PAN Biowest, Nuaillé, France) at 37 °C in an atmosphere of 5% CO₂ in air.

Establishment of MLL/AF4-positive ALL cell lines expressing both S100A6 siRNA and luciferase

First, we produced MLL/AF4-positive ALL cell line (SEM) transduced with lentiviral vectors express luciferase (SEM-Luc) as described previously.⁹ Second, to examine the long-term effects of S100A6 inhibition, we produced SEM-Luc transduced with lentiviral vectors expressing S100A6 siRNA (SEM-Luc-S100A6 siRNA). As a control, SEM-Luc transduced with lentiviral vectors expressing control siRNA were produced (SEM-Luc-control siRNA). The methods used for establishment of SEM-Luc-S100A6 siRNA and SEM-Luc-control siRNA were as described previously.^{4,9,10}

Real-time quantitative PCR analysis of S100A6 and β -actin

We determined the levels of S100A6 mRNA expression in leukemia cells. To activate S100A6 mRNA expression, SEM-Luc-S100A6 siRNA cells or SEM-Luc-control siRNA cells were incubated for 48 h under TNF- α (5 ng/mL) based on a previous study.⁴ Total RNA was extracted and treated with DNase using an RNeasy Mini kit and RNase-Free DNase set (Qiagen, Germantown, MD, USA) and converted to cDNA using an RNA PCR kit (Takara, Shiga, Japan). Portions of unamplified cDNA were subjected to PCR with SYBR Green PCR Core Reagents (PE Applied Biosystems, Foster City, CA, USA). Incorporation of SYBR Green dye into the PCR products was

¹Department of Hematology, Nippon Medical School, Tokyo, Japan and ²Department of Biochemistry and Molecular Biology, Division of Gene Therapy Research Center for Advanced Medical Technology, Nippon Medical School, Tokyo, Japan. Correspondence: Dr H Tamai, Department of Hematology, Nippon Medical School, Sendagi 1-1-5, Bunkyo-Ku, Tokyo 113-8603, Japan.

E-mail: s6056@nms.ac.jp

³These authors contributed equally to this work.

Received 30 September 2013; revised 17 December 2013; accepted 23 December 2013; published online 3 March 2014

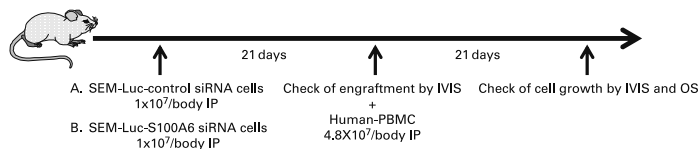


Figure 1. The protocol for murine transplantation experiments. 1×10^7 /body of (A) SEM-Luc-S100A6 siRNA cells or (B) SEM-Luc-control siRNA cells were injected into groups of five SCID mice by IP. Twenty-one days after injection of SEM cells, confirmation of engraftment of SEM cells was performed using IVIS; mice in each group were injected with 4.8×10^7 /body of human PBMCs. In addition to OS rate, tumor growth 21 days after injection of human PBMCs was assessed by IVIS.

monitored in real-time with an ABI PRISM 7700 sequence detection system (PE Applied Biosystems), thereby allowing determination of the threshold cycle at which exponential amplification of PCR products began. The threshold cycle values for cDNAs corresponding to β -actin and target genes were used to calculate the abundance of the target transcripts relative to that of β -actin mRNA. The oligonucleotide primers of S100A6 were as described previously.⁴

In vitro analysis of cell growth of SEM-Luc-S100A6 siRNA and SEM-Luc-control siRNA

The generated leukemia cell lines (SEM-Luc-S100A6 siRNA and SEM-Luc-control siRNA) were incubated *in vitro* with or without TNF- α (0, 1, 10 and 100 ng/mL) for 48 h before counting cells to examine the effects of TNF- α on leukemia cells, as described previously.⁴

Separation of human peripheral blood mononuclear cells (PBMCs)

Human PBMCs were obtained by separation of heparinized blood from a healthy donor on a Ficoll-Histopaque gradient. The PBMCs were washed twice and resuspended in RPMI 1640 supplemented with 25 mM HEPES buffer, 2 mM glutamine, 100 U/mL penicillin, 100 pg/mL streptomycin and 10% heat-inactivated FCS. (This medium is designated FCS-RPMI.)

Murine transplantation experiments and *in vivo* imaging

The protocol for murine transplantation experiments is shown in Figure 1. For *in vivo* analysis, 1×10^7 /body of SEM-Luc-S100A6 siRNA cells or SEM-Luc-control siRNA cells were injected into groups of five SCID mice by IP. Twenty-one days after injection of SEM cells, confirmation of engraftment of SEM cells was performed using an *in vivo* imaging system (IVIS); mice in each group were injected with 4.8×10^7 /body of human PBMCs by IP. In addition to OS rate, tumor growth 21 days after injection of human PBMCs was assessed by IVIS, as described previously.⁷ Each mouse was killed at the time of dying or over day 100 on survival. All animal experiments were performed in accordance with the regulations established by the Ethical Committee of Nippon Medical School and were approved by the Animal Care and Committee of Nippon Medical School.

Examination of serum concentrations of human TNF- α by ELISA

The serum concentrations of human TNF- α three weeks after injection of human PBMCs were measured by ELISA in each group of five mice. ELISA was performed as described previously.¹¹

Statistical analysis

The results of cell growth and gene expression assays were analyzed by Student's *t*-test, assuming unequal variances and two-tailed distributions. Data are shown as the means \pm s.d. of at least three samples. For survival analyses, event time distributions were estimated using the method of Kaplan and Meier, and differences in survival rates were compared using the log-rank test. In all analyses, $P < 0.05$ was taken to indicate statistical significance.

RESULTS

The expression of S100A6 mRNA was inhibited only in SEM-Luc-S100A6 siRNA cells under 5 ng/mL of TNF- α .

RQ-PCR analysis showed that S100A6 mRNA expression was significantly inhibited in SEM-Luc-S100A6 siRNA cells ($P = 0.005$) in

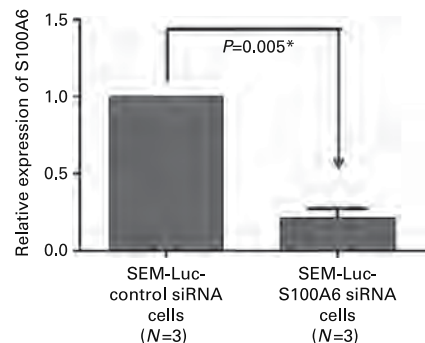


Figure 2. RQ-PCR analysis of S100A6 mRNA in the presence of TNF- α (5 ng/mL). S100A6 mRNA expression was significantly inhibited in SEM-Luc-S100A6 siRNA cells in comparison with SEM-Luc-control siRNA cells under TNF- α (5 ng/mL).

comparison with those in SEM-Luc-control siRNA cells under 5 ng/mL of TNF- α (Figure 2).

SEM-Luc-S100A6 siRNA cells were sensitive to TNF- α , while SEM-Luc-control siRNA cells showed resistance

There were no significant differences between the growth of SEM-Luc-S100A6 siRNA and SEM-Luc-control siRNA cells *in vitro* without TNF- α ($P = 0.890$) (Figure 3a). However, the growth of SEM-Luc-S100A6 siRNA cells was significantly inhibited by TNF- α in comparison with SEM-Luc-control siRNA cells ($P = 0.012$ for 1 ng/mL of TNF- α , $P = 0.005$ for 10 ng/mL of TNF- α and $P = 0.012$ for 100 ng/mL of TNF- α) (Figure 3b).

No significant differences in serum concentration of human TNF- α were observed between SEM-Luc-S100A6 siRNA-injected and SEM-Luc-control siRNA-injected mice

In the *in vivo* analysis, there were no significant differences between the serum concentrations of human TNF- α 3 weeks after injection of human PBMCs in SEM-Luc-S100A6 siRNA-injected mice and SEM-Luc-control siRNA-injected mice (145.0 ± 5.0 vs 150.0 ± 40.0 pg/mL, respectively, $P = 0.95$) (Figure 4a).

Significant differences in tumor growth were observed between SEM-Luc-S100A6 siRNA-injected mice and SEM-Luc-control siRNA-injected mice

Although there were no significant differences in tumor size between SEM-Luc-S100A6 siRNA-injected mice and SEM-Luc-control siRNA-injected mice ($2.59 \pm 0.15 \times 10^5$ vs $3.45 \pm 0.22 \times 10^5$ p/s, respectively, $P = 0.52$), there were significant differences in tumor size 3 weeks after injection of human PBMCs (6 weeks after SEM cell engraftment) between these two

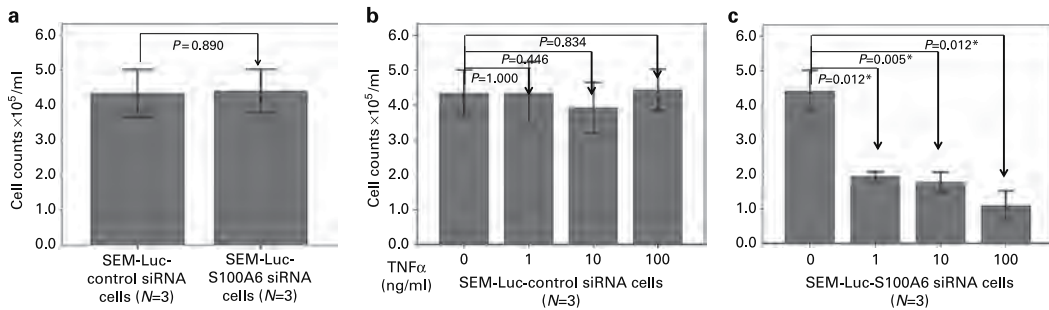


Figure 3. Growth of SEM-Luc-control siRNA cells and SEM-Luc-S100A6 siRNA cells *in vitro*. **(a)** Growth of SEM cells without TNF- α . There were no significant differences in growth between SEM-Luc-control siRNA cells and SEM-Luc-S100A6 siRNA cells *in vitro* without TNF- α . **(b)** Growth of SEM cells with TNF- α . No significant inhibition by TNF- α was observed in SEM-Luc-control siRNA cells *in vitro* with TNF- α . **(c)** Growth of SEM cells with TNF- α . Significant inhibition by TNF- α was observed in SEM-Luc-S100A6 siRNA cells *in vitro* with TNF- α .

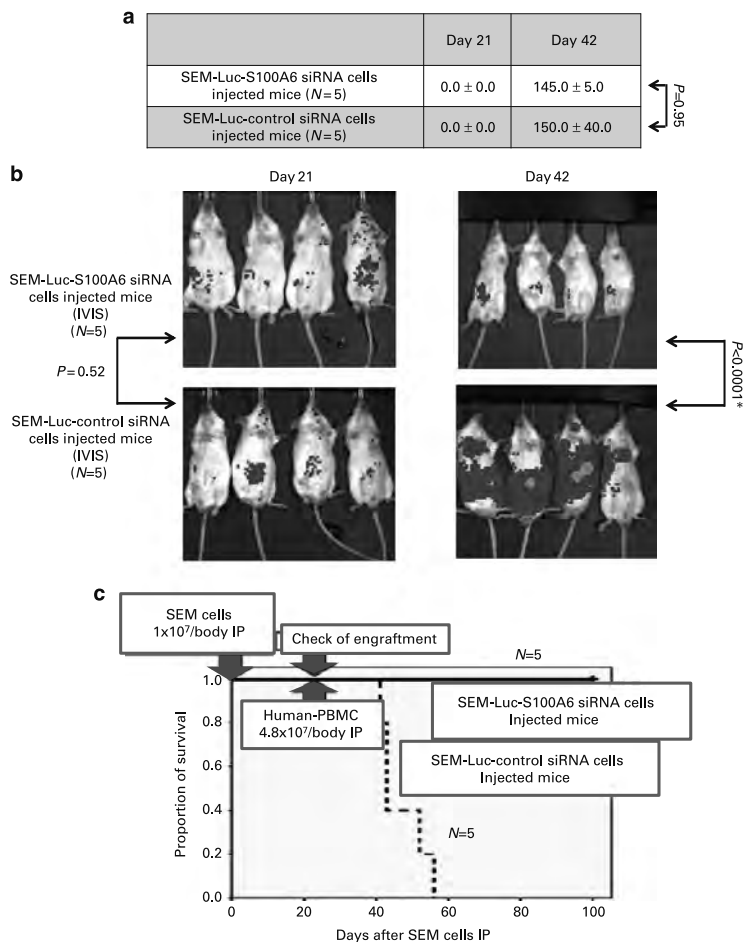


Figure 4. Comparison between SEM-Luc-control siRNA cell-injected mice and SEM-Luc-S100A6 siRNA cell-injected mice. **(a)** Serum concentration of human TNF- α of SEM-injected SCID mice. There were no significant differences between SEM-Luc-control siRNA cell-injected mice and SEM-Luc-S100A6 siRNA cell-injected mice. **(b)** Tumor growth in SEM-injected SCID mice. The growth rate was significantly lower in SEM-Luc-S100A6 siRNA cell-injected mice than in SEM-Luc-control siRNA cell-injected mice. **(c)** OS curves of SEM-injected SCID mice. Significantly longer survival was observed in SEM-Luc-S100A6 siRNA cell-injected mice compared with SEM-Luc-control siRNA cell-injected mice.

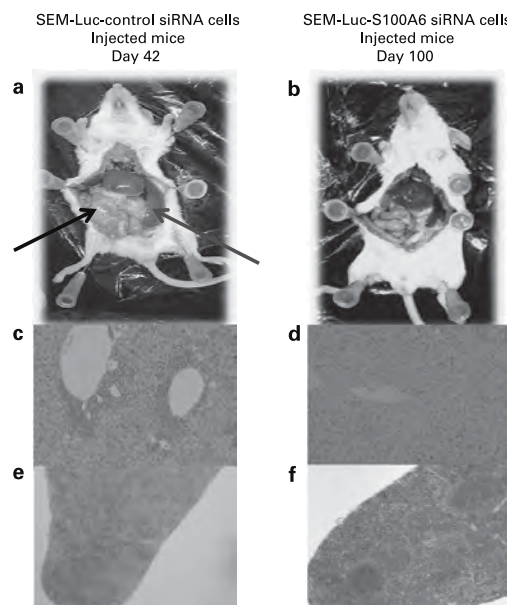


Figure 5. Comparison of macropathology and micropathology between SEM-Luc-control siRNA cell-injected mice and SEM-Luc-S100A6 siRNA cell-injected mice. (a) Macropathology of SEM-Luc-control siRNA-injected SCID mice. Red arrow: splenomegaly. Black arrow: massive tumor. (b) Macropathology of SEM-Luc-S100A6 siRNA-injected SCID mice. Splenomegaly and tumor were not observed. (c) Infiltration of the liver by lymphoma cells in SEM-Luc-control siRNA-injected mice. (d) No infiltration of the liver by lymphoma cells was observed in SEM-Luc-S100A6 siRNA-injected mice. (e) Disruption of the spleen structure by lymphoma cells in SEM-Luc-control siRNA-injected mice. (f) No disruption of the spleen structure by lymphoma cells was observed in SEM-Luc-S100A6 siRNA-injected mice. A full color version of this figure is available at the *Bone Marrow Transplantation* journal online.

groups ($2.98 \pm 0.80 \times 10^5$ vs $2.54 \pm 0.63 \times 10^6$ p/s, respectively, $P < 0.0001$) (Figure 4b).

SEM-Luc-S100A6 siRNA-injected mice showed significantly longer OS than SEM-Luc-control siRNA-injected mice

Figure 4c shows the OS curves of SEM-Luc-S100A6 siRNA-injected mice and SEM-Luc-control siRNA-injected mice. The difference in OS between the two groups of mice was significant (median > 100 days vs median 54 days, respectively, $P = 0.002$).

Macropathology of SEM-Luc-S100A6 siRNA-injected mice and SEM-Luc-control siRNA-injected mice

Figures 5a and b show the macropathology of SEM-Luc-control siRNA-injected mice and SEM-Luc-S100A6 siRNA-injected mice. Although SEM-Luc-control siRNA-injected mice showed massive tumors and splenomegaly on day 42 after SEM cell injection, no such tumors were observed in SEM-Luc-S100A6 siRNA-injected mice even on day 100 after SEM cell injection.

Micropathology of SEM-Luc-S100A6 siRNA-injected mice and SEM-Luc-control siRNA-injected mice

Histopathological analysis showed disruption of the spleen structure (Figure 5e) and infiltration of the liver and spleen by lymphoma cells in SEM-Luc-control siRNA-injected mice

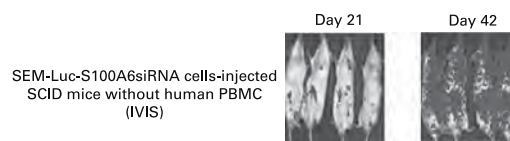


Figure 6. SCID mice could not inhibit the growth of SEM-Luc-S100A6 siRNA cells without human PBMCs.

(Figures 5c and e) in comparison with those in SEM-Luc-S100A6 siRNA-injected mice (Figures 5d and f).

DISCUSSION

The results of the present study indicate that inhibition of S100A6 can induce the GVL effect in MLL/AF4-positive ALL in a mouse model. We reported previously that MLL/AF4-positive ALL cell lines are resistant to TNF- α , which is the main factor involved in the GVL effect, by upregulation of S100A6 via inhibition of upregulation of the p53-caspase 8-caspase 3 pathway.⁴ The results of this study together with our previous findings suggest that inhibition of S100A6 may be a promising therapeutic target for MLL/AF4-positive ALL in combination with allo-HSCT because it induces GVL effects on MLL/AF4-positive ALL, which is otherwise resistant to GVL.

In an *in vivo* study, we used SCID mice which have functional natural killer (NK) cells without any conditioning. Therefore we previously examined whether only NK cells of SCID mice could inhibit or reject SEM-Luc-S100A6 siRNA cells. The results of that study are shown in Figure 6. Only NK cells of SCID mice could not inhibit the growth of SEM-Luc-S100A6 siRNA cells. This result showed that the inhibition of growth of SEM-Luc-S100A6 siRNA cells in PBMC-SCID mice is mainly due to human PBMCs. Interestingly, Spijkers-Hagelstein *et al.*¹² reported that overexpression of the S100 protein family members S100A8 and S100A9 in MLL/AF4-positive ALL was associated with failure to induce free-cytosolic Ca^{2+} and prednisolone resistance. These worthy data together with those of the present study suggest that high expression levels of S100 proteins by MLL/AF4-positive ALL may be the main factors in therapy resistance and poor prognosis of MLL/AF4-positive ALL.

The incidence of MLL/AF4-positive ALL shows a major peak in early infancy, which accounts for over 50% of ALL cases in infants less than 6 months of age; 10–20% of cases occur in older infants, 2% in children and up to 7% in adults.^{13–16} Although the 5-year OS of childhood ALL patients has improved to as much as 90% due to progress in chemotherapy and other supporting therapeutic modalities, including allo-HSCT,¹⁷ the prognosis is still poor for the remaining 10% of cases, which consist mainly of MLL/AF4-positive ALL and Ph chromosome-positive ALL. As use of BCR-ABL tyrosine kinase inhibitors targeting Ph chromosome-positive ALL has been explored, MLL/AF4-positive ALL is the greatest obstacle to overcoming childhood ALL.

Our results suggest that the development of drugs targeting S100 proteins may lead to improvements in MLL/AF4-positive ALL, which is the greatest obstacle to overcoming childhood ALL.

CONFLICT OF INTEREST

The authors declare no conflict of interest.

AUTHORSHIP

HT designed and conducted and performed the research, and wrote the paper. KM, HY, KD, TS and KI partially conducted the research.

REFERENCES

- 1 Harper DP, Aplan PD. Chromosomal rearrangements leading to MLL gene fusions: clinical and biological aspects. *Cancer Res* 2008; **68**: 10024–10027.
- 2 Pui CH, Gaynon PS, Boyett JM, Chessells JM, Baruchel A, Kamps W *et al*. Outcome of treatment in childhood acute lymphoblastic leukaemia with rearrangements of the 11q23 chromosomal region. *Lancet* 2002; **359**: 1909–1915.
- 3 Ringdén O, Karlsson H, Olsson R, Omazic B, Uhlén M. The allogeneic graft-versus-cancer effect. *Br J Haematol* 2009; **147**: 614–633.
- 4 Tamai H, Miyake K, Yamaguchi H, Takatori M, Dan K, Inokuchi K *et al*. Resistance of MLL-AFF1-positive acute lymphoblastic leukemia to tumor necrosis factor- α is mediated by S100A6 upregulation. *Blood Cancer J* 2011; **1**: e38.
- 5 Stomnicki ŁP, Nawrot B, Leśniak W. S100A6 binds p53 and affects its activity. *Int J Biochem Cell Biol* 2009; **41**: 784–790.
- 6 van Dieck J, Fernandez-Fernandez MR, Veprintsev DB, Fersht AR. Modulation of the oligomerization state of p53 by differential binding of proteins of the S100 family to p53 monomers and tetramers. *J Biol Chem* 2009; **284**: 13804–13811.
- 7 Tsoporis JN, Izhar S, Parker TG. Expression of S100A6 in cardiac myocytes limits apoptosis induced by tumor necrosis factor- α . *J Biol Chem* 2008; **283**: 30174–30183.
- 8 van Dieck J, Brandt T, Teufel DP, Veprintsev DB, Joerger AC, Fersht AR. Molecular basis of S100 proteins interacting with the p53 homologs p63 and p73. *Oncogene* 2010; **29**: 2024–2035.
- 9 Tamai H, Miyake K, Yamaguchi H, Takatori M, Dan K, Inokuchi K *et al*. AAV8 vector expressing IL24 efficiently suppresses tumor growth mediated by specific mechanisms in MLL/AF4-positive ALL model mice. *Blood* 2012; **119**: 64–71.
- 10 Miyake K, Flygare J, Kiefer T, Utsugisawa T, Richter J, Ma Z *et al*. Development of cellular models for ribosomal protein S19(RPS19)-deficient diamond-blackfan anemia using inducible expression of siRNA against RPS19. *Mol Ther* 2005; **11**: 627–637.
- 11 Utz JP, Limper AH, Kalra S, Specks U, Scott JP, Vuk-Pavlovic Z *et al*. Etanercept for the treatment of stage II and III progressive pulmonary sarcoidosis. *Chest* 2003; **124**: 177–185.
- 12 Spijkers-Hagelstein JA, Schneider P, Hulleman E, de Boer J, Williams O, Pieters R *et al*. Elevated S100A8/S100A9 expression causes glucocorticoidresistance in MLL-rearranged infant acute lymphoblastic leukemia. *Leukemia* 2012; **26**: 1255–1265.
- 13 Pui CH, Relling MV, Downing JR. Acute lymphoblastic leukemia. *N Engl J Med* 2004; **350**: 1535–1548.
- 14 Moorman AV, Harrison CJ, Buck GA, Richards SM, Secker-Walker LM, Martineau M *et al*. Karyotype is an independent prognostic factor in adult acute lymphoblastic leukemia (ALL): analysis of cytogenetic data from patients treated on the Medical Research Council (MRC) UKALLXII/Eastern Cooperative Oncology Group (ECOG) 2993 trial. *Blood* 2007; **109**: 3189–3197.
- 15 Pui CH, Kane JR, Crist WM. Biology and treatment of infant leukemias. *Leukemia* 1995; **9**: 762–769.
- 16 Pui CH, Ribeiro RC, Campana D, Raimondi SC, Hancock ML, Behm FG *et al*. Prognostic factors in the acute lymphoid and myeloid leukemias of infants. *Leukemia* 1996; **10**: 952–956.
- 17 Eden TO, Pieters R, Richards S. Childhood Acute Lymphoblastic Leukaemia Collaborative Group (CALLCG). Systematic review of the addition of vincristine plus steroid pulses in maintenance treatment for childhood acute lymphoblastic leukaemia - an individual patient data meta-analysis involving 5,659 children. *Br J Haematol* 2010; **149**: 722–733.

ORIGINAL ARTICLE

Complex molecular genetic abnormalities involving three or more genetic mutations are important prognostic factors for acute myeloid leukemia

S Wakita^{1,8}, H Yamaguchi^{1,8}, T Ueki², K Usuki³, S Kurosawa⁴, Y Kobayashi⁵, E Kawata⁵, K Tajika⁶, S Gomi⁶, M Koizumi⁷, Y Fujiwara¹, S Yui¹, K Fukunaga¹, T Ryotokuji¹, T Hirakawa¹, K Arai¹, T Kitano¹, F Kosaka¹, H Tamai¹, K Nakayama¹, T Fukuda⁴ and K Inokuchi¹

We conducted a comprehensive analysis of 28 recurrently mutated genes in acute myeloid leukemia (AML) in 271 patients with *de novo* AML. Co-mutations were frequently detected in the intermediate cytogenetic risk group, at an average of 2.76 co-mutations per patient. When assessing the prognostic impact of these co-mutations in the intermediate cytogenetic risk group, overall survival (OS) was found to be significantly shorter ($P=0.0006$) and cumulative incidence of relapse (CIR) significantly higher ($P=0.0052$) in patients with complex molecular genetic abnormalities (CMGAs) involving three or more mutations. This trend was marked even among patients aged ≤ 65 years who were also *FLT3*-ITD (*FMS*-like tyrosine kinase 3 internal tandem duplications)-negative (OS: $P=0.0010$; CIR: $P=0.1800$). Moreover, the multivariate analysis revealed that CMGA positivity was an independent prognostic factor associated with OS ($P=0.0007$). In stratification based on *FLT3*-ITD and *CEBPA* status and 'simplified analysis of co-mutations' using seven genes that featured frequently in CMGAs, CMGA positivity retained its prognostic value in transplantation-aged patients of the intermediate cytogenetic risk group (OS: $P=0.0002$, CIR: $P<0.0001$). In conclusion, CMGAs in AML were found to be strong independent adverse prognostic factors and simplified co-mutation analysis to have clinical usefulness and applicability.

Leukemia (2016) 30, 545–554; doi:10.1038/leu.2015.288

INTRODUCTION

Genomic analysis of acute myeloid leukemia (AML) patients has revealed the involvement of various chromosomal abnormalities and molecular genetic mutations in the onset of AML.^{1–3} Numerous cohort studies have sought to determine the significance of the recurrent genetic abnormalities in AML patients and have revealed strong associations between genetic abnormalities and the pathogenesis and prognosis of the disease.⁴ These discoveries have spurred a new phase in prognostic stratification and therapeutic strategies. To date, chromosomal analysis has been the most important prognostic factor for transplantation-aged AML patients, but $\sim 60\%$ of patients are classified as having intermediate cytogenetic risk.⁵ Since the latter half of the 1990s, numerous genetic mutations associated with AML have been identified, and attempts have been made to stratify prognoses based on them. Among these mutations, *FMS*-like tyrosine kinase 3 internal tandem duplications (*FLT3*-ITD), *nucleophosmin 1* (*NPM1*) mutations and *CCAAT/enhancer-binding protein A* (*CEBPA*) mutations are prognostically significant,^{6–15} and many large-scale cohort studies have shown that these mutations can predict long-term prognosis.^{16,17} Guidelines of the European Leukemia Net (ELN) and National Comprehensive Cancer Network (NCCN), which are widely used in clinical settings, have incorporated these prognostic factors.^{18,19} Recently, new recurrent mutations in DNA methylation modifiers, such as *DNA methyltransferase 3a*

(*DNMT3A*), *Tet methylcytosine dioxygenase 2* (*TET2*), *isocitrate dehydrogenase 1* (*IDH1*) and *isocitrate dehydrogenase 2* (*IDH2*),^{20–24} as well as cohesin-related genes,^{25–31} were detected at high frequency and are now gaining attention. It remains unclear whether these genetic mutations are associated with the prognosis of a certain subset of AML patients. Moreover, substantial advances of genomic analysis in recent years have made it possible to identify new mutations, with ≥ 50 such mutations recurrently being detected in AML patients.^{25,30,32} Yet, attempts at prognostic stratification using these new mutations have been chaotic, and the complex results have made stratification difficult to apply in clinical settings.

The clinical application of *FLT3*-ITD and mutations in *NPM1* and *CEBPA*, which has been established as important, has some unsolved problems. For example, *FLT3*-ITD is a strong adverse prognostic factor, with patients harboring the mutation at initial presentation losing it on relapse in 30% of cases.^{33–36} However, the reasons underlying relapse and resistance to treatment have not been sufficiently explained. Although many studies have reported high remission rates associated with *NPM1* mutations, some patients lose the *NPM1* mutations on relapse, and others newly acquire certain mutations, such as *FLT3*-ITD, that result in relapse.³⁷ Notably, in certain cases, such patients acquire resistance to therapy. Moreover, although a mutation in one location of the *CEBPA* gene does not serve as a prognostic factor,

¹Department of Hematology, Nippon Medical School, Tokyo, Japan; ²Department of Hematology, Nagano Red Cross Hospital, Nagano, Japan; ³Department of Hematology, NTT Medical Center Tokyo, Tokyo, Japan; ⁴Department of Hematopoietic Stem Cell Transplantation, National Cancer Center Hospital, Tokyo, Japan; ⁵Department of Hematology, Japanese Red Cross Kyoto Daini Hospital, Kyoto, Japan; ⁶Department of Hematology, Yokohama Minami Kyousai Hospital, Yokohama, Japan and ⁷Department of Gastroenterology, Asahi General Hospital, Chiba, Japan. Correspondence: Dr H Yamaguchi, Department of Hematology, Nippon Medical School, 1-1-5 Sendagi, Bunkyo-Ku, Tokyo 113-8603, Japan.

E-mail: y-hiroki@fd6.so-net.ne.jp

⁸These two authors contributed equally to this work.

Received 30 May 2015; revised 4 October 2015; accepted 7 October 2015; accepted article preview online 21 October 2015; advance online publication, 13 November 2015

mutations in two locations, which consist of biallelic mutations involving an N-terminal mutation on one allele and a C-terminal mutation on the other (that is, double mutations) in most cases, are associated with a favorable prognosis. The mechanisms underlying this biological paradox, in which a single mutation is associated with a worse prognosis than a double mutation, have yet to be explained.^{7,9,38}

Deep sequencing technology may help address some of these outstanding questions. In fact, deep sequencing-based genomic analysis of AML patients has started to clarify the clonal evolution process resulting from the acquirement of genetic mutations. In 2012, Ding et al.³⁹ reported the whole-genome analysis of primary and relapsed AML using next-generation sequencers. Two possibilities regarding AML relapse were proposed: (1) founding clones gain mutations and evolve into relapse clones and (2) subclones with different mutations exist among founding clones, and a subclone from this population expands at relapse. They also reported that in addition to the major mutations, mutations in *WAC*, *SMC3*, *DIS3*, *DDX41* and *DAXX* are also observed at relapse.³⁹ After this initial study, the acquirement of numerous genetic mutations was found to be strongly associated with AML onset, with further co-mutations contributing to clonal diversity and leading to the generation of treatment-resistant clones.^{40,41} Many studies have reported that combined chromosomal abnormalities (complex karyotypes) are associated with treatment resistance and adverse prognosis in AML.^{5,42–44} Yet, no study has assessed the relationship between co-mutations and prognosis. The present study aimed to determine the significance of newly reported genetic mutations and the impact of co-mutations comprising them on prognosis. To this end, we conducted a comprehensive analysis of 28 recurrently mutated genes in AML.

MATERIALS AND METHODS

Patients

The target population included 271 *de novo* AML patients (excluding M3) treated at Nippon Medical School Hospital or its affiliated institutions. A comprehensive genetic mutational analysis, as described below, was conducted among patients with $\geq 20\%$ blasts in bone marrow or peripheral blood. The study was conducted in accordance with the Declaration of Helsinki. Informed consent was obtained from patients, and the analysis and treatments were conducted while respecting the welfare and free will of the patients. This protocol was approved by our institutional review board.

Screening for chromosomal abnormalities

G-band analysis was performed on bone marrow samples obtained from patients at initial presentation. When obtaining bone marrow samples was difficult, peripheral blood was used instead. For patients suspected of being M2, M3, or M4eo based on the FAB (French–American–British) classification, fluorescence *in situ* hybridization analysis was used to additionally search for *RUNX1-RUNX1T1*, *PML-RARA* and *CBFB-MYH11* mutations.

Screening for molecular genetic abnormalities in all exons of 20 genes and hot spots of 8 genes

An oligonucleotide library was generated by emulsion PCR using order-made probes designed against the exons of the following 20 genes: *TET2* (HUGO Gene Nomenclature Committee (HGNC): 25941), *DNMT3A* (HGNC: 2978), *ASXL1* (HGNC: 18318), *KMT2A* (HGNC: 7132; the HGNC nomenclature of *MLL* has recently changed to *KMT2A*), *RUNX1* (HGNC: 10471), *KIT* (HGNC: 6342), *TP53* (HGNC: 11998), *PTPN11* (HGNC: 9644), *GATA2* (HGNC: 4171), *WT1* (HGNC: 12796), *STAG2* (HGNC: 11355), *RAD21* (HGNC: 9811), *SMC1A* (HGNC: 11111), *SMC3* (HGNC: 2468), *DAXX* (HGNC: 2681), *BCOR* (HGNC: 20893), *BCORL1* (HGNC: 25657), *NF1* (HGNC: 7765), *DDX41* (HGNC: 18674) and *PHF6* (HGNC: 18145). The library was sequenced with the next-generation sequencer, the Ion torrent personal genome machine (Thermo Fisher Scientific, Waltham, MA, USA). With respect to detected mutations, NCBI (National Center for Biotechnology Information) and COSMIC

(Catalogue Of Somatic Mutations In Cancer) databases were used to search for polymorphisms and cancer-related mutations. For newly identified mutations, we searched for genetic polymorphisms using Sanger sequencing with remission-stage samples.

Genes located in known hot spots (*FLT3*-ITD and *FLT3*-TKD, *NPM1*, *IDH1*, *IDH2*, *NRAS* and *KRAS*), those for which probe design for emulsion sequencing was difficult (*CEBPA*) and those for which analysis with Ion torrent personal genome machine (Thermo Fisher Scientific) was difficult (partial tandem duplication of the *KMT2A* gene (*KMT2A*-PTD)) were analyzed using previously reported methods.³⁶

Statistical analysis

The primary end point was overall survival (OS). A hazard ratio (HR) of 0.632 and 50% of proportion of OS were assumed for the sample size calculation. Recruitment of ~180 patients allowed for a power of 80% for detecting a difference of that size with a type I error of 5%. Retrospectively assessed this study, there were 184 intermediate cytogenetic risk patients, whom 99 died during the period. Consequently, our analysis provided a 80% statistical power to detect HR of 0.621 with a significance level (α) of 0.05 (two-tailed) regarding OS. OS was defined as the time interval from the date of diagnosis to the date of death. Cumulative incidence of relapse (CIR) for patients who had achieved complete remission (CR) was calculated from the time interval from the date of CR to the date of relapse.

The χ^2 test was used to test the association between categorical variables and the presence and absence of mutations. Fisher's exact test was used if the expected frequency of an event was < 5 in any cell of a 2×2 table. The nonparametric Mann–Whitney *U*-test was used to determine the statistical significance of differences in median values. All statistical tests were two sided. Moreover, the Kaplan–Meier method and log-rank test were used to analyze OS and CIR. With respect to prognostic factors, multivariate analysis was conducted with the Cox proportional hazards model. A stepwise backward procedure selection model was used to extract independent events. Events at a significance level of $P \leq 0.20$ were analyzed. Statistical analyses were performed using GraphPad Prism (version 6.00 for Windows, GraphPad Software, La Jolla, CA, USA) and IBM SPSS Statistics (version 21.0 for Windows, IBM Corporation, Armonk, NY, USA), and power calculation was performed using GraphPad StatMate (version 2.00 for windows).

RESULTS

Clinical characteristics

Of the 271 patients, 57.9% were male, with a median age of 54.9 years (range, 17–86 years). The median observation period was 772.7 days. As demonstrated in Supplementary Table 1, the Chromosomal Classification according to the 2013 NCCN guidelines classified these patients into the following: favorable cytogenetic risk (47 patients), intermediate cytogenetic risk (184 patients) and poor cytogenetic risk (40 patients). Prognostic stratification was possible for CR rate, OS and CIR based on chromosomal analysis of the present cohort, as in previous reports (CR rate: favorable cytogenetic risk, 93.6%; intermediate cytogenetic risk, 63.2%; poor cytogenetic risk, 32.4%; $P < 0.0001$; 5-year OS: favorable cytogenetic risk, 56.1%; intermediate cytogenetic risk, 28.7%; poor cytogenetic risk, 11.7%; $P = 0.0001$; and 5-year CIR: favorable cytogenetic risk, 51.7%; intermediate cytogenetic risk, 70.5%; poor cytogenetic risk, 91.3%; $P = 0.0003$) (Supplementary Table 2a).

Impact of each mutation on prognosis

In the favorable and poor cytogenetic risk groups, none of the mutations were associated with remission rate (data not shown). In the intermediate cytogenetic risk group, mutations in *NPM1*, *CEBPA* (particularly double mutations) and *PTPN11* were significantly associated with a high remission rate (Supplementary Table 2b).

In the favorable and poor cytogenetic risk groups, none of the mutations predicted OS (data not shown). In the intermediate cytogenetic risk group, mutations in the following were identified as significant adverse prognostic factors: *TP53* ($P < 0.0001$),

FLT3-ITD ($P=0.0003$) and *DNMT3A* ($P=0.0065$), whereas *CEBPA* double mutation (*CEBPA* dm) was identified as a significant favorable prognostic factor ($P=0.0068$) (Supplementary Table 2b). In patients aged ≤ 65 years in the intermediate cytogenetic risk group, mutations in the following were identified as significant prognostic factors: *FLT3*-ITD ($P=0.0001$), *DNMT3A* ($P=0.0053$) and *TET2* ($P=0.0060$), whereas *CEBPA* dm was identified as a significant favorable prognostic factor ($P=0.0135$) (Supplementary Table 2c). On the other hand, *NPM1* mutations that showed a tendency for favorable prognosis in previous studies were not significantly associated with OS and CIR, even if we assess for patients of the intermediate cytogenetic risk group excluding *FLT3*-ITD-positive patients (5-year OS: positive, 43.48%; negative, 49.63%; $P=0.2168$).

Analysis of genetic mutations

The rate of detection of each mutation is shown in Figure 1a, and the number of mutations per patient is shown in Figure 1b. Many mutations were detected in the intermediate cytogenetic risk group, and were often found in combination, with an average of

2.76 mutations per patient. Mutations in the *KIT* gene were detected at high frequency in the favorable cytogenetic risk group, and mutations in the *TP53* gene were detected at high frequency in the poor cytogenetic risk group (in particular, in complex karyotype cases) (*KIT* mutation \times favorable cytogenetic risk: $P < 0.0001$; *TP53* mutation \times poor cytogenetic risk: $P=0.0019$).

In the intermediate cytogenetic risk group, which had a high frequency of co-mutations, significant coexistence was detected for mutations in the following genes: *FLT3*-ITD \times *NPM1*, *FLT3*-ITD \times *DNMT3A*, *NPM1* \times *PTPN11*, *NPM1* \times *DNMT3A*, *NPM1* \times *TET2* and *DNMT3A* \times *IDH2*. Mutations of the following genes were mutually exclusive: *FLT3*-ITD \times *NRAS*, *FLT3*-ITD \times *CEBPA*, *CEBPA* \times *NPM1*, *NPM1* \times *KMT2A*-PTD and *CEBPA* \times *DNMT3A* (Figure 2).

Co-mutations

Characteristics of patients with CMGAs harboring ≥ 3 mutations. Complex molecular genetic abnormalities (CMGAs) harboring ≥ 3 mutations were detected in 63.0% of patients with the intermediate cytogenetic risk. Table 1 summarizes the

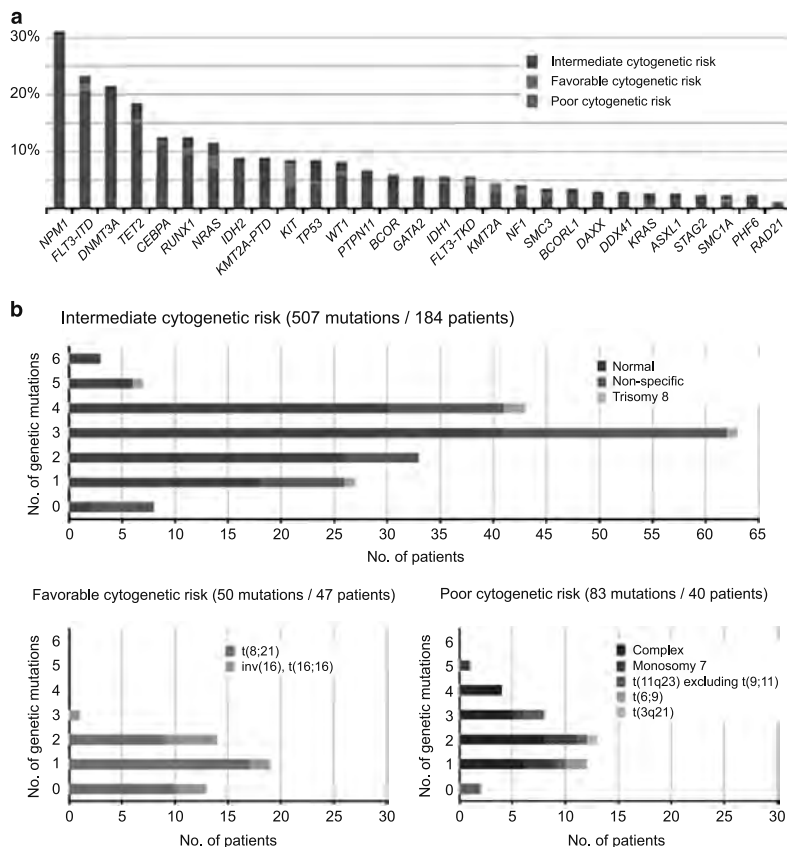


Figure 1. (a) Frequency of analyzed genetic mutations in the *de novo* AML cohort. Blue represents intermediate cytogenetic risk, green represents favorable cytogenetic risk and red represents poor cytogenetic risk. Many of the mutations were detected in the intermediate cytogenetic risk group, although mutations in *KIT* and *TP53* genes were frequently detected in the favorable and poor cytogenetic risk groups, respectively (*KIT* mutation \times favorable cytogenetic risk: $P < 0.0001$; *TP53* mutation \times poor cytogenetic risk: $P=0.0019$). (b) Number of genetic mutations according to cytogenetic risk. Mean numbers of mutations detected per patient by cytogenetic risk were as follows: intermediate cytogenetic risk, 2.76/patient; poor cytogenetic risk, 2.08/patient; and favorable cytogenetic risk, 1.06/patient. There was a high frequency of co-mutations in the intermediate cytogenetic risk group, and a trend for few co-mutations in the favorable cytogenetic risk group.

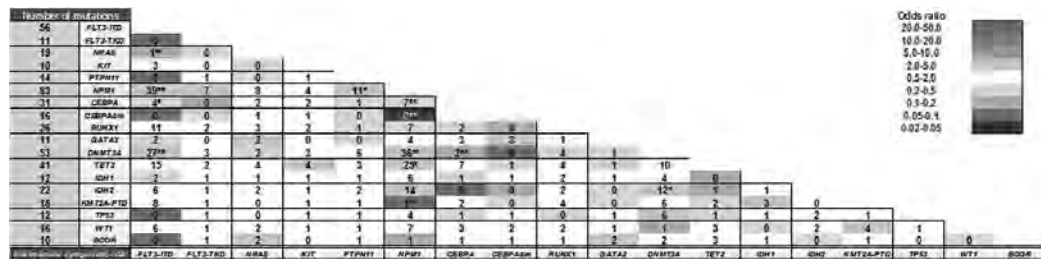


Figure 2. Pairwise associations among genetic mutations found in the intermediate cytogenetic risk group. We listed only genetic mutations detected over 10 patients in this figure. Associations are colored by odds ratio. Blue depicts mutually exclusive gene pairs, and red depicts gene pairs that are co-mutated more than expected by chance. * $P < 0.05$; ** $P < 0.01$.

characteristics of CMGA-positive patients. There were no significant differences in age, chromosomal analysis and treatment between CMGA-positive and -negative patients. When assessing the mutations comprising the CMGAs, mutations in *NPM1* ($P < 0.0001$), *DNMT3A* ($P < 0.0001$), *FLT3-ITD* ($P < 0.0001$), *TET2* ($P = 0.0001$) and *IDH1/2* ($P = 0.0048$) were strongly involved in CMGAs in the intermediate cytogenetic risk group, and mutations in *WT1* and *KMT2A-PTD* were also included in CMGAs at a high frequency. However, *CEBPA* dm ($P = 0.0019$) were mutually exclusive with CMGAs.

Analysis of prognosis of survival and remission. In the intermediate cytogenetic risk group, patients with CMGAs had a significantly shorter OS than those without CMGAs (5-year OS: CMGA-positive, 18.1%; CMGA-negative, 45.9%; $P = 0.0006$), but a significantly higher CIR (5-year CIR: CMGA-positive, 83.2%; CMGA-negative, 52.6%; $P = 0.0052$). This trend was also significant among patients aged ≤ 65 years old (5-year OS: CMGA-positive, 24.1%; CMGA-negative, 58.9%; $P < 0.0001$; 5-year CIR: CMGA-positive, 79.2%; CMGA-negative, 48.1%; $P = 0.0073$). Moreover, as CMGA positivity was a significant prognostic factor for *FLT3-ITD* negative patients aged ≤ 65 years in the intermediate cytogenetic risk group (5-year OS: CMGA-positive, 28.36%; CMGA-negative, 63.20%; $P = 0.0010$; 5-year CIR: CMGA-positive, 75.68%; CMGA-negative, 44.55%; $P = 0.1800$), CMGA positivity could be considered an adverse prognostic factor independent of *FLT3-ITD* (Figures 3a–f).

Similarly, in analysis of AML with normal karyotype only (NK-AML), CMGA positivity was a significant adverse prognostic factor for OS and CIR (5-year OS: CMGA-positive, 29.0%; CMGA-negative, 52.6%; $P = 0.0088$; 5-year CIR: CMGA-positive, 76.5%; CMGA-negative, 47.0%; $P = 0.0048$). This trend was also significant among patients aged ≤ 65 years (5-year OS: CMGA-positive, 31.9%; CMGA-negative, 68.7%; $P = 0.0006$; 5-year CIR: CMGA-positive, 76.0%; CMGA-negative, 40.3%; $P = 0.0029$). In analysis of *FLT3-ITD*-negative NK-AML, CMGA positivity was a significant adverse factor in patients aged ≤ 65 years, affecting OS with a trend toward higher CIR (5-year OS: CMGA-positive, 43.0%; CMGA-negative, 74.8%; $P = 0.0066$; 5-year CIR: CMGA-positive, 69.1%; CMGA-negative, 33.9%; $P = 0.0566$) (Figures 4a–f).

In the intermediate cytogenetic risk group, when one point was allotted for each chromosomal aberration and the points added to the number of co-mutations, cases with more than three points also had a significantly shorter OS (5-year OS: CMGA-positive, 19.5%; CMGA-negative, 48.7%; $P = 0.0021$), and this trend was also significant among both patients aged ≤ 65 years (5-year OS: CMGA-positive, 25.1%; CMGA-negative, 64.0%; $P = 0.0003$) and *FLT3-ITD*-negative patients aged ≤ 65 years (5-year OS: CMGA-positive, 43.0%; CMGA-negative, 74.8%; $P = 0.0066$). However, there was no significant difference in CIR between the groups (Supplementary Figures 1A–F).

Multivariate analysis. In order to establish the importance of CMGA positivity, we conducted multivariate analyses to assess the effects of the following factors on OS and CIR for patients aged ≤ 65 years in the intermediate cytogenetic risk group: sex (male or female), white blood cell count on initial visit ($\geq 20\,000/\mu\text{l}$ or $< 20\,000/\mu\text{l}$), induction therapy (idarubicin plus cytarabine and daunorubicin plus cytarabine or not), post-remission therapy (hematopoietic stem cell transplantation on first CR or not), *FLT3-ITD* (positive or negative), *NPM1* mutation (positive or negative), *CEBPA* dm (positive or negative), *TET2* mutation (positive or negative), *DNMT3A* (positive or negative), *TP53* (positive or negative), *NRAS* (positive or negative), *KMT2A-PTD* (positive or negative) and CMGA (positive or not). Multivariate analyses with Cox proportional hazards models revealed that CMGA positivity (HR: 3.717, $P = 0.0007$, 95% confidence interval (CI): 1.7331–7.9722), hematopoietic stem cell transplantation on first CR as a post-remission therapy (HR: 0.362, $P = 0.0037$, 95% CI: 0.1826–0.7194) and *NPM1* mutation positivity (HR: 0.504, $P = 0.0355$, 95% CI: 0.2665–0.9547) were independent prognostic factors associated with OS (Table 2). With respect to CIR, hematopoietic stem cell transplantation on first CR as a post-remission therapy (HR: 0.258, $P = 0.0004$, 95% CI: 0.1218–0.5457) and *FLT3-ITD* positivity (HR: 2.179, $P = 0.0298$, 95% CI: 1.0791–4.4005) were independent prognostic factors. However, CMGA positivity did not reach statistical significance (HR: 1.792, $P = 0.1164$, 95% CI: 0.8651–3.7110) (Table 2).

Prognostic stratification based on a simplified CMGA analysis for clinical application. Our results indicate that CMGAs are useful in prognostic stratification. However, in order to apply CMGAs to clinical settings, comprehensive mutational analysis with next-generation sequencers is necessary. This is not a trivial issue, given the associated high costs.

When stratifying based on a 'simplified analysis of co-mutations' using 7 genes (*NPM1*, *DNMT3A*, *TET2*, *IDH1/2*, *WT1* and *KMT2A-PTD*) that were found to be present at high frequency in CMGAs, along with the status of *FLT3-ITD* and *CEBPA* dm, we found that CMGA positivity (that is, ≥ 3 co-mutations) was a strong adverse prognostic factor of patients of the intermediate cytogenetic risk group on OS and CIR, similar to *FLT3-ITD* positivity (5-year OS: *FLT3-ITD*-positive, 16.24%; *FLT3-ITD*-negative/*CEBPA* dm-positive, 68.38%; *FLT3-ITD*-negative/*CEBPA* dm-negative/CMGA-positive, 18.18%; *FLT3-ITD*-negative/*CEBPA* dm-negative/CMGA-negative, 30.84%; $P = 0.0003$; 5-year CIR: *FLT3-ITD*-positive, 87.50%; *FLT3-ITD*-negative/*CEBPA* dm-positive, 38.81%; *FLT3-ITD*-negative/*CEBPA* dm-negative /CMGA-positive, 100%; *FLT3-ITD*-negative/*CEBPA* dm-negative/CMGA-negative, 64.06%; $P \leq 0.0001$) (Figures 5a and b). Among patients aged ≤ 65 years, 'simplified analysis of co-mutations' was also useful for further classification significantly (5-year OS: *FLT3-ITD*-positive, 20.97%; *FLT3-ITD*-negative/*CEBPA* dm-positive, 74.07%; *FLT3-ITD*-negative/*CEBPA* dm-negative/

Table 1. Characteristics of patients harboring complex molecular genetic abnormalities (CMGAs)

Intermediate cytogenetic risk group, n = 184	All patients			Age ≤ 65 years		
	CMGA-positive, n = 116 (80)	CMGA-negative, n = 68 (46)	P-value	CMGA-positive, n = 73 (58)	CMGA-negative, n = 48 (31)	P-value
Male/female	60/56 (36/44)	37/31 (24/22)	0.7612 (0.4638)	39/34 (28/30)	26/22 (15/16)	1.0000 (1.0000)
Age (years)	56.2 (54.0) 18–85 (18–79)	52.5 (54.0) 17–86 (18–86)	0.1988 (0.8931)	46.6 (47.2) 18–65 (18–65)	43.6 (44.6) 17–65 (18–65)	0.3050 (0.4933)
FAB subtype						
M0	9 (5)	5 (4)		5 (3)	3 (3)	
M1	38 (23)	17 (12)		24 (18)	11 (7)	
M2	27 (21)	23 (16)		17 (14)	17 (12)	
M4	25 (21)	8 (6)		18 (16)	6 (4)	
M5	14 (9)	8 (5)		9 (7)	7 (4)	
M6	1 (0)	3 (1)		0 (0)	2 (1)	
M7	0 (0)	0 (0)		0 (0)	0 (0)	
Not determined	2 (1)	4 (2)	0.0749 (0.6350)	0 (0)	2 (1)	0.2809 (0.6307)
Cytogenetic mutation						
Normal karyotype: 126	80	46		58	31	
Trisomy 8: 5	4	1		3	1	
Others: 40	26	14		11	14	
Not determined: 13	6	7	0.2500	1	6	1.0000
Induction therapy						
IDA/AraC or DNR/AraC	61 (47)	35 (24)		44 (35)	31 (20)	
Others	55 (33)	33 (22)	1.0000 (0.5761)	29 (23)	17 (11)	0.7037 (0.8199)
HSCT on first CR						
Auto-HSCT	1 (1)	1 (1)		1 (1)	1 (1)	
Allo-HSCT	21: MRD10, MUD10, CB1 (14: MRD6, MUD7, CB1)	10: MRD5, MUD3, CB2 (4: MRD1, MUD2, CB1)	0.5000 (0.3151)	21: MRD10, MUD10, CB1 (14: MRD6, MUD7, CB1)	9: MRD5, MUD2, CB2 (3: MRD1, MUD1, CB1)	0.5000 (0.6220)
Achieving CR (%)	65.7% (66.7%)	48.8% (67.4%)	<u>0.0245</u> (1.0000)	65.2% (67.3%)	65.4% (71.0%)	1.0000 (0.8113)
OS						
Median OS (days)	459 (487)	1315 (not reached)		491 (542)	Not reached (not reached)	
5-Year OS	18.1% (29.0%)	45.9% (52.6%)	<u>0.0006</u> (0.0088)	24.1% (31.9%)	58.9% (68.7%)	<u>< 0.0001</u> (0.0006)
CIR						
Median CIR (days)	284 (279)	1505 (not reached)		344 (284)	Not reached (not reached)	
5-Years CIR	83.2% (76.5%)	52.6% (47.0%)	<u>0.0052</u> (0.0048)	79.2% (76.0%)	48.1% (40.3%)	<u>0.0073</u> (0.0029)
Genetic mutations included in CMGA						
NPM1	73 (60)	10 (10)	<u>< 0.0001</u> (<u>< 0.0001</u>)	49 (43)	4 (4)	<u>< 0.0001</u> (<u>< 0.0001</u>)
DNMT3A	48 (36)	5 (4)	<u>< 0.0001</u> (<u>< 0.0001</u>)	33 (27)	2 (1)	<u>< 0.0001</u> (<u>< 0.0001</u>)
FLT3-ITD	49 (39)	7 (6)	<u>< 0.0001</u> (<u>< 0.0001</u>)	36 (30)	5 (4)	<u>< 0.0001</u> (0.0005)
TET2	34 (23)	7 (7)	<u>0.0031</u> (0.1274)	19 (19)	3 (3)	<u>0.0072</u> (0.0200)
WT1	14 (7)	2 (0)	0.0545 (NA)	8 (8)	2 (1)	NA (NA)
KMT2A-PTD	15 (10)	3 (2)	0.0735 (NA)	11 (5)	2 (0)	0.0742 (NA)
IDH1	11 (8)	1 (1)	NA (NA)	4 (4)	1 (1)	NA (NA)
IDH2	18 (13)	4 (4)	0.0610 (0.2869)	9 (8)	2 (2)	NA (NA)
IDH1/2	28 (21)	5 (5)	<u>0.0048</u> (0.0428)	13 (12)	3 (3)	0.0986 (0.2424)
CEBPA	15 (10)	15 (13)	0.1469 (0.0332)	11 (10)	15 (12)	0.1258 (0.0382)
CEBPA double mutation	4 (2)	12 (11)	0.0019 (NA)	3 (2)	12 (11)	<u>0.0012</u> (NA)
CEBPA single mutation	11 (8)	4 (2)	0.5779 (NA)	8 (8)	3 (1)	NA (NA)

Abbreviations: AraC, cytarabine; CB, cord blood; CIR, cumulative incidence of relapse; CR, complete remission; DNR, daunorubicin; FAB, French–American–British; HSCT, hematopoietic stem cell transplantation; IDR, idarubicin; MRD, HLA-matched related donor; MUD, HLA-matched unrelated donor; NA, not applicable; OS, overall survival. The data of the normal karyotype are given in parenthesis. The underlines represent significant differences.

CMGA-positive, 25.00%; *FLT3*-ITD-negative/*CEBPA* dm-negative/CMGA-negative, 42.34%; $P = 0.0002$; 5-year CIR: *FLT3*-ITD-positive, 84.73%; *FLT3*-ITD-negative/*CEBPA* dm-positive, 33.71%; *FLT3*-ITD-negative/*CEBPA* dm-negative/CMGA-positive, 100%; *FLT3*-ITD-negative/*CEBPA* dm-negative/CMGA-negative, 59.11%; $P < 0.0001$) (Figures 5c and d).

DISCUSSION

In the present study, we conducted a comprehensive analysis of genetic mutations of 271 patients with *de novo* AML and clarified previously unknown partnerships between mutations repeatedly detected in AML. Whereas many of the mutations analyzed in this

study were detected in the intermediate cytogenetic risk group, *KIT* mutations were frequently detected in the favorable cytogenetic risk group and *TP53* mutations in the poor cytogenetic risk group (Figure 1a). The coexistence and mutual exclusivity of many of the mutations detected in the intermediate cytogenetic risk group became evident through our analyses (Figure 2). These results demonstrate the existence of strong partnerships between cytogenetic and genetic mutations.

Our findings suggest the possibility that genetic mutations can predict prognosis and response to chemotherapy in AML patients. We also confirmed that, in Japanese cohorts, *FLT3*-ITD is an adverse prognostic factor, and that *CEBPA* dm are a favorable prognostic factor, as reported previously. However, although

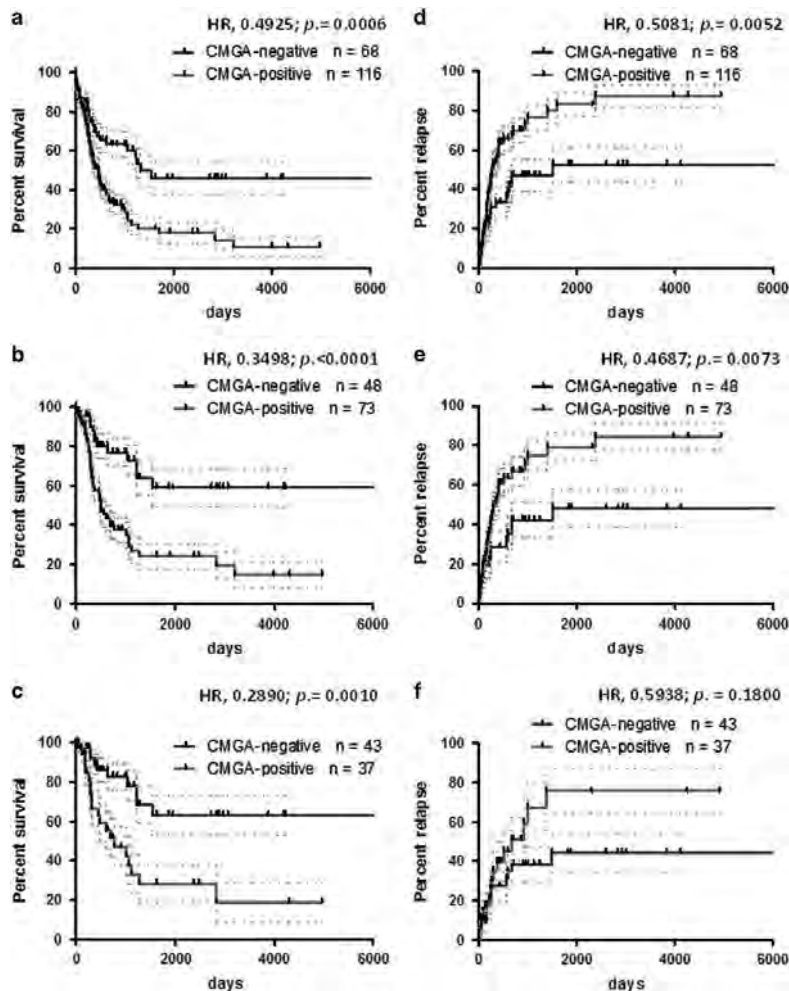


Figure 3. Prognostic impact of CMGAs in the intermediate cytogenetic risk group. Error bars represent s.e.m. (a) Kaplan–Meier curves of survival based on the presence or absence of CMGAs (all patients). (b) Kaplan–Meier curves of survival based on the presence or absence of CMGAs (patients aged ≤ 65 years). (c) Kaplan–Meier curves of survival based on the presence or absence of CMGAs (patients aged ≤ 65 years and *FLT3*-ITD-negative). (d) Kaplan–Meier curves of CIR based on the presence or absence of CMGAs (all patients). (e) Kaplan–Meier curves of CIR based on the presence or absence of CMGAs (patients aged ≤ 65 years). (f) Kaplan–Meier curves of CIR based on the presence or absence of CMGAs (patients aged ≤ 65 years and *FLT3*-ITD-negative).

NPM1-positive AML patients had a high remission rate consistent with previous reports, the relapse rate was also high (Supplementary Tables 2a–c). Thus, even if patients were *FLT3*-ITD negative, there was no trend for a favorable prognosis. This is consistent with the findings reported by the Japan Adult Leukemia Study Group (JALSG),⁴⁵ and may reflect racial differences.

CMGA positivity strongly predicted survival and relapse in AML patients. This result not only made possible the stratification of intermediate cytogenetic risk/*FLT3*-ITD-negative patients, for whom prognosis was previously considered difficult to predict based on genetic mutations, but also explains the genetic significance of each of the independently reported mutations in the clinical context. In other words, the combination of genetic

mutations (that is, co-mutations) is the most important adverse prognostic factor, and our results demonstrate that the impact of previously known *FLT3*-ITD and *CEBPA* dm on prognosis arises from (1) the high frequency of coexistence of multiple co-mutations with *FLT3*-ITD and (2) the mutual exclusivity of many co-mutations and *CEBPA* dm (Table 1). Our data also suggest that the unfavorable prognosis of Japanese *FLT3*-ITD-negative, *NPM1* mutation-positive AML patients may result from background co-mutations. Western studies have shown a trend of favorable prognosis in AML with mutated *NPM1* when the patient is in the intermediate cytogenetic risk group and is also *FLT3*-ITD negative. As mentioned above, in the univariate analysis, *NPM1* mutation positivity was not a favorable prognostic factor in our cohort, even if the patient was *FLT3*-ITD negative. The multivariate analysis,

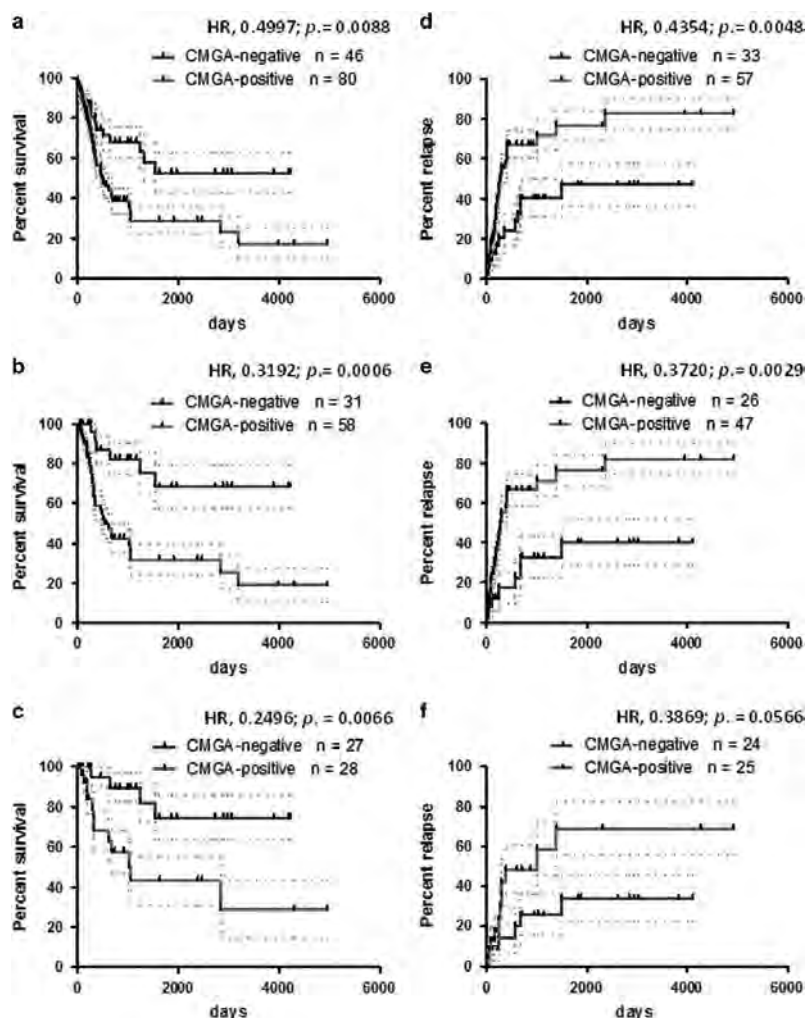


Figure 4. Prognostic impact of CMGAs in AML with normal karyotype. Error bars represent s.e.m. (a) Kaplan–Meier curves of survival based on the presence or absence of CMGAs (all patients). (b) Kaplan–Meier curves of survival based on the presence or absence of CMGAs (patients aged ≤ 65 years). (c) Kaplan–Meier curves of survival based on the presence or absence of CMGAs (patients aged ≤ 65 years and *FLT3*-ITD-negative). (d) Kaplan–Meier curves of CIR based on the presence or absence of CMGAs (all patients). (e) Kaplan–Meier curves of CIR based on the presence or absence of CMGAs (patients aged ≤ 65 years). (f) Kaplan–Meier curves of CIR based on the presence or absence of CMGAs (patients aged ≤ 65 years and *FLT3*-ITD-negative).

however, identified *NPM1* as an independent prognostic factor. This suggests that the overlapping of mutations may cancel the favorable character of AML with mutated *NPM1*. Focusing on the subset of our cohort consisting of patients aged ≤ 65 years with mutated *NPM1*, we did indeed find that all four of the patients without CMGAs achieved long-term survival (CMGA-positive: $n = 4$; 5-year OS, 100%; CMGA-negative: $n = 49$; 5-year OS, 30.37%. HR: 0.3230; $P = 0.0742$). Recent advances in knowledge have led to the conclusion that AML with mutated *NPM1* has a heterogeneous background involving a variety of co-mutation patterns. So far, several large cohort studies have tried to distinguish a poor-prognosis group of AML with mutated *NPM1* without *FLT3*-ITD by other genetic mutations, but without success. In particular, *TET2*

and *IDH1* mutations were expected to be prognostic factors, but no consensus has been reached because their predictive value differed between reports.^{23,24,46–50} Our proposed system for prognostic stratification using CMGAs may aid the evaluation of unexpected risk associated with these mutations. Furthermore, recent studies also revealed changeability in the co-mutation pattern of AML with mutated *NPM1*.^{37,51} For instance, Krönke *et al.*³⁷ performed a comparative mutation analysis of primary and relapse samples from 53 AML patients with mutated *NPM1* using deep sequencing and reported changes in mutation patterns in 34 patients, including 9 patients who acquired *FLT3*-ITD. The study also reported that, regardless of the co-presence of a *DNMT3A* mutation that was continuously detected from primary onset,

Table 2. Multivariate analysis of overall survival (OS) and cumulative incidence of relapse (CIR) based on complex molecular genetic abnormalities (CMGAs)

Intermediate cytogenetic risk group, age ≤ 65 years	OS				CIR			
	HR	P-value	95.0% CI		HR	P-value	95.0% CI	
CMGA positive	3.717	<u>0.0007</u>	1.7331	7.9722	1.792	0.1164	0.8651	3.7110
HSCT on first CR	0.362	<u>0.0037</u>	0.1826	0.7194	0.258	<u>0.0004</u>	0.1218	0.5457
<i>NPM1</i> mutation-positive	0.504	<u>0.0355</u>	0.2665	0.9547	—	—	—	—
<i>CEBPA</i> double mutation-positive	0.247	0.0629	0.0568	1.0779	0.430	0.1857	0.1234	1.5004
<i>FLT3</i> -ITD-positive	1.582	0.1513	0.8454	2.9619	2.179	<u>0.0298</u>	1.0791	4.4005
<i>NRAS</i> mutation-positive	0.516	0.1926	0.1904	1.3966	0.247	0.0596	0.0579	1.0579
<i>KMT2A</i> -PTD mutation-positive	—	—	—	—	1.905	0.1111	0.8620	4.2109
WBC < 20 000/μl	—	—	—	—	0.583	0.1150	0.2980	1.1404

Abbreviations: CI, confidence interval; CR, complete remission; HR, hazard ratio; HSCT, hematopoietic stem cell transplantation; PTD, partial tandem duplication; WBC, white blood cell count. The underlines represent significant differences.

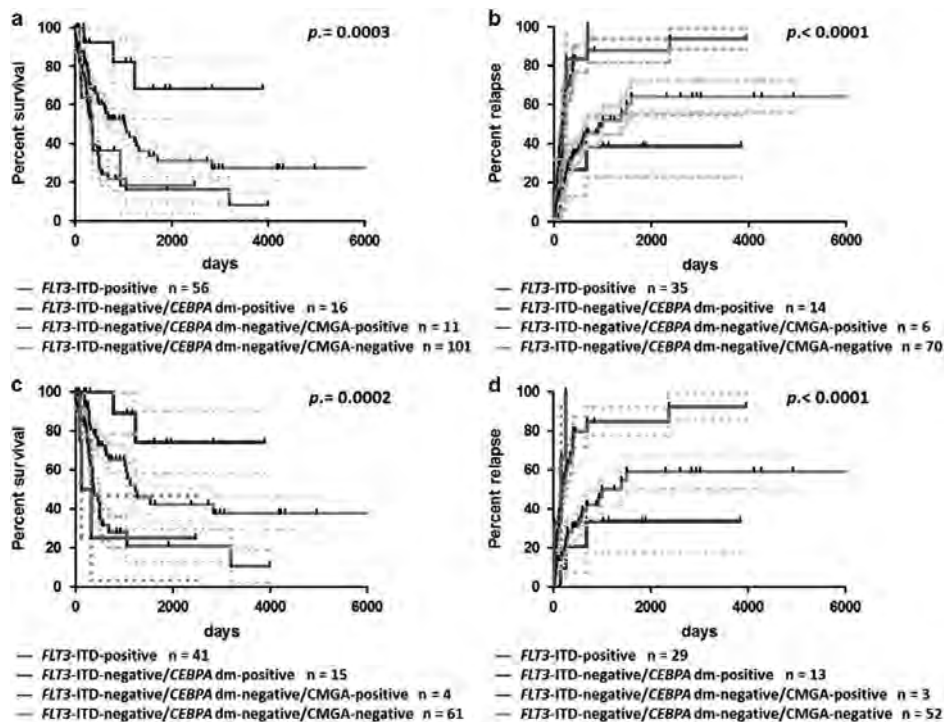


Figure 5. Development of a new prognostic risk stratification method based on CMGAs. Error bars represent s.e.m. (a) Kaplan–Meier curves of survival for the intermediate cytogenetic risk group based on stratification using the simplified CMGA analysis. (b) Kaplan–Meier curves of CIR for the intermediate cytogenetic risk group based on stratification using the simplified CMGA analysis. (c) Kaplan–Meier curves of survival for the intermediate cytogenetic risk group (patients aged ≤ 65 years) based on stratification using the simplified CMGA analysis. (d) Kaplan–Meier curves of CIR for the intermediate cytogenetic risk group (patients aged ≤ 65 years) based on stratification using the simplified CMGA analysis.

there were five patients in whom *NPM1* mutations were lost on relapse, all of whom were resistant to intensive salvage therapy.³⁷ The findings of the present study suggest that some cases of AML with mutated *NPM1* may exhibit genetic changeability in AML clones owing to genetic instability, leading to the evolution of a therapy-resistant clone. Overlapping of genetic mutations, which

probably reflects genetic instability, may be predictive of AML relapse owing to clonal evolution.

We believe it is important to focus on not only the importance of karyotypic instability in AML and myelodysplastic syndrome based on previous reports,^{52,53} but also genetic instability in NK-AML. Interestingly, many of the genetic mutations found to

comprise CMGAs were mutations in DNA methylation modifiers. Although such mutations were detected together with many other mutations, they were stably detected in primary and relapsed AML, unlike mutations in *NPM1* and *FLT3-ITD*.^{36,54,55} Furthermore, in recent years, analysis of leukemic stem cells with droplet digital PCR has revealed that mutations that coexist with *DNMT3A* and *IDH1* mutations could be detected in preleukemic hematopoietic stem cells that are pluripotent like normal hematopoietic stem cells.⁵⁶ Other studies have shown that clonal hematopoiesis accompanied by small amounts of *DNMT3A* and *TET2* mutations are observed in the serum of ~10% of healthy elderly individuals,⁵⁷ and mutations in DNA methylation modifiers could be thought of as founder gene mutations that cause preleukemia. The findings of many of these studies suggest the possibility that DNA methylation modifiers act to protect hematopoietic stem cells from the accumulation of genetic mutations. *TP53* has been referred to as 'the guardian angel of the genome,' reflecting its property of protecting the genome from karyotypic instability. DNA methylation modifiers may represent another such 'guardian angel of the genome,' through their ability to protect against molecular genetic abnormalities. Future research aimed at determining how genetic mutations accumulate in AML may lead to the development of novel therapeutic strategies against the disease.

Our proposed system for prognostic stratification using CMGAs covers molecular mutations, but does not include chromosomal aberrations. Adding an assessment of chromosomal instability may improve the predictive value of our stratification. It may however be necessary to examine chromosomal abnormalities in more detail in order to clarify the entire picture of genetic instability. The chromosomal analyses with G-band technique used in this study were somewhat crude, particularly in light of the fact that only dividing cells could be detected, that results are affected during sample preparation for morphological analysis and analysts' skill and experience, and the difficulty of chromosomal analysis of copy number alterations and uniparental disomies. In recent years, studies have shown that loss of heterozygosity because of copy number alterations and uniparental disomies, which were difficult to detect with G-band analysis in previous studies, is an important genomic abnormality associated with the pathogenesis of NK-AML.^{58–60} Detailed chromosomal analysis using virtual karyotyping with methods such as single-nucleotide polymorphism arrays may be of key importance when elucidating the mechanisms underlying genetic instability.

Finally, we propose using CMGAs in prognostic stratification. The importance of CMGAs not only extends to explaining the correlations between complex genetic mutations, but may also contribute to the detection for unpredictable risk of patients who are classified into the intermediate cytogenetic risk group (Figure 5). Previous genomic analyses of AML not only clarified the complex nature of the involved genetic mutations, but also complicated the genetic mutation-based prognostic stratification. However, clinical application of genomic analysis that are more practical and convenient in actual clinical settings are being contemplated. Complex prognostic stratification in the post-genomic era might be simplified by placing more focus on genetic co-mutations.

CONFLICT OF INTEREST

The authors declare no conflict of interest.

AUTHOR CONTRIBUTIONS

SW and HY were the principal investigators and take primary responsibility for the paper. SW, HY, TU, KU, SK, YK, EK, KT, SG, MK, HT, KN, TF and KI recruited the

patients. SW, HY, KA, TK and FK performed the laboratory work for this study. SW, HY, YF, SY, KF, TR, TH and KI analyzed the data and wrote the paper.

REFERENCES

- Estey E, Döhner H. Acute myeloid leukaemia. *Lancet* 2006; **368**: 1894–1907.
- Mardis ER, Ding L, Dooling DJ, Larson DE, McLellan MD, Chen K *et al*. Recurring mutations found by sequencing an acute myeloid leukemia genome. *N Engl J Med* 2009; **361**: 1058–1066.
- Ley TJ, Ding L, Walter MJ, McLellan MD, Lamprecht T, Larson DE *et al*. *DNMT3A* mutations in acute myeloid leukemia. *N Engl J Med* 2010; **363**: 2424–2433.
- Schlenk RF, Döhner H. Genomic applications in the clinic: use in treatment paradigm of acute myeloid leukemia. *Hematology Am Soc Hematol Educ Program* 2013; **2013**: 324–330.
- Grimwade D, Hills RK, Moorman AV, Walker H, Chatters S, Goldstone AH *et al*. Refinement of cytogenetic classification in acute myeloid leukemia: determination of prognostic significance of rare recurring chromosomal abnormalities among 5876 younger adult patients treated in the United Kingdom Medical Research Council trials. *Blood* 2010; **116**: 354–365.
- Preudhomme C, Sagot C, Boissel N, Cayuela JM, Tigaud I, de Botton S *et al*. Favorable prognostic significance of CEBPA mutations in patients with de novo acute myeloid leukemia: a study from the Acute Leukemia French Association (ALFA). *Blood* 2002; **100**: 2717–2723.
- Pabst T, Eyholzer M, Fos J, Mueller B U. Heterogeneity within AML with CEBPA mutations; only CEBPA double mutations, but not single CEBPA mutations are associated with favourable prognosis. *Br J Cancer* 2009; **100**: 1343–1346.
- Fröhling S, Schlenk RF, Stolze I, Bihlmayr J, Benner A, Kreitmeier S *et al*. CEBPA mutations in younger adults with acute myeloid leukemia and normal cytogenetics: prognostic relevance and analysis of cooperating mutations. *J Clin Oncol* 2004; **22**: 624–633.
- Wouters BJ, Löwenberg B, Erpelinck-Verschueren CA, van Putten WL, Valk PJ, Delwel R *et al*. Double CEBPA mutations, but not single CEBPA mutations, define a subgroup of acute myeloid leukemia with a distinctive gene expression profile that is uniquely associated with a favorable outcome. *Blood* 2009; **113**: 3088–3091.
- Kottaridis PD, Gale RE, Frew ME, Harrison G, Langabeer SE, Belton AA *et al*. The presence of a FLT3-internal tandem duplication in patients with acute myeloid leukemia (AML) adds important prognostic information to cytogenetic risk group and response to the first cycle of chemotherapy: analysis of 854 patients from the United Kingdom Medical Research Council AML 10 and 12 trials. *Blood* 2001; **98**: 1752–1759.
- Thiede C, Steudel C, Mohr B, Schaich M, Schäkel U, Platzbecker U *et al*. Analysis of FLT3-activating mutations in 979 patients with acute myelogenous leukemia: association with FAB subtypes and identification of subgroups with poor prognosis. *Blood* 2002; **99**: 4326–4335.
- Fröhling S, Schlenk RF, Breitnick J, Benner A, Kreitmeier S, Tobis K *et al*. Prognostic significance of activating FLT3 mutations in younger adults (16 to 60 years) with acute myeloid leukemia and normal cytogenetics: a study of the AML Study Group Ulm. *Blood* 2002; **100**: 4372–4380.
- Schnittger S, Schoch C, Kern W, Mecucci C, Tschulik C, Martelli MF *et al*. Nucleophosmin gene mutations are predictors of favorable prognosis in acute myelogenous leukemia with a normal karyotype. *Blood* 2005; **106**: 3733–3739.
- Döhner K, Schlenk RF, Habdank M, Scholl C, Rücker FG, Corbacioglu A *et al*. Mutant nucleophosmin (NPM1) predicts favorable prognosis in younger adults with acute myeloid leukemia and normal cytogenetics: interaction with other gene mutations. *Blood* 2005; **106**: 3740–3746.
- Thiede C, Koch S, Creutzig E, Steudel C, Illmer T, Schaich M *et al*. Prevalence and prognostic impact of NPM1 mutations in 1485 adult patients with acute myeloid leukemia (AML). *Blood* 2006; **107**: 4011–4020.
- Röllig C, Bornhäuser M, Thiede C, Taube F, Kramer M, Mohr B *et al*. Long-term prognosis of acute myeloid leukemia according to the new genetic risk classification of the European LeukemiaNet recommendations: evaluation of the proposed reporting system. *J Clin Oncol* 2011; **29**: 2758–2765.
- Mrózek K, Marcucci G, Nicolet D, Mahary KS, Becker H, Whitman SP *et al*. Prognostic significance of the European LeukemiaNet standardized system for reporting cytogenetic and molecular alterations in adults with acute myeloid leukemia. *J Clin Oncol* 2012; **30**: 4515–4523.
- Döhner H, Estey EH, Amadori S, Appelbaum FR, Büchner T, Burnett AK *et al*. Diagnosis and management of acute myeloid leukemia in adults: recommendations from an international expert panel, on behalf of the European LeukemiaNet. *Blood* 2010; **115**: 453–474.
- O'Donnell MR, Abboud CN, Altman J, Appelbaum FR, Arber DA, Attar E *et al*. Acute myeloid leukemia. *J Natl Compr Canc Netw* 2012; **10**: 984–1021.

- 20 Thol F, Damm F, Lüdeking A, Winschel C, Wagner K, Morgan M *et al*. Incidence and prognostic influence of DNMT3a mutations in acute myeloid leukemia. *J Clin Oncol* 2011; **29**: 2889–2896.
- 21 Chou WC, Chou SC, Liu CY, Chen CY, Hou HA, Kuo YY *et al*. TET2 mutation is an unfavorable prognostic factor in acute myeloid leukemia patients with intermediate-risk cytogenetics. *Blood* 2011; **118**: 3803–3810.
- 22 Figueroa ME, Abdel-Wahab O, Lu C, Ward PS, Patel J, Shih A *et al*. Leukemic IDH1 and IDH2 mutations result in a hypermethylation phenotype, disrupt TET2 function, and impair hematopoietic differentiation. *Cancer Cell* 2010; **18**: 553–567.
- 23 Marcucci G, Maharry K, Wu YZ, Radmacher MD, Mrózek K, Margeson D *et al*. IDH1 and IDH2 gene mutations identify novel molecular subsets within de novo cytogenetically normal acute myeloid leukemia: a Cancer and Leukemia Group B study. *J Clin Oncol* 2010; **28**: 2348–2355.
- 24 Boissel N, Nibourel O, Renneville A, Gardin C, Reman O, Contentin N *et al*. Prognostic impact of isocitrate dehydrogenase enzyme isoforms 1 and 2 mutations in acute myeloid leukemia: a study by the Acute Leukemia French Association group. *J Clin Oncol* 2010; **28**: 3717–3723.
- 25 The Cancer Genome Atlas Research Network. Genomic and epigenomic landscapes of adult de novo acute myeloid leukemia. *N Engl J Med* 2013; **368**: 2059–2074.
- 26 Welch JS, Ley TJ, Link DC, Miller CA, Larson DE, Koboldt DC *et al*. The origin and evolution of mutations in acute myeloid leukemia. *Cell* 2012; **150**: 264–278.
- 27 Rocquain J, Gelsi-Boyer V, Adélaïde J, Murati A, Carbuca N, Vey N *et al*. Alteration of cohesin genes in myeloid diseases. *Am J Hematol* 2010; **85**: 717–719.
- 28 Thol F, Bollin R, Gehlhaar M, Walter C, Dugas M, Suchanek KJ *et al*. Mutations in the cohesin complex in acute myeloid leukemia: clinical and prognostic implications. *Blood* 2014; **123**: 914–920.
- 29 Kon A, Shih LY, Minamino M, Sanada M, Shiraishi Y, Nagata Y *et al*. Recurrent mutations in multiple components of the cohesin complex in myeloid neoplasms. *Nat Genet* 2013; **45**: 1232–1237.
- 30 Kihara R, Nagata Y, Kiyoi H, Kato T, Yamamoto E, Suzuki K *et al*. Comprehensive analysis of genetic alterations and their prognostic impacts in adult acute myeloid leukemia patients. *Leukemia* 2014; **28**: 1586–1595.
- 31 Walter MJ, Shen D, Shao J, Ding L, White BS, Kandoth C *et al*. Clonal diversity of recurrently mutated genes in myelodysplastic syndromes. *Leukemia* 2013; **27**: 1275–1282.
- 32 Patel JP, Gönen M, Figueroa ME, Fernandez H, Sun Z, Racevskis J *et al*. Prognostic relevance of integrated genetic profiling in acute myeloid leukemia. *N Engl J Med* 2012; **366**: 1079–1089.
- 33 Kottaridis PD, Gale RE, Langabeer SE, Frew ME, Bowen DT, Linch DC *et al*. Studies of FLT3 mutations in paired presentation and relapse samples from patients with acute myeloid leukemia: implications for the role of FLT3 mutations in leukemogenesis, minimal residual disease detection, and possible therapy with FLT3 inhibitors. *Blood* 2002; **100**: 2393–2398.
- 34 Shih LY, Huang CF, Wu JH, Lin TL, Dunn P, Wang PN *et al*. Internal tandem duplication of FLT3 in relapsed acute myeloid leukemia: a comparative analysis of bone marrow samples from 108 adult patients at diagnosis and relapse. *Blood* 2002; **100**: 2387–2392.
- 35 Cloos J, Goemans BF, Hess CJ, van Oostveen JW, Waisfisz Q, Corthals S *et al*. Stability and prognostic influence of FLT3 mutations in paired initial and relapsed AML samples. *Leukemia* 2006; **20**: 1217–1220.
- 36 Wakita S, Yamaguchi H, Omori I, Terada K, Ueda T, Manabe E *et al*. Mutations of the epigenetics-modifying gene (DNMT3a, TET2, IDH1/2) at diagnosis may induce FLT3-ITD at relapse in de novo acute myeloid leukemia. *Leukemia* 2013; **27**: 1044–1052.
- 37 Krönke J, Bullinger L, Teleanu V, Tschürtz F, Gaidzik VI, Kühn MW *et al*. Clonal evolution in relapsed NPM1-mutated acute myeloid leukemia. *Blood* 2013; **122**: 100–108.
- 38 Li HY, Deng DH, Huang Y, Ye FH, Huang LL, Xiao Q *et al*. Favorable prognosis of biallelic CEBPA gene mutations in acute myeloid leukemia patients: a meta-analysis. *Eur J Haematol* 2015; **94**: 439–448.
- 39 Ding L, Ley TJ, Larson DE, Miller CA, Koboldt DC, Welch JS *et al*. Clonal evolution in relapsed acute myeloid leukaemia revealed by whole-genome sequencing. *Nature* 2012; **481**: 506–510.
- 40 Walter MJ, Shen D, Ding L, Shao J, Koboldt DC, Chen K *et al*. Clonal architecture of secondary acute myeloid leukemia. *N Engl J Med* 2012; **366**: 1090–1098.
- 41 Grimwade D, Walker H, Harrison G, Oliver F, Chatters S, Harrison CJ *et al*. The predictive value of hierarchical cytogenetic classification in older adults with acute myeloid leukemia (AML): analysis of 1065 patients entered into the United Kingdom Medical Research Council AML11 trial. *Blood* 2001; **98**: 1312–1320.
- 42 Slovak ML, Kopecky KJ, Cassileth PA, Harrington DH, Theil KS, Mohamed A *et al*. Karyotypic analysis predicts outcome of preremission and postremission therapy in adult acute myeloid leukemia: a Southwest Oncology Group/Eastern Cooperative Oncology Group Study. *Blood* 2000; **96**: 4075–4083.
- 43 Mrózek K. Cytogenetic, molecular genetic, and clinical characteristics of acute myeloid leukemia with a complex karyotype. *Semin Oncol* 2008; **35**: 365–377.
- 44 Haeflrich T, Kern W, Schoch C, Schnittger S, Sauerland C, Heinecke A *et al*. A new prognostic score for patients with acute myeloid leukemia based on cytogenetics and early blast clearance in trials of the German AML Cooperative Group. *Haematologica* 2004; **89**: 408–418.
- 45 Suzuki T, Kiyoi H, Ozeki K, Tomita A, Yamaji S, Suzuki R *et al*. Clinical characteristics and prognostic implications of NPM1 mutations in acute myeloid leukemia. *Blood* 2005; **106**: 2854–2861.
- 46 Paschka P, Schlenk RF, Gaidzik VI, Haddank M, Krönke J, Bullinger L *et al*. IDH1 and IDH2 mutations are frequent genetic alterations in acute myeloid leukemia and confer adverse prognosis in cytogenetically normal acute myeloid leukemia with NPM1 mutation without FLT3 internal tandem duplication. *J Clin Oncol* 2010; **28**: 3636–3643.
- 47 Green CL, Evans CM, Hills RK, Burnett AK, Linch DC, Gale RE. The prognostic significance of IDH1 mutations in younger adult patients with acute myeloid leukemia is dependent on FLT3/ITD status. *Blood* 2010; **116**: 2779–2782.
- 48 Metzeler KH, Maharry K, Radmacher MD, Mrózek K, Margeson D, Becker H *et al*. TET2 mutations improve the new European LeukemiaNet risk classification of acute myeloid leukemia: a Cancer and Leukemia Group B study. *J Clin Oncol* 2011; **29**: 1373–1381.
- 49 Gaidzik VI, Paschka P, Späth D, Haddank M, Köhne CH, Germing U *et al*. TET2 mutations in acute myeloid leukemia (AML): results from a comprehensive genetic and clinical analysis of the AML study group. *J Clin Oncol* 2012; **30**: 1350–1357.
- 50 Tian X, Xu Y, Yin J, Tian H, Chen S, Wu D *et al*. TET2 gene mutation is unfavorable prognostic factor in cytogenetically normal acute myeloid leukemia patients with NPM1+ and FLT3-ITD - mutations. *Int J Hematol* 2014; **100**: 96–104.
- 51 Krönke J, Schlenk RF, Jensen KO, Tschürtz F, Corbacioglu A, Gaidzik VI *et al*. Monitoring of minimal residual disease in NPM1-mutated acute myeloid leukemia: a study from the German-Austrian acute myeloid leukemia study group. *J Clin Oncol* 2011; **29**: 2709–2716.
- 52 Kern W, Haeflrich T, Schnittger S, Ludwig WD, Hiddemann W, Schoch C. Karyotype instability between diagnosis and relapse in 117 patients with acute myeloid leukemia: implications for resistance against therapy. *Leukemia* 2002; **16**: 2084–2091.
- 53 Horiike S, Misawa S, Kaneko H, Sasai Y, Kobayashi M, Fujii H *et al*. Distinct genetic involvement of the TP53 gene in therapy-related leukemia and myelodysplasia with chromosomal losses of Nos 5 and/or 7 and its possible relationship to replication error phenotype. *Leukemia* 1999; **13**: 1235–1242.
- 54 Hou HA, Kuo YY, Liu CY, Chou WC, Lee MC, Chen CY *et al*. DNMT3A mutations in acute myeloid leukemia: stability during disease evolution and clinical implications. *Blood* 2012; **119**: 559–568.
- 55 Welch JS. Subclonal architecture in acute myeloid leukemia. *Hematology Education: the education program for the annual congress of the European Hematology Association*. The EHA Learning Center: The Hague, The Netherlands, 2013, pp 23–29.
- 56 Shlush LI, Zandi S, Mitchell A, Chen WC, Brandwein JM, Gupta V *et al*. Identification of pre-leukaemic haematopoietic stem cells in acute leukaemia. *Nature* 2014; **506**: 328–333.
- 57 Genovese G, Kähler AK, Handsaker RE, Lindberg J, Rose SA, Bakhoum SF *et al*. Clonal hematopoiesis and blood-cancer risk inferred from blood DNA sequence. *N Engl J Med* 2014; **371**: 2477–2487.
- 58 Raghavan M, Smith LL, Lillington DM, Chaplin T, Kakkas I, Molloy G *et al*. Segmental uniparental disomy is a commonly acquired genetic event in relapsed acute myeloid leukemia. *Blood* 2008; **112**: 814–821.
- 59 Yi JH, Huh J, Kim HJ, Kim SH, Kim YK, Kim YK *et al*. Adverse prognostic impact of abnormal lesions detected by genome-wide single nucleotide polymorphism array-based karyotyping analysis in acute myeloid leukemia with normal karyotype. *J Clin Oncol* 2014; **32**: 4702–4708.
- 60 Walter MJ, Payton JE, Ries RE, Shannon WD, Deshmukh H, Zhao Y *et al*. Acquired copy number alterations in adult acute myeloid leukemia genomes. *Proc Natl Acad Sci USA* 2009; **106**: 12950–12955.

Supplementary Information accompanies this paper on the Leukemia website (<http://www.nature.com/leu>)

EUROPEAN
HEMATOLOGY
ASSOCIATIONFerrata Storti
Foundation**Haematologica** 2016
Volume 101(9):1074-1081

Clinical characteristics and prognosis of acute myeloid leukemia associated with DNA-methylation regulatory gene mutations

Takeshi Ryotokuji,^{1,*} Hiroki Yamaguchi,^{1,*} Toshimitsu Ueki,² Kensuke Usuki,³ Saiko Kurosawa,⁴ Yutaka Kobayashi,⁵ Eri Kawata,⁵ Kenji Tajika,⁶ Seiji Gomi,⁶ Junya Kanda,⁷ Anna Kobayashi,¹ Ikuko Omori,¹ Atsushi Marumo,¹ Yusuke Fujiwara,¹ Shunsuke Yui,¹ Kazuki Terada,¹ Keiko Fukunaga,¹ Tsuneaki Hirakawa,¹ Kunihito Arai,¹ Tomoaki Kitano,¹ Fumiko Kosaka,¹ Hayato Tamai,¹ Kazutaka Nakayama,¹ Satoshi Wakita,¹ Takahiro Fukuda,⁴ and Koiti Inokuchi¹

¹Department of Hematology, Nippon Medical School, Tokyo; ²Department of Hematology, Nagano Red Cross Hospital; ³Department of Hematology, NTT Medical Center Tokyo; ⁴Department of Hematopoietic Stem Cell Transplantation, National Cancer Center Hospital, Tokyo; ⁵Department of Hematology, Japanese Red Cross Kyoto Daini Hospital; ⁶Department of Hematology, Yokohama Minami Kyousai Hospital, Kanagawa; and ⁷Division of Hematology, Saitama Medical Center Jichi Medical University, Japan

*TR and HY contributed equally to this work

ABSTRACT

In recent years, it has been reported that the frequency of DNA-methylation regulatory gene mutations – mutations of the genes that regulate gene expression through DNA methylation – is high in acute myeloid leukemia. The objective of the present study was to elucidate the clinical characteristics and prognosis of acute myeloid leukemia with associated DNA-methylation regulatory gene mutation. We studied 308 patients with acute myeloid leukemia. DNA-methylation regulatory gene mutations were observed in 135 of the 308 cases (43.8%). Acute myeloid leukemia associated with a DNA-methylation regulatory gene mutation was more frequent in older patients ($P<0.0001$) and in patients with intermediate cytogenetic risk ($P<0.0001$) accompanied by a high white blood cell count ($P=0.0032$). DNA-methylation regulatory gene mutation was an unfavorable prognostic factor for overall survival in the whole cohort ($P=0.0018$), in patients aged ≤ 70 years, in patients with intermediate cytogenetic risk, and in *FLT3*-ITD-negative patients ($P=0.0409$). Among the patients with DNA-methylation regulatory gene mutations, 26.7% were found to have two or more such mutations and prognosis worsened with increasing number of mutations. In multivariate analysis DNA-methylation regulatory gene mutation was an independent unfavorable prognostic factor for overall survival ($P=0.0424$). However, patients with a DNA-methylation regulatory gene mutation who underwent allogeneic stem cell transplantation in first remission had a significantly better prognosis than those who did not undergo such transplantation ($P=0.0254$). Our study establishes that DNA-methylation regulatory gene mutation is an important unfavorable prognostic factor in acute myeloid leukemia.

Correspondence:

y-hiroki@fd6.so-net.ne.jp

Received: January 23, 2016.

Accepted: May 30, 2016.

Pre-published: May 31, 2016.

doi:10.3324/haematol.2016.143073

Check the online version for the most updated information on this article, online supplements, and information on authorship & disclosures: www.haematologica.org/content/101/9/1074

©2016 Ferrata Storti Foundation

Material published in *Haematologica* is covered by copyright. All rights reserved to the Ferrata Storti Foundation. Copies of articles are allowed for personal or internal use. Permission in writing from the publisher is required for any other use.



Introduction

Acute myeloid leukemia (AML) is a heterogeneous disease whose onset involves a variety of chromosomal abnormalities and gene mutations.^{1,2} To improve the outcome of AML treatment, it is very important to establish a prognosis from cytogenetic analysis and provide accordingly differentiated treatment.^{1,2} Standard

chemotherapy is given to patients with a favorable prognosis according to their cytogenetic profile, whereas allogeneic transplantation in first remission is actively promoted for patients with an unfavorable cytogenetic prognosis.³

Meanwhile, for the approximately 60% of cases that fall into the intermediate prognosis group, clinicians are seeking to provide a clear prognosis and differentiated therapy based on cytogenetic analysis, which have not been available for this group of patients. In the latter half of the 2000s, gene mutations in AML were successively discovered, and attempts have been made to use these to provide a differentiated prognosis. The most important of these gene mutations for differentiated prognosis are *FMS-like tyrosine kinase 3* internal tandem duplications (*FLT3*-ITD), *nucleophosmin 1* (*NPM1*) gene mutation, and *CCAAT/enhancer binding protein A* (*CEBPA*) gene mutation.⁴ In 2008, Richard *et al.* reported that AML cases that were *FLT3*-ITD-negative and *NPM1*-mutation-positive, or that were accompanied by *CEBPA* biallelic mutation, were associated with a favorable prognosis and that allogeneic hematopoietic stem cell transplantation in first remission was not indicated.^{9,10} It was also reported that *FLT3*-ITD-positive AML has a very unfavorable prognosis, which might be improved by allogeneic hematopoietic stem cell transplantation in first remission.¹⁰ These findings have been integrated as prognostic factors in the European Leukemia Net (ELN) and National Comprehensive Cancer Network (NCCN) guidelines,^{12,13} which are becoming widely applied in clinical practice.

However, these gene mutations are observed in only around 30% of cases with intermediate cytogenetic prognosis, meaning that differentiation of prognosis is still insufficient. In recent years, the use of next-generation sequencers has facilitated energetic exploration of gene mutations, leading to the discovery of other AML-related gene mutations,¹⁴⁻¹⁷ and mutations in the genes that regulate DNA methylation, such as *DNA methyltransferase 3 alpha* (*DNMT3A*), *Tet methylcytosine dioxygenase 2* (*TET2*), *isocitrate dehydrogenase 1* (*IDH1*), and *isocitrate dehydrogenase 2* (*IDH2*).¹⁸⁻²³ It has been suggested that these gene mutations may also have prognostic relevance in some cases of AML, but this view has yet to become established. Moreover, a further series of gene mutations has recently been discovered, so that differentiated prognosis based on gene mutations has actually become more confused.^{14,16,18,24}

The focus of the present study was DNA-methylation regulatory gene mutations (DMRGM), which are mutations of the genes that regulate gene expression through DNA methylation (*IDH1*, *IDH2*, *DNMT3A*, *TET2*). Studies have been carried out of the various DMRGM and other genes reported as indicating an unfavorable prognosis in AML.^{15-20,22, 25,25-30} Our group has also reported that AML with DMRGM at onset is associated with a high frequency of *FLT3*-ITD at relapse and has an unfavorable prognosis.³¹ However, since comprehensive gene mutation analysis using a next-generation sequencer is costly, there have so far been few reports on DMRGM-based prognostic analysis covering a large number of cases. In particular, there are very few reports on large cohorts in which there is a combined analysis of both *TET2* mutation, which is mutually exclusive with *IDH1* and *IDH2* mutations, and *DNMT3A* mutation.²⁰ Since *IDH1/2* mutations and *TET2* mutation are mutually complementary, DMRGM need to be subjected to integrated

analysis as a group, but there have so far been no reports of such analysis having been performed. We therefore analyzed the clinical characteristics of a group of AML patients with DMRGM and the prognostic impact of these mutations.

Methods

Patients

We studied 308 patients with *de novo* AML (excluding M3) treated at Nippon Medical School Hospital or its affiliated institutions. A comprehensive genetic mutational analysis, as described below, was conducted among patients with $\geq 20\%$ blasts in bone marrow or peripheral blood. The study was conducted in accordance with the Declaration of Helsinki; written informed consent was obtained from the participants, and the patients were analyzed and treated with respect for their welfare and free will. The study protocol was approved by our institutional review board.

Screening for cytogenetic mutations

G-band analysis was performed on bone marrow samples obtained from patients at initial presentation. When it was difficult to obtain bone marrow samples, peripheral blood was used instead. For patients suspected of having M2, M3, or M4e AML based on the French-American-British classification, fluorescence *in situ* hybridization analysis was used to search additionally for *RUNX1-RUNX1T1*, *PML-RARA*, and *CBFB-MYH11* mutations. The cytogenetic prognosis was then classified in accordance with the system recommended by the ELN.

Screening for molecular genetic abnormalities in all exons of 20 genes and hotspots of eight genes

An oligonucleotide library was generated by emulsion polymerase chain reaction using order-made probes designed against the exons of the following 20 genes: *TET2* (HGNC:25941), *DNMT3A* (HGNC:2978), *ASXL1* (HGNC:18318), *KMT2A* (HGNC:7132: the HGNC nomenclature of *MLL* has recently changed to *KMT2A*), *RUNX1* (HGNC:10471), *KIT* (HGNC:6342), *TP53* (HGNC:11998), *PTPN11* (HGNC:9644), *GATA2* (HGNC:4171), *WT1* (HGNC:12796), *STAG2* (HGNC:11355), *RAD21* (HGNC:9811), *SMC1A* (HGNC:11111), *SMC3* (HGNC:2468), *DAXX* (HGNC:2681), *BCOR* (HGNC:20893), *BCORL1* (HGNC:25657), *NF1* (HGNC:7765), *DDX41* (HGNC:18674), and *PHF6* (HGNC:18145). The library was sequenced with the next-generation sequencer Ion PGM™. With respect to detected mutations, the NCBI and COSMIC databases were used to search for polymorphisms and cancer-related mutations. For newly identified mutations, genetic polymorphisms were checked using Sanger sequencing with remission-stage samples.

Genes located in known hot spots (*FLT3*-ITD and *FLT3*-TKD, *NPM1*, *IDH1*, *IDH2*, *NRAS*, and *KRAS*), those for which probe design for emulsion sequencing was difficult (*CEBPA*), and those for which analysis with Ion PGM™ was difficult (*KMT2A*-PTD), were analyzed using previously reported methods.³¹

Statistical analysis

The primary endpoint was overall survival of DMRGM-positive AML patients in the study cohort. A hazard ratio of 0.707 and an overall survival rate of 50% were assumed for the sample size calculation. Recruitment of approximately 300 patients allowed for a power of 80% in detecting a difference of that size with a type I error of 5%. During the study period, there were 80 deaths among the 135 DMRGM-positive AML patients. This provided an 80%

statistical power to detect a hazard ratio of 0.542 with a significance level (alpha) of 0.05 (two-tailed) regarding overall survival, which was defined as the time interval from the date of diagnosis to the date of death. Relapse-free survival for patients who had achieved complete remission was calculated as the time interval from the date of complete remission to the date of relapse.

The χ^2 test was used to test the association between categorical variables and the presence and absence of mutations. The Fisher exact test was used if the expected frequency of an event was less than five in any cell of a 2×2 table. The non-parametric Mann-Whitney U test was used to determine the statistical significance of differences in median values. All statistical tests were two-sided. The Kaplan-Meier method and log-rank test were applied to analyze overall survival and relapse-free survival. With respect to prognostic factors, multivariate analysis was conducted with the Cox proportional hazards model. A stepwise backward procedure selection model was used to extract independent events. Events at a significance level of $P \leq 0.20$ were analyzed. Statistical analyses were performed using GraphPad Prism (version 6.00 for Windows, GraphPad Software, La Jolla, CA, USA) and IBM SPSS Statistics (version 21.0 for Windows, IBM Corp., Armonk, NY, USA), while the power calculation was performed using GraphPad StatMate (version 2.00 for Windows).

Results

Patients' background

The average age of the 308 patients studied was 54.1 years (range, 17-86 years). There were 181 males (58.8%) and 127 females (41.2%). Based on cytogenetic analysis, 60 cases (19.5%) were assigned to the favorable risk group, 51 (16.6%) to the unfavorable risk group, and 184 (59.7%) to the intermediate risk group. Overall, 148 (48.1%) had a normal karyotype (Table 1, *Online Supplementary Table S1*). Gene mutations were observed in 265 cases (86.0%), with the most frequent being *NPM1* mutation (88 cases, 28.6%), *DNMT3A* mutation (71, 23.1%), and *FLT3-ITD* (65, 21.1%) (*Online Supplementary Figure S1*, *Online Supplementary Table S2*). Gene mutations with an incidence of $\leq 3\%$ were excluded from the analysis as they were too infrequent to be studied as prognostic factors (*Online Supplementary Figure S1*).

Clinical characteristics of patients with DNA-methylation regulatory gene mutations

A *DNMT3A* mutation was found in 71 cases (23.1%), *TET2* mutation in 57 (18.5%), *IDH2* mutation in 28

Table 1. Clinical background of the AML patients studied.

	All n=308		DMRGM-positive n=135		DMRGM-negative n=173		P value
		%		%		%	
Age, years							
Mean	54.1		59.0		50.2		<0.0001
Range	17-86		18-86		17-82		
Sex							
Male	181	58.8	72	53.3	109	63.0	0.1025
Female	127	41.2	63	46.7	64	37.0	
White cell count, $\times 10^9/L$							
Mean	57.2		75.2		43.1		0.0032
Range	0.3-677		0.3-677		0.6-483		
Cytogenetic risk group							
Favorable	60	19.5	4	3.0	56	32.4	<0.0001
Intermediate	184	59.7	109	80.7	75	43.2	
Adverse	51	16.6	16	11.9	35	20.2	
Unknown	13	4.2	6	4.4	7	4.0	
FAB classification							
M0	17	5.5	5	3.7	12	6.9	0.3150
M1	75	24.4	42	31.1	33	19.1	0.0163
M2	115	37.3	39	28.9	76	43.9	0.0089
M4	40	13.0	22	16.3	18	10.4	0.1712
M4e	12	3.9	0	0.0	12	6.9	0.0015
M5	33	10.7	21	15.6	12	6.9	0.0246
M6	7	2.3	2	1.5	5	2.9	0.4729
M7	1	0.3	1	0.7	0	0.0	0.4383
Not determined	8	2.6	3	2.2	5	2.9	1.0000
Induction therapy							
(IDA/DNR/ACR)+AraC	292	94.8	125	82.6	167	96.5	0.2989
Others (AVV, VP16+AraC)	3	1.0	2	1.5	1	0.6	
Unknown	13	4.2	8	5.9	5	2.9	
Stem cell transplantation							
First CR	37	12.0	14	10.4	23	13.3	0.4831
Second CR	13	4.2	4	3.0	9	5.2	0.4015
\geq Third CR/disease	36	11.7	12	8.9	24	13.9	0.2122

CR: complete remission; IDA: idarubicin; DNR: daunorubicin; ACR: aclarubicin; AraC: cytarabine; AVV: cytarabine+etoposide+vincristine+vinblastine; VP16: etoposide.

(9.1%), and *IDH1* mutation in 17 (5.5%). *TET2* mutation was more frequent in older patients (average 63.5 years, $P<0.0001$) (Online Supplementary Table S3). High white blood cell counts were found in patients with mutations of *DNMT3A* (average $86.6 \times 10^9/L$, $P=0.0028$) and *TET2* (average $80.7 \times 10^9/L$, $P=0.0389$). Mutations in *DNMT3A* ($P<0.0001$), *TET2* ($P=0.0087$), and *IDH2* ($P=0.0199$) were more frequent in the intermediate cytogenetic risk group (Online Supplementary Table S3).

A DMRGM was found in 135 cases (43.8%), indicating that this group of gene mutations occurs with very high frequency in AML. There were 99 cases (73.3%) with one DMRGM (DMRGM1), 34 (25.2%) with two (DMRGM2), and two (1.5%) with three (DMRGM3). No cases had four or more DMRGM (Figure 1). Compared to AML without DMRGM (non-DMRGM), AML with DMRGM was more frequent in older patients (DMRGM: average 59.0 years; non-DMRGM: average 50.2 years; $P<0.0001$), in patients with high white blood cell count (DMRGM: average $75.2 \times 10^9/L$; non-DMRGM: average $43.1 \times 10^9/L$; $P=0.0032$), and in the intermediate cytogenetic risk group (DMRGM: 80.7%; non-DMRGM: 43.4%; $P<0.0001$) (Table 1).

Overlapping gene mutations

DNMT3A mutation was frequently present together with *FLT3*-ITD ($P=0.0005$), *FLT3*-TKD ($P=0.0200$), and mutations of *PTPN11* ($P=0.0254$), *NPM1* ($P<0.0001$), and *IDH2* ($P=0.0002$), but was mutually exclusive with *NRAS* mutation ($P=0.0364$) and *CEBPA* double mutation (*CEBPA* dm, $P=0.0265$). *TET2* mutation was frequently present together with *NPM1* mutation ($P=0.0031$) and *CEBPA* monoallelic mutation ($P=0.0441$), but was mutually exclusive with *NRAS* mutation ($P=0.0229$), *IDH1* mutation ($P=0.0497$), and *IDH2* mutation ($P=0.0380$) (Online Supplementary Table S4). DMRGM was frequently present together with *FLT3*-ITD ($P=0.0007$) and mutations of *PTPN11* ($P=0.0190$) and *NPM1* ($P<0.0001$), but was mutually exclusive with mutations of *NRAS* ($P=0.0035$) and *WT1* ($P=0.0241$) (Online Supplementary Table S4).

Prognostic analysis in all subjects

With regards to overall survival, the factors associated

with an unfavorable prognosis were age >70 years ($P<0.0001$), adverse cytogenetic risk ($P<0.0001$), *FLT3*-ITD ($P<0.0001$), *KMT2A*-PTD ($P=0.0152$), *DNMT3A* mutation ($P=0.0017$), *TET2* mutation ($P=0.0043$), and *TP53* mutation ($P<0.0001$). In recent years, the development of a non-myeloablative regimen for hematopoietic stem cell transplantation has made it possible also for patients aged 65 to 69 years to undergo allogeneic hematopoietic stem cell transplantation. In the present study, analysis of prognosis was therefore stratified between patients aged ≤ 70 and >70 years. Favorable cytogenetic risk ($P<0.0001$), allogeneic hematopoietic stem cell transplantation (in first or second remission) ($P<0.0001$), and *CEBPA* dm ($P=0.0282$) were associated with a favorable prognosis (Online Supplementary Table S5).

As regards relapse-free survival, the factors associated with an unfavorable prognosis were adverse cytogenetic risk ($P=0.0210$), *FLT3*-ITD ($P<0.0001$), *TET2* mutation ($P=0.0219$), and *TP53* mutation ($P=0.0011$), whereas allogeneic hematopoietic stem cell transplantation (in first remission) ($P<0.0001$) and *NRAS* mutation ($P=0.0142$) were associated with a favorable prognosis (Online Supplementary Table S5).

Stratified analysis of *FLT3*-ITD-negative patients aged below 70 years with intermediate cytogenetic prognosis

Age >70 years, adverse cytogenetic risk, and *FLT3*-ITD were powerful poor prognostic factors. Rates of overall survival and relapse-free survival were therefore analyzed following stratification based on age ≤ 70 years, intermediate cytogenetic prognosis, and *FLT3*-ITD negativity. For overall survival, *DNMT3A* mutation was associated with an unfavorable prognosis ($P=0.0429$). On the other hand, allogeneic hematopoietic stem cell transplantation (in first or second remission) was associated with a favorable prognosis ($P=0.0283$) (Online Supplementary Table S5). For relapse-free survival, *TP53* mutation was associated with an unfavorable prognosis ($P=0.0068$), while, allogeneic hematopoietic stem cell transplantation (in first remission) was associated with a favorable prognosis ($P=0.0008$) (Online Supplementary Table S5).

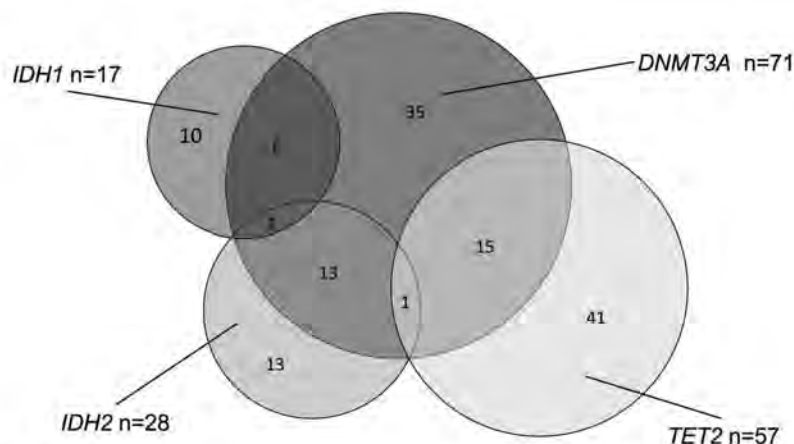


Figure 1. Frequency and overlap of DMRGM. There were 173 cases of DMRGM-negative AML (DMRGM0), 99 cases with one DMRGM (DMRGM1: 10 cases with *IDH1*, 13 with *IDH2*, 35 with *DNMT3A*, and 41 with *TET2*), 34 cases with two DMRGM (DMRGM2: 6 with *IDH1*+*DNMT3A*, 13 with *IDH2*+*DNMT3A*, and 15 with *DNMT3A*+*TET2*), and two cases with three DMRGM (DMRGM3: 1 with *IDH1*+*IDH2*+*DNMT3A* and 1 with *IDH2*+*DNMT3A*+*TET2*).

Prognostic impact of DNA-methylation regulatory gene mutations

The significance of DMRGM as a prognostic factor was investigated. With regards to overall survival, cases with DMRGM had a significantly poorer prognosis than cases without DMRGM ($P=0.0018$) (Figure 2A). Furthermore, patients with DMRGM tended to have a higher rate of relapse than patients without DMRGM, but the difference was not statistically significant (Figure 2B). Additionally, overall and relapse-free survival rates were analyzed following stratification based on age ≤ 70 years, intermediate cytogenetic risk, and *FLT3*-ITD negativity. With regards to overall survival, cases with DMRGM had a significantly poorer prognosis than cases without DMRGM ($P=0.0409$) (Figure 2C). However, there was no significant difference in relapse-free survival between patients with and without DMRGM (Figure 2D).

Prognostic impact of number of DNA-methylation regulatory gene mutations

Overall and relapse-free survival rates were studied relative to the number of DMRGM mutations. The greater the number of DMRGM, the poorer the prognosis (DMRGM0 versus DMRGM2+3; $P<0.0001$; DMRGM1 versus DMRGM2+3; $P=0.0244$; DMRGM0 versus DMRGM1:

$P=0.0651$) (Figure 3A). As far as concerns relapse-free survival, DMRGM2+3 was associated with a poorer prognosis than DMRGM0 ($P=0.0244$) and DMRGM1 ($P=0.0824$) (Figure 3B). Additionally, overall and relapse-free survival rates were analyzed following stratification based on age ≤ 70 years, intermediate cytogenetic risk, and *FLT3*-ITD negativity. The overall survival rate of patients with DMRGM2+3 was significantly lower than that of patients with DMRGM0 ($P=0.0189$) (Figure 3C). The relapse-free survival rate of patients with DMRGM2+3 tended to be worse than that of patients with DMRGM1, but not significantly so ($P=0.0600$) (Figure 3D).

Prognostic significance of DNA-methylation regulatory gene mutation combinations

In the present analysis, prognosis was poor for patients with DMRGM, but was found to be poorer still for those with DMRGM2+3. We, therefore, investigated whether the combinations of DMRGM influence prognosis in patients with DMRGM2+3. The 15 patients with *DNMT3A* mutation accompanied by *TET2* mutation (*DNMT3A* mutation/*TET2* mutation⁺) were compared with the 20 patients with *DNMT3A* mutation accompanied by *IDH* mutation (*DNMT3A* mutation/*IDH1* or *IDH2* mutation⁺). No clear significant difference was

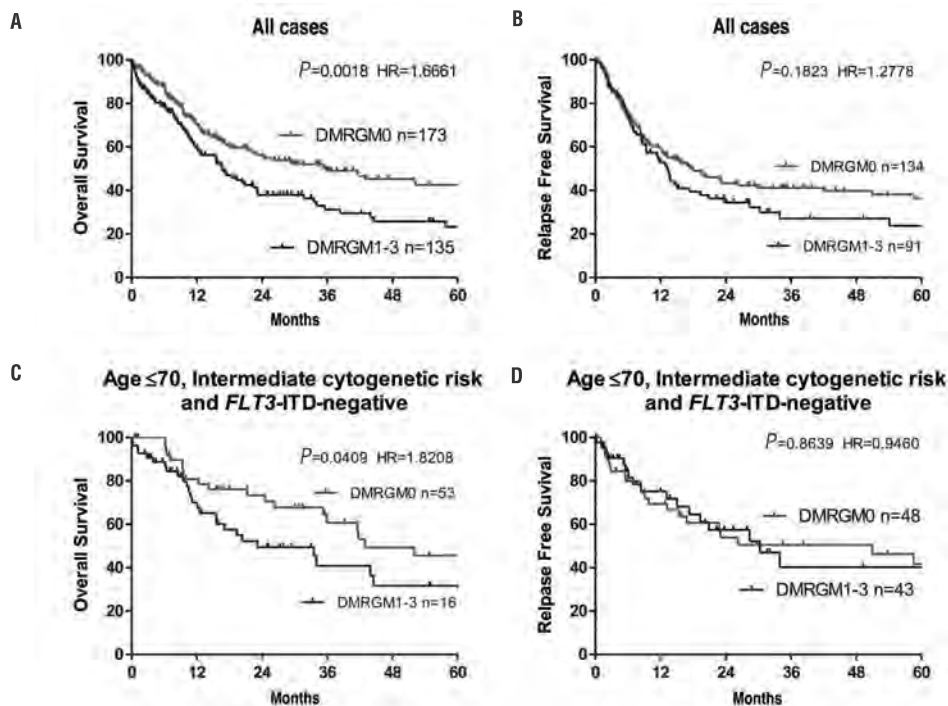


Figure 2. Overall and relapse-free survival rates in AML cases with and without DMRGM. (A) Overall survival rate for all cases. (B) Relapse-free survival rate for all cases. (C) Overall survival rate in *FLT3*-ITD-negative cases aged ≤ 70 years with intermediate cytogenetic prognosis. (D) Relapse-free survival rate in *FLT3*-ITD-negative cases aged ≤ 70 years with intermediate cytogenetic prognosis. HR: Hazard ratio.

established in overall survival rate (Online Supplementary Figure S2A), but *DNMT3A* mutation/*TET2* mutation⁺ was associated with a poorer relapse-free survival rate ($P=0.0349$) (Online Supplementary Figure S2B).

Multivariate analysis

Multivariate analysis (Cox proportional hazard model) via the step-wise method was carried out using the following variables: age >70 years, poor cytogenetic risk, transplantation time (in first or second complete remission), DMRGM, and gene mutation associated with poor prognosis. The following were identified as independent unfavorable prognostic factors for overall survival: age >70 years ($P=0.0001$); adverse cytogenetic risk ($P<0.0001$); DMRGM ($P=0.0424$); *FLT3*-ITD ($P<0.0001$); and *TP53* mutation ($P=0.0003$) (Table 2), whereas the independent unfavorable prognostic factors for relapse-free survival were: unfavorable cytogenetic risk ($P=0.0005$); *FLT3*-ITD ($P<0.0001$); *TP53* mutation ($P=0.0089$); and *KMT2A*-PTD ($P=0.0236$) (Table 2).

Efficacy of allogeneic transplantation in first remission for patients with DNA-methylation regulatory gene mutation-positive acute myeloid leukemia

The efficacy of allogeneic transplantation in first remission for patients with DMRGM aged ≤ 70 years was examined. In terms of overall survival, patients with DMRGM who underwent allogeneic stem cell transplantation in

first remission [SCT (1st CR)/DMRGM⁺] had a significantly more favorable prognosis than those who did not undergo such transplantation [SCT(1st CR)/DMRGM⁻] ($P=0.0254$) (Figure 4A). Likewise, in terms of relapse-free survival, SCT (1st CR)/DMRGM⁺ cases had a significantly more favorable prognosis than SCT (1st CR)/DMRGM⁻ cases ($P=0.0049$) (Figure 4B). A similar analysis was undertaken in cases aged ≤ 70 years, cases with intermediate cytogenetic risk, and *FLT3*-ITD-negative cases, but as the number of SCT(1st CR)/DMRGM⁺ cases was low, at just seven, the efficacy of allogeneic stem cell transplantation in first remission is not shown here.

Discussion

It was confirmed that DMRGM are very frequently present in AML, being observed in 135 of the 308 cases (43.8%) studied. A DMRGM was an unfavorable prognostic factor for overall survival in the whole group and in patients aged ≤ 70 years, in patients with an intermediate cytogenetic risk group, and in *FLT3*-ITD-negative patients. Allogeneic stem cell transplantation in first remission may improve the prognosis of cases with DMRGM mutation.

Until now, the significance of individual DMRGM as prognostic factors in AML has not been clear. Regarding *DNMT3A*, the most frequent of the DMRGM, Ley *et al.* reported that *DNMT3A* R882 mutation and non-R882

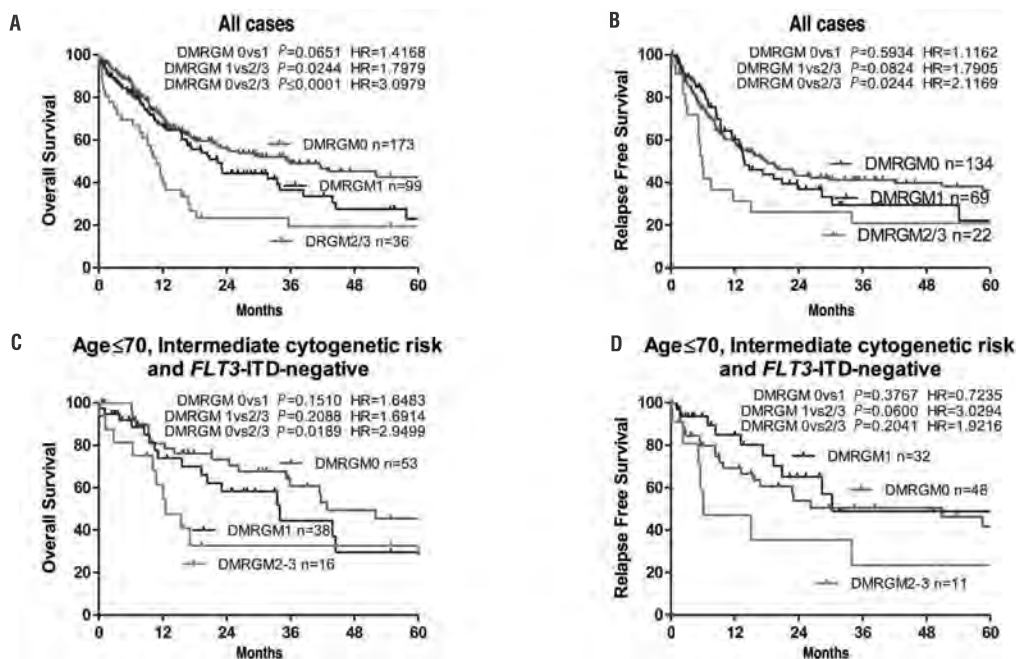


Figure 3. Overall and relapse-free survival rates in AML patients with no DMRGM, one DMRGM, and two or more DMRGM (A) Overall survival rate for all cases. (B) Relapse-free survival rate for all cases. (C) Overall survival rate in *FLT3*-ITD-negative cases aged ≤ 70 years with intermediate cytogenetic prognosis. (D) Relapse-free survival rate in *FLT3*-ITD-negative cases aged ≤ 70 years with intermediate cytogenetic prognosis. HR: Hazard ratio.

mutation are both associated with unfavorable prognosis, independently of whether *FLT3*-ITD is present.¹⁸ Meanwhile, Patel *et al.* reported that patients with intermediate cytogenetic risk who have a *DNMT3A* mutation do not have an unfavorable prognosis even if *FLT3*-ITD is not present.²⁴

Because of the expense associated with comprehensive gene mutation analysis using a next-generation sequencer, there have so far been few reports on DMRGM-based prognostic analysis involving a large number of patients. Such studies consist of the one by Patel *et al.*, based on 398 cases, and one by Hou *et al.*, based on 500 cases.^{24,25} Our analysis covered four DMRGM – *IDH1*, *IDH2*, *DNMT3A*, and *TET2* – in 308 cases of AML, a large cohort suggesting reliable results. Moreover, ours is the first study in which AML prognosis was explored with division into groups based on DMRGM.

Our study revealed that the greater the number of DMRGM, the poorer the prognosis is. It has been reported that increasing numbers of DMRGM are associated with unfavorable outcome in a number of hematologic malignancies. For example, Papaemmanuil *et al.* described that leukemia-free survival in patients with myelodysplastic syndromes becomes shorter with increasing number of gene mutations.³² Guglielmelli *et al.* also reported that, in primary myelofibrosis, the greater the number of mutations of *ASXL1*, *EZH2*, *SRSF2*, and *IDH1/2*, the poorer the patients' prognosis is.³³ We have also reported recently that three or more gene mutations is an unfavorable prognostic factor in *de novo* AML.³⁴ According to whole-exon mutation analysis using a next-generation sequencer, there are on average 2.5–5.0 gene mutations per case in AML,^{14,18,34} and it has been established that the onset of AML requires the combination of a number of gene mutations.^{16,17} These findings suggest that cases with a large number of gene mutations have a correspondingly high level of genomic instability and point to the strong possibility of mutations in genes not yet examined.³⁴ This is thought to result in a poorer prognosis. Our finding that prognosis in AML worsens with increasing number of DMRGM suggests that to improve prognostic analysis in AML it will be important not only to focus on each individual gene mutation, but also to seek to identify overall genomic instability in individual cases.

In a whole-exon analysis of 12,380 healthy subjects, Genovese *et al.* found that healthy subjects in whom DMRGM mutations were observed had a high rate of myeloid malignancies in hematopoietic organs a number of years later.³⁵ Shlush *et al.* demonstrated that, in AML with *DNMT3A* mutation, the mutation also occurred in hematopoietic stem cells with normal differentiation potential, so that even in cases in which chemotherapy induced remission, the *DNMT3A* mutation remaining in the stem cells subsequently led the resulting blood cells to proliferate and cause relapse of the leukemia.³⁶ If this finding applies to all DMRGM-positive AML cases, then chemotherapy alone cannot be expected to be effective in DMRGM-positive AML. As indicated by Patel *et al.*, for young patients with DMRGM-positive AML, allogeneic hematopoietic stem cell transplantation in first remission may be the only curative therapy available. The findings above indicate that the prognosis of patients with DMRGM-positive AML is unfavorable,

Table 2. Multivariate analysis of prognostic factors.

	Hazard ratio	P value	95% Confidence interval
Overall survival			
Age > 70 years	2.2901	0.0001	1.5049 – 3.4848
Adverse cytogenetic risk	2.7025	<0.0001	1.7472 – 4.1802
SCT (first or second CR)	0.2917	<0.0001	0.1658 – 0.5133
DMRGM	1.5782	0.0424	1.0158 – 2.4521
<i>FLT3</i> -ITD	2.6250	<0.0001	1.7393 – 3.38945
<i>RUNX1</i>	0.6524	0.0918	0.3971 – 1.0719
<i>TP53</i>	2.5915	0.0003	1.5488 – 4.3362
<i>KMT2A</i> -PTD	1.5755	0.0983	0.9191 – 2.7010
<i>GATA2</i>	0.5523	0.1717	0.2358 – 1.2939
Relapse free survival			
Age > 70 years	1.4937	0.1443	0.8716 – 2.5599
Adverse cytogenetic risk	2.6814	0.0005	1.5347 – 4.6848
SCT (first remission)	0.1466	<0.0001	0.0670 – 0.3211
<i>FLT3</i> -ITD	3.1407	<0.0001	2.0494 – 4.8131
<i>NRAS</i>	0.5634	0.0888	0.2910 – 1.0909
<i>RUNX1</i>	0.6602	0.1802	0.3597 – 1.2117
<i>TP53</i>	2.3102	0.0089	1.2341 – 4.3244
<i>KMT2A</i> -PTD	2.2479	0.0236	1.1147 – 4.5330

SCT: stem cell transplantation, CR: complete remission.

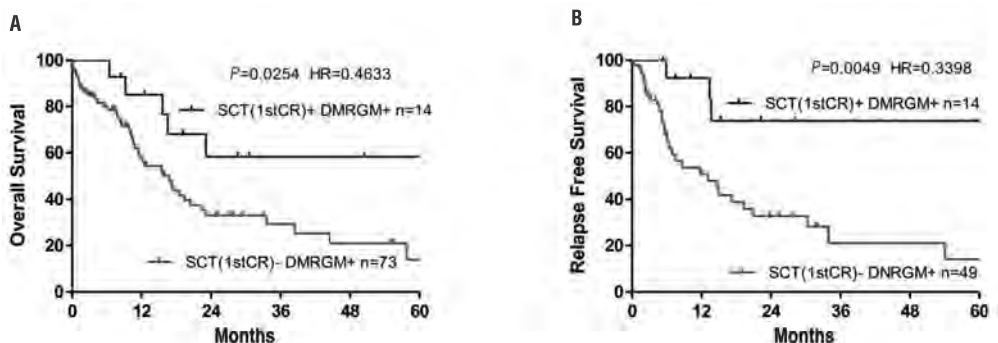


Figure 4. Efficacy of allogeneic stem cell transplantation in first remission for DMRGM-positive AML cases aged 70 years or below. (A) Overall survival rate for all cases. (B) Relapse-free survival rate for all cases. HR: hazard ratio; SCT: stem cell transplantation; 1stCR: first complete remission.

that the outcome worsens with increasing numbers of such mutations and that these patients should be treated with allogeneic hematopoietic stem cell transplantation in first remission.

One of the issues that needs to be considered when going forward with this research is that the subjects in this study were of Japanese ethnicity. So far, there have been no reports on the relation of ethnicity to frequency of gene

mutations and prognosis in AML. Whether the present research findings would be replicated in cohorts of patients of other ethnicities is an area that requires investigation in the future. Moreover, the present study did not include patients treated with azacitidine or other demethylating agents. The efficacy of demethylating agents in DMRGM-positive AML is therefore another area requiring investigation.

References

- Valk PJ, Verhaak RG, Beijen MA, et al. Prognostically useful gene-expression profiles in acute myeloid leukemia. *N Engl J Med*. 2004;350(16):1617-1628.
- Bullinger L, Döhner K, Bair E, et al. Use of gene-expression profiling to identify prognostic subclasses in adult acute myeloid leukemia. *N Engl J Med*. 2004;350(16):1605-1616.
- Schlenk RF, Döhner K, Mack S, et al. Prospective evaluation of allogeneic hematopoietic stem-cell transplantation from matched related and matched unrelated donors in younger adults with high-risk acute myeloid leukemia: German-Austrian trial AMLHD98A. *J Clin Oncol*. 2010;28(30):4642-4648.
- Preudhomme C, Sagot C, Boissel N, et al. Favorable prognostic significance of CEBPA mutations in patients with de novo acute myeloid leukemia: a study from the Acute Leukemia French Association (ALFA). *Blood*. 2002;100(8):2717-2723.
- Pabst T, Eyholzer M, Fos J, Mueller BU. Heterogeneity within AML with CEBPA mutations; only CEBPA double mutations, but not single CEBPA mutations are associated with favourable prognosis. *Br J Cancer*. 2009;100(8):1343-1346.
- Kottanidis PD, Gale RE, Frew ME, et al. The presence of a FLT3-internal tandem duplication in patients with acute myeloid leukemia (AML) adds important prognostic information to cytogenetic risk group and response to the first cycle of chemotherapy: analysis of 854 patients from the United Kingdom Medical Research Council AML 10 and 12 trials. *Blood*. 2001;98(6):1752-1759.
- Schnittger S, Schoch C, Kern W, et al. Nucleophosmin gene mutations are predictors of favorable prognosis in acute myelogenous leukemia with a normal karyotype. *Blood*. 2005;106(12):3733-3739.
- Döhner K, Schlenk RF, Habdank M, et al. Mutant nucleophosmin (NPM1) predicts favorable prognosis in younger adults with acute myeloid leukemia and normal cytogenetics: interaction with other gene mutations. *Blood*. 2005;106(12):3740-3746.
- Schlenk RF, Döhner K, Krauter J, et al. Mutation and treatment outcome in cytogenetically normal acute myeloid leukemia. *N Engl J Med*. 2008;358(18):1909-1918.
- Taskesen E, Bullinger L, Corbacioglu A, et al. Prognostic impact, concurrent genetic mutations, and gene expression features of AML with CEBPA mutations in a cohort of 1182 cytogenetically normal AML patients: further evidence for CEBPA double mutant AML as a distinctive disease entity. *Blood*. 2011;117(8):2469-2475.
- Brunet S, Labopin M, Esteve J, et al. Impact of FLT3 internal tandem duplication on the outcome of related and unrelated hematopoietic transplantation for adult acute myeloid leukemia in first remission: a retrospective analysis. *J Clin Oncol*. 2012;30(7):735-741.
- Döhner H, Estey EH, Amadori S, et al. Diagnosis and management of acute myeloid leukemia in adults: recommendations from an international expert panel, on behalf of the European LeukemiaNet. *Blood*. 2010;115(3):453-474.
- O'Donnell MR, Abboud CN, Altman J, et al. Acute myeloid leukemia. *J Natl Compr Canc Netw*. 2012;10(8):984-1021.
- The Cancer Genome Atlas Research Network. Genomic and epigenomic landscapes of adult de novo acute myeloid leukemia. *N Engl J Med*. 2013;368(22):2059-2074.
- Kihara R, Nagata Y, Kiyoi H, et al. Comprehensive analysis of genetic alterations and their prognostic impacts in adult acute myeloid leukemia patients. *Leukemia*. 2014;28(8):1586-1595.
- Döhner H, Weisdorf DJ, Bloomfield CD. Acute myeloid leukemia. *N Engl J Med*. 2015;373(12):1136-1152.
- Xie M, Lu C, Wang J, et al. Age-related mutations associated with clonal hematopoietic expansion and malignancies. *Nat Med*. 2014;20(12):1472-1478.
- Ley TJ, Ding L, Walter MJ, et al. DNMT3A mutations in acute myeloid leukemia. *N Engl J Med*. 2010;363(25):2424-2433.
- Thol F, Damm F, Lüdeking A, et al. Incidence and prognostic influence of DNMT3a mutations in acute myeloid leukemia. *J Clin Oncol*. 2011;29(21):2889-2896.
- Chou WC, Chou SC, Liu CY, et al. TET2 mutation is an unfavorable prognostic factor in acute myeloid leukemia patients with intermediate-risk cytogenetics. *Blood*. 2011;118(14):3803-3810.
- Figueroa ME, Abdel-Wahab O, Lu C, et al. Leukemic IDH1 and IDH2 mutations result in a hypermethylation phenotype, disrupt TET2 function, and impair hematopoietic differentiation. *Cancer Cell*. 2010;18(6):553-567.
- Marcucci G1, Maharry K, Wu YZ, et al. IDH1 and IDH2 gene mutations identify novel molecular subsets within de novo cytogenetically normal acute myeloid leukemia: a Cancer and Leukemia Group B study. *J Clin Oncol*. 2010;28(14):2348-2355.
- Boissel N, Nibourel O, Renneville A, et al. Prognostic impact of isocitrate dehydrogenase enzyme isoforms 1 and 2 mutations in acute myeloid leukemia: a study by the Acute Leukemia French Association group. *J Clin Oncol*. 2010;28(23):3717-3723.
- Patel JP, Gönen M, Figueroa ME, et al. Prognostic relevance of integrated genetic profiling in acute myeloid leukemia. *N Engl J Med*. 2012;366(12):1079-1089.
- Hou HA, Kuo YY, Liu CY, et al. DNMT3A mutations in acute myeloid leukemia: stability during disease evolution and clinical implications. *Blood*. 2012;119(2):559-568.
- Marcucci G, Metzeler KH, Schwind S, et al. Age-related prognostic impact of different types of DNMT3A mutations in adults with primary cytogenetically normal acute myeloid leukemia. *J Clin Oncol*. 2012;30(7):742-750.
- Aslanyan MG, Kroeze LI, Langemeijer SM, et al. Clinical and biological impact of TET2 mutations and expression in younger adult AML patients treated within the EORTC/GIMEMA AML-12 clinical trial. *Ann Hematol*. 2014;93(8):1401-1412.
- Ribeiro AF, Pratzcorona M, Erpelinck-Verschueren C, et al. Mutant DNMT3A: a marker of poor prognosis in acute myeloid leukemia. *Blood*. 2012;119(24):5824-5831.
- Gaidzik VI, Schlenk RF, Paschka P, et al. Clinical impact of DNMT3A mutations in younger adult patients with acute myeloid leukemia: results of the AML Study Group (AMLSC). *Blood*. 2013;121(23):4769-4777.
- Gaidzik VI, Paschka P, Späth D, et al. TET2 mutations in acute myeloid leukemia (AML): results from a comprehensive genetic and clinical analysis of the AML study group. *J Clin Oncol*. 2012;30(12):1350-1357.
- Wakita S, Yamaguchi H, Omori I, et al. Mutations of the epigenetics-modifying gene (DNMT3a, TET2, IDH1/2) at diagnosis may induce FLT3-ITD at relapse in de novo acute myeloid leukemia. *Leukemia*. 2013;27(5):1044-1052.
- Papaemmanuil E, Gerstung M, Malcovati L, et al. Clinical and biological implications of driver mutations in myelodysplastic syndromes. *Blood*. 2013;122(22):3616-3627.
- Guglielmelli P, Lasho TL, Rotunno G, et al. The number of prognostically detrimental mutations and prognosis in primary myelofibrosis: an international study of 797 patients. *Leukemia*. 2014;28(9):1804-1810.
- Wakita S, Yamaguchi H, Ueki T, et al. Complex molecular genetic abnormalities involving three or more genetic mutations are important prognostic factors for acute myeloid leukemia. *Leukemia*. 2016;30(5):545-554.
- Genovese G, Köhler AK, Handsaker RE, et al. Clonal hematopoiesis and blood-cancer risk inferred from blood DNA sequence. *N Engl J Med*. 2014;371(26):2477-2487.
- Shlush LI, Zandi S, Mitchell A, et al. Identification of pre-leukaemic haematopoietic stem cells in acute leukaemia. *Nature*. 2014;506(7488):328-333.

Amlexanox Downregulates S100A6 to Sensitize *KMT2A/AFF1*-Positive Acute Lymphoblastic Leukemia to TNF α Treatment

Hayato Tamai¹, Hiroki Yamaguchi¹, Koichi Miyake², Miyuki Takatori³, Tomoaki Kitano¹, Satoshi Yamanaka¹, Syunsuke Yui¹, Keiko Fukunaga¹, Kazutaka Nakayama¹, and Koiti Inokuchi¹



Abstract

Acute lymphoblastic leukemias (ALL) positive for *KMT2A/AFF1* (*MLL/AF4*) translocation, which constitute 60% of all infant ALL cases, have a poor prognosis even after allogeneic hematopoietic stem cell transplantation (allo-HSCT). This poor prognosis is due to one of two factors, either resistance to TNF α , which mediates a graft-versus-leukemia (GVL) response after allo-HSCT, or immune resistance due to upregulated expression of the immune escape factor S100A6. Here, we report an immune stimulatory effect against *KMT2A/AFF1*-positive ALL cells by treatment with the anti-allergy drug amlexanox, which we found

to inhibit S100A6 expression in the presence of TNF- α . In *KMT2A/AFF1*-positive transgenic (Tg) mice, amlexanox enhanced tumor immunity and lowered the penetrance of leukemia development. Similarly, in a NOD/SCID mouse model of human *KMT2A/AFF1*-positive ALL, amlexanox broadened GVL responses and extended survival. Our findings show how amlexanox degrades the resistance of *KMT2A/AFF1*-positive ALL to TNF α by downregulating S100A6 expression, with immediate potential implications for improving clinical management of *KMT2A/AFF1*-positive ALL. *Cancer Res*; 77(16); 4426–33. ©2017 AACR.

Introduction

The most prevalent mixed-lineage leukemia (MLL) rearrangement in acute lymphoblastic leukemia (ALL) generates the *KMT2A/AFF1* (*MLL/AF4*) fusion gene due to the t(4;11)(q21;q23) chromosomal translocation. ALL with t(4;11)(q21;q23) has a bimodal age distribution with a major peak of incidence in early infancy and accounts for over 50% of ALL cases in infants < 6 months old, 10% to 20% in older infants, 2% in children, and up to 7% in adults (1). Despite recent improvements in the overall treatment outcome for ALL patients, including allogeneic hematopoietic stem cell transplantation (allo-HSCT), *KMT2A/AFF1*-positive ALL is still associated with a poor prognosis (2). The complete remission (CR) rate in children is as high as 88%, but the median overall survival (OS) is only 10 months, indicating an extremely poor prognosis. In adult patients with ALL, the CR rate is 75%, but the prognosis is also poor, with a median OS of 7 months (1).

The poor prognosis of *KMT2A/AFF1*-positive ALL has been suggested to be due to resistance to TNF α , which is the factor

involved in the graft-versus-leukemia (GVL) effect, or tumor immunity by upregulation of S100A6 expression followed by interference with the p53–caspase pathway (3). S100A6 is a 10.5-kDa Ca²⁺-binding protein belonging to the S100 protein family, which has been reported to interact with and alter the conformation of p53 (4–7). Upregulation of S100A6 expression in *KMT2A/AFF1*-positive ALL inhibits p53 acetylation followed by inhibition of caspase apoptotic pathway upregulation in the presence of TNF α (8).

Here, we focused on amlexanox (2-amino-7-isopropyl-5-oxo-5H-chromeno[2,3-b] pyridine-3-carboxylic acid), a common anti-allergic drug, which targets S100A6. Amlexanox was reported to inhibit the translocation pathway of endogenous S100A6 in endothelial cells (9). Amlexanox has also been reported to bind to S100A13, which is another member of the S100 protein family (10). S100A13 and acidic fibroblast growth factor (FGF1) are involved in a wide range of important biological processes, including angiogenesis, cell differentiation, neurogenesis, and tumor growth. Generally, the biological function of FGF1 is to recognize a specific tyrosine kinase on the cell surface and initiate the cell signal transduction cascade. Amlexanox binds S100A13 and FGF1 and inhibits the heat shock–induced release of S100A13 and FGF1 (10). Amlexanox has been used in a number of recent metabolic studies. Reilly and colleagues reported that amlexanox acted as an inhibitor of IKK ϵ and TBK1 (11). They showed that treatment with amlexanox resulted in reduced inflammation, marked improvement in insulin sensitivity, and reduced hepatosteatosis in mice with genetic or dietary obesity (11). The present study was performed to examine the effects of amlexanox in *KMT2A/AFF1*-positive ALL.

¹Department of Hematology, Nippon Medical School, Tokyo, Japan. ²Department of Biochemistry and Molecular Biology, Division of Gene Therapy Research Center for Advanced Medical Technology, Nippon Medical School, Tokyo, Japan. ³Research Center for Life Science, Nippon Medical School, Tokyo, Japan.

H. Yamaguchi and K. Miyake contributed equally to this article.

Corresponding Author: Hayato Tamai, Nippon Medical School, Sendagi 1-1-5, Bunkyo-Ku, Tokyo 113-8603, Japan. Phone: 81-3-3822-2131; Fax: 81-3-5685-1793; E-mail: s6056@nms.ac.jp

doi: 10.1158/0008-5472.CAN-16-2974

©2017 American Association for Cancer Research.

Materials and Methods

Cell culture

The *KMT2A/AFF1*-positive human ALL cell line RS4;11 was purchased from ATCC. The *KMT2A/AFF1*-positive ALL cell line SEM was purchased from Deutsche Sammlung von Mikroorganismen und Zellkulturen GmbH (DSMZ). The cell lines were obtained in 3 years and used within 6 months after receipt or resuscitation. To check mycoplasma we used a PCR-based method, indirect staining and an agar and broth culture. SEM, SEM transduced with a lentiviral vector expressing luciferase (SEM-Luc), and RS4;11 cells were cultivated in RPMI 1640 (Sigma-Aldrich) supplemented with 10% FBS (PAN Biowest) at 37°C under 5% CO₂.

In vitro analysis of SEM and RS4;11 cell growth

SEM and RS4;11 were seeded in 6-well plates (2×10^5 cells/well) and incubated *in vitro* with TNF α (0 and 10 ng/mL; Wako) or Human peripheral blood mononuclear cells (PBMC; 2×10^5 cells/well) and amlexanox (Tokyo Chemical Industry; 0, 10, and 100 μ g/mL) for 48 hours before counting cells to examine the effects of TNF α and amlexanox on leukemia cells.

Western blotting analysis

Western blotting analysis was performed as described previously (3). SEM and RS4;11 cells were incubated for 48 hours and collected for Western blotting analysis. Equal aliquots of lysates from cell lines or homogenized mouse spleen were subjected to 10% SDS-PAGE, transferred onto polyvinylidene difluoride membranes, and immunoblotted with the following primary antibodies (Abs): anti-S100A6 (calcylin) Ab (Santa Cruz Biotechnology), anti-caspase-3, anti-cleaved caspase-3 Ab (Cell Signaling Technology), anti-p53 (Santa Cruz Biotechnology), anti-acetyl-p53 (Millipore), and anti- β -actin Ab (Millipore). Can Get Signal (Toyobo) was used to promote the reaction between primary Ab and antigen (Ag).

Animal experiments using the *KMT2A/AFF1* transgenic mouse model

KMT2A/AFF1 transgenic (Tg) mice, which show CD45R/B220⁺ leukemia by 12 months of age, at which time lymphoma cells will have infiltrated the bone marrow (BM) and spleen, were established previously (12). This *KMT2A/AFF1* Tg mouse model has an essentially normal immune system. We divided 10 male *KMT2A/AFF1* Tg mice at the age of 4 months into two groups: the amlexanox group ($n = 5$) fed a diet containing amlexanox (0.02%) for 10 months, and the control group ($n = 5$). All *KMT2A/AFF1* Tg mice were killed at the age of 14 months for histopathological and Western blotting analysis. All animal experiments were performed in accordance with the regulations established by the Ethical Committee of Nippon Medical School and were approved by the Animal Care and Committee of Nippon Medical School (Approval number: 28-026).

Histopathology and immunopathology

For histopathological analysis, mice were killed and tissues of interest were fixed in 4% paraformaldehyde. Hematoxylin and eosin (H&E) staining was performed using standard protocols. For immunopathological analysis, the slides were fixed for 30 minutes in 4% paraformaldehyde, microwaved for 5 minutes in Vector Antigen Unmasking Solution (pH 6.0; Vector Laborato-

ries) for Ag retrieval, rinsed twice for 10 minutes each time in PBS, and incubated for 15 minutes in 3% hydrogen peroxide in methanol to quench endogenous peroxidase activity. For CD45R/B220 staining, the pretreated slides were incubated for 60 minutes with anti-CD45R/B220 (BD Pharmingen) primary Abs. To visualize anti-CD45R/B220 Ab binding, the slides were incubated for 30 minutes with FITC-conjugated anti-rat IgG (Jackson ImmunoResearch Laboratories). Nuclei were counterstained with Mayer's hematoxylin. The photomicrographs shown in the figures were taken with a SPOT Insight digital camera controlled using SPOT Advanced Version 4.0.9 software (Diagnostic Instruments) with a Nikon Eclipse 80i microscope equipped with Nikon Plan 2 \times /0.08 NA and Plan 40 \times /0.75 NA objectives. Comparison of CD45R/B220-positive tumor cells between the control group and amlexanox group was performed by counting the numbers of CD45R/B220-positive cells/mm².

Separation of human PBMCs

Human PBMCs were obtained by separation of heparinized blood from a healthy donor on a Ficoll-Histopaque gradient. The PBMCs were washed twice and resuspended in RPMI 1640 supplemented with 25 mmol/L HEPES buffer, 2 mm glutamine, 100 U/mL penicillin, 100 pg/mL streptomycin, and 10% heat-inactivated FCS (designated as FCS-RPMI).

Animal experiments using PBMC-NOD/SCID mice

For *in vivo* analysis, 5×10^5 /body of SEM-Luc cells were injected intraperitoneally (i.p.) into three groups of 10 nonobese diabetic/severe combined immunodeficiency (NOD/SCID) mice. Each group of 10 mice was divided into two groups: the amlexanox + PBMC group ($n = 5$) fed a diet containing amlexanox (0.02%), and the PBMC group ($n = 5$) fed a diet without amlexanox. Feeding with each diet was started when SEM-Luc cells were injected and supplied consistently until mice died. Mice in each group were injected i.p. with 4×10^7 /body of human PBMCs every 2 weeks. Non-PBMC-injected mice fed a diet without amlexanox were used as controls. In addition to overall survival (OS) rate, tumor growth after injection of human PBMCs was assessed using an *in vivo* imaging system (IVIS) as described previously (3).

Statistical analysis

The results of cell growth were analyzed by the Student *t* test, assuming unequal variances and two-tailed distributions. Data are shown as the means \pm standard deviation of at least three samples. For survival analyses, event time distributions were estimated using the method of Kaplan and Meier, and differences in survival rates were compared using the log-rank test. In all analyses, $P < 0.05$ was taken to indicate statistical significance.

Results

Both SEM and RS4;11 cells were sensitive to TNF α in the presence of 100 μ g/mL of amlexanox, while both SEM and RS4;11 cells showed resistance without amlexanox

First, to analyze the effects of amlexanox on *KMT2A/AFF1*-positive ALL cell lines, SEM and RS4;11 were seeded in 6-well plates (2×10^5 cells/well) and incubated *in vitro* with TNF α (0 and 10 ng/mL; Wako) and amlexanox (Tokyo Chemical Industry; 0, 10, and 100 μ g/mL). After 48 hours of incubation, viable cells were counted using Trypan blue exclusion. *KMT2A/AFF1*-positive

Tamai et al.

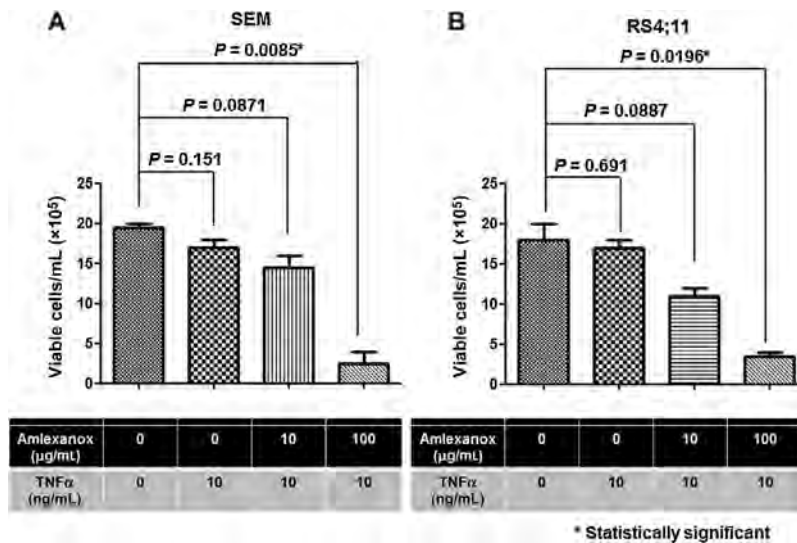


Figure 1. Effects of amlexanox on *KMT2A/AFL1*-positive ALL cell lines with or without TNFα. The figure presents a summary of growth inhibition of *KMT2A/AFL1*-positive ALL cell lines by administration of amlexanox with or without TNFα (A, SEM; B, RS4;11). Although there was no significant inhibition by 10 ng/mL of TNFα without amlexanox, significant inhibition was observed with 10 ng/mL of TNFα in the presence of 100 μg/mL of amlexanox.

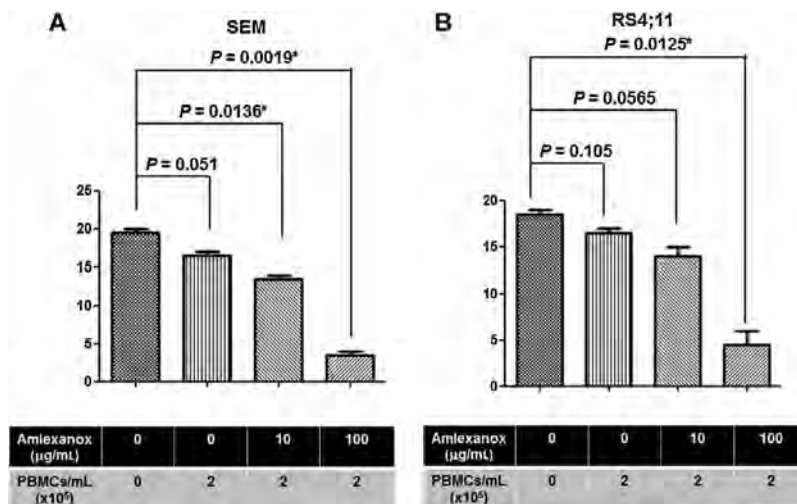
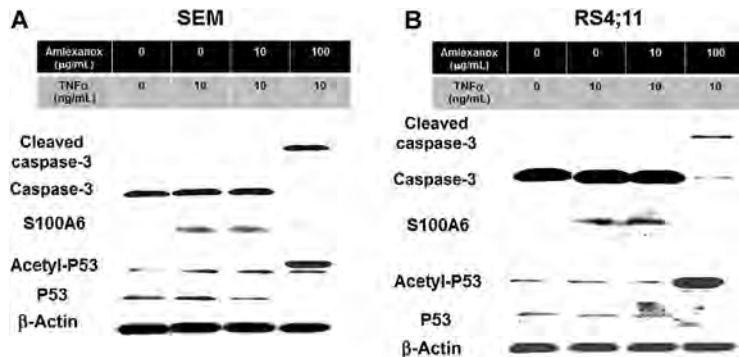


Figure 2. Effects of amlexanox on *KMT2A/AFL1*-positive ALL cell lines with or without PBMCs (2×10^5 cells/well). SEM and RS4;11 were incubated with PBMCs (2×10^5 cells/well) instead of 10 ng/mL of TNFα and viable cells were counted. SEM cells showed significant growth inhibition by incubation with PBMCs in the presence of 10 or 100 μg/mL of amlexanox ($P = 0.0136$ or 0.0019 ; A). RS4;11 cells also showed significant growth inhibition by incubation with PBMCs in the presence of 100 μg/mL of amlexanox ($P = 0.0125$; B).

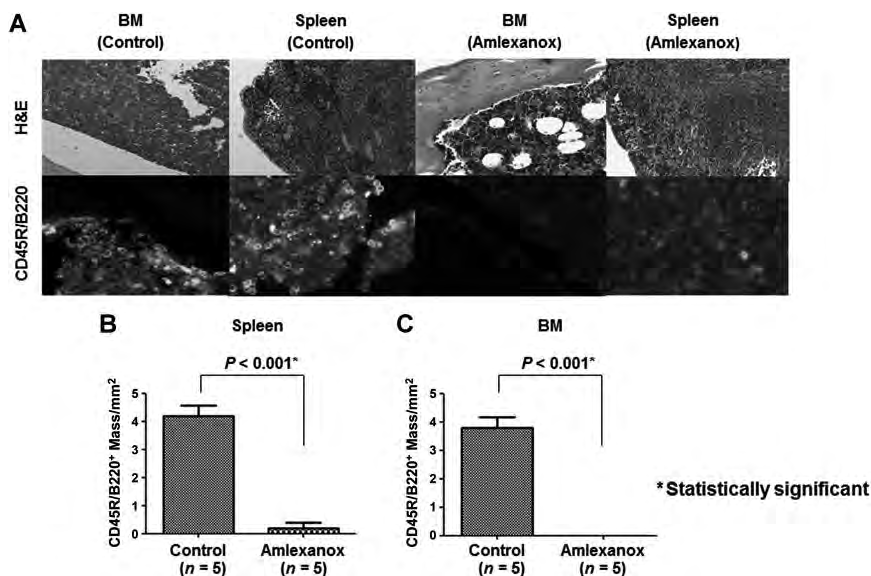
Figure 3.

Mechanism underlying the effects of amlexanox on *KMT2A/AFI*-positive ALL. **A** and **B**, Western blotting of lysates of *KMT2A/AFI*-positive cell lines with amlexanox. Western blotting analysis showed that 100 $\mu\text{g/mL}$ of amlexanox suppressed S100A6 activation and induced apoptosis by upregulation of acetyl p53/p53 and cleaved caspase-3/ caspase (A, SEM; B, RS4;11).



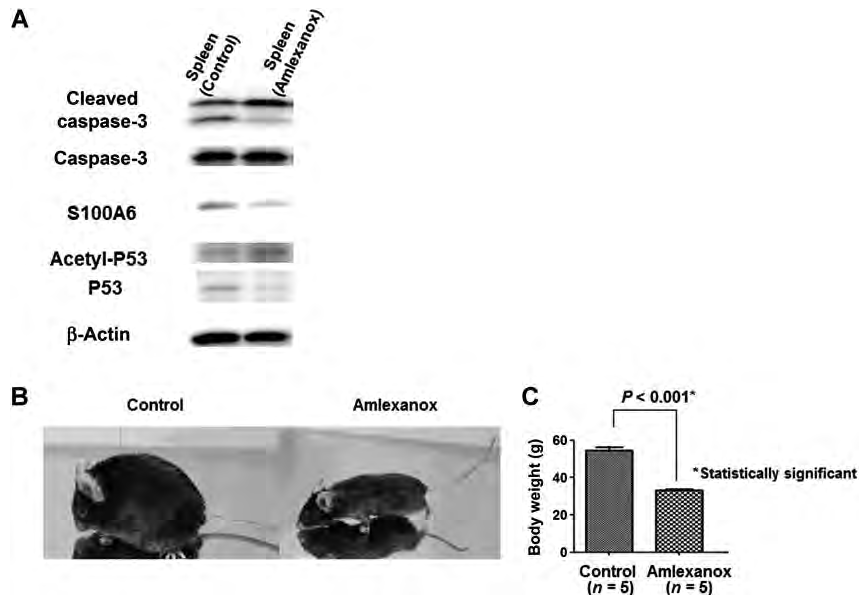
ALL cells (SEM or RS4;11) showed no significant growth inhibition by 10 ng/mL of TNF α in the absence or presence of 10 $\mu\text{g/mL}$ of amlexanox (Fig. 1A and B). However, both cell lines showed significant growth inhibition by 10 ng/mL of TNF α in the presence of 100 $\mu\text{g/mL}$ of amlexanox ($P = 0.0085$ for SEM, $P = 0.0196$ for RS4;11; Fig. 1A and B). Next, to examine direct evidence that amlexanox increases cell-mediated anti-leukemia effects, SEM

and RS4;11 cells were incubated with PBMCs (2×10^5 cells/well) instead of 10 ng/mL of TNF α and viable cells were counted. SEM cells showed significant growth inhibition on incubation with PBMCs in the presence of 10 or 100 $\mu\text{g/mL}$ of amlexanox ($P = 0.0136$ or 0.0019; Fig. 2A). RS4;11 cells also showed significant growth inhibition on incubation with PBMCs in the presence of 100 $\mu\text{g/mL}$ of amlexanox ($P = 0.0125$; Fig. 2B). These results

**Figure 4.**

Results of amlexanox in *KMT2A/AFI* Tg mice. **A**, Comparison of the results of immunohistopathological analyses (H&E and CD45R/B220) between one mouse from the amlexanox group (amlexanox#1) and one mouse from the control group (control#1). Although CD45R/B220 $^{+}$ pro-B-cell leukemia infiltration (green fluorescence) was observed in the spleen and BM of control#1, no leukemia infiltration was observed in amlexanox#1. Although H&E staining in amlexanox#1 showed normocellular BM, control#1 showed hypercellular BM because of leukemia infiltration. Although H&E-stained spleen sections from amlexanox#1 showed normal structure of the spleen, control#1 showed destruction of the normal structure. **B** and **C**, Comparison of CD45R/B220 $^{+}$ leukemia mass/ mm^2 between the control group ($n = 5$) and amlexanox group ($n = 5$). Both the spleen (**B**) and BM (**C**) of the amlexanox group had significantly less CD45R/B220 $^{+}$ leukemia cell invasion in comparison with the control group (both $P < 0.001$).

Tamai et al.

**Figure 5.**

Comparison of *KMT2A/AFF1* Tg mice between the amlexanox group and control group. **A**, Western blotting analysis confirmed *in vivo* that upregulation of S100A6 was inhibited and p53 acetylation and cleaved caspase-3 were activated in the amlexanox group. **B** and **C**, At the age of 14 months, *KMT2A/AFF1* Tg mice in the amlexanox group had significantly lower body weight than those in the control group ($P < 0.001$).

indicated that amlexanox increases both TNF α and cell-mediated antileukemia effects.

Downregulation of S100A6 by amlexanox leads to growth suppression of *KMT2A/AFF1*-positive human ALL cells through the p53–caspase-3 pathway in the presence of TNF α

To analyze the molecular mechanism underlying the effect of amlexanox on the *KMT2A/AFF1*-positive human ALL cells, SEM and RS4;11 were incubated for 48 hours, and collected for Western blotting analysis. As shown in Fig. 3, S100A6 was activated in the presence of 10 ng/mL TNF α , and activated S100A6 was decreased and both acetyl-p53/p53 ratio and cleaved caspase-3/caspase-3 ratio were increased in cells treated with 100 μ g/mL of amlexanox in the presence of 10 ng/mL of TNF α in the *KMT2A/AFF1*-positive human ALL cell line (Fig. 3A and B).

Amlexanox inhibited infiltration of pro-B-cell leukemia in the *KMT2A/AFF1* Tg mouse model

To examine whether amlexanox in combination with tumor immunity suppressed the development of *MLL/AF4*-positive ALL, we used *KMT2A/AFF1*-positive Tg mice in which the immune system is normal (12). *In vivo* analysis was performed using *KMT2A/AFF1*-positive Tg mice, which we established previously and show CD45R/B220⁺ pro-B-cell leukemia by 12 months of age (12). Although pro-B cell-leukemia infiltration was observed in all five mice in the control group, no leukemia occurred in four

of five mice in the amlexanox group at the age of 14 months. Figure 4A (top) shows a comparison of the results of H&E staining between one mouse from the amlexanox group (amlexanox#1) and one mouse from the control group (control#1). Although the normal structure of the spleen was disrupted in control#1, no such effect was seen in the spleen of amlexanox#1. Although BM of control#1 was hypercellular with tumor cells, that of amlexanox#1 was normocellular with no tumor invasion. Figure 4A (bottom) shows a comparison of the results of immunohistopathologic analysis between one mouse from the amlexanox group (amlexanox#1) and one mouse from the control group (control#1). Although the spleen and BM of control#1 showed CD45R/B220⁺ leukemia infiltration, no leukemia was observed in amlexanox#1.

Figure 4B shows a comparison of CD45/B220⁺ leukemia mass/mm² between the control group ($n = 5$) and amlexanox group ($n = 5$). Both the spleen and BM of the amlexanox group had significantly less CD45/B220⁺ leukemia cell invasion in comparison with the control group (both $P < 0.001$).

Amlexanox inhibits S100A6 upregulation followed by the p53–caspase-3 apoptotic pathway in *KMT2A/AFF1* Tg mice

To examine the mechanism underlying the suppression of leukemia by amlexanox in *KMT2A/AFF1* Tg mice, we performed Western blotting analysis of the lysates from the spleens of *KMT2A/AFF1* Tg mice in the amlexanox group and compared the

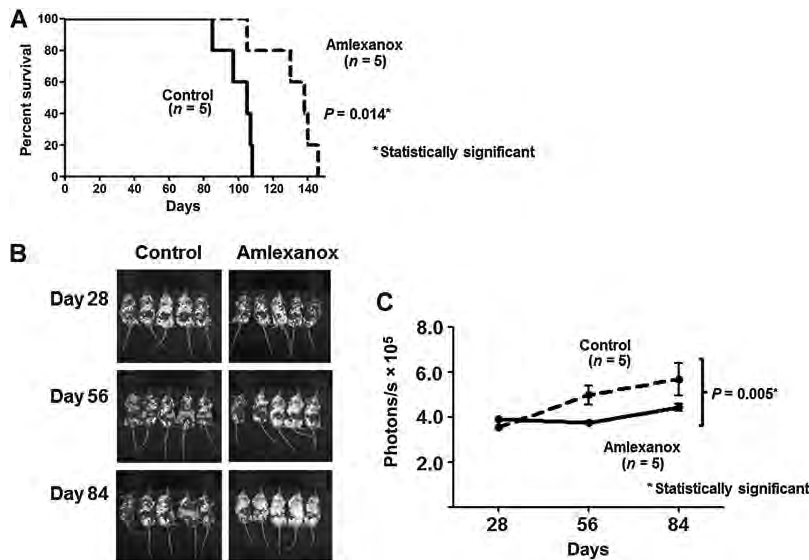


Figure 6.

Results of amlexanox in PBMC-NOD-SCID mice. **A**, OS curves of PBMC-NOD-SCID mice injected with 5×10^5 body of *KMT2A/AFF1*-positive ALL cells. The amlexanox + PBMC group showed significantly prolonged OS in PBMC-NOD-SCID mice injected with 5×10^5 /body of *KMT2A/AFF1*-positive ALL cells. **B** and **C**, Figure 5B and C show comparisons of SEM-Luc volumes between the PBMC + amlexanox group and control group. On day 84 after transplantation, the SEM-Luc volume was significantly lower in the amlexanox + PBMC group than in the control group ($P = 0.003$).

results with those for *KMT2A/AFF1* Tg mice in the control group. Western blotting analysis indicated the inhibition of S100A6 and upregulation of p53 acetylation as well as cleaved caspase-3 levels in the amlexanox group in comparison with the control group (Fig. 5A).

Amlexanox-treated *KMT2A/AFF1*Tg mice were significantly smaller than those in the control group

Reilly and colleagues reported that amlexanox reduced obesity in mice by inhibition of IKK ϵ and TBK1 (11), and this may be a problem when considering use of amlexanox in human infants. Therefore, we monitored body weight of mice treated with amlexanox. As shown in Fig. 5B, *KMT2A/AFF1* Tg mice in the amlexanox group had significantly lower weight at the age of 14 months than those in the control group (Fig. 5C; $P < 0.001$).

Comparison of PBMC-NOD/SCID mice transplanted with SEM-Luc

To examine whether amlexanox in combination with GVL effect could suppress the development of *KMT2A/AFF1*-positive ALL, we used PBMC-NOD/SCID mice transplanted with *KMT2A/AFF1*-positive ALL. As shown in Fig. 6A, PBMC-NOD/SCID mice transplanted with SEM-Luc in the amlexanox + PBMC group showed significantly longer survival than those in the control group ($P = 0.011$). The PBMC group did not show significantly longer survival than those in the control group ($P = 0.93$).

Figure 6B and C show comparisons of the volumes of SEM-Luc between the amlexanox + PBMC group and control group. On day 84 following transplantation, the volume of SEM-Luc was significantly lower in the amlexanox group than the control group ($P = 0.003$). There was no significant difference in SEM-Luc between the PBMC group and control group ($P = 0.120$).

Discussion

The results presented here suggested that amlexanox inhibits the resistance of *KMT2A/AFF1* (*MLL/AF4*)-positive ALL to TNF α by downregulating S100A6 expression. The results of this study indicated that amlexanox blocks upregulation of S100A6 expression followed by interference with the p53-caspase pathway in *KMT2A/AFF1*-positive ALL both *in vitro* and *in vivo*. The hypothetical mechanism underlying these effects is shown in Fig. 7. With respect to the genomic mechanism of *KMT2A/AFF1*, *KMT2A* is an H3K4 histone methyltransferase, and leukemia transformation by *KMT2A* fusion requires the H3 lysine 79 (H3K79) methyltransferase DOT1L, which is recruited to the *KMT2A* fusion transcriptional complex. Suppression of DOT1L inhibited expression of *AFF1* target genes, indicating that H3K79 methylation is a distinguishing feature of *KMT2A/AFF1*-positive ALL and plays a key role in maintenance of *AFF1*-driven gene expression (13). However, our therapeutic target of *KMT2A/AFF1*-positive ALL is not this genomic mechanism but the resistance of *KMT2A/AFF1* (*MLL/AF4*)-positive ALL to TNF α by downregulating S100A6 expression.

Tamai et al.

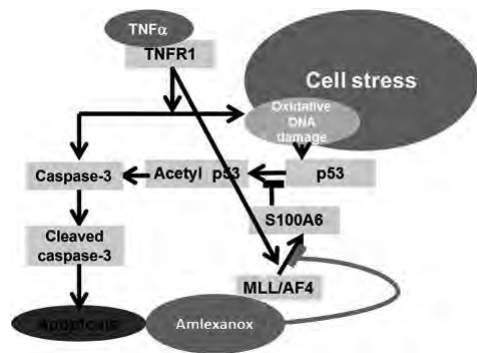


Figure 7. Working hypothesis for the effect of amlexanox on *KMT2A/AFF1*-positive ALL. Amlexanox induces the caspase-3 apoptotic pathways in *KMT2A/AFF1*-positive ALL through downregulation of S100A6, followed by p53 acetylation.

We previously reported that the poor prognosis of *KMT2A/AFF1*-positive ALL may be caused by resistance to TNF α , which is the factor involved in the GVL effect, or tumor immunity by upregulation of S100A6 expression followed by interference with the p53–caspase apoptotic pathway (3). Amlexanox, known as an anti-allergic drug, may exploit the GVL effect or tumor immunity in *KMT2A/AFF1*-positive ALL because it inhibits the resistance of *KMT2A/AFF1*-positive ALL to TNF α . *In vivo* analysis using *KMT2A/AFF1*-positive Tg mice showed that amlexanox in combination with tumor immunity may suppress the development of *MLL/AF4*-positive ALL. Therefore, using amlexanox after CR may be effective to suppress relapse of *KMT2A/AFF1*-positive ALL.

The GVL effect on *KMT2A/AFF1*-positive ALL may also be induced by amlexanox in PBMC-NOD/SCID mice. Specifically, allogeneic hematopoietic stem cell transplantation (allo-HSCT) is expected to show beneficial effects in combination with amlexanox despite its lack of efficacy in *KMT2A/AFF1*-positive ALL patients reported to date (2). Interestingly, Spijkers-Hagelstein and colleagues reported that overexpression of the S100 protein family members S100A8 and S100A9 in *KMT2A/AFF1*-positive ALL was associated with failure to induce free-cytosolic Ca²⁺ and prednisolone resistance (14). These observations taken together with our previous study suggest that high levels of S100 protein expression by *KMT2A/AFF1*-positive ALL may be the main factors involved in therapy resistance and poor prognosis of *KMT2A/AFF1*-positive ALL. Amlexanox was also reported to bind to

another member of the S100 protein family, S100A13 (10). Although there have been no reports regarding the relations between amlexanox and S100A8 and S100A9, it is possible that this drug affects these proteins.

Another major advantage of the use of amlexanox is that it is already a commonly used anti-allergy drug and its cost is not high in contrast to almost all other molecular target drugs. However, there is a problem when considering use of amlexanox as treatment for human infants. As reported by Reilly and colleagues, amlexanox prevents weight gain by inhibition of IKK- ϵ and TBK1 (11). Our *KMT2A/AFF1* Tg mice fed amlexanox were also significantly smaller than those fed the control diet ($P < 0.001$; Fig. 5B and C). This is an important problem for the treatment of infants, although it would not be an issue in adults. Despite these problems, treatment targeting S100A6 by amlexanox may increase tumor immunity and the effects of hematopoietic stem cell transplantation against *KMT2A/AFF1*-positive leukemia, thus making it useful for treatment of *KMT2A/AFF1*-positive leukemia.

Disclosure of Potential Conflicts of Interest

No potential conflicts of interest were disclosed.

Authors' Contributions

Conception and design: H. Tamai, H. Yamaguchi, K. Inokuchi
Development of methodology: H. Tamai, H. Yamaguchi
Acquisition of data (provided animals, acquired and managed patients, provided facilities, etc.): H. Tamai, H. Yamaguchi, K. Inokuchi
Analysis and interpretation of data (e.g., statistical analysis, biostatistics, computational analysis): H. Tamai, H. Yamaguchi, M. Takatori, T. Kitano
Writing, review, and/or revision of the manuscript: H. Tamai, H. Yamaguchi, K. Miyake, S. Yamanaka, K. Fukunaga, K. Nakayama, K. Inokuchi
Administrative, technical, or material support (i.e., reporting or organizing data, constructing databases): H. Tamai, H. Yamaguchi
Study supervision: H. Tamai, H. Yamaguchi, K. Miyake, K. Inokuchi

Acknowledgments

The authors thank Dr. R. Van Etten of Harvard Medical School for the kind gift of the pMSCVneop230 BCR/ABL plasmid for establishment of our *KMT2A/AFF1* Tg mice.

Grant Support

H. Tamai was supported in part by grant 40465349 from the Ministry of Health and Welfare of Japan and the Ministry of Education, Science, and Culture of Japan. H. Tamai was also supported by grants from SENSHIN Medical Research Foundation.

The costs of publication of this article were defrayed in part by the payment of page charges. This article must therefore be hereby marked *advertisement* in accordance with 18 U.S.C. Section 1734 solely to indicate this fact.

Received November 1, 2016; revised March 11, 2017; accepted June 6, 2017; published OnlineFirst June 23, 2017.

References

- Tamai H, Inokuchi K. 11q23/MLL acute leukemia: update of clinical aspects. *J Clin Exp Hematop* 2010;50:91–8.
- Pui CH, Gaynon PS, Boyett JM, Chessells JM, Baruchel A, Kamps W, et al. Outcome of treatment in childhood acute lymphoblastic leukaemia with rearrangements of the 11q23 chromosomal region. *Lancet* 2002;359:1909–15.
- Tamai H, Miyake K, Yamaguchi H, Shimada T, Dan K, Inokuchi K. Inhibition of S100A6 induces GVL effects in *MLL/AF4*-positive ALL in human PBMC-SCID mice. *Bone Marrow Transplant* 2014;49:699–703.
- Soomnicki EP, Nawrot B, Les'niak W. S100A6 binds p53 and affects its activity. *Int J Biochem Cell Biol* 2009;41:784–90.
- van Dieck J, Fernandez-Fernandez MR, Veprintsev DB, Fersht AR. Modulation of the oligomerization state of p53 by differential binding of proteins of the S100 family to p53 monomers and tetramers. *J Biol Chem* 2009;284:13804–11.
- Tsoporis JN, Izhar S, Parker TG. Expression of S100A6 in cardiac myocytes limits apoptosis induced by tumor necrosis factor- α . *J Biol Chem* 2008;283:30174–83.



Amlexanox Suppresses *KMT2A/AFF1 (MLL/AF4)*-Positive ALL

7. van Dieck J, Brandt T, Teufel DP, Veprintsev DB, Joerger AC, Fersht AR. Molecular basis of S100 proteins interacting with the p53 homologs p63 and p73. *Oncogene* 2010;29:2024–35.
8. Tamai H, Miyake K, Yamaguchi H, Takatori M, Dan K, Inokuchi K, et al. Resistance of MLL-AFF1-positive acute lymphoblastic leukemia to tumor necrosis factor- α is mediated by S100A6 upregulation. *Blood Cancer J* 2011;1:e38.
9. Hsieh HL, Schäfer BW, Cox JA, Heizmann CW. S100A13 and S100A6 exhibit distinct translocation pathways in endothelial cells. *J Cell Sci* 2002;115:3149–58.
10. Rani SG, Mohan SK, Yu C. Molecular level interactions of S100A13 with amlexanox: inhibitor for formation of the multiprotein complex in the nonclassical pathway of acidic fibroblast growth factor. *Biochemistry* 2010;49:2585–92.
11. Reilly SM, Chiang SH, Decker SJ, Chang L, Uhm M, Larsen MJ, et al. An inhibitor of the protein kinases TBK1 and IKK- ϵ improves obesity-related metabolic dysfunctions in mice. *Nat Med* 2013;19:313–21.
12. Tamai H, Miyake K, Yamaguchi H, Takatori M, Dan K, Inokuchi K, et al. AAV8 vector expressing IL24 efficiently suppresses tumor growth mediated by specific mechanisms in MLL/AF4-positive ALL model mice. *Blood* 2012;119:64–71.
13. Sanjuan-Pla A, Bueno C, Prieto C, Acha P, Stam RW, Marschalek R, et al. Revisiting the biology of infant t(4;11)/MLL-AF4⁺ B-cell acute lymphoblastic leukemia. *Blood* 2015;126:2676–85.
14. Spijkers-Hagelstein JA, Mimoso Pinhanos S, Schneider P, Pieters R, Stam RW. Src kinase-induced phosphorylation of annexin A2 mediates glucocorticoid resistance in MLL-rearranged infant acute lymphoblastic leukemia. *Leukemia* 2013;27:1063–71.

ORIGINAL ARTICLE

WILEY **Cancer Science**

Dasatinib cessation after deep molecular response exceeding 2 years and natural killer cell transition during dasatinib consolidation

Takashi Kumagai¹  | Chiaki Nakaseko² | Kaichi Nishiwaki³ | Chikashi Yoshida⁴ | Kazuteru Ohashi⁵ | Naoki Takezako⁶ | Hina Takano⁷ | Yasuji Kouzai⁸ | Tadashi Murase⁹ | Kosei Matsue¹⁰  | Satoshi Morita¹¹ | Junichi Sakamoto¹² | Hisashi Wakita¹³ | Hisashi Sakamaki⁵ | Koiti Inokuchi¹⁴ | on behalf of the Kanto CML and Shimousa Hematology Study Groups

¹Department of Hematology, Ome Municipal General Hospital, Tokyo, Japan

²Department of Hematology, Chiba University Hospital, Chiba, Japan

³Division of Clinical Oncology and Hematology, Department of Internal Medicine, Jikei University School of Medicine, Kashiwa Hospital, Chiba, Japan

⁴Department of Hematology, National Hospital Organization, Mito Medical Center, Higashiibarakigun, Japan

⁵Hematology Division, Tokyo Metropolitan Cancer and Infectious Diseases Center, Komagome Hospital, Tokyo, Japan

⁶Department of Hematology, National Hospital Organization Disaster Medical Center, Tachikawa, Japan

⁷Department of Hematology, Musashino Red Cross Hospital, Musashino, Japan

⁸Department of Hematology, Tokyo Metropolitan Tama Synthesis Medical Center, Tokyo, Japan

⁹Department of Laboratory Medicine, Dokkyo Medical University Koshigaya Hospital, Saitama, Japan

¹⁰Division of Hematology/Oncology, Department of Internal Medicine, Kameda Medical Center, Kamogawa, Japan

¹¹Department of Biomedical Statistics and Bioinformatics, Kyoto University Graduate School of Medicine, Kyoto, Japan

¹²Tokai Central Hospital, Kakamigahara, Japan

¹³Division of Hematology and Oncology, Japanese Red Cross Society, Narita Red Cross Hospital, Narita, Japan

¹⁴Department of Hematology, Nippon Medical School, Tokyo, Japan

Correspondence

Takashi Kumagai, Department of Hematology, Ome Municipal General Hospital, Tokyo, Japan.
Email: kumamed1_2001@yahoo.co.jp

Funding information

Epidemiological and Clinical Research Information Network (ECRIN); Bristol-Myers Squibb (BMS)

Tyrosine kinase inhibitors (TKI) improve the prognosis of patients with chronic myelogenous leukemia (CML) by inducing substantial deep molecular responses (DMR); some patients have successfully discontinued TKI therapy after maintaining DMR for ≥ 1 year. In this cessation study, we investigated the optimal conditions for dasatinib discontinuation in patients who maintained DMR for ≥ 2 years. This study included 54 patients with CML who were enrolled in a D-STOP multicenter prospective trial, had achieved DMR, and had discontinued dasatinib after 2-year consolidation. Peripheral lymphocyte profiles were analyzed by flow cytometry. The estimated 12-month treatment-free survival (TFS) was 62.9% (95% confidence interval: 48.5%-74.2%). During dasatinib consolidation, the percentage of total lymphocytes and numbers of CD3⁺ CD56⁺ natural killer (NK) cells, CD16⁺ CD56⁺ NK cells and CD56⁺ CD57⁺ NK-large granular lymphocytes (LGL) were significantly higher in

This is an open access article under the terms of the Creative Commons Attribution-NonCommercial License, which permits use, distribution and reproduction in any medium, provided the original work is properly cited and is not used for commercial purposes.

© 2017 The Authors. *Cancer Science* published by John Wiley & Sons Australia, Ltd on behalf of Japanese Cancer Association.

patients with molecular relapse after discontinuation but remained unchanged in patients without molecular relapse for >7 months. At the end of consolidation, patients whose total lymphocytes comprised <41% CD3⁺ CD56⁺ NK cells, <35% CD16⁺ CD56⁺ NK cells, or <27% CD56⁺ CD57⁺ NK-LGL cells had higher TFS relative to other patients (77% vs 18%; $P < .0008$; 76% vs 10%; $P < .0001$; 84% vs 46%; $P = .0059$, respectively). The increase in the number of these NK cells occurred only during dasatinib consolidation. In patients with DMR, dasatinib discontinuation after 2-year consolidation can lead to high TFS. This outcome depends significantly on a smaller increase in NK cells during dasatinib consolidation.

KEYWORDS

chronic myelogenous leukemia, dasatinib, natural killer, stop, tyrosine kinase inhibitors

1 | INTRODUCTION

Chronic myelogenous leukemia (CML) is caused by the BCR-ABL1 fusion gene on the Philadelphia chromosome. This leukemia tends to transform into an acute form and was, therefore, historically associated with a poor prognosis.^{1,2} However, the advent of tyrosine kinase inhibitor (TKI) imatinib, which inhibits functions of BCR-ABL1 protein, has dramatically improved the prognosis of CML patients.³ More recently, second-generation TKI, such as dasatinib and nilotinib, have been found to induce faster and deeper molecular responses compared to imatinib.^{4,5} Most patients who receive TKI therapy survive for more than a decade. Recent data have revealed that an increasing number of patients may gradually achieve a deep molecular response (DMR) if they continue to use second-generation TKI for several years.^{6,7} However, increasing concern surrounds the long-term adverse effects and financial burden associated with TKI.^{8–12}

To address these concerns, the possibility of imatinib cessation has been extensively studied. In a prospective study first presented by a French group (STIM study), approximately 39% of CML patients who maintained DMR for ≥ 2 years while using first-line imatinib could safely stop taking the drug after >6 months,¹³ although patients who had received therapy for >5 years or had a low Sokal score were significantly more successful. An Australian group also found that imatinib could be stopped after a 2-year DMR consolidation period (TWISTER trial).¹⁴ Regarding second-generation TKI, a Japanese prospective study demonstrated that approximately 49% of CML patients who achieved DMR for >1 year during second-line dasatinib therapy could successfully discontinue treatment for >6 months,¹⁵ and attempts to discontinue nilotinib yielded similar observations.^{16,17} Therefore, the second-generation TKI appear to better enable chronic-phase CML patients to achieve therapy discontinuation.

The optimal conditions for successful TKI discontinuation regarding the type of TKI, depth of DMR, duration and amount of TKI administration or consolidation after DMR, and criteria for molecular relapse are yet to be determined. Currently, several of the additional TKI discontinuation trials needed to elucidate these conditions are

under way.¹⁸ Dasatinib induces increases in the populations of lymphocytes, large granular lymphocytes (LGL), natural killer (NK) cells and cytotoxic T cells, as well as a decrease in regulatory T cells (Tregs), especially in patients with good clinical responses,^{19,20} and a recent report found an association between an expanded NK cell population and successful TKI cessation.^{15,21} Therefore, the potential association between dasatinib-induced lymphocyte changes in number and successful discontinuation of dasatinib is an area of growing interest.

In the ongoing Japanese multicenter prospective D-STOP trial, we have attempted to discontinue dasatinib following a 2-year consolidation in patients with CML who had achieved DMR. During this period, we monitored the peripheral lymphocyte profiles via flow cytometry to investigate their associations with successful discontinuation. Here we show that dasatinib specifically increased NK cells during consolidation, but not during discontinuation, and demonstrate that a lower percentage of NK cells during consolidation significantly increases the likelihood that a patient will achieve a longer treatment-free survival (TFS).

2 | MATERIALS AND METHODS

2.1 | Study design and patients

The D-STOP trial (NCT01627132) is a multicenter, single-arm, phase 2 study conducted over 22 centers in Japan. Figure 1 presents the study schema for D-STOP. Patients diagnosed with chronic-phase CML and who achieved DMR after receiving any TKI were eligible for 2-year dasatinib consolidation therapy with the intent to maintain DMR. The inclusion criteria were as follows: age ≥ 15 years, performance status (ECOG score) of 0–2, and no severe primary organ dysfunction involving the liver, kidney or lungs. All previous treatments were permitted except for allogeneic hematopoietic stem-cell transplantation. The exclusion criteria were as follows: other chromosomal abnormalities in addition to the Philadelphia chromosome, a history of BCR-ABL1 mutation, and/or other active malignant disorders. The D-STOP trial was approved by the ethics committees of

the participating institutes. All participants provided written informed consent in accordance with the Declaration of Helsinki.

2.2 | Real-time quantitative RT-PCR

During the dasatinib-consolidation phase, real-time quantitative RT-PCR (RQ-PCR) analyses were performed every 3 months in the central laboratory (Bio Medical Laboratories [BML], Tokyo, Japan) to measure molecular responses¹⁹ according to the *BCR-ABL1* International Scale (IS) and the laboratory's conversion factor,²² as previously described.¹⁵ In summary, *ABL1* was used as an internal control, and the cut-off corresponded to *BCR-ABL1* of 0.0069% IS or molecular response of 4.0 (detectable disease with a *BCR-ABL1* <0.01% IS or undetectable disease in cDNA with >10 000 *ABL1* transcripts).²³ Patients with DMR confirmation every 3 months during a 2-year dasatinib consolidation period subsequently entered the discontinuation phase. Following dasatinib cessation, DMR were monitored by RQ-PCR every month for the first year (clinical cut-off), followed by every 3 months for the remaining 2 years (total = 3 years).

If *BCR-ABL1* >0.0069% IS was detected at any point during the consolidation or discontinuation phase, an additional RQ-PCR was performed within 1 month. Two successive *BCR-ABL1* positive results confirmed a molecular relapse. For relapses occurring during the discontinuation phase, dasatinib was restarted at the previously effective dose. After dasatinib recommencement, the response was assessed by RQ-PCR at 1, 3, 6 and 12 months. Dasatinib dose reduction was permitted at any time in response to adverse events based on physicians' judgment.

2.3 | Flow cytometric analysis

The whole peripheral blood lymphocyte profiles were established by the central laboratory (BML) before and after 3, 6, 12 and

24 months of dasatinib consolidation. Blood samples were collected more than a few hours after dasatinib intake. Peripheral white blood cell counts were measured using an automated cell count analyzer. The flow cytometry methods have been previously described.^{15,19,24} In brief, the lymphocyte fraction was determined using forward-scatter vs side-scatter gating (Figure S1A), and immunophenotypic examinations were performed using two-color or three-color flow cytometry on a FACSCalibur system with CellQuest software, version 3.3 (Becton Dickinson, Franklin Lakes, NJ, USA). All antibodies used in this study were purchased from Becton Dickinson. The defined lymphocyte subsets comprised NK cells (CD3⁻ CD56⁺ and CD16⁺ CD56⁺ cells), NK-cell LGL (NK-LGL, CD56⁺ CD57⁺), helper T cells (CD4⁺ CD8⁻), cytotoxic T cells (CD4⁻ CD8⁺), T-cell LGL (T-LGL) (CD3⁺ CD57⁺)¹⁹ and regulatory T cells (Tregs) (CD4⁺ CD25⁺ CD127^{dim/-})²⁵ (Figure S1B).

2.4 | Definition of the endpoint

The primary endpoint was the 12-month rate of TFS, defined as the time from the discontinuation of dasatinib to the date of molecular relapse. To establish the predictive factors associated with treatment-free remission, we evaluated patients by sex, age at discontinuation, Sokal risk score at diagnosis, duration of *BCR-ABL1* transcript negativity before consolidation, duration of TKI therapy before consolidation, total dose of dasatinib, and type of TKI used when DMR was achieved. We also assessed the above-described lymphocyte subsets before and after 3, 6, 12 and 24 months of dasatinib consolidation while in TFS. Safety was evaluated throughout the consolidation period and adverse events were classified using the Common Terminology Criteria for Adverse Events, version 4.0.

2.5 | Statistical analysis

In this study, a sample size of at least 50 patients was determined to demonstrate that patients who discontinued dasatinib remained in TFS at a power >80% when compared with data from a previous study.¹³ Each continuous variable was separated into two groups using the cut-off points calculated by the concordance index.

A Kaplan–Meier analysis was used to calculate the proportion of patients in treatment-free remission, and a log-rank test was used to statistically compare the stratified groups (two or more). Cox proportional hazards analysis of significant predictors in the univariate analysis was used to calculate the factors contributing to successful discontinuation. Strongly correlated explanatory variables were independently entered into the Cox regression model. Factors significant in at least one of the tested models were considered possible independent predictors of relapse risk.

Receiver operating characteristic (ROC) curves were generated to determine the cut-off values of lymphocytes (%), NK cells (% and counts) and clinical data for the Kaplan–Meier analysis. Optimal thresholds along ROC curves were determined by searching for plausible values where the sum of the sensitivity and specificity were maximized. A *P*-value <0.05 was considered significant. The statistical

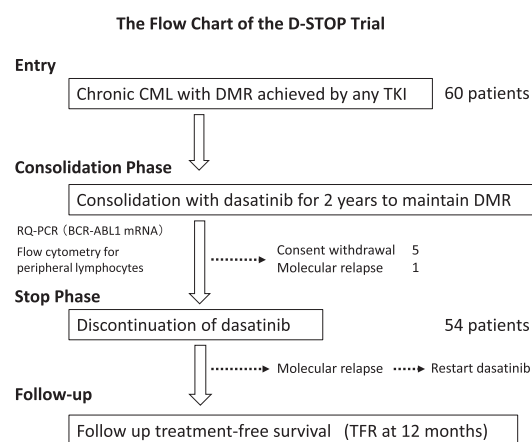


FIGURE 1 Flow chart of the D-STOP trial. CML, chronic myelogenous leukemia; DMR, deep molecular response; RQ-PCR, real-time quantitative PCR; TFR, treatment-free survival

software EZR on R commander (R Project for Statistical Computing, Vienna, Austria) was used for statistical analysis calculations.²⁶

3 | RESULTS

3.1 | Treatment-free survival after dasatinib discontinuation

As shown in Figure 1, 60 patients with a confirmed DMR between 1 February 2012 and 31 January 2014 were enrolled into the dasatinib consolidation phase. Of these patients, 6 were excluded during consolidation because of consent withdrawal or fluctuations in the *BCR-ABL1* transcript levels suggestive of a molecular relapse. Safety analyses revealed no severe (grade ≥ 3) treatment-related toxic effects during the consolidation phase. A total of 54 patients (32 male, 22 female) were included in the dasatinib-discontinuation (STOP) phase (Table 1).

The median age at treatment discontinuation was 56 (range: 27–84) years. The median duration of TKI treatment was 92 (36–177) months, and the median duration of *BCR-ABL1* negativity before treatment cessation was 51 (24–173) months. Patients were followed up for a median of 16 (3–24) months after discontinuation. In total, 34, 19 and 1 patient used imatinib, dasatinib and an unknown agent, respectively, at the time of DMR achievement before consolidation. No patient received interferon-alpha.

Regarding the clinical endpoint, the estimated overall probabilities of TFS were 68.5% (95% confidence interval [CI]: 54.3–79.1) at 6 months and 62.9% (95% CI: 48.5–74.2) at 12 months (Figure 2). Twenty patients experienced relapses during discontinuation phase, and most relapses occurred within 6 (and maximum 7) months. The loss of major molecular response (MMR) was observed in 20% of the relapsed patients. All relapsed patients responded to dasatinib

within 3 months of recommencing treatment. MMR was achieved within 6 months in all patients and DMR within 12 months in 16 of the 19 patients evaluable within this period. No loss of a hematologic response, complete cytogenetic response or progression to advanced disease was observed.

The clinical factors that affected molecular relapse during the discontinuation phase were analyzed (Figure 3). However, no significant associations of the 12-month TFS rate were observed with patient characteristics such as sex (Figure 3A), Sokal score at diagnosis (Figure 3B), *BCR-ABL1* mRNA negative duration (Figure 3C), duration of TKI treatment (Figure 3D), age at discontinuation (Figure 3E), total dose of dasatinib (Figure 3F) and type of TKI used when DMR was achieved (Figure 3G).

At present, the last patient discontinued dasatinib more than 24 months ago and the actual late TFS rate at 24 months was calculated as 57%. This is consistent with the results of previous reports, which indicated that the most molecular relapses occur within 6 months after cessation, with a small percentage of patients experiencing late relapse.^{27,28} We will report our final results at 3-year follow-up.

3.2 | Clinical data during consolidation therapy

Physicians were free to determine the dose of dasatinib during the consolidation phase. Of the 60 patients who entered the consolidation phase, 35% and 52% experienced transient suspension and reduction of dasatinib, respectively. The etiologies of the drug suspensions included 20 non-hematological adverse events (G2–3) (13 pleural effusions, 1 chronic heart failure, 1 elongation of corrected QT in ECG, 1 renal failure, 1 hematochezia, 1 diarrhea, 1 general

TABLE 1 Characteristics of the patients

Age at discontinuation (y)	56 (27–84)
Sex	
Male	32
Female	22
Performance status	
≤ 1	54
Sokal score at diagnosis ^a	
Low	24
Intermediate	11
High	6
Type of TKI when achieving DMR	
Imatinib	34
Dasatinib	19
Unknown	1
<i>BCR-ABL</i> (–) duration (mo)	51 (24–173)
Duration of TKI treatment (mo)	92 (36–177)

DMR, deep molecular response; TKI, tyrosine kinase inhibitor.

^aSokal scores were not available for 13 patients.

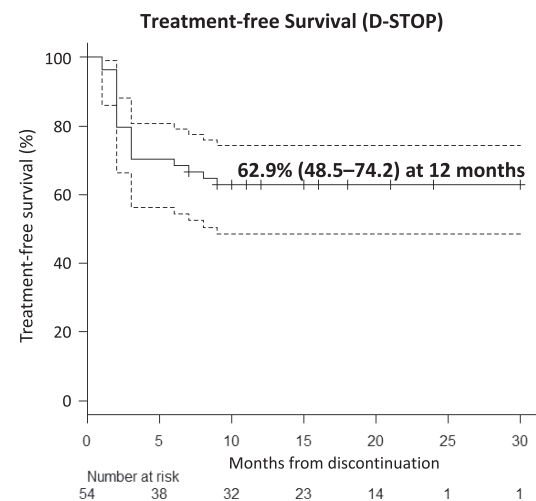


FIGURE 2 Estimated treatment-free survival in the D-STOP trial. The estimated treatment-free survival of the patients who discontinued dasatinib (y-axis) and the duration (months) of discontinuation (x-axis) are shown. The dotted line indicates the 95% confidence interval

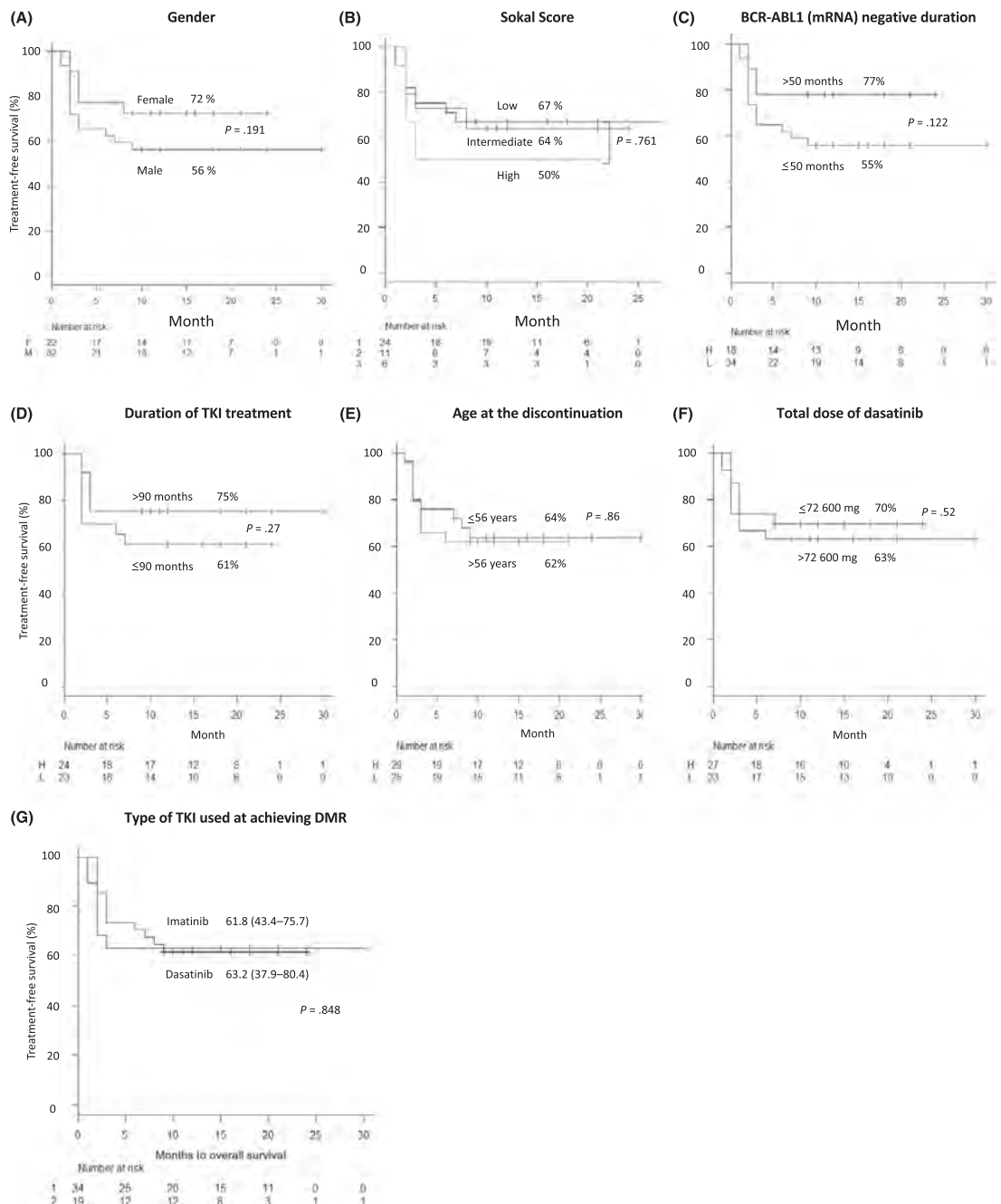


FIGURE 3 Estimated treatment-free survival according to patients' characteristics. The estimated treatment-free survival rates according to patient characteristics, including sex (A), Sokal score (B), BCR-ABL1 mRNA-negative duration (C), duration of tyrosine kinase inhibitor (TKI) treatment (D), age at discontinuation (E), total dose of dasatinib (F), and the type of TKI when achieving a deep molecular response (G) are presented along the y-axis. In all figures, the duration (months) of discontinuation is shown along the x-axis. The cut-off levels of each type of clinical data were determined using receiver operating characteristic (ROC) curve analyses as described in the Methods

fatigue and 1 unknown) and 2 hematological adverse events (\geq G3) (anemia and pancytopenia). The etiologies of the dose reductions included 31 non-hematological adverse events (G2–3) (13 pleural effusions, 1 elongation of corrected QT in ECG, 1 liver dysfunction, 1 renal failure, 1 hematochezia, 2 diarrhea, 1 general fatigue, 2 alopecia, 1 fever, 1 appetite loss, and others) and 3 hematological adverse events (\geq G3) (1 anemia, 1 thrombocytopenia and 1 pancytopenia). Pleural effusions were the major reasons for dose change. No patient withdrew from the study due to adverse events. Thirty-four patients switched from imatinib to dasatinib at the start of consolidation. Patients switching to dasatinib for the first time during consolidation took 80.1% of the scheduled dose (100 mg/d) ($n = 30$).

3.3 | Lymphocyte profiles during consolidation therapy

We divided patients in the D-STOP trial into S (successful) and F (failed) groups, which, respectively, comprised those who discontinued dasatinib and remained in remission for >7 months ($n = 34$) and those who relapsed during the observation period ($n = 20$). The absolute lymphocyte counts did not differ significantly between S and F groups before or after dasatinib consolidation therapy ($P = .25$ and $.24$, respectively) (data not shown). However, the relative lymphocyte count after consolidation increased significantly relative to the baseline values in F group ($P = .0091^*$) (Figure 4A(ii)).

We further assessed the proportion (%) of each lymphocyte subset among the total lymphocyte population and the absolute cell counts using flow cytometry. The proportion of $CD3^+ CD56^+$ NK cells did not differ between S and F groups before consolidation ($P = .95$); by contrast, this value increased significantly in F group during the consolidation period ($P = .00016^*$) but remained stable in S group ($P = .69$). After consolidation, both the proportion (Figure 4A(iii)) and absolute number of $CD3^+ CD56^+$ NK cells (Figure 4A(iii)) were significantly higher in F group than in S group ($P = .0043^*$ and $P = .015^*$, respectively). In the S group, this NK cell population transiently increased at 12 months ($P = .0094^*$) and returned to baseline levels after consolidation ($P = .75$), resulting in a significant difference between the two groups after consolidation (Figure 4A(iii)).

Regarding $CD16^+ CD56^+$ NK cells, the proportions among total lymphocytes and cell counts in both groups exhibited similar changes during the consolidation period (Figure S2A-1,A-2). The proportions of $CD56^+ CD57^+$ NK-LGL cells among total lymphocytes did not differ significantly between the two groups before consolidation ($P = .52$); during the consolidation period, this proportion increased in F group ($P = .0009^*$) while remaining stable in S group ($P = .36$). After consolidation, the proportion of $CD56^+ CD57^+$ NK-LGL cells was significantly higher in F group compared with S group ($P = .0051^*$) (Figure S2B-1). The absolute $CD56^+ CD57^+$ cell count also increased during the consolidation period in F group ($P = .0004^*$), whereas in S group this value increased transiently at

12 months ($P = .0011^*$) but returned to the baseline level after 24 months ($P = .46$) (Figure S2B-2).

Based on these observations, we our results were as follows. The patients with a relative lymphocyte change $<140\%$ (as determined by ROC analysis) after consolidation had a significantly higher TFS rate (76%) than those with a change $\geq 140\%$ (38%) ($P = .022^*$) (Figure 4B(ii)). The difference of $CD3^+ CD56^+$ proportions also led to a marked disparity in the TFS rates at 12 months between the patients with $CD3^+ CD56^+$ proportions of $<41\%$ and $\geq 41\%$ (ROC analysis) among total lymphocytes at the end of consolidation (77% vs 18%, respectively; $P = .0008^*$) (Figure 4B(iii)). A marked difference in TFS was also observed between patients with a $CD16^+ CD56^+$ proportion of $<35\%$ vs those with a proportion $\geq 35\%$ (ROC analysis) after consolidation (76% vs 10%, respectively; $P < .0001^*$) (Figure 4B(iii)). A significant difference in the TFS at 12 months between patients with a $CD56^+ CD57^+$ NK-LGL proportion of $<27\%$ (ROC analysis) and those with a proportion of $\geq 27\%$ after consolidation was also observed (84% vs 46%, respectively; $P = .0059^*$) (Figure 4B(iv)). Based on these results, we concluded that the increases in NK and NK-LGL cells during the consolidation period correlated negatively with successful discontinuation.

Multivariate analysis was performed using factors such as sex, Sokal score, BCR-ABL-1 negative duration, duration of TKI treatment, patient age, total dasatinib dose, switching from imatinib to dasatinib before consolidation, the existence of imatinib resistance and levels of $CD56^+ CD3^+$ NK cells ($<41\%$) at the end of consolidation. In the univariate analysis, factors with P -values of $\geq .30$ were excluded. Lower levels of $CD3^+ CD56^+$ NK cells at the end of consolidation were an independent predictive factor for TFS (Figure S3). The final results will be reported at 3-year follow-up.

Regarding the cytotoxic T ($CD4^+ CD8^+$), T-LGL ($CD3^+ CD57^+$) and regulatory T (Tregs; $CD4^+ CD25^+ CD127^{dim/-}$) cell subsets, no significant differences in the proportions among total lymphocytes or absolute cell counts were observed between S and F groups before or after consolidation (Figure S4A-1, A-2, B-1, B-2, D-1 and D-2). However, F group exhibited significant increases in cytotoxic T cells (Figure S4A-2, $P = .0009^*$) and T-LGL (Figure S4B-2, $P = .028^*$) during consolidation. In contrast, the S group exhibited only a significant decrease in Tregs (Figure S4D-2, $P = .035^*$).

The proportion of helper T cells ($CD4^+ CD8^-$) among total lymphocytes was significantly lower in F group than in S group after consolidation (Figure S4C-1). However, as the absolute cell counts did not differ between the two groups during consolidation (Figure S4C-2), the difference appeared to arise from a relative increase in total lymphocytes in F group (Figure 4A(i)) and was not considered important. In summary, small and occasionally significant changes in T cell subsets were observed.

3.4 | Changes in natural killer cell populations throughout the dasatinib discontinuation study

Rapid decreases in the lymphocyte, $CD3^+ CD56^+$ NK cell and $CD56^+ CD57^+$ NK-LGL populations were observed after dasatinib

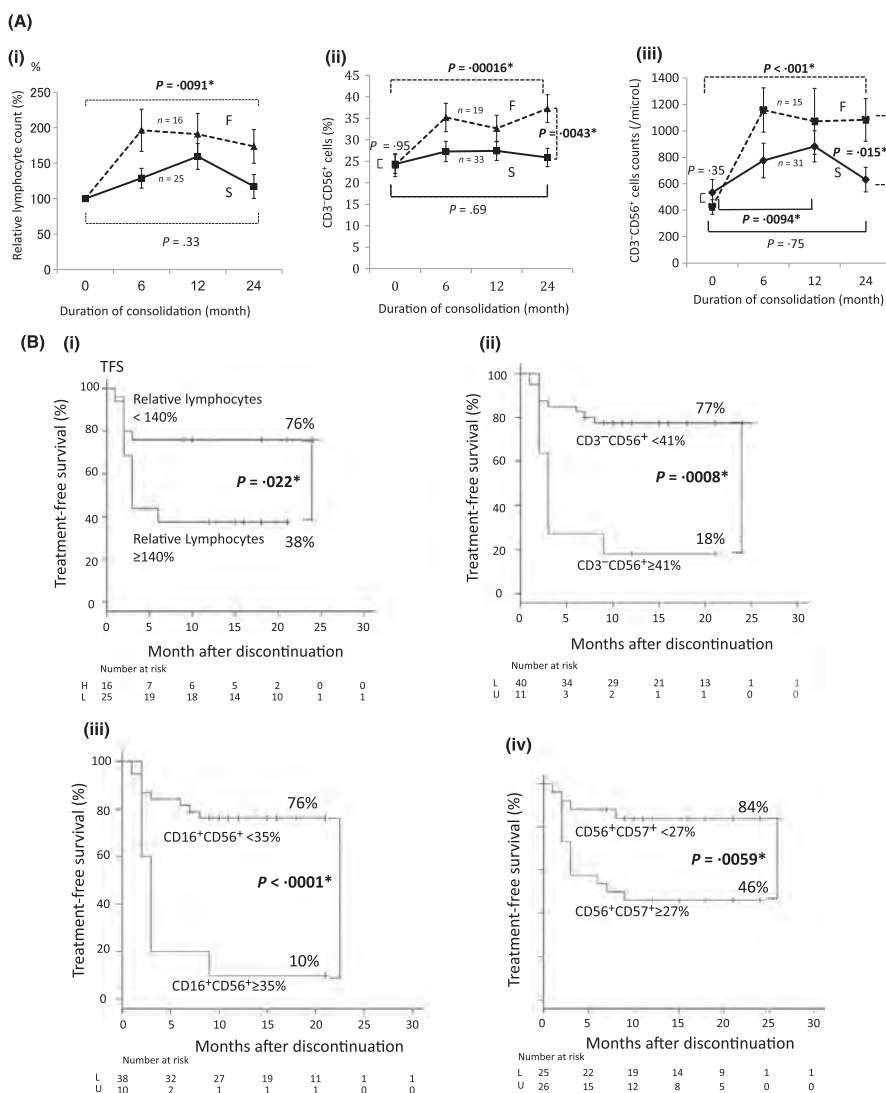


FIGURE 4 Changes in the numbers of total lymphocytes and natural killer (NK) cell subsets during consolidation therapy with dasatinib after achieving a deep molecular response. In all figures, the solid line indicates the successful (S) group, which comprised patients who achieved successful discontinuation without relapse for >7 mo ($n = 34$); the dotted line denotes the failed (F) group, which comprised patients with a molecular relapse during the observation period ($n = 20$). Data are presented as averages \pm SE. The x-axis indicates the duration of consolidation (months). The following data are presented on the y-axes: (A(i)) Relative proportion of lymphocytes (%) compared to the baseline levels just before consolidation. (A(ii)) Proportion (%) of CD3⁺CD56⁺ NK cells during consolidation. (A(iii)) Absolute number of CD3⁺CD56⁺ NK cells during consolidation. (B(i)) Treatment-free survival (TFS) rates of patients with lymphocyte counts $\geq 140\%$ or $< 140\%$ relative to the baseline at the end of consolidation. The cut-off level was determined using a receiver operating characteristic (ROC) curve analysis as described in the Methods. (B(ii)) TFS rates of the patients with CD3⁺CD56⁺ NK cell proportions (%) $\geq 41\%$ or $< 41\%$ at the end of consolidation. The cut-off level was determined using an ROC curve analysis as described in the Methods. (B(iii)) TFS rates of the patients with CD16⁺CD56⁺ NK cell proportions (%) $\geq 35\%$ or $< 35\%$ at the end of consolidation. The cut-off level was determined using an ROC curve analysis as described in the Methods. (B(iv)) TFS rates of the patients with CD56⁺CD57⁺ NK-LGL proportions (%) of $\geq 27\%$ or $< 27\%$ at the end of consolidation. The cut-off level was determined using an ROC curve analysis as described in the Methods

discontinuation, and no significant differences remained between the S and F groups after 3 months (Figure 5A). We note that although NK cell counts may also have shifted over time, we did not collect additional data.

In F group, the lymphocyte population increased significantly after dasatinib re-treatment for a molecular relapse (Figure 5B), indicating that dasatinib specifically increased NK cells. Before consolidation, S group tended to have a higher average NK cell count compared with F group; however, this trend reversed after 3 months (Figure 5C). When we determined the cut-off level before consolidation, patients with a higher than average NK cell count tended to have higher TFS (data not shown), whereas during consolidation, F group was more likely to exhibit a larger dasatinib-specific lymphocyte increase (%) from the baseline (Figure 4A(i-iii)).

At the start of consolidation, some patients switched from imatinib to dasatinib. These patients were specific to the D-STOP study and were not included in previous cessation studies. These patients did not affect the TRF rate (Figure 1G). However, the relative increase in lymphocyte levels in the failed patients during consolidation ($157.6 \pm 26.3\%$) tended to be higher than that in patients who continued dasatinib ($117.4 \pm 13.7\%$). Therefore, such a patient population might emphasize our results over those of other studies.^{13-15,21}

We considered the underlying mechanism of these NK cell changes during dasatinib discontinuation (Figure 5D). Before consolidation, NK cells tended to be higher in discontinuation-successful patients (Figure 5C). Although these cells increased to a great extent in the discontinuation-failed patients during consolidation (Figure 4A, B), the population contracted rapidly after discontinuation (Figure 5A). During discontinuation, NK cell numbers are reportedly higher among successful patients.^{15,21,29,30} We observed that in the failed patients, the lymphocyte population increased again after re-starting dasatinib, suggesting a direct effect of TKI on this cell population (Figure 5B).

4 | DISCUSSION

The results of this study demonstrate the feasibility of achieving a high TFS rate with dasatinib consolidation for ≥ 2 years after achieving DMR; the dasatinib-induced increase in NK cells during consolidation was found to correlate negatively with successful discontinuation.

We compared the D-STOP and DADI trials,¹⁵ which included similar numbers of patients (63 and 54, respectively) with similar median ages (59 [24-84] and 56 [27-84]) years, respectively, to evaluate favorable conditions for dasatinib discontinuation. Both trials defined DMR at discontinuation and molecular relapse using RQ-PCR data obtained at BML.^{15,22} Patients in the DADI trial achieved DMR during second-line dasatinib therapy after first-line imatinib therapy.¹⁵ By contrast, patients in the D-STOP trial underwent dasatinib consolidation after achieving DMR via treatment with any TKI, although the majority of patients had initially used imatinib (34 patients) or dasatinib (19 patients). Interestingly, the TFS rates of imatinib-treated and dasatinib-treated patients were extremely similar,

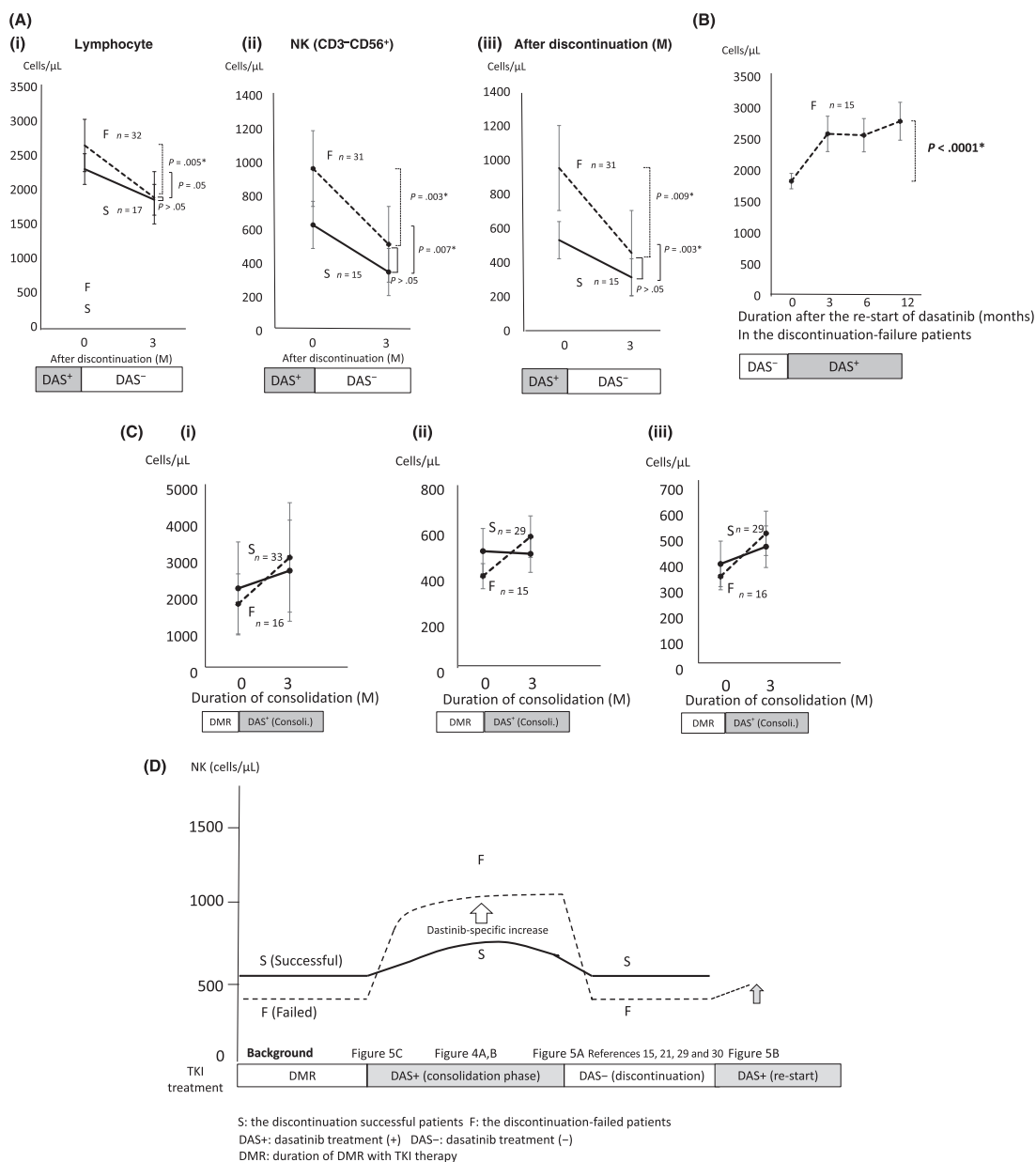
with no significant differences (Figure 3G), indicating that the type of TKI used to achieve DMR was not important for successful discontinuation. The most significant difference between 2 studies was the duration of consolidation, which was 2 years in the D-STOP but only 1 year in the DADI trial.¹⁵ In the D-STOP study, the rate of imatinib resistance was 14.8% (8/54), which was lower than that in the DADI study (20.6%, 13/63).¹⁵ As imatinib resistance was a predictive factor for poor TFS in DADI, this may affect the TFS in the D-STOP study. In contrast, the estimated TFS at 12 months in imatinib-resistant patients and others were 62.5% (95% CI, 22.9-86.1) and 62.9% (95% CI, 47.3-75.1) ($P = .94$), respectively, in the D-STOP study. These were not significantly different, and further analysis is necessary. The different TFS observed in D-STOP (62.9% at 12 months) relative to DADI (49% at 6 months) might be attributable to these factors.

We previously reported that a relative increase in the levels of NK cells with initial dasatinib was associated with higher DMR achievement. Increased levels of NK cells may function to exclude CML cells before achieving DMR.¹⁹ Such patients with increased levels of NK cells could achieve DMR and enter a cessation-study such as the D-STOP. After the achievement of DMR, levels of NK cells may continue to increase or stabilize during consolidation. The D-STOP trial indicated that patients with stable NK cells during consolidation were more successful in cessation.

After achieving DMR, NK cells may function differently for the immune surveillance to prevent molecular relapses. This was indicated by the previous reports that stated that the patients with successful discontinuation had larger and more functional NK cells than the failed patients.^{15,21,29,30}

To explain the greater increase in NK cells following dasatinib consolidation in the failed patients during DMR in the D-STOP trial, we first hypothesized that NK cells of the successful patients and those of the failed patients responded differently to dasatinib during DMR. NK cells in the failed patients who had lower immune surveillance capability may respond more and increase after dasatinib administration. The increase in NK cells seemed dasatinib-specific and might be attributable to the inhibition of multiple kinases, such as c-KIT, PDGF, SRC and Src family kinases, in addition to ABL1.³¹ Although SRC has been reported to be associated with NK cell function and signal transduction,³² the reason underlying dasatinib-induced specific increase in NK cells during consolidation in the failed patients remains unclear. Differences in the immune functions, maturation, and genomic as well as epigenomic structures of NK cells of the successful patients and failed patients is a topic for future research.

Another hypothesis is that the increase in NK cells during DMR occurs through the off-target effects of dasatinib only when residual CML cells with high expansion capacity are excluded by NK cells, even though present in a small number (<MR4). Therefore, levels of NK cells stabilize when there are few residual CML cells with high expansion capacity, as is observed in the successful patients. In contrast, the levels of NK cells may increase with residual CML cells with high expansion capacity, such as imatinib-resistant CML cells to be excluded by NK cells, as observed in the failed patients.



Such an increase in NK cells during consolidation was also induced specifically by dasatinib in DADI (Figure S3 in Imagawa¹⁵); however, similar increases were not reported for imatinib cessation. Levels of NK cells were high in successful patients during discontinuation;^{15,21,29,30} however, in the D-STOP study, they were high during the consolidation phase in those who failed (Figure 5A). The levels of NK cells should be reversed before and

after dasatinib cessation. In Figure 5, we proposed the possibility of reversing the levels of NK cells before and after dasatinib cessation. After 3 months, the sample size was not sufficient because data collection was not scheduled for all patients, and data could not be collected from those who relapsed in <3 months and restarted dasatinib with further rise in the lymphocyte levels (Figure 5B).

FIGURE 5 Natural killer (NK) cell changes throughout the dasatinib-discontinuation study. (A) (i) Lymphocytes, (ii) NK cells (CD3⁺ CD56⁺) and (iii) NK-large granular lymphocytes (NK-LGL; CD57⁺ CD56⁺) significantly decreased rapidly after dasatinib discontinuation in both the successful (S) and failed (F) groups (x-axis: months after discontinuation of dasatinib, y-axis: counts of lymphocytes, CD3⁺ CD56⁺ NK cells or CD56⁺ CD57⁺ NK-LGL). Cell counts of lymphocytes, NK and NK-LGL did not differ significantly between patient groups after 3 mo ($P = .89$, $P = .064$ and $P = .065$, respectively). (B) A rapid and significant increase in lymphocytes was observed after 12 mo of dasatinib re-start for F patients with molecular relapses ($P < .0001^*$) (x-axis: months after dasatinib re-start, y-axis: lymphocyte counts). (C) The average counts of (i) lymphocytes, (ii) NK cells (CD3⁺ CD56⁺) and (iii) NK-LGL (CD57⁺ CD56⁺) were lower in F patients ($n = 20$) relative to S patients ($n = 34$) before dasatinib-consolidation; this pattern reversed after 3 mo of consolidation (x-axis: months after dasatinib consolidation, y-axis: lymphocyte counts). (D) The suggested hypothesis of NK cell transition during the dasatinib discontinuation study (x-axis: treatments including the period of deep molecular response [DMR] induced by tyrosine kinase inhibitor [TKI] therapy [DMR], dasatinib consolidation therapy {DAS⁺ (consolidation phase)}, dasatinib discontinuation {DAS⁻ (discontinuation)} and dasatinib re-treatment for molecular relapses in discontinuation-failed patients {DAS⁺ (re-start)}, y-axis: NK cell counts). Dasatinib discontinuation-successful patients (S) are indicated by the solid line; failed (F) patients are indicated by the dotted line. Patients who achieved DMR before consolidation therapy and were discontinuation-successful tended to have a higher average NK cell count (as in C). During dasatinib consolidation, NK cells increased specifically in response to dasatinib much more in the F group than in the S group, as shown in Figure 4A,B. A similar increase may not occur during imatinib consolidation.²³ However, NK cells rapidly decreased to the basal level after discontinuation, as in Figure 5A. During discontinuation, NK cells were higher in group S, as previously reported.^{15,21,29,30} Furthermore, lymphocytes increased again after re-starting dasatinib in the F group, further supporting a specific effect of dasatinib (B). Consoli., consolidation with dasatinib; DAS⁺, duration with dasatinib treatment; DAS⁻, duration without dasatinib treatment; DAS→DAS, patients who continued dasatinib before and during consolidation; DMR, duration of DMR with TKI therapy; F, failed group; IM→DAS, patients who switched imatinib to dasatinib just before consolidation; S, successful group

In conclusion, we have demonstrated that a 2-year consolidation with dasatinib after achieving DMR was feasible and yielded a high TFS rate after discontinuation. However, despite earlier reports that a larger NK cell population during discontinuation correlated with improved TFS,^{15,21,27,28} we observed that a transient increase in NK cells during dasatinib consolidation was unfavorable for successful discontinuation.

D-STOP showed that an increase in the levels of NK cells during dasatinib consolidation was negatively correlated with successful cessation. Therefore, patients with stable levels of NK cells with dasatinib consolidation after DMR may be good candidates for discontinuation. These findings may provide new insights into optimal TKI cessation.

ACKNOWLEDGMENTS

This study was supported by the Epidemiological and Clinical Research Information Network (ECRIN) and Bristol-Myers Squibb (BMS). We thank Yumi Miyashita at ECRIN for collecting the data and Narutaka Sakurada and Yoshinori Yamamoto at BML for performing flow cytometry and RQ-PCR. We thank Ishida Tadao (Department of Gastroenterology, Rheumatology and Clinical Immunology, Sapporo Medical University, Sapporo), Hiroyuki Sugawara (Department of Hematology, Sumitomo Hospital, Osaka), Sakae Tanosaki (Department of Hematology, Tokyo Doai Memorial Hospital, Tokyo), Masayuki Koizumi (Department of Hematology, Asahi Chuo Hospital, Chiba), Megumi Akiyama (Department of Hematology, Yokosuka Kyosai Hospital, Kanagawa), Hiroshi Inoue (Department of Hematology, Inoue Memorial Hospital, Chiba), Iwai Kazuya (Department of Hematology, Shizuoka City Shizuoka Hospital, Shizuoka) and Akira Ohwada (Department of Hematology, Tokyo Metropolitan Bokutoh Hospital, Tokyo) for participating in this study. We are grateful to Professor Junia V. Melo for critically commenting on and editing the manuscript.

DISCLOSURE STATEMENT

T.K. received lecture fees from Bristol-Myers Squibb, Novartis and Pfizer. C.N. received honoraria from Bristol-Myers Squibb, Pfizer and Novartis, and grants from Bristol-Myers Squibb and Pfizer. K.N. received research funding from Novartis. C.Y. received honoraria and speakers bureau from Bristol-Myers Squibb and Pfizer, and honoraria, speakers bureau and grants from Otsuka. K.M. received honoraria from Celgene. S.M. received honoraria from Bristol-Myers Squibb. J.S. received remuneration from Yakult Honsha. I.K. received research grants from Bristol-Myers Squibb, and honoraria from Bristol-Myers Squibb, Novartis, Celgene and Pfizer.

ORCID

Takashi Kumagai  <http://orcid.org/0000-0001-6850-4545>

Kosei Matsue  <http://orcid.org/0000-0002-8669-9865>

REFERENCES

- Faderl S, Talpaz M, Estrov Z, O'Brien S, Kurzrock R, Kantarjian HM. The biology of chronic myeloid leukemia. *N Engl J Med*. 1999;341:164-172.
- Lugo TG, Pendergast AM, Muller AJ, Witte ON. Tyrosine kinase activity and transformation potency of bcr-abl oncogene products. *Science*. 1990;247:1079-1082.
- Druker BJ, Guilhot F, O'Brien SG, et al. Five-year follow-up of patients receiving imatinib for chronic myeloid leukemia. *N Engl J Med*. 2006;355:2408-2417.
- Kantarjian H, Shah NP, Hochhaus A, et al. Dasatinib versus imatinib in newly diagnosed chronic-phase chronic myeloid leukemia. *N Engl J Med*. 2010;362:2260-2270.
- Saglio G, Kim DW, Issaragrisil S, et al. ENESTnd investigators. Nilotinib versus imatinib for newly diagnosed chronic myeloid leukemia. *N Engl J Med*. 2010;362:2251-2259.

6. Cortes JE, Saglio G, Kantarjian HM, et al. A. Final 5-year study results of DASISION: the dasatinib versus imatinib study in treatment-naïve chronic myeloid leukemia patients trial. *J Clin Oncol*. 2016;34:2333-2340.
7. Hochhaus A, Saglio G, Hughes TP, et al. Long-term benefits and risks of frontline nilotinib vs imatinib for chronic myeloid leukemia in chronic phase: 5-year update of the randomized ENESTnd trial. *Leukemia*. 2016;30:1044-1054.
8. Padula WV, Larson RA, Dusetzina SB, et al. Cost-effectiveness of tyrosine kinase inhibitor treatment strategies for chronic myeloid leukemia in chronic phase after generic entry of imatinib in the United States. *J Natl Cancer Inst*. 2016;108:djw003.
9. Rochau U, Sroczynski G, Wolf D, et al. Cost-effectiveness of the sequential application of tyrosine kinase inhibitors for the treatment of chronic myeloid leukemia. *Leuk Lymphoma*. 2015;56:2315-2325.
10. Efficace F, Cannella L. The value of quality of life assessment in chronic myeloid leukemia patients receiving tyrosine kinase inhibitors. *Hematology Am Soc Hematol Educ Program*. 2016;2016:170-179.
11. Cortes J, Kantarjian H. Chronic myeloid leukemia: sequencing of TKI therapies. *Hematology Am Soc Hematol Educ Program*. 2016;2016:164-169.
12. Steegmann JL, Baccarani M, Breccia M, et al. European LeukemiaNet recommendations for the management and avoidance of adverse events of treatment in chronic myeloid leukaemia. *Leukemia*. 2016;30:1648-1671.
13. Mahon FX, Réa D, Guilhot J, et al. Discontinuation of imatinib in patients with chronic myeloid leukaemia who have maintained complete molecular remission for at least 2 years: the prospective, multicentre Stop Imatinib (STIM) trial. *Lancet Oncol*. 2010;11:1029-1035.
14. Ross DM, Branford S, Seymour JF, et al. Safety and efficacy of imatinib cessation for CML patients with stable undetectable minimal residual disease: results from the TWISTER study. *Blood*. 2013;122:515-522.
15. Imagawa J, Tanaka H, Okada M, et al. Discontinuation of dasatinib in patients with chronic myeloid leukaemia who have maintained deep molecular response for longer than 1 year (DADI trial): a multicentre phase 2 trial. *Lancet Haematol*. 2015;2:e528-e535.
16. Mahon FX, Richter J, Guilhot J, et al. Interim analysis of a pan European stop tyrosine kinase inhibitor trial in chronic myeloid leukemia: the EURO-SKI study. *Blood*. 2014;124:151.
17. Mahon FX, Baccarani M, Mauro MJ, et al. Treatment-free remission (TFR) following nilotinib (NIL) in patients (pts) with chronic myeloid leukemia in chronic phase (CML-CP): ENESTfreedom, ENESTop, ENESTgoal, and ENESTpath. *J Clin Oncol*. 2014;32:TPS7124.
18. Sauße S, Richter J, Hochhaus A, Mahon FX. The concept of treatment-free remission in chronic myeloid leukemia. *Leukemia*. 2016;30:1638-1647.
19. Kumagai T, Matsuki E, Inokuchi K, et al. Relative increase in lymphocytes from as early as 1 month predicts improved response to dasatinib in chronic-phase chronic myelogenous leukemia. *Int J Hematol*. 2014;99:41-52.
20. Mustjoki S, Eklblom M, Arstila TP, et al. Clonal expansion of T/NK-cells during tyrosine kinase inhibitor dasatinib therapy. *Leukemia*. 2009;23:1398-1405.
21. Ilander M, Olsson-Strömberg U, Schlums H, et al. Increased proportion of mature NK cells is associated with successful imatinib discontinuation in chronic myeloid leukemia. *Leukemia*. 2017;31:1108-1116.
22. Yoshida C, Fletcher L, Ohashi K, et al. Harmonization of molecular monitoring of chronic myeloid leukemia therapy in Japan. *Int J Clin Oncol*. 2012;17:584-589.
23. Cross NC, White HE, Colomer D, et al. Laboratory recommendations for scoring deep molecular responses following treatment for chronic myeloid leukemia. *Leukemia*. 2015;29:999-1003.
24. Iriyama N, Fujisawa S, Yoshida C, et al. Early cytotoxic lymphocyte expansion contributes to a deep molecular response to dasatinib in patients with newly diagnosed chronic myeloid leukemia in the chronic phase: results of the D-first study. *Am J Hematol*. 2015;90:819-824.
25. Liu W, Putnam AL, Xu-Yu Z, et al. CD127 expression inversely correlates with FoxP3 and suppressive function of human CD4 + T reg cells. *J Exp Med*. 2006;203:1701-1711.
26. Kanda Y. Investigation of the freely available easy-to-use software 'EZ' for medical statistics. *Bone Marrow Transplant*. 2013;48:452-458.
27. Etienne G, Guilhot J, Rea D, et al. Long-term follow-up of the French Stop Imatinib (STIM1) study in patients with chronic myeloid leukemia. *J Clin Oncol*. 2017;35:298-305.
28. Rea D, Nicolini FE, Tulliez M, et al. Discontinuation of dasatinib or nilotinib in chronic myeloid leukemia: interim analysis of the STOP 2G-TKI study. *Blood*. 2017;129:846-854.
29. Hughes A, Clarkson J, Tang C, et al. CML patients with deep molecular responses to TKI have restored immune effectors and decreased PD-1 and immune suppressors. *Blood*. 2017;129:1166-1176.
30. Ohyashiki K, Katagiri S, Tauchi T, et al. Increased natural killer cells and decreased CD3(+)/CD8(+)/CD62L(+) T cells in CML patients who sustained complete molecular remission after discontinuation of imatinib. *Br J Haematol*. 2012;157:254-256.
31. Weisberg E, Manley PW, Cowan-Jacob SW, Hochhaus A, Griffin JD. Second generation inhibitors of BCR-ABL for the treatment of imatinib-resistant chronic myeloid leukaemia. *Nat Rev Cancer*. 2007;7:345-356.
32. Hassold N, Seystahl K, Kempf K, et al. Enhancement of natural killer cell effector functions against selected lymphoma and leukemia cell lines by dasatinib. *Int J Cancer*. 2012;131:E916-E927.

SUPPORTING INFORMATION

Additional Supporting Information may be found online in the supporting information tab for this article.

How to cite this article: Kumagai T, Nakaseko C, Nishiwaki K, et al. Dasatinib cessation after deep molecular response exceeding 2 years and natural killer cell transition during dasatinib consolidation. *Cancer Sci*. 2018;109:182-192. <https://doi.org/10.1111/cas.13430>



Research paper

Therapeutic effects of tyrosine kinase inhibitors and subtypes of *BCR-ABL1* transcripts in Japanese chronic myeloid leukemia patients with three-way chromosomal translocations



Koiti Inokuchi^{a,*}, Kazutaka Nakayama^{a,1}, Tetsuzo Tauchi^b, Tomoiku Takaku^c, Norio Yokose^d, Hiroki Yamaguchi^a, Takashi Kumagai^e, Norio Komatsu^c, Kazuma Ohyashiki^b

^a Department of Hematology, Nippon Medical School, Tokyo, Japan

^b Department of Hematology, Tokyo Medical University, Tokyo, Japan

^c Department of Hematology, Juntendo University School of Medicine, Tokyo, Japan

^d Department of Hematology, Chiba Hokusoh Hospital, Nippon Medical School, Japan

^e Department of Hematology, Ome Municipal General Hospital, Tokyo, Japan

ARTICLE INFO

Keywords:

BCR-ABL1 transcripts

CML

TKI

Three-way translocation

The best response

Molecular biological effects

ABSTRACT

We analyzed the clinical responses to tyrosine kinase inhibitors (TKIs) and the molecular and cytogenetic characteristics of 18 chronic myeloid leukemia (CML) patients with 3-way chromosomal translocations. The patients were 14 men and 4 women, aged 23–75 years (median 57 years). The Sokal risk was low in 12 patients, intermediate in 4 patients, and high in 2 patients. Newly identified translocation breakpoints were seen in 7 of the 18 patients. Three patients had the same breakpoints of t(9;22;11)(q34;q11.2;q23).

The best responses to TKIs were partial cytogenetic response (PCyR) in 2 patients, complete cytogenetic response (CCyR) in 3 patients, molecular response (MR) 3.0 in 7 patients, MR 4.0 in 3 patients, and MR 4.5 or higher in 3 patients. A total of 66.7% of patients did not achieve MR 4.0 or higher. In 3 patients in whom TKIs resulted in MR 4.5 or higher for more than 2 years, TKI treatment was discontinued. However, all of them exhibited a loss of MR3.0, at 2, 6, and 20 months after the discontinuation of treatment, respectively, and TKI treatment needed to be restarted. According to Kaplan-Meier survival curve analysis, the overall survival (OS) was 100 months in 56% of the patients. The 60-months cumulative incidences of CCyR, MR3.0, MR4.0 and MR4.5 were 88.9%, 72.2%, 33.3%, and 16.7%, respectively. In the 11 analyzable patients, the *BCR-ABL1* mRNA subtype was e14a2 type in 4 patients and e13a2 type in 7 patients.

1. Introduction

Chronic myelogenous leukemia (CML) develops when reciprocal translocation between chromosome 9 and 22 leads to formation of the Philadelphia (Ph) chromosome, which contains the *BCR-ABL1* fusion gene [1,2]. In about 5% of CML patients, translocations involving a single or multiple chromosomes occur in addition to that between chromosomes 9 and 22 [3,4]. These are called variant (or complex) translocations. Of these, abnormalities of 3 chromosomes that occur in a single step are called 3-way translocations. A 2-step mechanism has also been hypothesized, but it is thought to be less likely [5].

To date, nearly all CML patients with 3-way translocations have been identified in case reports or investigations with small numbers of patients. Several of these reports were published around the time that

the treatment with tyrosine kinase inhibitors (TKIs) was established, and the effect of TKIs is thought to be similar in CML with 3-way translocations as in the usual form of CML [4,5]. However, 2 studies showed poor prognosis in CML with chromosomal abnormalities in addition to the Ph translocation [6,7].

Even in reports of Ph variants have only assessed major molecular response (MMR) [4–6]. There are no studies of the response to TKI in such cases, or analysis of the achievement of deep molecular response (DMR). In the era of TKI therapy, 40%–60% of CML patients no longer require treatment after DMR; however, among these patients there are still no reports of patients with 3-way translocations. At the molecular biological level, the *BCR-ABL1* mRNA subtype e13a2 (b2a2) is thought to be associated with worse outcomes than the e14a2 (b3a2) type [8,9], and there have been no reports regarding these subtypes in CML

* Corresponding author at: Department of Hematology, Nippon Medical School, 1–1–5 Sendagi, Bunkyo–Ku, Tokyo, 113–8603, Japan.

E-mail address: inokuchi@nms.ac.jp (K. Inokuchi).

¹ KI and KN contributed equally to this work.

<https://doi.org/10.1016/j.leukres.2018.01.005>

Received 8 August 2017; Received in revised form 30 December 2017; Accepted 2 January 2018

Available online 03 January 2018

0145-2126/ © 2018 Elsevier Ltd. All rights reserved.

patients with this 3-way translocations. There are also no reports of CML with 3-way translocations in Japanese populations. Here we report the clinical and molecular characteristics and TKI therapy outcomes of 18 Japanese CML patients with 3-way translocation.

2. Patients and methods

2.1. Patients

This study retrospectively investigated 18 CML patients with 3-way translocations involving chromosomes other than 9 and 22. The patients were followed at 5 institutions: Nippon Medical School Hospital, Nippon Medical School Chiba Hokusoh Hospital, Juntendo University, Tokyo Medical University, and Ome Municipal General Hospital Department of Hematology. These institutions followed 306 CML patients during a 15-year period (from 2002 to 2016); only 18 (5.9%) could be screened for CML with 3-way translocations.

2.2. Cytogenetic analysis

Cytogenetic responses were estimated based on the prevalence of Ph-positive interphase among at least 20 G-banded cells in each bone marrow sample. G-banded bone marrow metaphases (24 or 48 h of culture) at diagnosis were interpreted according to the International System for Human Cytogenetic Nomenclature (ISCN 2009). We used fluorescence *in situ* hybridization (FISH) with BCR and ABL double-color probes to detect Ph-positive leukocytes [10,11].

2.3. Definition of response

During the TKI treatment, conventional cytogenetic and FISH analysis was performed on bone marrow cells at baseline, after 6 and 12 months of treatment, and every 6 months thereafter or if disease progression stopped. Cytogenetic response was estimated based on the results of conventional banding analysis. The criteria for cytogenetic responses according to the percentage of Ph-positive peripheral leukocytes in interphase were as follows: complete cytogenetic response (CCyR), 0%; partial cytogenetic response (PCyR), 1%–35%; minor CyR, 36%–65%; minimal CyR, 66%–95%; no cytogenetic response, 96%–100%.

2.4. Evaluation of treatment response and molecular analysis

Molecular response measurement followed the ELN recommendations for *BCR-ABL1* messenger RNA quantification by reverse transcription quantitative polymerase chain reaction (RQ-PCR). Quantification of *BCR-ABL1* transcripts by RQ-PCR analysis was performed to assess the molecular response. Patient peripheral blood samples were obtained before and at 1, 3, 6, 9, 12, 15, and 18 months after starting TKI treatment, and the analysis of *BCR-ABL1* transcripts was performed by Biomedical Laboratories (Tokyo, Japan) [12,13,14]. The values were corrected using *GAPDH* and converted to *BCR-ABL1*^{IS}, as described [12,13,14]. A DMR was defined as a *GAPDH* –corrected *BCR-ABL1* transcript value of less than 50 copies/μg RNA, which ensures < 0.01% of *BCR-ABL1*^{IS} [12,13].

MR3.0, MR4.0, and MR4.5 were defined as detectable *BCR-ABL1*^{IS} values of < 0.1%, < 0.01%, and < 0.0032%, respectively. After TKI discontinuation, *BCR-ABL1* transcripts were quantified in the peripheral blood at the same frequency as in the STIM study, namely monthly during the first 12 months, every 2–3 months during the second year, and every 3–6 months for up to 5 years.

The loss of a major molecular response (MR) was defined as a *BCR-ABL1*^{IS} > 0.1% IS; MR3.0.

2.5. Determination *BCR-ABL1* transcript subtypes and detection of *ABL1* gene mutations

Subtypes of *BCR-ABL1* transcripts were determined using our previously described methods [15]. At first we used the RNA STAT-60 reagent (Tel-test, Friends wood, TX, USA) for total RNA extraction and recently QIAamp RNA Blood MiniKit, QIAGEN, Hilden, Germany) [16]. Patients with *BCR-ABL1* transcripts e13a2 (previously named b2a2), e14a2 (previously named b3a2), and e13a2 (b2a2) coexpressed with e14a2 (b3a2) were identified [15]. Mutation analysis of the *ABL1* gene was performed as previously described [16]. Briefly, mRNA was collected from the peripheral blood or bone marrow samples and was analyzed for *BCR-ABL1* gene point mutations using denaturing high-performance liquid chromatography (D-HPLC) and sequencing [17].

3. Results

3.1. Patient characteristics

A summary of karyotypes and molecular biological, and clinical characteristics of the 18 CML patients with 3-way chromosome translocations is shown in Table 1.

The patients all had Ph-positive, major *BCR-ABL1*-positive CML, and consisted of 14 men and 4 women, treated at 5 institutions. Thus, there were considerably more men than women. Their ages ranged from 23 to 75 years (mean age 57 years). At initial presentation, 1 patient (Case 8) was in the accelerated phase, while the remaining 17 patients were in the chronic phase. The Sokal risk was low in 11 patients, intermediate in 5 patients, and high in 2 patients. Karyotype was determined based on the International System for Human Cytogenetic Nomenclature (ISCN2009). At least 20 metaphases were analyzed. All patients had a 3-way translocation.

The chromosomes other than 9 and 22 that were involved in the variant translocations varied widely, as follows: chromosome 1 (2 patients), 2 (2 patients), 3 (2 patients), 6 (1 patient), 7 (1 patient), 8 (1 patient), 11 (3 patients), 12 (1 patient), 14 (2 patients), 17 (2 patients), and 21 (1 patient). New translocation breakpoints not reported in previous reports [4–7] were present in 7 of the 18 patients. In several cases the same breakpoints occurred in multiple patients; especially, t(9;22;11)(q34;q11.2;q23) in 3 patients and t(1;9;22)(q21;q34;q11) in 2 patients. In Case 17, the monosomy 5 karyotype abnormality was present in 4/24 cells.

All 18 patients had the major *BCR-ABL1* mRNA. The *BCR-ABL1* mRNA subtypes, in the 11 analyzable patients were the b3a2 type in 4 patients and the b2a2 type in 7 patients.

3.2. Clinical course and TKI treatment

All CML patients underwent treatment with TKIs. The clinical course of each patient is shown in Fig. 1. The initial TKI was imatinib in 6 patients, nilotinib in 3 patients, and dasatinib in 9 patients. Eight patients had to be switched to another TKI (second or third TKI) because of intolerance (interstitial pneumonia, pulmonary hypertension, bronchiolitis obliterans etc.), insufficient therapeutic effect, or the requirements of a clinical trial. Six of 18 patients switched to a second line treatment during the 5-year study period.

Of the 7 patients who began treatment with imatinib, 2 patients (Cases 1, 16) switched to nilotinib because of intolerance and 4 patients (Cases 2, 3, 15, 18) switched to a second TKI (nilotinib or dasatinib) because of insufficient response.

Three patients (Cases 1, 8, 9) achieved an MR of 4.0 or higher using dasatinib, and continued intensive therapy with this drug for more than 2 years. This response persisted, so we stopped dasatinib treatment. However, there was a loss of MR3.0 in 2 patients (Cases 1, 9) at 6 months and 2 months after the discontinuation of treatment, respectively, and a loss of MR3.0 in the 20th month in 1 patient, and dasatinib

Table 1
Summary of each CML patient characteristics with 3-way translocations.

case	age at diagnosis	sex	type of 3-way translocations	duration of OS (Mo)	WBC (/μl)	Hb (g/μl)	Plt	Blast(%)	eosino	baso	Sokal state	bcr/abl subtype	additional chromosome or genetic mutation
1	57	M	t(9;22;21)(q34;q11;q22)	140	50100	7.6	77.1	1	1.5	6	low	e14a2	
2	75	M	t(7;9;22)(q36;q34;q11.2)	96	114600	9.9	32.5	4	4.5	6	high	e14a2	
3	57	M	t(9;22;11)(q34;q11.2;q23)	80	204400	7.1	99.1	4	3	1.5	low	e14a2	T315I, F359V
4	30	M	t(9;22;17)(q34;q11.2;q25)	81	467080	11.1	10.8	3	3	2	low	e13a2	
5	23	M	t(8;9;22)(q22;q34;q11.2)	32	209600	9.6	36.7	0	6.5	5	low	e13a2	
6	65	M	t(2;9;22)(p13;q34;q11.2)	30	24100	14.1	19.5	0	0	4.5	low	e13a2	
7	45	M	t(9;22;12)(q34;q11.2;q25)	27	92500	10.7	24.5	0	0	3	low	e13a2	
8	35	F	t(9;22;11)(q34;q11.2;q23)	64	6970	11.8	78.6	8	2	4	high	e13a2	
9	64	M	t(9;22;14)(q34;q11.2;q13)	72	79950	14	68.5	0.5	1	6	int	e14a2	
10	31	M	t(2;9;22)(q24;q34;q11.2)	12	11800	12.8	24.2	0	1	1.5	low	ND	
11	73	M	t(9;22;11)(q34;q11.2;q23)	27	25800	11.6	41.3	3	0.6	10.2	int	ND	
12	64	M	t(9;22;14)(q34;q11.2;q32)	48	96900	12	29.5	3	2.5	9.5	int	ND	
13	64	F	t(9;17;22)(q34;q23;q11)	44	53200	11.2	55.1	0.5	3.5	2	low	ND	
14	49	M	t(3;9;22)(p12;q34;q11)	40	47900	13	80.6	0.5	3.5	4	low	ND	
15	43	F	t(1;9;22)(q21;q34;q11)	86	122400	8.6	93.3	1	4.5	6	low	ND	
16	68	F	t(1;9;22)(q21;q34;q11)	49	32600	16.9	29.2	0	3.5	10	low	ND	
17	45	M	t(3;9;22)(q26;q34;q11.2)	22	41600	14.7	52.5	0.5	3	7.5	low	e13a2	monosomy 5 (4/24)
18	62	M	t(6;9;22)(q21;q34;q11.2)	196	76500	11.6	63.7	0	4.5	14.5	int	e13a2	M244 V, Q252H

Abbreviations: F, female; int, intermediate; M, male; ND, not determined.

had to be restarted.

In Case 2 the disease worsened and the patient died at 96 months. In Case 3, double *ABL1* gene mutations of T315I and F359 V were seen during imatinib therapy (Table 1), and allogeneic transplantation was performed. Despite having acquired molecular CR, the patient died from post-transplant complications at about 5 months after transplantation. In Case 18, M244 V and Q252H double *ABL1* gene mutations were observed after administration of imatinib for 106 months, and a switch was made to nilotinib. There was still no improvement, and another switch was made to dasatinib. After the start of dasatinib, the M244 V and Q252H double *ABL1* gene mutations rapidly disappeared, and good control from minimal CyR to PCyR, and persisted for 8 years.

3.3. Cytogenetic and molecular responses, and the overall survival (OS)

The best responses with TKI treatment in the 18 analyzed patients were PCyR in 2 patient, CCyR in 3 patients, MR3.0 in 7 patients, MR4.0 in 3 patients, and MR4.5 or higher in 3 patients. MR4.0 was not achieved in 11/18 patients (66.7%) (Fig. 2).

The 60-months cumulative incidences of CCyR, MR3.0, MR4.0 and MR4.5 were 88.9% 72.2%, 33.3%, and 16.7%, respectively (Fig. 3).

Kaplan-Meier survival curve analysis showed that OS for the entire sample at 60 months was 100%, and at 100 months was 56% (Fig. 4).

4. Discussion

A previous study demonstrated poor prognosis in CML patients with 3-way translocations that developed following the conventional t(9;22) translocation by a 2-step mechanism [5]. In this study, none of the 18 patients showed 2 cutting points on the third chromosome in the karyotype, and there were breakpoints on the third chromosome at the initial visit.

Thus, it was considered probable that breakpoints on the third chromosome were caused by a 1-step mechanism, and we assumed that the prognosis of these 18 patients was the same as that of CML with standard Ph. On the other hand, regarding a new deletion such as 9q that occurs in der (9), the possibility of becoming TKI resistant has been reported [7], but the corresponding abnormality was not found in the current 18 patients. These patients exhibited 7 new translocation breakpoints that were not reported in previous studies. [4–7] Three patients had the same breakpoint, t (9; 22; 11) (q34; q11.2; q23), and the breakpoint at 11q23 was seen for the first time in a 3-way translocation. This translocation may be specific to Japanese patients. The therapeutic effect of TKI varied in these 3 cases was varied (Case 3, CCyR; Case 8, MR > 4.5; Case 11, MR 4.0), and it was unclear whether the overall molecular biological response was good or bad.

The *BCR/ABL1* mRNA subtype was e14a2 type in 4 patients and e13a2 type in 7 patients; this frequency seems to be reversed compared to the usual ratio in CML patients, namely 70% e14a2 and 30% e13a2. [8,15,18] This reversed ratio may be one characteristic of CML with 3-way translocation. The probability of the e13a2 subtype is lower in DMR; thus, it may be necessary to analyze this subtype in patients with 3-way translocations, because CML patients with the e13a2 subtype are poorly controlled compared with those with subtype e14a2 [8,18]. However, the worse outcome of e13a2 patients is still a matter of discussion [19].

None of the patients exhibited an obvious early resistance after the start of TKI. However, in 6 patients in whom MR3.0 was maintained, MR4.0 or greater was not achieved even with the long-term use of a TKI. Six of the 18 patients in this study switched to a second-line treatment during the 5-year study period. It can not be said that the number of patients who change TKI treatment is not large [20].

The above results (Figs. 2 and 3) indicate that it may be more difficult to obtain DMR with TKI in CML patients with 3-way translocations than in patients with the usual form of CML. In all 3 patients in whom good control of MR > 4.0 continued for 2 years and dasatinib

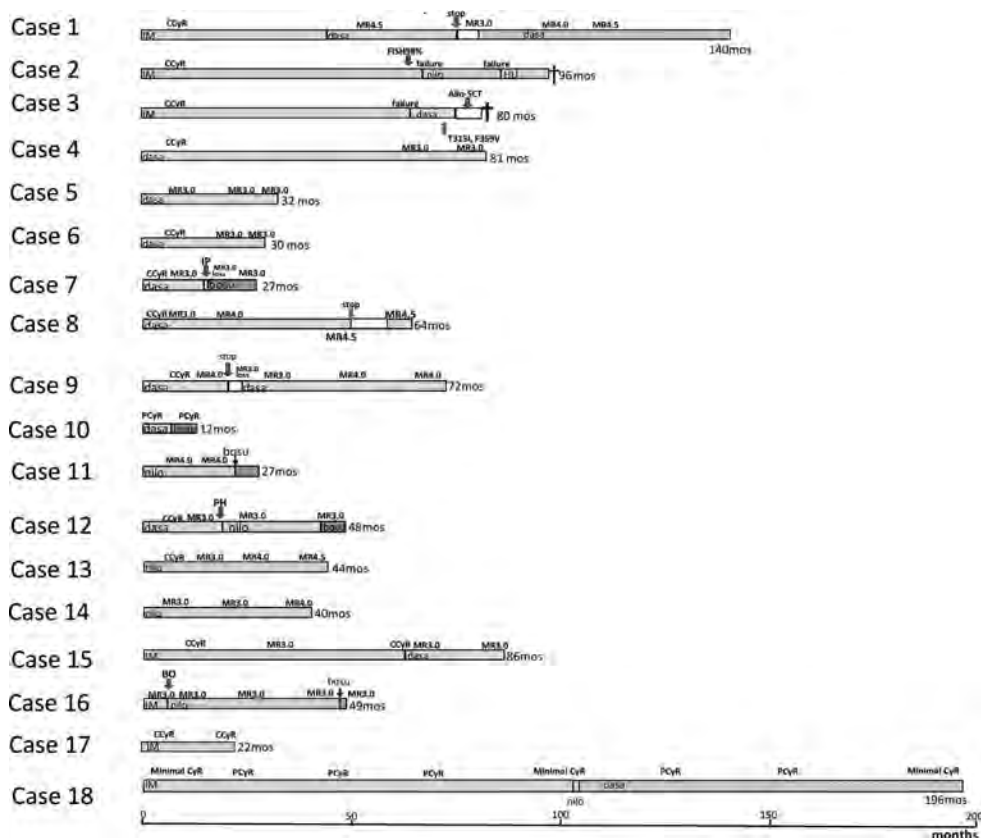


Fig. 1. Clinical course of each patient with a 3-way translocation.

BO: bronchiolitis obliterans; Bosu:bosutinib; CCyR: complete cytogenetic response; dasa: dasatinib; IM: imatinib; IP: interstitial pneumonia; nilo: nilotinib; PH: pulmonary hypertension; PCyR: partial cytogenetic response; mos: months.

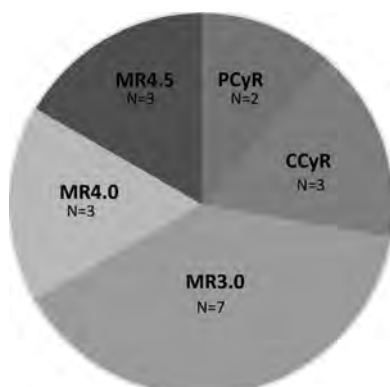


Fig. 2. Best responses during the TKI therapy.

CCyR: complete cytogenetic response; N = : Number of patients; PCyR: partial cytogenetic response.

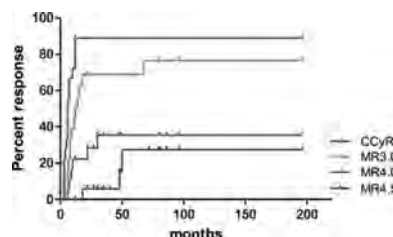


Fig. 3. Cumulative incidences of CCyR, MR3.0, MR4.0 and MR4.5.

Vertical lines indicate censored patients. CCyR: complete cytogenetic response; MR: molecular response.

was discontinued, there was a loss of MR3.0. Further investigations of a larger number of CML patients with 3-way translocation will be needed to determine the indications for treatment discontinuation.

While several studies have shown worse overall survival (OS) with imatinib treatment in patients with a showing a variant Ph translocation [6,7], there are also many reports showing less impact on OS [4,5]. There are no comprehensive reports to date on the DMR (MR4.0 and MR4.5), and in this study the effect of TKIs in CML with 3-way translocation was limited to CCyR and MR 3 in many patients. This is the

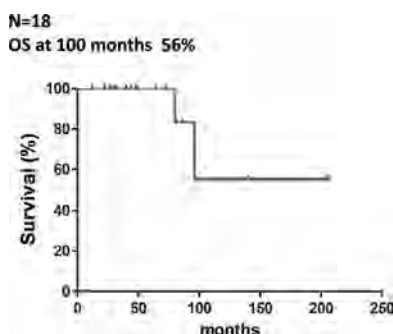


Fig. 4. Overall survival (OS) of 18 cases receiving TKI treatment. Vertical lines indicate censored patients.

first report demonstrating MR 4 or higher in this population, but only about 33.8% of patients reached this level (Figs. 2 and 3). Many of the patients who received imatinib as the initial TKI had poor responses and had to be switched to a second TKI; it is necessary to investigate the role of imatinib as a first TKI in additional patients with 3-way translocation.

The cumulative CCyR, MR3.0, MR4.0 and MR4.5 rates were higher for TKIs-treated Japanese patients as compared with total international patients in DASSION analysis [21,22]. When the rates of cumulative molecular responses were compared between standard Japanese CML and this CML with 3-way translocations, the cumulative CCyR and MR3.0 rates of CML patients with 3-way translocations were the same as those of Japanese standard CML [21]. However, the cumulative MR4.0 and MR4.5 rates at any time seemed to be lower in the CML with three-way translocation versus standard CML patients. The possible explanation for the difference of the cumulative MR4.0 and MR4.5 rates between standard CML and CML with three-way translocation may be molecular abnormalities due to the three-way translocation. The molecular abnormalities due to chromosomal translocation may influence on the cumulative MR4.0 and MR4.5 rates. Gene mutations in the driver gene have been reported to influence on the effectiveness of the molecular response [23].

Past reports have suggested that disease progression may be related to the location of the breakpoint on the third chromosome involved in 3-way translocation [6,7]. In this study, these breakpoints were not identified in all patients, but 3 patients had a breakpoint at 11q23, which is known to be associated with refractory leukemia, and there is a possibility that the MLL gene is located here and serves some kind of role related to tumorigenesis and prognosis [23]. In addition, 11q23 may be an abnormal chromosomal translocation peculiar to Japanese people. Multiple other breakpoints that have been indicated to be associated with tumorigenesis were also seen in the patients in this study. The 21q22 chromosome band is where the AML1 gene is located [24] and other genes that function as multiple myeloma or cancer genes have been reported at breakpoints 17q25, 17q23, 1q21, 7q36, 2q24, and 14q32 [25–27]. Gene analysis of these breakpoints is desirable, as is further investigation of the relationship with prognosis or MR in a larger number of patients. Gene mutation analysis has been performed in CML [23], and, in patients with a mutation in the driver gene, acquisition of DMR has been poor. The relationship of the acquisition of DMR with *BCR-ABL1* mRNA subtype is also an issue that will need to be examined in the future.

This study investigated 18 CML patients with a 3-way translocation, the first to do so in a Japanese population. It will be necessary to conduct investigations with a larger number of patients with 3-way translocations, including evaluations of racial differences.

Author's contribution

Koiti Inokuchi contributed to the study concept and design, interpreted and analyzed the data and wrote the article. Kazutaka Nakayama interpreted and analyzed the data, and performed experiments, and analyzed the data, and wrote the manuscript draft. Norio Yokose, Tetsuzo Tauchi, Hiroki Yamaguchi, Tomoiku Takaku and Takashi Kumagai were the institutional principle investigators; all were responsible for obtaining institutional IRB approvals, performing data collection and review, and submitting the manuscript.

Conflict of interest

No author has any conflict of interest to report in regard to this study.

Acknowledgement

The authors would like to thank Shinichiro Okamoto and Takehiko Mori, Keio University Hospital for the support in providing data for this research.

References

- [1] J.D. Rowley, A new consistent chromosomal abnormality in chronic myelogenous leukemia identified by quinacrine fluorescence and giemsa staining, *Nature* 243 (1973) 290–293.
- [2] A. de Klein, A.G. van Kessel, G. Grosveld, et al., A cellular oncogene is translocated to the Philadelphia chromosome in chronic myelogenous leukemia, *Nature* 300 (1982) 765–767.
- [3] K.S. Reddy, V.A. Sulcova, FISH study of variant Philadelphia rearrangement, *Cancer Genet. Cytogenet.* 118 (2000) 121–131.
- [4] A. Fabarius, A. Leitner, A. Hochhaus, et al., Impact of additional cytogenetic aberrations at diagnosis on prognosis of CML: long-term observation of 1151 patients from the randomized CML Study IV, *Blood* 118 (2011) 6760–6768.
- [5] G. Marzocchi, F. Castagnetti, S. Luatti, et al., Variant Philadelphia translocations: molecular-cytogenetic characterization and prognostic influence on frontline imatinib therapy, a GIMEMA Working Party on CML analysis, *Blood* 117 (2011) 6793–6800.
- [6] S. Luatti, F. Castagnetti, G. Marzocchi, et al., Additional chromosomal abnormalities in Philadelphia-positive clone: adverse prognostic influence on frontline imatinib therapy: a GIMEMA Working Party on CML analysis, *Blood* 120 (2012) 761–767.
- [7] A.G. Reid, B.J. Huntly, C. Grace, A.R. Green, E.P. Nacheva, Survival implications of molecular heterogeneity in variant Philadelphia-positive chronic myeloid leukaemia, *Br. J. Haematol.* 121 (2003) 419–427.
- [8] P. Jain, H. Kantarjian, K.P. Patel, et al., Impact of BCR-ABL transcript type on outcome in patients with chronic-phase CML treated with tyrosine kinase inhibitors, *Blood* 127 (2016) 1269–1275.
- [9] M. Futaki, K. Inokuchi, H. Matsuo, K. Miyake, K. Dan, T. Nomura, Relationship of the type of *bcr-abl* hybrid mRNA to clinical courses and transforming activity in Philadelphia-positive chronic myelogenous leukemia, *Leukemia Res* 16 (1992) 1071–1075.
- [10] K. Inokuchi, T. Shinohara, M. Futaki, et al., Establishment of a cell line with variant BCR/ABL breakpoint expressing P180BCR/ABL from late-appearing Philadelphia-positive acute biphenotypic leukemia, *Genes. Chromosomes Cancer* 23 (1998) 227–238.
- [11] M. Inami, K. Inokuchi, K. Nakayama, et al., Simultaneous novel BCR-ABL gene mutation and increased expression of BCR-ABL mRNA caused clinical resistance to ST1571 in double-Ph-positive acute biphenotypic leukemia, *Int. J. Hematol.* 78 (2003) 173–175.
- [12] N. Iriyama, S. Fujisawa, C. Yoshida, et al., Shorter halving time of BCR-ABL1 transcripts is a novel predictor for achievement of molecular responses in newly diagnosed chronic-phase chronic myeloid leukemia treated with dasatinib: results of the D-first study of Kanto CML study group, *Am. J. Hematol.* 90 (2015) 282–287.
- [13] T. Kumagai, E. Matsuki, K. Inokuchi, et al., Relative increase in lymphocytes from as early as 1 month predicts improved response to dasatinib in chronic-phase chronic myelogenous leukemia, *Int. J. Hematol.* 99 (2014) 41–52.
- [14] K. Inokuchi, T. Kumagai, E. Matsuki, et al., Efficacy of molecular response at 1 or 3 months after the initiation of dasatinib treatment can predict an improved response to dasatinib in imatinib-resistant or imatinib-intolerant Japanese patients with chronic myelogenous leukemia during the chronic phase, *J. Clin. Exp. Hematop.* 54 (2014) 197–204.
- [15] K. Inokuchi, T. Inoue, A. Tojo, et al., A possible correlation between the type of *bcr-abl* hybrid messenger RNA and platelet count in Philadelphia-positive chronic myelogenous leukemia, *Blood* 78 (1991) 3125–3127.
- [16] M. Inami, K. Inokuchi, H. Yamaguchi, et al., Oral administration of imatinib to P230 BCR/ABL-expressing transgenic mice changes clones with high BCR/ABL

- complementary DNA expression into those with low expression, *Int. J. Hematol.* 84 (2006) 346–353.
- [17] M. Inami, K. Inokuchi, K. Nakayama, H. Tamura, T. Shimada, K. Dan, Simultaneous novel *BCR-ABL* gene mutation and increased expression of *BCR-ABL* mRNA caused clinical resistance to STI571 in double-Ph-positive acute biphenotypic leukemia, *Int. J. Hematol.* 78 (2003) 173–175.
- [18] B. Hanfstein, M. Lauseker, R. Hehlmann, et al., Distinct characteristics of e13a2 versus e14a2 *BCR-ABL* driven chronic myeloid leukemia under first-line therapy with imatinib, *Haematologica* 99 (2014) 1441–1447.
- [19] M. Pfeiffermann, D. Evtimova, S. Saussele, et al., No influence of *BCR-ABL*1 transcript types e13a2 and e14a2 on long-term survival: results in 1494 patients with chronic myeloid leukemia treated with imatinib, *J. Cancer Res. Clin. Oncol.* 143 (2017) 843–850.
- [20] T.L. Holyoake, D. Vetrie, The chronic myeloid leukemia stem cell: stemming the tide of persistence, *Blood* 129 (2017) 1595–1606.
- [21] H. Nakamae, S. Fujisawa, M. Ogura, et al., Dasatinib versus imatinib in Japanese patients with newly diagnosed chronic phase chronic myeloid leukemia: a sub-analysis of the DASISION 5-year final report, *Int. J. Hematol.* 105 (2017) 792–804.
- [22] J.E. Cortes, G. Saglio, H.M. Kantarjian, et al., Final 5-year study results of DASISION: the dasatinib versus imatinib study in treatment-naïve chronic myeloid leukemia patients trial, *J. Clin. Oncol.* 34 (2016) 2333–2340.
- [23] T. Kim, M.S. Tydel, H.J. Kim, et al., Spectrum of somatic mutation dynamics in chronic myeloid leukemia following tyrosine kinase inhibitor therapy, *Blood* 129 (2017) 38–47.
- [24] H. Tamai, K. Inokuchi, 11q23/MLL acute leukemia: update of clinical aspects, *J. Clin. Exp. Hematop.* 50 (2010) 91–98.
- [25] C. Roumier, P. Fenaux, M. Lafage, M. Imbert, V. Eclache, C. Preudhomme, New mechanisms of AML1 gene alteration in hematological malignancies, *Leukemia* 17 (2003) 9–16.
- [26] I. Hanamura, J.P. Stewart, Y. Huang, et al., Frequent gain of chromosome band 1q21 in plasma-cell dyscrasias detected by fluorescence in situ hybridization: incidence increases from MGUS to relapsed myeloma and is related to prognosis and disease progression following tandem stem-cell transplantation, *Blood* 108 (2006) 1724–1732.
- [27] R. Zhang, J.Y. Lee, X. Wang, et al., Identification of novel genomic aberrations in AML-M5 in a level of array CGH, *PLoS One* 11 (9) (2014) e87637, <http://dx.doi.org/10.1371/journal.pone.0087637>.

Prognostic impact of low allelic ratio *FLT3*-ITD and *NPM1* mutation in acute myeloid leukemia

Masahiro Sakaguchi,^{1,*} Hiroki Yamaguchi,^{1,*} Yuho Najima,² Kensuke Usuki,³ Toshimitsu Ueki,⁴ Iekuni Oh,⁵ Sinichiro Mori,⁶ Eri Kawata,⁷ Nobuhiko Uoshima,⁷ Yutaka Kobayashi,⁷ Shinichi Kako,⁸ Kenji Tajika,⁹ Seiji Gomi,⁹ Katsuhiro Shono,¹⁰ Kensuke Kayamori,¹¹ Masao Hagihara,¹² Junya Kanda,¹³ Hitoji Uchiyama,¹⁴ Junya Kuroda,¹⁵ Naoyuki Uchida,¹⁶ Yasushi Kubota,¹⁷ Shinya Kimura,¹⁷ Saiko Kurosawa,¹⁸ Nana Nakajima,¹ Atsushi Marumo,¹ Ikuko Omori,¹ Yusuke Fujiwara,¹ Shunsuke Yui,¹ Satoshi Wakita,¹ Kunihito Arai,¹ Tomoaki Kitano,¹ Kazuhiko Kakahana,² Yoshinobu Kanda,^{5,8} Kazuteru Ohashi,² Takahiro Fukuda,¹⁸ and Koiti Inokuchi¹

¹Department of Hematology, Nippon Medical School, Tokyo, Japan; ²Division of Hematology, Tokyo Metropolitan Cancer and Infectious Diseases Center, Komagome Hospital, Tokyo, Japan; ³Department of Hematology, NTT Medical Center Tokyo, Tokyo, Japan; ⁴Department of Hematology, Nagano Red Cross Hospital, Nagano, Japan; ⁵Division of Hematology, Department of Medicine, Jichi Medical University, Tochigi, Japan; ⁶Hemato-Oncology Department, St Luke's International Hospital, Tokyo, Japan; ⁷Department of Hematology, Japanese Red Cross Kyoto Daini Hospital, Kyoto, Japan; ⁸Division of Hematology, Jichi Medical University Saitama Medical Center, Saitama, Japan; ⁹Department of Hematology, Yokohama Minami Kyousai Hospital, Kanagawa, Japan; ¹⁰Department of Hematology, Chiba Aoba Municipal Hospital, Chiba, Japan; ¹¹Department of Hematology, Chiba University Hospital, Chiba, Japan; ¹²Department of Hematology, Eiju General Hospital, Tokyo, Japan; ¹³Department of Hematology and Oncology, Graduate School of Medicine, Kyoto University, Kyoto, Japan; ¹⁴Department of Hematology, Japanese Red Cross Kyoto Daiichi Hospital, Kyoto, Japan; ¹⁵Division of Hematology and Oncology, Kyoto Prefectural University of Medicine, Kyoto, Japan; ¹⁶Department of Hematology, Federation of National Public Service Personnel Mutual Aid Associations, Toranomon Hospital, Tokyo, Japan; ¹⁷Division of Hematology, Respiratory Medicine and Oncology, Department of Internal Medicine, Faculty of Medicine, Saga University, Saga, Japan; and ¹⁸Department of Hematopoietic Stem Cell Transplantation, National Cancer Center Hospital, Tokyo, Japan

Key Points

- The ELN guideline classifying *FLT3*-ITD low allele ratio with *NPM1* mutation as having a favorable prognosis is questionable.
- Performing allo-HSCT during CR1 irrespective of the *FLT3*-ITD allele ratio and *NPM1* mut status significantly improves outcome.

In the opinion of the European LeukemiaNet (ELN), nucleophosmin member 1 gene mutation (*NPM1* mut)-positive acute myeloid leukemia (AML) with an *fms*-like kinase 3-internal tandem duplication (*FLT3*-ITD) allele ratio (AR) <0.5 (low AR) has a favorable prognosis, and allogeneic hematopoietic stem cell transplant (allo-HSCT) in the first complete remission (CR1) period is not actively recommended. We studied 147 patients with *FLT3*-ITD gene mutation-positive AML, dividing them into those with low AR and those with AR of ≥ 0.5 (high AR), and examined the prognostic impact according to allo-HSCT in CR1. Although *FLT3*-ITD AR and *NPM1* mut are used in the prognostic stratification, we found that *NPM1* mut-positive AML with *FLT3*-ITD low AR was not associated with favorable outcome (overall survival [OS], 41.3%). Moreover, patients in this group who underwent allo-HSCT in CR1 had a significantly more favorable outcome than those who did not (relapse-free survival [RFS] $P = .013$; OS $P = .003$). Multivariate analysis identified allo-HSCT in CR1 as the sole favorable prognostic factor (RFS $P < .001$; OS $P < .001$). The present study found that prognosis was unfavorable in *NPM1* mut-positive AML with *FLT3*-ITD low AR when allo-HSCT was not carried out in CR1.

Introduction

Acute myeloid leukemia (AML) is a heterogeneous hematological malignancy characterized by myeloblast invasion of the bone marrow, peripheral blood, and other tissues in association with impaired differentiation and autonomous proliferation of hematopoietic stem cells. Induction therapy achieves complete remission (CR) in 60% to 80% of cases. However, the subsequent 5-year survival rate remains at $\sim 40\%$.¹ Allogeneic hematopoietic stem cell transplantation (allo-HSCT) is a useful treatment aimed at cure of AML. However, non-relapse mortality in allo-HSCT is as high as $\sim 20\%$,² and allo-HSCT therefore needs to be applied appropriately based on a consideration of the prognosis. To allow this, prognostic stratification plays an

important role, but at present, chromosomal analysis places more than half of patients in the intermediate prognosis group, suggesting that this form of stratification is as yet insufficient. Our current tasks are to achieve more detailed prognostic stratification and a more accurate understanding of when hematopoietic stem cell transplant is indicated.

The prognostic factors in AML include age, white blood cell count at initial presentation, and chromosomal abnormality. The advent of the next-generation sequencer has enabled prognostic stratification to additionally take account of gene mutations.³ It has been suggested that the gene mutations nucleophosmin member 1 (*NPM1*), CCAAT/enhancer-binding protein α (*CEBPA*), and fms-like kinase 3-internal tandem duplication (*FLT3*-ITD) may act as prognostic factors in AML of normal karyotype, and these mutations are also used in the prognostic classification of the European LeukemiaNet (ELN). However, they are found in only ~30% of patients in the intermediate prognosis group. A more detailed stratification is therefore required going forward.

FLT3, a member of the type III receptor tyrosine kinase family, consists of a ligand-binding extracellular domain, a single transmembrane domain, a cytoplasmic domain containing the juxta-membrane domain, tyrosine kinase domain 1, and tyrosine kinase domain 2. *FLT3*-ITD gene mutation was first reported in 1996 by Nakao et al⁴ and is observed in ~25% of AML patients.⁵ In the *FLT3*-ITD gene mutation, the ITD is inserted into the *FLT3* gene on chromosome 13, and its length varies from 3 to several hundred nucleotides.⁶ The *FLT3*-ITD gene mutation promotes proliferative activation through persistent phosphorylation of the *FLT3* receptor and simultaneously suppresses apoptosis.⁷⁻⁹ In clinical terms, *FLT3*-ITD gene mutation is associated with increased white blood cell count, elevation of myeloblast proportion, and risk of relapse from CR and has been reported to carry an unfavorable prognosis.^{5,10,11} For this reason, allo-HSCT in the first complete remission (CR1) is recommended in *FLT3*-ITD-positive AML patients of transplant-eligible age.¹²⁻¹⁶

In *FLT3*-ITD gene mutation-positive AML cases, there was for many years no settled opinion regarding the status as prognosis-regulating factors of *FLT3*-ITD allele ratio (AR), the size of the ITD insertion mutation, the presence in ITD of tyrosine kinase domain 1, and the presence of the *NPM1* gene mutation (*NPM1* mut).¹²⁻²¹ In recent years, however, it has been reported that the inclusion of *FLT3*-ITD AR may make possible more detailed prognostic stratification in *NPM1* mut-positive AML.^{12,22-24} In response to these findings, the ELN proposed a new prognostic classification in 2017.²⁵ In the opinion of the ELN, *NPM1* mut-positive AML with *FLT3*-ITD AR <0.5 has a favorable prognosis, and allo-HSCT in CR1 is not actively recommended. In contrast, the guideline of the National Comprehensive Cancer Network classifies *FLT3*-ITD gene mutation as a poor prognostic factor.²⁶ Although it involves only a certain proportion of *FLT3*-ITD-positive cases, this is the first time that *FLT3*-ITD-positive AML has been classified in the favorable prognosis group, and there appears to be a fair number of clinicians who view the ELN recommendation with skepticism. The present study therefore aimed to examine the prognostic impact of *FLT3*-ITD AR and explore whether allo-HSCT is indicated in *FLT3*-ITD-positive AML.

Materials and methods

Patients

The study was a retrospective analysis of the 147 *FLT3*-ITD-positive cases among de novo AML patients diagnosed at Nippon

Medical School Hospital or partner research institutions in the period since the year 2000 after excluding therapy-related AML, AML arising from myelodysplastic syndromes, and acute promyelocytic leukemia (M3). None of the patients was treated with *FLT3* inhibitors. All samples were obtained at diagnosis after obtaining written informed consent in accordance with the Declaration of Helsinki. All the experiments were approved by the ethics committee of each institution.

Screening for cytogenetic abnormalities

G-band analysis was carried out using bone marrow aspirate sampled at the time of initial presentation. In cases where sampling was difficult, peripheral blood was used for the test instead. The cytogenetic prognosis was then classified in accordance with the system recommended by the ELN.

Gene mutation analysis

Following reference to existing studies,^{11,27,28} 5'-GCAATT-TAGGTATGAAAGCCAGC-3' was used as the forward primer and 5'-CTTTCAGCATTTTGACGGCAAC-3' as the reverse primer. Approximately 1 ng DNA was added to a mixture of 0.2 μ M of the respective primer with TaKaRa Taq (Takara Bio, Shiga, Japan) (5 μ L Ex Taq Buffer, 4 μ L dDNP mixture, and 0.25 μ L TaKaRa Ex Taq polymerase), and the whole mixture was brought to an overall volume of 50 μ L with sterile purified water. The resulting mixture was subjected to polymerase chain reaction amplification at 95°C for 3 minutes, followed by 35 cycles at 98°C for 5 seconds, 64°C for 30 seconds, 72°C for 1 minute, and 72°C for 7 minutes. The amplified products were electrophoresed through 2% agarose gels and visualized under UV light with ethidium bromide staining. Cases in which an additional higher molecular weight band was observed were judged to be *FLT3*-ITD gene mutation-positive (*FLT3*-ITD). The AR and mutant size of *FLT3*-ITD patient samples were measured by fragment analysis using Applied Biosystems 3130 and 3130xl Genetic Analyzers (Thermo Fisher, Carlsbad, CA). *FLT3*-ITD AR was calculated as the ratio of the area under the curve of mutant to wild-type alleles (*FLT3*-ITD/*FLT3*wt). *FLT3*-ITD allele frequency (AF) was calculated as the area under the curve of mutant alleles as a percentage of mutant and wild-type alleles. In cases with >1 mutant, all *FLT3*-ITD mutants were aggregated. Mutant size was calculated by subtracting the total number of bases with wild-type *FLT3* from the total number of bases containing mutant *FLT3*. As in previous reports, screening was carried out for *NPM1* mut and *CEBPA* mutation.^{29,30}

Statistical analysis

CR in the present study was defined according to the criteria for CR (bone marrow blasts <5%, absence of circulating blasts and blasts with Auer rods, absence of extramedullary disease, absolute neutrophil count $\geq 1.0 \times 10^9$ /L, and platelet count $\geq 100 \times 10^9$ /L) or those for CR with incomplete hematologic recovery (the same except for residual neutropenia [$<1.0 \times 10^9$ /L] or thrombocytopenia [$<100 \times 10^9$ /L]) in the ELN's Response Criteria in AML.²⁵ Relapse was defined as a return to $\geq 5\%$ blast cells in the bone marrow after successful achievement of CR. Primary induction failure was defined as nonresponse to remission induction. Overall survival (OS) was defined as the time interval measured from the date of diagnosis to the date of death. Relapse-free survival (RFS) for patients who had achieved CR was calculated as the time interval from the date of CR to the

Table 1. Clinical background of the AML patients with *FLT3*-ITD

	All (N = 147)	AR		P
		<0.5 (n = 59)	≥0.5 (n = 88)	
Age, median (range), y	56 (18-90)	54 (21-86)	54 (18-90)	.853
Sex				.172
Male	66	30	36	
Female	77	26	51	
Unknown	4	3	1	
ECOG-PS, 0/1/2/3/4	41/46/6/3/3	21/17/1/1/0	20/29/5/2/3	
WBC count, median (range), $\times 10^9/L$	56.1 (1.0-677.0)	47.2 (1.0-620.0)	75.6 (1.3-677.0)	.342
Hb, median (range), g/dL	8.4 (3.3-15.1)	8.4 (3.3-15.0)	8.6 (4.1-15.1)	.799
Plt count, median (range), $\times 10^9/L$	50.0 (5.0-630.0)	55.0 (6.0-630.0)	49.0 (5.0-540.0)	.515
LDH, median (range), IU/L	719 (151-5930)	718 (151-5930)	765 (156-4144)	.437
FAB				
M0	6	1	5	.402
M1	51	17	34	.220
M2	37	19	18	.108
M4	29	13	16	.565
M5	17	4	13	.190
Not determined	7	5	2	.117
Chromosomal aberrations				
t(8,21)	4	2	2	1.000
inv(16)	1	1	0	.401
Normal	106	40	66	.354
Trisomy 8	3	0	3	.274
11q23	0	0	0	1.000
Complex	4	1	3	.649
Unknown	8	4	4	.558
Gene mutation				
<i>FLT3</i> -TKD	0	0	0	1.000
<i>NPM1</i>	83	31	52	.432
<i>CEBPA</i> (sm)	8	5	3	.268
<i>CEBPA</i> (dm)	3	3	0	.063
Induction therapy				
(IDA/DNR/ACR) + Ara-C	108	41	67	.371
AVV, BHAC-DM, CAG	25	12	13	.382
Others	14	6	8	.827
Stem cell transplantation				
All	65	26	39	.976
In CR1	31	16	15	.142

Data are numbers of patients, except as noted. Some data are missing due to the unavailability of certain follow-up data in a retrospective study.

ACR, aclarubicin; Ara-C, cytarabine; AVV, cytarabine + etoposide + vincristine + vinblastine; BHAC-D, enocitabine + daunorubicin + 6-mercaptopurine; CAG, cytarabine + cytarabine + granulocyte colony-stimulating factor; dm, double mutation; DNR, daunorubicin; ECOG-PS, Eastern Cooperative Oncology Group performance status; *FLT3*-TKD, fms-like kinase 3-tyrosine kinase domain; IDA, idarubicin; Plt, platelet; sm, single mutation; WBC, white blood cell.

date of relapse. These were defined according to the ELN.²⁵ An χ^2 test was used for the analysis of nominal variables. Where a figure of <5 appeared in any field of the 2×2 table, a Fisher's exact test was used for analysis. The nonparametric Mann-Whitney *U* test was used to determine the statistical significance of differences in median values. All statistical tests were 2 sided. To analyze OS

and RFS, the Kaplan-Meier method and the log-rank test were used. Events at a significance level of $P < .05$ were analyzed. Statistical analyses were performed using GraphPad Prism (version 7.03 for Windows; GraphPad Software, La Jolla, CA), and EZR (version 1.36; Saitama Medical Center, Jichi Medical University, Saitama, Japan).³¹

Results

Patient background

Patient background is shown in Table 1. The median age was 56 years. There were 66 males and 77 females. The median follow-up period was 0.95 years (345 days). Cytogenetic test results found normal karyotype in 106 cases, t(8;21) in 4, inv(16) in 1, trisomy 8 in 3, and complex karyotype in 4. Gene mutations other than *FLT3*-ITD consisted of *NPM1* in 83 cases and *CEBPA* biallelic mutation in 3. Induction therapy consisted in 108 cases of standard chemotherapy in the form of an anthracycline-type drug (idarubicin, daunorubicin, or aclarubicin) combined with cytarabine. Allo-HSCT was carried out in 65 patients, in 31 of whom it took place during CR1.

Study of *FLT3*-ITD AR

The median value for *FLT3*-ITD AF was 36.98% (range 2.08% to 100%), similar to that of a previous report,¹² in which the median value for *FLT3*-ITD AF was 35% (range 1% to 96%) (supplemental Figure 1A). The characteristic distribution of AF and mutant size in the 124 cases with a single *FLT3*-ITD mutant is shown in supplemental Figure 1B-C.

RFS and OS were studied with the cutoff values for *FLT3*-ITD AR set variously at 0.25 (AF 20%), 0.5 (AF 33.3%), and 1.0 (AF 50%). When the cutoff value was set at *FLT3*-ITD AR 0.25, RFS and OS were found to be significantly more favorable in the low-AR group than in the high-AR group (RFS $P = .030$; OS $P = .037$) (supplemental Figure 2A). When the cutoff value was set at *FLT3*-ITD AR 0.5, RFS and OS were again significantly more favorable in the low-AR group (RFS $P = .008$; OS $P = .015$) (Figure 1). In contrast, when the cutoff value was set at *FLT3*-ITD AR 1.0, no significant difference in RFS or OS was observed between the low-AR group and the high-AR group (RFS $P = .174$; OS $P = .624$) (supplemental Figure 2B). These findings indicate that a cutoff value set at *FLT3*-ITD AR 0.5 was the most appropriate for prognostic stratification.

Based on the above results, the patients were divided into 2 groups: a low-AR group with AR of <0.5 (low AR) and a high-AR group with AR of ≥ 0.5 (high AR). The patient background of the 2 groups (Table 1) showed no significant difference in any factors.

Impact of AR on CR1 success rate, relapse rate, and CR2 success rate

The success rate of CR1, the relapse rate, and the success rate of the second complete remission (CR2) in the low-AR and high-AR groups are summarized in Table 2. The overall success rate of CR1 was 68.6% (94/137), with no significant difference found between the low-AR and high-AR groups (low AR 62.7% vs high AR 64.8%, $P = .985$). The relapse rate was examined with analysis restricted to cases in which allo-HSCT was not performed during CR1. The relapse rate was 84.4% (38/45) overall, with no significant difference noted between the low-AR and high-AR groups (low AR 85.7% vs high AR 83.9%, $P = 1.000$). Next, we examined the efficacy in these cases of postrelapse second induction therapy. The overall success rate of CR2 was 31.8% (7/22 patients), with no significant difference found between low-AR and high-AR groups (low AR 20.0% vs high AR 35.3%, $P = .637$). Relapse cases where transplant was not carried out in CR1 were thus associated with poor outcome irrespective of AR, with a probability of achieving second remission of $\sim 30\%$.

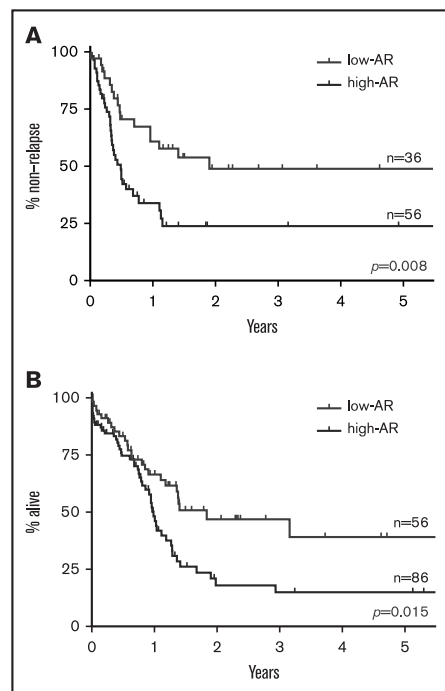


Figure 1. Impact on RFS and OS of *FLT3*-ITD AR with cutoff value set at 0.5.

(A) RFS. (B) OS. RFS and OS were found to be significantly more favorable in the low-AR group than in the high-AR group (RFS at 5 years: low-AR group 48.9% vs high-AR group 23.8%, $P = .008$; OS at 5 years: low-AR group 39.1% vs high-AR group 15.0%, $P = .015$).

Impact of AR on OS and RFS

Taking all cases of *FLT3*-ITD-positive AML, the 5-year RFS was 34.3%, and the 5-year OS was 25.8% (supplemental Figure 3). The overall relapse rate was 58.2% (53/91 patients).

In stratified analysis focusing on patients <70 years of age who have intermediate prognosis based on karyotype, the low-AR group was also found to have significantly better outcomes in both RFS and OS than the high-AR group (RFS $P = .017$; OS $P = .049$) (Figure 2A).

When analysis was restricted to *NPM1* mut-positive cases, RFS and OS were again found to be significantly more favorable in the low-AR group than the high-AR group (RFS $P = .026$; OS $P = .041$) (Figure 2B). Table 3 shows patient background stratified by AR status in cases positive and negative for *NPM1* mut. No significant difference in patient background was observed between the low-AR and high-AR groups in the *NPM1* mut-positive cases. Thus, although cases with low-AR *FLT3*-ITD accompanied by *NPM1* mut are classified according to the ELN recommendation²⁵ as having favorable prognosis, our results indicate an associated OS of $\leq 50\%$, which, far from being favorable, represents an intermediate outcome. Moreover, although high-AR *FLT3*-ITD cases additionally positive for *NPM1* mut are classified by the

Table 2. Outcome data according to *FLT3*-ITD AR level

	AR		OR (95% CI)	P
	<0.5 (n = 59)	≥0.5 (n = 88)		
All patients				
PIF	17 (28.9)	26 (29.5)	0.993 (0.477-2.063)	.985
CR1	37 (62.7)	57 (64.8)		
Excluding patients who received allo-HSCT in CR1				
Relapse after CR1	12 (20.3)	26 (29.5)	0.867 (0.171-4.576)	1.000
Nonrelapse after CR1	2 (3.9)	5 (5.7)		
Resistant to reinduction	4 (6.8)	11 (12.5)	0.458 (0.058-4.063)	.637
CR2	1 (1.7)	6 (6.8)		

Values represent n (%) of patients.

CI, confidence interval; OR, odds ratio; PIF, primary induction failure.

ELN guidelines²⁵ in the intermediate group, according to our findings, this group has OS of ≤25%, corresponding to an unfavorable outcome.

Prognostic impact of AR and allo-HSCT

FLT3-ITD-positive AML patients who did not undergo allo-SCT had significantly less favorable outcome (Figure 3A). In the group in which allo-HSCT was performed, cases with low AR had significantly more favorable outcome in RFS and OS than cases with high AR (RFS: low AR vs high AR, $P = .012$; OS: low AR vs high AR, $P = .004$) (Figure 3B). In the group in which allo-HSCT was not performed, no significant difference in RFS and OS was found between the low-AR and high-AR groups, both of which had unfavorable outcomes (RFS: low AR vs high AR, $P = .812$; OS: low

AR vs high AR, $P = .967$) (Figure 3B) (supplemental Table 1A). Cases with *FLT3*-ITD low AR are classified by the ELN recommendation as having good prognosis, but in our analysis, cases in this group not undergoing allo-HSCT had a very poor outcome.

In the group in which allo-HSCT was performed in CR1, no significant difference in RFS and OS was found between cases with low AR and those with high AR, with both groups having a favorable outcome (RFS: low AR vs high AR, $P = .501$; OS: low AR vs high AR, $P = .266$) (Figure 4A) (supplemental Table 1B).

Among *NPM1* mut-positive AML cases with *FLT3*-ITD where allo-HSCT was performed in CR1, no significant difference in RFS and OS was found between cases with low AR and those with high AR, with both groups having a favorable outcome (RFS: low AR vs high AR, $P = .372$; OS: low AR vs high AR, $P = .695$) (Figure 4B) (supplemental Table 1C).

Significance of allo-HSCT in CR1 in cases with low-AR *FLT3*-ITD

Among cases with low-AR *FLT3*-ITD, those undergoing allo-HSCT in CR1 had a significantly more favorable outcome than those who did not receive allo-HSCT in CR1 (RFS: $P < .001$; OS: $P < .001$) (Figure 4A). Moreover, in cases with low-AR *FLT3*-ITD, even with stratification for *NPM1* mut, those who underwent allo-HSCT in CR1 had a significantly more favorable outcome than those that did not have allo-HSCT in CR1 (RFS $P = .013$; OS $P = .003$) (Figure 4B). To allow for the possibility that age influenced the decision on whether to carry out transplant in CR1, an analysis stratified by age of <70 years was performed in the low-AR *FLT3*-ITD group. However, the result of this stratified analysis also showed that performing transplant in CR1 significantly improved outcome, regardless of whether *NPM1* mut was also present (low AR, RFS $P < .001$; OS $P < .001$) (low AR + *NPM1* mut, RFS $P = .044$; OS $P = .028$) (supplemental Figure 4; supplemental Tables 2 and 3).

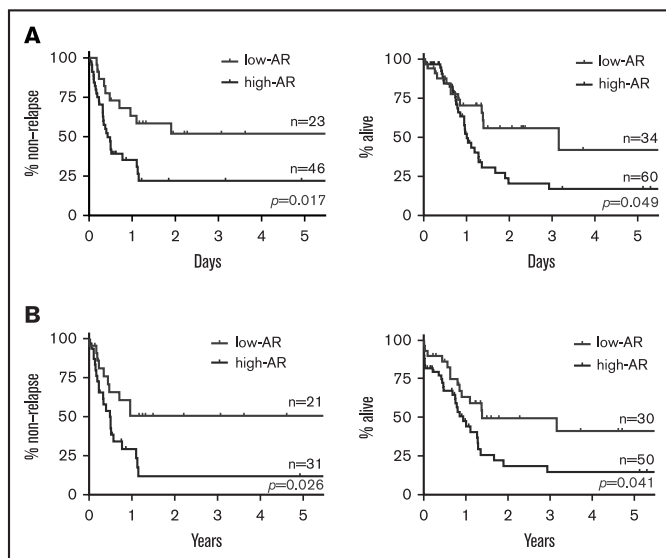


Figure 2. Impact on RFS and OS of *FLT3*-ITD AR focus on patients younger than 70 years with intermediate prognosis based on karyotype and *NPM1* mut. (A) RFS (left) and OS (right) of patients <70 years with intermediate prognosis based on karyotype stratified for *FLT3*-ITD AR. The low-AR group was found to have significantly better outcomes in both RFS and OS than the high-AR group (RFS at 5 years: low-AR group 51.9% vs high-AR group 22.8%, $P = .017$; OS at 5 years: low-AR group 41.9% vs high-AR group 17.1%, $P = .049$). (B) RFS (left) and OS (right) of *NPM1* mut-positive cases stratified for *FLT3*-ITD AR. When analysis was restricted to *NPM1* mut-positive cases, RFS and OS were again found to be significantly more favorable in the low-AR group than the high-AR group (RFS at 5 years: low-AR group 50.5% vs high-AR group 11.7%, $P = .026$; OS at 5 years: low-AR group 41.3% vs high-AR group 14.7%, $P = .041$). However, in contrast to the classification of the ELN guidelines,²⁵ the low-AR group, with a 5-year survival rate of 41.3%, was found to have not a good but an intermediate prognosis, and the high-AR group, with a 5-year survival rate of 14.7%, was found to have not an intermediate but an unfavorable prognosis.

Table 3. Clinical background of AML patients with and without *NPM1* mut

	All (n = 146)	<i>NPM1</i> + (n = 83)			P	<i>NPM1</i> - (n = 63)			P
		AR <0.5 (n = 31)	AR ≥0.5 (n = 52)			< 0.5 (n = 27)	≥ 0.5 (n = 36)		
Age (y), median (range)	56 (18-90)	58 (26-80)	56 (18-90)		.873	52 (21-96)	55 (20-90)		.673
Sex									
Male	66	13	15		.240	17	21		.797
Female	77	17	36		.239	8	15		.430
Unknown	4	1	1		1.000	2	0		.180
ECOG-PS, 0/1/2/3/4	41/45/6/3/3	12/9/1/0/0	11/19/3/2/2			9/7/0/3/0	9/10/2/0/1		
WBC count, median (range), $\times 10^9/L$	60.4 (1.0-677.0)	49.9 (1.0-470.5)	85.6 (2.1-677.0)		.519	36.2 (1.1-620.0)	48.9 (1.3-450.1)		.0570
Hb, median (range), g/dL	8.5 (3.5-15.1)	8.9 (3.3-14.3)	8.5 (4.4-14.9)		.756	8.0 (4.1-15.0)	8.7 (4.1-15.1)		.926
PLt count, median (range), $\times 10^9/L$	50.0 (5.0-630.0)	49.0 (11.0-160.0)	45.0 (5.0-339.0)		.708	82.0 (6.0-630.0)	50.0 (6.0-540.0)		.602
LDH, median (range), IU/L	718 (151-5930)	588 (204-3788)	695 (156-4144)		.093	718 (151-5930)	819 (157-3915)		.891
FAB									
M0	6	0	2		.526	1	3		.629
M1	51	13	22		1.000	4	12		.144
M2	36	7	8		.556	11	10		.296
M4	29	5	8		1.000	8	8		.566
M5	17	4	10		.554	0	3		.253
Not determined	7	2	2		.927	3	0		.073
Chromosomal aberrations									
t(8;21)	4	0	0		1.000	2	2		1.000
inv(16)	1	0	0		1.000	1	0		.429
Normal	105	23	46		.130	16	20		.802
Trisomy 8	3	0	0		1.000	0	3		.253
11q23	0	0	0		1.000	0	0		1.000
Complex	4	0	1		1.000	1	2		1.000
Unknown	8	2	3		1.000	2	1		.572
Gene mutation									
<i>FLT3</i> -TKD	0	0	0		1.000	0	0		1.000
<i>CEBPA</i> (km)	8	2	1		.553	3	2		.643
<i>CEBPA</i> (dm)	3	0	0		1.000	3	0		.0073
Induction therapy									
(IDA/DNR/ACR) + Ara-C	108	24	39		1.000	17	28		.262
AVW, BHAC-DM, CAG	24	5	6		.739	6	7		1.000
Others	14	2	7		.473	4	1		.155
Stem cell transplantation									
AI	65	12	22		.821	14	17		.801
In CR1	31	8	6		.130	8	9		.777

Data are numbers of patients, except as noted. Some data are missing due to the unavailability of certain follow-up data in a retrospective study.
 HU, hydroxyurea.

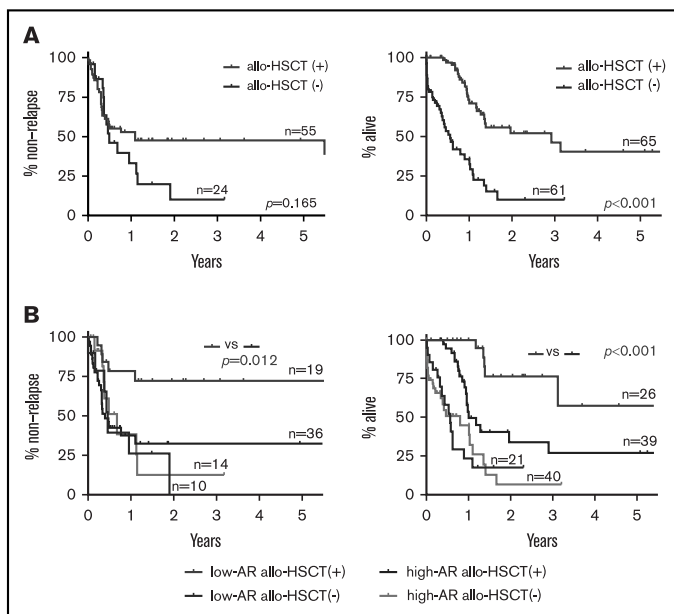


Figure 3. Impact on RFS and OS of *FLT3*-ITD AR and allo-HSCT. (A) Comparison of RFS (left) and OS (right) with and without allo-HSCT. The group in which transplant was carried out had significantly better OS than the nontransplant group. Additionally, although the difference was not significant, RFS showed a superior tendency in the transplant group compared with the nontransplant group (RFS at 3 years: allo-HSCT [+] 47.4% vs allo-HSCT [-] 9.9%, $P = .165$; OS at 3 years: allo-HSCT [+] 46.1% vs allo-HSCT [-] 10.1%, $P < .001$). (B) RFS (left) and OS (right) with and without allo-HSCT and stratified for AR. When analysis was restricted to *FLT3*-ITD low-AR cases, RFS and OS were again found to be significantly more favorable in the allo-HSCT (+) group than the allo-HSCT (-) group (RFS at 2 years: allo-HSCT [+] group 72.6% vs allo-HSCT [-] group 0.0%, $P = .012$; OS at 2 years: allo-HSCT [+] group 76.5% vs allo-HSCT [-] group 17.4%, $P < .001$). Among *FLT3*-ITD high-AR cases, the transplant group had significantly better OS than the nontransplant group. Additionally, although the difference was not significant, RFS showed a superior tendency in the transplant group compared with the nontransplant group (RFS at 5 years: allo-HSCT [+] group 32.4% vs allo-HSCT [-] group 12.7%, $P = .784$; OS at 2 years: allo-HSCT [+] group 33.7% vs allo-HSCT [-] group 6.4%, $P = .002$).

The findings presented above suggest that prognosis in *FLT3*-ITD-positive AML could be improved by performing allo-HSCT in CR1 irrespective of *FLT3*-ITD AR and *NPM1* mut.

Prognostic factor analysis

The results of prognostic factor analysis carried out using Cox proportional hazard regression analysis are shown in Table 4. Favorable prognostic factors associated with significant difference in RFS in univariate analysis were white blood cell count of $\leq 20 \times 10^9/L$ (HR, 0.415; $P < .001$), AR < 0.5 (HR, 0.460; $P = .010$), and allo-HSCT in CR1 (HR, 0.083; $P < .001$). In multivariate analysis, the only favorable prognostic factor associated with significant difference was allo-HSCT in CR1 (HR, 0.066; $P < .001$). Prognostic factors associated with significant difference in OS in univariate analysis were white blood cell count of $20 \times 10^9/L$ or below (HR, 0.544; $P = .024$), age (HR, 1.039; $P < .001$), AR < 0.5 (HR, 0.555; $P = .017$), allo-HSCT (HR, 0.248; $P < .001$), and allo-HSCT in CR1 (HR, 0.113; $P < .001$). In multivariate analysis, the prognostic factor associated with significant difference was age (HR, 1.033; $P < .001$) and allo-HSCT in CR1 (HR, 0.092; $P < .001$).

Discussion

We found that *FLT3*-ITD low AR with *NPM1* mut was not associated with favorable outcome and that careful interpretation was required with respect to the ELN recommendation, which classifies such cases as having favorable prognosis. In *FLT3*-ITD-positive AML, we additionally found that performing allo-HSCT during CR1 irrespective of AR and *NPM1* mut significantly improves outcome. Although *FLT3*-ITD AR is used in the prognostic stratification of *FLT3*-ITD-positive AML, low AR was not associated with favorable prognosis and was not a factor influencing therapeutic strategy.

AML with low-AR *FLT3*-ITD accompanied by *NPM1* mut is reported in some studies to have intermediate outcome, with 5-year OS of 35% to 47%,^{12,22,23,32} while elsewhere it is reported to be associated with good outcome, with a 3-year OS of ~60%.²⁴ However, as the reports quoted include some whose analysis is restricted to cases with intermediate cytogenetic prognosis^{23,32} or to cases aged 60 years or below,²² and one that excludes cases having undergone allo-HSCT,²⁴ their results need to be interpreted with care. When our data are supplemented with the findings of these reports, AML with low-AR *FLT3*-ITD and *NPM1* mut appears to be of intermediate outcome, rather than belonging in the favorable prognostic classification proposed by the ELN.

So what should we conclude as to whether to perform allo-HSCT in CR1 for the treatment of AML with low-AR *FLT3*-ITD combined with *NPM1* mut? Pratorcora et al reported no usefulness of allo-HSCT in CR1 in patients who were *NPM1* mut-positive and had wild-type or low-AR *FLT3*-ITD; however, as the group that received allo-HSCT in CR1 did show a clear tendency to more favorable outcome than the group that did not receive allo-HSCT in CR1, questions remain regarding the conclusion of the study.²² Meanwhile, Ho et al report that, in a group with *FLT3*-ITD AR < 0.8 , patients who received allo-HSCT in CR1 and those that received chemotherapy without allo-HSCT in CR1 had similar therapeutic outcomes, with a 5-year OS of ~60%.³³ However, no stratification for *NPM1* mut was carried out, and in the group that received chemotherapy rather than allo-HSCT in CR1, information is lacking as to whether allo-HSCT was performed after first relapse, making the results difficult to interpret. Kim et al analyzed outcome comparing patients with AF $< 50\%$ and mutant size < 70 bp with other cases.³⁴ Focusing only on patients with a normal karyotype, they found that the group with AF $< 50\%$ and

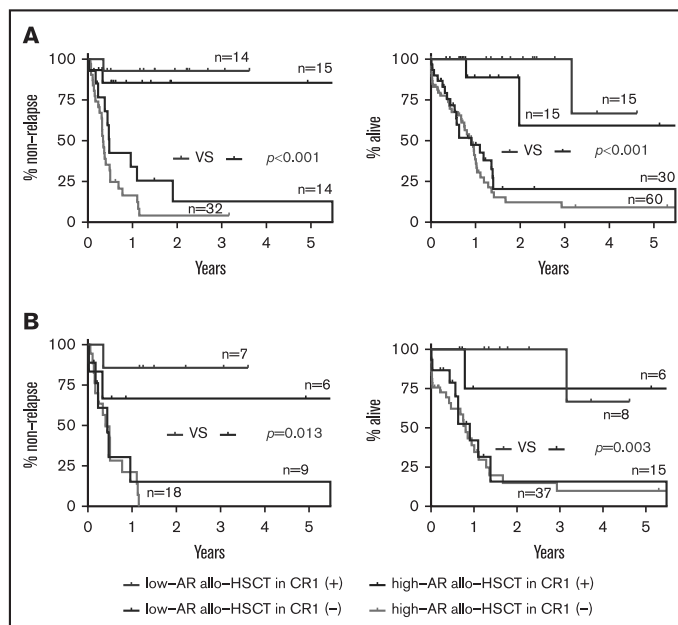


Figure 4. Impact on RFS and OS of allo-HSCT in CR1 and FLT3-ITD AR. (A) RFS (left) and OS (right) with and without allo-HSCT in CR1 and stratified for FLT3-ITD AR. Among FLT3-ITD low-AR cases, the group in which transplant was carried out in CR1 had significantly more favorable RFS and OS than the group in which transplant was not carried out in CR1 (RFS at 3 years: allo-HSCT in CR1 [+] group 92.9% vs allo-HSCT in CR1 [-] group 12.8%, $P < .001$; OS at 4 years: allo-HSCT in CR1 [+] group 66.7% vs allo-HSCT in CR1 [-] group 20.4%, $P < .001$). Similarly, among FLT3-ITD high-AR cases, RFS and OS were significantly more favorable in the group with transplant in CR1 than in the group without transplant in CR1 (RFS at 3 years: allo-HSCT in CR1 [+] group 85.6% vs allo-HSCT in CR1 [-] group 4.1%, $P < .001$; OS at 4 years: allo-HSCT in CR1 [+] group 66.7% vs allo-HSCT in CR1 [-] group 9.9%, $P = .030$). (B) RFS (left) and OS (right) in patients positive for both FLT3-ITD and NPM1 mut, showing results with and without allo-HSCT in CR1 and stratified for FLT3-ITD AR. Among FLT3-ITD low-AR cases, RFS and OS were significantly more favorable in the group with transplant in CR1 than in the group without transplant in CR1 (RFS at 3 years: allo-HSCT in CR1 [+] group 85.7% vs allo-HSCT in CR1 [-] group 15.2%, $P = .013$; OS at 4 years: allo-HSCT in CR1 [+] group 66.7% vs allo-HSCT in CR1 [-] group 15.6%, $P = .003$). Among FLT3-ITD high-AR cases similarly, RFS and OS were significantly more favorable in the group with transplant in CR1 than in the group without transplant in CR1 (RFS at 3 years: allo-HSCT in CR1 [+] group 66.7% vs allo-HSCT in CR1 [-] group 0.0%, $P = .036$; OS at 4 years: allo-HSCT in CR1 [+] group 75.0% vs allo-HSCT in CR1 [-] group 9.9%, $P = .030$). The group without allo-HSCT in CR1 includes cases that did not receive allo-HSCT.

mutant size <70 bp had a 5-year OS of $\sim 35\%$, rising to $\sim 65\%$ if allo-HSCT was performed, which is equivalent to the outcome associated with wild-type FLT3. However, this study also did not stratify for NPM1 mut and did not indicate at which stage allo-HSCT was performed. We carried out stratification for NPM1 mut in cases with FLT3-ITD low AR, and our analysis took account of the stage at which allo-HSCT was performed, the relapse rate in cases not undergoing allo-HSCT in CR1, and the rate of successful second remission following the first relapse. As a result, we found that allo-HSCT in CR1 significantly improved outcomes in this group of patients. Therefore, in contrast to the ELN recommendation against allo-HSCT in CR1 for NPM1 mut-positive AML with FLT3-ITD low AR, we recommend that NPM1 mut-positive AML with FLT3-ITD low AR should be treated with allo-HSCT in CR1 if a suitable donor is available.

One potential problem with the present study lies in the small number of cases of FLT3-ITD low-AR AML in which allo-HSCT was not performed in CR1. In clinical practice since 2010, based on the view that FLT3-ITD-positive AML patients have poor prognosis,

allo-HSCT in CR1 is frequently and actively pursued when a suitable donor is available. We therefore included in the present study a retrospective analysis of cases from a period when genetic mutation analysis was not carried out as a prognostic factor. This makes possible a comparison within FLT3-ITD-positive AML cases between those in which allo-HSCT was carried out in CR1 and those in which it was not. Given the above and the improvement in allo-HSCT treatment techniques, it is possible that our results may have been influenced by the period in which treatment was received. As the present study was a retrospective one, a further problem is that we could not perform an analysis of the reasons why transplant was not possible in CR1 (eg, comorbid infectious disease).

The multikinase inhibitor midostaurin has been shown to improve the therapeutic result when administered concomitantly with chemotherapy.³⁵ In the relevant report, allo-HSCT in CR1 was carried out in 28.1% of the midostaurin group and in 22.7% of the placebo group, and the 4-year OS rate was found to show a more favorable tendency in the midostaurin group. However, as no account was taken of AR,

Table 4. Multivariate analysis of prognostic factor

	Univariate analysis			Multivariate analysis		
	HR	95% CI	P	HR	95% CI	P
RFS						
WBC count $<20 \times 10^9/L$	0.415	0.216-0.800	$<.001$	1.113	0.474-2.614	.805
Age	1.017	0.998-1.036	.077			
Not poor cytogenetic prognosis	1.008	0.245-4.148	.991			
AR <0.5	0.460	0.255-0.830	.010	0.578	0.284-1.178	.135
Presence of <i>NPM1</i> mut	1.536	0.903-2.614	.114			
Allo-HSCT at any time	0.641	0.343-1.197	.163	NA	NA	NA
Allo-HSCT at CR1	0.083	0.030-0.234	$<.001$	0.066	0.020-0.218	$<.001$
OS						
WBC count $<20 \times 10^9/L$	0.544	0.321-0.924	.024	0.754	0.376-1.513	.427
Age	1.039	1.023-1.055	$<.001$	1.033	1.016-1.051	$<.001$
Not poor cytogenetic prognosis	1.037	0.379-2.838	.944			
AR <0.5	0.555	0.343-0.898	.017	0.747	0.435-1.286	.293
Presence of <i>NPM1</i> mut	1.313	0.846-2.038	.225			
Allo-HSCT at any stage	0.248	0.150-0.409	$<.001$	NA	NA	NA
Allo-HSCT in CR1	0.113	0.045-0.281	$<.001$	0.092	0.028-0.302	$<.001$

HR, hazard ratio; NA, not available.

the impact of AR and midostaurin remains unclear. Going forward, it would be helpful to undertake a renewed analysis of prognosis based on the inclusion of AR. In the present study, 5-year OS in the low-AR group was 39.1%. If the use of *FLT3* inhibitors and other therapies succeeds in raising OS by $\sim 10\%$ to 15%, then in the future, patients in the low-AR group might be treated as if they belong to the favorable prognosis group. *FLT3* inhibitors may thus make it possible to avoid allo-HSCT.

The present study consisted of a prognostic analysis of AR in *FLT3*-ITD-positive AML before the advent of *FLT3* inhibitors. Going forward, the advent of *FLT3* inhibitors may bring about major changes in therapeutic methods and outcomes. For example, Döhner et al report that low-AR *FLT3*-ITD patients with *NPM1* mut have a 5-year OS of $\sim 50\%$ with chemotherapy alone, indicating intermediate prognosis as in our findings, but that chemotherapy supplemented with *FLT3* inhibitor treatment may improve 5-year OS to $\sim 70\%$, placing these patients in the favorable prognosis group.³⁶

For the present, however, we recommend allo-HSCT in CR1 for *FLT3*-ITD-positive AML in cases where a suitable donor is available, regardless of whether *NPM1* mut is also present.

References

- Ohtake S, Miyawaki S, Fujita H, et al. Randomized study of induction therapy comparing standard-dose idarubicin with high-dose daunorubicin in adult patients with previously untreated acute myeloid leukemia: the JALSG AML201 Study. *Blood*. 2011;117(8):2358-2365.
- Kurosawa S, Yakushijin K, Yamaguchi T, et al. Changes in incidence and causes of non-relapse mortality after allogeneic hematopoietic cell transplantation in patients with acute leukemia/myelodysplastic syndrome: an analysis of the Japan Transplant Outcome Registry. *Bone Marrow Transplant*. 2013;48(4):529-536.
- Patel JP, Gönen M, Figueroa ME, et al. Prognostic relevance of integrated genetic profiling in acute myeloid leukemia. *N Engl J Med*. 2012;366(12):1079-1089.

Acknowledgment

The authors thank the physicians who cared for patients and collected clinical data during this study.

Authorship

Contribution: M.S. and H.Y. were the principal investigators and take primary responsibility for the paper; Y.N., K.U., T.U., I. Oh, S.M., E.K., N. Uoshima, Y. Kobayashi, S. Kako, K.T., S.G., K.S., K. Kayamori, M.H., J. Kanda, H.U., J. Kuroda, N. Uchida, Y. Kubota, S. Kimura, S. Kurosawa, K. Kakihana, Y. Kanda, T.F., and K.O. recruited the cases; M.S., H.Y., N.N., K.A., and T.K. performed the laboratory work for the study; and M.S., H.Y., N.N., A.M., I. Omori, Y.F., S.Y., S.W., and K.I. analyzed the data and wrote the paper.

Conflict-of-interest disclosure: The authors declare no competing financial interests.

ORCID profile: K. Kakihana, 0000-0001-5062-5795.

Correspondence: Hiroki Yamaguchi, Department of Hematology, Nippon Medical School, 1-1-5 Sendagi, Bunkyo-Ku, Tokyo 113-8603, Japan; e-mail: y-hiroki@fd6.so-net.ne.jp.

4. Nakao M, Yokota S, Iwai T, et al. Internal tandem duplication of the *flt3* gene found in acute myeloid leukemia. *Leukemia*. 1996;10(12):1911-1918.
5. Small D. *FLT3* mutations: biology and treatment. *Hematology Am Soc Hematol Educ Program*. 2006;2006:178-184.
6. Kayser S, Schlenk RF, Londono MC, et al; German-Austrian AML Study Group (AML-SG). Insertion of *FLT3* internal tandem duplication in the tyrosine kinase domain-1 is associated with resistance to chemotherapy and inferior outcome. *Blood*. 2009;114(12):2386-2392.
7. Hayakawa F, Towatari M, Kiyoi H, et al. Tandem-duplicated *Flt3* constitutively activates STAT5 and MAP kinase and introduces autonomous cell growth in IL-3-dependent cell lines. *Oncogene*. 2000;19(5):624-631.
8. Mizuki M, Fenski R, Halfter H, et al. *Flt3* mutations from patients with acute myeloid leukemia induce transformation of 32D cells mediated by the Ras and STAT5 pathways. *Blood*. 2000;96(12):3907-3914.
9. Brandts CH, Sargin B, Rode M, et al. Constitutive activation of Akt by *Flt3* internal tandem duplications is necessary for increased survival, proliferation, and myeloid transformation. *Cancer Res*. 2005;65(21):9643-9650.
10. Stirewalt DL, Radich JP. The role of FLT3 in haematopoietic malignancies. *Nat Rev Cancer*. 2003;3(9):650-665.
11. Kottaridis PD, Gale RE, Linch DC. *Flt3* mutations and leukaemia. *Br J Haematol*. 2003;122(4):523-538.
12. Gale RE, Green C, Allen C, et al; Medical Research Council Adult Leukaemia Working Party. The impact of FLT3 internal tandem duplication mutant level, number, size, and interaction with NPM1 mutations in a large cohort of young adult patients with acute myeloid leukemia. *Blood*. 2008;111(5):2776-2784.
13. Schlenk RF, Döhner K, Krauter J, et al; German-Austrian Acute Myeloid Leukemia Study Group. Mutations and treatment outcome in cytogenetically normal acute myeloid leukemia. *N Engl J Med*. 2008;358(18):1909-1918.
14. Bornhäuser M, Illmer T, Schaich M, Soucek S, Ehninger G, Thiede C; AML SHG 96 study group. Improved outcome after stem-cell transplantation in *FLT3/ITD*-positive AML. *Blood*. 2007;109(5):2264-2265, author reply 2265.
15. Brunet S, Labopin M, Esteve J, et al. Impact of *FLT3* internal tandem duplication on the outcome of related and unrelated hematopoietic transplantation for adult acute myeloid leukemia in first remission: a retrospective analysis. *J Clin Oncol*. 2012;30(7):735-741.
16. Meshinchi S, Arceci RJ, Sanders JE, et al. Role of allogeneic stem cell transplantation in *FLT3/ITD*-positive AML. *Blood*. 2006;108(1):400-401, author reply 400-401.
17. Schnittger S, Schoch C, Kern W, et al. Nucleophosmin gene mutations are predictors of favorable prognosis in acute myelogenous leukemia with a normal karyotype. *Blood*. 2005;106(12):3733-3739.
18. Döhner K, Schlenk RF, Habdank M, et al. Mutant *nucleophosmin (NPM1)* predicts favorable prognosis in younger adults with acute myeloid leukemia and normal cytogenetics: interaction with other gene mutations. *Blood*. 2005;106(12):3740-3746.
19. Verhaak RG, Goudswaard CS, van Putten W, et al. Mutations in *nucleophosmin (NPM1)* in acute myeloid leukemia (AML): association with other gene abnormalities and previously established gene expression signatures and their favorable prognostic significance. *Blood*. 2005;106(12):3747-3754.
20. Thiede C, Koch S, Creutzig E, et al. Prevalence and prognostic impact of *NPM1* mutations in 1485 adult patients with acute myeloid leukemia (AML). *Blood*. 2006;107(10):4011-4020.
21. Brown P, McIntyre E, Rau R, et al. The incidence and clinical significance of nucleophosmin mutations in childhood AML. *Blood*. 2007;110(3):979-985.
22. Pratorcorona M, Brunet S, Nomdedéu J, et al; Grupo Cooperativo Para el Estudio y Tratamiento de las Leucemias Agudas Mieloblásticas. Favorable outcome of patients with acute myeloid leukemia harboring a low-allelic burden *FLT3-ITD* mutation and concomitant *NPM1* mutation: relevance to post-remission therapy. *Blood*. 2013;121(14):2734-2738.
23. Schlenk RF, Kayser S, Bullinger L, et al; German-Austrian AML Study Group. Differential impact of allelic ratio and insertion site in *FLT3-ITD*-positive AML with respect to allogeneic transplantation. *Blood*. 2014;124(23):3441-3449.
24. Schnittger S, Bacher U, Kern W, Alpermann T, Haeflrich C, Haeflrich T. Prognostic impact of *FLT3-ITD* load in *NPM1* mutated acute myeloid leukemia. *Leukemia*. 2011;25(8):1297-1304.
25. Döhner H, Estey E, Grimwade D, et al. Diagnosis and management of AML in adults: 2017 ELN recommendations from an international expert panel. *Blood*. 2017;129(4):424-447.
26. NCCN Clinical Practice Guidelines in Oncology (NCCN Guidelines). Acute Myeloid Leukemia Version 2.2014. Available at: <http://williams.medicine.wisc.edu/aml.pdf>. Accessed 1 April 2017.
27. Zwaan CM, Meshinchi S, Radich JP, et al. FLT3 internal tandem duplication in 234 children with acute myeloid leukemia: prognostic significance and relation to cellular drug resistance. *Blood*. 2003;102(7):2387-2394.
28. Kottaridis PD, Gale RE, Frew ME, et al. The presence of a FLT3 internal tandem duplication in patients with acute myeloid leukemia (AML) adds important prognostic information to cytogenetic risk group and response to the first cycle of chemotherapy: analysis of 854 patients from the United Kingdom Medical Research Council AML 10 and 12 trials. *Blood*. 2001;98(6):1752-1759.
29. Wakita S, Yamaguchi H, Ueki T, et al. Complex molecular genetic abnormalities involving three or more genetic mutations are important prognostic factors for acute myeloid leukemia. *Leukemia*. 2016;30(3):545-554.
30. Wakita S, Yamaguchi H, Omori I, et al. Mutations of the epigenetics-modifying gene (*DNMT3a*, *TET2*, *IDH1/2*) at diagnosis may induce *FLT3-ITD* at relapse in de novo acute myeloid leukemia. *Leukemia*. 2013;27(5):1044-1052.
31. Kanda Y. Investigation of the freely available easy-to-use software 'EZ' for medical statistics. *Bone Marrow Transplant*. 2013;48(3):452-458.
32. Linch DC, Hills RK, Burnett AK, Khwaja A, Gale RE. Impact of FLT3(ITD) mutant allele level on relapse risk in intermediate-risk acute myeloid leukemia. *Blood*. 2014;124(2):273-276.

33. Ho AD, Schetelig J, Bochtler T, et al; Study Alliance Leukemia. Allogeneic stem cell transplantation improves survival in patients with acute myeloid leukemia characterized by a high allelic ratio of mutant *FLT3*-ITD. *Biol Blood Marrow Transplant*. 2016;22(3):462-469.
34. Kim Y, Lee GD, Park J, et al. Quantitative fragment analysis of FLT3-ITD efficiently identifying poor prognostic group with high mutant allele burden or long ITD length. *Blood Cancer J*. 2015;5(8):e336.
35. Stone RM, Mandrekar SJ, Sanford BL, et al. Midostaurin plus Chemotherapy for Acute Myeloid Leukemia with a *FLT3* Mutation. *N Engl J Med*. 2017; 377(5):454-464.
36. Döhner K, Thiede C, Larson RA, et al. Prognostic impact of NPM1/FLT3-ITD genotypes from randomized patients with acute myeloid leukemia (AML) treated within the international ratify study [abstract]. *Blood*. 2017;130(suppl 1). Abstract 467.